Solution-Phase and Automated Solid-Phase Synthesis of High-Mannose Oligosaccharides: Application to Carbohydrate Microarrays and Biological Studies

by

Daniel Martin Ratner

B.A., Chemistry (1999)
Pomona College

Submitted to the Department of Chemistry in partial fulfillment of the requirements for the degree of

Doctor of Philosophy

at the
Massachusetts Institute of Technology
September, 2004

Signature of Author_____
Department of Chemistry
August 19, 2004

Certified By_____
Peter H. Seeberger
Visiting Professor of Chemistry, MIT
Professor of Chemistry, ETH Zurich, CH
Thesis Supervisor

Accepted By_____
Robert W. Field
Professor of Chemistry
Chairman, Departmental Committee on Graduate Students

This doctoral thesis has been examined by a committee of the Department of Chemistry as follows:

Professor Daniel S. Kemp_____
Chair

Professor Peter H. Seeberger_____
Thesis Supervisor

Professor Barbara Imperiali_____
Department of Chemistry

Solution-Phase and Automated Solid-Phase Synthesis of High-Mannose Oligosaccharides: Application to Carbohydrate Microarrays and Biological Studies

by

Daniel Martin Ratner

Submitted to the Department of Chemistry
on August 19, 2004 in Partial Fulfillment of the
Requirements for the Degree of Doctor of Philosophy

ABSTRACT

Glycosylation is critical to cellular function in eukaryotic systems. *N*-linked modification of asparagine residues within nascent proteins is involved in numerous folding and processing pathways. *N*-linked glycans are also a common feature of viral-associated envelope glycoproteins, including gp120 and gp41 of the human immunodeficiency virus (HIV-1). These glycans are attractive targets for therapy and prophylaxis due to their numerous roles in HIV infectivity and immunoevasion.

This thesis describes the solution-phase synthesis of a series high-mannose type glycans using a linear synthetic approach. The synthetic mannans are used to study the potent anti-HIV microbicide cyanovirin-N, a novel 11 kDa protein isolated from the cyanobacterium (blue-green algae) *Nostoc ellipsosporum*. These studies established the structural basis for carbohydrate-binding by cyanovirin-N, which is responsible for its HIV inactivating properties.

Automated solid-phase synthesis and microfluidic reactors were employed in the development of new technologies for synthetic carbohydrate chemistry. Utilizing a carbohydrate synthesizer, the first automated solid-phase synthesis of the *N*-linked core pentasaccharide is detailed. In addition, the design, fabrication and application of a microreactor for optimizing the glycosylation reaction is described.

Utilizing a novel tri(ethylene glycol) linker with a reactive thiol handle, the fabrication of carbohydrate microarrays is depicted. A panel of oligosaccharides was selected to represent the major structural determinants of high-mannose type glycans on a single microarray. These microarrays were used study the glycan-dependent binding interactions of four gp120-binding proteins: the dendritic cell lectin DC-SIGN, the antibody 2G12, cyanovirin-N, and a recently identified anti-HIV protein, scytovirin.

Thesis Supervisor: Peter H. Seeberger
Title: Visiting Professor of Chemistry, MIT
Professor of Chemistry, ETH Zurich, CH

In my view, all that is necessary for faith is the belief that by doing our best we shall come nearer to success, and that success in our aims (the improvement of the lot of mankind, present and future) is worth attaining.

Rosalind Franklin (1920-1958)
Letter to her father
Summer, 1940

Acknowledgements

This thesis documents my serendipitous journey into synthetic carbohydrate chemistry. There many who deserve acknowledgement. I apologize in advance to those I neglect to mention on this page.

I met Peter Seeberger while visiting MIT as a prospective graduate student. Peter's vision, enthusiasm, and salesmanship drew me to MIT, and ultimately to his research group. My passion for carbohydrate chemistry was lit while working alone at night creating the world's first automated solid-phase oligosaccharide synthesizer (the Emil Fischer β-2000) out of space parts and a used peptide synthesizer donated by the Kemp group.

Along the way, I met a number of extraordinary people in the Seeberger Laboratory. I had the pleasure of publishing collaboratively with several of them, including Obadiah Plante, Erika Swanson, Matt Disney, Dan Snyder and Eddie Adams. In addition, I was fortunate to have the guidance of two fine mentors, Rodrigo Bohn Andrade and the 'teacher,' Hernan Orgueira.

Beyond the confines of the Building 18, I had the opportunity to collaborate with Drs. Barry O'Keefe, Angela Gronenborn and Pradman Qasba of the National Cancer Institute of Frederick, MD; Prof. David Walt of Tufts University; Prof. Milan Mrksich and his student Jing Su of the University of Chicago; and Prof. Klavs Jensen and his student Eddie Murphy of MIT's Dept. of Chemical Engineering. These collaborations shaped my thesis, and gave meaning to my molecules.

While studying at MIT, I met a living legend – a Gandalf for my academic journey. As both my thesis committee chair and acting research advisor (2003-2004), Professor Daniel S. Kemp is the most extraordinary individual I have ever worked with, and likely ever will. His generosity is largely responsible for my ability to finish this doctoral work at MIT.

To all those mentioned above, I owe many thanks. To my readers, Diana, Sharon and Ed, I thank you for wading through countless pages while catching my many mistakes (except for thiss one). To Bob, my lone labmate, I thank you for putting up with 15 months of non-stop National Public Radio (NPR). And to Sharon, thanks for the smiles and the Peet's French Roast.

Most of all, my deepest debt of gratitude is owed to my family. To my parents, who entrusted my elementary education to a bunch of hippies known collectively as Room Nine. I may have never learned my multiplication tables, or how to spell, but I was instilled with the sense that learning is fun.

To Shannon and Philip. There are no words to express my thanks. I love you both.

For

Jan "The Geeze" Jessen

List of Abbreviations

Ac	Acetyl
All	Allyl
Asn	Asparagine
Bn	Benzyl
Bu	Butyl
Bz	Benzoyl
calcd	Calculated
CVN	Cyanovirin-N
DBU	1,8-Diazabicyclo-undec-7-ene
DDQ	2,3-Dichloro-5,6-dicyano-1,4-benzoquinone
DMAP	4-(Dimethylamino)pyridine
DMDO	Dimethyldioxirane
DMF	*N,N*-Dimethylformamide
DTBP	Di-*t*-butyl pyridine
ESI MS	Electrospray ionization mass spectrometry
Et	Ethyl
equiv	Equivalent(s)
Gal	Galactose
GAPS	Gamma amino propyl silane
gCOSY	^{1}H, ^{1}H Gradient correlation spectroscopy
Glc	Glucose
GlcNAc	*N*-Acetyl glucosamine
h	Hour(s)
HPLC	Highh performance liquid chromatography
HRMS	High resolution mass spectrometry
HSQC	Heteronuclear Single Quantum Coherence spectroscopy
Hz	Hertz
IR	Infrared
Lev	Levulinoyl

MALDI-TOF	Matrix assisted laser desorption ionization – time of flight
Man	Mannose
Me	Methyl
min	Minute(s)
MS	Mass spectrometry
ms	molecular sieves
NMR	Nuclear magnetic resonance
obsd	Observed
Pent	4-pentenyl
Ph	Phenyl
Phth	Phthaloyl
PMB	*p*-methoxylbenzyl
ppm	Parts per million
s	second(s)
SPR	Surface plasmon resonance
TBAF	tetra-*n*-Butylammonium flouride
TBS	*tert*-Butyldimethylsilyl
TBSOTf	*tert*-Butyldimethylsilyl trifuoromethanesulfonate
TCA	Trichloroacetyl
TCEP	Tris(2-Carboxyethyl) Phosphine Hydrochloride
TES	Triethylsilane
TIPS	Triisopropylsilane
Tf	Trifluoromethanesulfonyl
TFA	Trifluoroacetic acid
TFAA	Trifluoroacetic anhydride
THF	Tetrahydrofuran
TLC	Thin-layer chromatography
TMSOTf	Trimethylsilyl trifuoromethanesulfonate
TROC	2,2,2-Trichloroethoxycarbonyl
v	Volume

Portions of this thesis were adopted with permission from the following journal articles, co-written by the author.

Ratner, D. M.; Adams, E. W.; Disney, M. D.; Seeberger, P. H. Tools for Glycomics: Mapping Interactions of Carbohydrates in Biological Systems. *ChemBioChem*, **2004**, In Press.

Adams,* E. W.; Ratner,* D. M.; Bokesh, H. R.; McMahon, J. B.; O'Keefe, B. R.; Seeberger, P.H. Oligosaccharide and Glycoprotein Microarrays as Tools in HIV-Glycobiology: A Detailed Analysis of Glycan Dependent gp120 / Protein Interactions. *Chem. Biol.* **2004**, *11*, 875-881..

Ratner, D. M.; Adams, E. W.; Su, J.; O'Keefe, B. R.; Mrksich, M.; Seeberger, P. H. Probing Protein-Carbohydrate Interactions with Microarrays of Synthetic Oligosaccharides. *ChemBioChem.* **2004**, 5, 379-383.

Ratner, D. M.; Swanson, E. R.; Seeberger, P. H. Automated Synthesis of the *N*-linked Core Pentasaccharide. *Org. Lett.* **2003**, *5*, 4717-4720.

Adams, E. W.; Uberfeld, J.; Ratner, D. M.; O'Keefe, B. R.; Walt, D, R.; Seeberger, P. H. Encoded Fiber-Optic Microsphere Arrays for Probing Protein-Carbohydrate Interactions. *Angew. Chem. Int. Ed.* **2003**, *42*, 5317-5320.

Barrientos, L. G.; Louis, J. M.; Ratner, D. M.; Seeberger, P. H.; Gronenborn, A. M. Solution Structure of a Circular-permuted Variant of the Potent HIV-inactivating Protein Cyanovirin-*N*: Structural Basis for Protein Stability and Oligosaccharide Interaction. *J. Mol. Biol.* **2003**, *325*, 211-223.

Shenoy, S. R.; Barrientos, L. G.; Ratner, D. M.; O'Keefe, B. R.; Seeberger, P. H.; Gronenborn, A. M.; Boyd, M. R. Multisite and Multivalent Binding Between Cyanovirin-*N* and Branched Oligomannosides: Calorimetric and NMR Characterization. *Chem. Biol.* **2002**, *9*, 1109-1118.

Botos, I.; O'Keefe, B. R.; Shenoy S. R.; Cartner, L. K.; Ratner, D. M.; Seeberger, P. H.; Boyd, M. R.; Wlodawer, A. Structures of the Complexes of a Potent Anti-HIV Protein Cyanovirin-*N* and High-Mannose Oligosaccharides. *J. Biol. Chem.* **2002**, *277*, 34336-34342.

Ratner, D. M.; Plante, O. J.; Seeberger, P. H. A Linear Synthesis of Branched High-Mannose Oligosaccharides from the HIV-1 Viral Surface Envelope Glycoprotein gp120. *Eur. J. Org. Chem.* **2002**, *5*, 826-833.

Table of Contents

Chapter 1

Introduction and Background

1.1 Introduction

The roots of carbohydrate chemistry can be traced back over a century, to the beginnings of modern organic chemistry and the pioneering days of Emil Fischer. Decades after the sugars were first described, accumulated evidence suggested that carbohydrates were implicated in far more than structural function (cell walls) and energy storage (glucose and glycogen). Over time, the somewhat obscure field of carbohydrate chemistry has grown into a respected discipline, pursued by industry and academia alike. Today it is widely accepted that carbohydrates are among the most structurally diverse biopolymers, and play a role in an innumerable variety of vital cellular processes. The field of glycobiology is devoted entirely to unraveling the secrets of this hitherto neglected dimension of biology. Following in the footsteps of genomics and proteomics, 'glycomics' is poised to join the informatics age of biological study.

Carbohydrates, in the form of oligosaccharides and glycoconjugates are implicated in cell-cell interactions,[1] fertilization,[2] development,[3] the immune response,[4] inflammation,[5] viral-host interactions,[6] bacterial pathogenicity,[7] and signal transduction.[8] In addition to shedding light on the mechanism of countless processes in biology, carbohydrates are being adopted for use in vaccine design against human pathogens[9] and cancers.[10] Just as the human milk oligosaccharides confer protection to infants against numerous pathogens,[11] carbohydrate-based pharmaceuticals and food-additives hope to achieve similar prophylaxis.

With this growing appreciation for glycobiology came increased demand for access to pure materials for study. This has proven challenging, due to the microheterogeneity of naturally isolated oligosaccharide and glycoconjugates. And, to the frustration of glycobiologists, no process exists for amplifying purified glycans. Unlike working with protein and nucleic acid, carbohydrate research is stymied by a lack of widely available automated synthesis, sequencing, or technologies analogous to cDNA microarray and siRNA (small interfering RNA) gene silencing. A complementary set of biophysical tools for studying carbohydrates has remained elusive, and this void has hindered the emergence of this field.

Progress in carbohydrate chemistry is generating new and exciting possibilities for obtaining pure, chemically defined, oligosaccharides and neoglycoconjugates. Access to these structures is provided by improved synthetic methods, including the development of an automated solid-phase synthesizer[12] and methods for enzymatic synthesis.[13] Over time, these advances are steadily closing the technological gap between glycomics and the more advanced disciplines of genomics and proteomics.

In an effort to furnish new tools for glycobiology, this thesis will explore chemical methods for the synthesis of high-mannose oligosaccharides related to the *N*-linked glycosylation pathway and describe the development of a carbohydrate microarray. The following sections will address (1) a brief overview of *N*-linked glycosylation, (2) introduce the glycobiology of the HIV-1 virus, as it relates to *N*-linked glycosylation, (3) examine some of the challenges to the chemical synthesis of carbohydrates, and (4) detail the objectives of this dissertation.

1.2 Glycosylation in Biological Systems

A powerful feature of carbohydrates in biological systems is their ability to modify other biomolecules to form glycoconjugates. The glycosylation of peptides has a profound effect on the structure and function of the modified proteins. Glycosyl modification of peptides falls into three major classes: *N*-linked glycan modification of asparagines residues; *O*-linked glycosylation of serine or threonine residues; and glycosylphosphatidyl inositol (GPI) coupling of the carboxy-terminus. *N*-linked glycosylation is the most common saccharide-modification of protein in eukaryotic cells,[14] and is the basis for the synthetic efforts described in this thesis.

1.2.1 *N*-linked Glycosylation

N-linked glycosylation takes place in the endoplasmic reticulum (ER) as a co-translational modification of growing nascent polypeptides.[15] The reaction is catalyzed by oligosaccharyl transferase (OT), which transfers the tetradecasaccharide **1-1** from a dolichylpyrophosphate carrier to an asparagine side chain as the nascent peptide emerges

from the translocon into the lumen of the ER.[16] Glycosylation is specific for the tripeptide sequon Asn-X-Ser/Thr,[17] and it is estimated that 90% of all such sequons are glycosylated.[18]

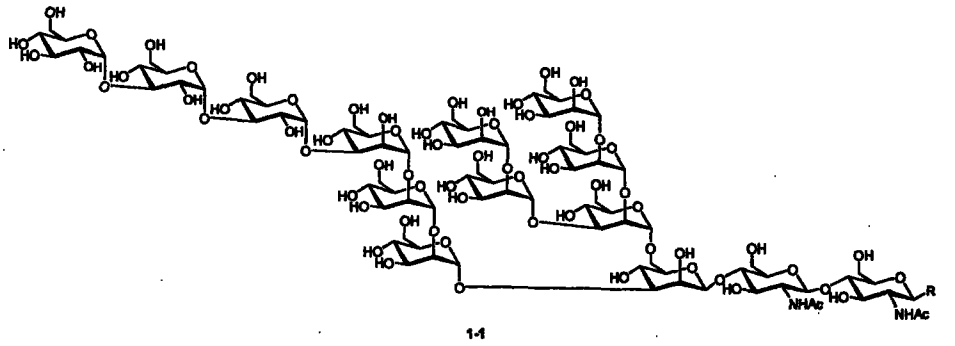

Figure 1.1 Tetradecasaccharide involved in the initial *N*-linked glycosylation of nascent peptides, transferred to asparagines side chain by oligosaccharyl transferase.

Immediately following OT glycosylation of the asparagines residue, the *N*-linked glycans proceed through a complex series of modifications. First, as the glycoprotein is moved to the Golgi complex for further modification, the terminal glucose and mannose residues are removed by ER glucosidases and mannosidases.[19] Numerous trimming and terminal glycosylations are possible in the Golgi, as the *N*-linked glycan is elaborated into its final form. Among the possible outcomes are complex, high-mannose and hybrid-type glycans (Figure 1.2).

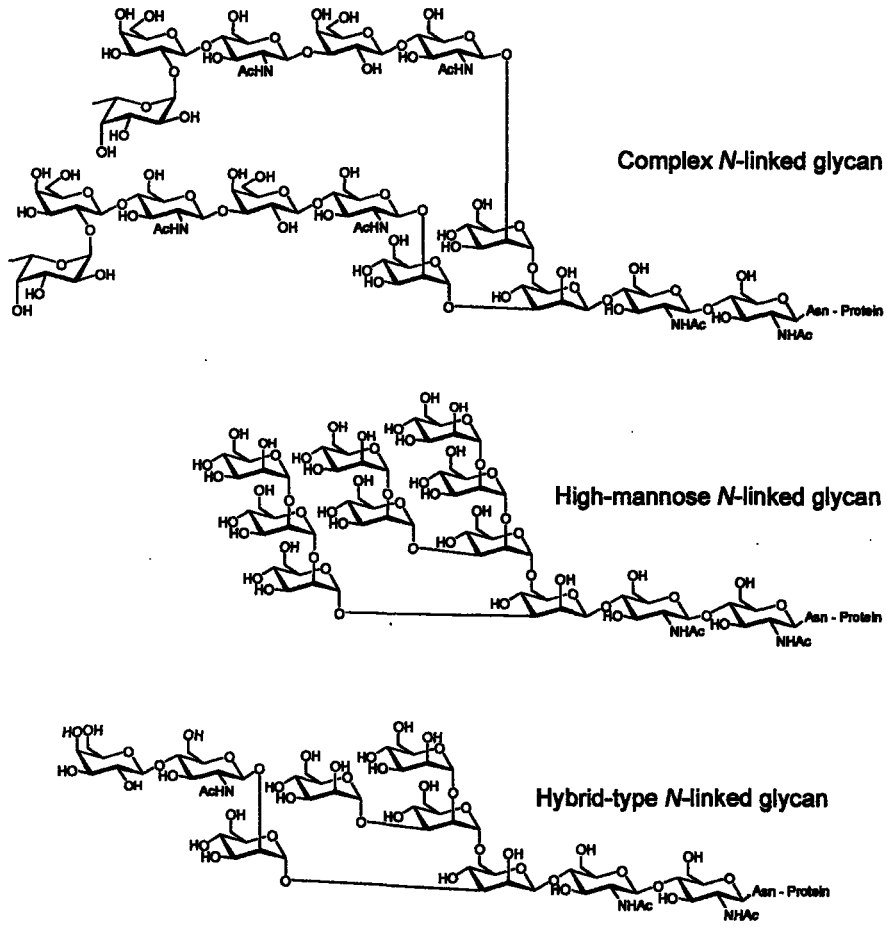

Figure 1.2 Examples of the three classes of *N*-linked glycans: complex, high-mannose and hybrid-type.

Correct protein folding is among the most vital functions of *N*-linked glycans during protein synthesis.[20] The large glycan structures can have a significant influence on the structure of a glycopeptide, thus directly affecting the folding process and protein stability.[21] Beyond these physical effects, *N*-linked glycans are involved in trafficking of unfolded proteins between the ER and Golgi and through the calnexin-calreticulin cycle, a crucial step in proper folding.[22]

N-linked glycans also play a central role in the quality control mechanism of protein synthesis within the cell. Even during unstressed conditions, misfolded side products are common during protein synthesis. Therefore cytosolic turnover of glycoproteins is essential to normal function within the cell. A misfolded protein is targeted for degradation through specific trimming of *N*-linked glycans, marking the

protein for ER-associated degradation.[23] Such ill-fated proteins are transported out of the ER into the cytosol where they are ubiquitinated and degraded by the 26S proteosome.

1.2.2 *N*-linked Glycans and the Glycobiology of HIV

Human immunodeficiency virus (HIV-1), the causative agent of acquired immune deficiency syndrome (AIDS), is an enveloped retrovirus highly decorated in glycoprotein. gp120, the major surface envelope glycoprotein of HIV-1, contains 24 sites of predicted *N*-linked glycosylation.[24] This makes the glycans a major contributor to the overall structure of the glycoprotein. In fact, 50% of the molecular mass of gp120 comprises oligosaccharide. The *N*-linked glycans are critical to HIV infectivity, as they contribute to both the proper folding of envelope glycoproteins, and increased cyto-pathogenicity of the virus.[25] Inhibition of *N*-linked glycosylation or downstream glycan processing has been proven to interfere with viral infectivity.[26]

Glycoprotein gp120 and integral membrane protein gp41 are attractive targets for developing therapies aimed at prophylaxis or decreasing HIV viral load in infected persons. gp120 and gp41 reside in the external viral membrane as a functional trimer of three non-covalently associated heterodimers.[27] This gp120/gp41 construct plays a vital role in HIV viral entry through interactions with CD4 molecules and members of the chemokine receptor family present on T lymphocytes, macrophages, dendritic cells, and brain microglia. One mode of HIV internalization by the host cell begins with CD4 binding of gp120. This exposes a chemokine receptor-binding domain on gp120 that subsequently reveals gp41, permitting insertion into the host cell membrane. Disrupting this process interferes with an important pathway in viral infection.

The prevalence of gp120 on the surface of HIV-1 makes it a major target of the humoral immune response.[28] As such, a great deal of effort in vaccine design has focused on immunizing against monomeric and oligomeric forms of gp120. This approach has been frustrated by *N*-linked glycan variability and steric masking of potential neutralization-sensitive epitopes of gp120.[29] The specific glycosylation pattern and structural composition of *N*-linked glycans is highly dependent on the host cell in which the virus was produced.[30] In addition, the predominance of the *N*-linked

glycosylation pathway in mammalian cells likely causes these modified proteins to be regarded as "self" or non-immunogenic, inhibiting a rigorous antibody response. The human monoclonal antibody 2G12 was recently described as an exception to the typical lackluster immune response to high-mannose oligosaccharides.[4] 2G12 demonstrates a nanomolar affinity for oligosaccharide clusters with an accessible Manα(1→2)Man motif.

1.2.2.1 High-Mannose Glycans and HIV

Up to 11 high-mannose oligosaccharides are among the 24 *N*-linked glycans on gp120.[31] Of these, five or six are the large octa- or nonamannose glycans (Man8 or Man9). The presence of Man8 or Man9 on virus glycoprotein is physiologically relevant because normal mammalian glycoproteins rarely contain large high-mannose glycans. To the contrary, ER and Golgi processing of native glycoproteins in mammalian systems seldom leaves high-mannose residues unmodified; non-viral glycoproteins presenting high-mannose glycans are typically targeted for rapid degradation.

By utilizing mannose-binding proteins the presence of high-mannose oligosaccharides on viral glycoprotein has been exploited as a means of blocking HIV viral entry into host cells. Pursued by the Molecular Targets Development Program of the National Cancer Institute, high-throughput screens of products derived from *Cyanobacteria* have yielded a number of protein candidates, capable of inhibiting viral entry into host cells. Among these compounds, cyanovirin-*N*,[32] an 11 kDa protein, and scytovirin,[33] a 9.6 kDa protein, are promising leads. Both proteins derive their anti-HIV activity by binding the high-mannose oligosaccharides present on gp120. It is believed that viral inhibition could be achieved by two possible mechanisms. Either by binding gp120 and preventing its receptor binding domains from interacting with their targets. Or, subsequent to protein binding, gp120 undergoes conformational changes that render its binding domains functionally inactive. *In vivo* prophylaxis studies with CVN have shown promise, and demonstrated no adverse effects upon host physiology.[34] This is possible because of the high degree to which endogenous proteins undergo *N*-linked glycan processing by the Golgi apparatus. Therefore, host cell-surface and secreted

proteins lack the high concentration of unprocessed *N*-linked glycans required for CVN targeting.

1.3 The Chemical Synthesis of Carbohydrates

The difficulty of isolating significant quantities of pure carbohydrate and glycoconjugate from natural sources poses a challenge to securing material for biological study. Preparing oligosaccharides and neoglycoconjugates by enzymatic and chemical synthesis offers a powerful solution. Both methods continue to make rapid progress towards developing new and more powerful methods for preparing structures of increasing complexity. Enzymatic syntheses, such as the novel 'superbug' and 'superbead' technology,[13,35] offer the superb control afforded by biology, utilize non-hazardous and environmentally friendly starting materials, and are suited for scale-up using batch fermentation-like methods. Chemical synthesis, on the other hand, gives the investigator access to materials that may be non-natural, and have no precedence for synthesis by biological systems. In addition, chemical synthesis generates homogenous product, free from undesired glycoforms. As such, both methods have much to contribute to the synthesis of complex saccharides.

1.3.1 The Glycosylation Reaction

Synthetic carbohydrate chemistry, the focus of this dissertation, is rooted in a tradition that reaches back over 100 years, to the first glycosylation reactions reported by Koenigs and Knorr.[36] Glycosylation is at the heart of carbohydrate synthesis, as it is the process of linking multiple carbohydrates to each other, or to other biomolecules. The glycosylation reaction involves the coupling of a glycosylating agent to a nucleophile (glycosyl acceptor). The path of a typical reaction begins with activation of the glycosyl donor, resulting in the departure of a leaving group at the anomeric position, and generation of an electrophilic cyclic oxocarbenium intermediate (Scheme 1.1). This species is subsequently reacted with a nucleophilic acceptor, typically a hydroxyl, generating a glycosidic linkage.

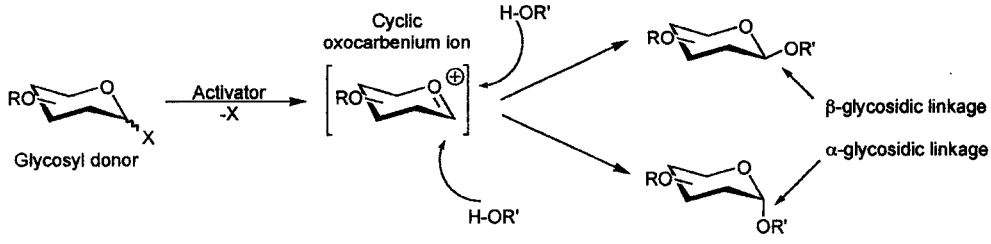

Scheme 1.1 Glycosylation reaction pathway.

Following the Koenigs and Knorr use of the glycosyl halide[36] several anomeric leaving groups have been used as glycosyl donors. Among others,[37] these have included the trichloroacetimidate,[38] glycosyl thioglycoside,[39] glycosyl sulfoxide,[40] glycosyl phosphate,[41] *n*-pentenyl glycoside[42] and 1,2-anhydrosugar (Figure 1.3).[43]

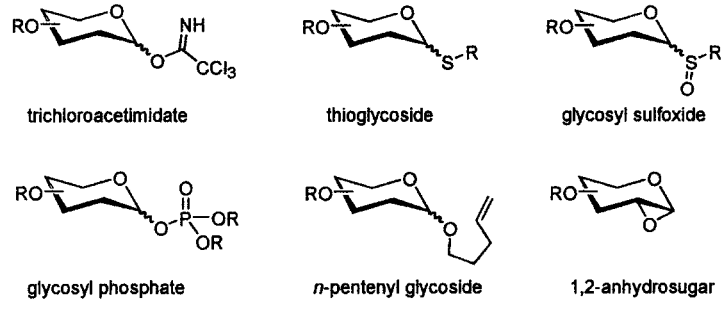

Figure 1.3 Common glycosyl donors.

There are many challenges to a chemical approach for synthesizing oligosaccharides. The typical pyranose sugar has five hydroxyl groups with similar reactivities. Coupling two monosaccharides can form up to 11 positional and anomeric isomers of the disaccharide product. To address this, synthetic chemistry must make extensive use of temporary protecting groups. The selection of the masking groups has a profound effect on the reactivity of both glycosyl donor and acceptor. Poorly selected protecting groups can complicate an otherwise straightforward synthesis.

Stereochemical control of the glycosylation reaction is crucial to any synthesis. As illustrated in Scheme 1.1, two stereochemical outcomes are possible for every glycosylation reaction. Approach of the nucleophile from the top face of the cyclic oxocarbenium ion results in a β-linkage, while approach from the bottom leads to the α-

linkage. Numerous factors contribute to the outcome of this reaction. These include solvent, choice of protecting groups (participating vs. non-participating), identity of the anomeric leaving group, the reactivity of the activator, matched vs. mismatched donor/acceptor pairs,[44] and the anomeric and exoanomeric effects.

1.3.2 β-Mannosides

Controlling the stereochemistry of glycosylation is particularly challenging when the desired outcome is a β-mannosidic linkage (Figure 1.4). The β-mannoside is ubiquitous in mammalian glycosylation, as it serves as the branching point for the core pentasaccharide of *N*-linked glycans. The biological relevance of this structure creates a strong rationale for its chemical synthesis.

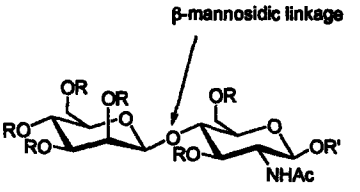

Figure 1.4 The β-mannosidic linkage.

Synthesis of β-mannosidic linkages must overcome two significant challenges that oppose its formation, the anomeric effect and steric repulsion (Figure 1.5). Interactions of the endocyclic oxygen lone pair with the non-bonding orbital of an axially oriented substituent favors the α-anomer for a pyranoside.[45] Lacking a substituent in the axial configuration at the anomeric carbon, the β-mannoside cannot benefit from this stabilizing interaction. And, due to 1,2-*cis* orientation of the β-mannoside, the axial functionality at C2 is sterically conflicted with the equatorially oriented anomeric substituent. Together, these contributions increase the likelihood that the β-mannosidic linkage will anomerize under the acidic conditions that are often used to initiate glycosylation.

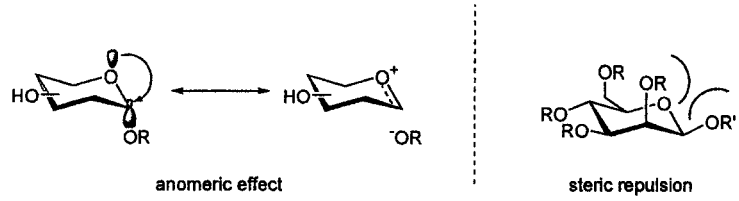

Figure 1.5 Anomeric effect stabilization of α-anomer; steric repulsion for 1,2-*cis*-mannopyranosyl.

The pressing biological significance of the β-mannoside has given rise to a number of synthetic approaches that overcome these challenges.[46] One method is based on generating a β-glucoside precursor. Unlike the β-mannoside, a 1,2-*trans*-pyranosyl β-glucoside is readily formed using a C2 participated group or the glycal assembly method pioneered by Danishefsky et al.[47] The β-glucoside can be transformed to yield the β-mannoside by epimerization of the C2 substituent (Scheme 1.2). Chapters 2 and 4 will utilize this method to generate a panel of high-mannose oligosaccharides possessing a β-mannoside core.

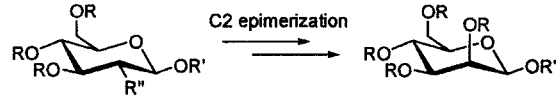

Scheme 1.2 Epimerization of β-Glucoside to form a β-mannoside.

Alternatively, direct S_N2-type displacement of an axial leaving group on the anomeric carbon gives the β-anomer as a product (Scheme 1.3). This method avoids formation of the planar oxocarbonium ion, decreasing the chance of an anomeric mixture. *In situ* generation of the anomeric α-triflate, a method developed by David Crich and colleagues,[48] typifies this synthetic approach and is utilized in Chapter 3 to prepare the *N*-linked core pentasaccharide.

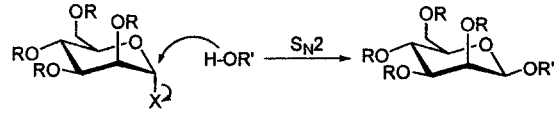

Scheme 1.3 S_N2 displacement of axial leaving group to furnish β-mannosides.

1.3.3 Automated Solid-Phase Synthesis of Oligosaccharides

The solution-phase synthesis of biomolecules is immensely successful at constructing large and complex structures; however these efforts remain time consuming and require significant labor. Repetitive chromatographic purification of intermediates is one of the most challenging steps during the synthesis of large structures. By eliminating these purification steps, the solid-phase paradigm has revolutionized the rapid synthesis of biopolymers. Ideally suited for automation, solid-phase synthesis was originally exploited for the automated synthesis of peptides,[49] and two decades later, oligonucleotides.[50]

Adopting the solid-phase paradigm for synthetic carbohydrate chemistry was slow to be realized. The challenge of developing methods compatible with the solid support and suitable linking chemistries was addressed by Danishefsky,[51] Kahne,[52] and Schmidt,[53] among others. Drawing from these successes, the Seeberger laboratory described the first automated solid-phase oligosaccharide synthesizer.[12] Utilizing an octenediol linker, oligosaccharides are elaborated on the solid support by sequential glycosylation and deprotection, until the final structure is realized (Scheme 1.4). The product is subsequently cleaved from the solid support by Grubbs' catalyst mediated olefin metathesis in the presence of ethylene to furnish the *n*-pentenyl glycoside. Most recently, the Le^y–Le^x tumor marker and the Lewis X and Lewis Y blood group antigens were prepared in an automated fashion using the carbohydrate synthesizer and an ester-based linker.[54]

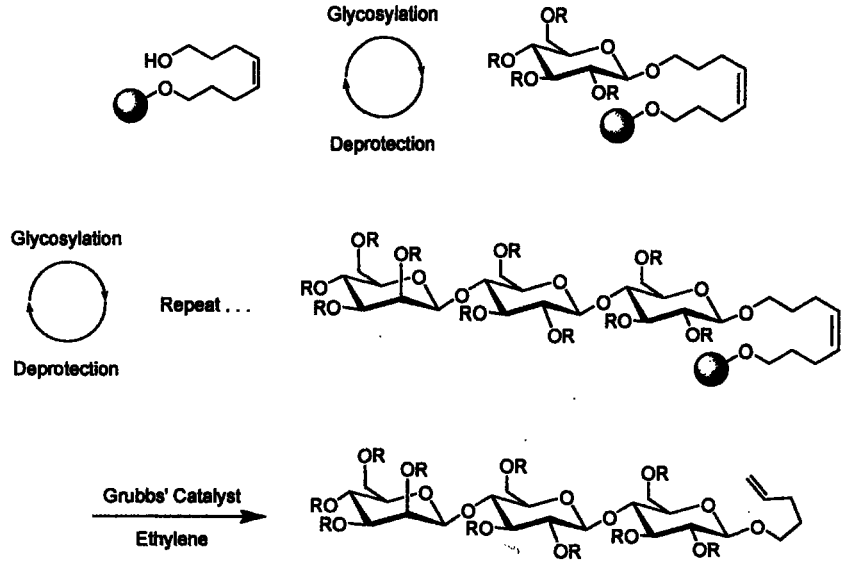

Scheme 1.4 Automated solid-phase oligosaccharide synthesis.

1.4 Dissertation Objectives

The Seeberger laboratory is devoted to advancing the burgeoning field of glycobiology through the development of practical tools based on synthetic carbohydrate chemistry. Progress towards this goal has been made with advances such as the automated solid-phase oligosaccharide synthesizer,[12,55] new protecting groups for carbohydrate synthesis,[56] and fully synthetic carbohydrate vaccines.[9a] In this tradition, the following dissertation aims to take a solution- and solid-phase approach to study the synthesis of *N*-linked high-mannose oligosaccharides and develop tools to aid ongoing investigations into their roles in HIV glycobiology.

Chapter 2 details a 'linear' strategy for the solution-phase synthesis of triantennary high-mannose oligosaccharides using monosaccharide building blocks. Based on this linear approach, Chapter 3 details construction of the core-pentasaccharide common to the three major classes of *N*-linked glycans. This study includes both a solution- and automated solid-phase synthesis, while addressing the challenging β-mannosidic linkage. Chapter 4 follows the development of a high-density carbohydrate microarray based on a new tri(ethylene glycol) linker and examines a preliminary microarray study of a panel of gp120-binding proteins. In this study we exploit the newly developed microarrays to study the glycan-dependent binding interactions of four gp120-

binding proteins: the dendritic cell lectin DC-SIGN,[57] the antibody 2G12, cyanovirin-*N*, and a recently identified anti-HIV protein, scytovirin.[58] Finally, Chapter 5 introduces the use of microfluidic devices to probe the glycosylation reaction.

This dissertation was motivated by a practical need for access to synthetically-derived oligosaccharides to advance the study of anti-HIV microbicides discovered at the NCI, National Institutes of Health. As an appendix to this thesis, Appendix A will briefly summarize the biophysical studies of the anti-HIV protein Cyanovirin-*N* using the synthetic mannosides prepared in Chapter 2. Appendix B summarizes the preparation of a panel of trisaccharides for use in an ongoing effort to establish the acceptor preferences of the enzyme β1,4-Galactosyltransferase-1, also in collaboration with the NCI.

References:

[1] Geijtenbeck, T.; Torensama, R.; van Vliet, S.; van Duijnhoven, G.; Adema, G.; van Kooyk, Y.; Figdor, C. *Cell* **2000**, 100, 575.

[2] Vacquier, V. D.; Moy, G. W. *Dev. Genetics* **1997**, 192, 125.

[3] Tiemeyer, M.; Goodman, C. S. *Development* **1996**, 122, 925.

[4] Scanlan, C. N.; Pantophlet, R.; Wormald, M. R.; Ollmann Saphire, E.; Stanfield, R.; Wilson, I. A.; Katinger, H.; Dwek, R. A.; Rudd, P. M.; Burton, D. R *J. Virol.* **2002**, *76*, 7306. Calarese, D. A.; Scanlan, C. N.; Zwick, M. B.; Deechongkit, S.; Mimura, Y.; Kunert, R.; Zhu, P.; Wormald, M. R.; Stanfield, R. L.; Roux, K. H.; Kelly, J. W.; Rudd, P. M.; Dwek, R. A.; Katinger, H.; Burton, D. R.; Wilson, I. A. *Science* **2003**, *300*, 2065.

[5] Kansas, G. *Blood* **1996**, 88, 3259.

[6] Geyer, H.; Geyer, R. Glycobiology of Viruses. In *Carbohydrates in Chemistry and Biology Part II: Biology of Saccharides, Vol. 4: Lectins and Saccharide Biology* **2001** Wiley-VCH-Weinheim, pp. 821-838

[7] Newburg, D. S. *Curr. Med. Chem.* **1999**, *6*: 117.

[8] Sacchettini, J. C.; Baum, L. G.; Brewer, C. F. *Biochemistry* **2001**, 40, 3009.

[9] a) Schofield, L.; Hewitt, M. C.; Evans, K.; Siomos, M. A.; Seeberger, P. H. *Nature* **2002**, *418*, 785. b) Nyame, A. K.; Kawar, Z. S.; Cummings, R. D. *Arch. Biochem. Biophys.* **2004**, *426* 182.

[10] Ragupathi, G.; Coltart, D. M.; Williams, L. J.; Koide, F.; Kagan, E.; Allen, J.; Harris, C.; Glunz, P. W.; Livingston, P. O.; Danishefsky, S. J. *Proc. Natl. Acad. Sci. U.S.A.* **2002**, *99*, 13699.

[11] Newburg, D. S.; Ruiz-Palacios, G. M.; Altaye, M.; Chaturvedi, P.; Meinzen-Derr, J.; Guerrero, M. D.; Morrow, A. L. *Glycobiology* **2004**, *14*, 253.

[12] Plante, O. J.; Palmacci, E. R.; Seeberger, P. H. *Science* **2001**, *291*, 1523.

[13] Chen, X.; Liu, Z. –Y.; Zhang, J. –B.; Zheng, W.; Kowal, P.; Wang, P. G. *ChemBioChem* **2002**, *3*, 47.

[14] Kornfield, R.; Kornfield, S. *Ann. Rev. Biochem.* **1985**, *54*, 631.

[15] For a review of *N*-linked glycosylation, and the role of *N*-linked glycans in biology, see: Helenius, A.; Aebi, M. *Science* **2001**, *291*, 2364. Imperiali, B.; Hendrickson, T. L. *Bioorg. Med. Chem.* **1995**, *3*, 1565. Imperiali, B.; O'Connor, S. E.; Hendrickson, T.; Kellenberger, C. *Pure. Appl. Chem.* **1999**, *71*, 777.

[16] Silberstein, S.; Gilmore, R. *FASEB J.* **1996**, *10*, 849.

[17] Bause, E. *Biochem. J.* **1983**, *209*, 331. Imperiali, B.; Rickert, W. W. *Proc. Natl. Acad. Sci. U.S.A.* **1995**, *92*, 597.

[18] Gavel, Y.; von Heijne, H. G. *Protein Eng.* **1990**, *3*, 433.

[19] Moremen, K. W.; Trimble, R. B.; Herscovics, A. *Glycobiology* **1994**, *4*, 113.

[20] Parodi, A. J. *Annu. Rev. Biochem.* **2000**, *69*, 69.

[21] Imperiali, B.; O'Connor, S. E. *Curr. Opin. Chem. Biol.* **1999**, *3*, 643.

[22] Helenius, A.; Trombetta, E. S.; Hebert, D. N.; Simons, J. F. *Trends Cell Biol.* **1997**, *7*, 193. Zapun, A.; Jakob, C. A.; Thomas, D. Y.; Bergeron, J. J. *Structure Fold. Des.* **1999**, *7*, R173.

[23] Klausner, R. D.; Sitia, R. *Cell* **1990**, *62*, 611. Plemper, R. K.; Worlf, D. H. *Trends Biochem. Sci.* **1999**, *24*, 266.

[24] Feizi, T.; Larkin, M. *Glycobiology*, **1990**, *1*, 17-23.

[25] Otteken, A.; Moss, B. *J. Biol. Chem.* **1996**, *271*, 97.

[26] Mehta, A.; Zitzmann, N.; Rudd, P. M.; Block, T. M.; Dwek, R. A. *FEBS Lett.* **1998**, *430*, 17.

[27] Wyatt, R.; and Sodroski, J. *Science* **1998**, *280*, 1884.

[28] Poignard, P.; Saphire, E. O.; Parren, P. W.; Burton, D. R. *Annu. Rev. Immunol.* **2001**, *19*, 253. Burton, D. R. *Proc Natl Acad Sci U S A* **1997**, *94*, 10018.

[29] Kwong, P. D.; Doyle, M. L.; Casper, D. J.; Cicala, C.; Leavitt, S. A.; Majeed, S.; Steenbeke, T. D.; Venturi, M.; Chaiken, I.; Fung, M.; Katinger, H.; Parren, P. W.; Robinson, J.; Van Ryk, D.; Wang, L.; Burton, D. R.; Freire, E.; Wyatt, R.; Sodroski, J.; Hendrickson, W. A.; Arthos, J. *Nature* **2002**, *420*, 678. Wyatt, R.; Kwong, P. D.; Desjardins, E.; Sweet, R. W.; Robinson, J.; Hendrickson, W. A.; Sodroski, J. G. *Nature* **1998**, *393*, 705.

[30] For examples of *N*-linked glycosylation of HIV in two cell lines (H9 T lymphocytes and CHO cells), see: Mizuochi, T.; Matthews, T. J.; Kato, M.; Hamako, J.; Titani, K.; Solomon, J. C.; Feizi, T. *J. Biol. Chem.* **1990**, *265*, 8519. Mizuochi, T.; Spellman, M. W.; Larkin, M.; Solomon, J. C.; Basa, L. J.; Feizi, T. *Biochem. J.* **1988**, *254*, 599.

[31] Yeh, J. C.; Seals, J. R.; Murphy, C. I. van Halbeek, H.; Cummings, R. D. *Biochemistry* **1993**, *32*, 11087.

[32] Boyd, M. R.; Gustafson, K. R.; McMahon, J. B.; Shoemaker, R. H.; O'Keefe, B. R.; Mori, T.; Gulakowski, R. J.; Wu, L.; Rivera, M. I.; Laurencot, C. M.; Currens, M. J.; Cardellina, J. H., 2nd; Buckheit, R. W.; Jr., Nara, P. L.; Pannell, L. K.; Sowder, R. C. 2nd; Henderson, L. E. *Antimicrob. Agents Chemother.* **1997**, *41*, 1521. Bolmstedt, A. J.; O'Keefe, B. R.; Shenoy, S. R.; McMahon, J. B.; and Boyd, M. R. *Mol. Pharmacol.* **2001**, *59*, 949.

[33] Bokesch, H. R.; O'Keefe, B. R.; McKee, T. C.; Pannell, L. K.; Patterson, G. M.; Gardella, R. S.; Sowder, R. C., 2nd; Turpin, J.; Watson, K.; Buckheit, R. W. Jr.; Boyd, M. R. *Biochemistry* **2003**, *42*, 2578.

[34] Tsai, C. C.; Emau, P.; Jiang, Y.; Tian, B.; Morton, W. R.; Gustafson, K. R.; Boyd, M. R. *AIDS Res. Hum. Retroviruses* **2003**, 19, 535.

[35] Zhang J.; Chen X.; Shao J.; Liu Z.; Kowal P.; Lu Y.; Wang P. G. *Meth. in Enzymol.* **2003**, 362, 106. Zhang, J. B.; Kowal, P.; Chen, X.; Wang, P. G. *Org. Biomolecular Chem.* **2003**, 1, 3048.

[36] Koenigs, W.; Knorr, E. *Chem. Ber.* **1901**, 34, 957.

[37] Toshima, K.; Tatsuta, K. *Chem. Rev.* **1993**, *93*, 1503.

[38] Schmidt, R. R.; Kinzy, W. *Adv. in Carb. Chem. and Biochem.* **1994**, *50*, 21.

[39] Garegg, P. J. *Adv. in Carb. Chem. and Biochem.* **1997**, *52*, 179.

[40] Kahne, D.; Walker, S.; Cheng, Y.; van Engen, D. *J. Am. Chem. Soc.* **1989**, *111*, 6881.

[41] Palmacci, E. R.; Plante, O. J.; Seeberger, P. H. *Eur. J. Org. Chem.* **2002**, 595.

[42] Fraser-Reid, B.; Konradsson, P.; Mootoo, D. R.; Udodong, U. J. *J. Chem. Soc. Chem. Comm.* **1988**, 823.

[43] Danishefsky, S. J.; Bilodeau, M. T. *Angew. Chem., Int. Ed.* **1996**, *35*, 1380.

[44] Spijker, N. M.; van Boeckel, C. A. A. *Angew. Chem. Int. Ed.* **1991**, *30*, 180.

[45] For a review of the anomeric effect, see Boons, G. -J. ed. *Carbohydrate Chemistry* **1998** Blackie Academic and Professional: London.

[46] For a review of β-mannoside formation, see: Pozsgay, V. "Stereoselective Synthsis of β-Mannosides," *Carbohydrates in Chemistry and Biology* Wiley-VCH **2000**, v.1, 319-343.

[47] Danishefsky, S. J.; Bilodeau, M. T. *Angew. Chem. Int., Ed. Engl.* **1996**, *35*, 1380-1419. Liu, K. K.; Danishefsky, S. J. *J. Org. Chem.* **1994**, *59*, 1892-1894.

[48] Crich, D.; Sun, S. X. *J. Am. Chem. Soc.* **1997**, *119*, 11217. Crich, D.; Sun, S. X.; *Tetrahedron.* **1998**, *54*, 8321.

[49] Merrifield, B. J. *J. Am. Chem. Soc.* **1963**, *85*, 2149.

[50] Caruthers, M. H. *Science* **1985**, *230*, 281.

[51] Danishefsky, S. J.; McClure, K. F.; Randolf, J. T.; Ruggeri, R. B. *Science*, **1993**, *260*, 1307.

[52] Yan, L.; Taylor, C. M.; Goodnow, R.; Kahne, D. E. *J. Am. Chem. Soc.* **1994**, *116*, 6953.

[53] Rademann, J.; Schmidt, R. R. *Tetrahderon Lett.* **1996**, *37*, 3989. Rademann, J.; Schmidt, R. R. *J. Org. Chem.* **1997**, *62*, 3650.

[54] Love, K. R.; Seeberger, P. H. *Angew. Chem. Int. Ed.* **2004**, *43*, 602.

[55] Plante, O. J. New Methods for the Synthesis of Carbohydrates: The First Automated Solid-Phase Oligosaccharide Synthesizer. Ph.D. Thesis, Massachusetts Institute of Technology, Cambridge, MA, June 2001.

[56] Plante, O. J.; Buchwald, S. L.; Seeberger, P. H. *J. Am. Chem. Soc.* **2000**, *122*, 7148-7149.

[57] Geijtenbeek, T. B.; Torensma, R.; van Vliet, S. J.; van Duijnhoven, G. C.; Adema, G. J.; van Kooyk, Y.; Figdor, C. G. *Cell* **2000**, *100*, 575.

[58] Bokesch, H. R.; O'Keefe, B. R.; McKee, T. C.; Pannell, L. K.; Patterson, G. M.; Gardella, R. S.; Sowder, R. C., 2nd; Turpin, J.; Watson, K.; Buckheit, R. W. Jr.; Boyd, M. R. *Biochemistry* **2003**, *42*, 2578.

Chapter 2

A Linear Synthesis of High-Mannose Oligosaccharides

Portions of this chapter were reprinted with permission, as they describe work found in the following publication:

Ratner, D. M.; Plante, O. J.; Seeberger, P. H. A Linear Synthesis of Branched High-Mannose Oligosaccharides from the HIV-1 Viral Surface Envelope Glycoprotein gp120. *Eur. J. Org. Chem.* 2002, *5*, 826-833.

2.1 Introduction

Chapter 2 describes a linear solution-phase synthesis of a high-mannose nonasaccharide pentyl glycoside. Envisioning the automated solid-phase assembly of complex carbohydrates, the synthesis of the nonasaccharide and the related tri- and hexamannoside demonstrates the facile assembly of highly branched structures in a stepwise fashion incorporating monosaccharide building blocks. A differentially protected core trisaccharide was prepared and further elongated in two high-yielding tri-mannosylations to furnish the triantennary structure. The tri-, hexa- and nonamannoside *n*-pentyl glycosides obtained via the described synthesis would serve as substrates for a detailed study of the carbohydrate-protein interactions responsible for binding of the anti-HIV protein cyanovirin-N to the glycoprotein gp120 (Appendix A).

This synthetic route would ultimately function as the template for preparing a series of high-mannose oligosaccharides used in the development of a number of synthetic tools for glycobiology. Most notably, Chapter 4 will focus on the development of a new method for preparing carbohydrate microarrays, based on analogs of the synthetic structures described below.

2.2 Target Identification and Significance

Carbohydrates are widely understood to play a vital role in HIV retroviral pathogenesis. The function of HIV-1 surface envelope glycoprotein gp120 in helper T lymphocyte (T_h) infection has been understood by biologists for some time.[1] Glycoprotein gp120 is highly glycosylated, containing up to 24 *N*-linked high-mannose

carbohydrates, which compose 50% of the molecular mass of the glycoprotein.[2] gp120 mediates viral fusion with the CD4 receptor on the surface of T_h cells. HIV fusion and subsequent lymphocyte infection occur upon binding of the glycoprotein and the CD4 receptor.

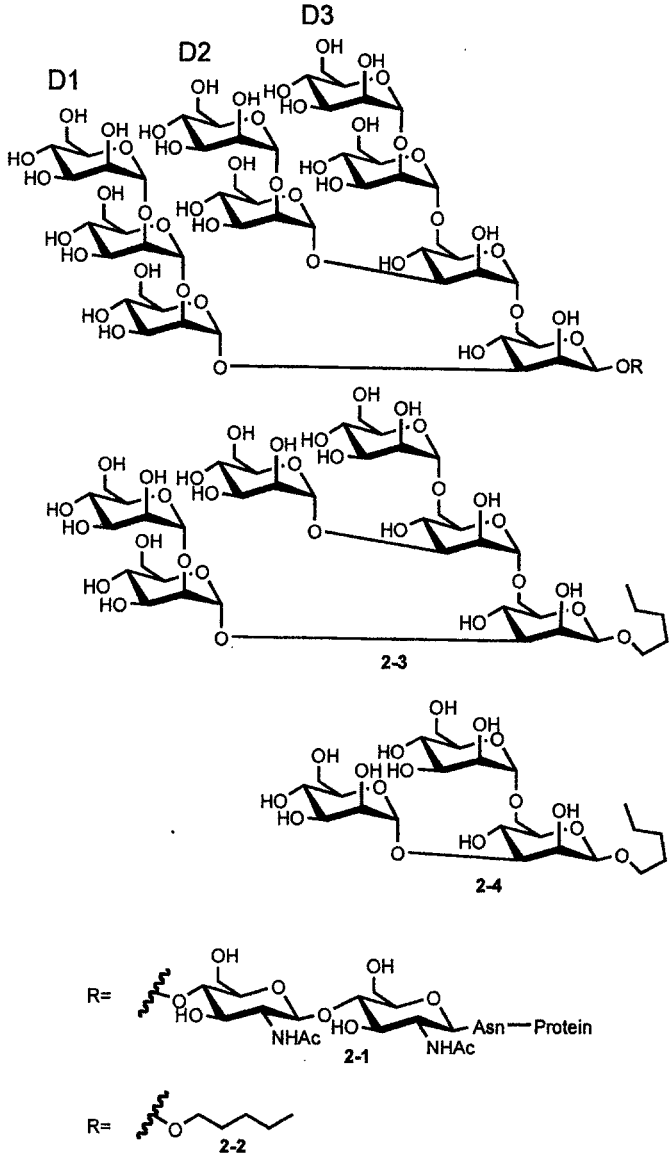

Figure 2.1 High-mannose oligosaccharide targets.

A novel protein has been recently discovered that exhibits potent anti-HIV activity. Isolated from the blue-green algae *Nostoc ellipsosporum*, cyanovirin-N (CVN) was found to bind viral gp120, thereby preventing lymphocyte infection.[1,3] CVN is a monomeric 11-kDa protein. Both natural and recombinant forms of the protein have

been shown to irreversibly inhibit a wide variety of HIV strains while exhibiting minimal toxicity to host cells. The mode of HIV inactivation by CVN has been studied and the protein's affinity for the gp120 high-mannose structure Man_9 **2-1** was established (Figure 2.1).[4] This affinity appears to be the mechanism through which CVN prevents gp120 from interacting with the CD4 receptor of the host lymphocyte. A detailed understanding of the specific interaction between CVN and Man_9 **2-1** could lead to the development of potential HIV preventatives and possibly even therapeutics. Access to synthetically derived mannosides as synthetic tools has therefore become particularly important in order to probe CVN-gp120 binding.

The total synthesis of high-mannose type viral surface glycans, that are found throughout nature as *N*-linked glycoconjugates, has been explored for the past two decades.[5] A synthesis of the high-mannose core structures of Man_9, isolated from calf thyroglobulin, was reported by Ogawa in 1981, a decade before the role of such structures in HIV pathogenesis was discovered.[5a] Two successful and highly convergent syntheses of the HIV-1 nonamannoside structure by Fraser-Reid[6] and Ley[7] were recently completed. However, the convergent nature of these solution-phase syntheses does not allow for their application to automated solid-phase synthesis.

Herein we describe a linear synthesis of the pentyl nonamannoside **2-2** and the related hexamannoside **2-3** and trimannoside **2-4** structures (Figure 2.1). The synthetic strategy was planned and executed with automated solid-phase synthesis in mind. Using three monomer building blocks, the nonamannoside was assembled in four glycosylation events. Two sequential tri-mannosylation reactions, using a single mannosyl donor, allowed for access to the completed structure in a minimal number of steps. The target structures are being utilized in biophysical studies focusing on the elucidation of cyanovirin-N and other natural product-binding to branched high-mannose structures (Appendix A).

2.3 Retrosynthesis

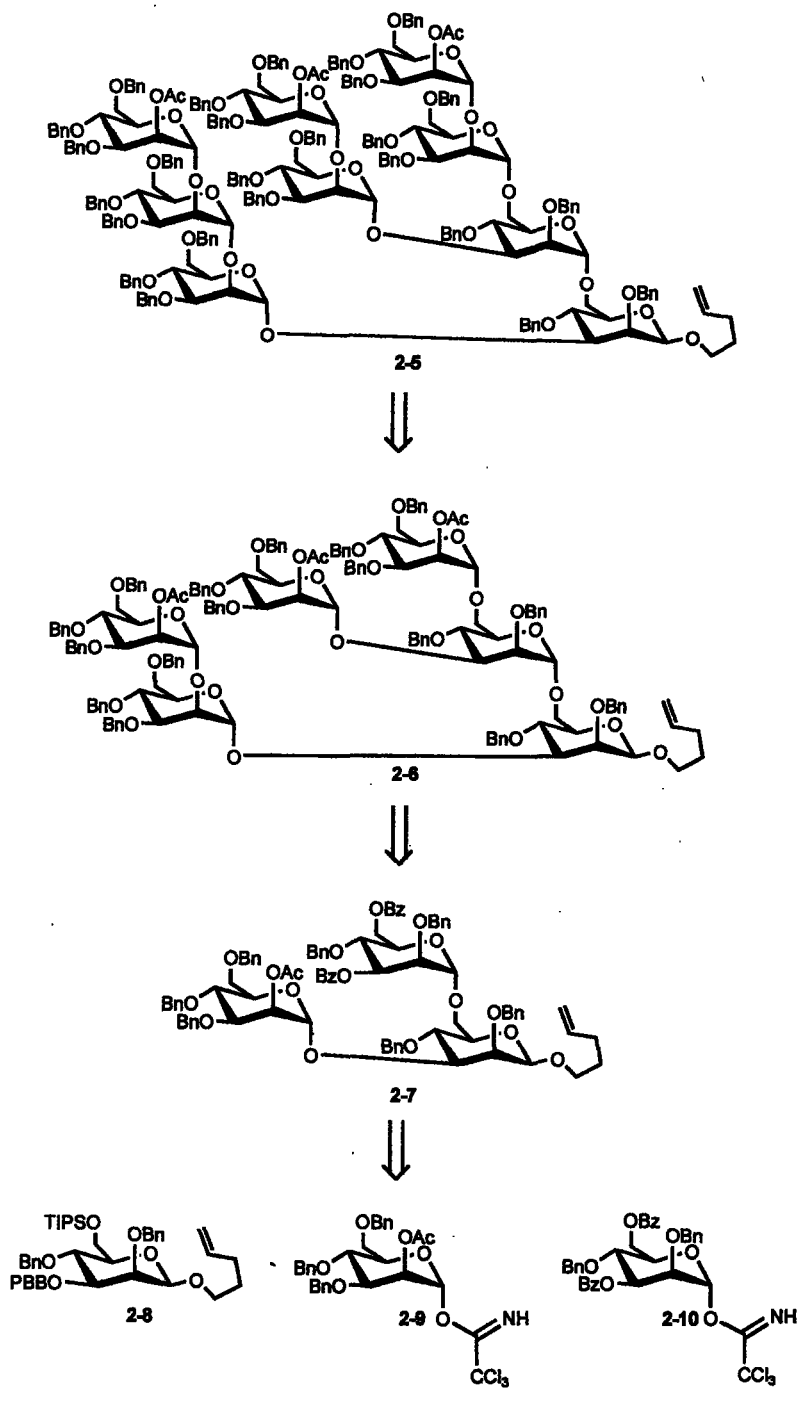

Scheme 2.1 Retrosynthetic analysis of nonamannoside **2-5**.

The retrosynthetic analysis of the *n*-pentyl Man_9 analog **2-2** (Scheme 2.1) was guided by our long-term goal of developing a synthetic strategy that could be applied to the solid support and eventually automated. We planned to obtain the fully protected

nonamannoside **2-5** via simultaneous tri-mannosylation of a hexasaccharide triol derived from **2-6**. This hexasaccharide would in turn be prepared by the tri-mannosylation of a trisaccharide core triol ensuing from **2-7**. The differentially protected trisaccharide **2-7** would be constructed from three protected monosaccharide building blocks **2-8, 2-9** and **2-10**. The stepwise nature of this strategy would facilitate access to a triply branched nonasaccharide using just four glycosylations. A solution-phase synthesis of the β-pentenyl glycoside analog of the natural structure was selected for our studies, based on our strategy for solid-phase oligosaccharide synthesis that furnishes the pentenyl glycoside upon cleavage from the solid support.[8] In addition to functioning as glycosyl donors, *n*-pentenyl glycosides are versatile handles that can be converted into a range of functional groups by transformation of the terminal olefin to a carboxylic acid, aldehyde, ester, thioether, thioester, or hydroxyl group.[9] In this fashion, the *n*-pentenyl moiety may allow for attachment of the products of our synthetic studies to a linker, fluorescent tag, or biomarker.

2.4 Synthesis of the *n*-Pentenyl β-mannoside

Initially, reliable synthetic access to the monosaccharide building blocks had to be established. The core 3,6-differentially protected β-mannoside **2-8** was the most synthetically challenging building block to be procured. Glycals have demonstrated their utility as intermediates in oligosaccharide assembly,[10] therefore we utilized them for the preparation of β-mannoside **2-8**. The synthesis of **2-8** commenced with benzylation of known glycal **2-11**[11] to yield differentially protected glucal **2-12** in 93% (Scheme 2.2). Stereospecific epoxidation of glycal **2-12** by treatment with dimethyldioxirane, followed by opening of the 1,2-anhydrosugar with 4-penten-1-ol in the presence of zinc chloride yielded β-glucoside **2-13** containing an C2 hydroxyl group (87%, two steps). Inversion of the C2 stereocenter was achieved via an oxidation-reduction sequence. Oxidation of the C2 hydroxyl under Pfitzner-Moffatt conditions (Ac_2O-DMSO) was followed by stereoselective reduction with sodium borohydride (74%, two steps) and benzylation to furnish the fully protected β-mannoside **2-8** in 98% yield. Selective removal of the halobenzyl ether at C3 was accomplished by palladium-catalyzed amination with *N*-

methyl aniline (92% yield) followed by treatment with dichloroacetic acid to afford monosaccharide acceptor **2-14** in 90% yield.[11]

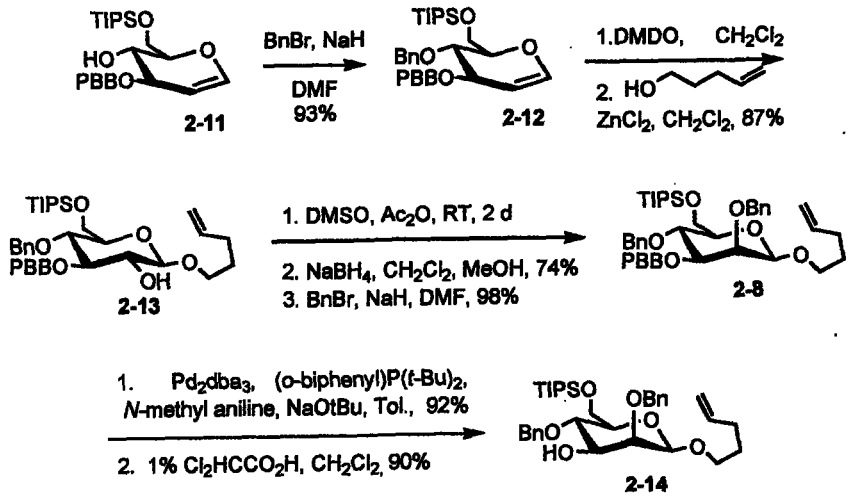

Scheme 2.2 Synthesis of core β-mannoside **2-14**.

2.5 Nonamannoside Assembly

At this stage only two other mannosyl monosaccharide building blocks were required for the completion of the nonamannoside; one with a temporary protecting group on C2 (**2-9**), and the other incorporating temporary protecting groups on C3 and C6 (**2-10**). The C3 hydroxyl of the reducing end β-mannoside is the point of attachment of a linear strand of α-(1→2) linked mannoses (branch D1). The C6 hydroxyl of the core *n*-pentenyl-β-mannoside is the origin of a 3,6-differentiated α-mannose that serves as the core for two branches (D2 and D3) of the triantennary structure (Figure 2.1). Differentially protected mannopyranosyl trichloroacetimidate **2-9**[12] as well as mannosyl donor **2-10**[13] were prepared using known procedures. Prepared on multi gram scale, **2-9** would serve as the source of seven of the nine mannoses in the final Man_9 structure.

With the three monosaccharide building blocks **2-8**, **2-9**, and **2-10** in hand the assembly of larger structures began. We first focused on the preparation of core trimannoside **2-7**. The α-selective mannosylation of the C3 hydroxyl of **2-14** with donor **2-9** afforded disaccharide **2-15** in 99% yield (Scheme 2.3). Removal of the C6 silyl ether

was accomplished in 91% yield using aqueous trifluoroacetic acid in THF to furnish disaccharide acceptor **2-16.**

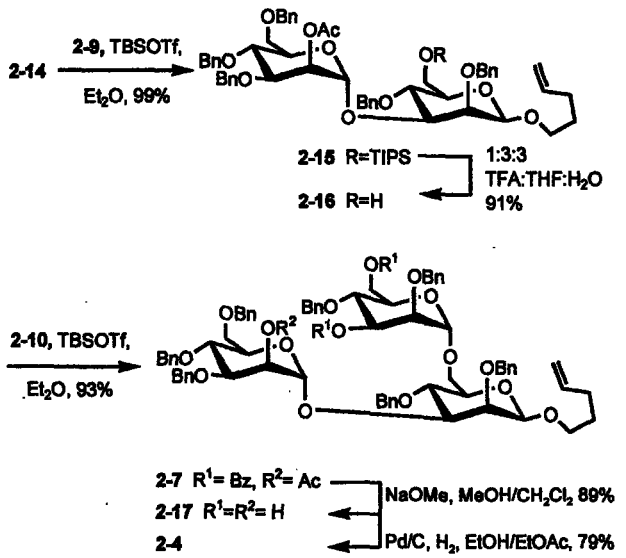

Scheme 2.3 Assembly of core trimannoside **2-7.**

Installation of the second mannose building block on C6 will serve as the root for branches D2 and D3. This required the use of a mannose donor that did not utilize a C2 participating ester group but rather a permanently blocked benzyl ether. Precedence for α-selectivity (favored by the anomeric effect) has been established previously in the case of similar mannosyl donors containing non-participating protecting groups on C2.[14] To aid the stereoselectivity of this glycosylation, diethyl ether was used as a solvent.[15] Unlike dichloromethane, diethyl ether is thought to contribute to α-selectivity by forming an exocyclic diethyl oxonium ion (Scheme 2.4). This species assumes an β-orientation due to the exoanomeric effect (a preference to place positively charge substituents of the C1 carbon of a pyranose in the equatorial conformation).[16] Nucleophilic attack by a glycosyl acceptor subsequently favors an axial approach (α-oriented).

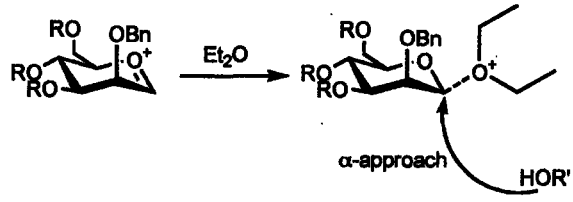

Scheme 2.4 Ethereal solvent participation favors α-selectivity.

Complete α-selectivity was achieved in the TBDMSOTf catalyzed glycosylation of disaccharide **2-16** with mannosyl donor **2-10** to yield the fully-protected core trisaccharide **2-7** in 93% (Scheme 2.3). Treatment of trisaccharide **2-7** with sodium methoxide accomplished the simultaneous cleavage of the C2 acetate and both benzoates to provide trisaccharide triol **2-17** in good yield (89%).

Simultaneous extension of the D1, D2 and D3 branches from the core trisaccharide was accomplished via two sequential tri-mannosylations with building block **2-9** (Scheme 2-5). Mannosylation of **2-17** with **2-9** (4.5 equivalents) yielded hexasaccharide **2-6** in a single step in 94% yield. Deprotection with sodium methoxide produced hexasaccharide triol **2-18** in quantitative yield. Trimannosylation of **2-18** using **2-9** furnished the fully protected high-mannose nonasaccharide **2-5** in 80% yield. In just three steps the initial trisaccharide **2-7** tripled in size to nonasaccharide **2-5** in 75% overall yield. Liberation of **2-5** from all protecting groups was accomplished in two steps by treatment with sodium methoxide to afford triol **2-19**, followed by Pd-catalyzed hydrogenation yielded the desired high-mannose pentyl glycoside **2-2** $(Man)_9$ in 88%. Fully deprotected hexasaccharide **2-3** (81%) and core trisaccharide **2-4** (79%) pentyl glycosides were prepared in similar fashion from **2-17** and **2-18**, respectively (Schemes 2.3 and 2.5).

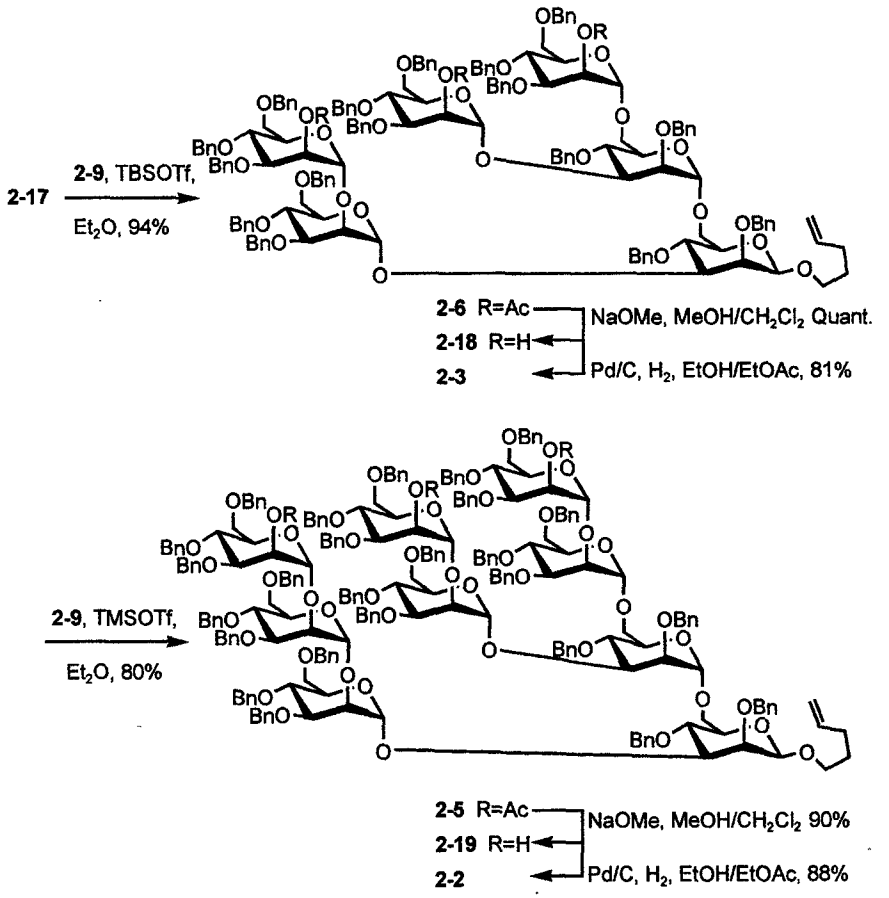

Scheme 2.5 Assembly of nonasaccharide **2-5**.

2.6 Constituent Linear Trisaccharide – D1 Arm

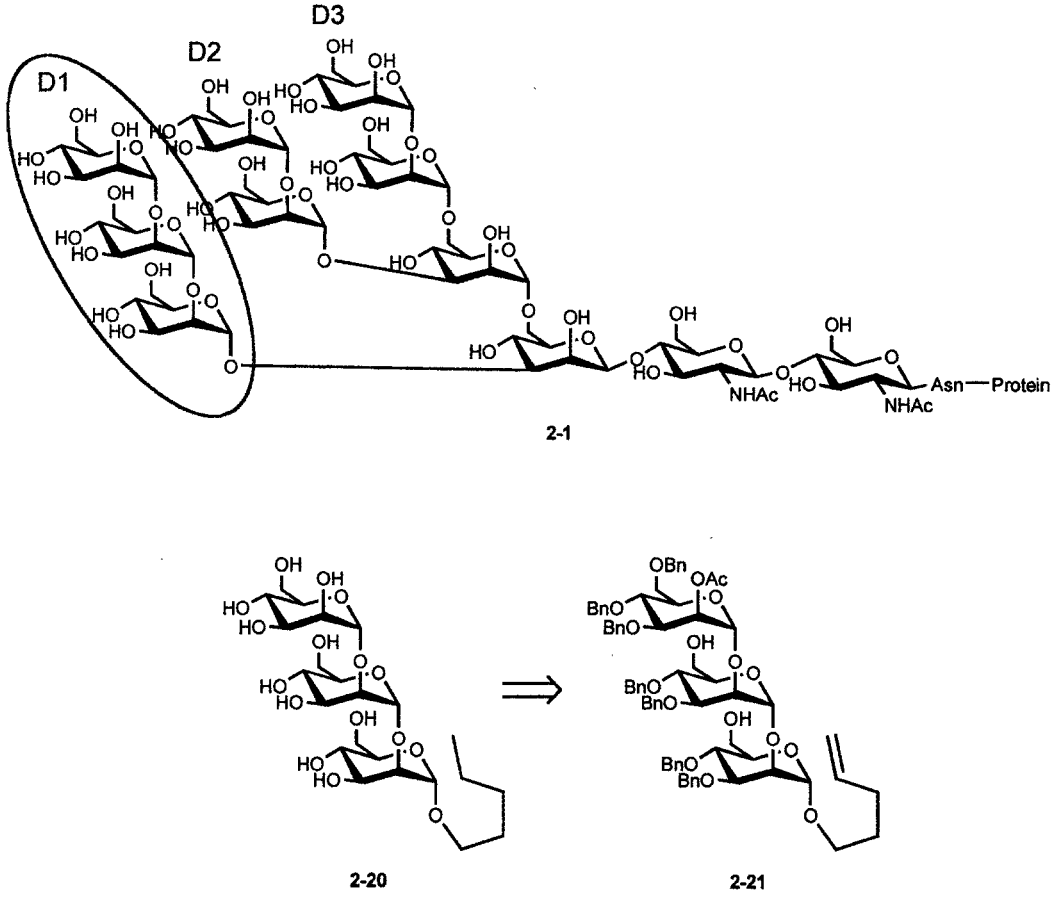

Scheme 2.6 Origin and retrosynthesis of D1 linear trimannoside.

Motivated by the interest in establishing the structural requirements for the high-mannose affinity of cyanovirin-N, attention was turned the linear trimannoside corresponding to the D1 arm of Man_9 (Scheme 2.6). *n*-Pentyl mannoside **2-20** was prepared via the deprotection of *n*-Pentenyl mannoside **2-21**. Utilizing both solution[6a] and automated solid-phase synthesis,[17] **2-21** was made via a literature procedure. **2-21** was treated with sodium methoxide to remove the C2 acetate protecting group (92% yield),[6b] and subsequently debenzylated via Pd-catalyzed hydrogenation yielding **2-20** in 96% yield.

2.7 Applications to Biology

The four high-mannose oligosaccharides **2-2, 2-3, 2-4** and **2-20** were subsequently used in biophysical studies to better understand the carbohydrate protein interactions between cyanovirin-N and gp120 (Appendix A).[18] Results of these studies elucidate the formation of very tight carbohydrate-protein interactions that form the basis for novel HIV preventatives and continue the effort towards developing general principles for protein-carbohydrate interactions.

2.8 Summary and Conclusions

The successful linear synthesis of high-mannose nonasaccharide pentyl glycoside **2-2,** trimannosides **2-4** and **2-20,** and hexamannoside **2-3** was accomplished using just three monomeric glycosyl building blocks. Construction of triantennary nonasaccharide **2-2** was achieved in four high-yielding glycosidation events; construction of a differentiated core trisaccharide was followed by two sequential trimannosylations. Overall yield for the synthesis of the nonasaccharide was comparable to previous convergent solution-phase syntheses.[6,7] Access to these synthetic structures has permitted further study of the anti-HIV microbicide activity exhibited by cyanovirin-N among other novel proteins isolated from natural sources. The linear strategy described herein for a solution-phase assembly of high-mannose oligosaccharides constitutes the basis for the automated synthesis of branched high-mannose motifs on the solid-support. In addition, the strategy established by this method would eventually serve as the basis of a novel scheme for the preparation of synthetic oligosaccharide microarrays and a host of potential tools for study in glycobiology.

References:

[1] Freed, E. O.; Martin, M. A. *J. Biol. Chem.* **1995**, *270*, 23883-23886. Bewley, C. A.; Gustafson, K. R.; Boyd, M. R.; Covell, D. G.; Bax, A.; Clore, G. M.; Gronenborn, A. M. *Nature Structural Biology* **1998**, *7*, 571.

[2] T. Feizi, "Glycobiology of AIDS," *Carbohydrates in Chemistry and Biology* Wiley-VCH **2000**, v.4, 851.

[3] Boyd, M. R.; Gustafson, K. R.; McMahon, J. B.; Shoemaker, R. H.; O'Keefe, B. R.; Mori, T.; Gulakowski, R. J.; Wu, L.; Rivera, M. I.; Laurencot, C. M.; Currens, M. J.; Cardellina II, J. H.; Buckheit, R. W.; Nara, P. L.; Pannell, L. K.; Sowder II, R. C.; Henderson, L. E. *Antimicrobial Agents and Chemotherapy* **1997**, *41*, 1521. Mori, T.; Boyd, M. R. *Antimicrobial Agents and Chemotherapy* **2001**, *45*, 664. O'Keefe, B. R.; Shenoy, S. R.; Xie, D.; Zhang, W.; Muschik, J. M.; Currens, M. J.; Chaiken, I.; Boyd, M. R. *Mol. Pharm.* **2000**, *58*, 982. Bewley, C. A. *J. Am. Chem. Soc.* **2001**, *123*, 1014.

[4] Bewley, C. A.; Otero-Quintero, S. *J. Am. Chem. Soc.* **2001**, *123*, 3892.

[5] a) Ogawa, T.; Kiyoaki, K.; Sasajima, K.; Matsui, M. *Tetrahedron* **1981**, *37*, 2779. b) Ogawa, T.; Sasajima, K. *Carbohydr. Res.* **1981**, *93*, 53. c) Ogawa, T.; Nukada, T. *Carbohydr. Res.* **1985**, *136*, 135. d) Ogawa, T.; Nakabayashi, S.; Kitajima, T. *Carbohydr. Res.* **1983**, *114*, 225.

[6] a) Merritt, J. R.; Fraser-Reid, B.; *J. Am. Chem. Soc.* **1992**, *114*, 8334. b) Merritt, J. R.; Naisang, E.; Fraser-Reid, B. *J. Org. Chem.* **1994**, *59*, 4443.

[7] Grice, P.; Ley, S. V.; Pietruszka, J.; Osborn, H.; Priepke, H.; Warriner, S. *Chem. Eur. J.* **1997**, *3*, 431. Ley, S. V.; Baeschlin, D. K.; Dixon, D. J.; Foster, A. C.; Ince, S. J.; Priepke, H. W. M.; Reynolds, D. J. *Chem. Rev.* **2001**, *101*, 53. Grice, P.; Ley, S. V.; Pietruszka, J.; Priepke, H. *Angew. Chem. Int. Ed.* **1996**, *35*, 197.

[8] Andrade, R. B.; Plante, O. J.; Melean, L. G.; Seeberger, P. H. *Org. Lett.* **1999**, *1*, 1811.

[9] Allen, J. R.; Harris, C. R.; Danishefsky, S. J. *J. Am. Chem. Soc.* **2001**, *123*, 1890. Fraser-Reid, B.; Udodong, U. E.; Wu, Z.; Ottosson, H.; Merritt, J. R.; Rao, C. S.; Roberts, C.; Madsen, R. *Synlett* **1992**, 927. Buskas, T.; Soderberg, E.; Konradsson, P.; Fraser-Reid, B. *J. Org. Chem.* **2000**, *65*, 958.

[10] Danishefsky, S. J.; Bilodeau, M. T. *Angew. Chem. Int. Ed.* **1996**, *35*, 1380. Liu, K. K.; Danishefsky, S. J. *J. Org. Chem.* **1994**, *59*, 1892.

[11] Plante, O. J.; Buchwald, S. L.; Seeberger, P. H. *J. Am. Chem. Soc.* **2000**, *122*, 7148.

[12] Rademann, J.; Geyer, A.; Schmidt, R. R. *Angew. Chem. Int. Ed.* **1998**, *37*, 1241.

[13] Mayer, T. G.; Kratzer, B.; Schmidt, R. R. *Angew. Chem. Int. Ed.* **1994**, *33*, 2177.

[14] Frick, W.; Bauer, A.; Bauer, J.; Wied, S.; Müller, G. *Biochem.* **1998**, *37*, 13421. Frick, W.; Mueller, G. Inositolglycans Having Insulin-Like Action, U.S. Patent 6,004,938, Dec. 21, **1999**.

[15] Wulff, G.; Rohle, G. *Angew. Chem. Int. Ed.* **1974**, *13*, 157. Wulff, G.; Schmidt, W. *Carbohydr. Res.* **1977**, *53*, 33. Wulff, G.; Schröder, U.; Wickelhaus, J. *Carbohydr. Res.* **1979**, *72*, 280.

[16] Lemieux, R. U. *Pure Appl. Chem.*, **1971**, *25*, 527.

[17] Andrade, R. B.; Plante, O. J.; Melean, L. G.; Seeberger, P. H. *Org. Lett.* **1999**, *1*, 1811. Palmacci, E. R.; Hewitt, M. C.; Seeberger, P. H. *Angew. Chem. Int. Ed.* **2001**, 40; 4433. Plante, O. J. New Methods for the Synthesis of Carbohydrates: The First Automated Solid-Phase Oligosaccharide Synthesizer. Ph.D. Thesis, Massachusetts Institute of Technology, Cambridge, MA, June 2001.

[18] Barrientos, L. G.; Louis, J. M.; Ratner, D. M.; Seeberger, P. H.; Gronenborn, A. M. *J. Mol. Biol.* **2003**, *325*, 211. Shenoy, S. R.; Barrientos, L. G.; Ratner, D. M.; O'Keefe, B. R.; Seeberger, P. H.; Gronenborn, A. M.; Boyd, M. R. *Chem. Biol.* **2002**, *9*, 1109. Botos, I.; O'Keefe, B. R.; Shenoy S. R.; Cartner, L. K.; Ratner, D. M.; Seeberger, P. H.; Boyd, M. R.; Wlodawer, A. *J. Biol. Chem.* **2002**, *277*, 34336.

Chapter 3

Solution-Phase and Automated Solid-Phase Synthesis of The Core Pentasaccharide of *N*-Linked Glycoproteins

Portions of this chapter describe work done in collaboration with Ms. Erika R. Swanson.[1] The Author wishes to thank Dr. Kerry R. Love for her assistance with the operation of the Automated Oligosaccharide Synthesizer, and Ms. Swanson for her assistance preparing the experimental section for publication. Elements of the automated synthesis detailed in this chapter were reprinted with permission, and may be found in the following publication:

Ratner, D. M.; Swanson, E. R.; Seeberger, P. H. Automated Synthesis of the *N*-linked Core Pentasaccharide. *Org. Lett.* **2003**, *5*, 4717-4720.

3.1 Introduction

Co-translational modification of proteins by glycosylation of asparagine residues includes three classes of *N*-linked oligosaccharides: high-mannose, hybrid and complex-type mannans.[2] In addition to the many functions of these branched glycans in mammalian cells, they are found on the glycoproteins of a variety of pathogens, including the viral envelope of HIV,[3] Ebola,[4] and some coronaviruses.[5] Rapid and reliable access to these branched glycans by automated synthesis would facilitate further investigation into the biological role of these glycoconjugates and their potential application as carbohydrate-based vaccines.[6] Currently, synthetic *N*-glycans are used to study carbohydrate/protein interactions using isothermal calorimetry,[7] carbohydrate arrays,[8] and the structural analysis of such complexes (Chapter 4 and Appendices A & B).[9]

The three major classes of *N*-linked glycans contain a common core pentasaccharide that has been a target of several recent syntheses in solution[10] and on solid support.[11] Figure 3.1 highlights this pentasaccharide for the complex and high-mannose type *N*-linked glycans. This pentasaccharide contains a number of synthetic challenges, including branching, β-(1→4) glucosamine linkages, and most notably, the daunting β-mannoside.[12]

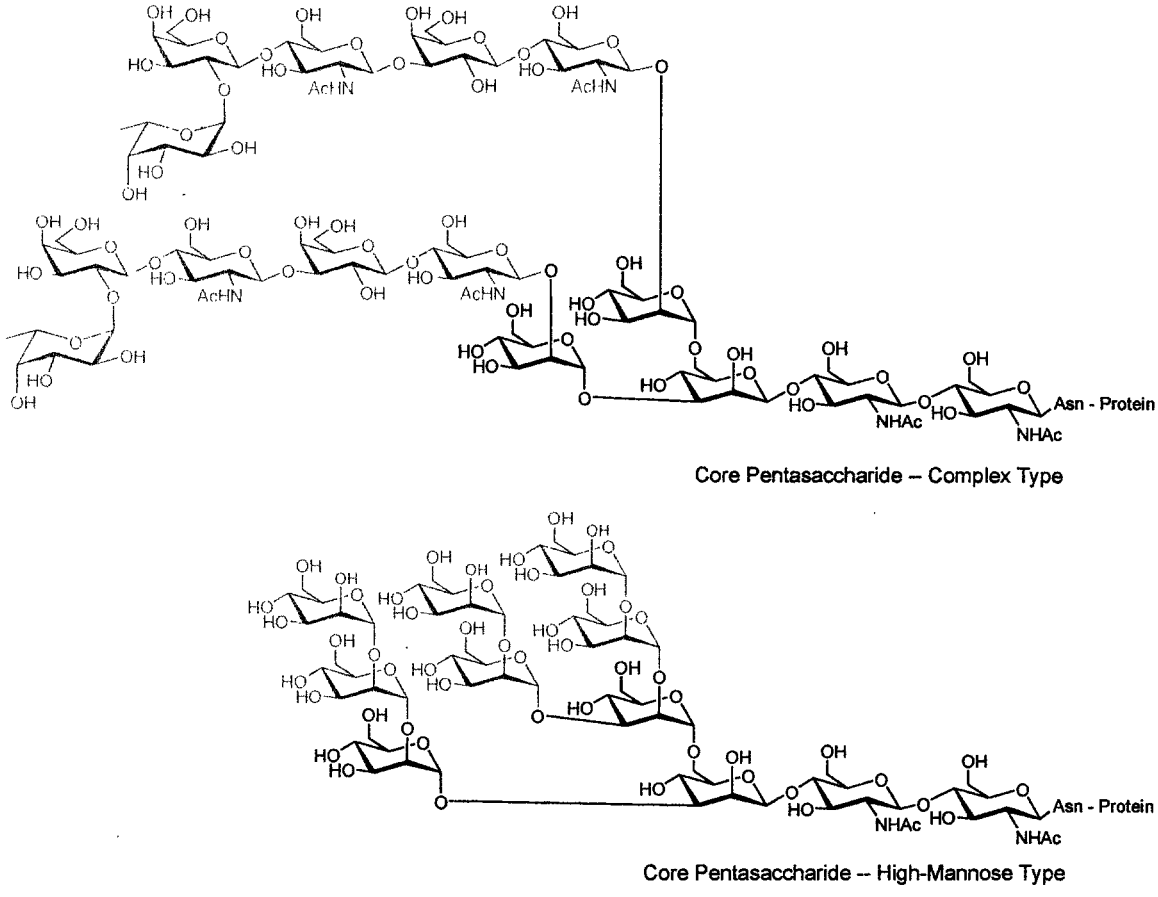

Figure 3.1 Complex and High-mannose type *N*-linked oligosaccharides, highlighting the core *N*-linked pentasaccharide $(Man_3)(GlcNAc)_2$.

Described is the first automated solid-phase synthesis of the core pentasaccharide of high-mannose *N*-linked glycoproteins *via* stepwise assembly from mono- and disaccharide building blocks. In order to accomplish this task, an analogous route for the solution-phase syntheses of the core pentasaccharide had to be established. The challenging β-mannosidic linkage was incorporated by the inclusion of a disaccharide trichloroacetimidate. These solution and automated syntheses provide rapid access to an oligosaccharide common to an entire class of glycoconjugates.

3.2 Retrosynthesis

Due to their unique branching motifs, synthetic access to high-mannose and complex-type *N*-linked oligosaccharides depends on the differentiation of the terminal

mannoses of the core pentasaccharide; a retrosynthetic analysis of the core pentasaccharide requires separate routes to establish precursors suitable for bi- and triantennary targets (Scheme 3.1). Differential protection of the core β-mannose on the C3 and C6 hydroxyl groups with orthogonal protecting groups (the *O*-acetate ester and *O*-triisopropylsilyl ether) result in **3-1** (a 3,6-di-*O*-acetyl core β-mannose, precursor to biantennary complex-type glycans) and **3-2** (3-*O*-acetyl-6-*O*-triisopropyl core β-mannose, for triantennary high-mannose type glycans). Careful examination of the two core trisaccharides revealed that access to both structures is achieved by three common building blocks: differentially protected reducing-end acceptor GlcNAc **3-3**, and two building blocks, **3-6** and **3-7**, for preparation of the β-mannoside-containing Manβ(1→4)GlcNAc disaccharide. A notable feature of this approach is that a single synthetic strategy may be applied for both classes of *N*-linked structures.

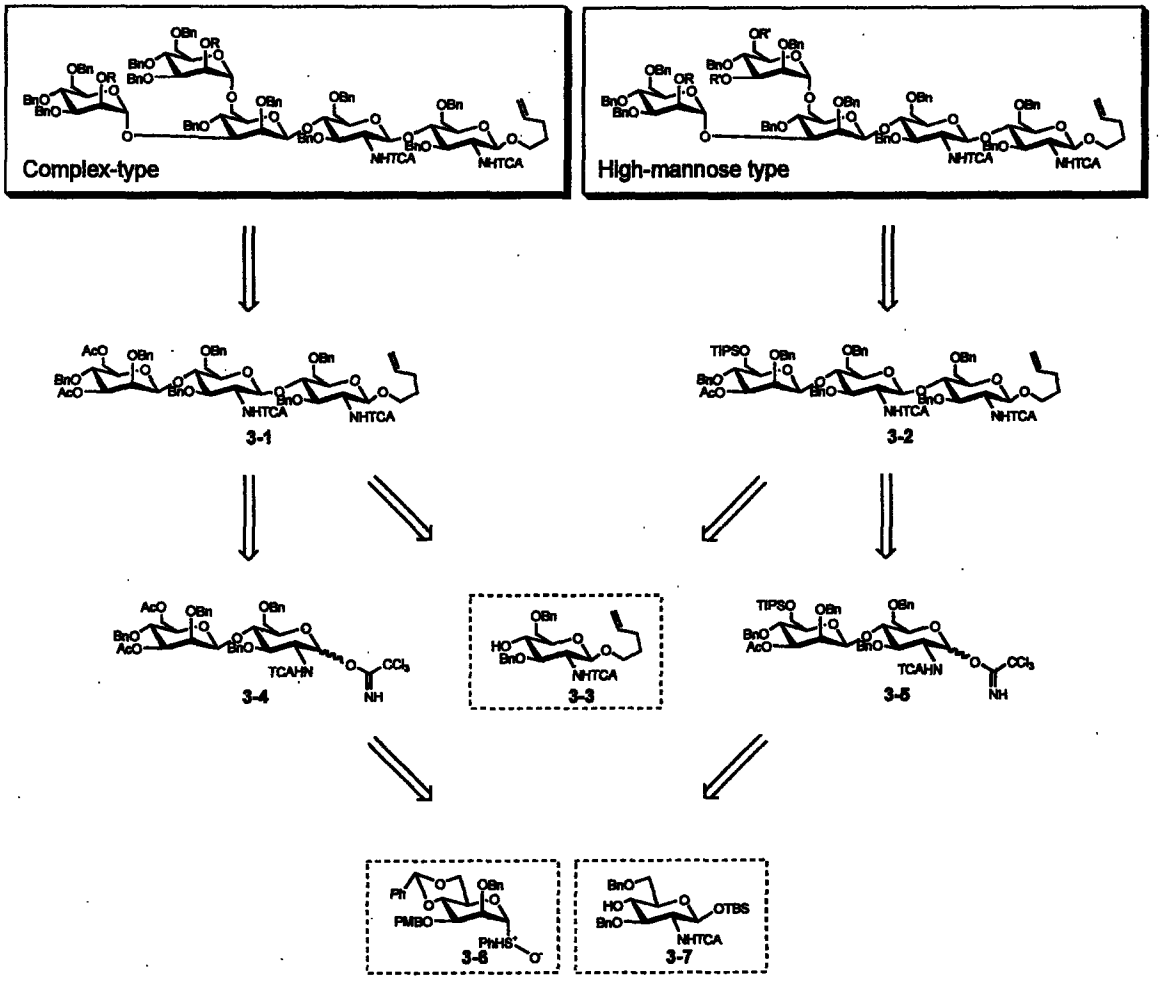

Scheme 3.1 Retrosynthesis of complex- and high-mannose type core pentasaccharides.

With automated solid-phase synthesis as our ultimate goal, the forward synthesis was planned with the inherent requirements of solid-phase oligosaccharide chemistry in mind. Namely, all reactions should be high-yielding, stereospecific, and compatible with the linking chemistry to the solid support. Based on this synthetic strategy, **3-8** and **3-9** were established as the synthetic targets to demonstrate the utility of this approach (Figure 3.2). Both pentasaccharides could be accessed using just five distinct building blocks, monosaccharides **3-10**, **3-11**,[13] and **3-12**,[13] and disaccharides **3-4** and **3-5** (Figure 3.3). In order to avoid anomeric mixtures on the solid support, the β-mannosidic linkage would be incorporated during the preparation of disaccharides **3-4** and **3-5**. Selective bi- and triantennary branching would be achieved *via* mannosylation of the differentiated trisaccharide cores by addition of mannosyl trichloroacetimidates **3-11** or **3-12**.

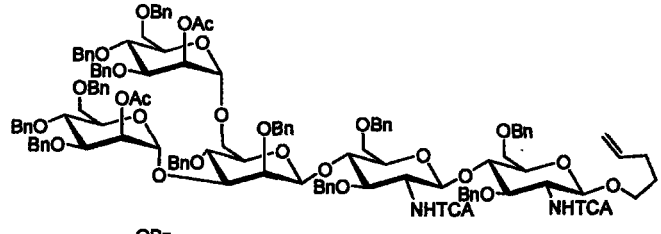

3-8

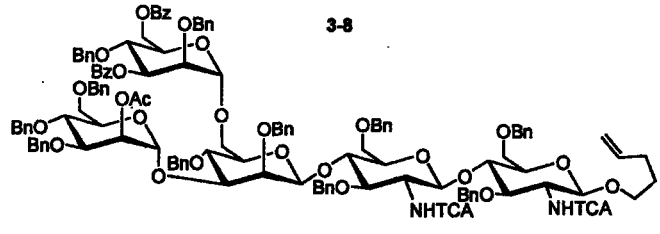

3-9

Figure 3-2 Targets for *N*-linked core pentasaccharides, complex-type **3-8**, and high-mannose type **3-9**. .

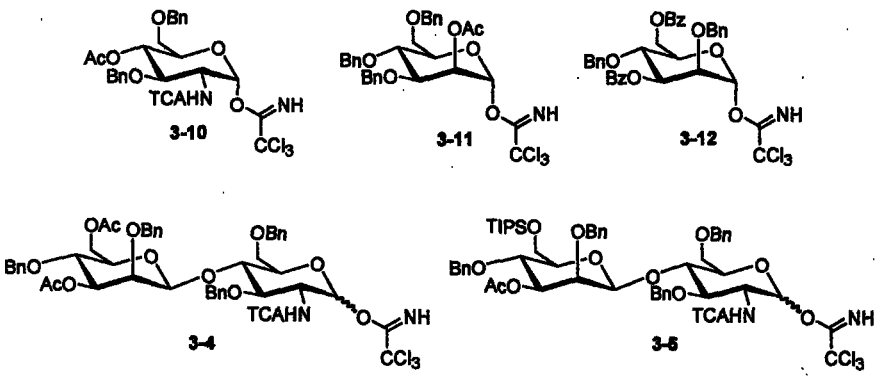

Figure 3-3 Building blocks required for the synthesis of **3-8** and **3-9**.

3.2.1 Protecting Group Strategy

The benzyl ether was selected as a 'permanent' protecting group due to its stability to a wide-range of reaction conditions. As in Chapter 2, the benzyl ether is typically removed only during the final deprotection of the synthetic structure. Protection of the C2-amine of the GlcNAc building blocks requires an additional set of protecting group manipulations. For the purpose of this synthesis, the trichloroacetimido group was selected for its stability and beneficial electronic effects. As a C2-participating group, the C2-trichloroacetimido glycosyl donors lend superior β-selectivity to glycosylation reactions.

As temporary protecting groups, the decision to utilize the acetate ester and triisopropylsilyl (TIPS) ether as orthogonal protected groups was based on a number of factors. A careful examination of the levulinate ester and *p*-methoxybenzyl (PMB) ether for both the C3 and C6 position of the β-mannoside ultimately concluded that they were not ideally suited for the synthetic route. Higher deprotection yields made the acetate more attractive than levulinate, and incompatibility of the C6 PMB ether with certain glycosylation conditions resulted in the unintentional deprotection of the PMB ether. Both the acetate and TIPS protecting groups were ultimately selected as temporary protecting groups in the building blocks (**3-4** and **3-5** and **3-10**) for their excellent stability, orthogonality, and ease of removal.

3.3 Monosaccharide Building Blocks

Upon identification of the necessary synthetic building blocks, glycosyl trichloroacetimidate **3-10** was prepared from known differentially protected glucosamine **3-13**[14] (Scheme 3.2). The 4,6-*O*-benzylidene group of **3-13** was opened selectively by treatment with TES/TFA/TFAA to afford **3-7** in 85% yield. Subsequent acetylation of the C4 hydroxyl (99% yield), was followed by desilylation. Treatment with DBU and trichloroacetonitrile furnished glycosyl trichloroacetimidate **3-10** in 76% yield.

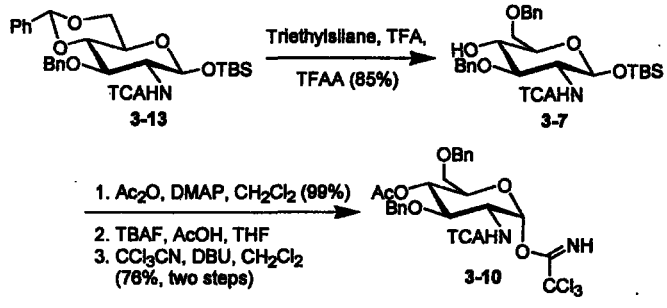

Scheme 3.2 Synthesis of glycosyl trichloroacetimidate **3-10**.

For the model solution-phase synthesis of both **3-8** and **3-9**, the *n*-pentenyl glycoside was used for the reducing-end GlcNAc. Solid-phase synthesis based on the octenediol linker,[15] developed by the Seeberger laboratory, furnishes the *n*-pentenyl glycoside following cleavage by Grubbs' olefin cross-metathesis in an atmosphere of ethylene.[16] The terminal GlcNAc for both pentasaccharides, **3-3**, was prepared by glycosylation of pent-4-en-1-ol (*n*-pentenyl alcohol) with glycosyl donor **3-10**. The crude *n*-pentenyl glycoside was subsequently reacted with a solution of sodium methoxide to furnish the differentiated GlcNAc C4 acceptor **3-3** in 94% over the two steps.

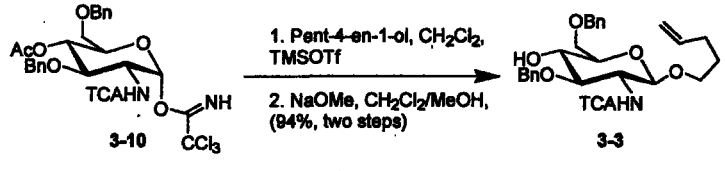

Scheme 3.3 Synthesis of *n*-pentenyl glycoside **3-3**.

3.4 Disaccharide Building Blocks

The β-mannoside-containing disaccharide **3-16**, a precursor common to both glycosyl trichloroacetimidates **3-4** and **3-5**, was prepared *via* direct β-mannosylation, using the Crich method.[17] Mannosylation of **3-7** by treatment of sulfoxide **3-6**[18] with triflic anhydride and di-*tert*butyl pyridine furnished the β-linked disaccharide **3-14** in 68% yield (Scheme 3.4). This procedure efficiently installed the β-mannosidic linkage without the need for tedious chromatographic separation of an anomeric mixture. The C3 *p*-methoxy benzyl ether was replaced with the base-labile acetate ester to yield **3-15** in 79% over two steps. Selective opening of the 4,6-*O*-benzylidene to expose the primary C6 hydroxyl was achieved by treatment with dichlorophenylborane and triethylsilane,[19] generating **3-16** in 88% yield.

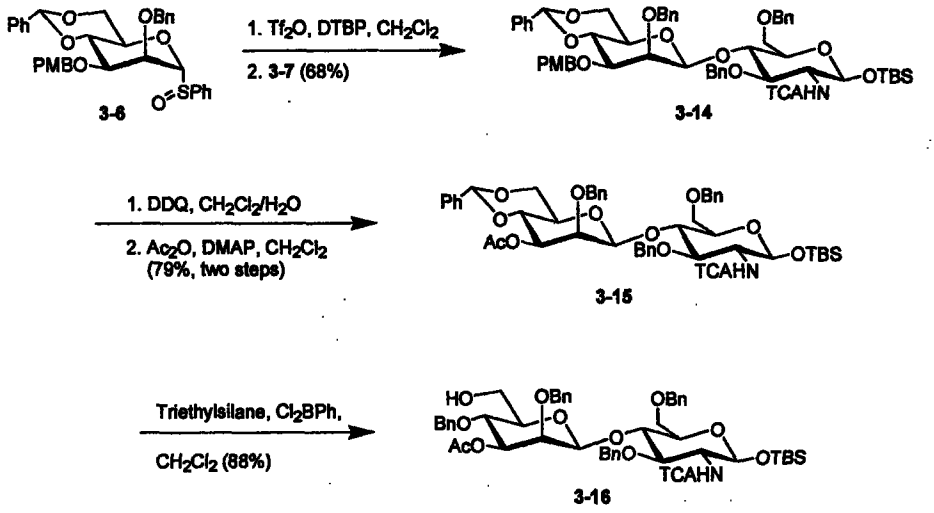

Scheme 3.4 Preparation of β-mannoside **3-16** by Crich method.

Disaccharide **3-16** was differentially protected on the C6 position with either an acetate ester or triisopropylsilyl ether to furnish glycosyl donors **3-4** and **3-5** respectively (Scheme 3.5). Acetylation of **3-16** yielded the 3,6-di-*O*-acetyl protected disaccharide **3-17** in 92% yield. Access to the disaccharide glycosyl trichloroacetimidate **3-4** was readily achieved by desilylation followed by treatment with trichloroacetonitrile and DBU to give **3-4** in 89% yield. Preparation of orthogonally protected **3-5** for the

preparation of *N*-linked high-mannose oligosaccharides was accomplished by silylation of the C6 hydroxyl with triisopropylsilyl chloride, yielding **3-18** in 80%. The anomeric *t*-butyldimethylsilyl ether (OTBS) was selectively deprotected by treatment with tetrabutylammonium fluoride. Following recovery of unreacted material, the anomeric lactol (95% isolated yield) was reacted with trichloroacetonitrile and DBU to produce trichloroacetimidate **3-5** in 90% yield.

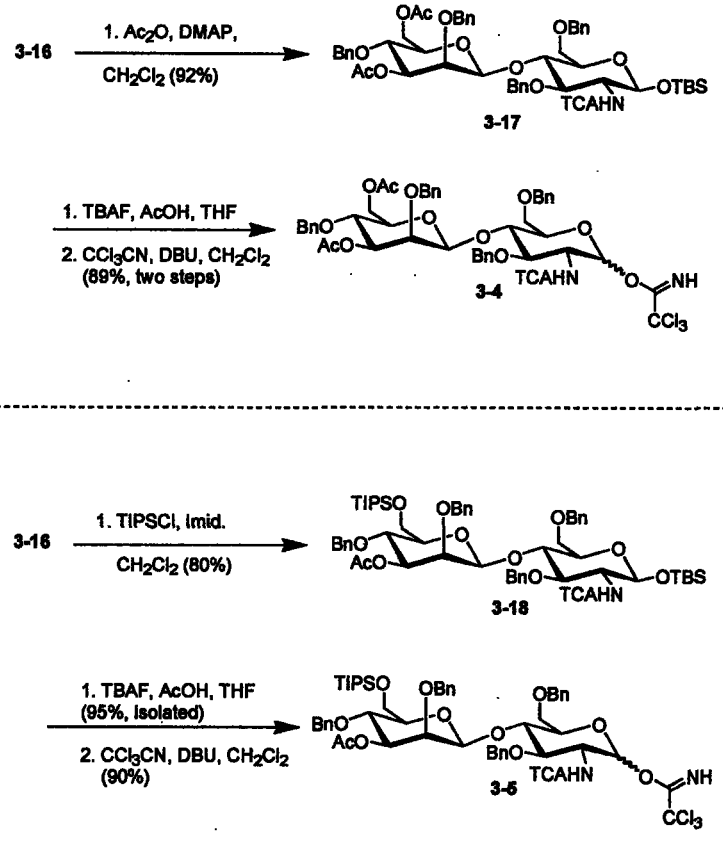

Scheme 3.5 β-Mannoside disaccharide trichloroacetimidates **3-4** and **3-5**.

3.5 Solution-Phase Synthesis

A solution-phase synthesis serves the useful purpose of establishing optimal conditions for glycosylation and provides reference material to determine the future success or failure of an automated synthesis. As such, the solution phase synthesis of **3-8** and **3-9** was used to confirm the two synthetic routes.

3.5.1 Solution-Phase Synthesis of Complex-Type Core Pentasaccharide

Having prepared the necessary building blocks **3-3**, **3-4**, and **3-11**, the proposed chemistry was tested with the solution-phase synthesis of the complex-type core pentasaccharide **3-8** (Scheme 3.6). *n*-Pentenyl glycoside acceptor **3-3** was glycosylated in 65% yield with disaccharide glycosyl donor **3-4** to give trisaccharide **3-1**. This single glycosylation step established the *N*-linked core chitobiose $(GlcNAc)_2$, and incorporated the β-mannoside. Utilization of the participating trichloroacetimido functionality in the C2 position of the glycosyl donor resulted in stereochemical control of the glycosylation reaction, yielding only the β-anomer. Deprotection of the C3 and C6 acetate protecting groups by treatment with methanolic sodium methoxide gave trisaccharide acceptor **3-19** in high yield (98%). Finally, using the simultaneous mannosylation method established in Chapter 2, **3-19** was dimannosylated with mannosyl trichloroacetimidate **3-11** to give the fully protected core pentasaccharide **3-8** in 98% yield.

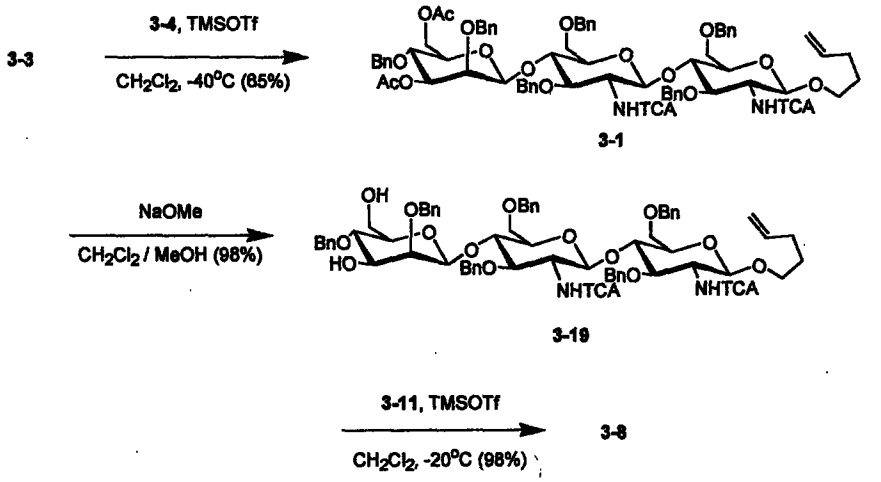

Scheme 3.6 Construction of complex-type core pentasaccharide **3-8**.

The high yields for both glycosylation and deprotection steps in this synthesis made the construction of **3-8** an ideal candidate for the initial attempt at an automated synthesis of the core pentasaccharide. It should also be noted that glycosylation with disaccharide **3-4** was performed as it would be during solid-phase synthesis –without the use of molecular sieves (useful as a drying agent, to reduce decomposition of

glycosylating agent to lactol). The use of powdered molecular sieves would not be possible during solid-phase syntheses, therefore it is useful to model reactions in their absence.

3.5.2 Solution-Phase Synthesis of High-Mannose Type Core Pentasaccharide

Unlike the construction of **3-8**, the solution-phase synthesis of the high-mannose type core pentasaccharide **3-9** required an additional 3,6-differentiated mannosyl donor to serve as a second branching point for the triantennary structure. Therefore, a total of four building blocks were involved: **3-3**, the reducing-end *n*-pentenyl GlcNAc; **3-5**, the 3,6-differentiated disaccharide trichloroacetimidate; **3-11**, the C2-*O*-acetyl mannosyl donor, and **3-12**, a 3,6-di-*O*-benzoyl mannosyl trichloroacetimidate (Scheme 3.6). Glycosylation of *n*-pentenyl glycoside **3-3** using disaccharide trichloroacetimidate **3-5** furnished trisaccharide **3-2** in 73% yield (note use of 4Å molecular sieves). Treatment of **3-2** with sodium methoxide provided access to the C3 hydroxyl trisaccharide acceptor **3-20**, with an isolated yield of 84%. Mannosylation of the C3 position with donor **3-11** yielded tetrasaccharide **3-21** in 77% yield. Due to the lability of the TIPS ether, TBSOTf was employed as an activator over traditional TMSOTf. Acidic deprotection of the TIPS ether with trifluoroacetic acid gave the C6 hydroxyl tetrasaccharide acceptor **3-22** in 82% yield. Finally, **3-22** was mannosylated with mannosyl donor **3-12** to complete the fully protected high-mannose core pentasaccharide **3-9** (87%).

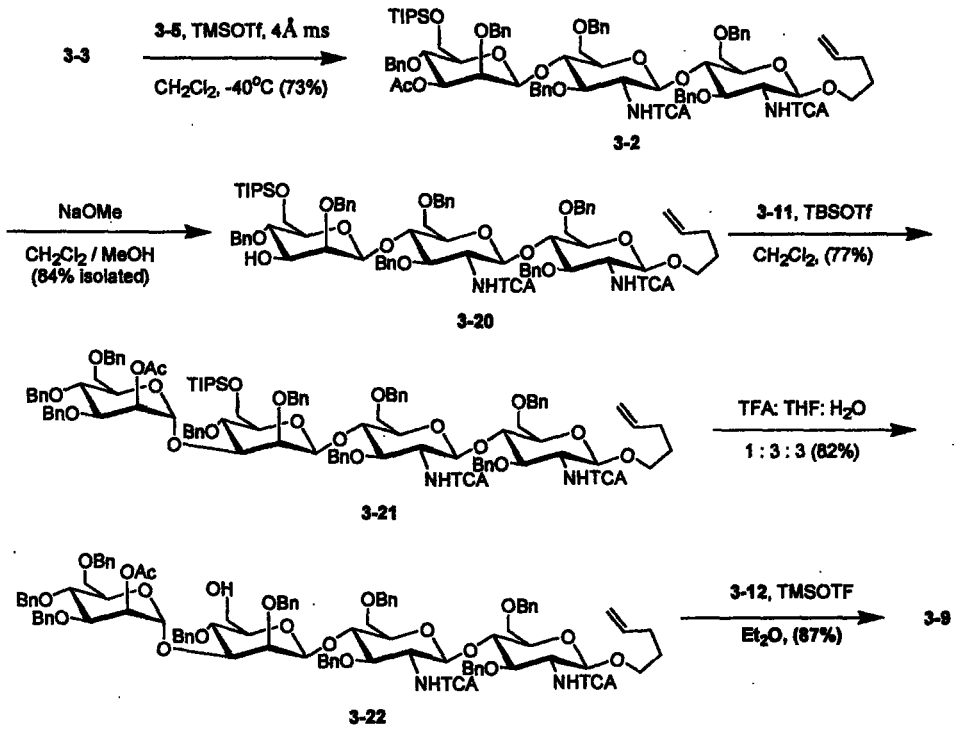

Scheme 3.7 Construction of high-mannose-type core pentasaccharide **3-9**.

3.6 Automated Solid-Phase Synthesis of Core Pentasaccharide

Following the successful solution-phase synthesis of both **3-8** and **3-9**, the automated solid-phase synthesis of *N*-linked core pentasaccharide **3-8** was attempted. With building blocks **3-10**, **3-4**, and **3-11** in hand, we used octenediol functionalized Merrifield resin **3-23** and an automated oligosaccharide synthesizer to construct **3-8** (Scheme 3.8).[20] The automated assembly made use of five programmed modules (Table 1): A) glycosylation, consisting of the addition of 3.5 equiv. of glycosylating agent and catalytic amounts of TMSOTf; B) methylene chloride wash; C) THF wash; D) acetate deprotection by the addition of 10 equivalents sodium methoxide in methanol twice; and E) pH neutralization with 0.2 M acetic acid in THF.

Module	Function	Reagent	Time (min)
A	Glycosylation	3.5 equiv donor and TMSOTf	21
B	Wash	CH_2Cl_2	9
C	Wash	THF	9.5
D	Deprotection	2 x 10 equiv. NaOMe	33
E	Wash	0.2 M AcOH / THF	12

Table 1. Conditions and reagents used in the automated synthesis of **3-8**.

Glycosylation of the linker with **3-10** (repeated once) utilized C2-trichloroacetamide participation to ensure anomeric selectivity at the reducing end. Glycosylation with disaccharide donor **3-4**, determined by solution-phase model studies to be the most challenging step, was repeated three times to ensure complete addition to the support-bound nucleophile. Finally, branching was introduced by glycosylation with mannosyl trichloroacetimidate **3-11** *via* a simultaneous dimannosylation of the C3 and C6 hydroxyl groups.

Following the final glycosylation, the resin was thoroughly washed and dried. Cleavage of the octenediol linker by olefin cross-metathesis was performed using Grubbs catalyst in an atmosphere of ethylene to furnish the *n*-pentenyl glycoside.[16] The resulting crude product, core pentasaccharide **3-8**, was purified by semi-preparative HPLC. Relative peak area analysis by HPLC showed 27% desired product **3-8**, with the remainder of isolated side-products consisting of (n-1) and (n-3) deletion sequences and decomposed Grubbs catalyst (HPLC traces in Experimental, Chapter 6, Section 6.3).

Total synthesis time for the automated construction of pentasaccharide **3-8** was less than six and a half hours. Starting from the monosaccharide and disaccharide building blocks, the desired pentasaccharide target was assembled and purified in less than three days, requiring only a single step for purification.

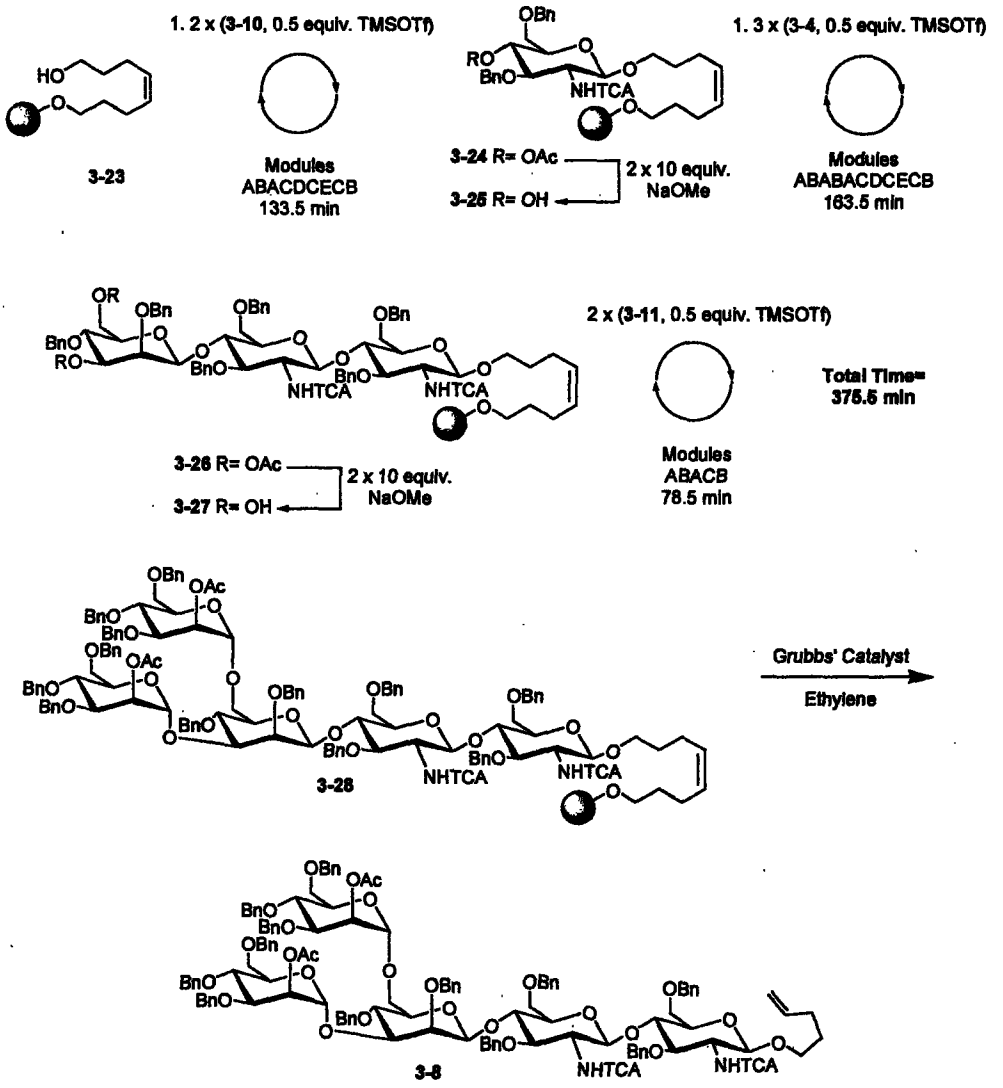

Scheme 3.8. Automated synthesis of pentasaccharide **1**.

3.7 Summary and Conclusions

The successful solution-phase syntheses of core pentasaccharides **3-8** and **3-9**, followed by the automated solid-phase synthesis of **3-8**, clearly demonstrated the utility of this synthetic approach for application to the solid-phase paradigm. Stereochemical control for all β(1→4) GlcNAc linkages was achieved by developing a method that included a C2 participating trichloroacetimide and a β-mannoside-containing disaccharide building block. In concert with the linear synthesis developed in Chapter 2,

these methods allowed for significant progress towards rapid synthetic access to complete *N*-linked oligosaccharides.

This work and other solid-phase oligosaccharide synthesis studies show that synthetically challenging and structurally diverse oligosaccharides can be rapidly prepared.[21] While existing methods for the construction of large oligosaccharides have been immensely successful, access to the mono- and disaccharide glycosyl donors remains one of the most challenging aspects of synthetic carbohydrate chemistry – leaving room for further advancement in the field. Currently, only a portion of the total time required for a synthesis similar to these is spent assembling the large structures. Significant time and effort is required to prepare the differentially protected building blocks. As the assembly of the two core pentasaccharides demonstrates, individual building blocks often find application in multiple syntheses, and are readily prepared in large scale. In addition, the opportunity for commercial expansion into the realm of synthetic carbohydrate chemistry makes the likelihood of purchasing fully protected glycosyl donors a real possibility in the near future.

References:

[1] Swanson, E. R. Synthesis of the Pentasaccharide Core of *N*-linked Glycoproteins. Masters Thesis, Massachusetts Institute of Technology, Cambridge, MA, February 2003.

[2] Dwek, R. A. *Chem. Rev.* **1996**, *96*, 683. Imperiali, B.; O'Connor, S. E. *Curr. Opin. Chem. Biol.* **1999**, *3*, 643.

[3] T. Feizi, "Glycobiology of AIDS," *Carbohydrates in Chemistry and Biology* Wiley-VCH **2000**, *4*, 851-863.

[4] Lin, G.; Simmons, G.; Pohlmann, S.; Baribaud, F.; Ni, H. P.; Leslie, G. J.; Haggarty, B.; Bates, P.; Weissman, D.; Hoxie, J. A.; Doms, R. W. *J. Virol.* **2003**, *77*, 1337.

[5] Delmas, B.; Laude, H. *Virus Research* **1991**, *20*, 107.

[6] Calarese, D. A.; Scanlan, C. N.; Zwick, M. B.; Deechongkit, S.; Mimura, Y.; Kunert, R.; Zhu, P.; Wormald, M. R.; Stanfield, R. L.; Roux, K. H.; Kelly, J. W.; Rudd, P.M.; Dwek, R. A.; Katinger, H.; Burton, D. R.; Wilson, I. A. *Science* **2003**, *300*, 2065.

[7] Shenoy, S. R.; Barrientos, L. G.; Ratner, D. M.; O'Keefe, B. R.; Seeberger, P. H.; Gronenborn, A. M.; Boyd, M. R. *Chem. Biol.* **2002**, *9*, 1109.

[8] Adams, E. W.; Uberfeld, J.; Ratner, D. M.; O'Keefe, B. R.; Walt, D, R.; Seeberger, P. H. *Angew. Chem. Int. Ed.* **2003**, *42*, 5317-5320. Ratner, D. M.; Adams, E. W.; Disney, M. D.; Seeberger, P. H. *ChemBioChem*, **2004**, In Press. Adams, E. W.; Ratner, D. M.; Bokesch, H. R.; McMahon, J. B.; O'Keefe, B. R.; Seeberger, P.H. *Chem. Biol.* **2004**, *11*, 875. Ratner, D. M.; Adams, E. W.; Su, J.; O'Keefe, B. R.; Mrksich, M.; Seeberger, P. H. *ChemBioChem.* **2004**, 5, 379-383.

[9] Barrientos, L. G.; Louis, J. M.; Ratner, D. M.; Seeberger, P. H.; Gronenborn, A. M. *J. Mol. Biol.* **2003**, *325*, 211. Botos, I.; O'Keefe, B. R.; Shenoy S. R.; Cartner, L. K.; Ratner, D. M.; Seeberger, P. H.; Boyd, M. R.; Wlodawer, A. *J. Biol. Chem.* **2002**, *277*, 34336.

[10] For a review of recent solution phase syntheses of the core pentasaccharide, see Yamazaki, F.; Kitajima, T.; Nukada, T.; Ito, Y.; Ogawa, T. *Carbohydrate Res.* **1990**, *201*,

15. Unverzagt, C. *Angew. Chem. Int. Ed.* **1994**, *33*, 1102. Meritt, J. R.; Naisang, E.; Fraser-Reid, B. *J. Org. Chem.* **1994**, *59*, 4443. Dan, A.; Ito, Y.; Ogawa, T. *J. Org. Chem.* **1995**, *60*, 4680. Matsuo, I.; Nakahara, Y.; Ito, Y.; Nukada, T.; Ogawa, T. *Bioorg. Med. Chem.* **1995**, *3*, 1455. Dan, A.; Ito, Y.; Ogawa, T. *Tetrahedron Lett.* **1995**, *36*, 7487. Seeberger, P. H.; Cirillo, P. F.; Hu, S. H.; Beebe, X.; Bilodeau, M. T.; Danishefsky, S. J. *Enantiomer.* **1996**, *1*, 311. Guo, Z.W.; Nakahara, Y.; Nakahara, Y.; Ogawa, T. *Bioorg. Med. Chem.* **1997**, *5*, 1917. Danishefsky, S. J.; Hu, S.; Cirillo, P. F.; Eckhardt, M.; Seeberger, P. H. *Chem. Eur. J.* **1997**, *3*, 1617. Matsuo, I.; Isomura, M.; Ajisaka, K. *J. Carb. Chem.* **1999**, *18*, 841. Takatani, M.; Nakama, T.; Kubo, K.; Manabe, S.; Nakahara, Y.; Ito, Y.; Nakahara, Y. *Glycoconjugate. J.* **2000**, *17*, 361. Wang, Z. G.; Zhang, X. F.; Live, D.; Danishefsky, S. J. *Angew. Chem. Int. Ed. Engl.* **2000**, *39*, 3652. Dudkin, V. Y.; Miller, J. S.; Danishefsky, S. J. *Tet. Lett.* **2003**, *44*, 1791. Miller, J. S.; Dudkin, V. Y.; Lyon, G. J.; Muir, T. W.; Danishefsky, S, J. *Angew. Chem. Int. Ed. Engl.* **2003**, *42*, 431. Pratt, M. R.; Bertozzi, C. R. *J. Am. Chem. Soc.* **2003**, *125*, 6149.

[11] Wu, X.; Grathwohl, M.; Schmidt, R. R. *Angew. Chem. Int. Ed. Engl.* **2002**, *41*, 4489.

[12] Gridley, J. J.; Osborn, H. M. I. *J. Chem. Soc., Perkin Trans. 1* **2000**, *10*, 1471.

[13] Mayer, T. G.; Kratzer, B.; Schmidt, R. R. *Angew. Chem. Int. Ed. Engl.* **1994**, *33*, 2177.

[14] Melean, L. G.; Love, K. R.; Seeberger, P. H. *Carb. Res.* **2002**, *337*, 1893.

[15] Ratner, D. M.; Seeberger, P. H.; "Octenediol." *Encyclopedia of Reagents for Organic Synthesis.* **2003**.

[16] Andrade, R. B.; Plante, O. J.; Melean, L. G.; Seeberger, P. H. *Org. Lett.* **1999**, *1*, 1811.

[17] Crich, D.; Sun, S. X. *J. Am. Chem. Soc.* **1997**, *119*, 11217. Crich, D.; Sun, S. X. *Tetrahedron.* **1998**, *54*, 8321.

[18] Crich, D.; Li, H. M.; Yao, Q. J.; Wink, D. J.; Sommer, R. D.; Rheingold, A. L. *J. Am. Chem. Soc.* **2001**, *123*, 5826.

[19] Sakagami, M.; Hamana, H. *Tetrahedron Lett.* **2000**, *41*, 5547.

[20] Plante, O. J.; Palmacci, E. R.; Seeberger, P. H. *Science,* **2001**, *291*, 1523. Plante, O. J. New Methods for the Synthesis of Carbohydrates: The First Automated Solid-Phase Oligosaccharide Synthesizer. Ph.D. Thesis, Massachusetts Institute of Technology, Cambridge, MA, June 2001.

[21] Love, K. R.; Seeberger, P. H. *Angew. Chem. Int. Ed.* **2004**, *43*, 602.

Chapter 4

Synthetic Tools for Glycobiology: Carbohydrate Microarrays

This chapter describes work completed in close collaboration with Mr. Eddie W. Adams. Microarrays were printed with the assistance of Mr. Sean Milton of the MIT BioMicro facility. Portions of this chapter were reprinted with permission, and may be found in the following publications:

Ratner, D. M.; Adams, E. W.; Disney, M. D.; Seeberger, P. H.; Tools for Glycomics: Mapping Interactions of Carbohydrates in Biological Systems. *ChemBioChem*, **2004**, In Press.

Adams, E. W.; Ratner, D. M.; Bokesch, H. R.; McMahon, J. B.; O'Keefe, B. R.; Seeberger, P.H. Oligosaccharide and Glycoprotein Microarrays as Tools in HIV-Glycobiology: A Detailed Analysis of Glycan Dependent gp120 / Protein Interactions. *Chem. Biol.* **2004**, *11*, 875-881.

Ratner, D. M.; Adams, E. W.; Su, J.; O'Keefe, B. R.; Mrksich, M.; Seeberger, P. H. Probing Protein-Carbohydrate Interactions with Microarrays of Synthetic Oligosaccharides. *ChemBioChem.* **2004**, 5, 379-383.

Adams, E. W.; Uberfeld, J.; Ratner, D. M.; O'Keefe, B. R.; Walt, D, R.; Seeberger, P. H. Encoded Fiber-Optic Microsphere Arrays for Probing Protein-Carbohydrate Interactions. *Angew. Chem. Int. Ed.* **2003**, *42*, 5317-5320.

4.1 Introduction

There is growing interest in microarray-based methods to study the roles of nucleic acids, proteins, and carbohydrates in biology. In particular, efforts in the emerging field of glycomics stand to benefit significantly from assay miniaturization through the construction of high-density oligosaccharide and glycoprotein microarrays. Research with carbohydrates is stymied by the fact that no 'biological amplification' strategy comparable to the polymerase chain reaction or cloning exists for the procurement of usable quantities of complex oligosaccharides. Investigators must rely

upon arduous isolation techniques to derive oligosaccharides from natural sources or prepare these complex structures via chemical synthesis. While the chip-based format does not circumvent these challenges, it does offer significant advantages over conventional methods. Most notably, microarrays are able to screen several thousand binding events in parallel while requiring a minimal amount of analyte and ligand for study. Making the most of precious synthetic or naturally procured materials, these miniaturized assays frequently require only picomoles of material per array, while enabling several experiments to be carried out on a single glass slide.

The motivation behind developing a system for arraying carbohydrates is based on the desire to have microarrays that are fully compatible with existing high-throughput screening technologies and will enable efficient covalent immobilization of oligosaccharides drawn from solution phase synthesis, automated solid-phase synthesis[1] and natural sources. Such carbohydrate arrays will be useful tools in the identification of carbohydrate-protein interactions and will help define the exact oligosaccharide structures involved in binding events. In addition, carbohydrate arrays could be used to rapidly screen for compounds that selectively inhibit protein-oligosaccharide interactions.

Here we describe an approach that begins with a high-density microarray system to study carbohydrate-protein interactions using synthetic oligosaccharide structures covalently immobilized to chemically modified glass slides. Using technologies available to many researchers, these carbohydrate arrays are printed at high-density using DNA microarray printing robotics and analyzed with conventional DNA array scanners.

4.1.1 Other Linking Schemes for Carbohydrate Microarrays

Many methods for preparing carbohydrate microarrays have been described to date: nitrocellulose coated slides for non-covalent immobilization of microbial polysaccharides and neoglycolipid modified oligosaccharides;[2] polystyrene microtiter plates for presenting lipid-bearing carbohydrates;[3] self-assembled monolayers modified by Diels-Alder mediated coupling of cyclopentadiene-derivatized saccharides;[4] thiol-derivatized glass slides modified with maleimide functionalized oligosaccharides;[5] and, thiol functionalized carbohydrates immobilized on maleimide-derived gold slides.[6]

While each of these approaches offer advantages in their own right, they do not meet the criteria we have set out to achieve. Specifically, we propose a microarray that encompasses covalent immobilization of oligosaccharide, resists non-specific binding by proteins and other biopolymers, and uses common high-throughput screening (HTS) technology.

4.2 New Linker Chemistry

Our laboratory developed a single linking chemistry for the purposes of streamlining the development process of new tools for glycobiology. With the input of Mr. Eddie W. Adams, the 2-(2-(2-mercaptoethoxy)ethoxy)ethyl linker was selected for the preparation of neoglycoconjugates.[7] This linker chemistry was selected based on its compatibility with existing synthetic methods, the ease of temporarily masking the thiol functionality with a protecting group, and the reliability of thiol-based conjugation chemistries – in particular, thiol-maleimide and thiol-iodoacetyl couplings. The orthogonal reactivity of a terminal thiol to the functional groups presented by carbohydrates allows for defined covalent immobilization of oligosaccharides to a functionalized surface, creating a cell surface-like environment on the chip.[8] In addition, the hydrophilic nature of the tri(ethylene oxide) linker increases the solubility of the immobilized structures on the surface, bringing them off the surface and into solution. The linker also resists non-specific binding by proteins.

The proposed chemistry consists of incorporating 2-[2-(2-benzylsulfanyl-ethoxy)-ethoxy]-ethanol[9] at the reducing end of the synthetic glycoside (Scheme 4.1). Following synthesis of the complete structure, all temporary protecting groups are removed, including the thiobenzyl ether masking the thiol functionality of the linker. The newly deprotected thiol-functionalized saccharide can subsequently be reacted with surfaces or structures modified with thiol-reactive moieties, such as maleimide or iodoacetyl groups.

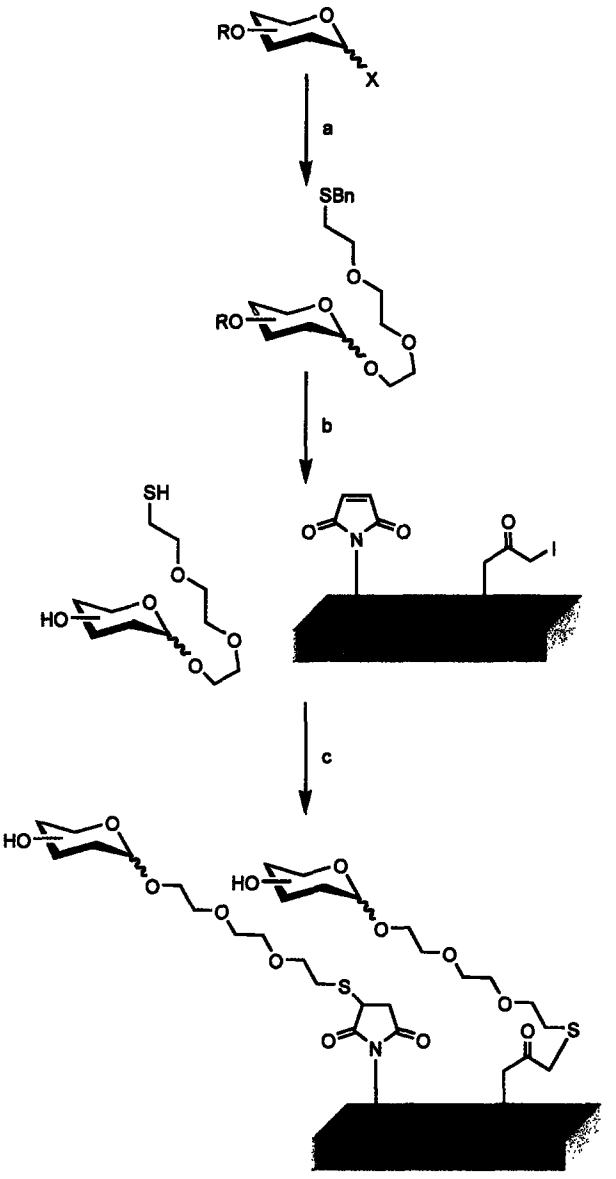

Scheme 4.1 2-(2-(2-mercaptoethoxy)ethoxy)ethanol as a linker for preparing neoglycoconjugates. a) Linker synthetically incorporated into the reducing-end of mono or oligosaccharide. b) 'Global' deprotection of all protecting groups from carbohydrate and thiol. c) Reduced thiol coupled to maleimide or iodoacetyl functionalized structure.

We adopted two surface chemistries for the preparation of our carbohydrate microarrays. Both strategies involve maleimide functionalization of glass slides, presenting a chemical handle to form stable bonds between the slide and thiol-containing synthetic oligosaccharides. In one case, bovine serum albumin (BSA) derivatized aldehyde glass slides were functionalized with succinimidyl 4-(*N*-maleimidomethyl)-

cyclohexane-1-carboxylate (SMCC) to present a maleimide reactive surface.[7] Alternatively, amine-derivatized Corning® GAPS II slides were directly modified with SMCC prior to incubation with thiol-presenting saccharides.[10]

4.3 Synthesis of Oligosaccharides for Carbohydrate Microarrays

For this initial study, the structures required for microarray fabrication were prepared synthetically. The precision afforded by organic synthesis permitted the construction of a panel of oligosaccharides that would be immensely difficult to prepare by enzymatic methods.

4.3.1 Oligosaccharide Targets

A panel composed of 8 carbohydrates was selected for this high-mannose carbohydrate microarray study (Figure 4.1). The 2-[2-(2-mercapto-ethoxy)-ethoxy]-ethyl glycosides were synthesized in a manner analogous to the *n*-pentyl high-mannose oligosaccharides prepared for Chapter 2. Targets **4-1** through **4-7** were selected to represent the major structural determinants of the *N*-linked high-mannose nonasaccharide Man_9. Galactose **4-8** was included as a representative non-mannosyl pyranoside.

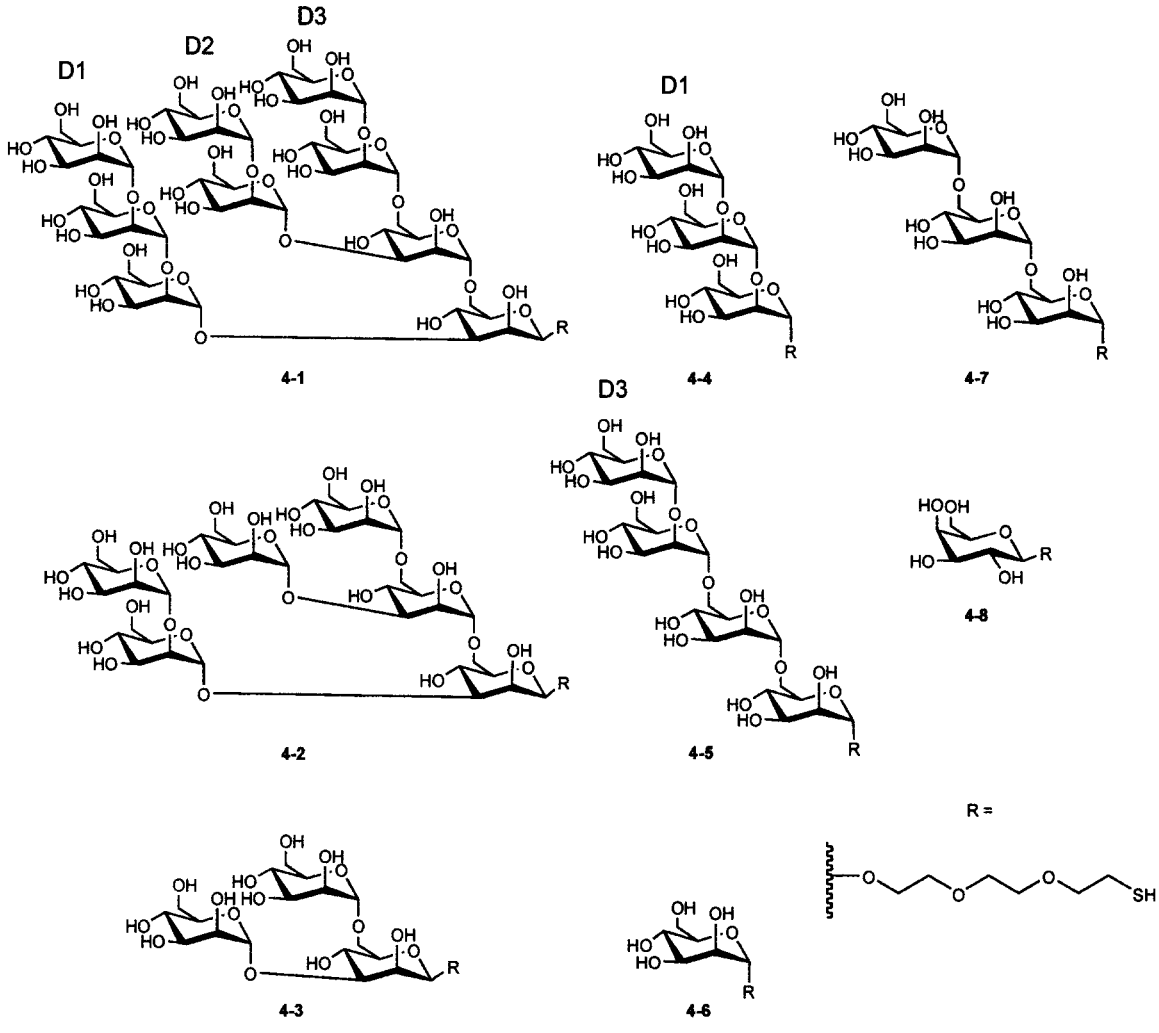

Figure 4.1 Oligosaccharides containing the 2-[2-(2-mercapto-ethoxy)-ethoxy]-ethyl-linker necessary for immobilization to thiol-reactive partners. Correct reducing-end stereochemistry indicated by "–R".

4.3.2 Retrosynthesis of Branched Mannans

Adopting methods developed during the solution-phase studies of high-mannose oligosaccharides in Chapter 2, the branched mannans required for this study were analyzed with the same retrosynthetic approach (Scheme 4.2). Given the success of the linear strategy for the construction of the branched structures, nonasaccharide **4-9** would be derived from the simultaneous trimannosylation of hexasaccharide **4-10**, which in turn

would arise from differentiated core trisaccharide **4-11**. Finally, three monosaccharide building blocks (**4-12**, **4-13**, and **4-14**) would be required for construction of the branched structures. A notable difference from the synthesis of Chapter 2 is the introduction of the 2-[2-(2-benzylsulfanyl-ethoxy)-ethoxy]-ethyl moiety in place of the *n*-pentenyl handle.

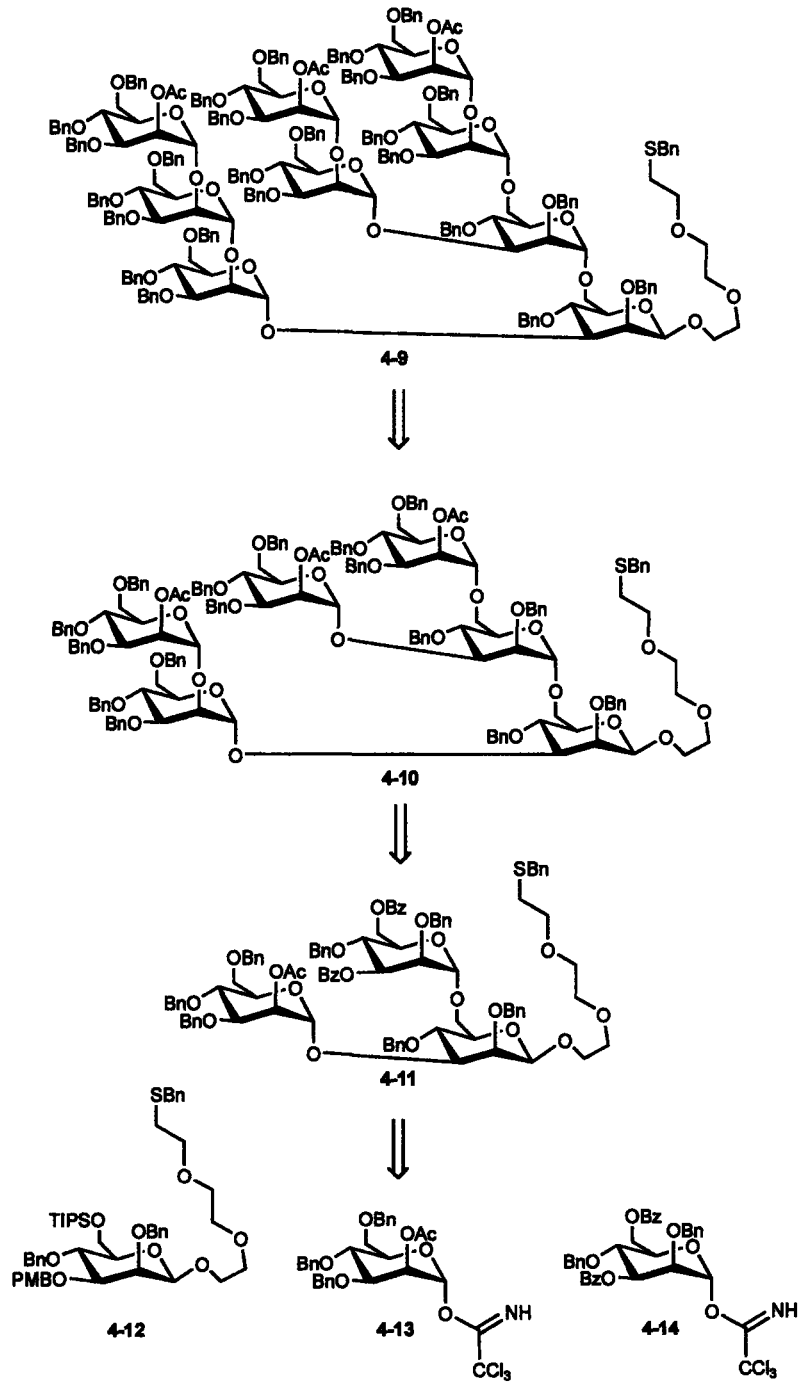

Scheme 4.2 Retrosynthetic analysis of nonamannoside **4-9**.

4.3.3 The 2-[2-(2-benzylsulfanyl-ethoxy)-ethoxy]-ethanol Linker

Prior to proceeding with the proposed synthesis, it was necessary to test the utility of the 2-[2-(2-benzylsulfanyl-ethoxy)-ethoxy]-ethyl linker in place of the well-established *n*-pentenyl moiety. To accomplish this, 2-[2-(2-benzylsulfanyl-ethoxy)-ethoxy]-ethanol was glycosylated with mannosyl donor **4-13**, with an encouraging yield of 99% (Scheme 4.3). 2-[2-(2-benzylsulfanyl-ethoxy)-ethoxy]-ethyl mannoside **4-15** was subjected to a dissolving metal reduction with sodium metal in liquid ammonia to furnish deprotected monosaccharide **4-6** in 76% yield. This simple procedure demonstrated the ability of the new linker to be glycosylated cleanly and stereoselectively. In addition, the thiobenzyl ether was established as a suitable protecting group to mask the thiol until the final deprotection.

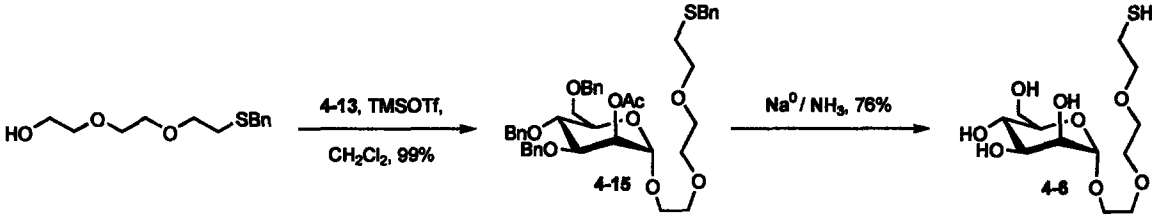

Scheme 4.3 Glycosylation of 2-[2-(2-benzylsulfanyl-ethoxy)-ethoxy]-ethanol with **4-13**.

4.3.4 Synthesis of β-Mannoside

Synthesis of core β-mannoside **4-19** proceeded via the same glycal-based approache detailed in Chapter 2, section 2.4. Glycal **4-16** was stereospecifically epoxidized by treatment with dimethyldioxirane, followed by opening of the 1,2-anhydrosugar with 2-[2-(2-benzylsulfanyl-ethoxy)-ethoxy]-ethanol in the presence of zinc chloride (Scheme 4.4). This yielded β-glucoside **4-17** with a C2 hydroxyl group (53%, two steps). Oxidation of the C2 hydroxyl under Pfitzner-Moffatt conditions (Ac_2O-DMSO) was followed by stereoselective reduction with sodium borohydride (36%, two steps) to furnish β-mannoside **4-18**. Benzylation of the C2 hydroxyl (90% yield) was followed by treatment of the C3 *p*-methoxybenzyl ether with 2,3-dichloro-5,6-

dicyano-1,4-benzoquinone (DDQ) to yield the C3 hydroxyl-containing mannoside **4-19** in 93%.

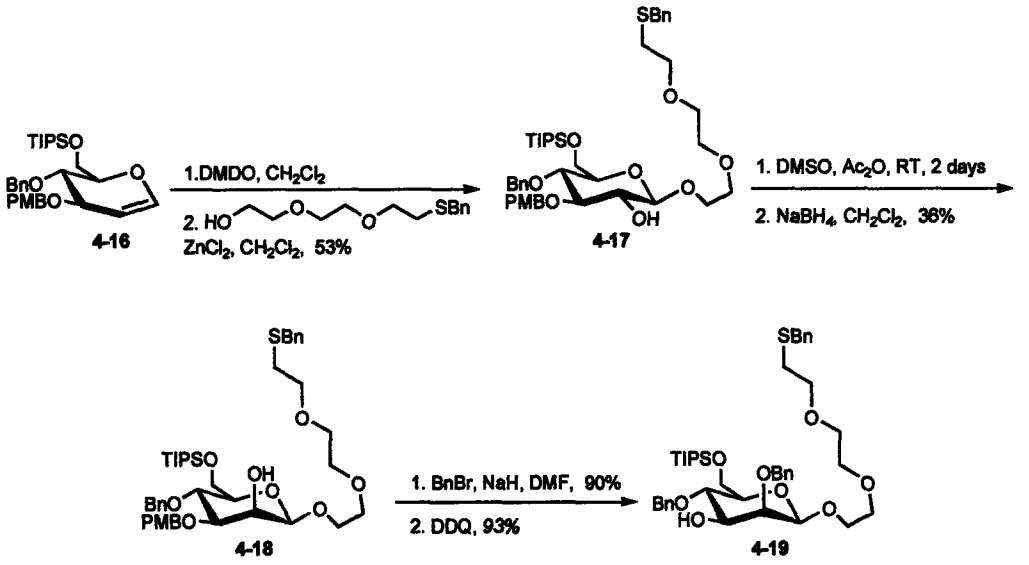

Scheme 4.4 Assembly of core β-mannoside.

4.3.5 Synthesis of Branched Oligosaccharides

With the differentiated core β-mannoside containing the new linker, it was possible to assemble the series of branched high-mannose oligosaccharides. Glycosylation of acceptor **4-19** with **4-13**, activated by addition of TBSOTf, yielded a 1:1 mix of desired product disaccharide **4-20** and the corresponding orthoester **4-21** (Scheme 4.5). Orthoester formation was not observed by TLC, and was unexpected following the results of similar chemistry developed in Chapter 2. However, the presence of orthoester **4-21** was firmly established by ^{1}H and ^{13}C NMR (Chapter 6, Appendix C). Unlike the *n*-pentenyl mannoside acceptor of Chapter 2, the flexible thiobenzyl ether-containing linker appears to affect the outcome of this glycosylation to favor formation of the orthoester (for discussion of orthoester formation, see Chapter 5, section 5.5.2).

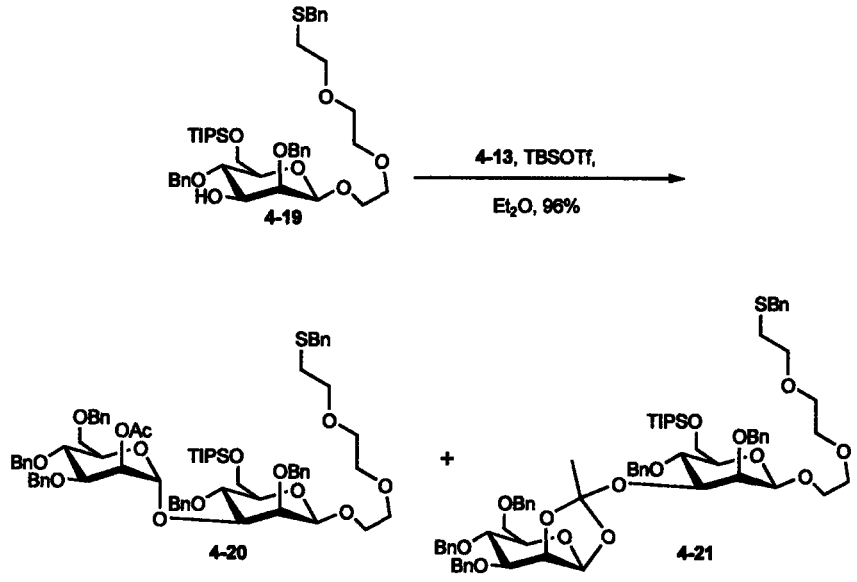

Scheme 4.5 Unexpected formation of orthoester **4-21** upon glycosylation of **4-19** with mannosyl donor **4-13**.

Orthoester **4-21** and disaccharide **4-20** were found to co-elute by silica gel chromatography, necessitating another means of isolating desired disaccharide **4-20**. An answer was found in the relative reactivity to acid of the orthoester vs. the glycoside. Proper glycosidic linkages are stable to weak acid, while the orthoester is readily hydrolyzed. Subjecting the 1:1 mix of **4-20** and **4-21** to 80% acetic acid resulted in the recovery of monosaccharide **4-19** and disaccharide **4-20** in 61% isolated mass recovery (Scheme 4.6). Disaccharide **4-20** was subsequently treated with TFA to remove the C6 TIPS ether to furnish disaccharide acceptor **4-22**. Mannosylation of **4-22** with **4-14** yielded core trisaccharide **4-11** in 81% yield. Prior to further elongation, trisaccharide **4-11** was subjected to treatment with sodium methoxide to remove the C2, C3 and C6 esters, yielding triol **4-23** in 85% yield.

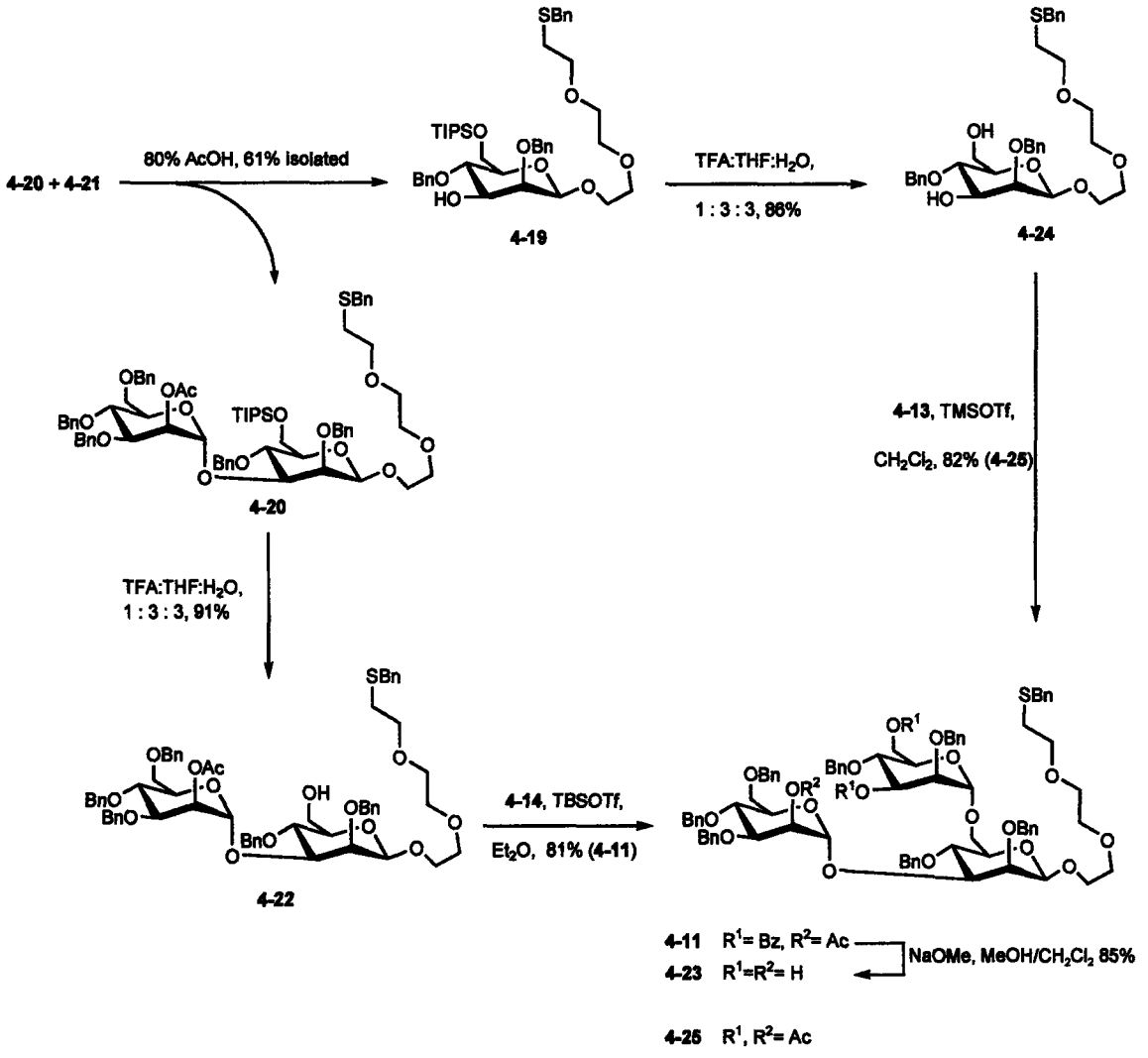

Scheme 4.6 Construction of trisaccharides **4-23** and **4-25**.

Recovered **4-19**, isolated from hydrolyzed orthoester **4-21**, was treated with TFA to furnish the C3,C6 diol **4-24** in 86% yield. Dimannosylation, by treatment of **4-24** with **4-13**, gave symmetrical trisaccharide **4-25**. While unsuitable for further differentiation or elongation, **4-25** was an ideal candidate for deprotection to generate branched trisaccharide **4-3**. By using reclaimed **4-19** to construct the non-differentiated core trisaccharide **4-25**, it was possible to commit the entirety of differentiated core trisaccharide **4-23** towards the construction of larger structures. This strategy made the best use of material on-hand, by avoiding a repeat of the difficult glycosylation of **4-19** with glycosyl donor **4-13**.

Completion of the hexa- and nonasaccharide proceeded by the trimannosylation of triol-acceptor **4-23** with donor **4-13** (Scheme 4.7). Hexasaccharide **4-10**, isolated in 84% yield, was subjected to methanolic sodium methoxide to furnish triol **4-26** (91%). Finally, nonasaccharide **4-9** was secured in 71% yield following the trimannosylation of **4-28** in diethyl ether.

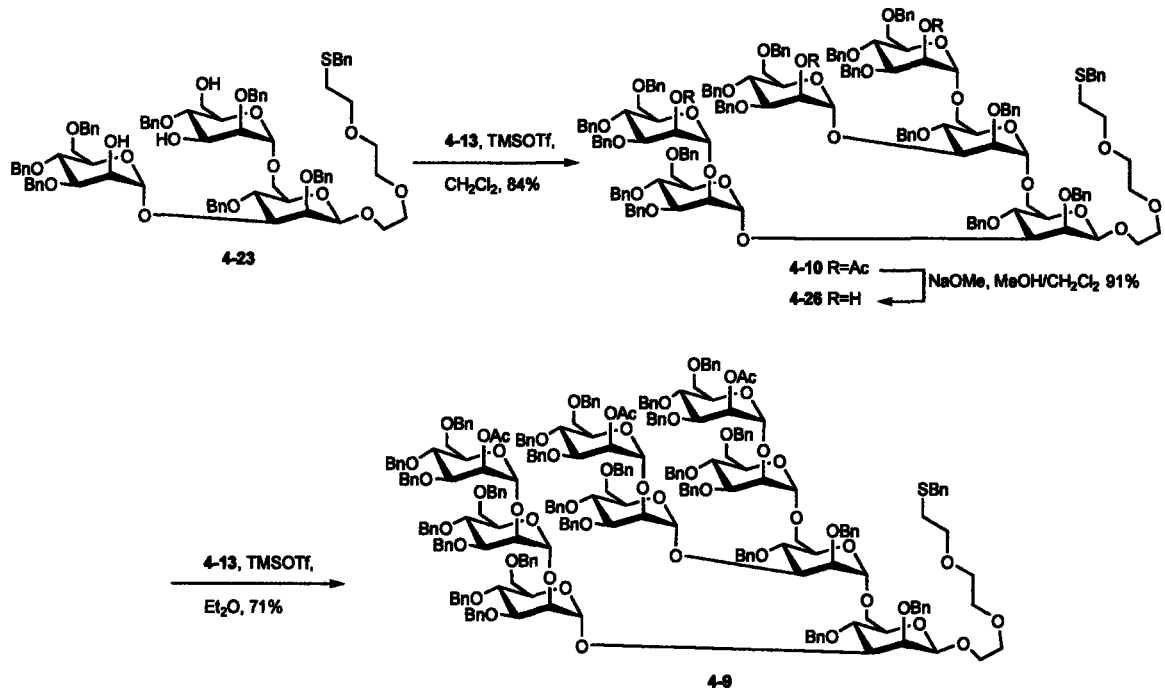

Scheme 4.7 Assembly of hexasaccharide **4-10** and nonasaccharide **4-9**.

The syntheses of fully protected tri-, hexa- and nonasaccharide **4-25**, **4-10** and **4-9** containing the tri(ethylene glycol) linker were successfully completed. Assembly of the high-mannose structures was accomplished with similar success to the initial completion of the *n*-pentenyl glycosides described in Chapter 2. While the thiobenzyl ether-containing linker reduced the yields of some key steps in the assembly, the impact was minor and did not affect the overall ability to prepare the complete structures.

4.3.6 Synthesis of Linear D1 Trisaccharide

A major structural constituent of the high-mannose nonasaccharide, the linear α(1→2) trimannoside was assembled by three sequential mannosylations of 2-[2-(2-benzylsulfanyl-ethoxy)-ethoxy]-ethanol with mannose donor **4-13** (Scheme 4.8). Unlike the D1 trisaccharide prepared by automated solid-phase synthesis for use in Chapter 2, inclusion of the new linker required a return to solution-phase synthesis for its creation. Beginning with **4-15** (Scheme 4.2), the C2 acetate was removed with sodium methoxide, quenched with acidic Amberlite-IR120 resin, and glycosylated with **4-13** in 70% yield (3 steps). Disaccharide **4-27** was similarly treated to furnish the C2 hydroxyl in 93% yield and glycosylated with **4-13** to give fully protected D1 trisaccharide **4-28** (91% yield).

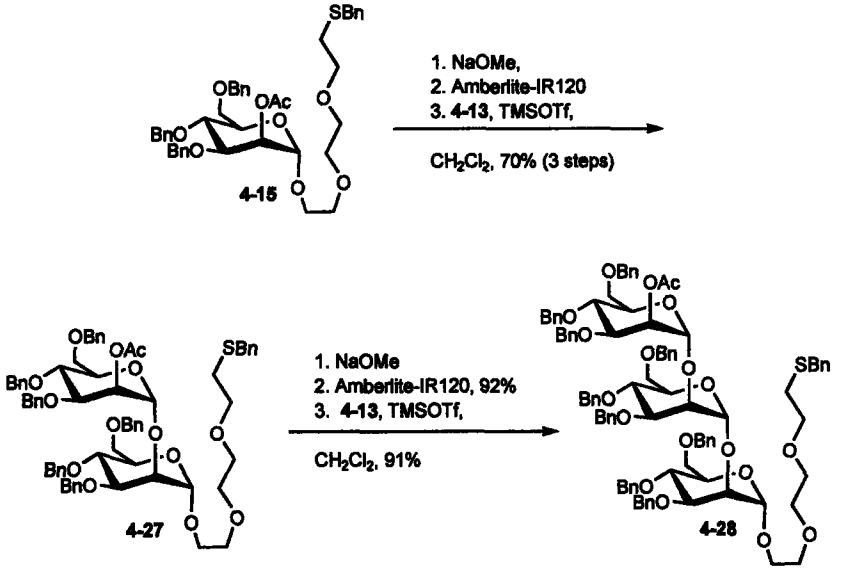

Scheme 4.8 Rapid solution-phase synthesis of linear D1 trimannoside **4-28**.

4.3.7 Retrosynthesis of Linear D3 Arm

As detailed in Figure 4.1, among the structures desired for study was the D3 arm tetrasaccharide **4-5**, and the truncated structure **4-7**. By including both structures on a microarray, in addition to the D1 trisaccharide, it would be possible to simultaneously establish whether D1, D3 or both arms are required for protein-binding of high-mannose oligosaccharides. The truncated D3 arm trisaccharide **4-7**, which is missing the terminal

α(1→2) mannose, contains only α(1→6) mannoses. Including this compound in the array adds an element of structural specificity, necessary for identifying the specific type of linkage required for protein-binding.

Retrosynthesis of the D3 arm trisaccharide was based on a linear assembly method, similar to the preparation of D1 trisaccharide **4-28** (Scheme 4.9). Fully protected D3 tetrasaccharide **4-29** could be truncated to trisaccharide **4-30** by the removal of a single α(1→2) mannoside. Cleavage of the α(1→6) mannose of **4-30** revealed the differentiated core disaccharide **4-31**. The complete assembly was based on three monosaccharide mannosyl donors **4-13**, **4-32** and **4-33**. Building blocks **4-32** and **4-33** differentiate the C2 and C6 positions with temporary protecting groups, permitting chemistries to be selectively accomplished at each position. Inclusion of either the C2 acetate or benzoate esters ensures stereospecific mannosylations to yield α-selective glycosylations. Mannosyl donor **3-33** was envisioned due to the relative stability of the benzoate ester. With magnesium methoxide, it is possible to selectively remove a C2 *O*-acetate in the presence of benzoyl protecting groups.[11] This chemistry permits differential elongation of **4-30**, by mannosylating on the C2 position of the non-reducing end mannose.

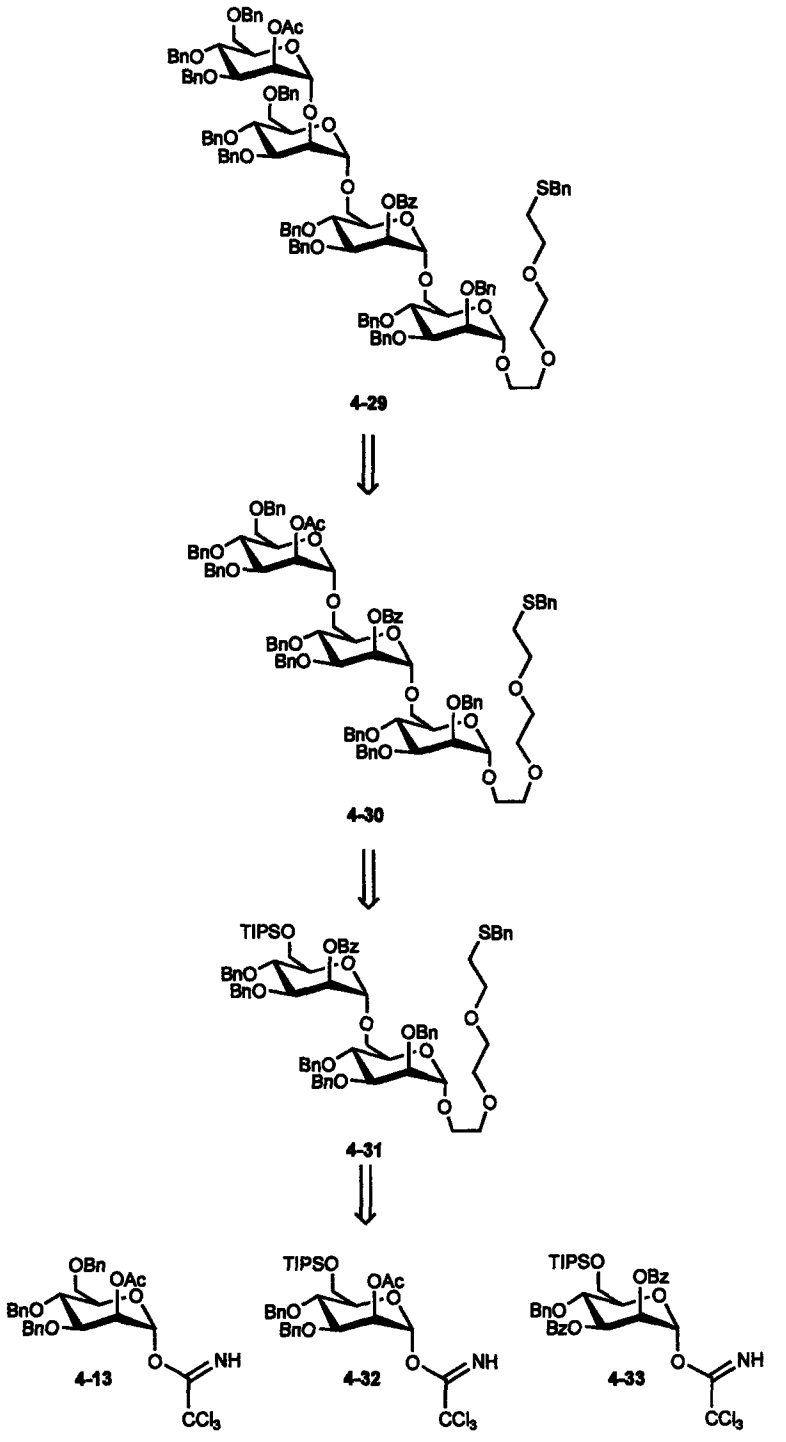

Scheme 4.9 Retrosynthesis of linear D3 tetrasaccharide **4-29**.

4.3.8 Synthesis of D3 Tetrasaccharide and Truncated Trisaccharide

Access to mannose donor **4-33** was accomplished in 5 steps, starting with mannose donor **4-32**[12] (Scheme 4.10). Allyl alcohol was glycosylated with **4-32** in 66% yield and subsequently reacted with sodium methoxide to yield allyl mannoside **4-34** in 82%. The C2 hydroxyl was reacted with benzoyl chloride in 92% yield, and fully protected allyl glycoside converted to the lactol by reaction with palladium chloride. Reacting the lactol with trichloroacetonitrile in the presence of DBU yielded mannosyl trichloroacetimidate **4-33** in 80% (2 steps).

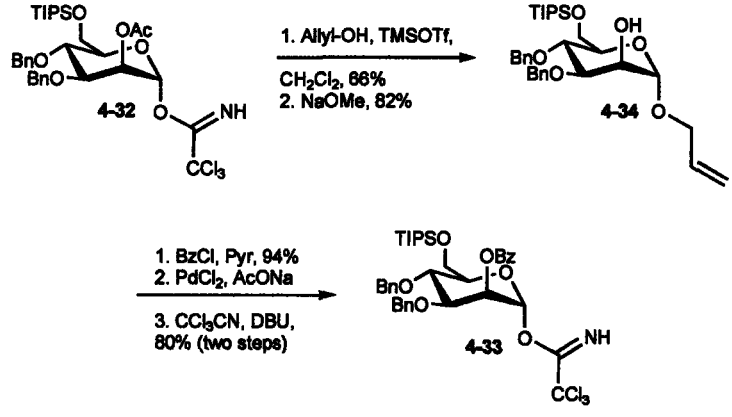

Scheme 4.10 Retrosynthesis of linear D3 arm tetrasaccharide **4-29**.

With the three donors necessary for completing the D3 tetrasaccharide available, assembly commenced with the mannosylation of 2-[2-(2-benzylsulfanyl-ethoxy)-ethoxy]-ethanol by mannosyl donor **4-32** to yield **4-35** in 99% (Scheme 4.11). Conversion of the C2 acetate to a more stable benzyl ether was achieved via acetate removal with sodium methoxide (98%) followed by benzylation with benzyl bromide in DMF (88%). Mannoside **4-36** was subjected to TBAF in refluxing Et_2O to furnish the C6 hydroxyl in 44% yield. Glycosylation with **4-33** gave disaccharide **4-31** in 98% yield. Avoiding the low yielding TBAF deprotection, disaccharide **4-31** was treated with TFA to remove the C6 silyl ether in 78% yield. The disaccharide acceptor was subsequently mannosylated in 77% yield with mannosyl building block **4-13** to give trisaccharide **4-30**. Trisaccharide **4-30** would serve dual purposes, as the fully protected version of the truncated D3 arm **4-7** and the precursor for preparing tetrasaccharide **4-29**. A portion of

4-30 was treated with magnesium methoxide to selectively remove the C2 acetate in the presence of the C2 benzoate. Selective deprotection was achieved in 71% yield to give the trisaccharide acceptor which was mannosylated with **4-13** to furnish fully protected D3 tetrasaccharide **4-29** in 95% yield.

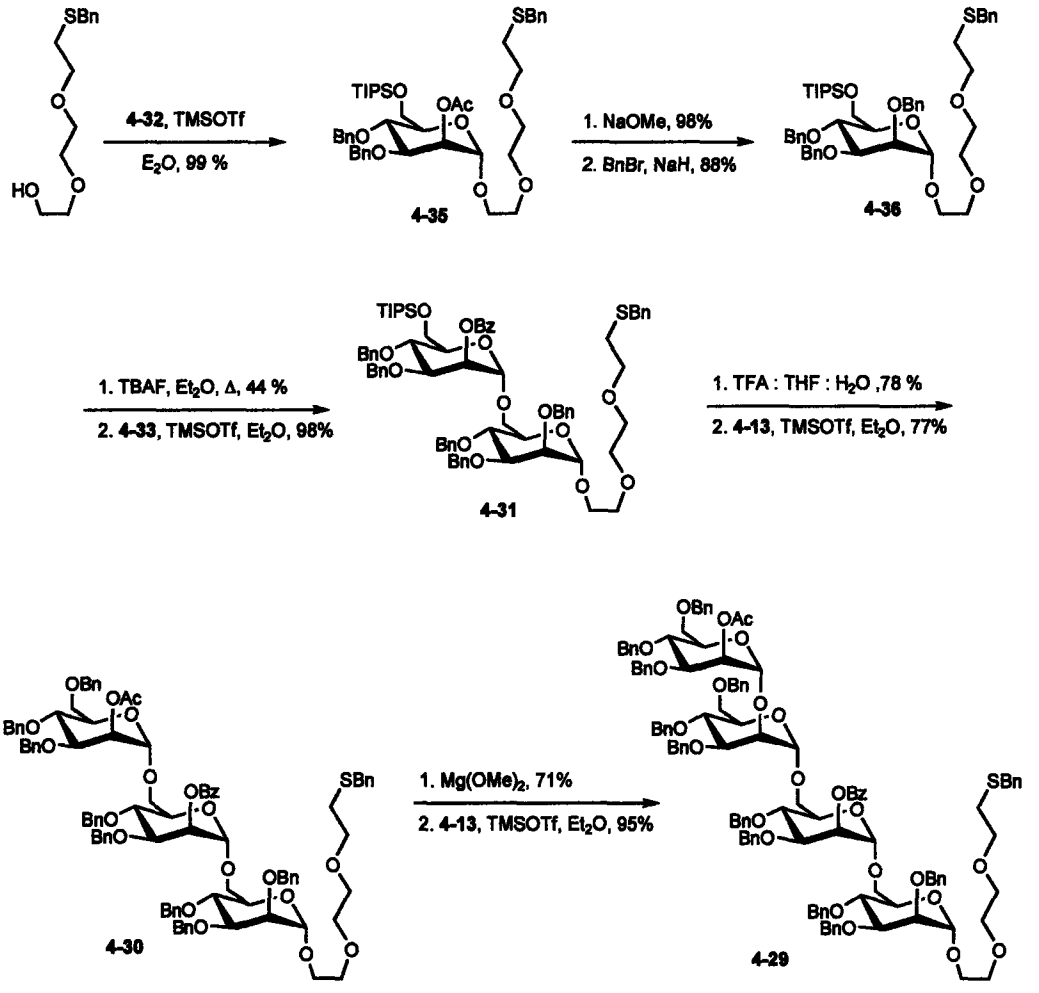

Scheme 4.11 Construction of linear D3 arm tetrasaccharide **4-29**.

4.3.9 Monosaccharide Galactose Control

As a non-mannose control for non-specific carbohydrate-binding on the microarray, galactose was selected as an ideal monosaccharide candidate. Cross reactivity between galactose- and mannose-binding proteins is minimal, and preparation of the required structure was easily achieved using a simple galactosyl phosphate

(Scheme 4.12). Galactosyl donor **4-37** was reacted with of 2-[2-(2-benzylsulfanyl-ethoxy)-ethoxy]-ethanol and stoichiometric TMSOTf, furnishing **4-38** in 73% yield.

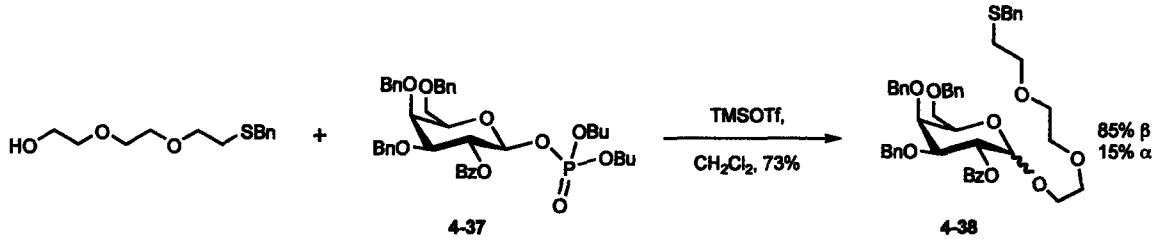

4-37 4-38

Scheme 4.12 Preparation of galactoside **4-38**.

4.3.10 Preparation of Fully Deprotected Oligosaccharides

Preparation of large quantities of oligosaccharide for study remains a strong advantage of synthetic carbohydrate chemistry. However, to make this possible, it is necessary to remove all protecting groups to furnish biologically useful material. With the benzyl ether as the most common 'permanent' protecting group, deprotection is typically achieved by hydrogenation with H_2 and a palladium catalyst. This process also necessitates that protecting groups not labile to hydrogenation, such as esters, be removed with an additional step. In the case of the structures prepared for this study, inclusion of a masked thiol requires that another deprotection chemistry be used, as a thiol would poison the palladium catalyst.

For the purpose of global deprotection, a sodium-based dissolving metal reduction was chosen for its versatility and simplicity.[13] By adding protected saccharides to a solution of sodium metal dissolved in liquid ammonia, the stringent conditions of the dissolving metal reduction simultaneously cleave esters, many amides, and benzyl ethers. Table 4.1 illustrates the isolated yields for the deprotection of the linker-containing oligosaccharides prepared for this study (Figure 4.1, see Chapter 6, section 6.4 for experimental detail).

Table 4.1 Yields for dissolving sodium-metal reductions of protected oligosaccharides. General procedure and characterization detailed in Chapter 6, section 6.4.

Starting Material	Product	Yield
4-9	**4-1**	60%
4-10	**4-2**	71%
4-11	**4-3**	82%
4-28	**4-4**	53%
4-29	**4-5**	91%
4-15	**4-6**	76%
4-30	**4-7**	71%
4-38	**4-8**	43%

4.3.11 Oxidation of Thiol-Modified Carbohydrates

Following deprotection, 2-[2-(2-benzylsulfanyl-ethoxy)-ethoxy]-ethyl glycosides become 2-[2-(2-mercapto-ethoxy)-ethoxy]-ethyl glycosides, thereby presenting a primary thiol at the end of a flexible tri(ethylene glycol) handle. Upon exposure to the atmosphere, solutions of these thiol-modified glycosides readily oxidize to the symmetrical disulfide (Scheme 4.13). Normal handling results in solutions that contain a mixture of both reduced and oxidized material, which is readily observed by TLC and mass spectrometry.

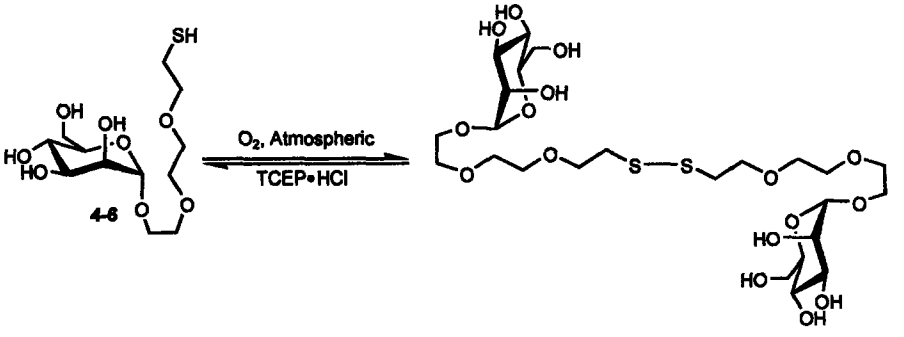

Scheme 4.13 Oxidation of thiol-modified glycoside to form dimeric disulfide.

Solutions of thiol-containing oligosaccharide must be reduced prior to coupling because the disulfide is not useful as a coupling partner to thiol-reactive species, such as the maleimide or iodoacetyl functionalities. To achieve this, tris(2-carboxyethyl) phosphine hydrochloride (TCEP·HCl) was used as a water-soluble phosphine for reduction. Solutions of dimerized glycoside were reduced by incubation at room temperature for 1 hour with 1 equivalent TCEP·HCl. TCEP has been shown to be reactive towards the maleimide group,[14] therefore a minimal quantity of TCEP was used in all reductions. Also, TCEP·HCl is known to decompose in phosphate buffered saline (PBS). Therefore, the reductions were run in pH 7.2 PBS, which maintained the desired pH for coupling, and ensured that unreacted TCEP would slowly degrade before it had an opportunity to interfere with the desired reaction.

4.4 Microarray Design and Fabrication

The design and fabrication of our carbohydrate microarrays was based on standard 25 x 75 mm glass-slide microarray technology. Two closely related surface chemistries were developed for the purpose of covalently attaching the carbohydrates to the surface of the microarray. These methods would ultimately serve as the basis for our microarray platform, utilized in a number of biological studies.

4.4.1 Microarray Layout and Design

The layout of our carbohydrate arrays was based on 16- and 32-pin printing methods using a standard DNA microarray printer (additional details in Chapter 6). We settled upon a 32-pin printing pattern that typically consisted of 8 synthetic oligosaccharides printed at 4 different concentrations (Figure 4.2). Each compound was printed either 36 or 100 times, in 6 x 6 or 10 x 10 grids respectively. Printing the structures in redundant grids permitted software-based statistical analysis of fluorescence for protein binding of each carbohydrate structure. Orientation on the chip was established by an identifying barcode on the bottom of the chip.

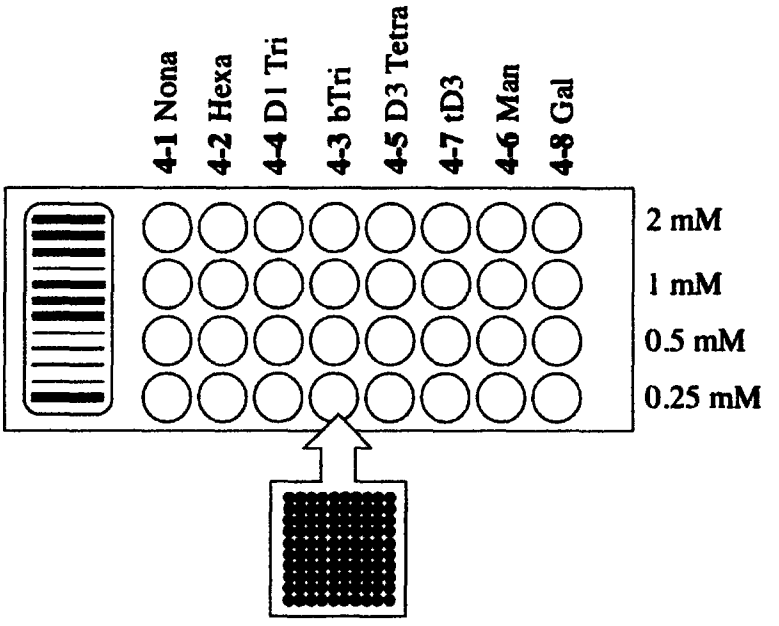

Figure 4.2 Layout of typical high-mannose oligosaccharide microarray (25 mm x 75 mm). Concentrations represent those of the solutions of oligosaccharide printing on the microarray.

4.4.2 Carbohydrate Microarrays Derived from BSA-Coated Glass Slides

Inspired by the success of protein microarrays based on BSA-derivatized glass surfaces,[15] the first microarrays were prepared by an analogous method. BSA is known to block many non-specific protein binding events. Therefore, having a surface coated with BSA is effective at reducing background binding, while presenting many usable amine functionalities (in the form of lysine side-chains) for surface derivatization. These characteristics made the BSA-based microarray attractive as a means of fabricating the first microarrays.

4.4.2.1 BSA Microarray Fabrication

Aldehyde-presenting glass slides were incubated with a buffered solution of BSA. Following Schiff's base formation, thereby immobilizing the BSA, the slides were rinsed, and functionalized with SMCC to create a thiol-reactive surface. Reduced thiol-

containing carbohydrates were subsequently printed on the maleimide-derivatized glass slides using a DNA microarray printer (16 or 32 pin). Following incubation, the slides were rinsed, and incubated in a solution of 3-mercaptopropionic acid. This last step effectively quenches unreacted maleimide sites on the glass slide, rendering the surface inert to non-specific binding by proteins. A particular concern was possible cross-reactivity of unreacted maleimide on the array's surface with free cysteine residues of any screened peptide.

4.4.2.2 Microarray Proof of Principle: Concanavalin A

To demonstrate the ability of the system to detect protein-carbohydrate interactions as a proof of principle, we used a well-known mannose/glucose specific lectin, Concanavalin A (ConA). Linker derivatized mannose **4-6** and galactose **4-8** were printed as 120 μm spots using a microarray printing robot. Both structures were printed as solutions ranging from 10 to 0.05 mM in PBS. Following incubation, the remaining maleimide groups were quenched with a 1 mM solution of 3-mercaptopropionic acid. The carbohydrate microarrays were incubated with fluorescein isothiocyanate (FITC)-labeled ConA, thoroughly rinsed with buffer, dried by centrifugation and scanned with a fluorescence slide scanner. As anticipated, FITC-labeled ConA was observed on the spots corresponding to immobilized mannose, while no fluorescence was associated with the spots that presented galactose (Figure 4.3). This result confirms that the microarray platform can be used for the immobilization of carbohydrates while maintaining specificity in carbohydrate-protein interactions. By utilizing proteins conjugated to fluorophores of non-overlapping excitation and emission spectra, we shall see that it is also possible to extend this technology to include two or more colors, as previously demonstrated.[15] We observed very high signal-to-noise ratios in this experiment, presumably due to minimal non-specific protein-surface interactions. Analogous observations have been made previously for protein microarrays that make use of derivatized BSA for the immobilization of small molecules.[15]

Figure 4.3 Mannose and Galactose microarray, printed at varying concentration, screened against FITC-labeled ConA

4.4.2.3 Carbohydrate-Binding by Cyanovirin-N

Having evaluated our carbohydrate microarrays with monosaccharide-lectin interactions, we sought to extend this system to include more biologically relevant and complex oligosaccharide structures. Here we selected a series of high-mannose type oligosaccharides of key importance in the *N*-linked glycosylation pathway and also found on the glycoproteins of a variety of infectious agents such HIV,[16] influenza virus and trypanosomes.[17,18] To this end, the following structures were printed at varying concentrations on the BSA-coated slides: **4-1**, nonamannoside; **4-2**, hexamannoside; **4-4**, linear trimannoside; **4-3**, branched trimannoside; **4-6**, mannose and **4-8**, galactose.

We chose the protein cyanovirin-N (CVN) as a model for the study of protein-oligosaccharide binding events.[19] Isolated from the blue-green algae *Nostoc ellipsosporum*, CVN was found to bind the high-mannose oligosaccharides of gp120, thereby inhibiting HIV's ability to infect target cells.[20] Natural and recombinant forms of CVN have been shown to irreversibly inactivate a wide variety of HIV strains while exhibiting minimal toxicity to host cells.[21] The ability of CVN to bind high-mannose oligosaccharides makes it an ideal test case for a carbohydrate array containing synthetic oligosaccharides of different lengths and complexity.

The carbohydrate microarrays were incubated with 4,4-difluoro-5-(4-phenyl-1,3-butadienyl)-4-bora-3a,4a-diaza-s-indacene-3-undecanoic acid (BODIPY)-labeled CVN,

rinsed with buffer, dried, and scanned by a microarray fluorescence scanner. As predicted by isothermal calorimetry (Appendix A), fluorescence was detected at spots corresponding to the immobilized D1 linear trimannoside **4-4**, hexamannoside **4-2** and nonamannoside **4-1** (Figure 4.4) while the branched trimannoside **4-3**, mannose **4-6** and galactose **4-8** showed no binding activity.

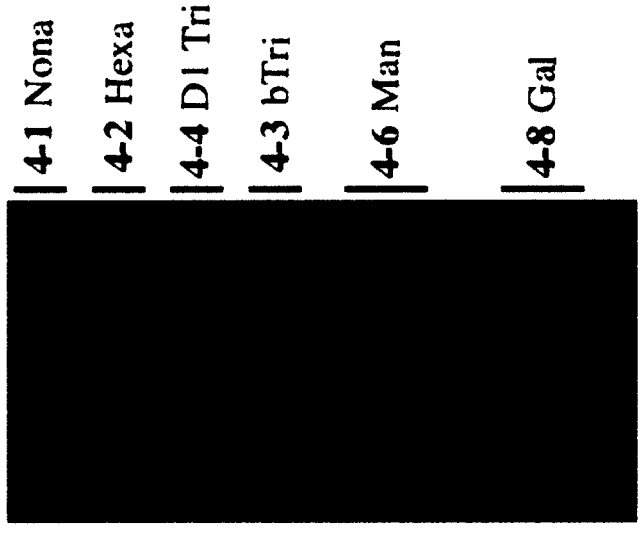

Figure 4.4 High-mannose oligosaccharide series (**4-1**, nonamannoside; **4-2**, hexamannoside; **4-4**, linear trimannoside; **4-3**, branched trimannoside), mannose (**4-6**) and galactose (**4-8**), arrayed at concentrations ranging between 2 and 0.25 mM and incubated with BODIPY-labeled CVN.

Ultimately, the specific aim of this first experiment was not to establish the carbohydrate binding profile of CVN. The panel of oligosaccharides under review was relatively small, comprising only a portion of the structural determinants of the high-mannose nonasaccharide Man_9. In addition, prior biophysical studies had already established much of the binding information, including data on precise affinities of CVN for the various oligosaccharides. Instead, the goal of this initial study was to establish the viability of the microarray format to quickly establish carbohydrate binding profiles for labeled proteins. Past studies of CVN binding for D1 tri-, branched tri-, hexa- and nonamannoside, required multi-milligram quantities of material, and many months of

experimentation. In contrast, the microarray experiment detailed above required nanograms of material, and could be completed in two hours.

4.4.3 Carbohydrate Microarrays Derived from GAPS II Slides

Encouraged by the microarray results with BSA-derivatized slides, we were determined to repeat these successes with the GAPS II slides. Amine coated GAPS II slides are frequently used to prepare DNA microarrays. As such, they are readily available, and relatively inexpensive. Unlike aldehyde slides, the GAPS II slides already possess a reactive amine handle for surface derivatization. This makes it unnecessary to coat the slides with BSA. However, it also creates the need for alternative surface-chemistries to resist non-specific adsorption of proteins to the surface.

To prepare thiol-reactive surfaces, the GAPS II slides were directly reacted with a solution of SMCC to prepare a monolayer of maleimide functionality on the surface of the GAPS II slide. Reduced thiol-modified carbohydrates could be directly printed on these SMCC modified slides. Following incubation with the oligosaccharides, the unreacted maleimides of the surface were treated with 2-(2-(2-mercaptoethoxy)ethoxy)ethanol. This quenching step served the dual purpose of reacting free maleimide, and generating a uniform tri(ethylene oxide) monolayer on the surface of the glass slide. Polymers of ethylene oxide are widely known to be highly resistant to binding by proteins.[22] As such, treating surfaces with tri(ethylene oxide) is an effective means of generating a biologically inert surface.

The results obtained with the GAPS II carbohydrate microarrays were very similar when compared to those of the BSA-derivatized slides (Figure 4.5). Due to the availability of the GAPS II slides, their compatibility with standard DNA printers and scanners, and the ease of functionalizing the surface, we ultimately chose these microarrays for the remainder of our biological studies.

Figure 4.5 FITC-ConA detection of high-mannose oligosaccharide series on a GAPS II slide. From left to right: **4-1**, nonamannoside; **4-2**, hexamannoside; **4-4**, linear trimannoside; **4-3**, branched trimannoside; **4-5**, D3 tetramannoside; **4-7**, truncated-D3 trimannoside; **4-6**, mannose; **4-8**, galactose. Structures were printed at 2 mM.

4.4.4 Surface Density of Immobilized Carbohydrate

Multivalency can play a critical role in binding events between protein and carbohydrate. High-density clusters of oligosaccharide frequently result in a large increase in affinity of a particular lectin for the carbohydrate cluster. For instance, abnormal glycosylation in certain cancerous cells can result in antigenic clusters of otherwise non-antigentic glycans.[23] The density of immobilized carbohydrate on the surface of a microarray is believed to approximate multivalent display of saccharide.[24]

Addressing the precise density of immobilized saccharide displayed on the microarray surface remains challenging. It may be possible to measure surface functionalization through colorimetric methods, analogous to those used to calculate loading on solid-phase resins.[25] However, such methods have not been attempted on this new microarray system.

Without determining the exact surface densities, it was necessary to establish a functional range of concentrations for printing oligosaccharides. If protein-carbohydrate binding data is to be extracted from microarray experiments, we must first establish that we can effectively saturate all possible sites on the surface of the array. To do this, both BSA and GAPS II microarrays were prepared consisting of a dilution series of oligosaccharide. Microarrays were printed with solutions of four oligosaccharides (**4-1**, **4-2**, **4-3** and **4-4**), ranging in concentration from 0.0078 mM to 1.0 mM. The arrays were subsequently screened with BODIPY-labeled CVN (Figure 4.6).

Figure 4.6 Dilution series microarray to establish the ideal concentration range for printed oligosaccharide. The microarray illustrates CVN binding of a dilution series of immobilized oligosaccharides **4-1**, **4-2**, **4-3** and **4-4**.

The fluorescence of bound BODIPY-labeled CVN was measured for each concentration of printed oligosaccharide. The intensity of fluorescence, corresponding to the amount of bound protein, was plotted as a function of the concentration of printed oligosaccharide (Figure 4.7). These results indicate that for the branched oligosaccharides (nonasaccharide **4-1** and hexasaccharide **4-2**) the fluorescence of bound protein does not increase significantly above printed oligosaccharide concentrations of 0.2 to 0.3 mM. For the linear trimannoside **4-4** the fluorescence of bound CVN levels-off slightly above 1 mM. Following these results, all carbohydrate microarrays prepared for biological study were printed at concentrations from 0.25 to 2 mM to ensure saturation.

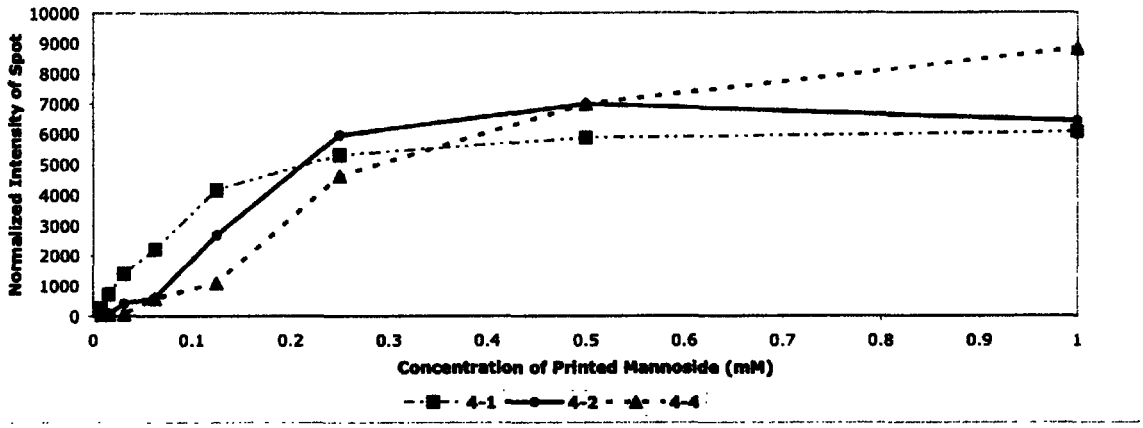

Figure 4.7 Fluorescence of bound BODIPY-labeled CVN as a function of concentration of printed oligosaccharide.

4.4.5 Carbohydrate / Glycoprotein Hybrid Microarrays

A hybrid microarray that displays carbohydrate, glycoprotein, and deglycosylated protein on a single chip would greatly increase the versatility of the existing microarray system. Such an array could establish the importance of the peptide-backbone context in a particular protein-carbohydrate binding event. To accomplish this, two surface chemistries had to be used on a single glass slide.

To prepare the hybrid microarrays, GAPS II slides were derivatized with SMCC (for a maleimide surface) and ethylene-glycol-bis(succinimidylsuccinate) (EGS, functionalizing the surface with an amine-reactive *N*-hydroxysuccinimide ester). By dipping the two opposite halves of a single GAPS II slide into the respective reagents, it was possible to prepare a slide with both surface chemistries. Such slides could be printed with both thiol-modified oligosaccharides and proteins by printing onto the side corresponding to the appropriate surface chemistry. Finally, the slides could be quenched with 2-(2-(2-mercatoethoxy)ethoxy)ethanol to react with remaining maleimide, and BSA to bind unreacted NHS ester.

As a proof of principle, a hybrid microarray consisting of four oligosaccharides and four glycoproteins was prepared using the aforementioned method. High-mannose oligosaccharides **4-1**, **4-2**, **4-3** and **4-4** were printed on the maleimide side of the glass

slide and gp120 and gp41 (natural and recombinant) were printed on the NHS-modified side. BODIPY-labeled CVN screening of the hybrid microarray resulted in the expected binding profile (Figure 4.8).

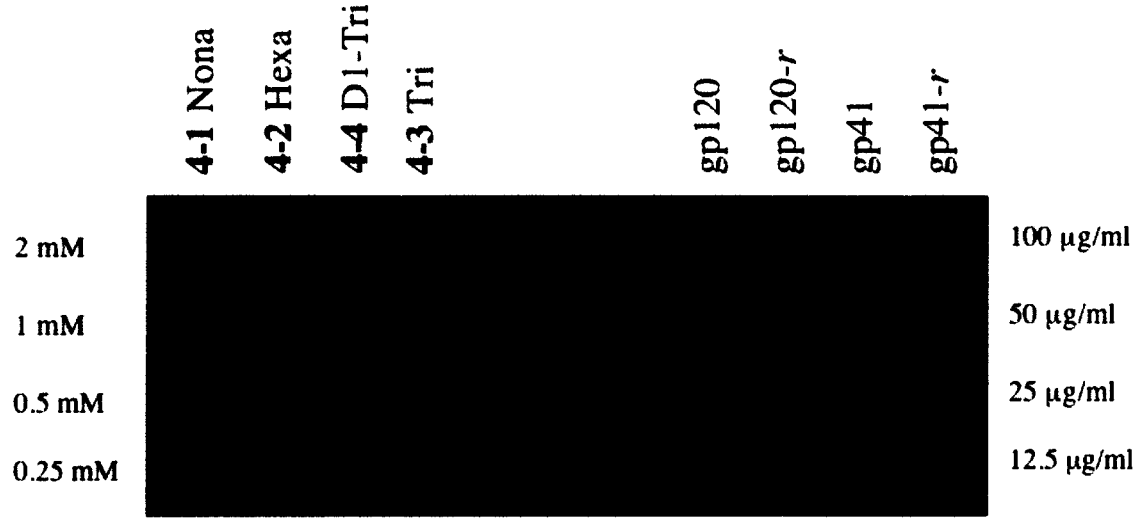

Figure 4.8 Carbohydrate/glycoprotein hybrid-microarray screened against BODIPY-labeled CVN. Note, missing fluorescence for **4-1** at 2 mM is due to failure of the microarray printer to contact the surface of the glass slide.

4.5 Microarray Applications to Biological Studies – HIV Glycobiology[10]

The following study of HIV glycobiology was done with the invaluable assistance Mr. Eddie W. Adams. In addition to collaboratively designing and fabricating the carbohydrate microarrays, Ed was personally responsible for the glycoprotein microarray experiment and he prepared the neoglycocopeptides using the synthetic mannans described in section 4.3.

Given the nature of the mannans prepared for this study, HIV glycobiology was the logical application for our recently developed microarrays. Defining HIV envelope glycoprotein interactions with host factors or binding partners advances our understanding of the infection process and provides a basis for the design of vaccines and agents that interfere with HIV entry. For this study, carbohydrate and glycoprotein microarrays were employed to analyze glycan-dependent gp120-protein interactions. In

concert with the aforementioned thiol-based linking chemistries, the carbohydrate arrays combine the advantages of microarray technology with the flexibility and precision afforded by organic synthesis. With these microarrays we individually and competitively determined the binding profiles of five gp120 binding proteins, established the carbohydrate structural requirements for these interactions, and identified a potential strategy for HIV-vaccine development.

A glycan-based microarray study of HIV offers an exciting opportunity for ongoing efforts in studying the virus. The density of carbohydrate present on gp120 prevents efficient generation of potent, neutralizing antibodies. These same oligosaccharides may be viewed as targets for a new class of anti-HIV agents. Thus, a detailed analysis of HIV-glycans will help define the immunology of HIV as well as guide efforts towards prophylaxis. Tools like the high-mannose microarrays easily identify additional biologically relevant carbohydrate/protein interactions and can aid future investigations in the field.

4.5.1 HIV-Binding Proteins

We exploited the oligosaccharide and glycoprotein microarrays to study the glycan-dependent binding interactions of four gp120-binding proteins: the dendritic cell lectin DC-SIGN,[26] the antibody 2G12, cyanovirin-N, and a recently identified anti-HIV protein, scytovirin.[27] We also investigated the non-glycan dependent interactions of CD4 with gp120 in the presence of these potential inhibitors. These miniaturized assays substantially decreased the amount of carbohydrate required for study, in addition to the volume and quantity of analyte to be studied. Also, fluorescence-based detection allowed multiple binding events to be analyzed simultaneously.

The five gp120-binding proteins were selected for study based on their respective roles in HIV biology. Due to their involvement in the internalization of HIV by the host cell, gp120 and gp41 are valuable molecular targets for developing therapies aimed at decreasing viral load and for prophylaxis in preventing viral transmission.

The high-spatial density of gp120 on the virion surface makes it the primary target of the humoral immune response to HIV.[28,29] Accordingly, most vaccine design

efforts to generate effective, neutralizing antibodies against HIV have been based on monomeric and oligomeric forms of gp120. However, the steric masking of potential neutralization-sensitive epitopes of gp120 by *N*-linked high-mannose oligosaccharides frustrates both natural and vaccine-promoted humoral responses.[30,31] In addition, these oligosaccharides are found on numerous host proteins, and are likely to be regarded as "self" or non-immunogenic, thereby preventing a rigorous antibody response. A notable exception to this immunological tolerance of high-mannose oligosaccharides is the human monoclonal antibody 2G12, which is capable of binding Manα(1→2)Man presenting-oligosaccharide clusters with nanomolar affinity.[32,33]

There is growing interest in small molecule inhibitors and HIV-binding proteins as prophylactic measures to prevent HIV entry into host cells.[34,35] High-throughput screens of natural products derived from *Cyanobacteria* have yielded a number of promising anti-HIV agents capable of inhibiting viral entry. Two of these compounds, cyanovirin-N (CVN) and scytovirin, 11 and 9.7 kDa proteins respectively, achieve their anti-viral activity by binding the high-mannose oligosaccharides present on HIV gp120.[36,37] This interaction is thought to prevent gp120's receptor binding domains from interacting with their targets; alternatively, conformational changes in the glycoprotein subsequent to protein binding may render theses binding domains functionally inactive. As most cell-surface and secreted glycoproteins undergo processing in the Golgi, extensively modifying *N*-linked oligosaccharides, CVN and scytovirin are likely to target virus-associated oligosaccharide but not endogenous glycoprotein. This has been demonstrated by *in vivo* prophylaxis studies with CVN that have not shown any adverse effects upon host physiology.[38]

4.5.2 Microarray Results and Discussion

Initially, we sought to determine if the glycan-binding profiles of the above proteins are dependent on the polypeptide backbone to which the high-mannose oligosaccharides are appended. To evaluate the role of the polypeptide backbone, microarrays bearing natural and modified glycoproteins, as well as neoglycoproteins were fabricated. Included among these proteins were gp120, gp41, de-glycosylated

gp210 (p120), ovalbumin (OVA), nonamannoside-modified OVA (OVA4-1), and mannosylated BSA. Each slide was incubated with one fluorophore-labeled protein, washed and scanned to establish binding (Figure 4.9a).

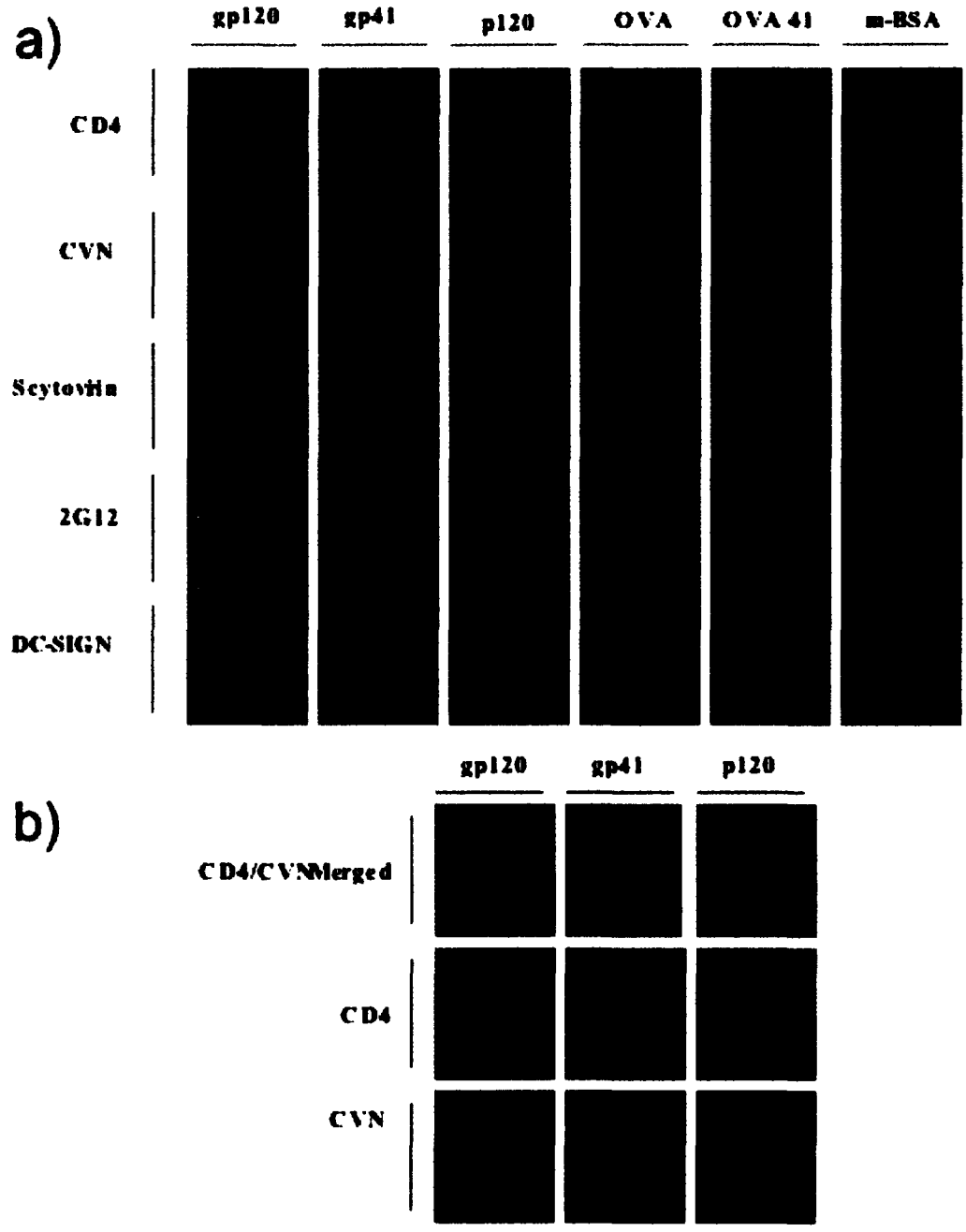

Figure 4.9 Glycoprotein binding. a) Glycoprotein microarrays incubated with fluorescently-labeled proteins. b) Sequential incubations of glycoprotein microarray with CD4 and CVN.

As anticipated, gp120 was bound by each of the proteins. Additional experiments proved that co-incubation of each protein with $(Man)_9(GlcNAc)_2$ successfully inhibited the respective interactions with gp120 (E. W. Adams, *data not shown*) in accordance with the known specificities of these proteins. However, CD4 interactions with gp120 were not inhibited by co-incubation with the free glycan. All five proteins were also shown to interact with gp41. Again, these interactions were inhibited by co-incubation with $(Man)_9(GlcNAc)_2$ except in the case of CD4. While recognition of the high-mannose oligosaccharides on gp41[39] has been described for CVN[40] and scytovirin,[27] this is the first demonstration of gp41 binding by DC-SIGN and 2G12. The physiological relevance of the observed g41 binding by DC-SIGN requires further study as it has not yet been determined if gp41 is exposed upon DC-SIGN-gp120 interactions. It also remains to be determined whether interactions between 2G12 and exposed gp41 can effectively inhibit viral entry.

Sequential incubations with fluorophore-labeled binding partners were used to determine if CVN, among of the aforementioned glycan-dependent gp120-binding proteins, could inhibit CD4-gp120 interactions. To accomplish this, soluble CD4 was incubated with the glycoprotein microarray, followed by addition of CVN. Bound CD4 was detected with a fluorophore-labeled anti-CD4 monoclonal antibody. To control for anti-CD4 binding of the array, independent control incubations revealed little to no non-specific binding (E. W. Adams, *data not shown*). Alternatively, soluble CD4 was added to the arrays only after pre-incubation with potential inhibitor CVN. In agreement with previous studies, we observed that CD4 bound gp120 pretreated with CVN, suggesting that CVN does not block or disrupt the CD4 binding site on gp120.[41] Interestingly, we observed that CVN completely displaced bound CD4 from gp120 pretreated with soluble CD4 (Figure 4.9b). However, CD4 bound to non-glycosylated gp120 (p120) was not disrupted by incubation with CVN, indicating the glycan-dependent nature of CVN's mode of action.

Neoglycoproteins were employed to study the peptide context in which glycans are presented. Ovalbumin, a glycoprotein bearing both hybrid and complex-type oligosaccharides, is not bound by any of the proteins. In contrast, ovalbumin modified

with high-mannose nonasaccharide **4-1** (OVA**4-1**) via a non-natural linkage is bound by DC-SIGN, CVN, scytovirin and, to a lesser extent, 2G12. This observation suggests that carbohydrate recognition by these proteins is largely insensitive to the underlying polypeptide chain, supporting the hypothesis that the density of the displayed carbohydrate determines binding.[42]

The observed binding of 2G12 to OVA**4-1** prompted us to investigate whether 2G12 would bind arrays of oligosaccharides. Epitope mapping studies with 2G12 have shown that it binds a conserved group of *N*-linked high-mannose oligosaccharides present on gp120, making it an effective neutralizing antibody against a number of primary HIV isolates.[32] If 2G12 could bind high-mannose oligosaccharides in the absence of a peptide backbone, a vaccine composed of clusters of these oligosaccharides might generate a 2G12-like response to gp120 glycans.

2G12-carbohydrate interactions were evaluated with microarrays of the eight aforementioned glycans (Figure 4.10). A carbohydrate binding profile was made for a given protein by comparing the integrated fluorescence between the spots of different immobilized oligosaccharide (Figure 4.11). Incubation of 2G12 with the microarray revealed antibody binding at spots corresponding to oligosaccharides **4-1**, **4-2**, **4-4**, and **4-5**, but not to the branched trimannoside **4-3** or mannose **4-6** (Figure 4.11b). The only structural motif in common for oligosaccharides **4-4** and **4-5** is the Manα(1→2)Man linkage, suggesting that this glycosidic linkage alone is necessary for recognition by 2G12. Based on the observation that incubation of gp120 with an α(1→2) mannosidase greatly diminished 2G12 binding, previous studies[32,43] have concluded that 2G12 recognizes the Manα(1→2)Man linkages present in Man_9. A single microarray allowed for rapid confirmation of this structural requirement for 2G12 recognition based on the diversity of glycosidic linkages attained by chemical synthesis. In addition, the microarray enabled direct verification of 2G12 binding to carbohydrates in the absence of a polypeptide backbone.

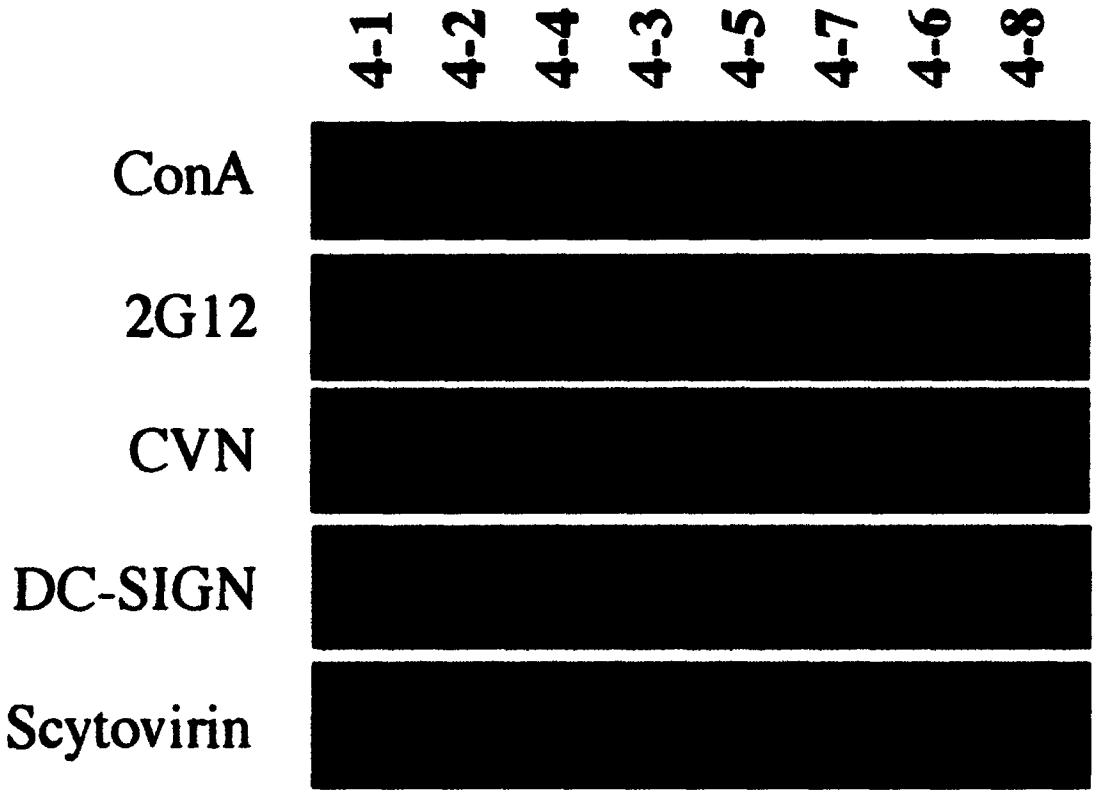

Figure 4.10 Carbohydrate microarrays containing synthetic mannans **4-1** through **4-7** and galactose **4-8**, printed at 2 mM. False color image of incubations with fluorescently labeled ConA, 2G12, CVN, DC-SIGN and Scytovirin.

We used our microarrays to study the carbohydrate-recognition profile of the cyanobacterial protein, scytovirin.[27] Scytovirin is a 9.7 kDa protein isolated from aqueous extracts of the cyanobacterium *Scytonema varium*. The protein binds gp120, gp160 and gp41 and has potent anticytopathic activity against primary isolates of HIV-1. Initial studies demonstrated that scytovirin binds HIV gp120 through a carbohydrate-dependent mechanism that is blocked by soluble $(Man)_9(GlcNAc)_2$, and $(Man)_8(GlcNAc)_2$, but not $(Man)_7(GlcNAc)_2$. However, structural determination has not established which specific mannose residues are missing from the truncated high-mannan $(Man)_7(GlcNAc)_2$.

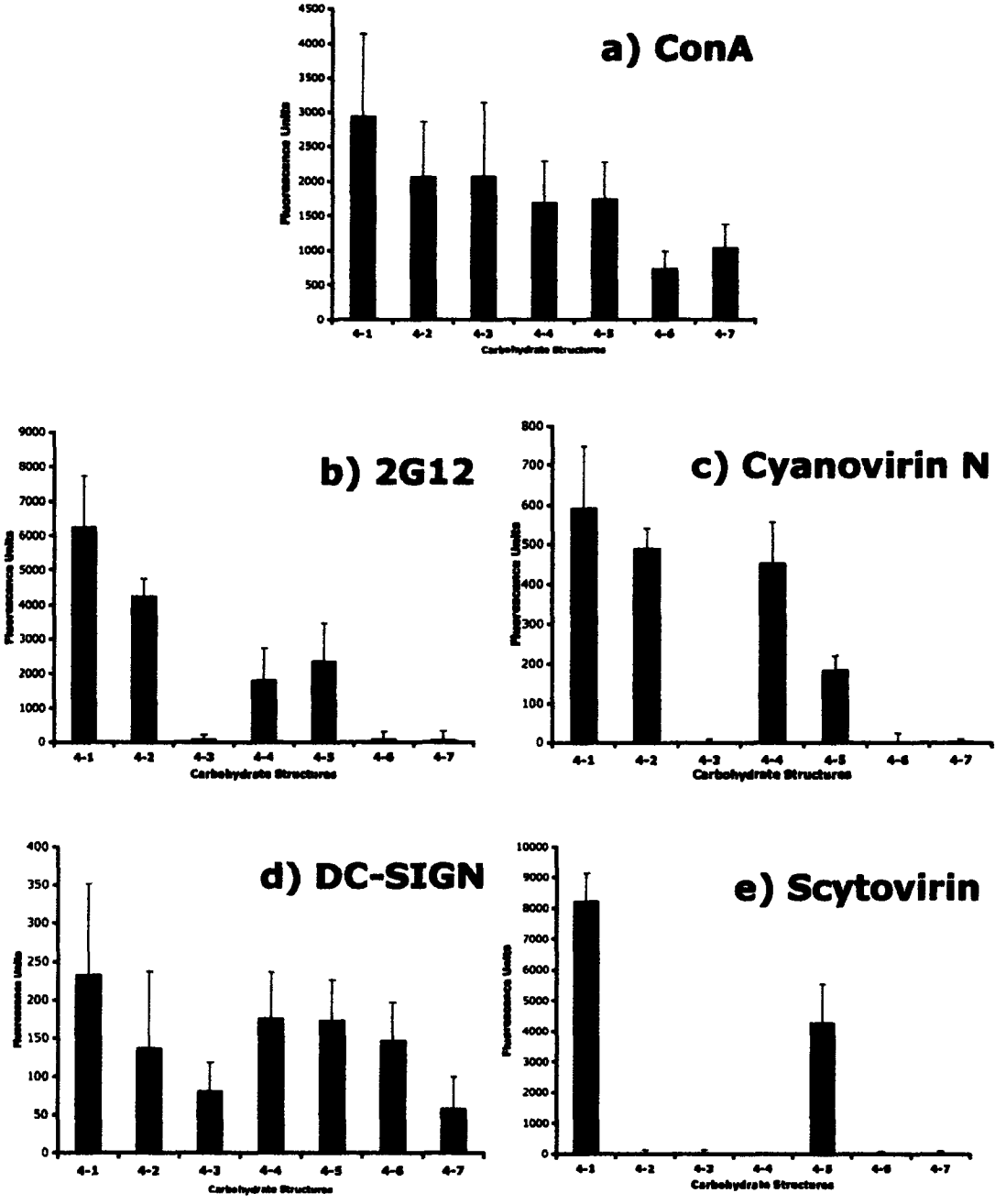

Figure 4.11 Comparison of the high-mannose binding profiles of five fluorescently labeled proteins incubated against synthetic mannans **4-1** through **4-7**. a) Concanavalin A, b) Antibody 2G12, c) Cyanovirin-N, d) DC-SIGN, and e) Scytovirin.

Analysis of scytovirin's carbohydrate binding profile with our microarrays revealed that of all the structures present, scytovirin bound only **4-1** and **4-5** (Figure

4.11e). This finding suggests that the terminal α(1→2) mannose linkage is necessary for recognition of the underlying α(1→6) trimannoside moiety unique to the D3 arm. If the Manα(1→6)Man linkages alone were sufficient for scytovirin binding, oligosaccharides **4-2** and **4-3** also should have been bound. Likewise, if Manα(1→2)Man glycosidic linkages alone were sufficient for recognition by scytovirin, structures **4-2** and **4-4** would have been bound. These results suggest that recognition of high-mannose oligosaccharides by scytovirin occurs by a markedly different mechanism than that observed for both 2G12 and CVN. Both 2G12 and CVN bind terminal Manα(1→2)Man independent of the underlying linkages found in the D1, D2 and D3 arms (Figures 4.11b and 4.11c).

To confirm the role of the terminal Manα(1→2)Man glycosidic linkage in binding of the D3 arm by scytovirin, **4-7**, a truncated derivative of the D3 arm lacking the terminal Manα(1→2)Man linkage was prepared to screen CVN, 2G12 and scytovirin. None of the proteins bound oligosaccharide **4-7** (Figures 4.11b,c,e), confirming the specificity of 2G12 and CVN for Manα(1→2)Man linked saccharides and the necessity of this linkage for recognition of the D3 arm by scytovirin. This mechanism of high-mannose oligosaccharide recognition by scytovirin has not been described for any other high-mannose binding protein. On-going NMR and crystallographic studies using these synthetic mannans should elucidate how scytovirin's tertiary structure dictates specific interactions with the D3 arm.

As part of a continuing investigation into oligosaccharide-mediated targeting of dendritic cell lectins (E. W. Adams, *unpublished data*) DC-SIGN was the last gp120-binding protein selected for microarray analysis. This 44kDa C-type lectin is expressed by dermal dendritic cells (DCs) in mucosal tissue, by interstitial DCs, and on DCs in the lymph nodes.[44] DC-SIGN is known to bind gp120 in a carbohydrate-dependent manner via the glycoprotein's high-mannose oligosaccharides.[44,45] This interaction promotes internalization of virus by the DC to a non-lysosomal compartment, where HIV appears to be protected from degradation and remains infectious for several days.[46] Finally, DC - $CD4^+$ T cell interaction leads to productive infection of the recipient lymphocyte. Incubation of the labeled-extracellular domain of DC-SIGN with synthetic mannan

carbohydrate arrays bearing structures **4-1** through **4-8** revealed that all mannose-containing structures were bound by DC-SIGN (Figures 4.10 and 4.11d).

4.5.3 Conclusions of Microarray Studies

The rapid identification of proteins and small molecules that interfere with HIV-host entry is a central pursuit in the effort to combat viral spread. The glycans associated with HIV envelope glycoproteins continue to be of great interest for their involvement in the infectious process, their antigenicity, and their ability to neutralize the humoral response. Evidence supports the theory that HIV eludes the immune response, in part, through an evolving glycan-shield.[47] A microarray-based approach to study agents that bind these glycans will further efforts to circumvent HIV's evasion mechanisms. For the first application of our microarray technology, we demonstrated their use for the study of gp120 binding proteins and defined the carbohydrate structural requirements sufficient for binding.

4.6 Additional Tools for Glycobiology

Introduction of a reactive handle on synthetic glycans (such as a thiol or an amine) provides access to a host of glycoconjugate-based tools.[48] The carbohydrate microarrays detailed above were a logical extension of this technology. By creating a cell surface-like environment on a highly miniaturized platform, it was possible to rapidly probe carbohydrate binding events. The synthesis of neoglycopeptides, such as ova**4-1** and mannosylated-BSA described herein, was also a useful application of the same linking chemistry. However, oligosaccharide and neoglycoprotein microarrays are but one technique made possible by the tri(ethylene glycol)-based linking chemistry.

A panel of synthetic tools for biophysical studies can be accessed using the aforementioned thiol-based conjugation scheme (Figure 4.12). Conjugating chemically defined saccharides in a precise manner to various biomarkers and reporters opens the doors to research that may not be possible using conventional techniques. To demonstrate the potential for these methods to aid investigations in glycobiology, we

prepared a number of additional tools using the same synthetic structures involved in the microarray fabrication. The tri(ethylene glycol)-modified saccharides were used to prepare self-assembled monolayers on gold surfaces for use in surface plasmon resonance experiments. Fluorescently-encoded microsphere microarrays were also fabricated as an extension of the microarray format. Additionally, monovalent and multivalent fluorescent conjugates were synthesized for *in vivo* fluorescent microscopy to examine endocytosis of complex mannans by the dendritic cell lectin DC-SIGN.

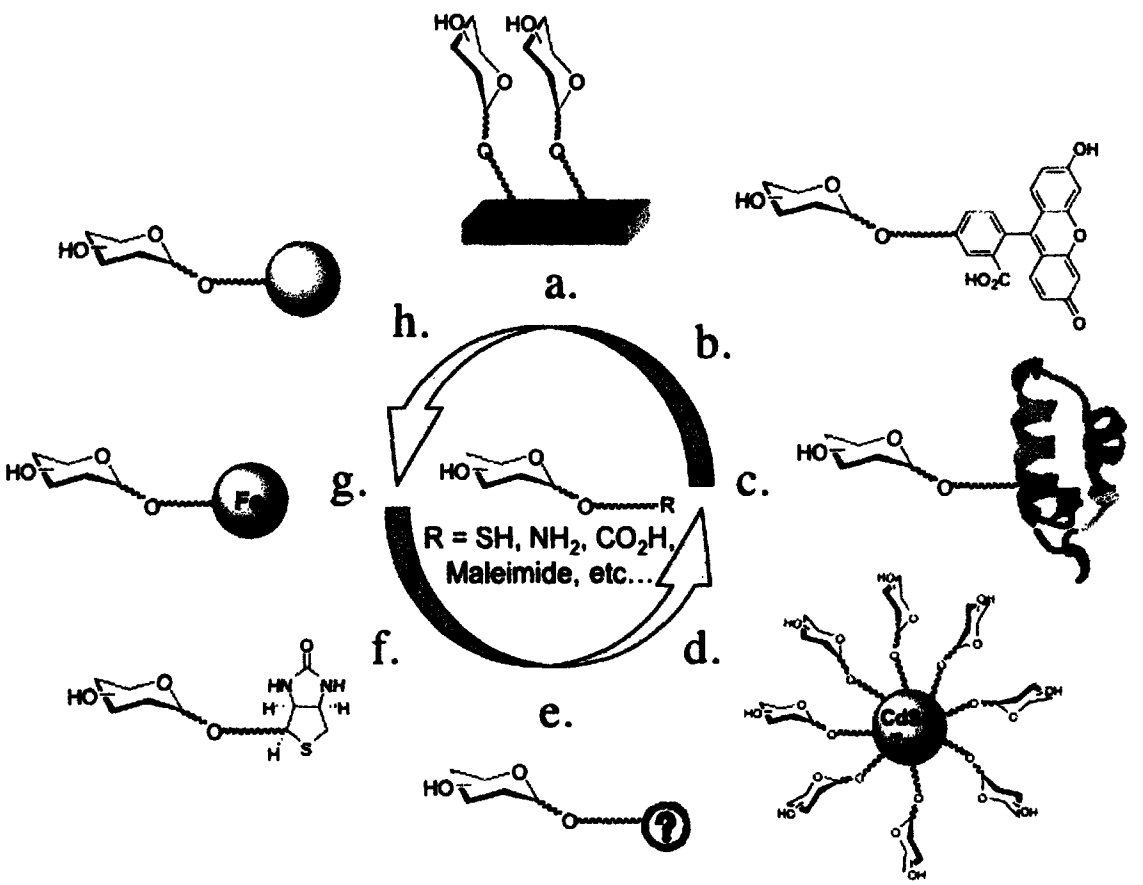

Figure 4.12 Synthetic tools for glycobiology: a. modified surfaces for microarrays and SPR; b. monovalent fluorescent conjugates; c. neoglycoproteins and carbohydrate vaccines; d. multivalent quantum dot conjugates; e. future neoglycoconjugates; f. affinity tag (biotin, etc.) conjugates; g. magnetic particle conjugates; h. latex microsphere and sepharose affinity resin conjugates.

4.6.1 Self-Assembled Monolayers and Surface Plasmon Resonance[7]

Following carbohydrate microarray-based ligand identification, the same carbohydrates can be immobilized to the self-assembled monolayers for a more complete characterization of activity. Monolayers are well suited to quantitative investigation of protein-ligand interactions, because they allow excellent control over the density of immobilized carbohydrate and because they present the ligands in a homogenous environment at the interface. In collaboration with Prof. Milan Mrksich of the University of Chicago, we adopted a previously reported method to immobilize the thiol-functionalized carbohydrates to a monolayer that presents maleimide and tri(ethylene glycol) groups in a ratio of 1:50.[49] MALDI-TOF Mass spectrometry confirmed that the immobilization reactions proceeded in quantitative yield.[50] Surface plasmon resonance (SPR) spectroscopy was used to measure the binding of CVN to monolayers presenting the linear trimannoside **4-4**. The initial SPR experiment illustrated that the amount of bound CVN increases with the density of immobilized trimannoside (Figure 4.13a). The ability to control the density of immobilized carbohydrate is an important advantage with the monolayer substrates, particularly because many proteins, including CVN, bind in divalent modes and show a strong dependence on the density of ligand. Indeed, we found that at higher densities of carbohydrate, a higher fraction of the protein remains tightly bound, reflecting the divalent binding mode. In a second experiment, we demonstrated that this platform is useful for testing the ability of carbohydrates to inhibit the interaction between CVN and immobilized **4-4**, and therefore to rapidly identify ligands for CVN. Figure 4.13b shows that linear mannoside **4-4** and nonamannoside **4-1** inhibit the binding of CVN, but that branched trimannoside **4-3** has no effect on binding, all in agreement with the results described in the microarray study.

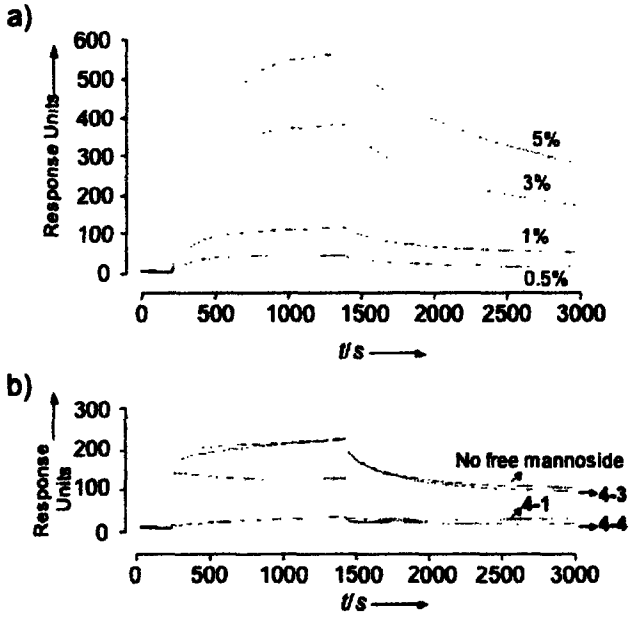

Figure 4.13 SPR experiments showing CVN binding to self-assembled monolayers of synthetic mannans. a) Real-time binding of CVN (0.1 μM in PBS) to SAM of D1 linear trimannoside **4-4** at surface densities ranging from 0.5 to 5.0%. b) Inhibition study of CVN binding to **4-4** SAM (1% density) using soluble nonamannoside **4-1** (0.02 mM), linear trimannoside **4-4** (0.2 mM), an branched trimannoside **4-3** (0.2 mM).

4.6.2 Encoded Microsphere Microarrays[51]

In contrast to the aforementioned microarrays, a system was developed that uses optically addressable, internally encoded microspheres to define the position and structure of a series of carbohydrates on a fiber optic microarray. This was accomplished in collaboration with Prof. David Walt of Tufts University.[51] While solid-phase carbohydrate libraries have been employed previously,[52] miniaturization of the assay, combined with fluorescently-encoded microspheres, allows for rapid screening while requiring amounts of material comparable to or less than that required by microarrays. To detect binding, the immobilized microsphere array is incubated with a fluorophore labeled-carbohydrate binding protein. The binding profile is determined by measuring the fluorescence of beads that emit at both the wavelength of an internal code, which is

used as a marker for the carbohydrate displayed on a microsphere (an entrapped fluorescent dye) and the labeled protein. Fluorescence colocalization indicates a binding event. Using this system, we examined the binding profiles of Concanavalin A and cyanovirin-N (Figure 4.14).

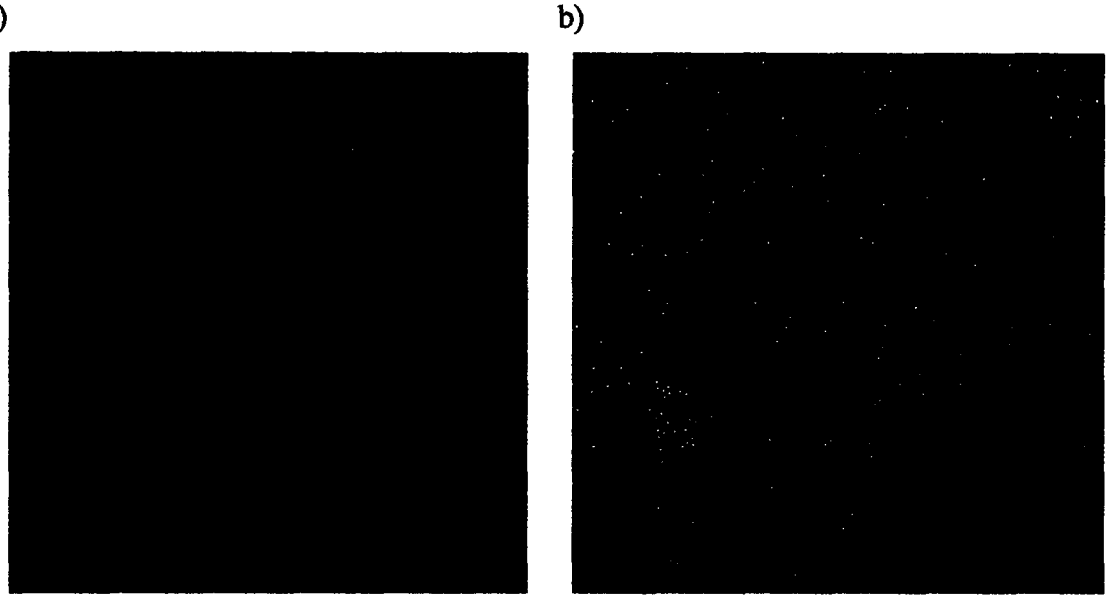

Figure 4.14 Internally-encoded, randomly oriented microsphere array bearing structures **4-1** through **4-4** and **4-6** and incubated with BODIPY-labeled cyanovirin-N. Specific binding events were observed by detecting BODIPY emission at 520 nm. a) Fluorescence at 520 nm prior to BODIPY-CVN incubation; b) fluorescence at 520 nm post-BODIPY-CVN incubation.

4.6.3 Monovalent Fluorescent Conjugates

The microarray format may not be the most appropriate tool for all applications. One such application is the study of cell-surface receptors with presumed carbohydrate-binding activity (i.e., lectins). One limitation to microarray studies is the need for purified receptor. In addition, the density of immobilized oligosaccharide on the microarray surface restricts observation to binding of clustered or multivalent arrays of carbohydrate. While it may be possible to immobilize carbohydrate at densities sufficiently low to approximate monovalent presentation of oligosaccharide, the

microarray format is not ideal for examining monovalent protein-carbohydrate interactions.

To establish a direct method of detecting oligosaccharide-receptor interactions, monovalent oligosaccharide-fluorophore conjugates were prepared. These probes serve as reporters to enable tracking of receptor-carbohydrate interactions via fluorescence microscopy and flow cytometry. Thiol-modified oligosaccharides were covalently linked to maleimido-FITC. These fluorescent glycoconjugates could subsequently be used to observe cell-surface lectin affinity for the monomeric oligosaccharide in solution. To test these conjugates, a panel of high-mannose oligosaccharide-fluorescein conjugates were used to follow the concentration-dependent binding and endocytosis of complex mannans by the dendritic cell lectin DC-SIGN in DC-SIGN-transfected HeLa cells and monocyte-derived dendritic cell, which express a high level of endogenous DC-SIGN (E. W.Adams., *unpublished results*; Figure 4.15).

Figure 4.15 DC-SIGN-mediated endocytosis of monovalent oligosaccharide-fluorescein conjugates. Transiently transfected HeLa cells expressing DC-SIGN endocytose **4-1**(nonasaccharide)-fluorescein. Left panel: confocal microscopy image of **4-1**-fluorescein (green) and phalloidin staining (blue); middle panel: phycoerythrin labeled anti-DC-SIGN antibody staining of DC-SIGN's subcellular localization; right panel: merge of first two panels showing colocalization of internalized oligosaccharide and DC-SIGN (E. W. Adams, *unpublished data*).

4.6.4 Multivalent Oligosaccharide Platforms for Cell Biology

Semiconductor nanocrystal (quantum dot)-based systems were explored as platforms to present multiple oligosaccharide monomers (>100) on a single particle.

Such conjugates permit the direct assessments of the effect of multivalency on oligosaccharide binding to cell-surface lectins. Early nanoparticle-based multivalent platforms for evaluating multivalent oligosaccharide interactions were based on carbohydrate-modified gold nanoparticles.[53] The success of these nanoparticle studies led us to believe that quantum dots could enhance the utility of the nanoparticle platform. Given the high quantum yields in aqueous systems and unique photophysical properties (e.g., their lack of excitation-induced photobleaching; their extremely narrow, non-overlapping emission spectrums; and the ability to achieve multiple wavelength emissions following excitation from a single excitation source), quantum dot-carbohydrate conjugates could be a powerful tool in studying the cell biology of cell-surface lectins.[54]

Thiol-modified oligosaccharides can be used for conjugation to modified quantum dots. Carboxy-bearing quantum dots, functionalized with 3-[2-pyridyldithio]propionyl hydrazide (PDPH), are reactive to the thiol-linker of the carbohydrates by way of disulfide exchange. By using quantum dots bearing defined densities of saccharide, the carbohydrate recognition by DC-SIGN and other mammalian lectins is being further elucidated.

4.7 Continuing Efforts Towards Synthetic Tools for Glycobiology

Efforts are ongoing towards extending the versatility of carbohydrate microarrays and additional synthetic tools for glycobiology. In addition to the methods described above, improvements are being made to the linker technology, and additional synthetic tools are being developed.

4.7.1 New Linking Chemistry for Natural Glycans

The microarrays detailed in this chapter relied upon synthetic access to the oligosaccharides of interest. While this afforded superb control over the panel of oligosaccharides acquired for the study, it is not without limitations. Synthetic carbohydrate chemistry continues to grow in its sophistication, and ability to synthesize

targets of increasing complexity. However, a unifying approach to all syntheses has not yet been adopted. Therefore, current methods require that each carbohydrate structure be approached as a total synthesis in its own right. This limits the ability to rapidly expand the panel of oligosaccharides available for study on the microarray.

Ongoing efforts are making significant gains towards a new method for preparing microarrays and other tools for glycobiology. Notably, this new approach utilizes carbohydrates isolated from natural sources. The purified carbohydrates are converted to the anomeric glycosylamine, and reacted with an amine-reactive linker to introduce the tri(ethylene glycol) linker, terminated in a thiol functionality (Scheme 4.14).

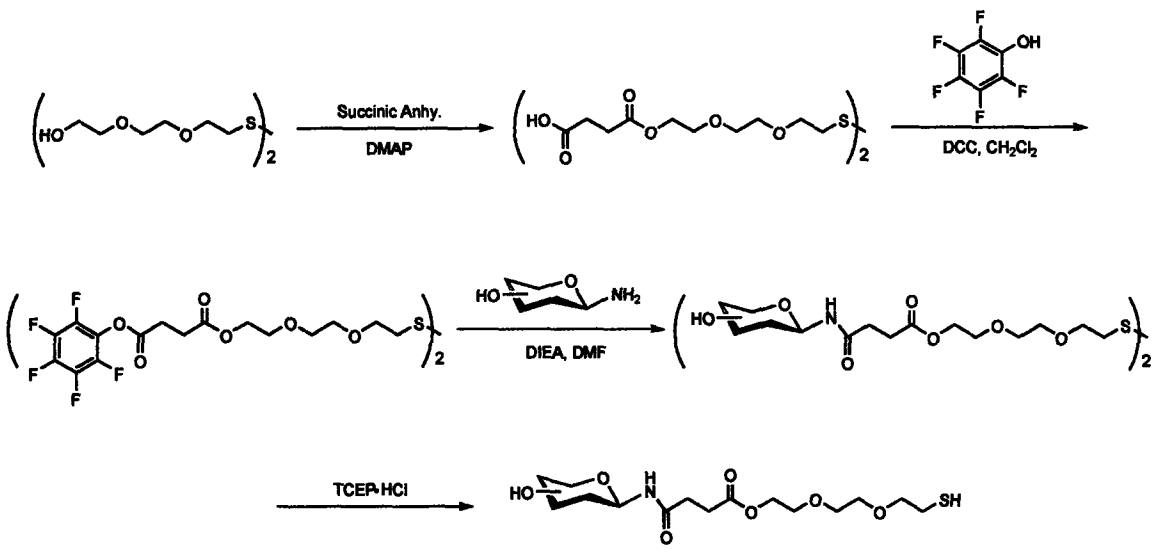

Scheme 4.14 Conjugation scheme for naturally isolated carbohydrates.

Presently, this method has been used to generate a carbohydrate microarray based on a series of naturally procured glycans. Included among these saccharides is the human milk oligosaccharide 2'-fucosyllactose (2'FL), which is widely reported to confer protection to infants from a number of intestinal pathogens.[55] Preliminary microarray studies using the new linking chemistry have been fruitful in demonstrating substrate specificity for two 2'FL-binding lectins (Figure 4.16). Efforts are ongoing to optimize these new chemistries, and to prepare a new set of microarrays and neoglycoconjugates based on these methods.

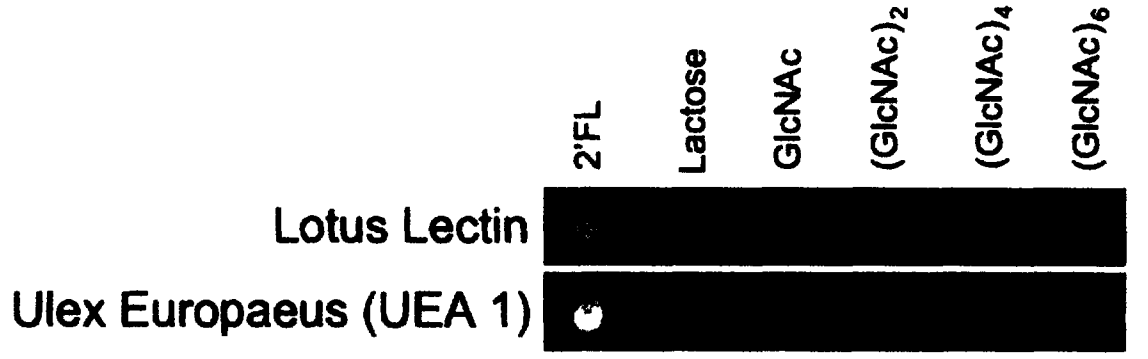

Figure 4.16 Microarrays of naturally isolated glycans screened against lectins with known specificity for 2'-fucosyllactose.

4.8 Summary and Conclusions

Inclusion of the thiol-containing tri(ethylene glycol) linker into synthetic oligosaccharides (and most recently isolated glycans) has enabled the preparation of a host of tools for use in biophysical studies related to glycobiology. HIV glycobiology served as a concrete and highly relevant demonstration of the utility of such an expanded set of synthetic tools for glycomics.

The carbohydrate microarray system described herein offers several features that make it attractive as a tool for glycomics: it requires small quantities of material, is fully amenable to HTS technologies, provides covalent immobilization of structures to a hydrophilic/non-fouling surface to control non-specific interactions, utilizes a linker system that may be introduced in the solution phase synthesis of any carbohydrate of interest, and can be extended to the preparation of self-assembled monolayers for a more complete characterization of activity.[56] We envision similar microarrays of diverse oligosaccharide structures will find a range of applications including epitope mapping of carbohydrate specific antibodies, and ligand identification for cell-surface lectins obtained from cell lysates.

Using our microarray platform we have defined the binding profile of a novel HIV-inactivating protein, scytovirin, and identified a new mechanism of recognition of high-mannose oligosaccharides. Our study of DC-SIGN has elaborated its carbohydrate-

binding profile to include unbranched oligosaccharide structures. Analyses of CVN and 2G12 have confirmed the necessity of Manα(1→2)Man linkages for carbohydrate recognition. Furthermore, our study of 2G12 has definitively demonstrated that 2G12 can bind high-density arrays of Manα(1→2)Man-containing oligosaccharides in the absence of a polypeptide backbone. We feel this finding and the synthetic derivatives of **4-1** employed in the analysis of 2G12 will prove particularly important in aiding the design of carbohydrate-based vaccines aimed at eliciting a 2G12-like response.

Expanding upon the success of the carbohydrate microarray as a tool for glycobiology, progress has begun towards the development of additional tools to aid biophysical studies. A number of these potential tools have now been explored with promising results. Like the carbohydrate microarrays, advances in neoglycopeptides, surface plasmon resonance, carbohydrate microsphere microarrays, and mono- and multivalent fluorescent conjugates have proven the versatility of these methods for biological investigation.

References:

[1] Plante, O. J.; Palmacci, E. R.; Seeberger, P. H. *Science* **2001**, *291*, 1523.

[2] Wang, D.; Liu, S.; Trummer, B. J.; Deng, C.; Wang, A. *Nat. Biotechnol.* **2002**, *20*, 275.

[3] Fazio, F.; Bryan, M. C.; Blixt, O.; Paulson, J. C.; Wong, C. –H. *J. Am. Chem. Soc.* **2002**, *124*, 14397.

[4] Houseman, B.; Mrksich, M. *Chem. Biol.* **2002**, *9*, 443.

[5] Park, S.; Shin, I. *Angew. Chem. Int. Ed.* **2002**, *41*, 3180.

[6] Houseman, B. T.; Gawalt E. S.; Mrksich M. *Langmuir* **2003**, *19*, 1522.

[7] Ratner, D. M.; Adams, E. W.; Su, J.; O'Keefe, B. R.; Mrksich, M.; Seeberger, P. H. *ChemBioChem* **2004**, *5*, 379.

[8] Kiessling, L. L.; Gestwicki, J. E.; Strong, L. E. *Curr. Opin. Chem. Biol.* **2000**, *4*, 696.

[9] Boden, N.; Bushby, R. J.; Clarkson, S.; Evans, S. D.; Knowles, P. F.; Marsh, A. *Tetrahedron* **1997**, *53*, 10939. Critchley, P.; Willand, M. N.; Rully, A. K.; Crout, D. H. G. *Org. BioMol. Chem.* **2003**, *6*, 928.

[10] Adams, E. W.; Ratner, D. M.; Bokesch, H. R.; McMahon, J. B.; O'Keefe, B. R.; Seeberger, P. H. *Chem. Biol.* **2004**, *11*, 875.

[11] Xu, Y. –C.; Bizuneh, A.; Walker, C. *Tet. Lett.* **1996**, *37*, 455. Xu, Y. –C.; Bizuneh, A.; Walker, C *J. Org. Chem.* **1996**, *61*, 9086. Xu, Y. –C.; Lebeau, E.; Walker, C. *Tet. Lett.* **1994**, *35*, 6207.

[12] Courtesy of M. C. Hewitt.

[13] Birch, A. J. *J. Chem. Soc.* **1945**, 809. Small, G. H.; Minnella, A. E.; Hall, S. S. *J. Org. Chem.* **1975**, *40*, 3151.

[14] Shafer, D. E.; Inman J. K.; Lees, A. *Anal. Biochem.* **2000**, *282*, 161.

[15] MacBeath, G.; Schreiber, S. L. *Science*, **2000**, *289*, 1760.

[16] Wyatt, R.; Sodroski, J. *Science* **1998**, 280, 1884.

[17] Matsumoto, A.; Yoshima, H.; Kobota, A. *Biochemistry* **1983**, 22, 188.

[18] Magez, S.; Radwanska, M.; Stijlemans, B.; Xong, H. V.; Pays, E.; De Baetselier, P. *J. Biol. Chem.* **2001**, 276, 33458.

[19] O'Keefe, B.; Shenoy, S.; Xie, D.; Zhang, W.; Muschik, J.; Currens, M.; Chaiken, I.; Boyd, M. *Mol. Pharmacol.* **2000**, 58, 982.

[20] Bolmstedt, A.; O'Keefe, B.; McMahon, B.; Boyd, J.; Boyd, M. *Mol. Pharmacol.* **2001**, 59, 949.

[21] Boyd, M.; Gustafson, K.; McMahon, J.; Shoemaker, R.; O'Keefe, B.; Mori, T.; Gulakowski, R.; Wu, L.; Rivera, M.; Laurencot, C.; Currens, M.; Cardellina II, J.; Buckheit Jr., R.; Nara, P.; Pannell, L.; Sowder II, R.; Henderson, L. *Antimicrob. Agents Chemother.* **1997**, 41, 1521.

[22] Hodneland, C. D.; Lee, Y. S.; Min, d. H.; Mrksich, M. *Proc. Natl. Acad. Sci. U.S.A.* **2002**, *90*, 5048. Houseman, B.T.; Huh, J.H.; Kron, S.J.; Mrksich, M. *Nat. Biotech.* **2002**, *20*, 270.

[23] Kudryashov, V.; Glunz, P. W.; Williams, L. J.; Hintermann, S.; Danishefsky, S. J.; Lloyd, K. O. *Proc. Natl. Acad. Sci. U.S.A.* **2001**, *98*, 3264.

[24] Houseman, B. T.; Mrksich, M. *Top. Curr. Chem.* **2002**, *218*, 1-44.

[25] Andrade, R. B.; Plante, O. J.; Melean, L. G.; Seeberger, P. H. Org. Lett. **1999**, *1*, 1811.

[26] Geijtenbeek, T. B.; Torensma, R.; van Vliet, S. J.; van Duijnhoven, G. C.; Adema, G. J.; van Kooyk, Y.; and Figdor, C. G. *Cell* **2000**, *100*, 575.

[27] Bokesch, H. R.; O'Keefe, B. R.; McKee, T. C.; Pannell, L. K.; Patterson, G. M.; Gardella, R. S.; Sowder, R. C. 2nd; Turpin, J.; Watson, K.; Buckheit, R. W. Jr.; Boyd, M. R. *Biochemistry* **2003**, *42*, 2578.

[28] Poignard, P.; Saphire, E. O.; Parren, P. W.; Burton, D. R. *Annu. Rev. Immunol.* **2001**, *19*, 253.

[29] Burton, D. R. *Proc. Natl. Acad. Sci. U. S. A.* **1997**, *94*, 10018.

[30] Kwong, P. D.; Doyle, M. L.; Casper, D. J.; Cicala, C.; Leavitt, S. A.; Majeed, S.; Steenbeke, T. D.; Venturi, M.; Chaiken, I.; Fung, M.; Katinger, H.; Parren, P. W.; Robinson, J.; Van Ryk, D.; Wang, L.; Burton, D. R.; Freire, E.; Wyatt, R.; Sodroski, J.; Hendrickson, W. A.; Arthos, J. *Nature* **2002**, *420*, 678.

[31] Wyatt, R.; Kwong, P. D.; Desjardins, E.; Sweet, R. W.; Robinson, J.; Hendrickson, W. A.; Sodroski, J. G. *Nature* **1998**, *393*, 705.

[32] Scanlan, C. N.; Pantophlet, R.; Wormald, M. R.; Ollmann Saphire, E.; Stanfield, R.; Wilson, I. A.; Katinger, H.; Dwek, R. A.; Rudd, P. M.; Burton, D.R. *J. Virol.* **2002**, *76*, 7306.

[33] Calarese, D. A.; Scanlan, C. N.; Zwick, M. B.; Deechongkit, S.; Mimura, Y.; Kunert, R.; Zhu, P.; Wormald, M. R.; Stanfield, R. L.; Roux, K. H.; Kelly, J. W.; Rudd, P. M.; Dwek, R. A.; Katinger, H.; Burton, D. R.; Wilson, I.A. *Science* **2003**, *300*, 2065.

[34] Chan, D. C.; Kim, P. S. *Cell* **1998**, *93*, 681.

[35] Howard, O. M.; Korte, T.; Tarasova, N. I.; Grimm, M.; Turpin, J. A.; Rice, W. G.; Michejda, C. J.; Blumenthal, R.; Oppenheim, J. J. *J. Leukoc. Biol.* **1998**, *64*, 6.

[36] Boyd, M. R.; Gustafson, K. R.; McMahon, J. B.; Shoemaker, R. H.; O'Keefe, B. R.; Mori, T.; Gulakowski, R. J.; Wu, L.; Rivera, M. I.; Laurencot, C. M.; Currens, M. J.; Cardellina, J. H. 2nd; Buckheit, R. W.; Jr., Nara, P. L.; Pannell, L. K.; Sowder, R. C. 2nd; Henderson, L. E. *Antimicrob. Agents. Chemother.* **1997**, *41*, 1521.

[37] Bolmstedt, A. J.; O'Keefe, B. R.; Shenoy, S. R.; McMahon, J. B.; Boyd, M. R. *Mol. Pharmacol.* **2001**, *59*, 949.

[38] Tsai, C. C.; Emau, P.; Jiang, Y.; Tian, B.; Morton, W. R.; Gustafson, K. R.; Boyd, M. R. *AIDS Res. Hum. Retroviruses* **2003**, *19*, 535.

[39] Johnson, W. E.; Sauvron, J. M.; Desrosiers, R. C. *J. Virol.* **2001**, *75*, 11426.

[40] O'Keefe, B. R.; Shenoy, S. R.; Xie, D.; Zhang, W.; Muschik, J. M.; Currens, M. J.; Chaiken, I.; Boyd, M. R. *Mol. Pharmacol.* **2000**, *58*, 982.

[41] Esser, M. T.; Mori, T.; Mondor, I.; Sattentau, Q. J.; Dey, B.; Berger, E. A.; Boyd, M. R.; Lifson, J. D. *J. Virol.* **1999**, *73*, 4360-4371.

[42] Shenoy, S. R.; Barrientos, L. G.; Ratner, D. M.; O'Keefe, B. R.; Seeberger, P. H.; Gronenborn, A. M.; Boyd, M. R. *Chem. Biol.* **2002**, *9*, 1109.

[43] Sanders, R. W.; Venturi, M.; Schiffner, L.; Kalyanaraman, R.; Katinger, H.; Lloyd, K. O.; Kwong, P. D.; Moore, J. P. *J. Virol.* **2002**, *76*, 7293.

[44] Geijtenbeek, T. B.; Kwon, D. S.; Torensma, R.; van Vliet, S. J.; van Dufijnhoven, G. C.; Middel, J.; Cornelissen, I. L.; Nottet, H. S.; KewalRamani, V. N.; Littman, D. R.; Figdor, C. G.; and van Kooyk, Y. *Cell* **2000**, *100*, 587.

[45] Feinberg, H.; Mitchell, D. A.; Drickamer, K.; Weis, W. I. *Science* **2001**, *294*, 2163.

[46] Kwon, D. S.; Gregorio, G.; Bitton, N.; Hendrickson, W. A.; Littman, D. R. *Immunity* **2002**, *16*, 135-144.

[47] Wei, X.; Decker, J. M.; Wang, S.; Hui, H.; Kappes, J. C.; Wu, X.; Salazar-Gonzalez, J. F.; Salazar, M. G.; Kilby, J. M.; Saag, M. S., Komarova, N. L.; Nowak, M. A.; Hahn, B. H.; Kwong, P. D.; Shaw, G. M. *Nature* **2003**, *422*, 307.

[48] Ratner, D. M.; Adams, E. W.; Disney, M. D.; Seeberger, P. H. *ChemBioChem* **2004**, in press.

[49] Houseman, B. T.; Gawalt, E. S.; Mrksich, M. *Langmuir*, **2003**, *19*, 1522.

[50] Su, J.; Mrksich, M. *Angew. Chem. Int. Ed.* **2002**, *41*, 4715.

[51] Adams, E. W.; Uberfeld, J.; Ratner, D. M.; O'Keefe, B. R.; Walt, D. R.; Seeberger, P. H. *Angew. Chem. Int. Ed.* **2003**, *42*, 5317.

[52] Liang, R.; Yan, L.; Loebach, J.; Ge, M.; Uozumi, Y.; Sekanina, K.; Horan, N.; Gildersleeve, J.; Thompson, C.; Smith, A.; Bizwas, K.; Still, W. C.; Kahne. D. *Science* **1996**, *274*, 1520.

[53] de la Fuente, J. M.; Barrientos, A. G.; Rojas, T. C.; Rojo, J.; Canada, J.; Fernandez, A.; Penades, S. *Angew. Chem. Int. Ed.* **2001**, *40*, 2257. Otsuka, H.; Akiyama, Y.; Nagasaki, Y.; Kataoka, K. *J. Am. Chem. Soc.* **2001**, *123*, 8226. Lin, C. C.; Yeh, Y. C.; Yang, C. Y.; Chen, C. L.; Chen, G. F.; Chen, C. C.; Wu, Y. C. *J. Am. Chem. Soc.* **2002**, *124*, 3508. Hernaiz, M. J.; de la Fuente, J. M.; Barrientos, A. G.; Penades, S. *Angew. Chem. Int. Ed.* **2002**, *41*, 1554. Nolting, B.; Yu, J. J.; Liu, G. Y.; Cho, S. J.; Kauzlarich, S.; Gervay-Hague, J. *Langmuir* **2003**, *19*, 6465. Barrientos, A. G.; de la Fuente, J. M.; Rojas, T. C.; Fernandez, A.; Penades, S. *Chem. Eur. J.*, **2003**, *9*, 1909. Lin, C. C.; Yeh, Y. C.; Yang, C.; Chen, G. F.; Chen, Y. C.; Wu, Y. C.; Chen, C. C. *Chem. Comm.* **2003**, 2920. Rojo, J.; Diaz, V.; de la Fuente, J. M.; Segura, I.; Barrientos, A. G.; Riese, H. H. ; Bernad, A.; Penades, S. *ChemBioChem*, **2004**, *5*, 291.

[54] Bruchez, M. Jr.; Maronne, M.; Gin, P.; Weiss, S.; Alivisatos, A. P. *Science* **1998**, *281*, 2013.

[55] Newburg, D. S.; Ruiz-Palacios, G. M.; Altaye, M.; Chaturvedi, P.; Meinzen-Derr, J.; Guerrero, M. D.; Morrow, A. L. *Glycobiology* **2004**, *14*, 253.

[56] Houseman, B.; Mrksich, M. *Chem. Biol.* **2002**, 9, 443.

Chapter 5

Development of First Microchemical Device for the Optimization of Glycosylation Reactions

This chapter described work done in close collaboration with Mr. Edward R. Murphy, a doctoral student in the laboratory of Prof. Klavs F. Jensen in Chemical Engineering, MIT. Details of this study have been submitted for publication:

Ratner, D. M.; Murphy, E. R.; Jhunjhunwala, M.; Snyder, D. A.; Jensen, F. K.; Seeberger, P. H. Glycosylation as a Challenge for Microreactor-based Reaction Optimization in Organic Chemistry. *Submitted for Review.*

5.1 Introduction

While glycosylation reactions have been carried out for more than a century, the union of glycosylating agent and nucleophile to form a glycosidic linkage remains a challenging undertaking.[1] Glycoside formation depends on the conformation, sterics, and electronics of both reaction partners. Due to the challenge of accurately predicting the reactivity of the coupling partners, it is difficult to foresee the outcome of the reaction. In addition, reaction variables such as concentration, stoichiometry, temperature, reaction time, and activator play an undisputable role in the outcome of a given glycosylation.[2]

In addition to glycosylations, synthetic chemistry relies on an innumerable variety of organic reactions to construct a diverse range of molecular targets. Many organic transformations depend on multiple factors that determine the outcome of the reaction. Serving as a model system, the glycosylation reaction encompasses many of the challenges common to most reactions. In both academic and industrial settings, much of the effort spent by synthetic organic chemists is consumed searching for optimal reaction conditions to achieve a particular transformation. Method optimization frequently requires the commitment of time and large quantities of valuable starting materials.[3] The ability to find ideal reaction conditions quickly and efficiently would have a major impact on the practice and pace of research and development in organic chemistry.

Among their many applications, microfluidic-based devices are capable of performing a wide range of single and multiphase organic reactions.[4] In addition to requiring small quantities of reagent, submillimeter reaction channels allow for the precise control of reaction variables, such as reagent mixing, flow rates, reaction time,

and heat and mass transfer. Microfluidic devices are also amenable to integrated reaction monitoring, using UV/VIS, IR, NMR, mass spectrometry (MS), and LC/MS.[5] Unlike conventional bench-top batch reactions, microreactors are easily scalable, rendering a device capable of both analytical and semi-preparative scales of production. Finally, the microreactor format is ideally suited for automation of reaction optimization.

Here, we describe the design, fabrication, and use of a continuous flow microreactor to study the glycosylation reaction as an example of a challenging organic transformation. Optimizing glycosylation yield, reaction time and reaction temperature was the primary goal, in addition to gaining an understanding of the formation of different side products. While this study focuses on the glycosylation reaction as a model, the microchemical-based approach is applicable to most organic reactions and will allow for rapid reaction optimization using minimal amounts of starting materials.

5.2 Microdevice Reactor Design and Fabrication

The device prepared for this study was designed and fabricated by Mr. Edward R. Murphy within the facilities of the MIT Microsystems Technology Laboratories (MTL). At the inception of this collaborative effort, Mr. Daniel A. Snyder (Seeberger laboratory) and Mr. Manish Jhunjhunwala (Jensen Laboratory) established a preliminary microreactor design. The following design was conceived from the lessons learned during their initial efforts.

5.2.1 Reactor Design

A typical glycosylation reaction consists of three components, a glycosyl donor (halide, trichloroacetimidate, phosphate, etc...), a nucleophilic acceptor, and an activator. In most cases, the donor and acceptor are mixed in an anhydrous non-nucleophilic solvent, activator is added, and the reaction proceeds. Depending on the particulars of the reaction, an additional reagent may be added at the end of the reaction to quench unreacted activator and cease progress of the reaction. The design of a microreactor specific for glycosylation reactions should be based on this three component system, with

the addition of an optional method for a chemical quench.

To accomplish this goal, a five-port silicon microreactor was designed with three primary inlets to mix and react glycosylating agent (donor), nucleophile (acceptor), and activator. To ensure complete mixing and residence times sufficient for the reaction, the reactor was split into a mixing and reaction zone. The primary inlet streams are combined and enter a narrow loop mixing zone. The mixed reactant stream subsequently enters a wider reaction zone that is terminated by a secondary inlet used to quench the reaction. Finally, the quenched reaction stream exits the reactor for collection and analysis. (Figure 5.1).

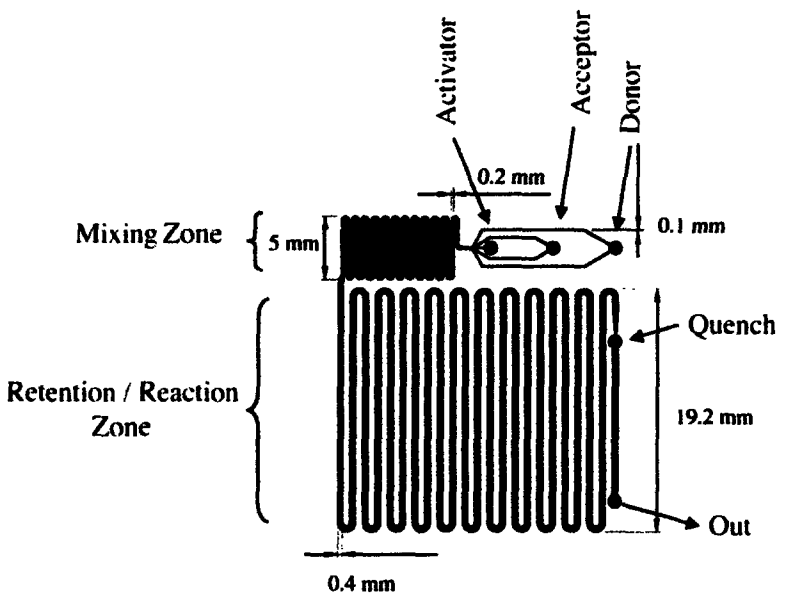

Figure 5.1 Microreactor layout design (Schematic by E. R. Murphy).

5.2.2 Microreactor Fabrication

Microfluidic channels were etched into a single crystal silicon wafer and capped by a Pyrex wafer via an anodic bond (Figure 5.2). This construction was chosen for its compatibility with a wide range of chemical reagents, as well as the high thermal conductivity of silicon – facilitating rapid thermal equilibration and temperature control.[6] Moreover, the silicon can be oxidized to create a glass surface throughout the resulting microchannels. Deep reactive ion etching techniques (DRIE)[7] make it easier to realize

deep aspect ratio structures in silicon than glass. Thus, the use of DRIE and subsequent oxidation and anodic bonding to Pyrex provides microreactors with glass surface properties. Additionally, the anodic bond, performed in a clean room environment, provides an hermetic seal at all points of contact between silicon and Pyrex. This seal prevents cross-channel contamination within the device, and excludes the introduction of moisture from the environment surrounding the microreactor.

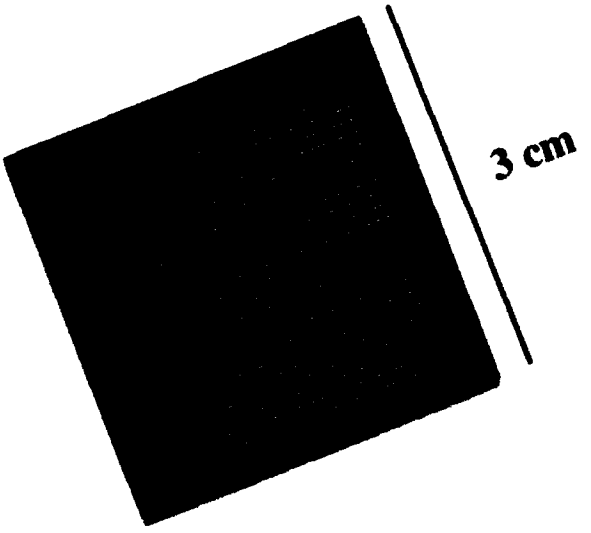

Figure 5.2 Microfluidic channels etched into silicon are clearly visible through the Pyrex cap (photo credit, Felice Frankel).

The flow channels and inlet ports for the device were patterned onto 650μm thick, double side polished (DSP), oxidized, silicon wafers using standard photolithographic techniques. The oxide layer was etched by buffered oxide etch (BOE) to produce a hard mask of the device pattern. The inlet ports on the back-side of the silicon wafer were then etched to a depth of 300μm using deep reactive ion etch (DRIE). Following the back-side etch, the flow channels were patterned and etched to a depth of 400μm as previously described.[7] The wafer was then anodically bonded to a Pyrex wafer and the copper pads were deposited around the inlet ports using electron beam deposition. The metal pads consisted of a 100nm thick titanium adhesion layer followed by a 500nm copper layer. The device was subsequently cut from the wafer and fitted with steel tube plumbing

(packaged).

Chemical compatibility was the primary concern in determining the packaging scheme. Traditional methods for packaging microdevices include epoxy bonding or compression seals. However, the nature of most solvents used in organic transformations posed a challenge to epoxy packaging methods. In particular, dichloromethane slowly dissolves most epoxies and o-rings used for compression seals. A solder-based packaging technique allowed the best chemical compatibility, as the inlet tubes were stainless steel with brass ferrules swaged to the exterior of these tubes. Lead-Tin solder was then applied around the exterior of the brass ferrule to complete the seal to the copper pads on the device (Figure 5.3). This arrangement brings the stainless steel tube in direct contact with the device. The only other surface exposed to the reactants is the 600nm thick metal layer.

Figure 5.3 Inlets and outlet are attached to the microdevice via lead-tin soldering (photo credit, Felice Frankel).

5.3 Functional Microreactor Setup

The flow of material through the device is controlled by syringe pump. An operational microreactor setup consists of four gas-tight syringes, one corresponding to each of the four inlets (donor, acceptor, activator and quench), a syringe pump to control

the flow, and stainless steel / Teflon plumbing (Figure 5.4). Thermal equilibrium of the microreactor is maintained by a water or acetone-bath in an insulated Dewar flask, monitored with a thermocouple.

a)

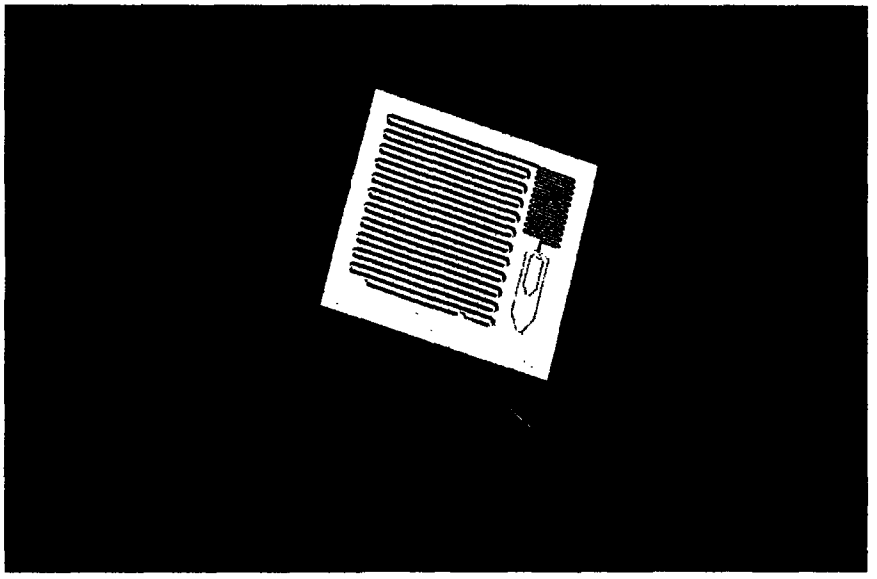

b)

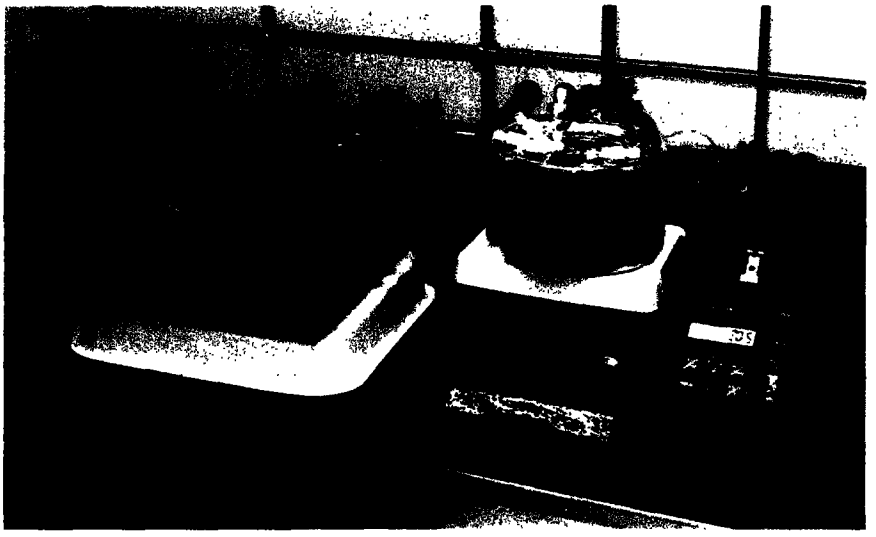

Figure 5.4 Microreactor device setup. a) Close-up of device including steel tubing and Teflon fittings (photo credit, Felice Frankel); b) Bench setup of functional microreactor.

Plumbing for the device consists of Hamilton syringes connected via 22 gauge

needles with Valco stainless steel fittings to 0.010 inch (inner diameter) Teflon tubing. The small inner diameter tubing is critical because of the high-pressures generated by the force required to drive material through the device. Even the slight elasticity of Teflon can cause large diameter tubing to swell, thus distorting the rate of flow through the device.

The smallest feature within the device is a 50 μm constriction-point at the end of the reaction zone, prior to the secondary inlet containing the quench. This constriction prevents back-flow through the device, ensuring uniform flow through the mixing and reaction zones. The small dimension of this constriction makes filtration of incoming solvent streams critical for optimal performance of the device. Therefore, all streams are separately passed through in-line steel frits (housed within the Teflon fittings) to pre-filter the incoming solutions prior to introduction to the reactor.

5.4 Microreactor Features

The micrometer scale of features in this device results in laminar flow within the channels; each fluid stream forms a lamina that mixes with the adjacent layers by diffusion (Figure 5.5).[8] The time required to mix laminae can be estimated by Equation (1) where w is the width to diffuse and $\mathcal{D}$ is the diffusivity of the component of interest.

$$t = \frac{w}{\mathcal{D}} \tag{1}$$

The mixing zone for this device is 119 mm long, 200μm wide, and 400μm deep. Prior to combining reagents in the mixing zone, the glycosyl donor and acceptor streams are each split in two. The resulting four streams are stacked with the activator stream, such that the donor must diffuse through the lamina resulting from the acceptor inlet before reaching the lamina of the activator (Figure 5.5). The stacking of laminae also creates a symmetrical concentration profile across the width of the mixing channel, reducing the diffusion width to 100μm – half that of the channel.

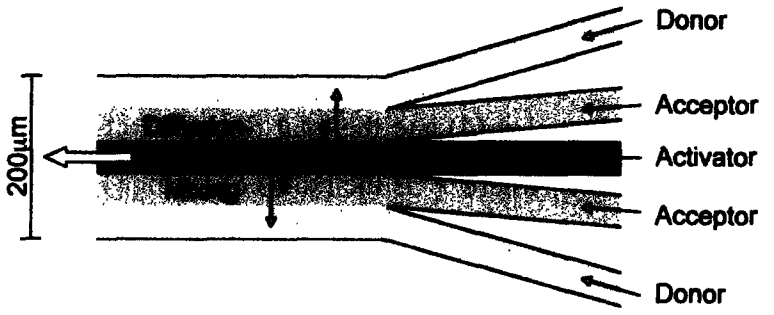

Figure 5.5 Schematic of diffusion-controlled mixing of glycosyl donor, acceptor and activator laminae in the mixing zone.

The reaction zone is a 400μm wide channel, 430 mm long, and 400μm deep. This feature was designed with a large volume to increase the residence time of the device. The output of the reaction zone combines with the secondary inlet before exiting the reactor. The volumes of the mixing and reaction zones are 9.5 μL and 68.8 μL respectively, giving a total reactor volume (pre-quench) of 78.3 μL. The residence time for this zone can be calculated according to Equation (2) where V is the volume of the section and Q is the total volumetric flow rate through that section.

$$\tau = \frac{V}{Q} \tag{2}$$

Stoichiometry within the microreactor is based on the concentration of components of the combined stream in the reactor. This, in turn, is determined by both the concentration of each reagent inside its source syringe and the flow rate of each stream. The flow rate of a given material stream is calculated according to Equation (3) where Q is the volumetric flow rate, r is the syringe internal radius and $\dot{h}$ is the linear speed of the syringe plungers.

$$Q = \pi r^2 \dot{h} \tag{3}$$

As the plunger speed ($\dot{h}$) is the same for all of the syringes, it is possible to calculate the concentration of reagents within the reactor. The total flow rate through the reaction zone is given by Equation (4) and the total flow rate after the quench has been added is given by Equation (5) where r_i^2 is the radius of syringe i (i.e. r_{donor}^2 is the radius of the syringe attached to donor port, etc...).

$$Q_{react} = \pi\left(r_{donor}^2 + r_{acceptor}^2 + r_{activator}^2\right)\dot{h} \tag{4}$$

$$Q_{react} = \pi\left(r_{donor}^2 + r_{acceptor}^2 + r_{activator}^2 + r_{quench}^2\right)\dot{h} \tag{5}$$

Thus the concentration inside the reaction zone of any component can be calculated by Equation (6).

$$C_i = C_{i,syringe}\frac{r_i^2}{r_{donor}^2 + r_{acceptor}^2 + r_{activator}^2} \tag{6}$$

5.5 Glycosylation in a Microchemical System

As a class of reactions, glycosylation covers a very broad range, encompassing a myriad of glycosyl donors, acceptors, and types of linkages.[2] Therefore, it was necessary to focus on a specific glycosylation reaction to be used as a model to test the utility of microchemical systems in optimizing organic reactions. For this purpose, two reactions utilizing a single mannosyl donor were employed in this study (sections 5.5.2 and 5.5.3). By examining these two simple reactions, it was possible to concentrate on overcoming the unanticipated and inevitable challenges that arise when designing an untested microchemical system. Additional details of the operation of the microdevice are available in Chapter 6 (section 6.5).

5.5.1 HPLC Internal Reference

Data generated by HPLC analysis of the microreactor glycosylations was normalized by an UV-active compound added to the quench syringe which enters through the secondary inlet (after the reaction zone). The HPLC standard normalizes the output stream for HPLC analysis by compensating for solvent evaporation and variability in the volume of collected sample. Because the glycosylation reaction was the subject of this study, α-D-methyl 2,3,4,6-tetra-*O*-benzyl mannoside **5-1**[9] was chosen as the ideal HPLC standard (Figure 5.6). This standard was selected for high UV/Vis absorbance, and compatibility with the reacting species.

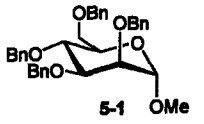

Figure 5.6 HPLC internal reference standard **5-1**.

5.5.2 Glycosylation of the Diisopropylidene Galactose Acceptor

Initially, the microchemical system was used to carry out the glycosylation by mannosyl trichloroacetimidate **5-2**[10] of diisopropylidene galactose **5-3** upon activation with 0.2 equivalents TMSOTf in anhydrous dichloromethane (Scheme 5.1). The reactor stream was quenched with a solution of triethylamine to terminate the reaction as it exited the reaction zone of the device. As detailed in section 5.4, the concentration of the reagents in the reactor was determined not only by the concentration inside the syringe but also the flow rate of each stream. Therefore, all flow rates were maintained in proportion to that of the donor inlet stream. The reaction temperature was varied from -78 to 20 °C, with glycosyl donor stream flow rates of 10, 20, 40 and 80 μl/ml, that resulted in reactor residence times (reaction time) of 26.7, 53.4, 106.8, and 213.5 seconds. Glycosylating agent **5-2** (1.2 equivalents) and nucleophile **5-3** (1.0 equivalents) were flowed through the microreactor with reaction zone concentrations of 0.0136 M and 0.0114 M respectively. The triethylamine quench also contained HPLC standard **5-1** (1.0 equivalent) and 25% dichloromethane to increase solubility.

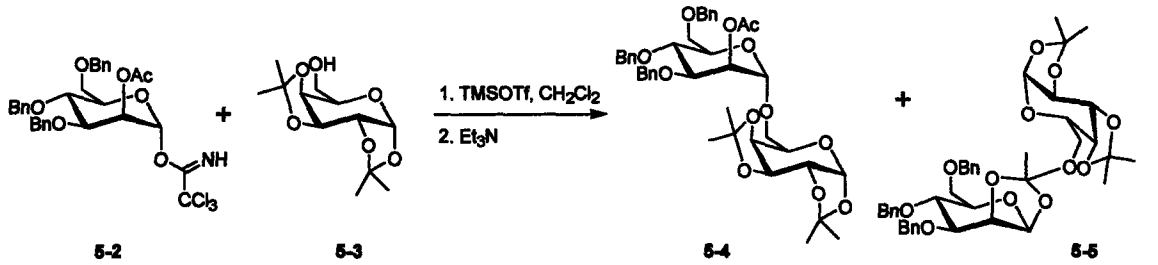

Scheme 5.1 Glycosylation of **5-3** with mannosyl donor **5-2**. In addition to product **5-4**, formation of orthoester **5-5** is frequently observed.

HPLC analysis of the crude samples, normalized with internal standard **5-1**, illustrates a clear relationship between reaction temperature, reaction time and formation of product **5-4** (Figure 5.7). For a given reaction time, the yield of product increases with temperature until maximum conversion is achieved. Correspondingly, at temperatures lower than the optimum, yield increases with increasing reaction time (i.e. decreasing flow rate).

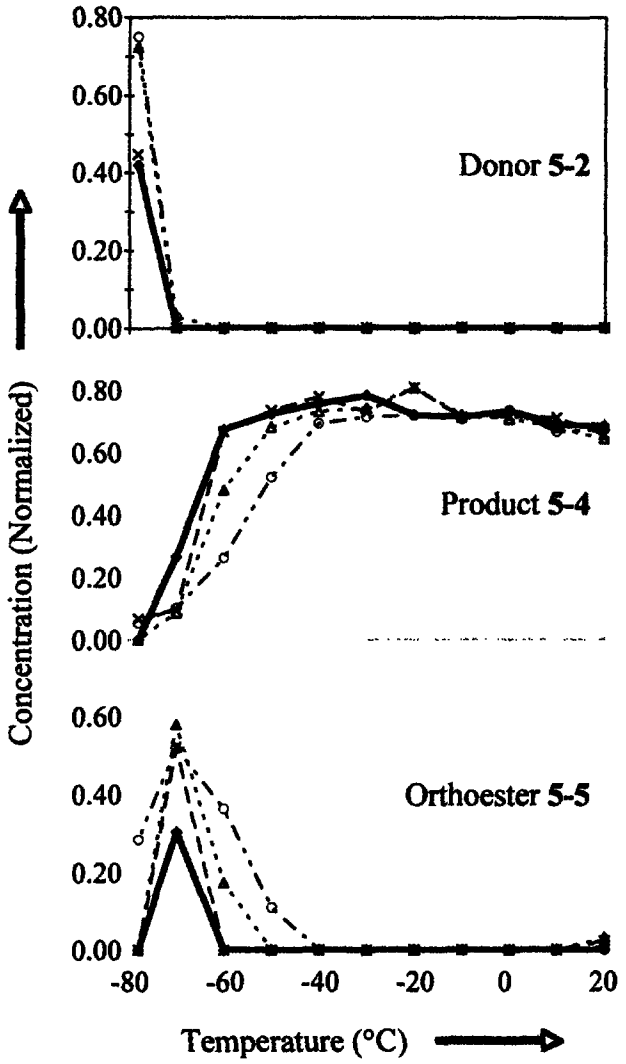

Figure 5.7 Normalized HPLC traces from glycosylation of **5-3** with **5-2**. . Legend, reaction times: 213.5 s, 106.8 s, 53.4 s, 26.7 s.

Notably, we were able to observe the formation of orthoester **5-5** as a major side product at lower temperatures. Formation of the orthoester is frequently encountered as an undesired product for glycosylations involving a donor with a C2 ester (especially the C2 acetate).[11] The orthoester is thought to occur when the C2 participating ester forms an acyloxonium ion from the oxycarbocation formed upon activation of the glycosyl donor (Scheme 5.2). The acyloxonium species can either react with the nucleophilic acceptor (R'OH) to form the desired product (a 1,2-*trans* linked *O*-glycoside), or the orthoester side-product. Orthoester formation is typically minimal for glycosylations activated with acidic TMSOTf, as the orthoester can rearrange to the *O*-glycoside in the presence of a

proton source. In the case of glycosylation of **5-3**, the rapid formation of orthoester was most pronounced around -70 °C, while at higher temperatures little or none was observed. With longer reaction times and higher temperatures, rearrangement of the orthoester to the desired product was evident.

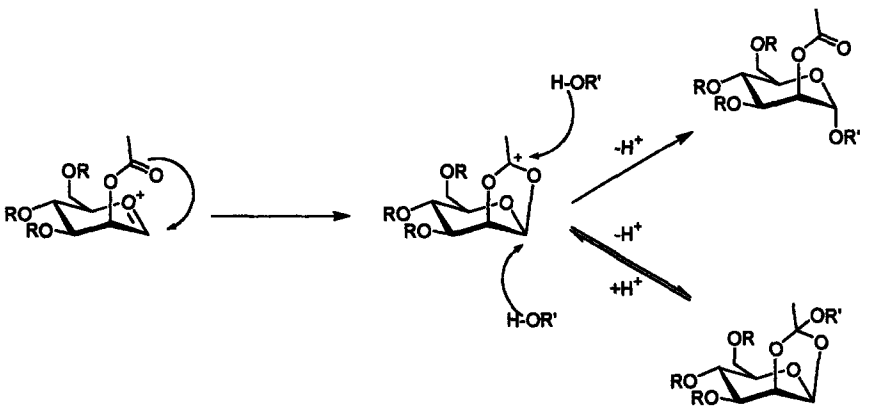

Scheme 5.2 Formation of orthoester is often observed for C2 acetate containing glycosyl donors.

Unlike batch reactions, the results from the microreactor study show that formation of the orthoester can be trapped, and profiled as a function of temperature and time. A typical batch process is followed by TLC until no additional product formation is observed. This process takes several minutes, and does not allow for live study of the proceeding reaction. In contrast, the experimental design of this microreactor-based study easily permits the examination of the progress of a reaction at set time intervals.

5.5.3 Glycosylation of a Hindered Acceptor

Following the initial efforts with the microreactor, a second model glycosylation was attempted with the device. α-D-methyl 2,3,4-tri-*O*-benzyl mannoside **5-6**[12] was mannosylated with **5-2** to yield disaccharide **5-7**[13] (Scheme 5.3). With the additional steric bulk of three benzyl ethers (including the axial C2 benzyl ether), **5-6** is less reactive as an acceptor for glycosylation than **5-3**. In addition, the benzyl ethers facilitate UV monitoring for HPLC analysis of unreacted acceptor in the reactor stream.

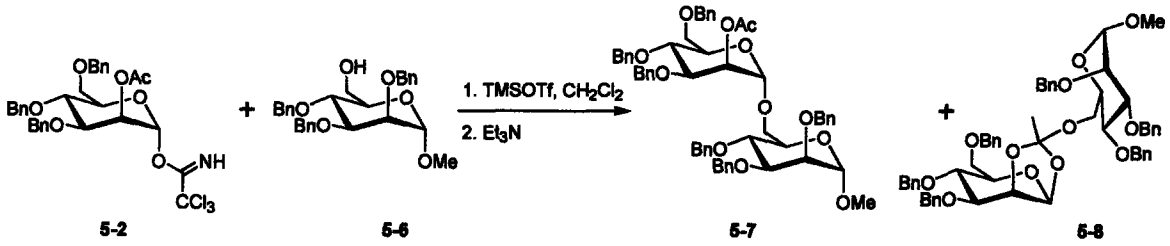

5-2 5-6 5-7 5-8

Scheme 5.3 Glycosylation of **5-6** with mannosyl donor **5-2** to form disaccharide **5-7**, and orthoester side product **5-8**.

In contrast to the results obtained for the coupling of **5-2** and **5-3**, microreactor-HPLC analysis of the union of **5-2** and **5-6** shows a unique reaction profile (Figure 5.8). Optimal product yields are obtained from -60 to -40 °C, the same temperature range that fosters formation of orthoester **5-8**. The reaction outcome appears optimal at -60 °C with a reaction time of just over 213 seconds, sufficient time for the orthoester to fully rearrange to the desired product. As Figure 5.8 illustrates, there is some evidence that orthoester **5-8** appears not as a side-product, but as an intermediate in the formation of the desired *O*-glycoside **5-7**. At low temperatures and short reaction times, it becomes clear that **5-8** forms as stable product much more rapidly than **5-7**.

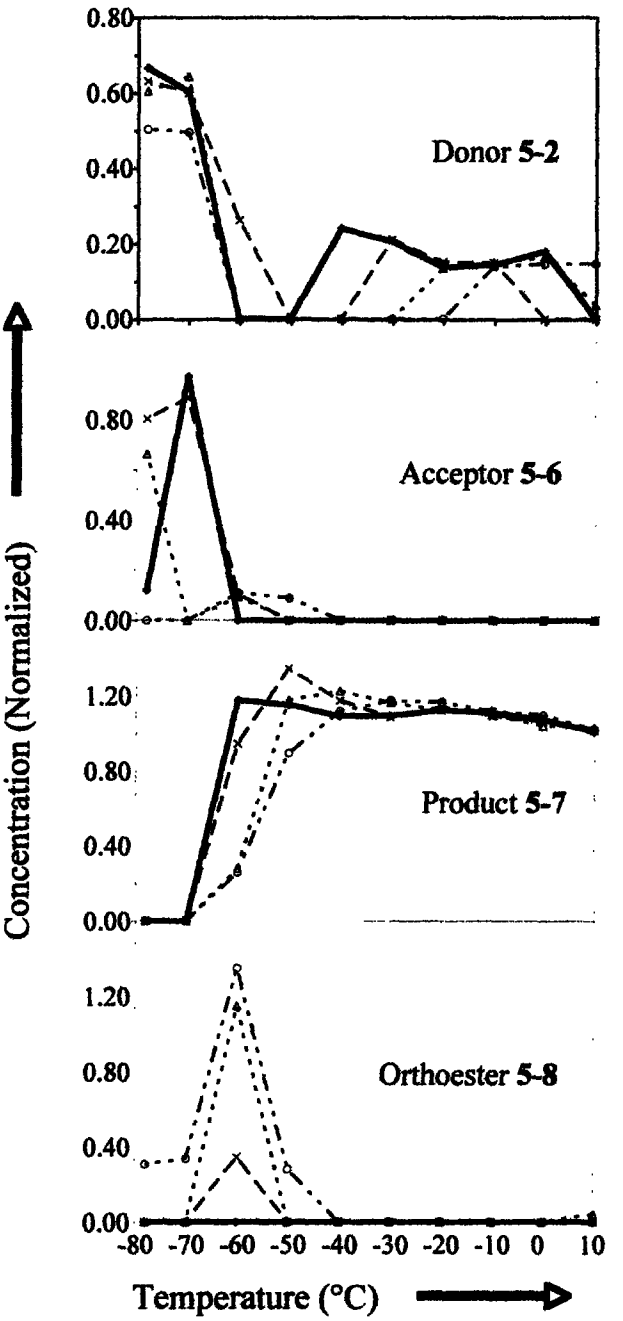

Figure 5.8 Normalized HPLC traces from glycosylation of **5-6** with **5-2**. . Legend, reaction times: ◆ 213.5 s, × ▪ 106.8 s, △ ▪ 53.4 s, ⊖ ▪ 26.7 s.

From the perspective of optimizing the reaction for large scale production, this analysis also demonstrates that nearly the same yield is achievable by running the reaction at -35 °C for 25.7 seconds. With very little change in overall yield, it is possible to increase production by nearly an order of magnitude over the slower reactions run at

lower temperatures (213 seconds at -60°C). This illustrates valuable knowledge regarding process development for scale-up, in addition to reaction optimization. This type of continuous-flow study offers significant advantage over a much more cumbersome and costly batchwise optimization for developing methods for semi-preparative or preparative scale production.

5.6 Summary and Conclusions

This study detailed the development of the first microchemical system for running glycosylation reactions. The microreactor proved its capacity for rapidly obtaining reaction profiles for two examples of this difficult organic transformation. The new setup allowed 44 reactions to be completed in a single afternoon, varying temperature and reaction time for the coupling. Each experiment required just over 2 mg of glycosylating agent per reaction, representing a significant improvement over traditional methods for optimizing the glycosylation reaction.

Microchemical devices are easily scaled for many applications. The continuous flow nature of the reactor permits the microanalytical scale presented herein to be adjusted to suit the needs of any particular study. Ultimately, the production capacity of a reactor is limited only by the size of the reagent reservoirs. Larger syringes, or solvent pumps, would permit a single device to easily produce 100 g of material in a day.

Following this success, one can envision a number of potential avenues for pursuit. While the reactions performed in this study served only as models for typical glycosylations, any number of current challenges to synthetic carbohydrate chemistry may be examined with these microchemical systems. Such efforts might include improving the yield of β-mannoside formation, profiling challenging sialic acid couplings, or improving methods for coupling with glucuronic and iduronic acid donors – a hurdle to the synthesis of heparin oligosaccharides.

Finally, a microchemical approach to combinatorial chemistry is also within consideration. Fabrication efforts are underway to multiplex an array of microreactors (3 by 3). Such an array of 9 reactors would easily permit the simultaneous glycosylation by

3 glycosyl donors of 3 glycosyl acceptors to form 9 unique disaccharide products. As fabrication methods continue to advance, possible applications for microchemical systems will rapidly expand. The versatility of the silicon-based microchemical system stands to fundamentally change method optimization and process development in academia and industry.

References:

[1] Lehmann, J. In *Carbohydrates: Structure and Biology*, Thieme: Stuttgart, **1998**, p. 1-45.

[2] For review, see: Toshima, K.; Tatsuta, K. *Chem. Rev.* **1993**, *120*, 1503. Nukada, T.; Berces, A.; Zgierski, M. Z.; Whitfield, D. M. *J. Am. Chem. Soc.* **1998**, *120*, 13291.

[3] Carlson, R. *Design and Optimization in Organic Synthesis*, Elsevier Science: Amsterdam, New York, **1992**.

[4] Jähnisch, K.; Hessel, V.; Löwe, H.; Baerns, M. *Angew. Chem. Int. Ed.* **2004**, *43*, 406. Pennemann, H.; Watts, P.; Haswell, S. J.; Hessel, V.; Löwe H. *Org. Process. Res. Dev.* **2004**, *8*, 422. Fletcher, P. D. I.; Haswell, S. J.; Pombo-Villar, E.; Warrington, B. H.; Watts, P.; Wong, S. Y. F.; Zhang, X. *Tetrahedron* **2002**, *58*, 4735.

[5] Schilling, M.; Nigge, W.; Rudzinski, A.; Neyer A.; Hergenröder, R. *Lab. Chip.* **2004**, *4*, 220. Jackman, R. J.; Floyd, T. M.; Ghodssi, R.; Schmidt, M. A.; Jensen, K.F. *J. Micromechanical and Microengineering* **2001**, *11*, 263. Lu, H.; Schmidt, M. A.; Jensen, K. F. *Lab. Chip.* **2001**, *1*, 22.

[6] Jensen, K. F. *Chem. Eng. Sci.* **2001**, 56, 293. Arana, L.; Schaevitz, S. B.; Franz, A. J.; Schmidt, M. A.; Jensen, K. F. *J. of MicroElectromechanical* Systems **2003**, *12*, 600.

[7] Losey, M. W.; Jackman, R. J.; Firebaugh, S. L.; Schmidt, M. A.; Jensen, K. F. *J. MicroElectromechanical Systems* **2002**, *11*, 709.

[8] As determined by Reynolds number calculation.

[9] Fügedi, P.; Lipták, A.; Neszmélyi, P. N. Carbohd. Res. **1982**, *107*, C5. Vasella, A.; Witzig, C.; Waldraff, C.; Uhlmann, P.; Briner, K.; Bernet, B.; Panza, L.; Husi, R. *Helv. Chim. Acta.* **1993**, *76*, 2847.

[10] Rademann, J.; Geyer, A.; Schmidt, R. R. *Angew. Chem. Int. Ed.* **1998**, *37*, 1241.

[11] Garegg, P. J.; Norberg, T. *Acta. Chem. Scand.* **1979**, *B33*, 116.

[12] Garegg, P. J.; Oscarson, S.; Tidén, A. –K. *Carbohyd. Res.* **1990**, *200*, 475.

[13] Ding, X. L.; Kong, F. Z. *J. Carbohyd. Chem.* **1998**, *17*, 915. Li, Z. –J.; Li, H.; Cai, M. –S. *Carbohyd. Res.* **1999**, *320*, 1.

Chapter 6

Experimental

6.1 General Methods

All commercial materials were used without further purification, unless otherwise noted. Dichloromethane (CH_2Cl_2) and diethyl ether (Et_2O) were purchased from J. T. Baker (Cycletainer™) and passed through neutral alumina columns prior to use. Toluene was purchased from J. T. Baker (Cycletainer™) and passed through neutral alumina and copper (II) oxide columns prior to use. Analytical thin-layer chromatography was performed on E. Merck silica gel 60 F_{254} plates (0.25 mm). Compounds were visualized by dipping the plates in a cerium sulfate-ammonium molybdate solution, followed by heating. Liquid chromatography was performed using forced flow of the indicated solvent on Silicycle Inc. silica gel (230-400 mesh). ^1H NMR spectra were obtained on either a Bruker Avance 400 (400 MHz) or Varian VXR-500 (500 MHz) and are reported in parts per million (δ) relative to chloroform (7.26 ppm). Coupling constants (*J*) are reported in Hz. ^{13}C NMR spectra were recorded on either a Bruker Avance 400 (100 MHz) or a Varian VXR-500 (125 MHz) and are reported in δ relative to $CDCl_3$ (77.23 ppm) as an internal reference. IR spectra were obtained on a Perkin-Elmer 1600 series FTIR spectrometer. ESI Mass spectrometry was performed on a Bruker Daltonics Apex 3 Tesla Fourier Transform Mass Spectrometer. Addition ESI mass spectrometry was performed on a Waters Micromass ZMD 4000 mass spectrometer. MALDI-TOF mass spectra were obtained on a PerSpective Biosystems Voyager Elite DE Spectrometer using 9:1 2,5-dihydroxybenzoic acid with 5-methoxysalicylic acid, 0.1 % TFA in 1:1 water:acetonitrile or α-cyano-4-hydroxycinnamic acid as the matrix.

6.2 Experimentals for Chapter 2

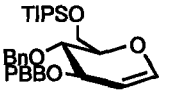

2-12

1,5-Anhydro-4-*O*-benzyl-3-*O*-(4-bromobenzyl)-2-deoxy-6-*O*-triisopropylsilyl-D-arabino-hex-1-enitol 2-12. 1,5-anhydro-3-*O*-(4-bromobenzyl)-2-deoxy-6-*O*-triisopropylsilyl-D-arabino-hex-1-enitol **2-11** (7.80 g, 16.5 mmol) was dissolved in DMF (125 mL) and cooled on an ice-bath to 0 °C. Sodium hydride (0.8 g, 60% in mineral oil,

19.9 mmol) was carefully added to the solution, and stirred for 20 min at 0 °C. Benzyl bromide (3.39 g, 19.9 mmol) was added to the reaction mixture and slowly warmed to room temperature for 2 h. Methanol (3 mL) was slowly added to quench the reaction, which was further diluted in 150 mL water. The solution was extracted with diethyl ether (3x 300 mL). After concentration *in vacuo* the resulting residue was purified by flash column chromatography on silica gel (2→5% EtOAc/hexanes) to afford 8.60 g (93%) of **2-12** as a clear oil. $[\alpha]^{24}_{D}$: -19.6° (*c* 1.1, CH_2Cl_2); IR (thin film) 2942, 2865, 1647, 1240, 1101, 682 cm^{-1}; ^1H NMR ($CDCl_3$) δ 7.46-7.44 (d, *J* = 8.2 Hz, 2H), 7.36-7.30 (m, 5H), 7.22-7.20 (d, *J* = 8.2 Hz, 2H), 6.41 (dd, *J* = 1.5, 6.1 Hz, 1H), 4.85-4.78 (m, 3H), 4.59 (d, *J* = 11.9 Hz, 1H), 4.52 (d, *J* = 12.2 Hz, 1H), 4.20-4.18 (m, 1H), 4.07-3.93 (m, 4H), 1.10-1.07 (m, 21H); ^{13}C NMR ($CDCl_3$) δ 145.1, 138.6, 137.7, 129.5, 128.6, 128.1, 128.0, 121.6, 99.5, 78.3, 76.0, 74.2, 74.1, 70.0, 62.0, 18.2, 18.2, 12.2; ESI MS *m/z* ($M + Na^+$) calcd 583.1849, found 583.1838.

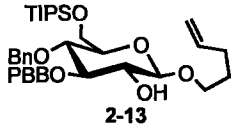

2-13

4-Pentenyl 4-*O*-benzyl-3-*O*-(4-bromobenzyl)-6-*O*-triisopropylsilyl-β-D-glucopyranoside 2-13. Glucal **2-12** (1.82 g, 3.23 mmol) was dissolved in CH_2Cl_2 (6 mL) and cooled to 0 °C. A 0.08 M solution of dimethyldioxirane in acetone (48.5 mL, 3.88 mmol) was added and the reaction was stirred for 15 min. After the solvent was removed the remaining residue was dried *in vacuo* for 1.5 h and subsequently dissolved in CH_2Cl_2 (10 mL). The solution was cooled to –78 °C followed by the addition of 4-penten-1-ol (1.61 mL, 16.15 mmol). A 1.0 M solution of $ZnCl_2$ in diethyl ether (3.55 mL, 3.55 mmol) was added and the reaction was warmed slowly to room temperature and stirred over 16 h. The reaction was diluted with EtOAc (200 mL) and washed with sat. aqueous $NaHCO_3$ (2 x 100 mL), water (2 x 100 mL) and brine (2 x 100 mL) and dried (Na_2SO_4). The organic phase was concentrated *in vacuo* and the resulting residue purified by flash column chromatography on silica gel (15% EtOAc/hexanes) to afford 1.86 g (87%) of **2-13** as a clear oil. $[\alpha]^{24}_{D}$: -20.8° (*c* 1.3, CH_2Cl_2); IR (thin film) 3456, 2941, 2865, 1115, 1069, 689 cm^{-1}; ^1H NMR ($CDCl_3$) δ 7.36 (d, *J* = 6.5 Hz, 2H), 7.26-7.16 (m, 7H), 5.79-

5.69 (m, 1H), 4.98-4.89 (m, 2H), 4.81 (d, J = 11.4, 1H), 4.82 (d, J = 11.6, 1H), 4.79 (d, J = 12.5, 1H), 4.63 (d, J = 11.6, 1H), 4.15 (d, J = 7.5, 1H), 3.92-3.76 (m, 3H), 3.60-3.51 (m, 4H), 3.25-3.21 (m, 1H), 2.28-2.27 (m, 1H), 2.08-2.02 (m, 2H), 1.68-1.61 (m, 2H), 1.07-0.89 (m, 21H); ^{13}C NMR ($CDCl_3$) δ 138.5, 138.3, 138.0, 131.7, 129.8, 128.7, 128.1, 128.0, 121.7, 115.1, 102.6, 84.6, 77.4, 76.4, 75.3, 75.1, 74.4, 69.2, 62.6, 30.5, 29.0, 18.2, 12.2; ESI MS m/z ($M + Na^+$) calcd 685.2530, found 685.2532.

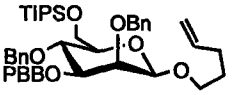

2-8

4-Pentenyl 2,4-di-*O*-benzyl-3-*O*-(4-bromobenzyl)-6-*O*-triisopropylsilyl-β-D-mannopyranoside 2-8. Glucoside **2-13** (0.564 g, 0.85 mmol) was azeotropically dried with toluene (3 x 3 mL) and dissolved in dimethyl sulfoxide (3.5 mL). Acetic anhydride (1.75 mL) was added and the reaction was allowed to stir 24 h at room temperature. After the solvent was removed *in vacuo*, addition of CH_2Cl_2 (20 mL) was followed by washing with water (2 x 20 mL) and drying of the organic phase (Na_2SO_4). After concentration *in vacuo* the residue was dissolved in 1:1 CH_2Cl_2:MeOH (10 mL) and cooled to 0 °C. $NaBH_4$ (0.161 g, 4.25 mmol) was slowly added and the reaction was stirred 16 h at room temperature. CH_2Cl_2 (100 mL) was added and the organic phase was washed with water (100 mL), 1% aqueous citric acid (2 x 100 mL), sat. aqueous $NaHCO_3$ (100 mL), brine (100 mL) and dried (Na_2SO_4). The organic phase was dried *in vacuo* to give a clear oil and purified by flash column chromatography on silica gel (6→7% EtOAc/hexanes) to afford 0.42 g (74%) of the desired 4-pentenyl 4-*O*-benzyl-3-*O*-(4-bromobenzyl)-6-*O*-triisopropylsilyl-β-D-mannopyranoside. $[\alpha]^{24}_D$: -32.0° (*c* 1.3, CH_2Cl_2); IR (thin film) 3439, 2940, 2864, 1638, 1105, 1069, 683 cm^{-1}; ^{1}H NMR ($CDCl_3$) δ 7.36 (d, J = 8.4 Hz, 2H), 7.29-7.17 (m, 7H), 5.78-5.68 (m, 1H), 4.97-4.87 (m, 2H), 4.80 (d, J = 10.9 Hz, 1H), 4.68- 4.53 (m, 3H), 4.32 (d, J = 0.9 Hz, 1H), 3.98 (m, 1H), 3.92-3.78 (m, 4H), 3.46-3.40 (m, 2H), 3.19-3.15 (m, 1H), 2.26 (d, J = 2.9 Hz, 1H), 2.04 (m, 2H), 1.67-1.60 (m, 21H), 1.05-0.97 (m, 2H); ^{13}C NMR ($CDCl_3$) δ 138.8, 138.5, 137.5, 131.9, 129.9, 128.9, 128.5, 128.2, 122.0, 115.2, 99.8, 82.0, 76.8, 75.6, 74.3, 71.0, 69.1, 68.9, 63.0, 30.7, 29.1, 18.4, 12.4; ESI MS m/z ($M + Na^+$) calcd 685.2530, found

685.2539. 4-Pentenyl 4-*O*-benzyl-3-*O*-(4-bromobenzyl)-6-*O*-triisopropylsilyl-β-D-mannopyranoside (1.00g, 1.5 mmol) was azeotropically dried with toluene (3 x 3 mL) and dissolved in DMF (15 mL). The solution was cooled to 0 °C and sodium hydride (90 mg, 60% in mineral oil, 1.81 mmol) was carefully added and the mixture was warmed to room temperature. Benzyl bromide (214 μL, 1.81 mmol) was added to the solution, and stirred for 2 h. The reaction was diluted with diethyl ether (100 mL), washed with water (100 mL), followed by extraction of the combined aqueous phase with diethyl ether (50 mL). The combined organic phase was washed with sat. aqueous $NaHCO_3$ (100 mL), water (100 mL), brine (100 mL), dried (Na_2SO_4) and concentrated to give a thick oil *in vacuo*. The residue was purified by flash column chromatography on silica gel (5 → 20% EtOAc/hexanes) to afford 1.17 g (98%) of **2-8**. $[\alpha]^{24}_D$: -54.0° (*c* 1.2, CH_2Cl_2); IR (thin film) 2940, 2865, 1454, 1361, 1107, 1070, 696 cm^{-1}; ^1H NMR ($CDCl_3$) δ 7.49-7.28 (m, 12H), 7.17 (d, J = 8.4 Hz, 2H), 5.92-5.82 (m, 1H), 5.08-4.85 (m, 5H), 4.68 (d, J = 11.0 Hz, 1H), 4.05-3.89 (m, 5H), 3.51-3.43 (m, 2H), 3.32-3.28 (m, 1H), 2.18 (m, 2 H), 1.79–1.72 (m, 1H), 1.16-1.04 (m, 21H) ; ^{13}C NMR ($CDCl_3$) δ 139.1, 138.7, 138.5, 137.6, 131.6, 129.4, 128.6, 128.4, 128.2, 127.9, 127.5, 121.7, 115.1, 102.0, 82.6, 77.4, 75.4, 75.0, 74.0, 73.7, 70.7, 69.1, 63.3, 30.6, 29.2, 18.2, 12.2; ESI MS *m/z* ($M + Na^+$) calcd 775.3000, found 775.3020.

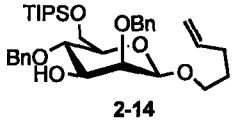

2-14

4-Pentenyl 2,4-di-*O*-benzyl-6-*O*-triisopropylsilyl-β-D-mannopyranoside 2-14. Glucoside **2-8** (0.507 g, 0.671 mmol) was azeotropically dried with toluene (3 x 3 mL) then for 1 h *in vacuo*. The residue was dissolved in toluene (2 mL) followed by the addition of *N*-methyl aniline (86 mg, 0.805 mmol). An oven-dried Schlenk flask was evacuated and backfilled with argon (5 x). The flask was charged with $Pd_2(dba)_3$ (12.3 mg, 2 mol %), (o-biphenyl)P(t-Bu)$_2$ (4 mol %), and NaOtBu (0.090 g, 0.939 mmol), evacuated and backfilled with argon (5 x). A rubber septum was installed and the aryl bromide/amine solution was added via cannula. The flask was sealed using a teflon screwcap and the reaction mixture was heated to 80 °C with stirring. After 18 h, the

reaction was cooled to room temperature, diluted with diethyl ether (20 mL), filtered through a pad of celite, and concentrated *in vacuo*. The crude product was purified by flash column chromatography on silica gel (2 → 5% EtOAc/hexanes) to yield 0.483 g (92%) of 4-pentenyl 4-*O*-benzyl-3-*O*-(4-(*N*-methyl-*N*-phenylamino)benzyl)-6-*O*-triisopropylsilyl-β-D-mannopyranoside. $[\alpha]^{24}_D$: -52.6° (*c* 1.5, CH_2Cl_2); IR (thin film) 2940, 2865, 1595, 1497, 1105, 1067, 696 cm^{-1}; ^1H NMR ($CDCl_3$) δ 7.51 (d, *J* = 6.9 Hz, 2H), 7.37-7.23 (m, 13H), 7.08-6.97 (m, 4H), 5.93-5.82 (m, 1H), 5.09-4.89 (m, 5H), 4.67 (d, *J* = 10.9 Hz, 1H), 4.54 (d, *J* = 11.5 Hz, 1H), 4.47 (d, *J* = 11.5 Hz, 1H), 4.40 (s, 1H), 4.06-3.90 (m, 5H), 3.55 (dd, *J* = 3.0, 9.4 Hz, 1H), 3.49-3.43 (m, 1H), 3.35-3.29 (m, 4H), 2.21-2.15 (m, 2H), 1.79-1.71 (m, 2H), 1.16-1.10 (m, 21H); ^{13}C NMR ($CDCl_3$) δ 149.3, 148.9, 139.3, 138.9, 138.5, 131.0, 129.4, 129.2, 128.5, 128.4, 128.3, 128.2, 127.8, 127.4, 121.6, 120.9, 120.6, 115.1, 102.0, 82.6, 75.4, 75.0, 74.1, 73.7, 71.5, 69.0, 63.4, 40.5, 30.6, 29.2, 18.2, 12.2; ESI MS *m/z* ($M + Na^+$) calcd 802.4479, found 802.4473. The aminated product (68 mg, 0.0876 mmol) was dissolved in CH_2Cl_2 (3 mL) followed by the addition of dichloroacetic acid (72 μL, 0.876 mmol), resulting in a transparent blue color. The reaction was stirred for 30 min at room temperature then diluted with CH_2Cl_2 (20 mL). Washing with sat. aqueous $NaHCO_3$ (2 x 30 mL), brine (30 mL), was followed by drying (Na_2SO_4) and concentration *in vacuo*. The crude product was purified by flash column chromatography on silica gel (2 → 5% EtOAc/ toluene) to afford 46.3 mg (90%) of **2-14**. $[\alpha]^{24}_D$: -31.4° (*c* 1.3, CH_2Cl_2); IR (thin film) 3446, 2940, 2865, 1734, 1455, 1249, 1085, 695 cm^{-1}; ^1H NMR ($CDCl_3$) δ 7.32-7.17 (m, 10H), 5.80-5.69 (m, 1H), 5.00-4.87 (m, 3H), 4.80 (d, *J* = 11.1 Hz, 1H), 4.56-4.53 (m, 2H), 4.39 (d, *J* = 0.4 Hz, 1H), 3.96-3.83 (m, 3H), 3.73 (d, *J* = 3.1 Hz, 1H), 3.64-3.53 (m, 2H), 3.41-3.35 (m, 1H), 3.20-3.17 (m, 1H), 2.48 (d, *J* = 9.7 Hz, 1H), 2.08-2.03 (m, 2H), 1.67-1.62 (m, 2H), 1.07-0.94 (m, 21H); ^{13}C NMR ($CDCl_3$) δ 138.8, 138.7, 138.4, 128.5, 128.2, 127.9, 115.0, 101.7, 77.9, 76.9, 76.7, 75.0, 74.6, 74.1, 69.1, 63.2, 30.6, 29.2, 18.2, 12.5; ESI MS *m/z* ($M + Na^+$) calcd 607.3425, found 607.3440.

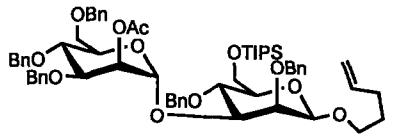

2-15

4-Pentenyl 2-*O*-acetyl-3,4,6-tri-*O*-benzyl-α-D-mannopyranosyl-(1→3)-2,4-di-*O*-benzyl-6-*O*-triisopropylsilyl-β-D-mannopyranoside 2-15. Mannosyl trichloroacetimidate **2-9** (65 mg, 0.10 mmol) and glycosyl acceptor **2-14** (30 mg, 0.0513 mmol) were azeotropically dried with toluene (3 x 3 mL) and dissolved in CH_2Cl_2 (1 mL). The solution was cooled to -20 °C for 15 min, followed by the addition TBDMSOTf (2.4 μL, 0.010 mmol), and stirred for 30 min at –20 °C. The reaction was quenched by addition of Et_3N (50 μL), and dried *in vacuo*. The crude product was purified by flash column chromatography on silica gel (2 → 5% EtOAc/toluene) to afford 54 mg (99%) disaccharide **2-15**. $[\alpha]^{24}_D$: -15.6° (*c* 1.4, CH_2Cl_2); IR (thin film) 2940, 2865, 1745, 1235, 1078, 697 cm^{-1}; ^1H NMR ($CDCl_3$) δ 7.32-7.04 (m, 25H), 5.79-5.69 (m, 1H), 5.44-5.43 (m, 1H), 5.12 (d, *J* = 1.2 Hz, 1H), 4.95-4.87 (m, 3H), 4.79 (d, *J* = 11.1 Hz, 1H), 4.70-4.35 (m, 8H), 4.29 (s, 1H), 3.93-3.54 (m, 9H), 3.52-3.51 (m, 2H) 3.33-3.27 (m, 1H), 3.17-3.13 (m, 1H), 2.06-1.99 (m, 5H), 1.64-1.57 (m, 2H), 1.04-0.93 (m, 21H); ^{13}C NMR ($CDCl_3$) δ 170.5, 139.2, 138.8, 138.4, 138.4, 138.3, 138.1, 128.6, 128.5, 128.4, 128.4, 128.3, 128.2, 127.9, 127.9, 127.8, 127.7, 127.6, 127.2, 114.9, 101.7, 99.9, 80.6, 78.3, 77.7, 77.2, 75.3, 75.0, 74.5, 73.9, 73.8, 73.6, 72.2, 72.1, 69.2, 69.1, 69.0, 63.0, 30.6, 29.2, 21.2, 18.2, 12.5; ESI MS *m/z* ($M + Na^+$) calcd 1081.5468, found 1081.5428.

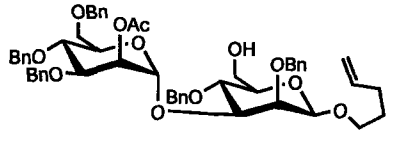

2-16

4-Pentenyl 2-*O*-acetyl-3,4,6-tri-*O*-benzyl-α-D-mannopyranosyl-(1→3)-2,4-di-*O*-benzyl-β-D-mannopyranoside 2-16. To a solution of disaccharide **2-15** (0.108g, 0.103 mmol) in THF (2 mL), water (2 mL) and trifluoroacetic acid (0.8 mL) were added. The turbid white solution was stirred for 2 h at room temperature. The reaction was diluted with diethyl ether (30 mL) and washed with sat. aqueous $NaHCO_3$ (2 x 20 mL), brine (20 mL), dried (Na_2SO_4) and concentrated. The residue was purified by flash column

chromatography on silica gel (10 → 30% EtOAc/hexanes) to afford 84.0 mg (91%) of disaccharide **2-16**. $[\alpha]^{24}_D$: -24.0° (*c* 0.5, CH_2Cl_2); IR (thin film) 3443, 2089, 1639, 1234, 698 cm^{-1}; ^1H NMR ($CDCl_3$) δ 7.42-7.17 (m, 25H), 5.90-5.80 (m, 1H), 5.55-5.54 (m, 1H), 5.26 (d, *J* = 1.5 Hz, 1H), 5.09-4.97 (m, 3H), 4.91 (d, *J* = 11.0 Hz, 1H), 4.84-4.78 (m, 2H), 4.73-4.43 (m, 8H), 4.43-3.75 (m, 9H), 3.69-3.63 (m, 2H), 3.44-3.41 (m, 1H), 3.39-3.31 (m, 1H), 2.22-2.12 (m, 6H), 1.78-1.70 (m, 2H); ^{13}C NMR ($CDCl_3$) δ 170.5, 138.7, 138.6, 138.3, 138.2, 137.9, 137.9, 128.6, 128.6, 128.5, 128.4, 128.3, 128.1, 128.0, 128.0, 127.8, 127.8, 127.8, 127.7, 127.6, 115.4, 101.8, 99.8, 80.0, 78.1, 77.5, 76.0, 75.4, 75.0, 74.4, 74.4, 72.3, 72.1, 69.7, 69.2, 68.9, 62.3, 30.4, 29.0, 21.2; ESI MS *m/z* ($M + Na^+$) calcd 925.4133, found 925.4141.

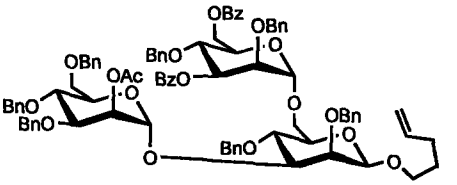

2-7

4-Pentenyl 2-*O*-acetyl-3,4,6-tri-*O*-benzyl-α-D-mannopyranosyl-(1→3)-[2,4-di-*O*-benzyl-3,6-di-*O*-benzoyl-α-D-mannopyranosyl-(1→6)]-2,4-di-*O*-benzyl-β-D-mannopyranoside 2-7. Mannosyl trichloroacetimidate **2-10** (94 mg, 0.150 mmol) and disaccharide **2-15** (80 mg, 0.088 mmol) were combined, azeotropically dried with toluene (3 x 3 mL) and dissolved in diethyl ether (2 mL). The solution was cooled to –20 °C for 15 min, followed by the addition of TBDMSOTf (4 μl, 0.018 mmol), and stirred for 30 min at -20 °C. The reaction was quenched by the addition of Et_3N (50 μL), and dried *in vacuo*. The crude product was purified by flash column chromatography on silica gel (5 → 10% EtOAc/toluene) to afford 120 mg (93%) of trisaccharide **2-7**. $[\alpha]^{24}_D$: +9.1° (*c* 1.0, CH_2Cl_2); IR (thin film) 2917, 1721, 1452, 1270, 1097, 1070, 698 cm^{-1}; ^1H NMR ($CDCl_3$) δ 7.98-7.92 (m, 4H), 7.49-7.31 (m, 4H), 7.25-6.95 (m, 36H), 6.86-6.83 (m, 1H), 5.64-5.55 (m, 2H), 5.42-5.40 (m, 1H), 5.11 (s, 1H), 4.85-4.73 (m, 5H), 4.62-4.40 (m, 10H), 4.35-4.16 (m, 5H), 4.03-3.65 (m, 12H), 3.53-3.46 (m, 2H), 3.27-3.21 (m, 2H), 1.97 (s, 3H), 1.94-1.88 (m, 2H), 1.51-1.42 (m, 2H); ^{13}C NMR ($CDCl_3$) δ 170.4, 166.8, 166.0, 139.0, 139.0, 138.8, 138.6, 138.3, 138.3, 137.9, 133.5, 133.3, 130.5, 130.5, 130.2, 128.9,

128.9, 128.8, 128.8, 128.7, 128.7, 128.6, 128.5, 128.4, 128.2, 128.2, 128.1, 128.0, 127.8, 127.7, 127.6, 115.2, 101.9, 100.1, 98.6, 80.7, 78.4, 77.8, 77.1, 76.1, 75.7, 75.5, 75.4, 75.2, 74.8, 74.6, 74.4, 73.8, 73.6, 72.5, 72.5, 72.5, 70.4, 69.6, 69.4, 69.3, 66.5, 64.0, 30.6, 29.3, 21.5; ESI MS *m/z* ($M + Na^+$) calcd 1475.6130, found 1475.6141.

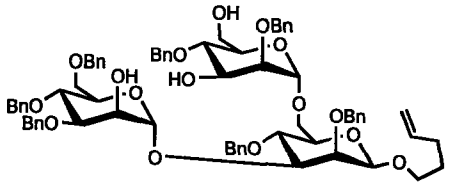

2-17

4-Pentenyl 3,4,6-tri-*O*-benzyl-α-D-mannopyranosyl-(1→3)-[2,4-di-*O*-benzyl-α-D-mannopyranosyl-(1→6)]-2,4-di-*O*-benzyl-β-D-mannopyranoside 2-17. Trisaccharide **2-7** (100 mg, 0.0687 mmol) was dissolved in CH_2Cl_2:MeOH (4 mL, 1:1). A solution of sodium methoxide in MeOH (450 μL, 25% w/v, 2 mmol) was added and the reaction was heated on an oil-bath to 45 °C for 1.5 h. The reaction was quenched with DOWEX-50W-hydrogen strongly acidic ion-exchange resin, filtered, and dried *in vacuo*. The resulting crude product was purified by flash column chromatography on silica gel (10 → 40% EtOAC/toluene) to afford 73.2 mg (89%) of trisaccharide **2-17**. $[\alpha]^{24}_D$: 11.0° (*c* 1.3, CH_2Cl_2); IR (thin film) 3470, 2922, 1453, 1364, 1072, 697 cm^{-1}; ^1H NMR ($CDCl_3$) δ 7.30-7.05 (m, 35H), 5.72-5.61 (m, 1H), 5.18 (d, *J* = 1.2 Hz, 1H), 5.11 (d, *J* = 0.97 Hz, 1H), 4.91-4.83 (m, 4H), 4.76-4.64 (m, 3H), 4.58-4.25 (m, 10H) 3.92-3.86 (m, 3H), 3.83-3.55 (m, 13H), 3.54-3.49 (m, 2H), 3.29-3.20 (m, 2H), 2.23 (bs, 2H), 2.00-1.94 (m, 2H), 1.84 (bs, 1H), 1.56-1.50 (m, 2H); ^{13}C NMR ($CDCl_3$) δ 139.0, 138.9, 138.9, 138.6, 138.4, 138.4, 138.4, 138.2, 138.2, 129.0, 129.0, 128.9, 128.8, 128.7, 128.7, 128.6, 128.4, 128.3, 128.3, 128.1, 128.1, 128.1, 128.1, 128.0, 127.9, 127.9, 127.8, 115.3, 102.1, 101.7, 98.0, 80.6, 80.3, 79.1, 77.9, 77.6, 76.9, 76.1, 75.7, 75.4, 75.2, 73.7, 73.0, 72.6, 72.2, 72.2, 71.7, 69.7, 69.4, 69.1, 66.5, 62.7, 30.6, 29.3; ESI MS *m/z* ($M + Na^+$) calcd 1225.5500, found 1225.5497.

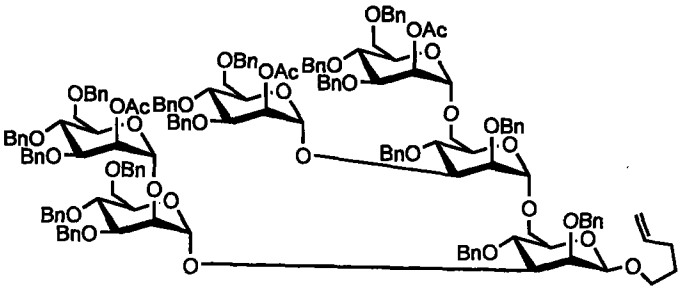

2-6

4-Pentenyl 2-*O*-acetyl-3,4,6-tri-*O*-benzyl-α-D-mannopyranosyl-(1→2)-3,4,6-tri-*O*-benzyl-α-D-mannopyranosyl-(1→3)-[2-*O*-acetyl-3,4,6-tri-*O*-benzyl-α-D-mannopyranosyl-(1→3)-[2-*O*-acetyl-3,4,6-tri-*O*-benzyl-α-D-mannopyranosyl-(1→6)]-2,4-di-*O*-benzyl-α-D-mannopyranosyl-(1→6)]-2,4-di-*O*-benzyl-β-D-mannopyranoside 2-6. Trisaccharide acceptor **2-17** (25 mg, 0.0207 mmol) and mannosyl trichloroacetimidate **2-9** (60 mg, 0.093 mmol, 4.5 eq) were combined, azeotropically dried with toluene (3 x 3 mL) and dissolved in CH_2Cl_2 (2 mL). The solution was cooled to –20 °C for 15 min, followed by the addition of TMSOTf (2.2 μL, 0.0123 mmol). The reaction mixture was stirred and warmed to room temperature over 40 min. The reaction was quenched by the addition of Et_3N (100 μL), and dried *in vacuo*. The crude product was purified by flash column chromatography on silica gel (2 → 20% EtOAc/toluene) to afford 51.3 mg (94%) of hexasaccharide **2-6**. $[\alpha]^{24}_D$: +34.9° (*c* 1.3, CH_2Cl_2); IR (thin film) 3029, 2916, 1744, 1235, 1076, 736, 697 cm^{-1}; ^1H NMR ($CDCl_3$) δ 7.40-7.10 (m, 80H), 5.77-5.70 (m, 1H), 5.53-5.52 (m, 3H), 5.24-5.20 (m, 2H), 5.03-4.98 (m, 3H), 4.94-4.90 (m, 3H), 4.89-4.81 (m, 5H), 4.76 (d, J = 2.3 Hz, 1H), 4.73 (app. s, 1H), 4.68-4.61 (m, 6H), 4.59-4.53 (m, 6H), 4.50-4.39 (m, 10H), 4.37-4.34 (m, 1H), 4.28-4.23 (m, 2H), 4.13-4.09 (m, 1H), 4.07-4.00 (m, 2H), 3.99-3.89 (m, 10H), 3.87-3.78 (m, 6H), 3.72-3.67 (m, 6H), 3.62-3.54 (m, 7H), 3.36-3.30 (m, 2H), 3.22-3.19 (m, 1H), 2.16 (s, 3H), 2.13 (s, 3H), 2.09 (s, 3H), 2.04-2.01 (m, 2H), 1.60-1.56 (m, 2H); ^{13}C NMR ($CDCl_3$) δ 170.4, 170.3, 170.3, 139.0, 138.9, 138.8, 138.7, 138.5, 138.5, 138.5, 138.4, 138.4, 138.3, 138.2, 138.0, 138.0, 129.2, 128.7, 128.7, 128.6, 128.6, 128.5, 128.5, 128.5, 128.4, 128.4, 128.4, 128.4, 128.3, 128.3, 128.2, 128.1, 128.0, 128.0, 127.9, 127.9, 127.9, 127.8, 127.8, 127.7, 127.7, 127.7, 127.7, 127.6, 127.6, 127.6, 127.6, 127.5, 127.5, 127.4, 127.4, 114.9, 101.7, 101.2, 100.0, 99.6, 98.4, 97.0, 81.7, 79.8, 78.4, 78.2, 77.8,

77.6, 77.5, 75.4, 75.3, 75.2, 75.2, 75.0, 74.9, 74.7, 74.2, 74.1, 73.6, 73.5, 73.4, 73.4, 72.6, 72.4, 72.3, 72.1, 72.0, 72.0, 72.0, 71.7, 71.4, 71.0, 69.5, 69.4, 69.0, 68.8, 68.7, 68.4, 66.3, 66.1, 31.0, 29.6, 21.9, 21.8; HSQC anomeric cross-peaks ($CDCl_3$) δ (5.22 x 101.1), (5.21 x 99.9), (5.06 x 99.5), (5.02 x 98.4), (4.93 x 97.0), (4.23 x 101.8); ESI MS *m/z* (M + Na^+) calcd 2648.1622, found 2648.1530.

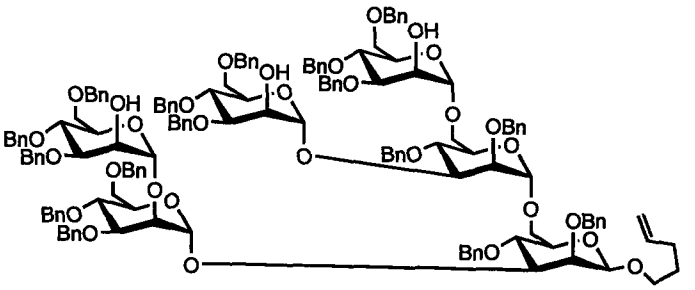

2-18

4-Pentenyl 3,4,6-tri-*O*-benzyl-α-D-mannopyranosyl-(1→2)-3,4,6-tri-*O*-benzyl-α-D-mannopyranosyl-(1→3)-[3,4,6-tri-*O*-benzyl-α-D-mannopyranosyl-(1→3)-[3,4,6-tri-*O*-benzyl-α-D-mannopyranosyl-(1→6)]-2,4-di-*O*-benzyl-α-D-mannopyranosyl-(1→6)]-2,4-di-*O*-benzyl-β-D-mannopyranoside 2-18. Hexasaccharide **2-6** (46 mg, 0.0175 mmol) was azeotropically dried with toluene (3 x 3 mL) and dissolved in CH_2Cl_2 (1.5 mL). MeOH (5 mL) was added followed by a solution of sodium methoxide in MeOH (120 μL, 25% w/v, 0.525 mmol). The reaction was stirred for 1 h, quenched with DOWEX-50W-hydrogen strongly acidic ion-exchange resin, filtered, and dried *in vacuo*. The resulting residue was purified by flash column chromatography on silica gel (5 → 20% EtOAc/toluene) to afford 45.7 mg (quant.) of hexasaccharide triol **2-18**. $[\alpha]^{24}_D$: +34.3° (*c* 1.0, CH_2Cl_2); IR (thin film) 3448, 3029, 2916, 1453, 1053, 697 cm^{-1}; ^1H NMR ($CDCl_3$) δ 7.48-6.81 (m, 80H), 5.67-5.57 (m, 1H), 5.16 (app. s, 1H), 5.11 (app. s, 1H), 5.02 (app. s, 1H), 4.97-4.86 (m, 2H), 4.83-4.78 (m, 3H), 4.75-4.69 (m, 5H), 4.65-4.53 (m, 4H), 4.51-4.45 (m, 12H), 4.40-4.35 (m, 8H), 4.30-4.22 (m, 3H), 4.13 (app. s, 1H), 4.02-3.99 (m, 4H), 3.92-3.82 (m, 3H), 3.81-3.64 (m, 14H), 3.62-3.43 (m, 13H), 3.36-3.33 (m, 1H), 3.24-3.19 (m, 1H), 3.13-3.10 (m, 1H), 2.28-2.07 (bs, 3H), 1.95-1.89 (m, 2H), 1.53-1.43 (m, 2H); ^{13}C NMR ($CDCl_3$) δ 139.5, 139.4, 139.3, 139.1, 139.0, 139.0, 138.9, 138.8, 138.8, 138.7, 138.7, 138.6, 129.3, 139.2, 129.1, 129.1, 129.1, 129.0, 129.0, 129.0, 128.9,

128.9, 128.8, 128.6, 128.6, 128.5, 128.5, 128.4, 128.4, 128.4, 128.3, 128.3.128.2, 128.1, 128.1, 128.0, 127.9, 115.4, 102.1, 102.1, 101.8, 101.8, 100.5, 97.5, 82.5, 80.8, 80.5, 80.3, 78.5, 78.4, 77.9, 76.2, 75.9, 75.8, 75.7, 75.5, 75.4, 75.2, 74.9, 74.9, 74.6, 74.2, 74.1, 74.0, 73.9, 73.2, 73.0, 72.8, 72.7, 72.6, 72.5, 72.3, 72.0, 72.0, 71.9, 70.1, 69.9, 69.7, 69.5, 69.4, 22.2, 21.8, 14.9; ESI MS *m/z* ($M + Na^+$) calcd 2522.1305, found 2522.1307.

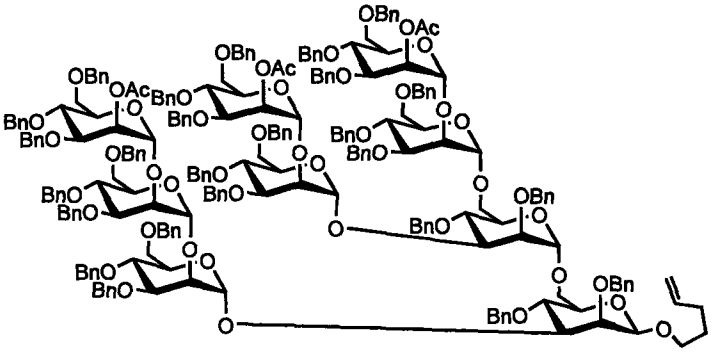

2-5

4-Pentenyl 2-*O*-acetyl-3,4,6-tri-*O*-benzyl-α-D-mannopyranosyl-(1→2)-3,4,6-tri-*O*-benzyl-α-D-mannopyranosyl-(1→2)-3,4,6-tri-*O*-benzyl-α-D-mannopyranosyl-(1→3)-[2-*O*-acetyl-3,4,6-tri-*O*-benzyl-α-D-mannopyranosyl-(1→2)-3,4,6-tri-*O*-benzyl-α-D-mannopyranosyl-(1→3)-[2-*O*-acetyl-3,4,6-tri-*O*-benzyl-α-D-mannopyranosyl-(1→2)-3,4,6-tri-*O*-benzyl-α-D-mannopyranosyl-(1→6)]-2,4-di-*O*-benzyl-α-D-mannopyranosyl-(1→6)]-2,4-di-*O*-benzyl-β-D-mannopyranoside 2-5. Hexasaccharide **2-18** (19 mg, 0.0075 mmol) and mannosyl trichloroacetimidate **2-9** (36 mg, 0.0561 mmol, 7.5 eq) were azeotropically dried with toluene (3 x 3 mL), dried an additional 1.5 h *in vacuo* and dissolved in diethyl ether (2mL). The solution was cooled to –20 °C for 15 min, followed by the addition of TMSOTf (1 μL, 0.005 mmol), and stirred for 30 min. The reaction was quenched by the addition of Et_3N (50 μL), and dried *in vacuo*. The crude product was purified by flash column chromatography on silica gel (2 → 18% EtOAc/toluene) affording 24 mg (80%) of nonasaccharide **2-5**. $[\alpha]^{24}_D$: +24.7° (*c* 0.9, CH_2Cl_2); IR (thin film) 3029, 2864, 1744, 1453, 1137, 1056, 736, 697 cm^{-1}; ^1H NMR ($CDCl_3$) δ 7.34-7.07 (m, 124H), 7.02-7.00 (m, 1H), 5.69-5.60 (m, 1H), 5.55-5.52 (m, 4H), 5.24-5.23 (m, 1H), 5.17 (m, 1H), 5.14 (m, 1H), 5.11-5.08 (m, 3H), 5.00-4.95 (m, 2H), 4.89-4.80 (m, 7H), 4.77-4.74 (m, 2H), 4.73-4.71 (m, 1H), 4.68-4.63 (m, 4H), 4.61-

4.60 (m, 2H), 4.58-4.56 (m, 4H), 4.55-4.54 (m, 6H), 4.51-4.45 (m, 9H), 4.43-4.30 (m, 12H), 4.22-4.16 (m, 3H), 4.13-4.08 (m, 4H), 4.06-3.97 (m, 5H), 3.94-3.82 (m, 21H), 3.78-3.73 (m, 4H), 3.67-3.55 (m, 10H), 3.52-3.50 (m, 3H), 3.46-3.35 (m, 5H), 3.30-3.26 (m, 1H), 3.18-3.13 (m, 2H), 2.13 (s, 3H), 2.12 (s, 3H), 2.08 (s, 3H), 1.98-1.94 (m, 2H), 1.55-1.48 (m, 2H); ^{13}C NMR ($CDCl_3$) δ 171.1, 171.0, 171.0, 132.5, 131.3, 130.3, 129.8, 129.3, 128.7, 128.3, 128.0, 128.0, 127.3, 126.6, 126.7, 126.2, 125.7, 115.0, 101.4, 101.4, 101.1, 100.7, 99.7, 99.5, 99.5, 99.3, 97.0, 82.2, 80.1, 79.9, 79.5, 79.2, 79.1, 78.4, 78.3, 77.4, 75.5, 75.4, 75.4, 75.2, 75.2, 75.2, 74.9, 74.9, 74.2, 73.5, 73.5, 73.4, 73.3, 73.3, 72.7, 72.8, 72.3, 72.2, 72.1, 72.0, 72.0, 71.9, 71.4, 71.4, 70.9, 70.8, 70.5, 69.4, 69.2, 69.2, 69.2, 69.0, 68.9, 68.8, 68.8, 68.8, 68.2, 68.2, 66.7, 66.6, 66.6, 66.6, 30.3, 29.1, 22.0, 21.3, 21.0, 20.5; HSQC anomeric cross-peaks ($CDCl_3$) δ (5.21 x 101.3), (5.18 x 101.2), (5.12 x 100.7), three (5.10 x 99.6), (5.00 x 99.6), (4.86 x 97.0), (4.16 x 102.0); ESI MS *m/z* (M + Na^+) calcd 3944.7437, found 3944.7440.

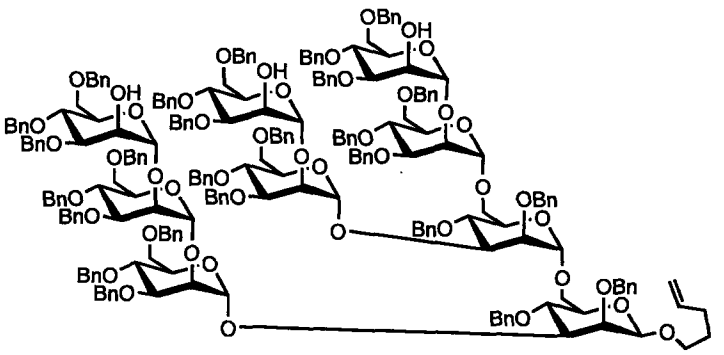

2-19

4-Pentenyl 3,4,6-tri-*O*-benzyl-α-D-mannopyranosyl-(1→2)-3,4,6-tri-*O*-benzyl-α-D-mannopyranosyl-(1→2)-3,4,6-tri-*O*-benzyl-α-D-mannopyranosyl-(1→3)-[3,4,6-tri-*O*-benzyl-α-D-mannopyranosyl-(1→2)-3,4,6-tri-*O*-benzyl-α-D-mannopyranosyl-(1→3)-[3,4,6-tri-*O*-benzyl-α-D-mannopyranosyl-(1→2)-3,4,6-tri-*O*-benzyl-α-D-mannopyranosyl-(1→6)]-2,4-di-*O*-benzyl-α-D-mannopyranosyl-(1→6)]-2,4-di-*O*-benzyl-β-D-mannopyranoside 2-19. Nonasaccharide **2-5** (14 mg, 0.0035 mmol) was dissolved in a mixture of CH_2Cl_2:MeOH (3 mL, 1:2) and cooled to 0 °C. A solution of sodium methoxide in MeOH (35 μL, 25% w/v) was added and the reaction was slowly warmed to room temperature over 1 h, quenched with DOWEX-50W-hydrogen strongly

acidic ion-exchange resin, filtered, and dried *in vacuo*. The resulting residue was purified by flash column chromatography on silica gel (5 → 30% EtOAc/toluene) affording 12 mg (90%) of nonasaccharide triol **2-19**. ^{1}H NMR ($CDCl_3$) δ 7.44-6.92 (m, 125H), 5.6-5.51 (m, 1H), 5.13 (m, 2H), 5.09-5.08 (m, 3H), 5.02 (app. s, 1H), 4.94 (app. s, 1H), 4.79 (d, J = 10.5 Hz, 1H), 4.77-4.70 (m, 9H), 4.66-4.28 (m, 41H), 4.27-3.30 (m, 56H), 3.27-3.07 (m, 3H), 2.29 (bs, 2H), 2.23 (bs, 1H), 1.88-1.85 (m, 2H), 1.43-1.37 (m, 2H).

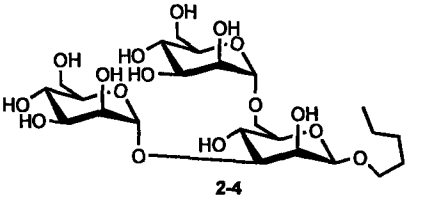

2-4

***n*-Pentyl α-D-mannopyranosyl-(1→3)-[α-D-mannopyranosyl-(1→6)]-β-D-mannopyranoside 2-4.** Activated palladium on carbon (100 mg, 10%) was suspended in ethanol (10 mL) and exposed to an atmosphere of hydrogen gas (balloon). After 30 min, trisaccharide triol **2-17** (70 mg, 0.0581 mmol) in EtOAc (5 mL) was added by cannula and stirred for 48 h under an atmosphere of hydrogen. The product was filtered through celite, dried *in vacuo*, to afford 6 mg (79%) trisaccharide **2-4**. $[\alpha]^{24}_D$: +35.0° (*c* 0.4, H_2O:EtOH 1:1); ^{1}H NMR (D_2O) δ 4.94 (app. s, 1H), 4.75 (app. s, 1H), 4.52 (app. s, 1H), 3.98 (d, J = 1.6 Hz, 1H), 3.91-3.90 (m, 1H), 3.83-3.47 (m, 19H), 3.40-3.37 (m, 1H), 1.46-1.43 (m, 2H), 1.17-1.15 (m, 4H), 0.73-0.70 (m, 3H); ^{13}C NMR (D_2O) δ 102.7, 100.0, 99.7, 81.1, 74.4, 73.6, 72.9, 70.7, 70.6, 70.4, 70.3, 70.2, 67.1, 67.0, 66.1, 65.8, 61.2, 28.7, 27.7, 22.1, 13.6; MALDI-TOF *m/z* ($M + Na^+$) calcd 595.22, found 596.77.

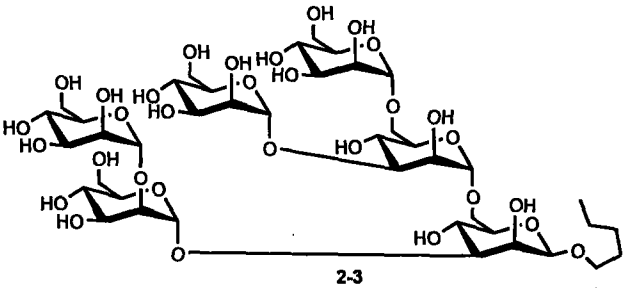

2-3

***n*-Pentyl α-D-mannopyranosyl-(1→2)-α-D-mannopyranosyl-(1→3)-[α-D-mannopyranosyl-(1→3)-[α-D-mannopyranosyl-(1→6)]-α-D-mannopyranosyl-**

(1→6)]-β-D-mannopyranoside 2-3. Activated palladium on carbon (50 mg, 10%) was suspended in ethanol (5 mL) and exposed to an atmosphere of hydrogen gas (balloon). After 30 min, hexasaccharide triol **2-18** (35 mg, 0.0139 mmol) in EtOAc (2 mL) was added by cannula and stirred for 48 h under an atmosphere of hydrogen. The product was filtered through celite, dried *in vacuo*, to afford 12 mg (81%) hexasaccharide **2-3**. $[\alpha]^{24}_{D}$: +54.5° (*c* 0.5, H_2O:EtOH 1:1); ^1H NMR (D_2O) δ 5.19 (app. s, 1H), 4.98 (app. S, 1H), 4.89 (app. s, 1H), 4.75 (app. s, 1H), 4.72 (app. s, 1H), 4.51 (app. s, 1H), 4.00 (app. s, 1H), 3.97-3.96 (m, 2H), 3.92-3.89 (m, 2H), 3.89-3.46 (m, 33H), 3.43-3.38 (m, 1H), 1.46-1.43 (m, 2H), 1.17-1.15 (m, 4H), 0.74-0.70 (m, 3H); MALDI-TOF *m/z* ($M + Na^+$) calcd 1081.38, found 1082.54.

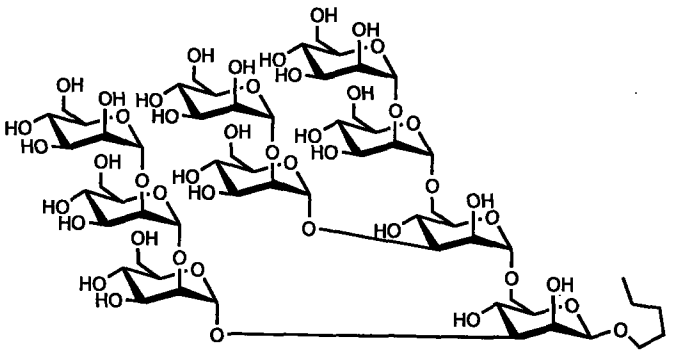

2-2

***n*-Pentyl α-D-mannopyranosyl-(1→2)-α-D-mannopyranosyl-(1→2)-α-D-mannopyranosyl-(1→3)-[α-D-mannopyranosyl-(1→2)-α-D-mannopyranosyl-(1→3)-[α-D-mannopyranosyl-(1→2)-α-D-mannopyranosyl-(1→6)]-α-D-mannopyranosyl-(1→6)]-β-D-mannopyranoside 2-2.** Activated palladium on carbon (50 mg, 10%) was suspended in ethanol (5 mL) and exposed to an atmosphere of hydrogen gas (balloon). After 30 min, nonasaccharide triol **2-19** (12 mg, 0.0031 mmol) in EtOAc (2 mL) was added by cannula and stirred for 48 h under an atmosphere of hydrogen. The product was separated by filtration through celite and dried *in vacuo* to yield 4.2 mg (88%) of fully deprotected nonasaccharide **2-2**. $[\alpha]^{24}_{D}$: +38.0° (*c* 0.05, H_2O:EtOH 1:1); ^1H NMR (D_2O) δ 5.26 (app. s, 1H), 5.19 (app. s, 1H), 5.16 (app. s, 1H), 5.00 (app. s, 1H), 4.89 (app. s, 3H), 4.72 (app. s, 1H), 4.51 (app. s, 1H), 4.00 (app. s, 1H), 3.99-3.91 (m, 7H), 3.87-3.84 (m, 4H), 3.82-3.79 (m, 3H), 3.76-3.73 (m, 6H), 3.72-3.68 (m, 6H), 3.66-3.58

(m, 12H), 3.57-3.52 (m, 5H), 3.52-3.46 (m, 5H), 3.40-3.38 (m, 1H), 1.46-1.44 (m, 2H), 1.18-1.16 (m, 5H), 0.74-0.71 (m, 3H); ^{13}C NMR (D_2O) δ 102.4, 102.4, 102.4, 100.9, 100.8, 100.8, 99.9, 99.7, 98.2, 79.1, 78.8, 78.8, 78.6, 74.2, 73.3, 73.3, 72.8, 71.2, 70.5, 70.3, 70.3, 70.3, 70.3, 70.3, 70.1, 69.7, 67.1, 66.9, 65.9, 65.7, 65.7, 65.7, 65.6, 65.6, 61.2, 61.2, 61.1, 61.1, 28.4, 27.5, 23.3, 21.9, 13.4; HSQC anomeric cross-peaks (D_2O) δ (5.26 x 100.9), (5.19 x 100.8), (5.16 x 100.8), (5.00 x 98.1), three (4.89 x 102.4), (4.72 x 99.8), (4.51 x 99.9); MALDI-TOF *m/z* ($M + Na^+$) calcd 1567.54, found 1569.09.

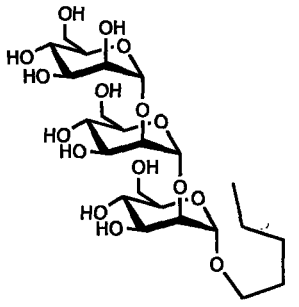

2-20

***n*-Pentyl α-D-mannopyranosyl-(1→2)-α-D-mannopyranosyl-(1→2)-α-D-mannopyranoside 2-20.** Trisaccharide **2-21** (90 mg, 0.0631 mmol) was dissolved in a mixture of CH_2Cl_2:MeOH (3 mL, 1:2) and cooled to 0 °C. A solution of sodium methoxide in MeOH (35 μL, 25% w/v) was added and the reaction was slowly warmed to room temperature over 1 h, quenched with DOWEX-50W-hydrogen strongly acidic ion-exchange resin, filtered, and dried *in vacuo*. The resulting residue was purified by flash column chromatography on silica gel (5 → 15% EtOAc/toluene) affording 80 mg (92%) of trisaccharide 4-Pentenyl 3,4,6-tri-*O*-benzyl-α-D-mannopyranosyl-(1→2)-3,4,6-tri-*O*-benzyl-α-D-mannopyranosyl-(1→2)-3,4,6-tri-*O*-benzyl-α-D-mannopyranoside. (See Chapter 2, ref. 6b for characterization) Activated palladium on carbon (50 mg, 10%) was suspended in ethanol (5 mL) and exposed to an atmosphere of hydrogen gas (balloon). After 30 min, the deacetylated trisaccharide (55 mg, 0.0397 mmol) in EtOAc (2 mL) was added by cannula and stirred for 48 h under an atmosphere of hydrogen. The product was filtered through celite, dried *in vacuo*, to afford 22.8 mg (96%) trisaccharide **2-20**. $[\alpha]^{24}_D$: +19.0° (*c* 0.09, H_2O:EtOH 1:1) ^1H NMR (D_2O) δ 5.28 (app. s, 1H), 5.06 (app. s, 1H), 4.98 (app. s, 1H), 4.04-4.02 (m, 1H), 3.98-3.96 (m, 1H), 3.89-3.79 (m, 6H), 3.76-

3.62 (m, 5H), 3.61-3.47 (m, 5H), 3.46-3.39 (m, 1H), 3.32-3.30 (m, 1H), 1.90 (app. s, 1H), 1.62-1.56 (m, 2H), 1.38-1.33 (m, 4H), 0.94-0.89 (m, 2H); ^{13}C NMR ($CDCl_3$) δ 104.3, 102.7, 100.0, 81.1, 80.5, 75.1, 74.7, 72.6, 72.3, 72.0, 69.4, 69.2, 68.9, 68.8, 63.4, 63.3, 63.2, 30.5, 29.8, 23.7, 14.6; MALDI-TOF *m/z* ($M + Na^+$) calcd 597.25, found 596.99.

6.3 Experimentals for Chapter 3

3-7

***tert*-Butyldimethylsilyl 3,6-di-*O*-benzyl-2-deoxy-2-trichloroacetimido-β-D-glucopyranoside 3-7.** Differentially protected glucosamine **3-13** (5.5 g, 8.9 mmol) was dissolved in CH_2Cl_2 (60 mL) and cooled to 0°C. Triethylsilane (8.5 mL, 53.5 mmol) was added and the resulting mixture was stirred for 10 min. Trifluoromethanesulfonic acid (3.4 mL, 44.5 mmol) and trifluoromethanesulfonic acid anhydride (1.3 mL, 8.9 mmol) were added simultaneously to the cooled solution and the mixture was stirred at 0°C for 30 min. The solution was warmed slowly to room temperature over a period of 1 h. The reaction mixture was poured into a saturated aqueous solution of Na_2CO_3. The aqueous layer was extracted with CH_2Cl_2 (2 x 20 mL) and the organic layer was dried over $NaSO_4$, filtered, and solvents removed *in vacuo*. Purification by flash silica column chromatography (10%→25% EtOAc/hexanes) afforded **3-7** as an oil (3.47 g, 63% yield). $[\alpha]^{24}_D$: -13.4° (*c* 1.8, CH_2Cl_2); IR (thin film) 2929, 2858, 1692, 1529, 1070, 838 cm^{-1}; ^1H NMR (400 MHz, $CDCl_3$) δ 7.40-7.27 (m, 10H), 6.99 (d, J = 8.1 Hz, 1H), 5.05 (d, J = 7.8 Hz, 1H), 4.83-4.76 (m, 2H), 4.64-4.57 (m, 2H), 3.95 (dd, J = 8.6, 10.5 Hz, 1H), 3.76-3.71 (m, 3H), 3.62-3.55 (m, 2H), 2.92 (s, 1H), 0.92 (s, 9H), 0.16 (s, 3H), 0.13 (s, 3H); ^{13}C NMR (400 MHz, $CDCl_3$) δ 161.9, 138.2, 137.8, 128.7, 128.6, 128.2, 128.0, 128.0, 127.8, 94.9, 92.7, 79.8, 74.4, 74.0, 73.8, 73.3, 70.7, 60.1, 25.8, 18.0, -4.0, -5.0; ESI MS *m/z* ($M^+ + Na^+$) calcd 640.1426, found 640.1400.

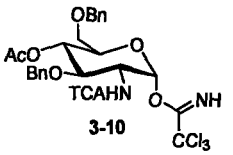

3-10

4-*O*-Acetyl-3,6-di-*O*-benzyl-2-deoxy-2-trichloroacetimido-α-D-glucopyranosyl trichloroacetimidate 3-10. A solution of **3-7** (1.06 g, 1.71 mmol) in CH_2Cl_2 (20 mL) was cooled to 0°C. Acetic anhydride (0.24 mL, 2.57 mmol) was added and the resulting solution was stirred for 5 min. Dimethylaminopyridine (314 mg, 2.57 mmol) was added and the reaction was allowed to warm slowly to room temperature while stirring overnight. The mixture was diluted with CH_2Cl_2 (30 mL) and the organic layer was washed with 5% HCl (2 x 30 mL). The organic layer was dried over Na_2SO_4, filtered, and solvents removed in vacuo to afford *tert*-butyldimethylsilyl 3,6-di-*O*-benzyl-2-deoxy-4-*O*-acetyl-2-trichloroacetimido-β-D-glucopyranoside (1.13 g, 99%). $[\alpha]^{24}_D$: +9.0° (*c* 1.7, CH_2Cl_2); IR (thin film) 3354, 1715, 1527, 1249, 1067 cm^{-1}; ^1H NMR (400 MHz, $CDCl_3$) δ 7.35-7.25 (m, 10H), 7.12 (d, J = 7.7 Hz, 1H), 5.20 (d, J = 7.8 Hz, 1H), 5.09 (Ψt, J = 9.4 Hz, 1H), 4.69 (d, J = 11.1 Hz, 1H), 4.59 (d, J = 11.1 Hz, 1H), 4.54 (s, 2H), 4.29 (Ψt, J = 10.3 Hz, 3H), 3.71-3.69 (m, 1H), 3.58-3.52 (m, 1H), 1.89 (s, 3H), 0.92 (s, 9H), 0.18 (s, 3H), 0.15 (s, 3H); ^{13}C NMR (100 MHz, $CDCl_3$) δ 169.9, 161.9, 138.0, 137.8, 128.6, 128.4, 128.0, 127.8, 127.8, 94.3, 92.7, 77.4, 74.1, 73.6, 73.4, 71.8, 69.8, 60.8, 25.8, 21.0, 18.0, -4.0, -5.1; ESI MS *m/z* (M^+ + Na^+) calcd 682.1532, found 682.1543. A solution *tert*-butyldimethylsilyl 3,6-di-*O*-benzyl-2-deoxy-4-*O*-acetyl-2-trichloroacetimido-β-D-glucopyranoside (1.13 g, 1.71 mmol) in THF (18 mL) was cooled to 0°C. Acetic acid (0.15 mL, 2.68 mmol) and then tetrabutylammonium fluoride (1.0 M in THF, 2.68 mL, 2.68 mmol) were added to the cooled solution. The reaction mixture was allowed to warm slowly to room temperature while stirring overnight. The reaction mixture was diluted with EtOAc and washed with $NaHCO_3$ (2 x 30 mL) and H_2O (1 x 30 mL). The organic layer was dried over Na_2SO_4, filtered, and solvents removed *in vacuo*. The crude material (887 mg, 1.62 mmol) was dissolved in CH_2Cl_2 (16 mL) and trichloroacetonitrile (4 mL). After stirring for 5 min, DBU (49 μL, 0.32 mmol) was added and the reaction mixture was allowed to stir for 1.5 h. The reaction mixture was passed through a silica plug, washed with EtOAc and solvents removed *in vacuo*. Purification by flash silica column chromatography (25% EtOAc/hexanes) afforded **3-10**

(942 mg, 76% two steps, 95:5 α:β). IR (thin film) 1747, 1722, 1678, 1514,1226, 1036 cm^{-1}; ^1H NMR (400 MHz, $CDCl_3$) δ 8.79 (s, 1H), 7.37-7.27 (m, 10H), 6.60 (d, J = 8.5 Hz, 1H), 6.49 (d, J = 3.5 Hz, 1H), 5.41 (Ψt, J = 9.7 Hz, 1H), 4.70-4.64 (m, 2H), 4.57-4.45 (m, 3H), 4.10-4.02 (m, 2H), 3.63-3.55 (m, 2H), 1.97 (s, 3H); ^{13}C NMR (100 MHz, $CDCl_3$) δ 169.3, 161.8, 159.9, 137.6, 137.0, 128.8, 128.4, 128.4, 128.3, 128.1, 127.8, 94.3, 92.1, 90.7, 76.0, 73.6, 73.0, 72.1, 69.9, 68.4, 53.5, 20.9; ESI MS *m/z* ($M^+ + Na^+$) calcd 710.9763, found 710.9762.

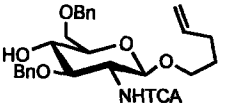

3-3

4-Pentenyl 3,6-di-*O*-benzyl-2-deoxy-2-trichloroacetimido-β-D-glucopyranoside 3-3. **3-10** (691 mg, 1.0 mmol) was coevaporated with toluene (3 x 5 mL) and dried under vacuum for 1 h. Donor **3-10** was dissolved in CH_2Cl_2 (10 mL) and cooled to -40°C. 4-penten-1-ol (0.15 mL, 1.5 mmol) was added and the resulting solution was stirred for 5 min. TMSOTf (18 μL, 0.1 mmol) was added and the mixture was stirred at -40°C for 15 min. The reaction was quenched by the addition of triethylamine (0.1 mL) and solvents removed in vacuo. Purification by flash silica column chromatography (20% EtOAc/hexanes) afforded an oil. The oil (633 mg, 1.0 mmol) was dissolved in MeOH (10 mL) and NaOMe (25% v/w, 23 μL, 0.1 mmol) was added. The mixture was stirred for 1.5 h at room temperature. Amberlite IR-120(plus) resin was added until pH 7 was reached. The reaction mixture was filtered, solvents removed in vacuo and purification by flash silica column chromatography (20% EtOAc/hexanes) afforded **3-3** (539 mg, 94%). $[\alpha]^{24}_D$: -14.1° (*c* 1.2, CH_2Cl_2); IR (thin film) 3325, 1690, 1641, 1532, 1124, 1067 cm^{-1}; ^1H NMR (400 MHz, $CDCl_3$) δ 7.39-7.28 (m, 10H), 6.94 (2, J = 7.5 Hz, 1H), 5.83-5.73 (m, 1H), 5.03-4.94 (m, 2H), 4.90 (d, J = 8.2 Hz, 1H), 4.81 (d, J = 11.2 Hz, 1H), 4.76 (d, J = 11.2 Hz, 1H), 4.64 (d, J = 12.0 Hz, 2H), 4.58 (d, J = 12.0 Hz, 1H), 4.05 (dd, J = 8.5, 10.4 Hz, 1H), 3.91-3.85 (m, 1H), 3.81-3.70 (m, 3H), 3.57-3.41 (m, 3H), 2.80 (s, 1H), 2.13-2.06 (m, 2H), 1.70-1.62 (m, 2H); ^{13}C NMR (100 MHz, $CDCl_3$) δ 162.0, 138.2, 138.1, 137.7, 128.8, 128.7, 128.3, 128.2, 128.1, 128.0, 115.2, 99.4, 92.7, 79.6, 75.0, 74.0,

73.9, 73.7, 70.7, 69.5, 58.7, 30.2, 28.9; ESI MS *m/z* ($M^+ + Na^+$) calcd 594.1187, found 594.1175.

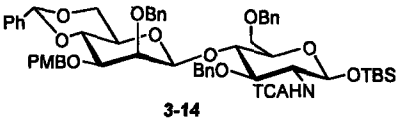

3-14

***tert*-butyldimethylsilyl 2-*O*-benzyl-4,6-*O*-benzylidene-3-*O*-*p*-methoxybenzyl-β-D-mannopyranosyl-(1→4)-3,6-di-*O*-benzyl-2-deoxy-2-trichloroacetimido-β-D-glucopyranoside 3-14.** Phenyl sulfoxide **3-6** (1.50 g, 2.56 mmol) and **3-7** (2.53 g, 4.09 mmol) were coevaporated separately (important!) with toluene (3 x 10 mL) and dried under vacuum overnight. Sulfoxide **3-6** was dissolved in CH_2Cl_2 (26 mL) and cooled to -78°C. Di-*t*-butyl pyridine (1.15 mL, 5.12 mmol) was added to the cooled solution and stirred for 10 min. Triflic anhydride (474 μL, 2.82 mmol) was added and the mixture was stirred for 5 min, during which time the colorless mixture turned orange. A solution of **3-7** in CH_2Cl_2 (10 mL) was slowly added to the reaction mixture via cannula and the reaction was stirred at -78°C for 1 h. The reaction was quenched with saturated $NaHCO_3$ (20 mL) and diluted with CH_2Cl_2 (30 mL). The organic layer was were washed with $NaHCO_3$ (2 x 30 mL), dried over Na_2SO_4, filtered, and solvents removed *in vacuo*. Purification by flash silica column chromatography (100% toluene → 25% EtOAc/toluene) afforded **3-14** (1.77 g, 68%). $[\alpha]^{24}_D$: -25.7° (*c* 3.1, CH_2Cl_2); IR (thin film) 3322, 2861, 1691, 1531, 1089 cm^{-1}; ^1H NMR (400 MHz, $CDCl_3$) δ 7.51-7.18 (m, 22H), 6.97 (d, J = 7.5 Hz, 1H), 6.87-6.85 (m, 2H), 5.54 (s, 1H), 5.19 (d, J = 7.7 Hz, 1H), 5.09 (d, J = 10.4 Hz, 1H), 4.85 (d, J = 2.6 Hz, 2H), 4.68-4.45 (m, 6H), 4.14-4.06 (m, 3H), 3.99 (t, J = 8.7 Hz, 1H), 3.80 (s, 3H) 3.79-3.77 (m, 1H), 3.68-3.39 (m, 6H), 3.16-3.15 (m, 1H), 2.37 (s, 1H), 0.90 (s, 9H), 0.15 (s, 3H), 0.12 (s, 3H); ^{13}C NMR (100 MHz, $CDCl_3$) δ 161.8, 159.3, 138.7, 138.6, 138.0, 137.8, 130.7, 129.3, 129.2, 129.1, 128.7, 128.6, 128.4, 128.4, 128.4, 128.3, 128.1, 127.9, 127.8, 126.3, 125.5, 113.9, 101.9, 101.5, 94.4, 92.7, 78.8, 78.3, 78.0, 77.4, 77.3, 75.2, 75.1, 74.8, 73.8, 72.5, 68.9, 68.7, 67.6, 60.7, 55.5, 25.9, 18.1, -4.0, -4.9; ESI MS *m/z* ($M^+ + Na^+$) calcd 1100.3312, found 1100.3278.

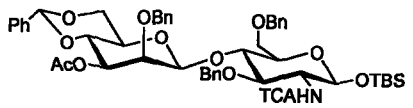

3-15

***tert*-Butyldimethylsilyl 3-*O*-acetyl-2-*O*-benzyl-4,6-*O*-benzylidene-β-D-mannopyranosyl-(1→4)-3,6-di-*O*-benzyl-2-deoxy-2-trichloroacetimido-β-D-glucopyranoside 3-15.** To a stirring solution of **3-14** (1.0 g, 0.93 mmol) in CH_2Cl_2 (4.5 mL) and H_2O (0.5 mL) was added 2,3-dichloro-5,6-dicyanobenzoquinone (252 mg, 1.11 mmol). After stirring for 45 min, the reaction mixture was diluted with CH_2Cl_2 (45 mL). The organic layer was washed with $NaHCO_3$ (2 x 25 mL), H_2O (1 x 25 mL), dried over Na_2SO_3, filtered and solvents removed *in vacuo*. Purification by flash silica column chromatography (20% EtOAc/hexanes) gave a white solid. ^1H NMR (400 MHz, $CDCl_3$) δ 7.36-733 (m, 2H), 7.29-7-12 (m, 18H), 6.86 (d, *J*= 7.5 Hz, 1H), 5.33 (s, 1H), 5.08 (d, *J*= 7.7 Hz, 1H), 4.97 (d, *J*= 10.4 Hz, 1H), 4.87 (d, *J*= 11.5 Hz, 1H), 4.60-4.52 (m, 3H), 4.42-4.37 (m, 2H), 4.05-3.91 (m, 3H), 3.62-3.58 (m, 4H), 3.50-3.36 (m, 3H), 3.30-3.24 (m, 1H), 3.05-2.99 (m, 1H), 2.27 (d, *J*= 8.7 Hz, 1H), 0.79 (s, 9H), 0.00 (s, 3H), -0.02 (s, 3H); ^{13}C NMR (100 MHz, $CDCl_3$) δ 162.1, 138.9, 138.4, 138.0, 137.6, 129.6, 129.5, 129.0, 129.0, 128.8, 128.7, 128.6, 128.5, 128.5, 128.4, 128.4, 128.4, 128.0, 126.7, 102.4, 102.2, 94.6, 92.9, 79.6, 79.3, 78.7, 77.7, 76.3, 75.2, 75.1, 74.2, 71.3, 69.0, 68.9, 67.4, 61.1, 26.1, 18.4, -3.8, -4.7. The solid (743 mg, 0.77 mmol) was dissolved in CH_2Cl_2 (8 mL) and cooled to 0°C. Acetic anhydride (147 μL, 1.55 mmol) was added and stirred for 5 min. Dimethylaminopyridine (114 mg, 0.93 mmol) was added and the stirring mixture was warmed slowly to room temperature over 2 h. The reaction was diluted with CH_2Cl_2 (15 mL) and washed with 5% HCl (2 x 15 mL), H_2O (1 x 15 mL), $NaHCO_3$ (2 x 15 mL). The organic layer was dried over Na_2SO_4, filtered, and solvents removed in vacuo. Purification by flash silica column chromatography (33% EtOAc/hexanes) afforded **3-15** (771 mg, 79% for two steps). $[\alpha]^{24}_D$: -45.0° (*c* = 0.7, CH_2Cl_2); IR (thin film) 3339, 2858, 1738, 1691, 1092, 1068 cm^{-1}; ^1H NMR (400 MHz, $CDCl_3$) δ 7.47-7.28 (m, 20H), 6.99 (d, *J* = 7.5 Hz, 1H), 5.48 (s, 1H), 5.22 (d, *J* = 7.7 Hz, 1H), 5.11 (d, *J* =10.4 Hz, 1H), 4.87-4.82 (m, 2H), 4.74-4.50 (m, 5H), 4.18-4.02 (m, 5H), 3.71 (dq, *J* = 2.3, 5.6 Hz, 2H), 3.57-3.52 (m, 2H), 3.41-3.38 (m, 1H), 3.23-3.22 (m, 1H), 1.99 (s, 3H), 0.92 (s, 9H), 0.16 (s, 3H), 0.13 (s, 3H); ^{13}C NMR (100 MHz, $CDCl_3$) δ 170.6, 161.8, 138.7, 138.2, 137.9,

137.4, 129.3, 128.8, 128.5, 128.4, 128.4, 128.4, 128.2, 128.2, 128.0, 128.0, 127.8, 126.4, 101.9, 101.3, 94.4, 92.7, 78.1, 77.3, 76.5, 75.9, 75.7, 75.1, 74.8, 73.8, 72.6, 68.8, 68.6, 67.5, 60.8, 25.8, 21.22, 18.1, -4.0, -4.9; ESI MS m/z ($M^+ + Na^+$) calcd 1022.2843, found 1022.2807.

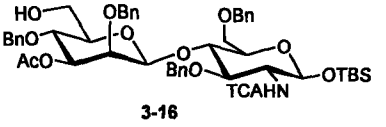

3-16

***tert*-Butyldimethylsilyl 3-*O*-acetyl-2,4-di-*O*-benzyl-β-D-mannopyranosyl-(1→4)-3,6-di-*O*-benzyl-2-deoxy-2-trichloroacetimido-β-D-glucopyranoside 3-16.** To a solution of **3-15** (265 mg, 0.265 mmol) in CH_2Cl_2 (2.7 mL) were added freshly dried 4Å molecular sieves (800 mg). After stirring for 1h, the mixture was cooled to -78°C. Triethylsilane (127 μL, 0.79 mmol) was added and the resulting solution was stirred for 5 min. Dichlorophenylborane (117 μL, 0.90 mmol) was added and the mixture was stirred for 30 min at -78°C. The reaction was quenched with the addition of triethylamine (0.5 mL) and methanol (0.5 mL) and diluted with CH_2Cl_2 (20 mL). The organic layer was washed with $NaHCO_3$ (2 x 20 mL), H_2O (1 x 20 mL), dried over Na_2SO_4, filtered, and solvents removed in vacuo. Purification by flash silica column chromatography (0 → 10% EtOAc/Tol) afforded **3-16** (234 mg, 88%) as a white solid. ^1H NMR (500 MHz, $CDCl_3$) δ 7.24-7.08 (m, 20H), 6.87 (d, *J*= 7.5 Hz, 1H), 5.05 (d, *J*=7.8 Hz, 1H), 4.97 (d, *J*= 10.7, 1H), 4.68 (d, *J*=11.9, 1H), 4.62 (dd, *J*= 3.2, 9.9, 1H), 4.54-4.36 (m, 7H), 4.00 (t, *J*= 8.8, 1H), 3.88 (t, *J*= 9.3, 1H), 3.78 (d, *J*=3.2, 1H), 3.73 (t, *J*=9.8, 1H), 3.62-3.44 (m, 3H), 3.41-3.36 (m, 1H), 3.29-3.20 (m, 2H), 3.05-2.98 (m, 1H), 1.78 (s, 3H), 1.58 (bs, 1H), 0.75 (s, 9H), 0.00 (s, 3H), -0.02 (s, 3H).

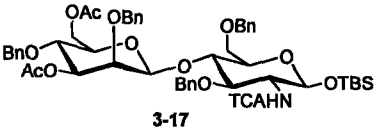

3-17

***tert*-Butyldimethylsilyl 3,6-di-*O*-acetyl-2,4-di-*O*-benzyl-β-D-mannopyranosyl-(1→4)-3,6-di-*O*-benzyl-2-deoxy-2-trichloroacetimido-β-D-glucopyranoside 3-17. 3-16** (170 mg, 0.17 mmol) was dissolved in CH_2Cl_2 (2 mL) and cooled to 0°C. Acetic anhydride

(32 μl, 0.34 mmol) was added and stirred for 5 min. Dimethylaminopyridine (25 mg, 0.20 mmol) was added and the stirring mixture was warmed slowly to room temperature over 2.5 h. The reaction mixture was then diluted with CH_2Cl_2 (15 mL) and washed with 5% HCl (2 x 15 mL), H_2O (1 x 15 mL), and $NaHCO_3$ (2 x 15 mL). The organic layer was dried over Na_2SO_4, filtered, and the solvents removed *in vacuo*. Purification by flash silica column chromatography (25% EtOAc/hexanes) afforded **3-17** (163 mg, 92%). $[\alpha]^{24}_D$: -23.5° (*c* 1.0, CH_2Cl_2); IR (thin film) 3342, 2858, 1742, 1691, 1234, 1073 cm^{-1}; ^1H NMR (400 MHz, $CDCl_3$) δ 7.39-7.22 (m, 20H), 6.93 (d, *J* = 7.5 Hz, 1H), 5.15-5.11 (m, 2H), 4.86-4.49 (m, 9H), 4.25-4.08 (m, 4H), 3.94 (d, *J* = 3.0 Hz, 1H), 3.85 (Ψt, *J* = 9.7 Hz, 1H), 3.74 (dd, *J* = 2.7, 11.1 Hz, 1H), 3.66 (dd, *J* = 3.4, 11.1 Hz, 1H), 3.54-3.37 (m, 3H), 1.93 (s, 3H), 1.89 (s, 3H), 0.89 (s, 9H), 0.14 (s, 3H), 0.10 (s, 3H); ^{13}C NMR (100 MHz, $CDCl_3$) δ 171.0, 170.4, 161.8, 139.0, 138.5, 138.0, 128.7, 128.7, 128.5, 128.4, 128.1, 128.1, 127.9, 127.9, 127.6, 100.8, 94.5, 92.7, 77.9, 77.7, 77.4, 76.2, 75.9, 75.1, 74.9, 74.3, 73.8, 73.6, 73.3, 68.9, 63.6, 60.4, 25.8, 21.2, 20.9, 18.1, -4.0 -4.9; ESI MS m/z ($M^+ + Na^+$) calcd 1066.3105, found 1066.3124.

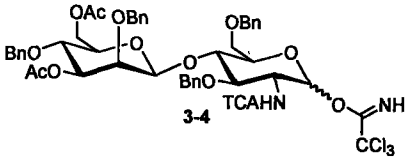

3-4

3,6-Di-*O*-acetyl-2,4-di-*O*-benzyl-β-D-mannopyranosyl-(1→4)-3,6-di-*O*-benzyl-2-deoxy-2-trichloroacetimido-α-D-glucopyranosyl trichloroacetimidate 3-4. A solution of **3-17** (330 g, 0.31 mmol) in THF (3 mL) was cooled to 0°C. Acetic acid (27 μL, 0.47 mmol) and then tetrabutylammonium fluoride (1.0 M in THF, 470 μL, 0.47 mmol) were added to the cooled solution. The reaction mixture was allowed to warm slowly to room temperature while stirring for 3 h. The reaction mixture was diluted with EtOAc and washed with $NaHCO_3$ (2 x 10 mL) and H_2O (1 x 10 mL). The organic layer was then dried over Na_2SO_4, filtered, and solvents removed in vacuo. The crude material (294 mg, 0.31 mmol) was dissolved in CH_2Cl_2 (3 mL) and trichloroacetonitrile (0.3 mL) and cooled to 0°C. After stirring for 5 min, DBU (9.3 μL, 0.062 mmol) was added and the reaction mixture was allowed to stir for 1.5 h. The reaction mixture was passed through a silica plug, washed with EtOAc and the solvents removed *in vacuo*.

Purification by flash silica column chromatography (25% EtOAc/hexanes) afforded **3-4** (298 mg, 89%, 95:5 α:β). IR (thin film) 1739, 1513, 1234, 1076, 1028 cm^{-1}; ^1H NMR (400 MHz, $CDCl_3$) δ 8.71 (s, 1H), 7.43-7.26 (m, 20H), 6.52 (d, J = 3.3 Hz, 1H), 6.46 (d, J = 7.6 Hz, 1H), 5.02 (d, J = 11.9 Hz, 1H), 4.87 (d, J = 12.1 Hz, 1H), 4.77-4.66 (m, 6H), 4.59-4.50 (m, 2H), 4.30-4.22 (m, 4H), 3.95-3.86 (m, 4H), 3.70 (s, 2H), 3.38-3.35 (m, 1H), 1.97 (s, 3H), 1.91 (s, 3H); ^{13}C NMR (100 MHz, $CDCl_3$) δ 170.9, 170.3, 162.0, 160.1, 138.4, 138.4, 137.9, 137.5, 128.8, 128.7, 128.7, 128.6, 128.6, 128.4, 128.4, 128.4, 128.3, 128.3, 128.2, 128.1, 128.1, 128.0, 127.9, 127.9, 127.9, 127.8, 100.6, 94.5, 92.1, 91.0, 76.7, 76.2, 75.8, 75.7, 75.0, 74.8, 73.9, 73.8, 73.7, 73.4, 73.1, 67.9, 63.1, 54.1, 21.1, 20.8; ESI MS m/z ($M^+ + Na^+$) calcd 1095.1336, found 1095.1343.

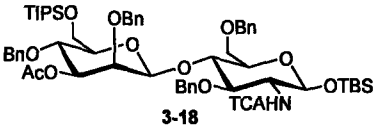

3-18

***tert*-Butyldimethylsilyl 3-*O*-acetyl-2,4-di-*O*-benzyl-6-*O*-triisopropylsilyl-β-D-mannopyranosyl-(1→4)-3,6-di-*O*-benzyl-2-deoxy-2-trichloroacetimido-β-D-glucopyranoside 3-18.** **3-16** (600 mg, 0.598 mmol) was dissolved in *N,N*-dimethylformamide (5.9 mL) to which triisopropylsilylchloride (231 mg, 1.19 mmol) and imidazole (122 mg, 1.79 mmol) was added. The mixture was stirred at RT for 36 h, diluted in diethylether (50 mL), washed with H_2O (3 x 40 mL), $NaHCO_3$ (2 x 40 mL) and brine (1 x 40 mL). The organic layer was then dried over Na_2SO_4, filtered, and solvents removed in vacuo. Purification by flash silica column chromatography (0 → 10% EtOAc/toluene) afforded **3-18** (551 mg, 80%). $[\alpha]^{24}_D$: -27.3° (*c* 1.1, CH_2Cl_2); IR (thin film) 2940, 2871, 1761, 1689, 1213, 1077 cm^{-1}; ^1H NMR (500 MHz, $CDCl_3$) δ 7.38-7.21 (m, 20H), 6.95 (d, J= 7.9 Hz, 1H), 5.06 (d, J= 7.1 Hz, 1H), 5.02 (d, J= 11.8 Hz, 1H), 4.86 (d, J= 12.0 Hz, 1H), 4.82 (dd, J= 3.1, 9.8 Hz, 1H), 4.74 (app. s, 1H), 4.70-4.56 (m, 6H), 4.15 (t, J= 8.1 Hz, 1H), 4.06 (t, J= 9.0 Hz, 1H), 3.97-3.83 (m, 3H), 3.83-3.74 (m, 2H), 3.72-3.58 (m, 3H), 3.30-3.24 (m, 1H), 1.91 (s, 3H), 1.00 (s, 21H), 0.90 (s, 9H), 0.15 (s, 3H), 0.12 (s, 3H); ^{13}C NMR (125 MHz, $CDCl_3$) δ 171.1, 162.3, 139.5, 139.2, 139.0, 138.7, 129.2, 129.1, 128.9, 128.8, 128.5, 128.4, 128.4, 128.3, 128.3, 128.2, 127.9, 101.1,

95.3, 78.1, 78.0, 77.4, 76.8, 75.7, 75.5, 75.4, 74.2, 74.0, 73.8, 69.8, 63.7, 59.7, 26.4, 21.7, 18.8, 18.7, 18.6, 12.6, -3.5, -4.4; ESI MS m/z ($M^+ + NH_4^+$) calcd 1175.48, found 1174.22.

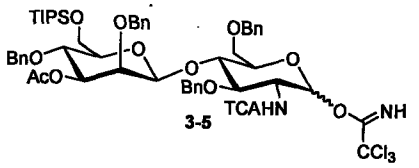

3-*O*-acetyl-2,4-di-*O*-benzyl-6-*O*-triisopropylsilyl-β-D-mannopyranosyl-(1→4)-3,6-di-*O*-benzyl-2-deoxy-2-trichloroacetimido-α-D-glucopyranosyl trichloroacetimidate 3-5. A solution of **3-18** (515 g, 0.444 mmol) in THF (3 mL) was cooled to 0°C. Acetic acid (37 μL, 0.622 mmol) and then tetrabutylammonium fluoride (1.0 M in THF, 577 μL, 0.577 mmol) were added to the cooled solution. The reaction mixture was allowed to warm slowly to room temperature while stirring for 4 h. The reaction mixture was diluted with EtOAc (50 mL) and washed with H_2O (3 x 40 mL) and $NaHCO_3$ (2 x 40 mL). The organic layer was then dried over Na_2SO_4, filtered, and solvents removed in vacuo. The crude material was filtered through a plug of silica gel to recover unreacted starting material to isolate pure lactol (407 mg, 95% isolated yield). The lactol (407 mg, 0.389 mmol) was dissolved in CH_2Cl_2 (5 mL) and trichloroacetonitrile (0.310 mL, 3.11 mmol) and cooled to 0°C. After stirring for 5 min, DBU (17.8 μL, 0.117 mmol) was added and the reaction mixture was allowed to stir for 2 h and slowly warmed to RT. The reaction mixture was passed through a silica plug, washed with EtOAc and the solvents removed *in vacuo*. Purification by flash silica column chromatography (0 → 20% EtOAc/toluene + 0.5% Et_3N) afforded **3-5** (410 mg, 90%). IR (thin film) 1721, 1536, 1212, 1066, 1033 cm^{-1}; ^1H NMR (400 MHz, $CDCl_3$) δ 8.58 (s, 1H), 7.32-7.06 (m, 20H), 6.43 (d, *J*= 3.4 Hz, 1H), 6.33 (d, *J*= 7.4 Hz, 1H), 4.91 (d, *J*= 12.5, 1H), 4.77-4.60 (m, 4H), 4.58-4.55 (m, 5H), 4.42 (d, *J*= 12.0, 1H), 4.23 (t, *J*= 9.6, 1H), 4.17-4.12 (m, 1H), 3.93 (t, *J*= 9.7, 1H), 3.86-3.74 (m, 5H), 3.62 (app. s, 2H), 3.15-3.11 (m, 1H), 1.84 (s, 3H), 1.52 (s, 3H), 0.93 (s, 18H); ^{13}C NMR (100 MHz, $CDCl_3$) δ170.8, 162.2, 160.5, 138.9, 137.8, 129.0, 128.8, 128.7, 128.6, 128.4, 128.4, 128.1, 128.1, 127.9, 127.9, 127.8, 100.6, 94.7, 77.7, 76.8, 76.6, 76.3, 75.6, 75.1, 7.51, 74.1, 73.9, 73.5, 68.2, 63.2, 54.4, 21.4, 18.5, 18.4, 12.4; ESI MS m/z ($M^+ + Na^+$) calcd 1209.27, found 1208.95.

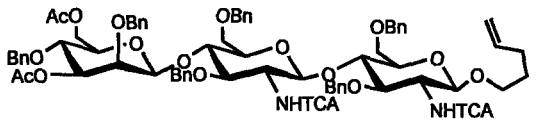

3-1

4-Pentenyl 3,6-di-*O*-acetyl-2,4-di-*O*-benzyl-β-D-mannopyranosyl-(1→4)-3,6-di-*O*-benzyl-2-deoxy-2-trichloroacetimido-β-D-glucopyranosyl-(1→4)-3,6-di-*O*-benzyl-2-deoxy-2-trichloroacetimido-β-D-glucopyranoside 3-1. A mixture of **3-4** (150 mg, 0.14 mmol) and **3-3** (120 mg, 0.21 mmol) were coevaporated with toluene (3 x 1 mL) and dried under vacuum overnight. The mixture was dissolved in CH_2Cl_2 (1.5 mL) and the resulting solution was cooled to -40°C. Following the addition of TMSOTf (2.5 μL, 0.014 mmol), the solution was warmed slowly to room temperature over a period of 2 h and triethylamine (0.1 mL) was added. The mixture was concentrated and filtered through a silica plug (50% EtOAc/hexanes) to remove baseline contaminants. The resulting oil was subjected to size exclusion chromatography (100% toluene) to remove the monosaccharide acceptor and the crude product was purified by flash silica column chromatography (40% EtOAc/hexanes) to afford **3-1** (136 mg, 65%). $[\alpha]^{24}_D$: -35.0° (*c* 1.0, CH_2Cl_2); IR (thin film) 1742, 1694, 1529, 1235, 1075 cm^{-1}; ^1H NMR (400 MHz, $CDCl_3$) δ 7.38-7.21 (m, 30H), 6.97 (d, J = 7.8 Hz, 1H), 6.60 (d, J = 8.0 Hz, 1H), 5.82-5.75 (m, 1H), 5.12 (d, J = 11.3 Hz, 1H), 5.03-4.87 (m, 4H), 4.81-4.62 (m, 8H), 4.56-4.49 (m, 4H), 4.42-4.39 (m, 1), 4.25-4.14 (m, 3H), 4.08-3.98 (m, 2H), 3.93 (d, J = 3.1 Hz, 1H), 3.90-3.84 (m, 2H), 3.78-3.73 (m, 3H), 3.69-3.59 (m, 3H), 3.55-3.44 (m, 3H), 3.34-3.30 (m, 1H), 3.26-3.24 (m, 1H) 2.14-2.07 (m, 2H), 1.93 (s, 3H), 1.87 (s, 3H), 1.71-1.64 (m, 2H); ^{13}C NMR (100 MHz, $CDCl_3$) δ 170.9, 170.4, 161.9, 161.9, 138.8, 138.5, 138.5, 138.2, 138.2, 137.9, 137.8, 128.8, 128.7, 128.7, 128.5, 128.5, 128.5, 128.3, 128.2, 128.1, 128.1, 128.0, 127.9, 127.9, 127.9, 127.8, 127.7, 127.7, 115.1, 100.8, 99.7, 98.9, 78.5 78.1, 77.9, 76.1, 76.1, 75.3, 75.2, 75.0, 75.0, 74.9, 74.4, 74.3, 73.6, 73.5, 73.4, 73.1, 69.4, 68.7, 68.6, 63.4, 58.2, 57.4, 30.2, 28.9, 21.1, 20.9; ESI MS m/z ($M^+ + Na^+$) calcd 1505.3430, found 1505.3423.

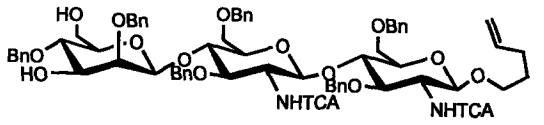

3-19

4-Pentenyl 2,4-di-*O*-benzyl-β-D-mannopyranosyl-(1→4)-3,6-di-*O*-benzyl-2-deoxy-2-trichloroacetimido-β-D-glucopyranosyl-(1→4)-3,6-di-*O*-benzyl-2-deoxy-2-trichloroacetimido-β-D-glucopyranoside 3-19. **3-11** (134 mg, 0.09 mmol) was dissolved in MeOH (1 mL) and NaOMe (25% v/w, 2.1 μL, 0.009 mmol) was added. The mixture was stirred overnight at room temperature. The reaction mixture was diluted with wet MeOH (5 mL), solvents removed in vacuo and purified by flash silica column chromatography (25% EtOAc/hexanes) afforded **3-19** (92 mg, 73%). $[\alpha]^{24}_{D}$: -32.2° (*c* 1.3, CH_2Cl_2); IR (thin film) 3332, 2872, 1694, 1529, 1073 cm^{-1}; ^1H NMR (400 MHz, $CDCl_3$) δ 7.42-7.22 (m, 30H), 6.93 (d, *J* = 7.8 Hz, 1H), 6.59 (d, *J* = 7.9 Hz, 1H), 5.83-5.76 (m, 1H), 5.11-4.96 (m, 5H), 4.85-4.75 (m, 4H), 4.68-4.47 (m, 7H), 4.33 (d, *J* = 12.1 Hz, 1H), 4.18 (Ψt, *J* = 8.3 Hz, 1H), 4.05-3.86 (m, 3H), 3.76-3.45 (m, 14H), 3.34 (dd, *J* = 5.4, 11.9 Hz, 1H), 3.26-3.23 (m, 1H), 3.08-3.04 (m, 1H), 2.33-2.31 (m, 1H), 2.14-2.08 (m, 2H), 1.72-1.64 (m, 2H); ^{13}C NMR (100 MHz, $CDCl_3$) δ 161.9, 161.9, 138.5, 138.4, 138.3, 138.2, 138.1, 137.6, 128.8, 128.8, 128.7, 128.7, 128.6, 128.5, 128.5, 128.2, 128.2, 128.1, 128.0, 127.9, 127.7, 127.2, 115.1, 101.2, 99.7, 98.6, 92.6, 92.6, 78.5, 78.4, 78.2, 78.1, 76.6, 75.7, 75.4, 75.4, 74.8, 74.8, 74.6, 74.2, 73.7, 73.5, 69.4, 68.5, 68.4, 62.3, 58.6, 57.7, 30.2, 28.8; ESI MS m/z ($M^+ + Na^+$) calcd 1421.3218, found 1421.3211.

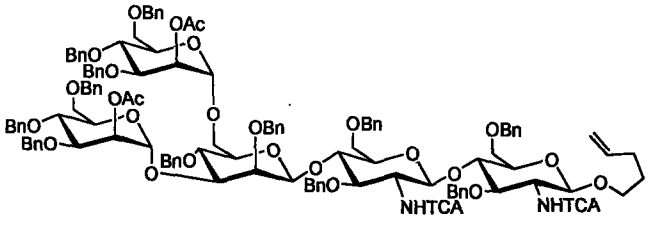

3-8

4-Pentenyl 2-*O*-acetyl-3,4,6-tri-*O*-benzyl-α-D-mannopyranosyl-(1→3)-[2-*O*-acetyl-3,4,6-tri-*O*-benzyl-α-D-mannopyranosyl-(1→6)]-2,4-di-*O*-benzyl-β-D-mannopyranosyl-(1→4)-3,6-di-*O*-benzyl-2-deoxy-2-trichloroacetimido-β-D-glucopyranosyl-(1→4)-3,6-di-*O*-benzyl-2-deoxy-2-trichloroacetimido-β-D-

glucopyranoside 3-8. 3-19 (76 mg, 0.0544 mmol) and **3-11** (104 mg, 0.163mml) were coevaporated together with toluene (3 x 2 ml), and dried overnight *in vacuo*. The mixture was dissolved in 500 µl dichloromethane and cooled to -20°C. 2 µl TMSOTf (0.0109 mmol) was added, and the reaction stirred for 20 minutes and warmed to RT. The reaction was quenched with 100 µl Et_3N, dried to an oil, and purified by flash silica column chromatography (5 → 20% EtOAc/toluene) to afford **3-8** (120 mg, 98%). IR (thin film) 2867, 1746, 1711, 1693, 1235, 1077 cm^{-1}; ^1H NMR (400 MHz, $CDCl_3$) δ 7.41-7.08 (m, 60H), 6.91 (d, J = 7.8 Hz, 1H), 6.40 (d, J = 7.9 Hz, 1H), 5.80-5.72 (m, 1H), 5.48-5.46 (m, 1H), 5.37-5.35 (m, 1H), 5.14-4.27 (m, 31H), 4.42-3.14 (m, 30H), 2.14-2.06 (m, 5H), 1.98 (s, 3H), 1.68-1.63 (m, 2H); ^{13}C NMR (100 MHz, $CDCl_3$) δ 170.3, 170.3, 161.9, 161.8, 138.9, 138.8, 138.7, 138.7, 138.6, 138.5, 138.5, 138.2, 138.2, 138.2, 138.0, 137.9, 128.8, 128.8, 128.7, 128.6, 128.6, 128.5, 128.5, 128.5, 128.5 128.4, 128.4, 128.3, 128.2, 128.1, 128.1, 128.0, 127.9, 127.9, 127.8, 127.8, 127.7, 127.7, 127.6, 127.5, 127.3, 115.1, 101.5, 99.8, 99.7, 99.0, 97.8, 92.7, 81.2, 78.5, 78.2, 78.1, 77.5, 77.2, 77.0, 75.5, 75.3, 75.2, 75.0, 75.0, 74.9, 74.5, 74.5, 74.4, 74.3, 74.2, 73.6, 73.5, 73.5, 72.5, 72.0, 71.7, 71.6, 71.5, 69.4, 69.2, 68.8, 68.6, 68.5, 66.7, 58.2, 57.4, 30.2, 29.9, 28.9, 28.9, 21.3, 21.2, 21.2; ESI MS m/z ($M^+ + Na^+$) calcd 2369.7303, found 2369.7401.

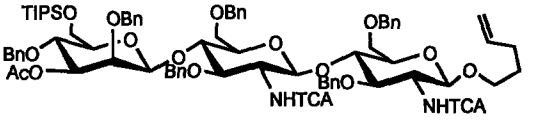

3-2

4-Pentenyl 3-O-acetyl-2,4-di-O-benzyl-6-O-triisopropylsilyl-β-D-mannopyranosyl-(1→4)-3,6-di-O-benzyl-2-deoxy-2-trichloroacetimido-β-D-glucopyranosyl-(1→4)-3,6-di-*O*-benzyl-2-deoxy-2-trichloroacetimido-β-D-glucopyranoside 3-2. A mixture of **3-3** (385 mg, 0.672 mmol) and **3-5** (400 mg, 0.336 mmol) were coevaporated with toluene (3 x 5 mL) and dried under vacuum overnight. The mixture was dissolved in CH_2Cl_2 (3 mL) and 500 mg 4Å MS and the resulting solution was cooled to -40°C. Following the addition of TMSOTf (12.1 µL, 0.0672 mmol), the solution was warmed slowly to room temperature over a period of 30 min and triethylamine (200 µL) was added. The mixture was filtered and concentrated to an oil, and purified by flash silica

column chromatography (0 → 15% EtOAc/toluene) to afford **3-2** (391 mg, 73%). $[\alpha]^{24}_D$: -33.1° (*c* 1.1, CH_2Cl_2); IR (thin film) 2949, 2887, 1777, 1643, 1541, 1211, 1079 cm^{-1}; ^1H NMR (500 MHz, $CDCl_3$) δ 7.40-7.24 (m, 20H), 7.24-7.12 (m, 10H), 7.00 (d, *J*= 7.9 Hz, ; 1H), 6.55 (d, *J*= 8.2 Hz, 1H), 5.83-5.73 (m, 1H), 5.04-4.81 (m, 5H), 4.79-4.72 (m, 2H), 4.70-4.55 (m, 9H), 4.50-4.38 (m, 3H), 4.13-4.03 (m, 2H), 3.98-3.82 (m, 5H), 3.80-3.56 (m, 7H), 3.55-3.49 (m, 2H), 3.48-3.42 (m, 1H), 3.33-3.28 (m, 1H), 3.24-3.19 (m, 1H), 2.14-2.20 (m, 2H), 1.89 (s, 3H), 1.72-1.60 (m, 2H), 0.97 (app. s, 21H); ^{13}C NMR (125 MHz, $CDCl_3$) δ 171.1, 162.3, 162.4, 139.5, 139.2, 139.1, 139.0, 138.8, 138.7, 138.4, 129.3, 129.2, 129.1, 129.0, 129.0, 128.9, 128.8, 128.7, 128.7, 128.5, 128.5, 128.4, 128.3, 128.3, 128.2, 127.9, 115.6, 101.2, 100.4, 100.0, 93.2, 93.3, 79.2, 78.7, 77.8, 77.0, 76.8, 76.1, 75.8, 75.7, 75.5, 75.4, 74.7, 74.3, 74.2, 74.1, 73.9, 69.9, 69.4, 69.1, 63.7, 58.0, 57.7, 30.7, 29.4, 18.8, 18.7, 12.7; ESI MS m/z (M^+ + Et_3NH^+) calcd 1698.60, found 1699.11.

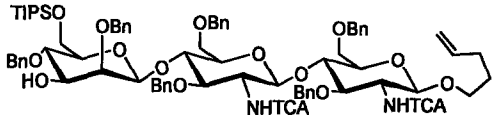

3-20

4-Pentenyl 2,4-di-O-benzyl-6-O-triisopropylsilyl-β-D-mannopyranosyl-(1→4)-3,6-di-O-benzyl-2-deoxy-2-trichloroacetimido-β-D-glucopyranosyl-(1→4)-3,6-di-*O*-benzyl-2-deoxy-2-trichloroacetimido-β-D-glucopyranoside 3-20. 4 μL Sodium methoxide (25% v/w, 0.0219mmol) was added to a solution of **3-2** in 3 ml (2:1 CH_2Cl_2:MeOH) and stirred 3 h at RT. Amberlite IR-120(plus) resin was added until pH 7 was reached. The reaction mixture was filtered, solvents removed in vacuo and purification by flash silica column chromatography (5-25% EtOAc/toluene) afforded **3-20** (230 mg, 84% isolated). $[\alpha]^{24}_D$: -37.1° (*c* 0.8, CH_2Cl_2); IR (thin film) 2913, 2878, 1615, 1532, 1209, 1072 cm^{-1}; ^1H NMR (500 MHz, $CDCl_3$) δ 7.38-7.27 (m, 18H), 7.27-7.23 (m, 4H), 7.23-7.16 (m, 8H), 6.96 (d, *J*= 8.0 Hz, 1H), 6.53 (d, *J*= 7.6 Hz, 1H), 5.81-5.73 (m, 1H), 5.08-4.86 (m, 6H), 4.82-4.73 (m, 1H), 4.70-4.54 (m, 7H), 4.45 (d, *J*= 12.4 Hz, 2H), 4.36 (d, *J*= 12.1 Hz, 1H), 4.11 (t, *J*= 7.8 Hz, 1H), 4.05 (t, *J*= 8.2 Hz, 1H), 3.99-3.90 (m, 2H), 3.90-3.82 (m, 1H), 3.80-3.61 (m, 8H), 3.60-3.41 (m, 8H), 3.33-3.27 (m, 1H), 3.20-3.16 (m, 1H), 2.14-2.04 (m, 2H), 1.70-1.60 (m, 3H), 0.96 (app. s, 21H); ^{13}C NMR (125 MHz, $CDCl_3$) δ 162.4,

162.3, 139.4, 139.2, 139.1, 139.0, 138.7, 138.3, 129.3, 129.3, 129.2, 129.2, 129.2, 129.1, 129.0, 128.9, 128.9, 128.8, 128.7, 128.7, 128.6, 128.6, 128.6, 128.5, 128.4, 128.3, 128.2, 128.0, 115.7, 101.9, 100.3, 99.8, 79.2, 79.2, 78.7, 78.0, 77.8, 77.3, 75.9, 75.8, 75.7, 75.7, 75.5, 75.2, 75.0, 74.8, 74.5, 74.3, 74.0, 69.9, 69.4, 69.1, 63.9, 59.3, 58.1, 57.8, 30.7, 29.4, 29.4, 18.8, 18.7, 12.7; ESI MS m/z ($M^+ + H^+$) calcd 1555.47, found 1554.66.

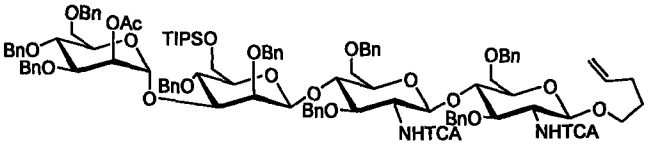

3-21

4-Pentenyl 3,4,6-tri-*O*-benzyl-α-D-mannopyranosyl-(1→2)-2,4-di-O-benzyl-6-O-triisopropylsilyl-β-D-mannopyranosyl-(1→4)-3,6-di-O-benzyl-2-deoxy-2-trichloroacetimido-β-D-glucopyranosyl-(1→4)-3,6-di-*O*-benzyl-2-deoxy-2-trichloroacetimido-β-D-glucopyranoside 3-21. Trisaccharide **3-20** (228 mg, 0.147 mmol) and mannosyl trichloroacetimidate **3-11** (140 mg, 0.220 mmol) were azeotropically dried with toluene (3 x 3 mL), dried an additional 4 h *in vacuo* and dissolved in dichloromethane (1 mL). The solution was cooled to –20 °C for 15 min, followed by the addition of TBSOTf (7 μL, 0.0293 mmol), and stirred for 30 min and warmed slowly to RT. The reaction was quenched by the addition of Et_3N (150 μL), and dried *in vacuo*. The crude product was purified by flash column chromatography on silica gel (2 → 15% EtOAc/toluene) affording of tetrasaccharide **3-21** (231 mg, 77%). $[\alpha]^{24}_D$: -21.4° (*c* 2.0, CH_2Cl_2); IR (thin film) 2931, 2887, 1799, 1722, 1682, 1254, 1099 cm^{-1}; ^1H NMR (500 MHz, $CDCl_3$) δ 7.42-7.10 (m, 45H), 6.97 (d, *J*= 8.1 Hz, 1H), 6.49 (d, *J*= 8.3, 1H), 5.83-5.75 (m, 1H), 5.48 (app. s, 1H), 5.17 (app. s, 1H), 5.04-4.82 (m, 7H), 4.80-4.50 (m, 14H), 4.49-4.29 (m, 7H), 4.10 (t, *J*= 7.5 Hz, 1H), 4.04 (t, *J*= 8.2 Hz, 1H), 3.97-3.81 (m, 10H), 3.77-3.44 (m, 16H), 3.29-3.24 (m, 1H), 3.16-3.11 (m, 1H), 2.12 (s, 3H), 2.12-2.02 (m, 3H), 1.73-1.61 (m, 2H), 0.96 (app. s, 21H); ^{13}C NMR (125 MHz, $CDCl_3$) δ 170.8, 162.4, 162.4, 139.6, 139.5, 139.2, 139.1, 138.8, 138.8, 138.7, 138.5, 138.4, 129.3, 129.2, 129.1, 129.1, 129.1, 129.0, 129.0, 128.8, 128.8, 128.8, 128.7, 128.6, 128.6, 128.5, 128.5, 128.4, 128.4, 128.4, 128.3, 128.3, 128.2, 128.2, 128.2, 128.0, 128.0, 127.9, 127.8, 127.6, 115.6, 101.6, 100.4, 100.2, 100.0, 81.4, 79.1, 79.0, 78.7, 78.1, 76.0,

75.9, 75.8, 75.7, 75.6, 75.6, 75.2, 74.8, 74.7, 74.2, 74.2, 74.1, 73.0, 72.5, 69.9, 69.6, 69.4, 69.3, 69.3, 63.7, 57.9, 57.6, 30.8, 29.4, 26.6, 21.8, 18.8, 18.7, 12.7, ; ESI MS m/z (M^{2+} + $2H^+$) calcd 1015.33, found 1014.77.

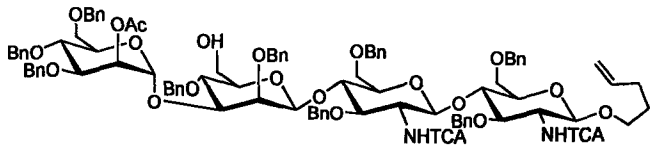

3-22

4-Pentenyl 3,4,6-tri-*O*-benzyl-α-D-mannopyranosyl-(1→2)-2,4-di-O-benzyl-β-D-mannopyranosyl-(1→4)-3,6-di-O-benzyl-2-deoxy-2-trichloroacetimido-β-D-glucopyranosyl-(1→4)-3,6-di-*O*-benzyl-2-deoxy-2-trichloroacetimido-β-D-glucopyranoside 3-22. Tetrasaccharide **3-21** (210 mg, 0.103 mmol) was dissolved in THF (3 mL). Water (3 mL) was slowly added with vigorous stirring followed by TFA (1 ml). The reaction was stirred for 3 hr at RT and diluted with diethyl ether (50 mL) and washed with sat. aqueous $NaHCO_3$ (2 x 30 mL), brine (30 mL), dried (Na_2SO_4) and concentrated. The residue was purified by flash column chromatography on silica gel (10 → 40% EtOAc/hexanes) to afford disaccharide **2-16** (159 mg, 82%). $[\alpha]^{24}_D$: -16.6° (*c* 0.3, CH_2Cl_2); IR (thin film) 3432, 1746, 1717, 1688, 1490, 1220, 1096, 1078, 698 cm^{-1}; ^1H NMR (500 MHz, $CDCl_3$) δ 7.44-7.39 (m, 4H), 7.37-7.15 (m, 41H), 6.92 (d, *J*=7.8 Hz, 1H), 6.54 (d, *J*= 7.5 Hz, 1H), 5.18 (s, 1H), 5.07 (d, *J*= 10.9 Hz, 1H), 5.04-4.96 (m, 4H), 4.89-4.73 (m, 7H), 4.66-4.60 (m, 3H), 4.57-4.52 (m, 2H), 4.50-4.40 (m, 7H), 4.26 (d, *J*= 12.0 Hz, 1H), 4.16 (t, *J*= 8.4 Hz, 1H), 4.02-3.94 (m, 3H), 3.92-3.86 (m, 3H), 3.84-3.79 (m, 4H), 3.78-3.72 (m, 2H), 3.72-3.54 (m, 9H), 3.54-3.40 (m, 4H), 3.30 (dd, *J*= 5.0, 12.0 Hz, 1H), 3.23-3.19 (m, 1H), 3.00-2.95 (m, 1H), 2.13 (s, 3H), 2.13-2.05 (m, 2H), 1.73-1.51 (m, 2H) ;^{13}C NMR (125 MHz, $CDCl_3$) δ 170.8, 162.5, 162.4, 139.3, 139.2, 139.1, 139.0, 138.8, 138.7, 138.6, 138.5, 138.4, 129.3, 129.3, 129.2, 129.2, 129.1, 129.1, 129.0, 129.0, 128.9, 128.8, 128.7, 128.7, 128.5, 128.5, 128.5, 128.4, 128.4, 128.4,128.3, 128.3, 128.1, 127.7, 101.4, 100.3, 100.2, 99.4, 81.1, 79.0, 78.8, 77.9, 76.3, 76.2, 75.7, 75.6, 75.6, 75.5, 75.4, 75.4, 75.2, 74.9, 74.2, 74.1, 73.1, 72.5, 70.0, 69.8, 69.4, 68.9, 62.6, 59.1, 58.2, 30.7, 29.4, 21.8; ESI MS m/z (M^+ + Et_3NH^+) calcd 1973.66, found 1974.61.

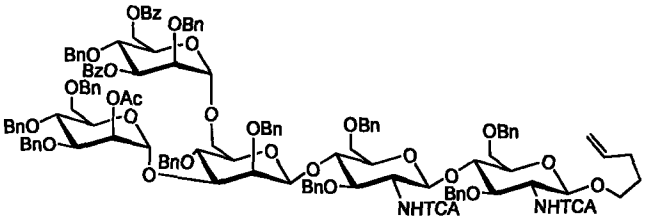

3-9

4-Pentenyl 2-*O*-acetyl-3,4,6-tri-*O*-benzyl-α-D-mannopyranosyl-(1→3)-[2,4-di-*O*-benzyl-3,6-di-*O*-benzoyl-α-D-mannopyranosyl-(1→6)]-2,4-di-*O*-benzyl-β-D-mannopyranosyl-(1→4)-3,6-di-O-benzyl-2-deoxy-2-trichloroacetimido-β-D-glucopyranosyl-(1→4)-3,6-di-*O*-benzyl-2-deoxy-2-trichloroacetimido-β-D-glucopyranoside 3-9. Tetrasaccharide **3-22** (131 mg, 0.0698 mmol) and mannosyl trichloroacetimidate **3-12** (43 mg, 0.0907 mmol) were azeotropically dried with toluene (3 x 3 mL), dried over night *in vacuo* and dissolved in diethylether (1 mL). The solution was cooled to –20 °C for 15 min, followed by the addition of TMSOTf (2.5 μL, 0.0140 mmol), and stirred for 45 min and warmed slowly to RT. The reaction was quenched by the addition of Et_3N (150 μL), and dried *in vacuo*. The crude product was purified by flash column chromatography on silica gel (0 → 40% EtOAc/toluene) affording of pentasaccharide **3-9** (147 mg, 87%). $[\alpha]^{24}_D$: -11.7° (c 0.09, EtOAc); IR (thin film) 2917, 2867, 1746, 1711, 1693, 1452, 1235, 1097, 1077, 698 cm^{-1}; ^1H NMR (400 MHz, $CDCl_3$) δ 7.88-7.98 (m, 4H), 7.45-7.20 (m, 4H), 7.20-6.90 (m, 55H), 6.89-6.78 (m, 2H), 5.65-5.55 (m, 1H), 5.51-5.45 (dd, *J*= 3.0, 9.6 Hz, 1H), 5.35-5.33 (m, 1H), 5.02 (app. s, 1H), 4.94-4.75 (m, 5H), 4.72-4.55 (m, 6H), 4.52-4.33 (m, 9H), 4.32-4.22 (m, 6H), 4.20-4.08 (m, 4H), 4.06-3.91 (m, 4H), 3.84-3.52 (m, 14H), 3.51-3.20 (m, 12H), 3.05-2.95 (m, 2H), 1.95 (app. s, 3H), 1.94-1.9 (m, 2H), 1.54-1.45 (m, 2H); ^{13}C NMR (100 MHz, $CDCl_3$) δ 172.0, 168.2, 167.8, 163.7, 163.6, 140.7, 140.5, 140.3, 140.3, 140.1, 140.0, 139.8, 139.7, 139.5, 135.3, 134.9, 132.0, 131.8, 131.7, 131.7, 130.5, 130.4, 130.4, 130.3, 130.3, 130.2, 130.2, 130.1, 130.0, 130.0, 129.8, 129.7, 129.7, 129.6, 129.6, 129.5, 129.5, 129.3, 129.3, 129.1, 129.0, 116.9, 103.0, 101.6, 101.3, 100.5, 100.0, 94.4, 82.7, 80.2, 79.9, 79.8, 79.7, 79.6, 79.2, 77.1, 77.0, 76.9, 76.8, 76.6, 76.3, 76.1, 75.9, 75.4, 75.3, 75.2, 75.1, 74.7, 74.3, 73.9, 72.0, 71.1, 71.0, 70.7, 70.4, 70.3, 68.4, 65.3, 60.4, 59.0, 32.0, 30.6, 23.0, ; ESI MS m/z ($M^+ + NH_4^+$) calcd 2440.77, found 2441.11.

Automated Synthesis of Core Pentasaccharide 3-8. Glycosylated resin from automated synthesis was dried *in vacuo* for 18 h over phosphorous pentoxide and transferred into a solid-phase round bottom flask with glass frit. The resin was swelled with 5 ml CH_2Cl_2, purged with an atmosphere of ethylene followed by the addition of 10 mol % Grubbs' catalyst (bis(tricyclohexylphosphine)benzylidene ruthenium (IV) dichloride. The reaction mixture was stirred for 24 h under an atmosphere of ethylene, an additional 10 mol% Grubbs' catalyst was added, and the reaction was allowed to stir an additional 24 h under an atmosphere of ethylene. Triethylamine (100 equiv.) and tris hydroxymethylphosphine (50 equiv.) were added, and the mixture stirred 2 h at room temperature. The reaction was diluted in CH_2Cl_2 and washed 3 times with water. The aqueous fractions were washed with additional CH_2Cl_2. The organic fractions were combined, dried over $MgSO_4$, filtered, and dried to yield adark oil.

The crude product was analyzed by HPLC (Figure 6.1-6.4, Waters Nova-pak© silica column (3.9 x 150 mm) with EtOAc/hexanes as the mobile phase), monitoring at 260 nm. A portion of the crude product was purified by semi-preparative HPLC using a Waters prep Nova-pak© silica column (7.8 x 300 mm) with a gradient of EtOAc/hexanes. Semi-preparative HPLC yielded 3 mg of **3-8** that corresponded to **3-8** made by solution phase synthesis.

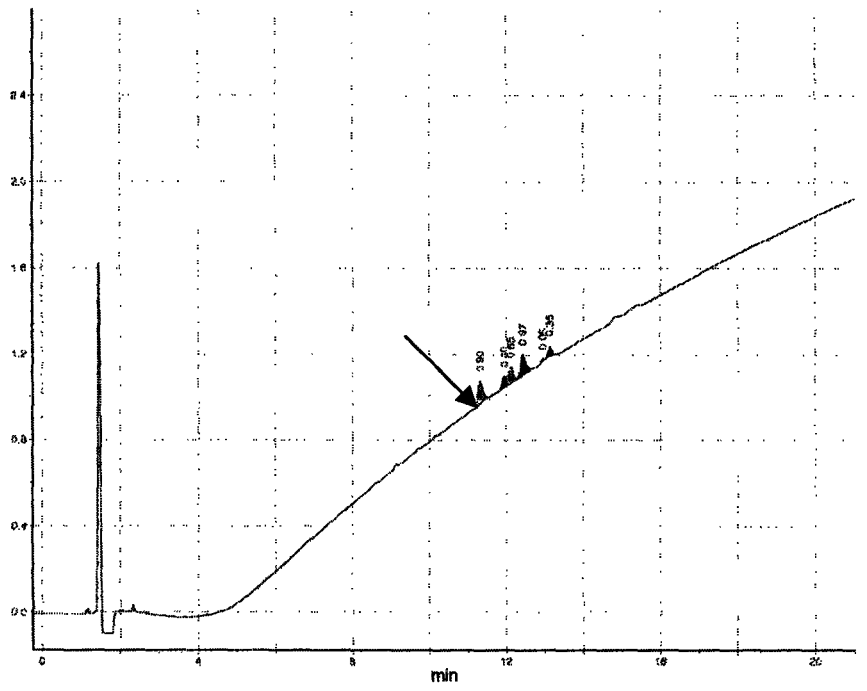

Figure 6.1 Analytical HPLC trace of crude **3-8** (arrow) cleavage product.

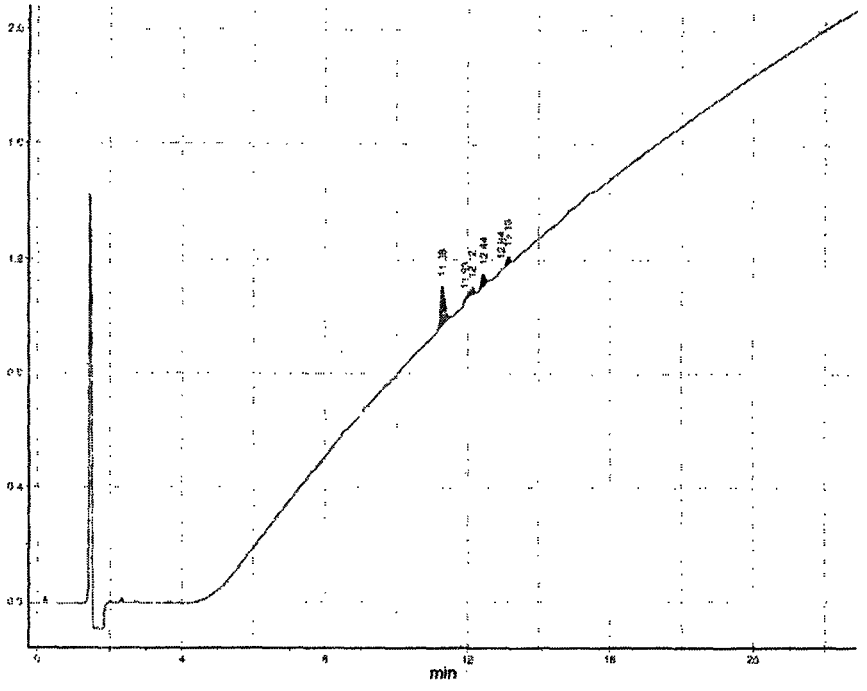

Figure 6.2 Analytical HPLC trace of cleavage product with added **3-8** (from solution phase synthesis).

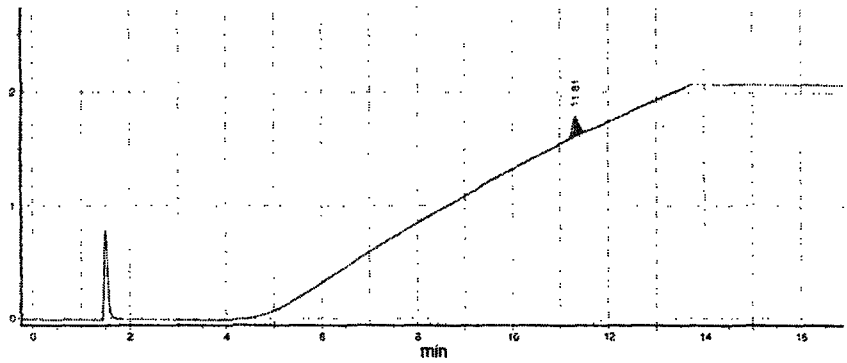

Figure 6.3 Analytical HPLC trace of semi-preparative HPLC purified **3-8**.

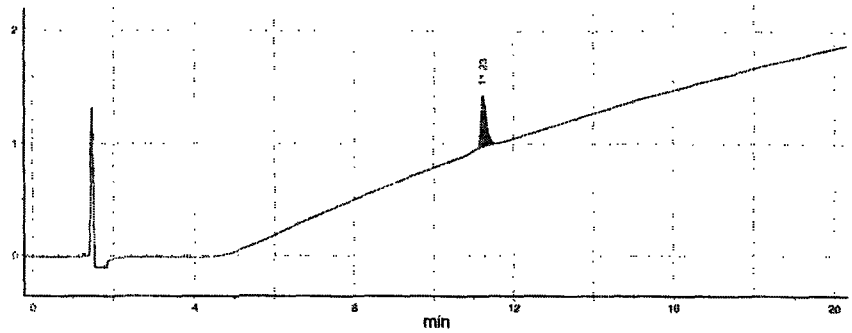

Figure 6.4 Analytical HPLC trace of purified **3-8** with added **3-8** (from solution-phase synthesis).

6.4 Experimentals for Chapter 4

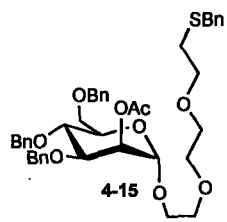

2-[2-(2-benzylsulfanyl-ethoxy)-ethoxy]-ethyl 2-*O*-acetyl-3,4,6-tri-*O*-benzyl-α-D-mannopyranoside 4-15. 2-[2-(2-benzylsulfanyl-ethoxy)-ethoxy]-ethanol (157 mg, 0.612 mmol) and mannosyl trichloroacetimidate **4-13** (300 mg, 0.471 mmol) were azeotropically dried with toluene (3 x 3 mL), dried an additional 1.5 h *in vacuo* and dissolved in dichloromethane (4.7mL). The solution was cooled to –20 °C for 15 min, followed by the addition of TMSOTf (17 μL, 0.0942 mmol), and stirred for 30 min while

warmed to RT. The reaction was quenched by the addition of Et_3N (100 μL), and dried *in vacuo*. The crude product was purified by flash column chromatography on silica gel (5 → 35% EtOAc/toluene) affording 340 mg (99%) of **4-15**. ^1H NMR (400 MHz, $CDCl_3$) δ 7.24-7.10 (m, 18H), 7.09-7.02 (m, 2H), 5.29 (m, 1H), 4.76 (d, *J*= 1.7 Hz, 1H), 4.73 (d, *J*= 10.7 Hz, 1H), 4.58 (d, *J*= 4.6, 1H), 4.55 (d, *J*= 5.6 Hz, 1H), 4.41-4.44 (m, 3H), 3.87 (dd, *J*= 3.4, 9.1 Hz, 1H), 3.77 (t, *J*= 9.6 Hz, 1H), 3.72-3.51 (m, 6H), 3.50-3.42 (m, 9H), 2.47 (t, *J*= 6.8 Hz, 2H), 2.02 (s, 3H); ^{13}C NMR (100 MHz, $CDCl_3$) δ 170.9, 138.8, 138.8, 138.6, 138.4, 129.4, 128.9, 128.8, 128.7, 128.5 ,128.3, 128.3, 128.1, 128.1, 128.0, 127.4, 98.3, 78.6, 75.6, 74.7, 73.9, 72.2, 71.8, 71.3, 70.7, 70.5, 69.2, 69.1, 67.3, 37.0, 31.0, 21.6; ESI MS m/z ($M^+ + H^+$) calcd 731.32, found 731.25.

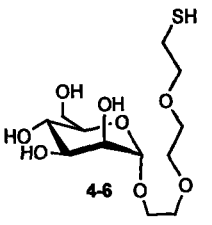

2-[2-(2-mercapto-ethoxy)-ethoxy]-ethyl α-D-mannopyranoside 4-6. Linker containing mannoside **4-15** (93 mg, 0.127 mmol) was dissolved in 5 ml freshly distilled THF. The solution was added to a stirring flask at -78 °C containing 30 ml NH_3 (liquid) with 100 mg sodium metal and methanol (15 μL, 0.508 mmol) . The solution was stirred at -78 °C for 45 minutes, maintaining deep blue color with addition of ~20 mg sodium. The reaction was quenched with the addition of methanol (5 mL). The mixture was slowly warmed to RT with stream of N_2 (g) to remove evaporating NH_3. When no trace of ammonia remains, the remaining mixture is neutralized with AcOH, and dried *in vacuo.* The resulting crude product is desalted on a sephadex G-25 column (1:1 EtOH:H_2O mobile phase) and dialyzed against 10 L H_2O (Spectra/Por® CE, MWCO 100) to afford 32 mg **4-6** (76%).^1H NMR (501 MHz, CD_3OD) δ 4.81 (s, 1H), 3.87-3.84 (m, 3H), 3.83-3.54 (m, 13H), 2.66 (t, *J*= 6.5 Hz, 1H), 1.91 (s, 1H); ^{13}C NMR (125 MHz, CD_3OD) δ; 101.8, 74.7, 72.6, 72.2, 71.7, 71.5, 68.7, 67.9, 63.0, 50.0, 24.8; ESI MS m/z ($M^+ + H^+$) calcd 329.12, found 329.19, + disulfide, calcd 655.22, found 655.31.

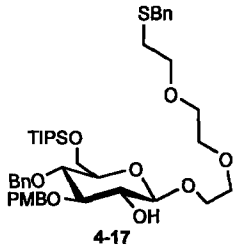

4-17

2-[2-(2-benzylsulfanyl-ethoxy)-ethoxy]-ethyl 4-*O*-benzyl-3-*O*-(4-methoxybenzyl)-6-*O*-triisopropylsilyl-β-D-glucopyranoside 4-17. Glucal **4-16** (2.66 g, 5.19 mmol) was dissolved in CH_2Cl_2 (6 mL) and cooled to 0 °C. A 0.08 M solution of dimethyldioxirane in acetone (77.8 mL, 6.23 mmol) was added and the reaction was stirred for 15 min. After the solvent was removed the remaining residue was dried *in vacuo* for 1.5 h and subsequently dissolved in CH_2Cl_2 (15 mL). The solution was cooled to –78 °C followed by the addition of 2-[2-(2-benzylsulfanyl-ethoxy)-ethoxy]-ethanol (2.66 g, 10.4 mmol). A 1.0 M solution of $ZnCl_2$ in diethyl ether (5.7 mL, 5.71 mmol) was added and the reaction was warmed slowly to room temperature and stirred over 16 h. The reaction was diluted with EtOAc (200 mL) and washed with sat. aqueous $NaHCO_3$ (2 x 100 mL), water (2 x 100 mL) and brine (2 x 100 mL) and dried (Na_2SO_4). The organic phase was concentrated *in vacuo* and the resulting residue was filtered through a 5 cm plug of silica gel (30% EtOAc/toluene) to afford 2.10 g (53%) of **4-17** as a crude oil. ^{1}H NMR (501 MHz, $CDCl_3$) δ 7.37-7.22 (m, 12H), 6.87-6.83 (m, 2H), 4.92-4.82 (m, 2H), 4.80-4.60 (m, 2H), 4.02-3.86 (m, 3H), 3.80 (s, 3H), 3.79-3.72 (m, 2H), 3.70-3.52 (m, 12H), 2.65 (t, *J*= 6.6 Hz, 2H), 1.09-1.06 (m, 21H) ESI MS m/z ($M^+ + NH_4^+$) calcd 802.44, found 801.98.

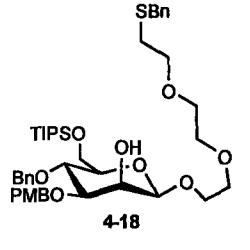

4-18

2-[2-(2-benzylsulfanyl-ethoxy)-ethoxy]-ethyl 4-*O*-benzyl-3-*O*-(4-methoxybenzyl)-6-*O*-triisopropylsilyl-β-D-mannopyranoside 4-18. Glucoside **4-17** (2.1 g, 2.67 mmol) was azeotropically dried with toluene (3 x 10 mL) and dissolved in dimethyl sulfoxide (10 mL). Acetic anhydride (5 mL) was added and the reaction was allowed to stir 48 h at room temperature. Solvent was removed *in vacuo*, the crude material was dissolved in 50

ml CH_2Cl_2 and washed with water (3 x 40 mL) and dried with Na_2SO_4. After concentration *in vacuo* the residue was dissolved in 1:1 CH_2Cl_2:MeOH (30 mL) and cooled to 0 °C. $NaBH_4$ (0.506 g, 13.4 mmol) was slowly added and the reaction was stirred 16 h at room temperature. CH_2Cl_2 (100 mL) was added and the organic phase was washed with water (100 mL), 1% aqueous citric acid (2 x 100 mL), sat. aqueous $NaHCO_3$ (100 mL), brine (100 mL) and dried (Na_2SO_4). The organic phase was dried *in vacuo* to give a clear oil and purified by flash column chromatography on silica gel (5→40% EtOAc/toluene) to afford 0.767 g (36%) of the desired β-mannoside **4-18**. ^1H NMR (501 MHz, $CDCl_3$) δ 7.36-17 (m, 12H), 6.87-6.85 (m, 2H), 4.91 (d, *J*= 10.8 Hz, 1H), 4.71-4.59 (m, 3H), 4.45 (s, 1H), 4.07 (d, *J*= 2.9 Hz, 1H), 4.00-3.85 (m, 4H), 3.80 (s, 3H), 3.76-3.64 (m, 5H), 3.63-3.56 (m, 6H), 3.52 (dd, *J*= 3.1, 9.1 Hz, 1H), 3.27-3.23 (m, 1H), 2.62 (t, *J*= 6.8 Hz, 2H), 2.32 (bs, 1H), 1.07 (app. s, 21H); ^{13}C NMR (125 MHz, $CDCl_3$) δ 159.8, 139.6, 130.7, 130.3, 129.6, 129.2, 129.2, 128.9, 128.5, 127.7, 114.4, 100.3, 81.8, 77.2, 74.6, 71.9, 71.7, 71.3, 71.1, 71.0, 69.1, 69.0, 68.9, 63.4, 56.1, 56.0, 37.2, 31.3, 18.2, 12.3; ESI MS m/z ($M^+ + NH_4^+$) calcd 802.44, found 802.11.

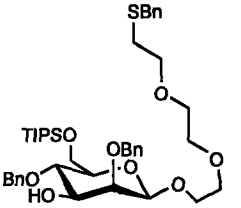

4-19

2-[2-(2-benzylsulfanyl-ethoxy)-ethoxy]-ethyl 2,4-di-*O*-benzyl-6-*O*-triisopropylsilyl-β-D-mannopyranoside 4-19. **4-18** (0.767g, 0.978 mmol) was azeotropically dried with toluene (3 x 3 mL) and dissolved in DMF (10 mL). The solution was cooled to 0 °C and sodium hydride (47 mg, 60% in mineral oil, 1.17 mmol) was carefully added and the mixture was warmed to room temperature. Benzyl bromide (139 μL, 1.17 mmol) was added to the solution, and stirred for 2 h. The reaction was quenched with the careful addtion of methanol (2 mL). The reaction was diluted with diethyl ether (100 mL), washed with water (100 mL), followed by extraction of the combined aqueous phase with diethyl ether (50 mL). The combined organic phase was washed with sat. aqueous $NaHCO_3$ (100 mL), water (100 mL), brine (100 mL), dried (Na_2SO_4) and concentrated to

give an oil *in vacuo*. The residue was purified by flash column chromatography on silica gel (0 → 10% EtOAc/toluene) to afford 769 mg (90%) of 2-[2-(2-benzylsulfanyl-ethoxy)-ethoxy]-ethyl 2,4-di-*O*-benzyl-3-*O*-(4-methoxybenzyl)-6-*O*-triisopropylsilyl-β-D-mannopyranoside. The aforementioned product (737 mg, 0.842 mmol) was dissolved in CH_2Cl_2 (4 mL) and H_2O (0.40 mL). To this mixture, DDQ (230 mg, 1.01 mmol) was added, and stirred for 1 hr at RT. The reaction was diluted in EtOAc:Et_2O (1:1, 150 mL), washed with water (2 x 50 mL), bicarb (2 x 50 mL) andbrine (1 x 60 mL), dried over $MgSO_4$ and concentrated to give an oil *in vacuo*. The resulting oil was purified by silica gel chromatography (0 → 20% EtOAc/toluene) to give 594 mg (93%) of β-mannoside acceptor **4-19**. ^{1}H NMR (400 MHz, $CDCl_3$) δ 7.31-7.13 (m, 15H), 4.97 (d, *J*= 11.8 Hz, 1H), 4.79 (d, *J*= 11.1 Hz, 1H), 4.56 (d, *J*= 1.6 Hz, 1H), 4.53 (d, *J*= 2.4 Hz, 1H), 4.45 (s, 1H), 3.95-3.83 (m, 3H), 3.76 (d, *J*= 3.2 Hz, 1H), 3.66-3.45 (m, 13H), 3.20-3.15 (m, 1H), 2.45 (app. bs, 2H), 2.42 (bs, 1H), 1.00 (app. s, 21H); ^{13}C NMR (100 MHz, $CDCl_3$) δ 139.1, 139.0, 138.8, 129.3, 128.9, 128.8, 128.7, 128.4, 128.4, 128.1, 128.0, 127.4, 101.9, 78.1, 77.8, 77.0, 75.2, 74.9, 74.4, 71.3, 71.0, 70.7, 68.8, 63.4, 37.0, 31.0, 18.4, 18.4, 12.7, 12.4, 12.1; ESI MS m/z ($M^+ + NH_4^+$) calcd 772.43, found 772.37.

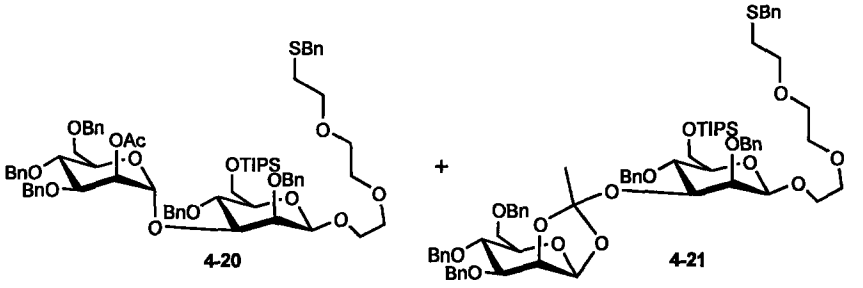

2-[2-(2-benzylsulfanyl-ethoxy)-ethoxy]-ethyl 2-*O*-acetyl-3,4,6-tri-*O*-benzyl-α-D-mannopyranosyl-(1→3)-2,4-di-*O*-benzyl-6-*O*-triisopropylsilyl-β-D-mannopyranoside 4-20 with orthoester contaminant. **4-19** (519 mg, 0.688 mmol) and mannosyl trichloroacetimidate **4-13** (657 mg, 1.03 mmol) were azeotropically dried with toluene (3 x 10 mL), dried an additional 12 h *in vacuo* and dissolved in diethyl ether (7.0 mL). The solution was cooled to –20 °C for 15 min, followed by the addition of TBSOTf (32 μL, 0.138 mmol), and stirred for 30 min at –20 °C. The reaction was quenched by the addition of Et_3N (100 μL), and dried *in vacuo*. The crude product appeared as a single

spot by TLC, and was purified by flash column chromatography on silica gel (5 → 35% EtOAc/toluene) affording 812 mg (96%) of the disaccharides **4-20** mixed (~1:1) with orthoester **4-21** (confirmed by ^{13}C NMR of orthoester carbon at δ 124.4). ^{1}H NMR (400 MHz, $CDCl_3$) δ 7.40-28 (m, 4H), 7.26-7.04 (m, 56H), 7.42-7.40 (m, 1H), 5.11 (d, *J*= 1.5 Hz, 1H), 5.06 (d, *J*= 2.6 Hz, 1H), 4.89-4.64 (m, 6H), 4.61-4.47 (m, 11H), 4.41-4.33 (m 7H), 3.93-3.81 (m, 9H), 3.81-3.73 (m, 7H), 3.67-41 (m, 30H), 3.33-3.29 (m, 1H), 3.21-3.12 (m, 2H), 2.53-2.48 (m, 2H), 2.00 (s, 3H), 1.66 (s, 3H), 0.98 (app. s, 42H); ^{13}C NMR (100 MHz, $CDCl_3$) δ 170.5, 139.8, 139.5, 139.1, 138.9, 138.8, 138.6, 138.6, 138.3, 138.2, 129.3, 128.9, 128.8, 128.8, 128.8, 128.7, 128.7, 128.6, 128.6, 128.5, 128.3, 128.2, 128.1, 128.0, 128.0, 127.9, 127.5, 127.4, 124.4, 101.9, 101.7, 100.1, 98.0, 80.7, 79.0, 78.5, 78.5, 76.6, 76.4, 75.6, 75.5, 75.2, 74.7, 74.3, 74.0, 73.8, 73.8, 72.5, 72.4, 72.3, 71.2, 70.9, 70.7, 69.5, 69.4, 69.3, 68.8, 63.5, 63.1, 37.0, 31.0, 25.7, 21.4, 18.4, 18.4, 12.4; ESI MS m/z ($M^+ + H^+$) calcd 1251.5875, found 1251.5861.

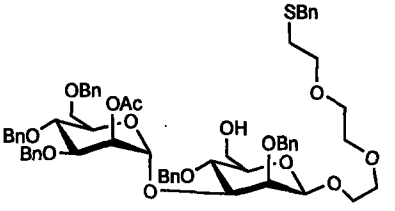

4-22

2-[2-(2-benzylsulfanyl-ethoxy)-ethoxy]-ethyl 2-*O*-acetyl-3,4,6-tri-*O*-benzyl-α-D-mannopyranosyl-(1→3)-2,4-di-*O*-benzyl-β-D-mannopyranoside 4-22. The mixture containing disaccharide **4-20** and orthoester **4-21** (812 mg) was dissolved in AcOH (50 mL, 80%), and stirred vigorously for 3 h at RT. The mixture was diluted in CH_2Cl_2 (100 mL) and washed with water (3 x 100 mL), sat. aqueous $NaHCO_3$ (2 x 50 mL), brine (50 mL) and dried (Na_2SO_4). The organic phase was dried *in vacuo*, and passed through a 10 cm plug of silica gel (10 % EtOAc/hexanes) to separate disaccharide **4-20** (248 mg) from C3 hydroxyl manoside **4-19** (132 mg). The crude isolate of **4-20** (248 mg, 0.202 mmol) was dissolved in THF (3 mL). Water (3 mL) was slowly added with vigorous stirring followed by TFA (1 mL). The reaction was stirred for 1 hr at RT, followed by additional TFA (1 mL). The mixture was stirred for an additional 1 h and diluted with diethyl ether (50 mL) and washed with water (3 x 50 ml), sat. aqueous $NaHCO_3$ (2 x 30 mL), brine (30

mL), dried ($MgSO_4$) and concentrated. The residue was purified by flash column chromatography on silica gel (5 → 30% EtOAc/toluene) to afford 197 mg (91%) of the C6 acceptor disaccharide **4-22**. ^1H NMR (400 MHz, $CDCl_3$) δ 7.27-7.06 (m, 30H), 5.45-5.43 (m, 1H), 5.19 (d, J = 1.3 Hz, 1H), 4.73-4.71 (m, 1H), 4.66-4.55 (m, 10H), 4.24-22 (m, 1H), 4.00 (d, J=11.1 Hz, 1H), 3.86 (d, J= 10.8 Hz, 1H), 3.84-3.60 (m, 6H), 3.54-3.50 (m, 10H), 3.26-2.19 (m, 2H), 2.63 (t, J=7.2 Hz, 2H), 2.44 (bs, 1H), 2.01 (s, 3H); ^{13}C NMR (100 MHz, $CDCl_3$) δ 171.0, 138.3, 137.5, 137.3, 137.2, 128.9, 128.9, 128.8, 128.5, 128.4, 128.4, 128.4, 128.3, 128.2, 127.9, 127.7, 127.6, 127.5, 127.5, 127.4, 126.9, 101.3, 97.8, 76.0, 74.2, 74.1, 74.1, 73.6, 73.4, 72.3, 71.3, 70.8, 70.3, 69.5, 69.2, 68.4, 66.7, 66.6, 65.4, 62.8, 62.3, 38.6, 33.4, 28.4, 17.6; ESI MS m/z ($M^+ + NH_4^+$) calcd 1090.50, found 1090.31.

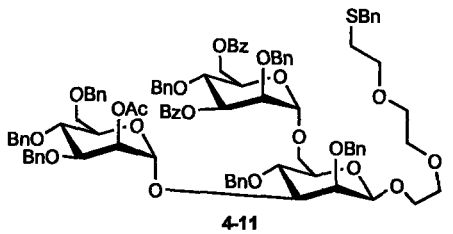

4-11

2-[2-(2-benzylsulfanyl-ethoxy)-ethoxy]-ethyl 2-*O*-acetyl-3,4,6-tri-*O*-benzyl-α-D-mannopyranosyl-(1→3)-[2,4-di-*O*-benzyl-3,6-di-*O*-benzoyl-α-D-mannopyranosyl-(1→6)]-2,4-di-*O*-benzyl-β-D-mannopyranoside 4-11. Disaccharide acceptor **4-22** (197 mg, 0.184 mmol) and mannosyl trichloroacetimidate **4-14** (172 mg, 0.275 mmol) were combined, azeotropically dried with toluene (3 x 5 mL) and dissolved in Et_2O (2 mL). The solution was cooled to –20 °C for 15 min, followed by the addition of TBSOTf (8.4 μL, 0.0367 mmol). The reaction mixture was stirred and warmed to room temperature over 40 min. The reaction was quenched by the addition of Et_3N (50 μL), and dried *in vacuo*. The crude product was purified by flash column chromatography on silica gel (2 → 30% EtOAc/toluene) to afford 241 mg (81%) of differentiated trisaccharide **4-11**. ^1H NMR (400 MHz, $CDCl_3$) δ 8.01-7.95 (m, 4H), 7.52-7.48 (m, 4H), 7.47-6.86 (m, 42H), 5.59 (dd, J= 3.2, 9.5 Hz, 1H), 5.44-5.43 (m, 1H), 5.13 (d, J= 9.4 Hz, 2H), 4.85-4.76 (m, 3H), 4.66-4.53 (m, 5H), 4.53-4.40 (m, 6H), 4.39-4.27 (m, 4H), 4.21 (t, J= 9.7 Hz, 1H), 4.06-3.99 (m 2H), 3.97-3.88 (m, 2H), 3.85-3.79 (m, 3H), 3.78-3.51 (m, 10H), 3.49-3.36 (m, 8H), 3.30-3.27 (m, 1H), 2.48 (app. bs, 2H), 1.99 (s, 3H); ^{13}C NMR (100 MHz,

$CDCl_3$) δ 170.4, 166.8, 166.0, 139.1, 139.1, 138.9, 138.6, 138.6, 138.3, 138.3, 138.0, 133.6, 133.4, 130.5, 130.2, 130.2, 129.4, 128.9, 128.9, 128.8, 128.8, 128.8, 128.7, 128.6, 128.6, 128.6, 128.5, 128.4, 128.2, 128.2, 128.1, 128.0, 128.0, 127.7, 127.4,101.9, 100.1, 98.6, 80.5, 78.4, 77.1, 76.1, 75.7, 75.6, 75.5, 75.2, 74.8, 74.6, 74.6, 73.8, 73.7, 73.2, 72.6, 72.5, 71.2, 70.9, 70.6,70.5, 69.3, 69.0, 66.4, 64.0, 37.0, 31.0, 21.9, 21.5, 14.7 ; ESI MS m/z ($M^+ + Na^+$) calcd 1645.65, found 1645.57.

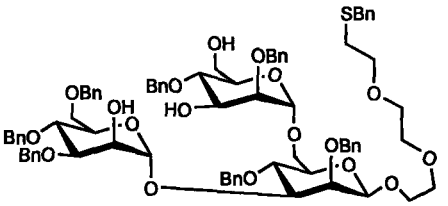

4-23

2-[2-(2-benzylsulfanyl-ethoxy)-ethoxy]-ethyl 3,4,6-tri-*O*-benzyl-α-D-mannopyranosyl-(1→3)-[2,4-di-*O*-benzyl-α-D-mannopyranosyl-(1→6)]-2,4-di-*O*-benzyl-β-D-mannopyranoside 4-23. Trisaccharide **4-11** (224 mg, 0.0687 mmol) was dissolved in CH_2Cl_2:MeOH (8 mL, 1:1). A solution of sodium methoxide in MeOH (450 μL, 25% w/v, 2 mmol) was added and the reaction was heated on an oil-bath to 45 °C for 1.5 h. The reaction was quenched with DOWEX-50W-hydrogen strongly acidic ion-exchange resin, filtered, and dried *in vacuo*. The resulting crude product was purified by flash column chromatography on silica gel (10 → 40% EtOAC/toluene) to afford 161 mg (85%) of trisaccharide triol **4-23**. ^{1}H NMR (400 MHz, $CDCl_3$) δ 7.28-7.02 (m, 40H), 5.16 (d, *J*=1.1 Hz, 1H), 5.07 (d, *J*= 1.0 Hz, 1H), 4.85-4.80 (m, 2H), 4.73-4.61 (m, 3H), 4.55-4.52 (m, 4H), 4.49-4.28 (m, 6H), 3.94-3.88 (m, 3H), 3.86-3.58 (m, 14H), 3.51-3.41 (m, 9H), 3.37-3.35 (m, 2H), 3.22-3.19 (m, 1H), 2.47 (t, *J*= 6.8 Hz, 2H), 2.00 (app. bs, 3H); ^{13}C NMR (100 MHz, $CDCl_3$) δ 137.6, 137.5, 137.5, 137.4, 137.1, 137.0, 136.8, 136.7, 128.0, 127.9, 127.5, 127.5, 127.4, 127.4, 127.4, 127.3, 127.2, 127.2, 127.2, 126.9, 126.9, 126.9, 126.8, 126.8, 126.7, 126.7, 126.6, 126.6, 126.5, 126.3, 126.0, 124.2, 100.6, 100.3, 96.5, 79.1, 78.8, 77.6, 77.2, 75.5, 74.5, 74.2, 74.0, 73.9, 73.7, 73.1, 73.1, 72.3, 71.6, 71.1, 70.8, 70.7, 70.4, 69.7, 69.5, 69.4, 69.1, 67.9, 67.6, 65.0, 61.2, 35.5, 29.5, 20.4; ESI MS m/z ($M^+ + Na^+$) calcd 1395.59, found 1395.66.

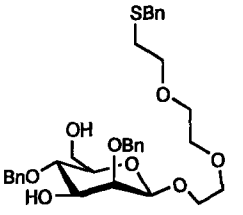

4-24

2-[2-(2-benzylsulfanyl-ethoxy)-ethoxy]-ethyl 2,4-di-*O*-benzyl-β-D-mannopyranoside 4-24. **4-19** (90 mg, 0.120 mmol) was dissolved in THF (1 mL). Water (300 μL) was slowly added with vigorous stirring followed by TFA (300 μL). The reaction was stirred for 3 hr at RT, diluted with diethyl ether (30 mL) and washed with water (3 x 20 ml), sat. aqueous $NaHCO_3$ (2 x 30 mL), brine (30 mL), dried ($MgSO_4$) and concentrated. The residue was purified by flash column chromatography on silica gel (10 → 30% EtOAc/toluene) to afford 62 mg (86%) of the C3,6 diol **4-24**. ^1H NMR (400 MHz, $CDCl_3$) δ 7.19-7.06 (m, 15H), 5.04 (d, *J*= 1.8 Hz, 1H), 4.64-4.62 (m, 4H), 3.99-3.95 (m, 2H), 3.74-3.66 (m, 6H), 3.60-3.54 (m, 8H), 3.35 (m, 1H), 3.02 (m, 1H), 2.66 (t, *J*= 6.9 Hz, 2H) 2.45 (app. bs, 2H); ^{13}C NMR (100 MHz, $CDCl_3$) δ 138.8, 137.3, 137.1, 128.9, 128.9, 128.8, 128.8, 128.7, 128.5, 128.4, 127.7, 127.7, 127.6, 127.6, 127.6, 127.4, 126.7, 100.1, 77.3, 74.1, 74.1, 72.9, 72.6, 72.4, 71.3, 70.9, 70.2, 65.7, 65.3, 59.8, 38.8, 33.3; ESI MS m/z ($M^+ + NH_4^+$) calcd 616.29, found 616.88.

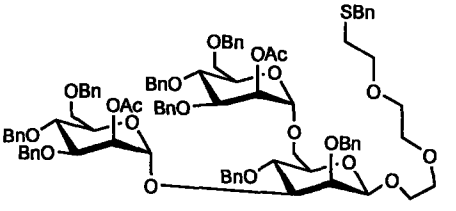

4-25

2-[2-(2-benzylsulfanyl-ethoxy)-ethoxy]-ethyl 2-*O*-acetyl-3,4,6-tri-*O*-benzyl-α-D-mannopyranosyl-(1→3)-[2-*O*-acetyl-3,4,6-tri-*O*-benzyl-α-D-mannopyranosyl-(1→6)]-2,4-di-*O*-benzyl-β-D-mannopyranoside 4-25. Mannosyl trichloroacetimidate **4-13** (172 mg, 0.269 mmol, 2.6 eq.) and monosaccharide diol **4-24** (62 mg, 0.104 mmol) were combined, azeotropically dried with toluene (3 x 3 mL) and dissolved in diethyl ether (1 mL). The solution was cooled to –20 °C for 15 min, followed by the addition of TMSOTf (4 μl, 0.021 mmol), and stirred for 30 min while warming slowly to RT. The

reaction was quenched by the addition of Et_3N (50 μL), and dried *in vacuo*. The crude product was purified by flash column chromatography on silica gel (5 → 25% EtOAc/toluene) to afford 131 mg (82%) of non-differentiated trisaccharide **4-25**. ^1H NMR (400 MHz, $CDCl_3$) δ 7.31-7.00 (m, 45H), 5.47-5.45 (m, 1H), 5.39-5.36 (m, 1H), 5.10 (d, *J*=1.8 Hz, 1H), 4.92-4.73 (m, 4H), 4.68-4.62 (m, 2H), 4.60-4.50 (m, 4H), 4.43-4.30 (m, 8H), 3.88-3.40 (m, 26H), 3.30-3.22 (m, 1H), 2.0 (t, *J*=6.8 Hz, 2H), 2.05 (s, 3H), 1.98 (s, 3H); ^{13}C NMR (100 MHz, $CDCl_3$) δ 170.7, 170.5, 139.2, 139.1, 139.0, 138.8, 138.7, 138.6, 138.3, 138.3, 138.1, 129.3, 128.9, 128.8, 128.8, 128.7, 128.6, 128.6, 128.5, 128.3, 128.3, 128.2, 128.1, 128.0, 128.0, 128.0, 127.9, 127.9, 127.7, 127.4, 102.0, 100.1, 98.3, 80.7, 78.5, 78.1, 77.6, 75.8, 75.5, 75.4, 75.3, 75.1, 74.6, 74.5, 74.5, 73.8, 73.7, 72.5, 72.4, 71.8, 71.8, 71.2, 70.9, 70.9, 70.7, 69.3, 69.2, 69.1, 68.8, 66.9, 37.0, 31.0, 21.6, 21.4; ESI MS m/z ($M^+ + NH_4^+$) calcd 1564.70, found 1565.01.

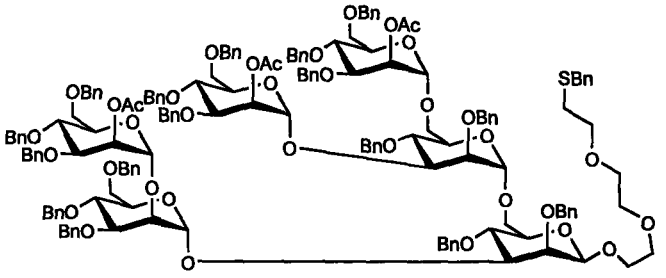

4-10

2-[2-(2-benzylsulfanyl-ethoxy)-ethoxy]-ethyl 2-*O*-acetyl-3,4,6-tri-*O*-benzyl-α-D-mannopyranosyl-(1→2)-3,4,6-tri-*O*-benzyl-α-D-mannopyranosyl-(1→3)-[2-*O*-acetyl-3,4,6-tri-*O*-benzyl-α-D-mannopyranosyl-(1→3)-[2-*O*-acetyl-3,4,6-tri-*O*-benzyl-α-D-mannopyranosyl-(1→6)]-2,4-di-*O*-benzyl-α-D-mannopyranosyl-(1→6)]-2,4-di-*O*-benzyl-β-D-mannopyranoside 4-10. Trisaccharide triol **4-25** (161 mg, 0.117 mmol) and mannosyl trichloroacetimidate **4-13** (336 mg, 0.527 mmol, 4.5 eq) were azeotropically dried with toluene (3 x 5 mL), dried an additional 10 h *in vacuo* and dissolved in CH_2Cl_2 (2mL). The solution was cooled to –20 °C for 15 min, followed by the addition of TMSOTf (13 μL, 0.070 mmol), and stirred for 30 min while warming to RT. The reaction was quenched by the addition of Et_3N (100 μL), and dried *in vacuo*. The crude product was purified by flash column chromatography on silica gel (5 → 40%

EtOAc/toluene) affording 276 mg (84%) of hexasaccharide **4-10.** ^{1}H NMR (400 MHz, $CDCl_3$) δ 7.30-6.92 (m, 80H), 5.43-5.40 (m, 3H), 5.10 (d, *J*= 2.8 Hz, 2H), 4.95-4.82 (m, 4H), 4.79-4.59 (m, 6H), 4.68-4.58 (m, 3H), 4.52-4.18 (m, 28H), 3.99-3.62 (m, 21H), 3.60-3.50 (m, 10H), 3.48-3.30 (m, 18H), 3.24 (d, *J*= 10.8 Hz, 1H), 3.10-3.02 (m, 1H), 2.44 (t, *J*= 10.8 Hz, 2H), 2.03 (s, 3H), 2.00 (s, 3H), 1.97 (s, 3H); ^{13}C NMR (100 MHz, $CDCl_3$) δ 170.7, 170.6, 170.6, 139.4, 139.2. 139.2, 139.1, 139.1, 138.9, 138.9, 138.9, 138.8, 138.8, 138.8, 138.7, 138.7, 138.7, 138.5, 138.4, 138.3, 129.5, 129.5, 129.0, 128.9, 128.9, 128.8, 128.8, 128.7, 128.7, 128.3, 128.3, 128.3, 128.0, 128.0, 127.9, 127.9, 102.1, 101.5, 100.3, 99.9, 98.8, 97.4, 81.9, 80.2, 78.7, 78.6, 78.1, 77.90, 75.7, 75.7, 75.6, 75.4, 75.3, 75.0, 74.7, 74.6, 74.5, 73.9, 73.9, 73.8, 73.7, 73.0, 72.7, 72.5, 72.3, 72.1, 71.7, 71.4, 71.3, 71.0, 69.4, 69.3, 69.1, 68.8, 66.7, 66.3, 37.1, 31.1, 22.0, 21.7, 21.5; MALDI-TOF m/z ($M^+ + Na^+$) calcd 2818.20, found 2817.55.

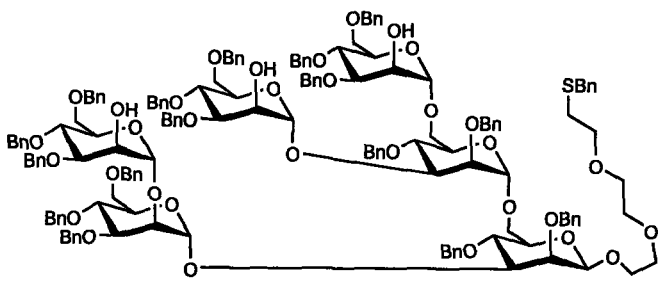

4-26

2-[2-(2-benzylsulfanyl-ethoxy)-ethoxy]-ethyl 3,4,6-tri-*O*-benzyl-α-D-mannopyranosyl-(1→2)-3,4,6-tri-*O*-benzyl-α-D-mannopyranosyl-(1→2)-3,4,6-tri-*O*-benzyl-α-D-mannopyranosyl-(1→3)-[3,4,6-tri-*O*-benzyl-α-D-mannopyranosyl-(1→2)-3,4,6-tri-*O*-benzyl-α-D-mannopyranosyl-(1→3)-[3,4,6-tri-*O*-benzyl-α-D-mannopyranosyl-(1→2)-3,4,6-tri-*O*-benzyl-α-D-mannopyranosyl-(1→6)]-2,4-di-*O*-benzyl-α-D-mannopyranosyl-(1→6)]-2,4-di-*O*-benzyl-β-D-mannopyranoside 4-26. Hexasaccharide **4-10** (117 mg, 0.0419 mmol) was azeotropically dried with toluene (3 x 3 mL) and dissolved in CH_2Cl_2 (2 mL). MeOH (4 mL) was added followed by a solution of sodium methoxide in MeOH (50 μL, 25% w/v, 0.22 mmol). The reaction was stirred for 1 h at 45 °C, quenched with DOWEX-50W-hydrogen strongly acidic ion-exchange resin, filtered, and dried *in vacuo*. The resulting residue was purified by flash column chromatography on silica gel (10 → 40% EtOAc/toluene) to afford 102 mg (91%) of

hexasaccharide triol **4-26**. ^{1}H NMR (500 MHz, $CDCl_3$) δ 7.48-7.10 (m, 80H), 5.27 (d, *J*= 22 Hz, 2H), 5.13 (d, *J*= 16.3 Hz, 2H), 5.03 (d, *J*= 12.5 Hz, 1H), 4.93-4.82 (m, 6H), 4.78-4.49(m, 27H), 4.48-4.34 (m, 3H), 4.15-3.81 (m, 23H), 3.79-3.46 (m, 28H), 3.26-3.22 (m, 1H), 2.60 (t, *J*= 6.8 Hz, 2H), 2.00 (app. s, 3H, -OH); ^{13}C NMR (125 MHz, $CDCl_3$) δ139.6, 139.5. 139.5, 139.5, 139.4, 139.3, 139.2, 139.2, 139.1, 139.0, 139.0, 138.9, 138.9, 138.9, 138.6, 138.5, 138.6, 129.8, 129.3, 129.0, 128.9, 128.9, 128.8, 128.7, 128.6, 128.5, 128.4, 128.3, 128.3, 128.1, 128.1, 127.6, 127.5, 102.2, 101.2, 100.0, 99.9, 98.7, 97.7, 80.2, 78.7, 78.5, 78.1, 77.90, 75.5, 75.5, 75.5, 75.4, 75.3, 75.1, 74.7, 74.6, 74.3, 73.9, 73.9, 73.8, 73.6, 73.1, 72.7, 72.5, 72.3, 72.1, 71.7, 71.4, 71.3, 71.0, 69.4, 69.3, 69.1, 68.8, 66.7, 66.3, 37.1, 31.1, 22.0; MALDI-TOF m/z ($M^+ + Na^+$) calcd 2692.17, found 2692.33.

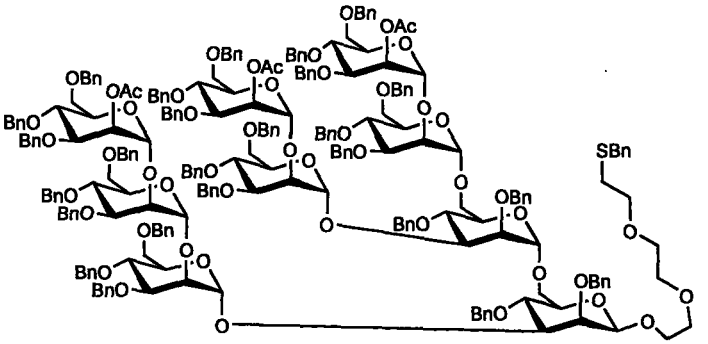

4-9

2-[2-(2-benzylsulfanyl-ethoxy)-ethoxy]-ethyl 2-*O*-acetyl-3,4,6-tri-*O*-benzyl-α-D-mannopyranosyl-(1→2)-3,4,6-tri-*O*-benzyl-α-D-mannopyranosyl-(1→2)-3,4,6-tri-*O*-benzyl-α-D-mannopyranosyl-(1→3)-[2-*O*-acetyl-3,4,6-tri-*O*-benzyl-α-D-mannopyranosyl-(1→2)-3,4,6-tri-*O*-benzyl-α-D-mannopyranosyl-(1→3)-[2-*O*-acetyl-3,4,6-tri-*O*-benzyl-α-D-mannopyranosyl-(1→2)-3,4,6-tri-*O*-benzyl-α-D-mannopyranosyl-(1→6)]-2,4-di-*O*-benzyl-α-D-mannopyranosyl-(1→6)]-2,4-di-*O*-benzyl-β-D-mannopyranoside 4-9. Hexasaccharide **4-26** (102 mg, 0.0382 mmol) and mannosyl trichloroacetimidate **4-13** (182 mg, 0.286 mmol, 7.5 eq) were azeotropically dried with toluene (3 x 5 mL), dried an additional 12 h *in vacuo* and dissolved in diethyl ether (2mL). The solution was cooled to –20 °C for 15 min, followed by the addition of TMSOTf (4 μL, 0.0229 mmol), and stirred for 30 min while warming to RT. The reaction was quenched by the addition of Et_3N (50 μL), and dried *in vacuo*. The crude

product was purified by flash column chromatography on silica gel (2 → 35 % EtOAc/toluene) affording 111 mg (71%) of nonasaccharide **4-9**. ^{1}H NMR (500 MHz, $CDCl_3$) δ 4.46-1.06 (m, 130H), 5.70 (app. s, 1H), 5.65-5.59 (m, 3H), 5.36-5.13 (m, 7H), 5.06-5.00 (m, 2H), 4.96-4.88 (m, 8H), 4.84-4.36 (m, 42H), 4.32-3.46 (m, 60H), 3.26-3.20 (m, 2H), 2.58 (t, *J*= 6.7Hz, 2H), 2.22 (s, 3H), 2.20 (s, 3H), 2.18 (s, 3H); . ^{13}C NMR (125 MHz, $CDCl_3$) δ Anomeric carbons: 102.1, 102.1, 100.2, 100.0, 100.0, 99.9, 93.8, 93.6, 92.8. MALDI-TOF m/z ($M^+ + Na^+$) calcd 4091.79, found 4091.82.

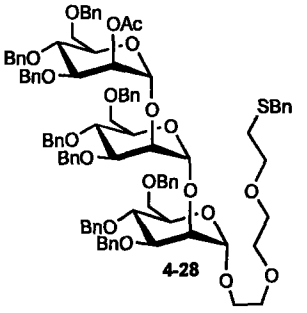

2-[2-(2-benzylsulfanyl-ethoxy)-ethoxy]-ethyl 2-*O*-acetyl-3,4,6-tri-*O*-benzyl-α-D-mannopyranosyl-(1→2)-3,4,6-tri-*O*-benzyl-α-D-mannopyranosyl-(1→2)-3,4,6-tri-*O*-benzyl-α-D-mannopyranoside 4-28. Beginning with mannoside **4-15** (400 mg, 0.549 mmol), the C2 acetate was removed by treatment with NaOMe (100 μL, 0.44 mmol) in 10 ml (1:1 CH_2Cl_2:MeOH), followed by neutralization with acidic Amberlite-IR-120 resin, furnishing 325 mg of crude monosaccharide C2 acceptor (86% crude). The crude acceptor was coevaporated (3 x 5 mL toluene) with mannosyl donor **4-13** (390mg, 0.0612 mol), dissolved in dichloromethane (5 mL), and cooled to 0 °C. Following treatment with TMSOTF (17 μL, 0.0942 mmol) the mixture was warmed to RT, quenched with Et_3N (50 μL) and dried *in vacuo*. Following silica gel chromatography (5 → 30 % EtOAc/toluene) 443 mg disccharide **4-27** (81%) was isolated. Disaccharide **4-27** (322 mg, 0.276 mmol) was deprotected analogously to **4-15** by treatment with NaOMe and quenched with Amberlite-IR-120 resin, furnishing the disaccharide C2 acceptor (285 mg, 0.254 mmol) in 92% yield. This disaccharide was coevaporated in toluene (3 x 5 ml) with **4-13** (210 mg, 0.330 mmol), dissolved in dichloromethane (3 ml), and cooled to 0 °C. TMSOTF (11.3 μL, 0.0508 mmol) was added, and the mixture warmed to room temperature. The reaction was quenched with Et_3N (100 μL) and dried *in vacuo*. The

resulting trisaccharide was purified by flash column chromatography on silica gel (10 → 40 % EtOAc/toluene) affording 369 mg (91%) of trimannoside **4-28**. ^{1}H NMR (500 MHz, $CDCl_3$) δ 7.36-7.14 (m, 50H), 5.56 (app. s, 1H), 5.21 (s, 1H), 5.07 (s, 1H), 4.95 (s, 1H), 4.87-4.82 (m, 3H), 4.70-4.42 (m, 15H), 4.31 (d, *J*= 12.0 Hz, 1H), 4.12 (s, 1H), 4.04 (s, 1H), 4.02-3.95 (m, 1H), 3.94-3.83 (m, 5H), 3.82-3.66 (m, 11H), 3.57-3.44 (m, 10H), 2.59 (d, *J*= 6.9 Hz, 2H), 2.15 (s, 3H); ^{13}C NMR (125 MHz, $CDCl_3$) δ 170.1, 139.3, 139.2, 139.2, 139.1, 139.1, 138.9, 138.7, 129.7, 129.2, 129.1, 129.1, 129.0, 129.0, 129.0, 129.0, 128.9, 129.8, 128.7, 128.5, 128.5, 128.4, 128.3, 128.2, 128.2, 128.1,127.7, 101.4, 100.2, 99.5, 80.2, 78.9, 76.9, 76.9, 76.8, 76.7, 76.5, 76.4, 74.9, 74.1, 74.0, 73.9, 72.0, 71.4, 71.1, 69.5, 67.2, 37.2, 31.2, 21.7; ESI MS m/z ($M^+ + NH_4^+$) calcd 1612.74, found 1613.01.

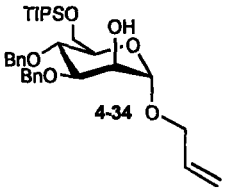

2-Propenyl 3,4-di-*O*-benzyl-6-*O*-triisopropylsilyl-α-D-mannopyranoside 4-34. Mannosyl trichloroacetimidate **4-32** (0.477 g, 0.796 mmol) was azeotropically dried with toluene (3 x 10 mL) and dissolved in CH_2Cl_2 (8 mL). The solution was cooled to -30 °C for 15 min, allyl alcohol (230 μL, 3.38 mmol), followed by TMSOTf (31 μL, 0.169 mmol) were added to the solution, and stirred for 30 min at –30 °C while warming to RT. The reaction was quenched by addition of Et_3N (500 μL), and dried *in vacuo*. The crude product was purified by flash column chromatography on silica gel (2 → 10% EtOAc/hexanes) to afford 477 mg (66%) of 2-Propenyl 2-*O*-acetyl-3,4-di-*O*-benzyl-6-*O*-triisopropylsilyl-α-D-mannopyranoside. ^{1}H NMR (500 MHz, $CDCl_3$) δ 7.37-7.25 (m, 10H), 5.94-5.81 (m, 1H), 5.37-5.35 (m, 1H), 5.30-5.16 (m, 2H), 4.91 (d, *J*= 10.8 Hz, 1H), 4.83 (d, *J*= 1.7 Hz, 1H), 4.70-4.55 (m, 3H), 4.19-3.89 (m, 8H), 3.70-3.65 (m, 1H), 2.12 (s, 3H), 1.10 (app. s, 21H). 2-Propenyl 2-*O*-acetyl-3,4-di-*O*-benzyl-6-*O*-triisopropylsilyl-α-D-mannopyranoside (316 mg, 0.528 mmol) was dissolved in methanol (3ml), into which sodium methoxide (12 μL, 25% wt, 0.0528 mmol) was added and stirred at RT for 16 h. The reaction was quenched with Amberlite-IR-120 resin, dried *in vacuo*, and purified by silica gel chromatography (5 → 20% EtOAc/hexanes) to furnish 240 mg

(82%) of **4-34** as an oil. ^{1}H NMR (500 MHz, $CDCl_3$) δ 7.42-7.26 (m, 10H), 5.96-5.88 (m, 1H), 5.29 (app. d, *J*= 18 Hz, 1H), 5.21 (d, *J*= 9.1 Hz, 1H), 4.93-4.91 (m, 2H), 4.77-4.67 (m, 3H), 4.25-4.21 (m, 1H), 4.09 (app. s, 1H), 4.03-3.91 (m 4H), 3.82 (t, *J*= 9.6 Hz, 1H), 3.80-3.71 (m, 1H), 2.47 (s, 1H), 1.12 (app. s, 21H); ^{13}C NMR (125 MHz, $CDCl_3$) δ 139.2, 138.7, 134.8, 134.3, 129.3, 129.3, 129.2, 129.2, 129.1, 129.1, 128.9, 128.7, 128.6, 128.6, 128.5, 128.5, 128.4, 118.2, 98.8, 81.4, 75.9, 75.2, 73.6, 72.8, 72.8, 69.4, 68.9, 63.7, 18.8, 12.7; ESI MS m/z ($M^+ + H^+$) calcd 557.33, found 557.19.

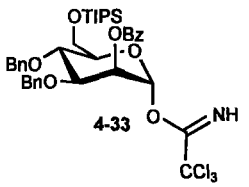

2-*O*-benzoyl-3,4-di-*O*-benzyl-6-*O*-triisopropylsilyl-α-D-mannopyranosyl trichloroacetimidate 4-33. Allyl mannoside **4-34** (236 mg, 0.424 mmol) was azeotroped with toluene (3 x 5 ml), dissolved in CH_2Cl_2 (2 mL) and cooled to 0 °C. To this solution benzoyl chloride (74 μL, 0.636 mmol) and pyridine (1 mL) were added. The mixture was stirred for 1.5 h, and warmed slowly to RT. The resulting mixture was diluted with CH_2Cl_2 (50 mL), washed with water (50 mL), sat. aqueous $NaHCO_3$ (50 mL), brine (50 mL) and dried (Na_2SO_4). The resulting crude product was purified by flash column chromatography on silica gel (4 → 10% EtOAC/toluene) to afford 264 mg (94%) 2-propenyl 2-*O*-benzoyl-3,4-di-*O*-benzyl-6-*O*-triisopropylsilyl-α-D-mannopyranoside. ^{1}H NMR (400 MHz, $CDCl_3$) δ 8.04-7.98 (m, 2H), 7.53-7.07 (m, 13H), 5.81-5.72 (m, 1H), 5.54-5.52 (m, 1H), 5.15 (dd, *J*= 1.5, 17.2 Hz, 1H), 5.06 (dd, *J*= 1.4, 11.3 Hz, 1H), 4.84 (d, *J*= 1.7 Hz, 1H), 4.79 (d, *J*= 10.7 Hz, 1H), 4.67 (d, *J*= 9.3 Hz, 1H), 4.56 (d, *J*= 9.3 Hz, 1H), 4.46 (d, *J*= 11.3 Hz, 1H), 4.09-3.84 (m, 6H), 3.64-3.61 (m, 1H), 0.99 (app. s, 21H). The benzoylated product (260 mg, 0.393 mmol) was dissolved in AcOH (3 mL) with water (100 μL). NaOAc (74 mg, 0.905 mmol) followed by $PdCl_2$ (80 mg, 0.452 mmol) were added the mixture. The slurry was vigorously stirred for 2 h at 50 °C. Additional NaOAc (74 mg, 0.905 mmol) and $PdCl_2$ (80 mg, 0.452 mmol) were added, and the reaction stirred another 2 h. The crude mixture was filtered through a 1 cm celite plug, diluted with EtOAc (100 ml) and washed with water (60 mL), sat. aqueous $NaHCO_3$ (60

mL), brine (60 mL) and dried (Na_2SO_4). The crude lactol was dried *in vacuo* to a yellow oil which was dissolved in CH_2Cl_2 (2 mL) and cooled to 0 °C. Trichloroacetonitrile (339 μL, 3.38 mmol) and DBU (17.6 μL, 0.118 mmol) were added, the reaction was stirred at 0 °C for 30 min and warmed to RT for 1 h. The crude product was subjected to silica gel column chromatography (0 → 10% EtOAC/hexanes), furnishing 174 mg desired trichloroacetimidate **3-33** and 62 mg recovered lactol (isolated yield 80%). ^{1}H NMR (500 MHz, $CDCl_3$) δ 8.68 (s, 1H), 8.17-8.14 (m, 2H), 7.63-7.26 (m, 13H), 6.42 (d, *J*= 1.8 Hz, 1H), 5.77-5.75 (m, 1H), 4.95 (d, *J*= 10.5 Hz, 1H), 4.83 (d, *J*= 11.4 Hz, 1H), 4.75 (d, *J*= 10.5 Hz, 1H), 4.65 (d, *J*= 11.5 Hz, 1H), 4.30 (t, *J*= 9.8 Hz, 1H), 4.18-4.14 (m, 2H), 4.03-3.94 (m, 2H), 1.13 (app. s, 21H); ^{13}C NMR (125 MHz, $CDCl_3$) δ 166.2, 160.7, 139.1, 138.4, 134.0, 130.8, 130.3, 129.1, 129.1, 129.0, 129.0, 128.9, 128.5, 96.5, 78.2, 76.3, 76.2, 74.2, 72.7, 68.5, 62.9, 18.8, 18.7, 12.8; ESI MS m/z ($M^+ + Na^+$) calcd 786.22, found 786.21.

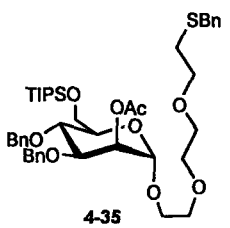

4-35

2-[2-(2-benzylsulfanyl-ethoxy)-ethoxy]-ethyl 2-*O*-acetyl-3,4-tri-*O*-benzyl-6-*O*-triisopropylsilyl-α-D-mannopyranoside 4-35. 2-[2-(2-benzylsulfanyl-ethoxy)-ethoxy]-ethanol (338 mg, 1.32 mmol) and mannosyl trichloroacetimidate **4-32** (618 mg, 0.879 mmol) were azeotropically dried with toluene (3 x 5 mL), dried an additional 2 h *in vacuo* and dissolved in Et_2O (9.0 mL). The solution was cooled to –20 °C for 15 min, followed by the addition of TMSOTf (32 μL, 0.176 mmol), and stirred for 15 min. The reaction was quenched by the addition of Et_3N (500 μL), and dried *in vacuo*. The crude product was purified by flash column chromatography on silica gel (5 → 10% EtOAc/toluene) affording 755 mg (99%) of **4-35**. ^{1}H NMR (400 MHz, $CDCl_3$) δ 7.23-7.10 (m, 15H), 5.25-5.24 (m, 1H), 4.77 (d, *J*= 10.7 Hz, 1H), 4.68 (d, *J*= 7.8 Hz, 1H), 4.59-4.51 (m, 2H), 4.41 (d, *J*= 11.1 Hz, 1H), 3.89-3.77 (m, 4H), 3.66-3.62 (m, 3H), 3.60-3.43 (m, 11H), 2.49 (t, *J*= 6.7 Hz, 2H), 1.98 (s, 3H), 0.096 (app. s, 21H); ^{13}C NMR (100 MHz, $CDCl_3$) δ 170.9, 139.0, 138.8, 138.5, 129.3, 128.9, 128.8, 128.5, 128.4, 128.1,

127.4, 97.9, 78.6, 75.7, 74.5, 73.3, 73.0, 72.2, 71.2, 71.0, 71.0, 70.7, 70.5, 69.3, 66.9, 63.0, 62.3, 37.0, 30.9, 21.4, 18.4, 18.4, 12.4; ESI MS m/z ($M^+ + NH_4^+$) calcd 814.44, found 814.59.

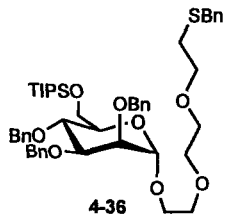

2-[2-(2-benzylsulfanyl-ethoxy)-ethoxy]-ethyl 2,3,4-tri-*O*-benzyl-6-*O*-triisopropylsilyl-α-D-mannopyranoside 4-36. To a solution of mannoside **4-35** (750 mg, 0.873 mmol) in methanol (8 mL), and CH_2Cl_2 (2 mL) was added sodium methoxide (20 μL, 25% wt, 0.0873 mmol). The solution was stirred 16 h at RT, additional sodium methoxide (8 μL, 0.0349 mmol) was added, and the reaction stirred an additional 2 h. The reaction was quenched with DOWEX-50W-hydrogen strongly acidic ion-exchange resin, filtered, and dried *in vacuo*. The residue was purified by flash column chromatography on silica gel (5 → 25% EtOAc/hexanes) to afford 582 mg (98%) of the C2 hydroxyl intermediate. This product (570 mg, 0.755 mmol) was azeotroped with toluene (3 x 5 ml), dissolved in DMF (7.5 mL), and cooled to 0 °C. Sodium hydride (60 mg, 60% in mineral oil, 1.51 mmol) was carefully added to the solution, and stirred for 20 min at 0 °C. Benzyl bromide (135 μL, 1.13 mmol) and TBAI (~10 mg) was added to the reaction mixture and slowly warmed to room temperature for 2 h. Methanol (3 mL) was slowly added to quench the reaction, which was further diluted in 150 mL water. The solution was extracted with diethyl ether (3x 50 mL). After concentration the combined organic phase *in vacuo,* the resulting residue was purified by flash column chromatography on silica gel (2 → 25% EtOAc/hexanes) to afford 560 mg (88%) of **4-36** as a clear oil. ^{1}H NMR (400 MHz, $CDCl_3$) δ 7.30-7.15 (m, 20H), 4.85 (d, *J*= 10.9 Hz, 1H), 4.78 (d, *J*= 1.7 Hz, 1H), 4.68-4.54 (m, 5H), 3.86-3.83 (m, 4H), 3.76-7.75 (m, 1H), 3.74-3.65 (m, 3H), 3.54-3.47 (m, 10H), 2.53 (t, *J*= 6.8 Hz, 2H), 0.99 (app. s, 21H); ^{13}C NMR (100 MHz, $CDCl_3$) δ 139.1, 139.1, 138.9, 138.8, 129.3, 128.9, 128.8, 128.7, 128.6, 128.5, 128.0, 128.0, 127.9,

127.4, 98.0, 80.7, 75.6, 75.4, 75.3, 73.9, 72.9, 72.5, 71.2, 71.0, 70.7, 70.6, 66.5, 63.5, 37.0, 30.9, 18.4, 18.4, 12.4; ESI MS m/z ($M^+ + NH_4^+$) calcd 862.47, found 862.71.

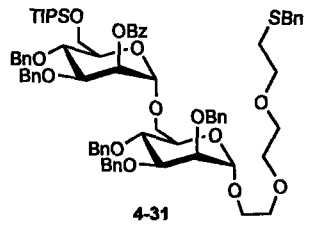

2-[2-(2-benzylsulfanyl-ethoxy)-ethoxy]-ethyl 2-*O*-benzoyl-3,4-di-*O*-benzyl-6-*O*-triisopropylsilyl-α-D-mannopyranosyl-(1→6)-2,3,4-tri-*O*-benzyl-α-D-mannopyranoside 4-31. To a solution of mannoside **4-36** (540 mg, 0.639 mmol) dissolved in Et_2O (7 mL) and CH_2Cl_2 (5 mL) was added TBAF (3.39 mL, 1.0 M in Et_2O, 3.39 mmol). The reaction was refluxed at 55 °C for 4 h, diluted with EtOAc (100 mL) and washed with sat. aqueous $NaHCO_3$ (60 mL), water (60ml), brine (60 mL) and dried (Na_2SO_4). The crude product was filtered through a plug of silica gel (10% EtOAc/toluene), to furnish 128 mg (44%) of the C6 hydroxyl acceptor. This product (128 mg, 0.186 mmol) and mannosyl donor **4-33** (180 mg, 0.242 mmol) were coevaporated with toluene (3 x 5 ml), and dissolved in Et_2O (2 mL). The solution was cooled to -20 °C, and TMSOTF (6.7 μL, 0.037 mmol) was added. The reaction was stirred at -20 °C for 30 min, quenched with Et_3N (200 μL), and dried *in vacuo* to an oil. The crude disaccharide was purified by silica gel column chromatography (2 → 30% EtOAc/hexans) to yield 236 mg (98%) of disaccharide **4-31**. ^1H NMR (500 MHz, $CDCl_3$) δ 8.16-8.14 (m, 2H), 7.61-7.18 (m, 33H), 5.76-7.75 (m, 1H), 5.04 (d, *J*= 1.4 Hz, 1H), 4.97-4.92 (m, 3H), 4.80-4.75 (m, 3H), 4.70-4.52 (m, 6H), 4.17-4.09 (m, 3H), 4.00-3.87 (m, 7H), 3.79-3.71 (m, 6H), 3.61-3.55 (m, 8H), 2.61 (t, *J*= 6.8 Hz, 2H), 1.12 (app. s, 21H); ^{13}C NMR (125 MHz, $CDCl_3$) δ 166.3, 139.6, 139.2, 139.2, 139.1, 139.1, 138.8, 130.8, 130.8, 130.8, 129.7, 129.7, 129.2, 129.2, 129.1, 129.1, 129.0, 129.0, 129.0, 128.9, 128.6, 128.4, 128.4, 128.3, 128.2, 127.7, 98.8, 98.4, 78.7, 78.1, 77.8, 75.9, 75.4, 73.4, 72.7, 72.0, 71.3, 71.0, 37.3, 31.3, 18.8, 18.8, 12.8; ESI MS m/z ($M^+ + Na^+$) calcd 1313.60, found 1314.00.

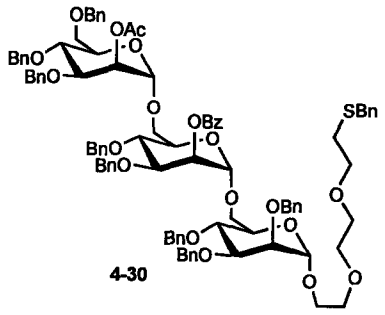

4-30

2-[2-(2-benzylsulfanyl-ethoxy)-ethoxy]-ethyl 2-*O*-acetyl-3,4,6-tri-*O*-benzyl-α-D-mannopyranosyl-(1→6)-2-*O*-benzoyl-3,4-di-*O*-benzyl-α-D-mannopyranosyl-(1→6)-2,3,4-tri-*O*-benzyl-α-D-mannopyranoside 4-30. Disaccharide **4-31** (240 mg, 0.186 mmol) was dissolved in THF (3 mL). Water (3 mL) was slowly added with vigorous stirring followed by TFA (1 mL). The reaction was stirred for 1 hr at RT, followed by the addition of additional TFA (2 mL). The mixture was stirred for an additional 1 h and diluted with diethyl ether (100 mL) and washed with water (3 x 50 ml), sat. aqueous $NaHCO_3$ (2 x 30 mL), brine (30 mL), dried ($MgSO_4$) and concentrated. The residue was purified by flash column chromatography on silica gel (10 → 50% EtOAc/hexanes) to afford 165 mg (78%) of the C6 acceptor disaccharide intermediate. ^1H NMR (500 MHz, $CDCl_3$) δ 8.13-8.11 (m, 2H), 7.63-7.20 (m, 33H), 5.77-5.76 (m, 1H), 5.11 (d, *J*= 1.8Hz, 1H), 4.98-4.94 (m, 3H), 4.78 (s, 2H), 4.75 (d, *J*= 11.6 Hz, 1H), 4.68-4.64 (m, 3H), 4.53 (d, *J*= 11.7 Hz, 2H), 4.14-4.11 (m, 1H), 4.02-3.90 (m, 5H), 3.81-3.74 (m, 8H), 3.62-3.55 (m, 9H), 2.61 (t, *J*= 6.85 Hz, 2H), 2.07 (m, 1H, -OH); ^{13}C NMR (125 MHz, $CDCl_3$) δ 166.2, 139.2, 139.2, 139.1, 139.1, 138.6, 133.9, 130.7, 130.6, 129.7, 129.2, 129.1, 129.1, 129.1, 128.9, 128.8, 128.6, 128.5, 128.4, 128.4, 128.4, 128.3, 128.3, 127.7, 98.7, 98.5, 80.9, 78.2, 75.9, 75.3, 74.6, 73.4, 72.7, 72.7, 71.8, 71.7, 71.6, 71.3, 71.0, 70.9, 69.5, 67.4, 67.2, 62.7, 37.3, 31.3. The resulting disaccharide acceptor (161 mg, 0.142 mmol) and mannosyl trichloroacetimidate **4-13** (135 mg, 0.213 mmol) were azeotropically dried with toluene (3 x 3 mL), dried an additional 2 h *in vacuo* and dissolved in diethyl ether (2mL). The solution was cooled to –20 °C for 15 min, followed by the addition of TMSOTf (5 μL, 0.0284 mmol), and warmed to RT. The reaction was quenched by the addition of Et_3N (500 μL), and dried *in vacuo*. The crude product was purified by flash column chromatography on silica gel (10 → 50% EtOAc/toluene) affording 176 mg (77%) of trisaccharide **4-30**. ^1H NMR (500 MHz, $CDCl_3$) δ 8.18-8.16 (m, 2H), 7.52-7.13 (m, 48H),

5.83-5.82 (m, 1H), 5.61-5.60 (m, 1H), 5.10 (d, *J*= 1.5 Hz, 1H), 5.05 (d, *J*= 1.5 Hz, 1H), 5.00-4.87 (m, 5H), 4.82-4.79 (m, 4H), 4.72-4.64 (m, 5H), 4.56-4.42 (m, 7H), 4.10 (dd, *J*= 3.0 Hz, 9.3 Hz, 1H), 4.01-3.88 (m, 10H), 3.84-3.72 (m, 7H), 3.71-3.55 (m, 15H), 2.62 (t, *J*= 6.9 Hz, 2H), 2.20 (s, 3H); ^{13}C NMR (125 MHz, $CDCl_3$) δ 171.0, 166.2, 139.3, 139.3, 139.2, 139.2, 139.2, 139.1, 138.9, 138.5, 138.4, 133.9, 130.8, 130.6, 129.7, 129.3, 129.3, 129.2, 129.1, 129.1, 129.0, 128.9, 128.9, 128.9, 128.6, 128.6, 128.5, 128.5, 128.4, 128.4, 128.3, 128.2, 128.1, 128.1, 127.7, 98.9, 98.8, 98.5, 81.0, 78.7, 78.6, 75.8, 75.7, 75.3, 75.3, 74.8, 74.7, 74.1, 73.4, 72.7, 72.3, 72.2, 71.9, 71.9, 71.6, 71.4, 71.3, 71.0, 70.9, 69.3, 69.3, 69.0, 67.3, 67.2, 66.6, 37.3, 31.3, 21.9; ESI MS m/z (M^+ + Na^+) calcd 1631.67, found 1632.03.

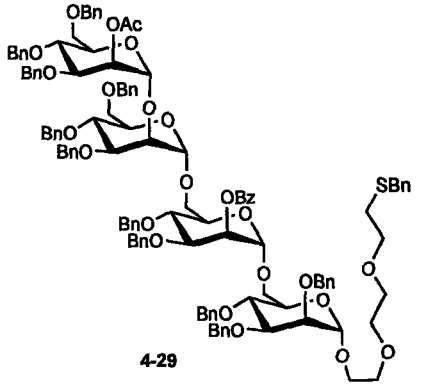

4-29

2-[2-(2-benzylsulfanyl-ethoxy)-ethoxy]-ethyl 2-*O*-acetyl-3,4,6-tri-*O*-benzyl-α-D-mannopyranosyl-(1→2)-3,4,6-tri-*O*-benzyl-α-D-mannopyranosyl-(1→6)-2-*O*-benzoyl-3,4-di-*O*-benzyl-α-D-mannopyranosyl-(1→6)-2,3,4-tri-*O*-benzyl-α-D-mannopyranoside 4-29. Trisaccharide **4-30** (170 mg, 0.106 mmol) was coevaporated with toluene (3 x 3 ml) and dissolved in a mixture of MeOH:Et_2O:THF (2 mL, 0.5 mL, and 0.5 mL, respectively). Stirring at RT, magnesium methoxide was added in 0.5 equiv aliquots over 4 h, until a total of 5 equiv (45 mg, 0.528 mmol). The reaction was quenched by the addition of AcOH (1 mL), and dried *in vacuo* to a white solid. Purification by flash silica column chromatography (5-50% EtOAc/toluene) afforded the trisaccharide C2 hydroxyl acceptor (117 mg, 71%). ^{1}H NMR (500 MHz, $CDCl_3$) δ 8.16-8.14 (m, 2H), 7.55-7.19 (m, 48H), 5.82-5.81 (m, 1H), 5.21 (d, *J*= 1.4 Hz, 1H), 5.11 (d, *J*= 1.7 Hz, 1H), 5.00-4.94 (m, 3H), 4.88-4.78 (m, 4H), 4.70-4.63 (m, 5H), 4.56-4.49 (m, 5H), 4.21-4.20 (m, 1H), 4.13 (dd, *J*= 2.0, 9.1 Hz, 1H), 4.01-3.86 (m, 10H), 3.81-3.71 (m, 9H),

3.64-3.57 (m, 11H), 2.63 (t, *J*= 6.9 Hz, 2H), 2.40 (s, 1H, -OH); ^{13}C NMR (125 MHz, $CDCl_3$) δ 166.2, 139.3, 139.2, 139.2, 139.2, 139.2, 139.1, 139.0, 138.6, 133.9, 130.9, 130.6, 129.8, 129.7, 129.2, 129.2, 129.1, 129.1, 129.1, 129.0, 129.0, 128.7, 128.6, 128.6, 128.5, 128.5, 128.4, 128.4, 128.4, 128.4, 128.3, 128.3, 128.2, 127.8, 100.1, 98.7, 98.5, 81.0, 80.7, 78.5, 75.8, 75.8, 75.3, 75.3, 75.0, 74.8, 74.2, 73.4, 72.7, 72.5, 72.0, 71.9, 71.9, 71.8, 71.6, 71.3, 71.0, 70.9, 69.4, 69.4, 69.0, 67.3, 67.2, 66.2, 37.3, 31.3. The resulting trisaccharide acceptor (117 mg, 0.0746 mmol) and mannosyl trichloroacetimidate **4-13** (71 mg, 0.112 mmol) were azeotropically dried with toluene (3 x 3 mL), and dissolved in diethyl ether (1 mL). The solution was cooled to –20 °C for 15 min, followed by the addition of TMSOTf (2.7 μL, 0.0149 mmol), and warmed to RT. The reaction was quenched by the addition of Et_3N (50 μL), and dried *in vacuo*. The crude product was purified by flash column chromatography on silica gel (5 → 30% EtOAc/toluene) affording 145 mg (95%) of tetrasaccharide **4-29.** ^{1}H NMR (500 MHz, $CDCl_3$) δ 8.17-8.16 (m, 2H), 7.47-7.17 (m, 63H), 5.82-5.81 (m, 1H), 5.62-5.61 (m, 1H), 5.17 (app. s, 1H), 5.12 (app. s, 1H), 5.08 (app. s, 1H), 4.99-4.89 (m, 6H), 4.82-4.79 (m, 4H), 4.72-4.43 (m, 20H), 4.23 (app. s, 1H), 4.13-4.07 (m, 1H), 4.06-3.94 (m, 12H), 3.89-3.71 (m, 12H), 3.67-3.55 (m, 14H), 2.64 (t, *J*= 6.7 Hz, 2H), 2.18 (s, 3H); ^{13}C NMR (125 MHz, $CDCl_3$) δ 170.9, 166.2, 139.4, 139.3, 139.3, 139.3, 139.3, 139.2, 139.2, 139.1, 139.0, 138.9, 138.8, 138.5, 133.9, 130.9, 130.6, 129.8, 129.7, 129.3, 129.2, 129.2, 129.2, 129.1, 129.1, 129.1, 129.0, 129.0, 128.9, 128.9, 128.9, 128.9, 128.9, 128.8, 128.8, 128.7, 128.7, 128.6, 128.6, 128.6, 128.5, 128.5, 128.5, 128.4, 128.3, 128.3, 128.2, 128.2, 128.2, 128.1, 128.1, 128.1, 128.0, 127.8, 100.3, 99.8, 99.0, 98.5, 81.0, 80.3, 78.9, 78.6, 78.1, 77.9, 77.6, 75.8, 75.6, 75.5, 75.4, 75.3, 75.2, 75.0, 74.7, 74.1, 74.0, 73.4, 72.8, 72.7, 72.7, 72.7, 72.5, 72.0, 71.8, 71.6, 71.3, 71.0, 70.9, 69.7, 69.6, 69.5, 69.4, 67.5, 67.2, 66.9, 37.4, 31.4, 30.5, 21.9; ESI MS m/z (M^{2+} + $2H^+$) calcd 1021.44, found 1021.51.

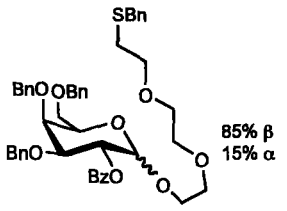

4-38

2-[2-(2-benzylsulfanyl-ethoxy)-ethoxy]-ethyl 2-*O*-benzoyl-3,4,6-tri-*O*-benzyl-α/β-D-galactopyranoside 4-38. Galactosyl phosphate **4-37** (345 mg, 0.462 mmol) and 2-[2-(2-benzylsulfanyl-ethoxy)-ethoxy]-ethanol were coevaporated with toluene (3 x 10 ml) and dissolved in CH_2Cl_2 (5 mL). The solution was cooled to -40 °C and TMSOTF (84 μL, 0.462 mmol) was added. The reaction was warmed to -20 °C quenched with Et_3N (500 μL) and dried *in vacuo*. The crude product was purified by silica gel column chromatography (5 → 20% EtOAc/toluene) to afford 267 mg (73%) galactoside **4-38.** ^1H NMR (500 MHz, $CDCl_3$) δ 8.10-8.08 (m, 2H), 7.60-7.44 (m, 3H), 7.39-7.25 (m, 20H), 5.57 (dd, *J*= 3.8, 10.5 Hz, 1H), 5.32 (d, *J*= 3.8 Hz, 1H), 5.00 (d, *J*= 11.6 Hz, 1H), 4.73 (d, *J*= 2.6 Hz, 2H), 4.65-4.45 (m, 3H), 4.16 (dd, *J*= 2.8, 9.1 Hz, 1H), 4.11-4.08 (m, 2H), 3.82-3.75 (m, 3H), 3.68-3.58 (m, 7H), 3.58-3.49 (m, 4H), 3.37-3.34 (m, 2H), 2.58 (t, *J*= 6.9 Hz, 2H); ^{13}C NMR (125 MHz, $CDCl_3$) δ 166.7, 139.2, 139.2, 139.0, 138.7, 133.8, 130.9, 130.5, 129.7, 129.2, 1291.2, 129.1, 129.1, 129.0, 129.0, 129.0, 128.9, 128.7, 128.6, 128.5, 128.4, 128.3, 128.3, 128.3, 127.7, 97.4, 78.1, 75.5, 75.2, 74.3, 73.3, 72.4, 71.5, 71.2, 70.9, 70.8, 70.1, 69.6, 68.2, 37.3, 31.3; ESI MS m/z ($M^+ + NH_4^+$) calcd 810.37, found 810.12.

General Procedure for the Dissolving Metal Reduction of Protected Oligosaccharides. Protected oligosaccharide was dissolved in anyhydrous THF and 1 equivalent methanol for every benzyl ether in the structure. The saccharide was added to a stirring solution of sodium metal dissolved in liquid ammonia. Following 45 minutes at -78 °C, the solution is quenched by addition of excess methanol, and the liquid ammonia is allowed to evaporate. The resulting product was neutralized by addition of acetic acid, dried *in vacuo*, purified by size-exclusion chromatography on Sephadex G-25 with 1:1

H_2O:EtOH mobile phase and dialyzed against 10 L H_2O (Spectra/Por® CE, MWCO 100, and MWCO 500 for **4-1** and **4-2**).

A Note on Disulfide Contamination. There were multiple opportunities for the following sulfhydryl-modified saccharides to partially oxidize to symmetric disfulides. Normal handling exposed the structures to atmospheric oxygen, and the formation of disulfide could be observed by TLC and in the following ^{1}H NMR spectra. This is most evident is the splitting of the methylene hydrogens adjacent to the thiol and in the ESI and MALDI-TOF MS.

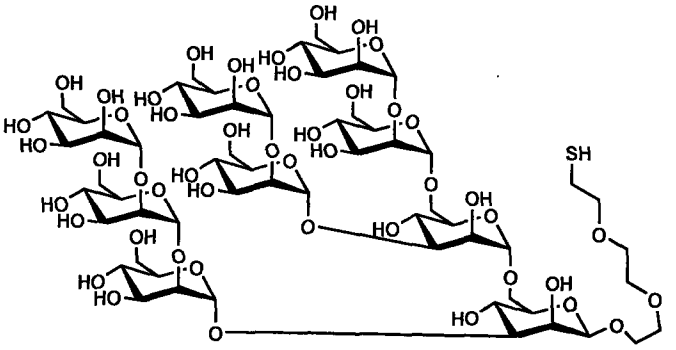

4-1

2-[2-(2-mercapto-ethoxy)-ethoxy]-ethyl α-D-mannopyranosyl-(1→2)-α-D-mannopyranosyl-(1→2)-α-D-mannopyranosyl-(1→3)-[α-D-mannopyranosyl-(1→2)-α-D-mannopyranosyl-(1→3)-[α-D-mannopyranosyl-(1→2)-α-D-mannopyranosyl-(1→6)]-α-D-mannopyranosyl-(1→6)]-β-D-mannopyranoside 4-1. Nonamannoside **4-9** (138 mg, 0.0338 mmol) was subjected to a dissolving metal reduction, and purified as described above to furnish 33 mg (60%) of **4-1**. ^{1}H NMR (500 MHz, D_2O/CD_3OD) δ 5.41 (s, 1H), 5.37 (s, 1H), 5.30 (s, 1H), 5.13 (s, 1H), 5.12 (s, 1H), 5.01 (app. s, 3H), 4.63 (s, 1H), 4.13-3.51 (m, 76H), 3.46-3.44 (m, 1H), 2.93 (t, *J*= 6.4 Hz, 2H, disulfide methylene), 2.68 (t, *J*= 6.1 Hz, 2H, sulfhydryl methylene); MATLDI-TOF MS m/z (M^+ + Na^+) calcd 1647.5, found 1647.5

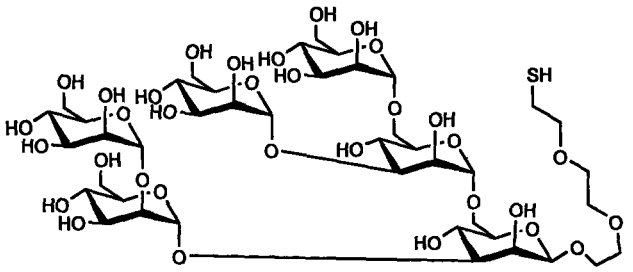

4-2

2-[2-(2-mercapto-ethoxy)-ethoxy]-ethyl α-D-mannopyranosyl-(1→2)-α-D-mannopyranosyl-(1→3)-[α-D-mannopyranosyl-(1→3)-[α-D-mannopyranosyl-(1→6)]-α-D-mannopyranosyl-(1→6)]-β-D-mannopyranoside 4-2. Hexasaccharide **4-10** (76 mg, 0.027 mmol) was subjected to a dissolving metal reduction, and purified as described above to furnish 22 mg (71%) of **4-2**. ^{1}H NMR (500 MHz, D_2O/CD_3OD) δ 5.37 (s, 1H), 5.10 (s, (1H), 5.00 (d, *J*= 1.6 Hz, 1H), 4.86 (app. s, 1H), 4.82 (app. s, 1H), 4.60 (d, *J*= 2.5 Hz, 1H), 4.13-4.11 (m, 3H), 4.06-4.05 (m, 1H), 4.01-3.59 (m, 68H), 3.46-3.40 (m, 1H), 2.93 (t, *J*= 6.4 Hz, 2H, disulfide methylene), 2.68 (t, *J*= 6.1 Hz, 2H, sulfhydryl methylene); MATLDI-TOF MS m/z ($M^+ + Na^+$) calcd 1161.37, found 1159.30.

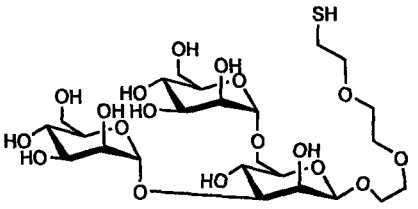

4-3

2-[2-(2-mercapto-ethoxy)-ethoxy]-ethyl α-D-mannopyranosyl-(1→3)-[α-D-mannopyranosyl-(1→6)]-β-D-mannopyranoside 4-3. Branched trisaccharide **4-25** (78 mg, 0.050 mmol) was subjected to a dissolving metal reduction, and purified as described above to furnish 27 mg (82%) of **4-3**. ^{1}H NMR (500 MHz, D_2O/CD_3OD) δ 5.08 (s, 1H), 4.83 (s, 1H), 4.59 (s, 1H), 4.12 (d, *J*= 3.7 Hz, 1H), 3.99-3.94 (m, 2H), 3.94-3.91 (m, 1H), 3.87-3.58 (m, 25H), 3.40-3.38 (m, 1H), 2.93 (t, *J*= 6.4 Hz, 2H, disulfide methylene), 2.67 (t, *J*= 6.1 Hz, 2H, sulfhydryl methylene); ^{13}C NMR (125 MHz, D_2O/CD_3OD) δ 103.3, 100.9, 100.6, 82.0, 76.1, 74.3, 73.7, 73.4, 71.9, 71.7, 71.3, 71.3, 71.2, 70.8, 70.7, 70.6, 70.4, 69.7, 68.7, 68.1, 67.8, 66.7, 66.5, 62.3, 62.1, 38.7, 23.9, 23.3; MATLDI-TOF MS m/z ($M^+ + Na^+$) calcd 675.21, found 676.0.

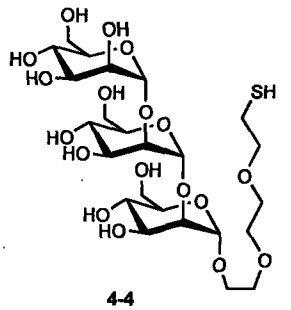

4-4

2-[2-(2-mercapto-ethoxy)-ethoxy]-ethyl α-D-mannopyranosyl-(1→2)-α-D-mannopyranosyl-(1→2)-α-D-mannopyranoside 4-4. Linear trisaccharide **4-28** (180 mg, 0.113 mmol) was subjected to a dissolving metal reduction, and purified as described above to furnish 39 mg (53%) of **4-4**. ^{1}H NMR (500 MHz, D_2O/CD_3OD) δ 5.27 (s, 1H), 5.10 (d, *J*= 1.2 Hz, 1H), 4.98 (d, *J*= 1.3 Hz, 1H), 4.03 (app. s, 1H), 3.97 (d, *J*= 1.5 Hz, 1H), 3.86-3.81 (m, 8H), 3.76-3.52 (m, 21H), 2.91 (t, *J*= 6.2 Hz, 2H, disulfide methylene), 2.66 (t, *J*= 6.4 Hz, 2H, sulfhydryl methylene); ^{13}C NMR (125 MHz, D_2O/CD_3OD) δ 103.4, 101.8, 99.3, 80.1, 79.6, 74.3, 73.9, 73.4, 71.7, 71.3, 71.2, 71.2, 70.8, 70.6, 70.5, 68.5, 68.3, 68.0, 67.2, 62.6, 62.4, 62.3, 48.8, 48.7, 48.0, 47.8, 24.0; ESI MS m/z (M^+ + H^+) calcd 653.23, found 653.20.

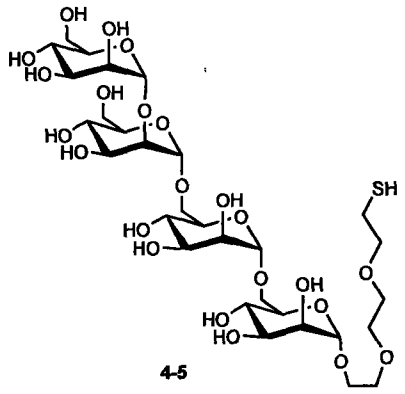

4-5

2-[2-(2-mercapto-ethoxy)-ethoxy]-ethyl α-D-mannopyranosyl-(1→2)-α-D-mannopyranosyl-(1→6)-α-D-mannopyranosyl-(1→6)-α-D-mannopyranoside 4-5. Tetrasaccharide **4-29** (88 mg, 0.0431 mmol) was dissolved in CH_2Cl_2 (1 mL) and MeOH (5 mL) and reacted with NaOMe (25% v/w, 25 μL, 0.1 mmol) at RT for 2 hr. The mixture was neutralized with with DOWEX-50W-hydrogen strongly acidic ion-exchange resin, filtered, and dried *in vacuo*. Prior to dissolving metal reduction, the crude material

was filtered through a 2 cm plug of silica gel (20% EtOAc/toluene), and dried. The material was subjected to a dissolving metal reduction, and purified as described above to furnish 32 mg (91%) of tetrasaccharide **4-5**. ^{1}H NMR (500 MHz, D_2O) δ 4.97 (d, *J*= 1.2 Hz, 1H), 4.86 (d, *J*=1.5 Hz, 1H), 4.71 (d, *J*= 1.2 Hz, 1H), 4.70 (d, *J*= 1.2 Hz, 1H), 3.90-3.89 (m, 1H), 3.84-3.78 (m, 6H), 3.74-3.60 (m, 12H), 3.59-3.50 (m, 17H), 3.44 (t, *J*= 9.7 Hz, 1H), 2.79 (t, *J*= 6.1 Hz, 2H, disulfide methylene). NOTE: Fully oxidized by sitting for prolonged period in solution under normal atmosphere. ESI MS m/z ($M^+ + H^+$) calcd 815.28, found 815.33.

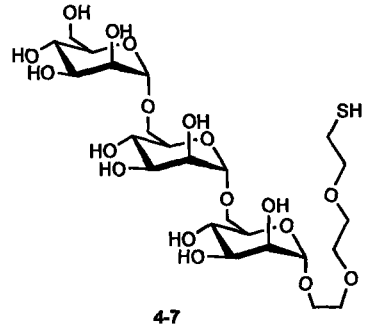

4-7

2-[2-(2-mercapto-ethoxy)-ethoxy]-ethyl α-D-mannopyranosyl-(1→6)-α-D-mannopyranosyl-(1→6)-α-D-mannopyranoside 4-7. Trisaccharide **4-30** (351 mg, 0.218 mmol) was dissolved in CH_2Cl_2 (1 mL) and MeOH (5 mL) and reacted with NaOMe (25% v/w, 25 μL, 0.1 mmol) at RT for 2 hr. The mixture was neutralized with with DOWEX-50W-hydrogen strongly acidic ion-exchange resin, filtered, and dried *in vacuo*. Prior to dissolving metal reduction, the crude material was filtered through a 2 cm plug of silica gel (10% EtOAc/toluene), and dried. The material was subjected to a dissolving metal reduction, and purified as described above to furnish 101 mg (71%) of trisaccharide **4-7**. ^{1}H NMR (500 MHz, D_2O) δ 4.74 (s, 1H, C1-H), 4.71 (app. s, 2H, 2 x C1-H), 3.82-3.73 (m, 5H), 3.71-3.61 (9H), 3.60-3.45 (m, 14H), 2.79 (t, *J*= 6.1 Hz, 2H, disulfide methylene), 2.57 (t, *J*= 6.1 Hz, 2H, sulfhydryl methylene); ^{13}C NMR (125 MHz, D_2O) δ 100.8, 100.1, 99.8, 73.3, 72.8, 71.4, 71.4, 71.3, 71.1, 70.6, 70.2, 70.1, 70.0, 69.8, 67.3, 67.2, 67.1, 66.1, 61.5, 37.8, 23.7; ESI MS m/z ($M^+ + H^+$) calcd 653.23, found 653.11.

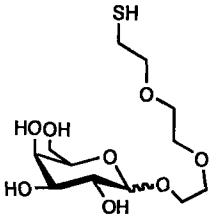

4-8

2-[2-(2-mercapto-ethoxy)-ethoxy]-ethyl α/β-D-galactopyranoside 4-8. Galactoside **4-38** (207.8 mg, 0.262 mmol) was subjected to a dissolving metal reduction, and purified as described above to furnish 37 mg (43%) of **4-8**. ^{1}H NMR (500 MHz, D_2O/CD_3OD) δ 4.85 (s, 1H, C1-H), 3.90-3.84 (m, 4H), 3.76-3.59 (m, 16H), 2.91 (t, *J*= 6.1 Hz, 2H, disulfide methylene), 2.66 (t, *J*= 6.1 Hz, 2H, sulfhydryl methylene); ^{13}C NMR (125 MHz, D_2O/CD_3OD) δ 103.8, 77.3, 75.7, 74.8, 74.7, 74.6, 74.5, 74.4, 73.7, 73.6, 71.4, 66.0, 42.6, 27.9. MATLDI-TOF MS m/z ($M^+ + Na^+$) calcd 351.11, found 352.0.

General Procedure for Functionalization of Adehyde Slides with BSA and Maleimide. SuperAldehyde slides (TeleChem International) were immersed in 50 mL phosphate buffered saline (PBS) containing 1% bovine serum albumin (BSA; w/v) and incubated overnight at room temperature. The slides were rinsed twice with distilled H_2O (100 mL), twice with 95% ethanol (50 mL) and dried under a stream of nitrogen. Subsequently, the slides were immersed in 45 mL of anhydrous DMF (Aldrich) containing 65 mg succinimidyl-4-(N-maleimidomethyl)cyclohexane-1-carboxylate (Pierce Chemical) and 100 mM N,N-Diisopropylethylamine (Aldrich). The slides were incubated in this solution for 24 h at room temperature, washed 4 times with 95% ethanol (50 mL) and stored in a vacuum dessicator until use.

General Procedure for Funtionalization of Corning® GAPS II Slides with Maleimide. Sulfhydryl-reactive slides were prepared in batches of two GAPS slides (Corning) incubated overnight at room temperature in 45 mL anhydrous *N,N*-dimethylformamide (DMF, Aldrich), 10 mg succinimidyl-4-(*N*-maleimidomethyl)cyclohexane-1-carboxylate (SMCC, Pierce Endogen) and 880 μL *N,N*-diisopropylethylamine (Aldrich). Slides were wash with 3 volumes methyl alcohol, dried under a stream of nitrogen, and stored in a dessicator prior to printing.

General Procedure for Microarray Printing. Thiol-containing oligosaccharides **1-7** were incubated at room temperature with 1 equivalent tris-(carboxyethyl)phosphine hydrochloride (TCEP, Pierce Endogen) in 1X PBS for 1 h. The structures were printed at concentrations ranging from 0.1 mM to 2 mM on maleimide-derivatized slides using a MicroGrid TAS array printer (30 % humidity, 120 μm spots with 300 μm spacing). Printed slides were incubated 12 h in a humidity chamber, washed 2 times with distilled H_2O, and then incubated for 1 h in 1 mM 2-(2-(2-mercaptoethoxy)ethoxy)ethanol in PBS (50 mL) to quench reactive maleimide groups. Alternatively, BSA derivatized slides were quenched for 1 h in 1 mM 3-mercaptopropionic acid in PBS (50 mL) to quench all remaining maleimide groups. Slides were rinsed with distilled H_2O (3 x 50 mL), 95% ethanol (3 x 50 mL) and stored in a dessicator prior to use.

General Procedure for Glycoprotein Microarray Fabrication and Neoglycopeptide Conjugates. See Adams, E. W.; Ratner, D. M.; Bokesch, H. R.; McMahon, J. B.; O'Keefe, B. R.; Seeberger, P.H. *Chem. Biol.* **2004**, *11*, 875-881.

6.5 Experimentals for Chapter 5

General Procedure for Running Microreactor Glycosylations. Prior to the introduction of reagents, the microchemical device was rinsed with 20 to 50 reactor volumes of anhydrous dichloromethane. Immediately before priming the device with reagent, 5 to 10 reactor volumes of 0.025 M TMSOTf in CH_2Cl_2 were flushed through the activator port and through the mixing and reaction zones of the device. This procedure ensures that the activator line is fully primed and free from air bubbles, and deactivates the surface of the reactor by silylation. Following the installation of the reagent containing syringes, the device was flushed with 10 to 20 reactor volumes to displace gas bubbles, and prime the remaining reagent lines.

Glycosyl donor and acceptor separately azeotroped with toluene, and dried overnight on vacuum. Samples were diluted with freshly distilled dichloromethane to the desired concentrations: 0.03 M for mannosyl donor, 0.025 M for the nucleophile

(acceptor), 0.025 M TMSOTf activator, and 0.05 M standard (**5-1**) in Et_3N with 25% by volume dichloromethane. The following gas-tight syringes were employed: 5.0 ml syringes for both glycosyl donor and nucleophile, a 2.5 ml syringe for the quench/standard, and a 1.0 ml syringe for the activator.

Sample collection was accomplished following equilibration of the temperature of the device (immersed in either a water or acetone bath, depending on temperature). 2.8 reactor volumes (220 μl) were delivered at the desired rate to flush the device, and equilibrate the reaction zone. Following the flush, 44 μl of material was collected for analysis, diluted with 20 μl hexanes, and the run was stopped. While maintaining the temperature, the device could be rerun at a different speed, or equilibrated to a different temperature.

HPLC Analysis. Collected samples were analyzed using a Waters Nova-pak© silica column (3.9 x 150 mm) with EtOAc/hexanes as the mobile phase, monitoring at 257.9 nm. The data was normalized by dividing the area of a given peak by the area corresponding to the standard. Figure 6.5 gives representative traces of the two glycosylation reactions.

a)

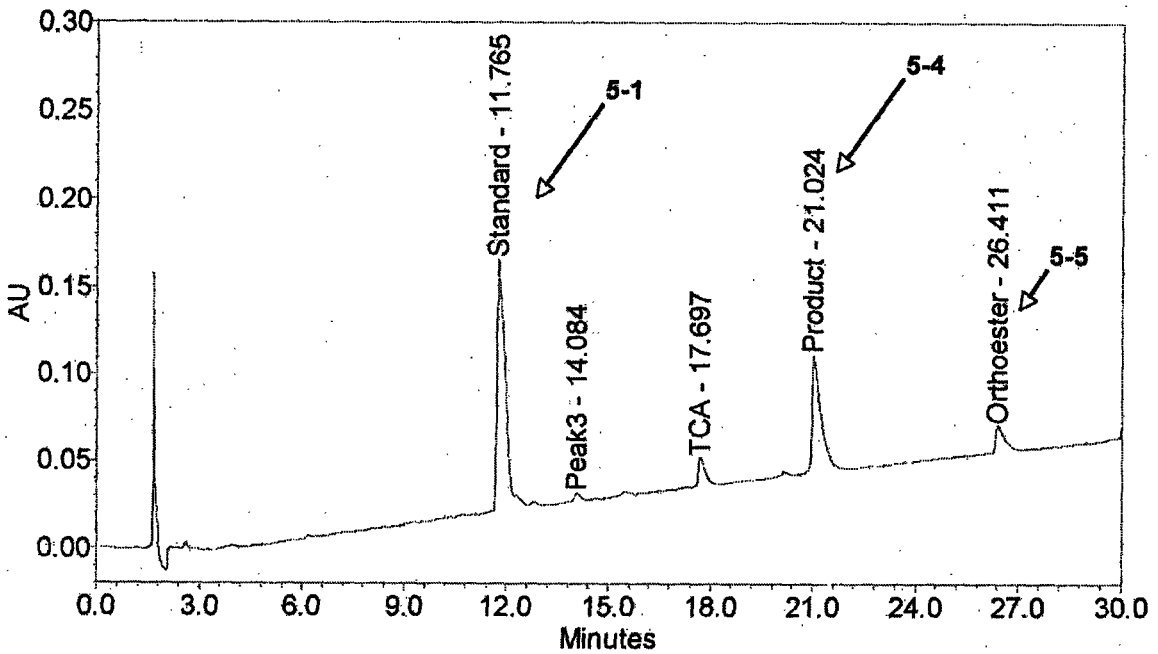

b)

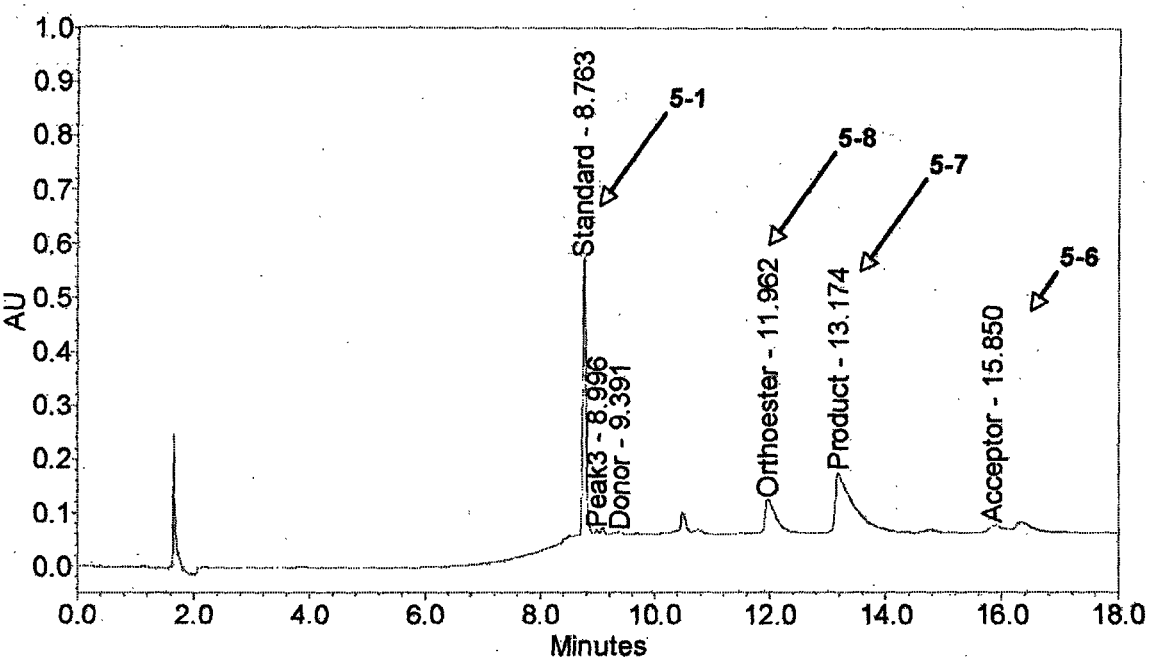

Figure 6.5 HPLC traces of glycosylation reactions monitored at 257.9 nm. a) Mannosylation of acceptor **5-3** with donor **5-2** (Scheme 5.1). b) Mannosylation of acceptor **5-6** with donor **5-2** (Scheme 5.2).

Appendix A

Biophysical Studies of Cyanovirin-N: Structural Elucidation of Carbohydrate-Binding

This appendix details the biophysical studies of Cyanovirin-N, done in collaboration with colleagues at the National Cancer Institute, NCI-Frederick, National Institutes of Health. The substrates prepared for these studies are described in Chapter 2 of this thesis. A full description of this work may be found in the following publications, parts of which are reprinted here with permission:

Shenoy, S. R.; Barrientos, L. G.; Ratner, D. M.; O'Keefe, B. R.; Seeberger, P. H.; Gronenborn, A. M.; Boyd, M. R. Multisite and Multivalent Binding Between Cyanovirin-N and Branched Oligomannosides: Calorimetric and NMR Characterization. *Chem. Biol.* **2002**, *9*, 1109-1118.

Botos, I.; O'Keefe, B. R.; Shenoy S. R.; Cartner, L. K.; Ratner, D. M.; Seeberger, P. H.; Boyd, M. R.; Wlodawer, A. Structures of the Complexes of a Potent Anti-HIV Protein Cyanovirin-N and High-Mannose Oligosaccharides. *J. Biol. Chem.* **2002**, *277*, 34336-34342.

Barrientos, L. G.; Louis, J. M.; Ratner, D. M.; Seeberger, P. H.; Gronenborn, A. M. Solution Structure of a Circular-permuted Variant of the Potent HIV-inactivating Protein Cyanovirin-N: Structural Basis for Protein Stability and Oligosaccharide Interaction. *J. Mol. Biol.* **2003**, *325*, 211-223.

A.1 Introduction

As of December 2003, an estimated 40 million people are infected by the human immunodeficiency virus (HIV)[1], with heterosexual contact accounting for greater than three-quarters of all cases.[2] Five million individuals contracted the virus in the past 12 months, and three million HIV/AIDS deaths were reported. Regional statistics show a disproportionate burden in developing nations, with a staggering 9% of the adult population of Sub-Saharan Africa infected with HIV/AIDS. Beyond the incalculable human toll, the explosion of HIV infection in regions like Southern Africa has become a destabilizing geopolitical force.

Efforts to develop an effective vaccine against HIV have been stymied by the high mutation rate of the virus,[3] and epitope masking of gp120 by *N*-linked glycans.[4] In the absence of a vaccine, the barrier method remains the most effect means of preventing viral spread during sexual contact. However, this method relies on the consent of the insertive partner. Recent advances, like the female condom, have made some headway towards empowering the non-insertive partner, however their high cost remains prohibitive for widespread adoption.

With unabated global proliferation of HIV and the absence of a vaccine, there is growing demand to develop anti-HIV microbicides to stem the spread of this disease. Towards this goal, high-throughput screens of products derived from the cyanobacterium (blue-green algae) *Nostoc ellipsosporum* have identified cyanovirin-N (CVN), an 11 kDa protein with potent virucidal properties.[5] Through carbohydrate-dependent binding of viral glycoprotein, CVN has been shown to greatly diminish the infectivity of HIV[6] and the Ebola virus.[7] Acting as a topical HIV preventive, CVN could become a powerful tool to control the spread of the virus through sexual contact.

Although CVN was known to act against HIV in a carbohydrate-dependent manner, no structural information was known for the complexes between CVN and high-mannose oligosaccharides. Studies using naturally derived high-mannose oligosaccharides $(Man)_8(GlcNAc)_2$ and $(Man)_9(GlcNAc)_2$ were plagued with problems of aggregation and precipitation.[8] Employing synthetic variants of Man9 enabled the detailed biophysical study of CVN-oligomannose complexes. In addition to avoiding aggregation and precipitation, the synthetic mannans permitted the investigation of CVN-binding of smaller branched and linear structures that comprise the triantennary high-mannose oligosaccharides.

Utilizing the synthetic structures detailed in Chapter 2 of this thesis, the precise mode of carbohydrate-binding was examined in detail for CVN. The following studies employed isothermal calorimetry, NMR titration, X-ray crystallography, and circular-permuted variants to probe CVN-carbohydrate complexes. Included below is a brief summary of the results from each of these studies. For full details, please refer to the original article.

A.2 Calorimetric and NMR Characterization of Multisite and Multivalent Binding of High-Mannose Oligosaccharides by Cyanovirin-N

This initial investigation used NMR and isothermal titration calorimetry to examine the multivalent interactions of branched high-mannose oligosaccharides to Cyanovirin-N.[9] It was demonstrated that CVN recognizes the Manα(1→2)Man-terminated arms of the triantennary nonamannoside, but there is no affinity for the internally-branched core trimannoside or the reducing-end $(GlcNAc)_2$. CVN was found to bind both the linear D1 trimannoside and synthetic nonamannoside in a similar fashion at two binding sites on the protein (Figure A.1).

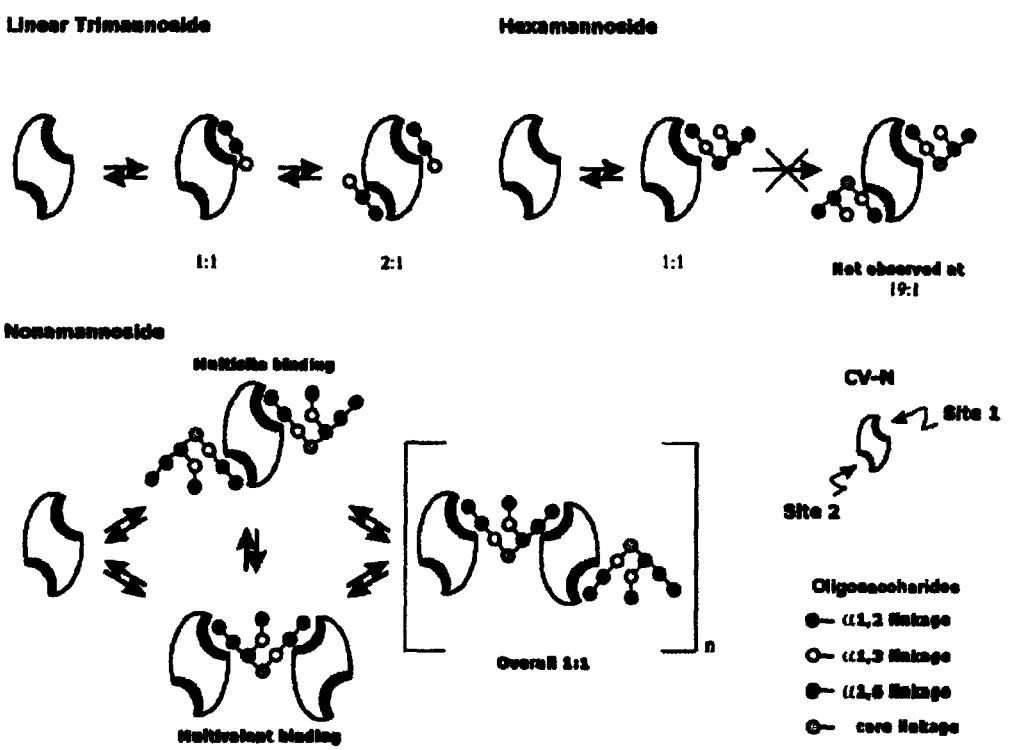

Figure A.1 Schematic of CVN binding of the synthetic structures D1 linear trimannoside, hexamannoside, and nonamannoside. The two binding sites of CVN are marked in blue and red. Reprinted with permission.[9]

The large size of the CVN-nonamannoside complexes suggested that two molecules of CVN were binding every nonamannoside, by interacting with the opposing D1 and D3 arms. The binding affinity of CVN was determined to be 3.48 μM for the linear trimannoside, 2.61 μM for the hexamannoside, and 270 nM for the synthetic nonamannoside. This binding information, coupled with the knowledge that CVN binds two nonamannosides, is believed to be responsible for the remarkably tight association of CVN for the branched nonamannose structures.

Isothermal titration calorimetry established that CVN binding of the mannosides was driven by enthalpic contributions, with the larger sugars exhibiting greater exothermic heats of binding. The negative ΔH of the CVN-carbohydrate association suggested that favorable polar/electrostatic, van der Waals, and hydrogen bonds were mediating the binding event. While the association was entropically disfavored, the enthalpies of binding were highly favorable and offset the entropic losses.

By characterizing the multisite and multivalent interactions of CVN and high-mannose oligosaccharides, it was possible to illuminate the biological activity of CVN. CVN has a nearly irreversible association with high-mannose oligosaccharides. By probing the mechanism of these remarkable interactions, it should be possible to develop new tools that, like CVN, can block viral-cell fusion by irreversibly binding and linking oligosaccharides on gp120.

A.3 X-Ray Crystal Structures of CVN-Oligomannose Complexes

Using X-ray crystallography, structures were determined for the complexes of wild-type CVN with $(Man)_9(GlcNAc)_2$ and the synthetic hexamannoside, reported at 2.5- and 2.4 Å respectively.[10] Understanding the structural basis for CVN binding of high-mannose oligosaccharides is important for developing the protein as a potential anti-HIV agent.

The 101-amino acid protein exists in solution as both a compact monomer and a dimer. In the crystal structure, CVN exists exclusively as a three-dimensional domain-swapped dimer with two primary sites near the hinge region and two secondary sites on

the opposite ends of the dimer. Crystal packing appears to thermodynamically favor the domain-swapped dimer, selectively trapping it as the crystal grows.

The crystal structures of the protein-carbohydrate complex revealed that at the binding interface of CVN with the nonamannoside, there are three stacked Manα(1→2)Man mannoses, with the remainder of the saccharide pointing into the solution. Similarly, the synthetic hexamannoside / CVN interface has two Manα(1→2)Man stacked mannoses, and the other sugars pointing into solution. These structures conclusively show the binding geometry of high-mannose sugars to CVN (Figure A.2).

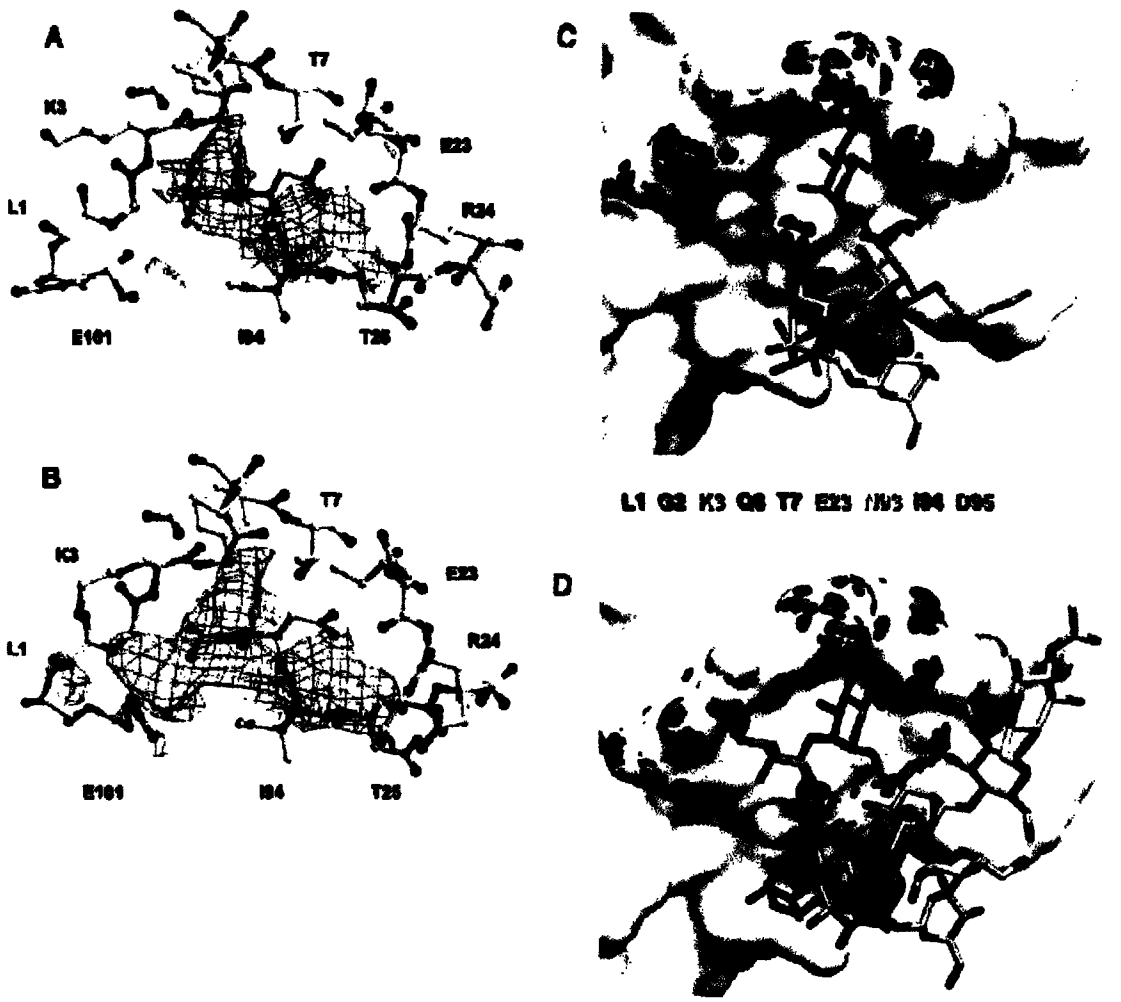

Figure A.2 Unbiased $F_o - F_c$ difference electron density maps of the binding interfaces contoured at 2.0-σ level and the atomic models of bound oligosaccharides. *A*) The

density for the complex with synthetic hexamannoside, visible for two stacked mannose rings: C (residue 505) and 4 (residue 504). *B*) the density for the complex with Man-9, visible for three stacked mannose rings: D1 (residue 506), C (residue 505), and 4 (residue 504). The final atomic coordinates of the oligosaccharides and the protein atoms in contact with them are shown for hexamannoside (*C*) and for Man-9 (*D*). *C* and *D* were generated with the program GRASP.[11] Reprinted with permission.[10]

The D1 and D3 arms of the nonamannoside were modeled into the electron density and refined. Only the D1 arm, with the repeated α(1→2)-linked mannoses could fit the density map. Additionally, the crystal structures of the protein-carbohydrate complexes revealed that the stacked Manα(1→2)Man rings were bound much more tightly than originally suggested by NMR studies. A total of ten hydrogen bonds were formed between the binding site and the stacked mannoses of the nonamannoside, and nine hydrogen bonds were observed for the hexamannoside.

A.4 Solution Structure of a Circular-permuted Variant of CVN

A detailed study of the structural determinants required for CVN's carbohydrate-binding activity is critical to understand CVN's mode of action and anti-HIV properties. This information also provides a rational basis for redesign and functional analysis. Towards this end, a circular permuted version of CVN (cpCVN) was studied to gain information on structure-function relationships that could not be achieved by single-site or deletion mutagenesis.[12]

Past studies had revealed that cpCVN adopted the wild-type CVN (wtCVN) fold, but had an anti-HIV activity that was 1000-fold lower in potency.[13] The difference in activity between cpCVN and wtCVN was reconciled in this study using NMR mapping experiments with the synthetic nonamannoside, hexamannoside and linear trimannoside prepared in Chapter 2. It is believed that ongoing efforts with cpCVN, and its comparison to wtCVN, will establish a rational approach to optimize and redesign this more potent variants of this anti-HIV microbicide.

A.5 Summary and Conclusions

Access to non-natural high-mannose oligosaccharides proved valuable in elaborating the precise mechanisms of CVN's high-mannose affinity. The synthetic mannans were useful in overcoming problems associated with aggregation and precipitation during formation of CVN-$(Man)_9(GlcNAc)_2$ complexes. In addition, the hexamannose and branched trimannose deletion sequences, in concert with the D1 arm linear trisaccharide, provided a means of ascertaining the structural determinants for high-mannose binding.

Efforts to develop and improve anti-HIV microbicides are ongoing. Now, with the combined advantage of carbohydrate microarrays, it is possible to quickly establish the structural determinants for protein-carbohydrate binding. This enables rapid screening of protein-carbohydrate binding events, which can in turn be examined in further detail using the biophysical techniques mentioned herein. For instance, based on the microarray results described in Chapter 4, the novel 9.6 kDa anti-HIV protein scytovirin[14] is currently undergoing structural analysis using the synthetic mannans it was found to bind in that study. This exemplifies the ability of synthetic carbohydrate-based tools to facilitate and expedite biophysical studies.

References:

[1] UNAIDS. World Health Organization. *AIDS Epidemic Update* December **2003**

[2] Piot, P. *Science* **1998**, *280*, 1844.

[3] Burton, D. R. *Proc. Natl. Acad. Sci. U.S.A.* **1997**, *94*, 10018.

[4] Losman, B.; Bolmstedt, A.; Schonning, K.; Bjorndal, A.; Westin, C.; Fenyo, E. M.; Olofsson, S. *AIDS Res. Hum. Retroviruses* **2001**, *17*, 1067.

[5] Boyd, M. R.; Gustafson, K. R.; McMahon, J. B.; Shoemaker, R. H.; O'Keefe, B. R.; Mori, T.; Gulakowski, R. J.; Wu, L.; Rivera, M. I.; Laurencot, C. M.; Currens, M. J.; Cardellina, J. H., 2nd; Buckheit, R. W.; Jr., Nara, P. L.; Pannell, L. K.; Sowder, R. C. 2nd; Henderson, L. E. *Antimicrob. Agents Chemother.* **1997**, *41*, 1521. Bolmstedt, A. J.; O'Keefe, B. R.; Shenoy, S. R.; McMahon, J. B.; and Boyd, M. R. *Mol. Pharmacol.* **2001**, *59*, 949.

[6] Tsai, C. C.; Emau, P.; Jiang, Y.; Tian, B.; Morton, W. R.; Gustafson, K. R.; Boyd, M. R. *AIDS Res. Hum. Retroviruses* **2003**, 19, 535.

[7] Barrientos, L. G.; O'Keefe, B. R.; Bray, M.; Anthony, S.; Gronenborn, A. M.; Boyd, M. R. *Antiviral Res.* **2003**, *58*, 47.

[8] Shenoy, S. R.; O'Keefe, B. R.; Bolmstedt, A. J.; Cartner, L. K.; Boyd, M. R. *J. Pharmacol. Exp. Ther.* **2001**, *297*, 704. Bewley, C. A.; Otero-Quintero, S. *J. Am. Chem. Soc.* **2001**, *123*, 3892.

[9] Shenoy, S. R.; Barrientos, L. G.; Ratner, D. M.; O'Keefe, B. R.; Seeberger, P. H.; Gronenborn, A. M.; Boyd, M. R. *Chem. Biol.* **2002**, *9*, 1109.

[10] Botos, I.; O'Keefe, B. R.; Shenoy S. R.; Cartner, L. K.; Ratner, D. M.; Seeberger, P. H.; Boyd, M. R.; Wlodawer, A. *J. Biol. Chem.* **2002**, *277*, 34336.

[11] Nicholls, A.; Shark, K.A.; Honig, B. *Proteins Struct. Funct. Gennet.* **1991**, *11*, 281.

[12] Barrientos, L. G.; Louis, J. M.; Ratner, D. M.; Seeberger, P. H.; Gronenborn, A. M. *J. Mol. Biol.* **2003**, *325*, 211.

[13] Barrientos, L.G.; Louis, J.M.; Hung, J.; Smith, T.H.; O'Keefe, B.R.; Gardella, R.S.; Gronenborn, A.M. *Proteins: Struct. Funct. Genet.* **2002**, *46*, 153.

[14] Bokesch, H.R.; O'Keefe, B.R.; McKee, T.C.; Pannell, L.K.; Patterson, G.M.; Gardella, R.S.; Sowder, R.C., 2nd; Turpin, J.; Watson, K.; Buckheit, R.W. Jr.; Boyd, M.R.; *Biochemistry* **2003**, *42*, 2578.

Appendix B

Synthetic Trisaccharide Acceptor Preferences of β1,4-Galactosyltransferase-1

The following describes an ongoing investigation into the acceptor preferences of the enzyme β-1,4-galactosyltransferase. This study was made possible by the synthesis of four trisaccharide structures for use in binding studies and X-ray crystal structure determination. Included below is a brief description of this project, focusing on the synthetic preparation of the four oligosaccharides. This collaboration is ongoing with colleagues at the NCI-Frederick, National Institutes of Health. The following manuscript is in preparation for submission:

Ramasamy, V.; Ramakrishnan, B.; Boeggeman, E.; Ratner, D. M.; Seeberger, P. H.; Qasba, P. K. Oligosaccharide Acceptor Preferences of β1,4-Galactosyltransferase-1: Crystal Structure of Met344His Mutant of Human β1,4-Galactosyltransferase-1 with the Trisaccharides of N-Glycan Moiety. *In Preparation.*

B.1 Introduction

The galactosyltransferase (GalTran) family of enzymes mediates the transfer of galactose (Gal) from UDP-Gal to a nascent oligosaccharide. The subfamilies of this enzyme include β1,4-, β1,3-, α1,3-, α1,4- and α1,6- variants, which differ by the position onto which they glycosylate the acceptor sugar, and the anomericity of the glycosidic linkage.[1] The galactosylation of oligosaccharides has a number of relevant physiological effects. For instance, the presence of Galα(1→3)Gal on the surface of animal tissue (pig cells) is a critical factor in the rejection of transplanted organs from non-human donors. Removing the α1,3-galactosyltransferase gene from pigs has been proposed as a potential solution to problems associated with xenotransplantation.[2]

The β1,4-galactosyltransferase subfamily has seven members, identified as T1 to T7. β1,4-galactosyltransferase-T1 (β1,4-Gal-T1) was the first to be identified, characterized and successfully cloned. β1,4-Gal-T1is a Golgi resident type II membrane enzyme, although it has also been found located in the cell surface acting as a lectin.[3] The catalytic domain of β1,4-Gal-T1 transfers Gal to a *N*-acetylglucosamine (GlcNAc) reside that is free or part of an oligosaccharide. The resulting disaccharide unit, Galβ(1→4)GlcNAc (*N*-acetyllactosamine), is a common motif in biological systems and

is known to be present in many active carbohydrate determinants. In addition, β1,4-Gal-T1 and α-lactalbumin form a lactose synthase complex, which produces lactose (Galβ(1→4)Glc) in the mammary gland during lactation.[4]

The mechanism for the catalytic activity of β1,4-Gal-T1 has been determined in detail,[5] and proceeds in a sequential order with the addition of Mn^{2+}, followed by UDP-α-Gal and the GlcNAc acceptor. The synthetic trisaccharides detailed below were used to examine the structural preference for the GlcNAc acceptor of β1,4-Gal-T1.

B.2 Synthetic Targets

Four trisaccharide targets were prepared for this study, each possessing a dimannose core and a non-reducing end GlcNAc moiety (Figure B.1). The targets were selected to represent a broad spectrum on *N*-linked glycan type acceptors with the GlcNAc acceptor presented in a variety of unique steric and conformational environments.

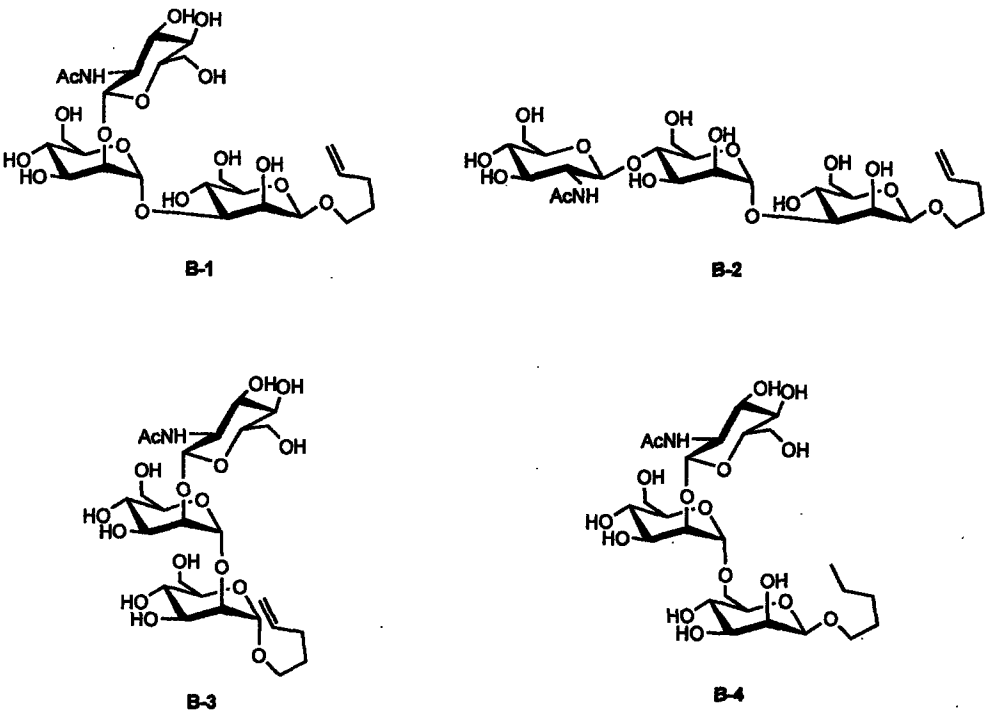

Figure B.1 GlcNAc-containing targets used as acceptors for β1,4-Gal-T1.

B.3 Retrosynthesis of Trisaccharides

Retrosynthetic analysis of the targets revealed four protected trisaccharides that would provide access to the desired products (Scheme B.1). With the exception of **B-3**, synthesis of the trisaccharide targets was based on the strategy developed in Chapter 2 to differentiate the core β-mannose on the C3 and C6 positions.

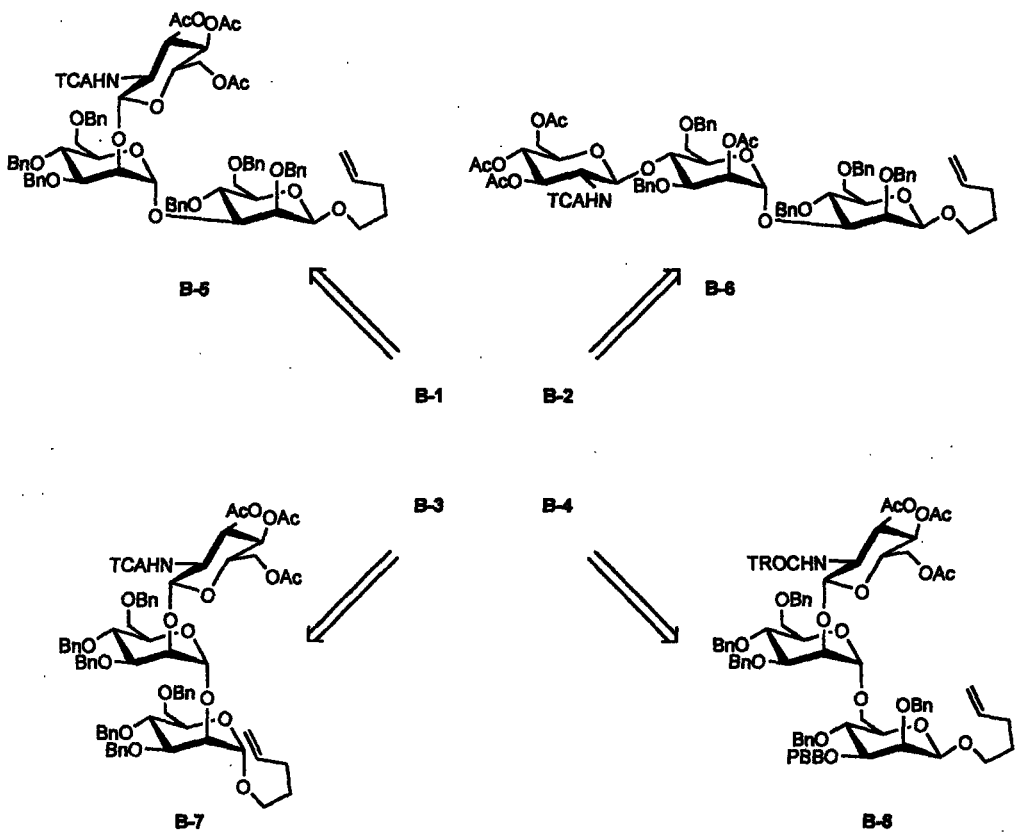

Scheme B.1 Retrosynthesis of trisaccharide targets.

Rapid access to the synthetic trisaccharides was the primary goal for this synthesis. Previously established building blocks were employed to expedite construction of the targets, as the significance of the trisaccharides was not in the challenge of their construction but in their application to elucidate the acceptor preferences of β1,4-Gal-T1.

Synthesis of these structures relied on intermediates used during the synthesis of the high-mannose oligosaccharides described in Chapters 2, 3 and 4 and a differentiated mannose used by the Seeberger laboratory in the construction of the *Leishmania* cap

tetrasaccharide.[6] Two additional glycosyl donors were employed for the incorporation of the GlcNAc resides. Trichloroacetimidate donors **B-9**[7] and **B-10**[8] were used in this study. Both donors used the acetate ester to protect their hydroxyl groups, however **B-9** used the trichloroacetimido protecting group on the C2 amine, and **B-10** included the trichloroethoxycarbamate (TROC).

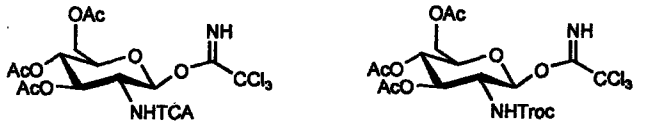

B-9 B-10

Figure B.2 Trichloroacetimidate donors **B-9** and **B-10**, for the installation of GlcNAc residues into the trisaccharide targets.

B.4 Synthesis of Protected Trisaccharides

Synthesis of the first trisaccharide, **B-5**, utilized a differentiated core β-mannoside. This differentiated monosaccharide **B-11** is analogous to **2-8** utilized in Chapter 2, and was prepared by established methods.[9] A benzyl ether was substituted onto the C6 hydroxyl by quantitative removal of the C6 silyl ether of **B-11** with TFA, followed by treatment with benzyl bromide to furnish **B-12** (96%). The PMB group was removed in 75% yield by treatment with DDQ to provide monosaccharide acceptor **B-13**. Glycosylation proceeded using the familiar mannosyl trichloroacetimidate **2-10** (99% yield) followed by deprotection of the C2 acetate using sodium methoxide to give disaccharide acceptor **B-14** in 78% yield. Trisaccharide **B-5** was accessed by glycosylation of **B-14** with GlcNAc donor **B-9** (77%).

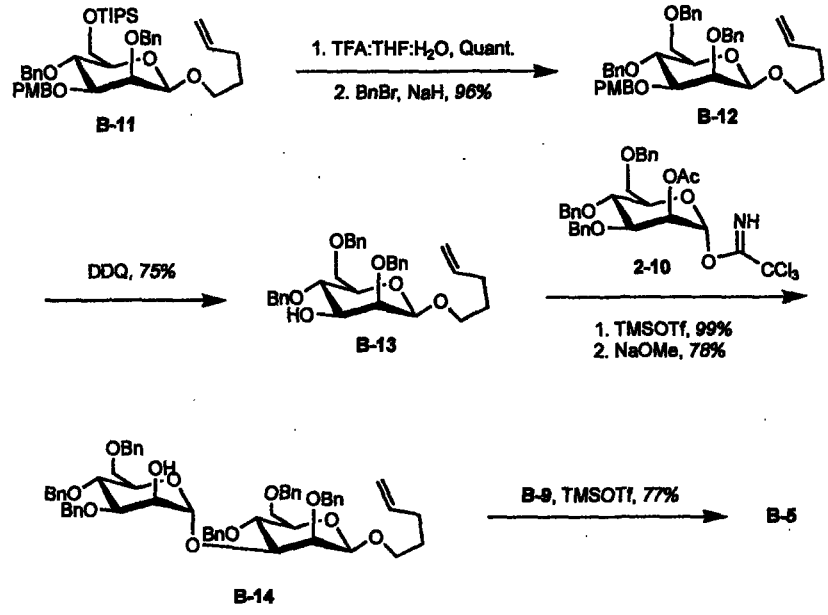

Scheme B.2 Construction of trisaccharide **B-5**.

Trisaccharide **B-6** was constructed using the core β-mannoside **B-13**. Glycosylation with the differentially protected mannosyl donor **B-15**[6] (99%) was followed by levulinoyl ester removal with hydrazine acetate to provide **B-16** in 60%. The disaccharide acceptor was glycosylated with **B-9** in 99% yield to furnish trisaccharide target **B-6**.

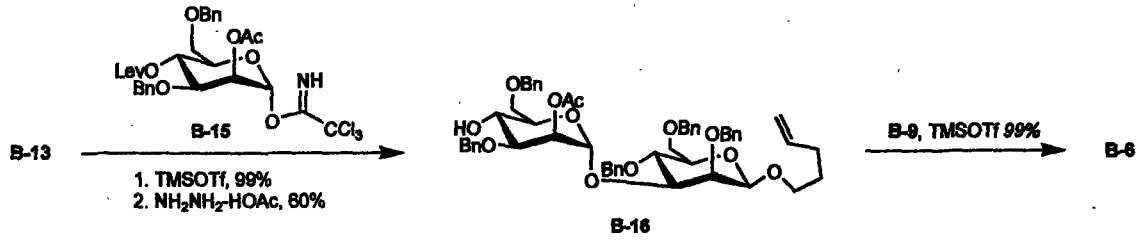

Scheme B.3 Construction of trisaccharide **B-6**.

The synthesis of **B-7** made use of a disaccharide intermediate involved in the construction of the D1 arm of the high-mannose nonasaccharide. Beginning with **B-17**,[9] the dimannoside acceptor was glycosylated with **B-9** in 86% yield trisaccharide **B-7**.

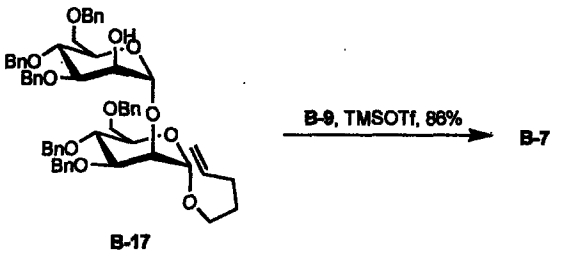

Scheme B.4 Synthesis of **B-7** utilized disaccharide acceptor **B-X** to expedite the synthesis.

Synthesis of the final trisaccharide **B-8** began with differentiated core β-mannoside **2-9**. Quantitative removal of the C6 triisopropylsilyl ether furnished the β-mannoside acceptor **B-18**. Glycosylation with mannosyl donor **2-10** (99% yield) followed by sodium methoxide removal of the C2 acetate yielded the disaccharide acceptor **B-19** in 95% yield. Trisaccharide **B-8** was secured by glycosylation of **B-19** with GlcNAc donor **B-10** in 37% yield.

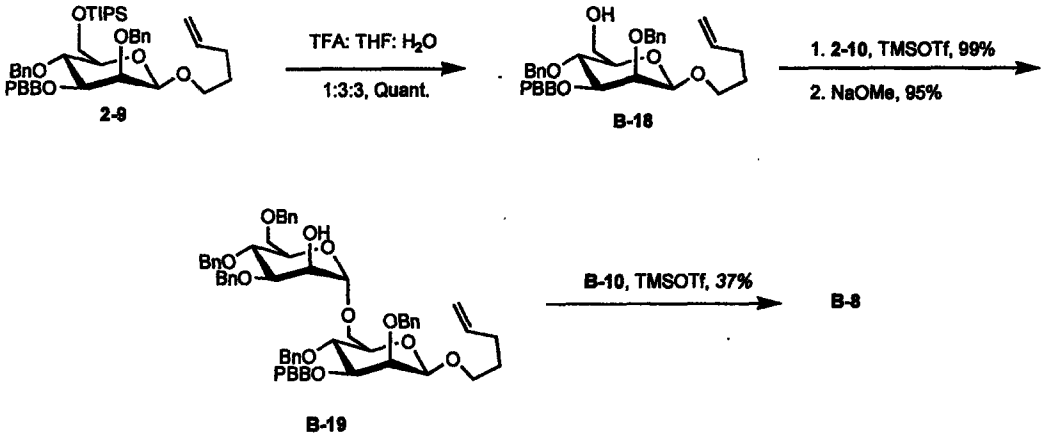

Scheme B.5 Construction of trisaccharide **B-8**.

B.5 Deprotection Strategy to Furnish Trisaccharide Targets

Deprotection of trisaccharide **B-5**, **B-6**, **B-7** was accomplished in a three step procedure: (1) removal of all protecting groups by a dissolving metal reduction, (2) per-*O*-acetylation of the deprotected structure using acetic anhydride and pyridine, and (3)

selective cleavage of the *O*-acetate esters by treatment with 0.05 M methanolic sodium methoxide (Table B.1).

Table B.1 Three-step deprotections to furnish trisaccharides **B-1**, **B-2**, and **B-3**.

Starting Material	Product	Overall Deprotection Yield
B-5	**B-1**	16%
B-6	**B-2**	23%
B-7	**B-3**	22%

The TROC carbamate on **B-8** was substituted with an *N*-acetate in 65% yield by treatment with elemental zinc in acetic acid, followed by standard acetylation to furnish **B-20**. The remaining benzyl ethers were removed by palladium-catalyzed hydrogenation, and the *O*-acetate esters were removed by treatment with 0.03 M sodium methoxide. Trisaccharide **B-4** was isolated in 91% following these two steps.

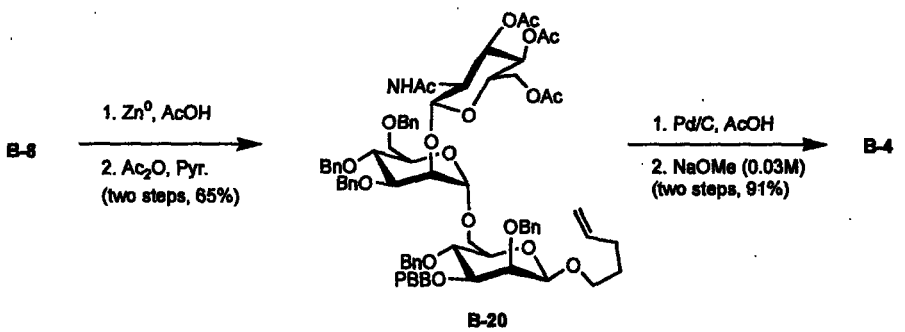

Scheme B.6 Deprotection of trisaccharide **B-8** to yield **B-4**.

All four trisaccharides were purified by Sephadex G-25 gel filtration. Trace organic contaminants were removed by repeated precipitation in cold diethyl ether from a minimum volume of DMSO.

B.6 Summary and Conclusions

The synthesis of these four trisaccharides illustrates the versatility of the monosaccharide building blocks used in synthetic carbohydrate chemistry. These

structures were constructed entirely from monosaccharide donors originally designed for other syntheses. It was therefore possible to construct this panel of oligosaccharides without requiring additional materials specific to this effort. The successful completion of these trisaccharides has provided valuable substrates for an ongoing biophysical study of β1,4-Gal-T1.

The work detailed in this thesis is predicated on the notion that providing access to defined oligosaccharides for biological study is one of the most valuable functions for synthetic carbohydrate chemistry. As with Chapters 2, 4 and Appendix A, this Appendix highlights this role of synthetic chemistry in an ongoing investigation. These four trisaccharides demonstrate the significant contribution that can be made when synthesis is applied to a specific biological need. While developments like the automated solid-phase oligosaccharide synthesizer are likely to greatly expand access to these types of structures, until synthetic means are more widely available to the non-expert, progress in the field is dependent on cross-discipline collaboration between glycobiologists and chemists with the synthetic capacity to generate structures of interest.

References:

[1] For a review of the galactosyltransferase family of enzymes, see: Amado, M.; Almeida, R.; Schwientek, T.; Clausen, H. *Biochim. Biophys. Acta.* **1999**, *1473*, 35. Hennet, T. *Cell Mol. Life. Sci.* **2002**, *59*, 1081.

[2] Liangxue, L.; Kolber-Simonds, D.; Park, K.-W.; Cheong, H.-T.; Greenstein, J.L.; Im, G.-S.; Samuel, M.; Bonk, A.; Rieke, A.; Day, B.N.; Murphy, C.N.; Carter, D.B.; Hawley, R.J.; Prather, R.S. *Science*, **2002**, *295*, 1089.

[3] Rodeheffer, C.; Shur, B.D. *Biochim. Biophys. Acta.* **2000**, *19*, 258.

[4] Brodbeck, U.; Denton, W.L.; Tanahashi, N.; Ebner, K.E. *J. Biol. Chem.* **1967**, *242*, 391. Brew, K.; Vanaman, T.C.; Hill, R.L. *Proc. Natl. Acad. Sci. U.S.A.* **1968**, *32*, 491.

[5] Ramakrishnan, B.; Boeggeman, E.; Ramasamy, V.; Qasba, P.K. *Curr. Opin. Struct. Biol.* **2004**, *in press*.

[6] Hewitt, M.C.; Seeberger, P.H. *Org. Lett.* **2001**, *3*, 3699.

[7] Blatter, G.; Beau, J. –M.; Jacquinet, J. –C. *Carbohydr. Res.* **1994**, *260*, 189.

[8] Ziegler, T. *Carbohydr. Res.* **1994**, *262*, 195.

[9] Plante, O. J. New Methods for the Synthesis of Carbohydrates: The First Automated Solid-Phase Oligosaccharide Synthesizer. Ph.D. Thesis, Massachusetts Institute of Technology, Cambridge, MA, June 2001.

Appendix C

Selected Spectra

Appendix C.2

Selected Spectra – Chapter 2

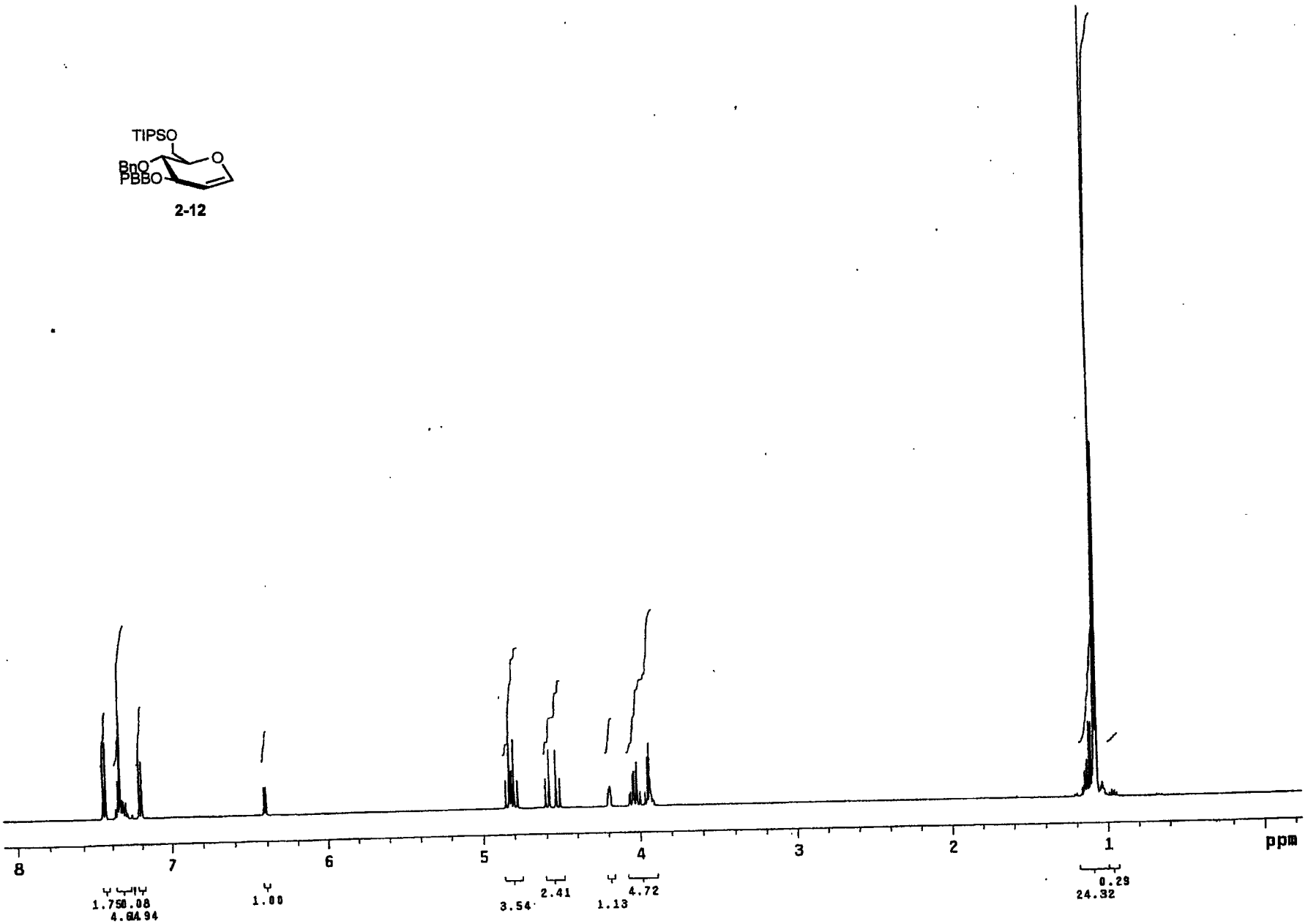
TIPSO
BnO
PBBO
O
2-12
8
7
6
5
4
3
2
1
ppm
1.75
8.08
4.64
9.4
1.00
3.54
2.41
1.13
4.72
0.29
24.32

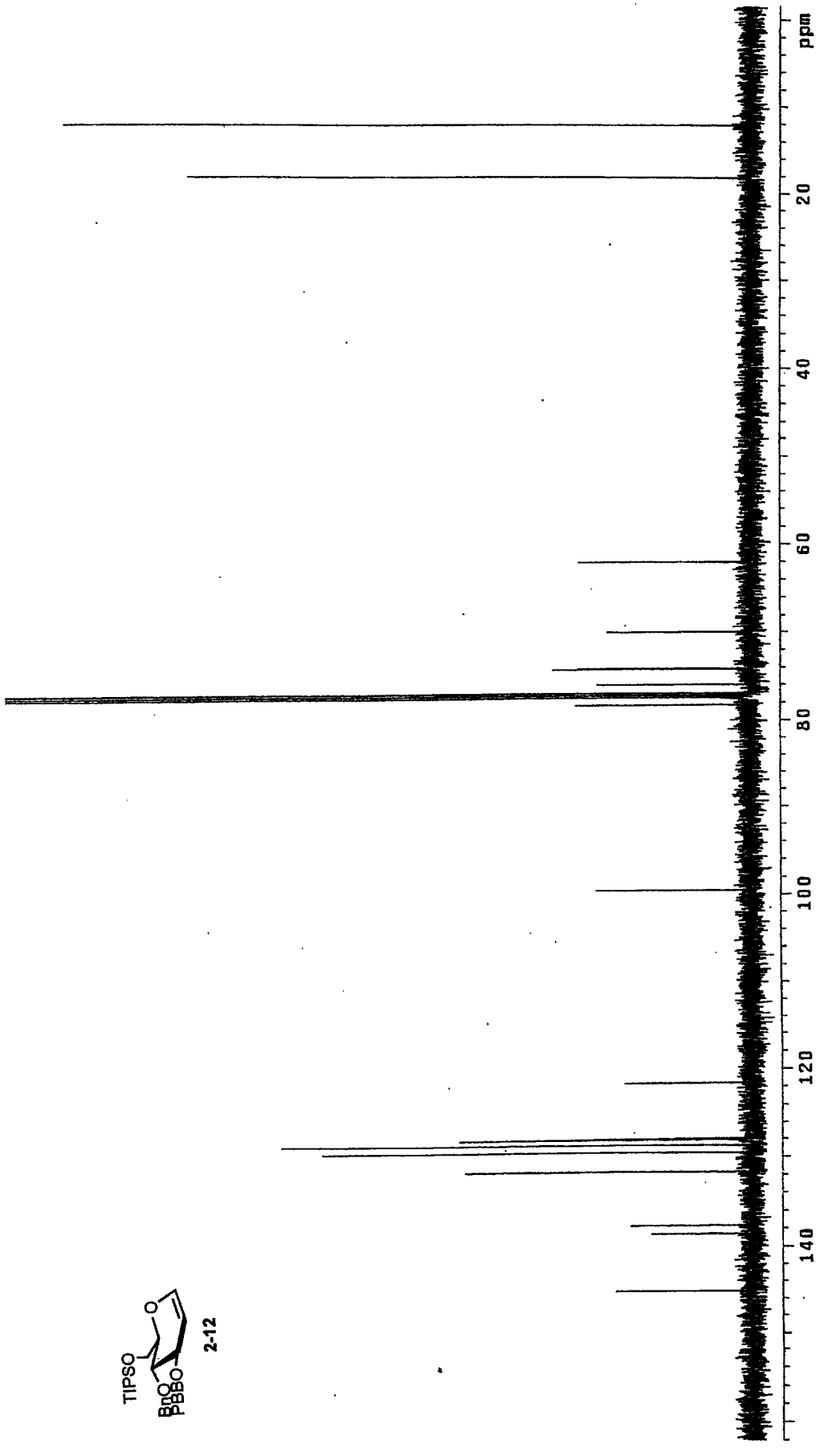
ppm
20
40
60
80
100
120
140
TIPSO
BnO
PBBO
2-12

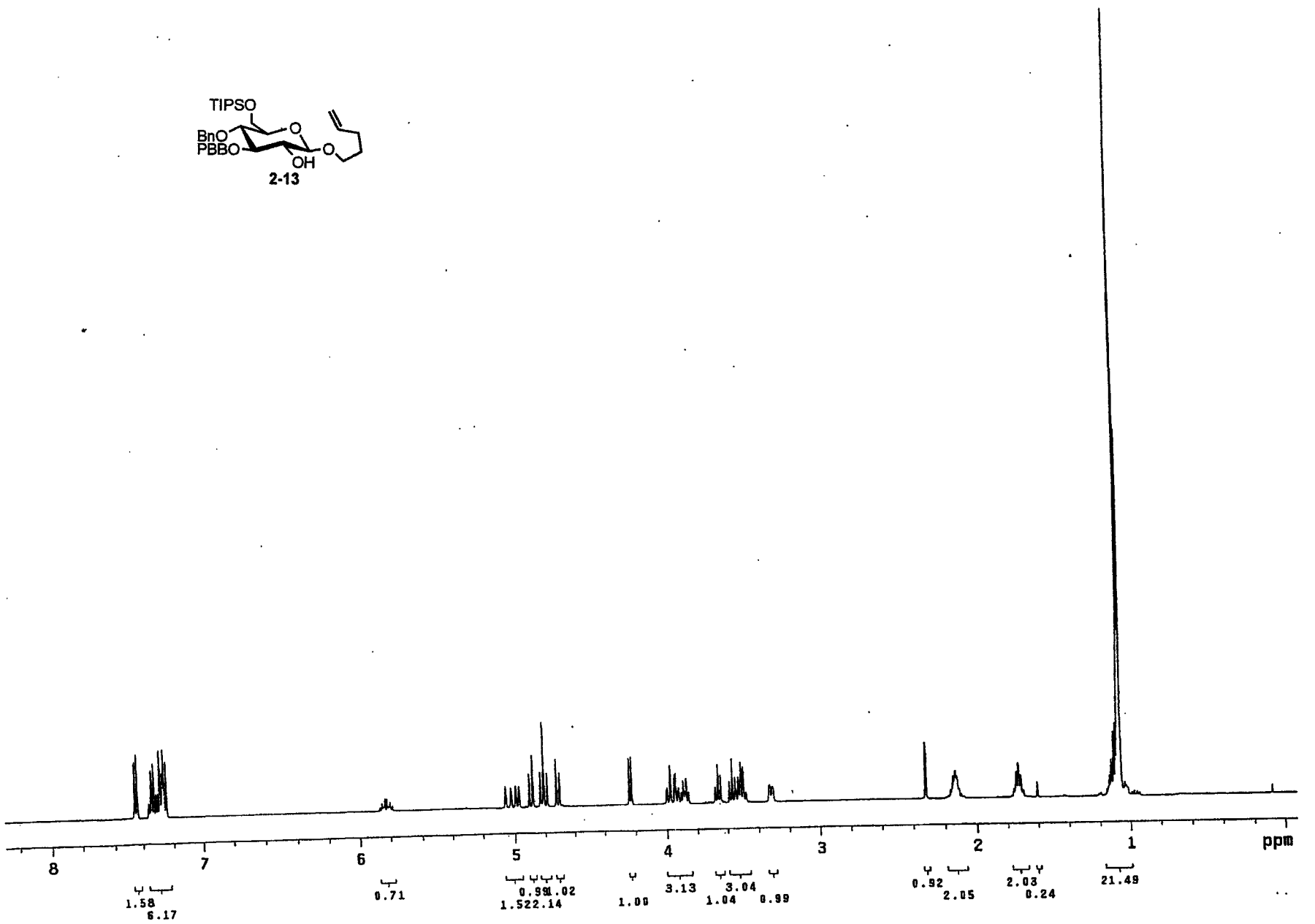
TIPSO
BnO
PBBO
OH
2-13
8
7
6
5
4
3
2
1
ppm
1.58
6.17
0.71
0.99
1.02
1.52
2.14
1.00
3.13
1.04
3.04
0.99
0.92
2.05
2.03
0.24
21.49

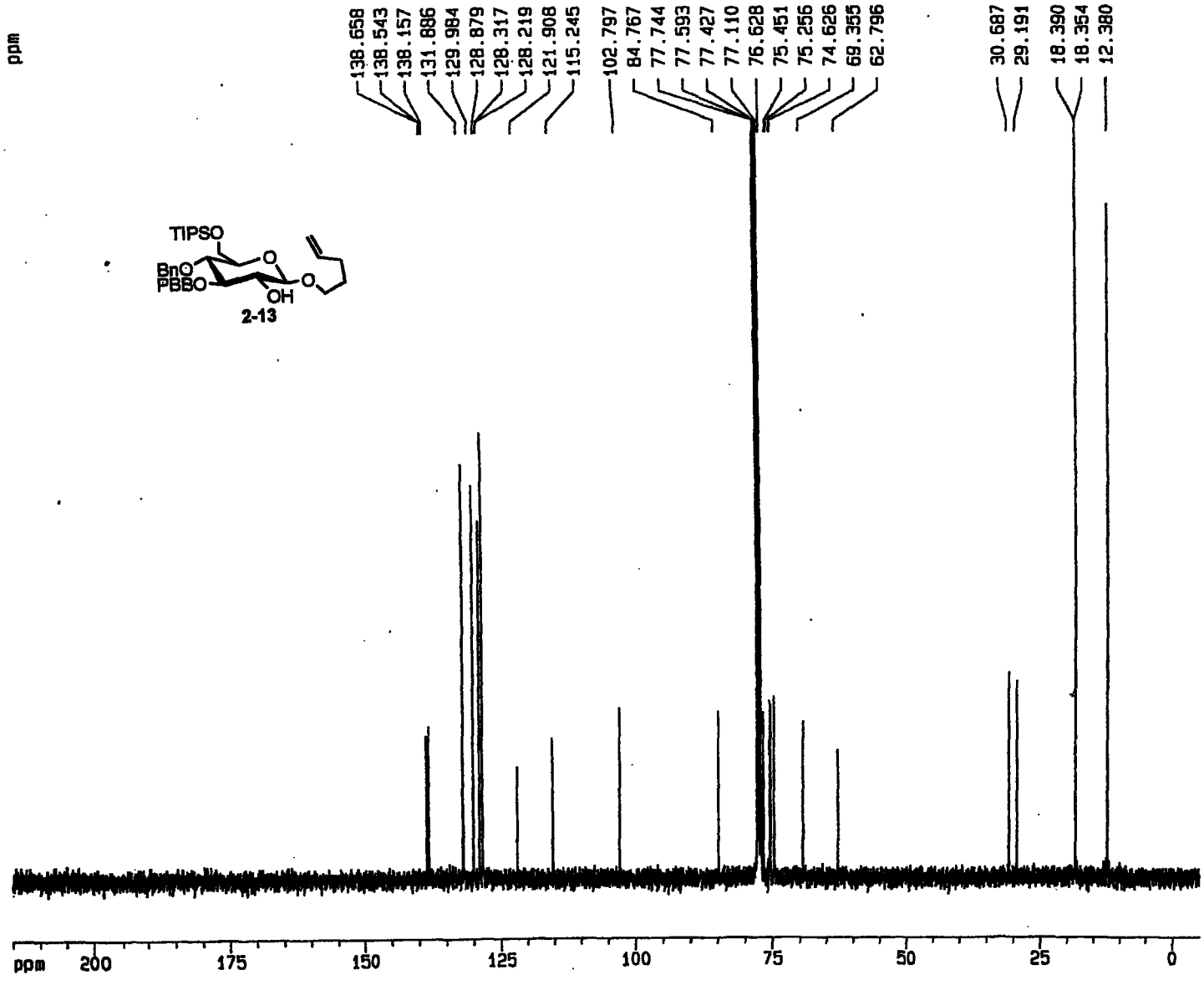

Current Data Parameters

NAME	OMR-I-257.1
EXPNO	11
PROCNO	1

F2 - Acquisition Parameters

Date_	20080914
Time	12.00
INSTRUM	spect
PROBHD	5mm BBO BB-1
PULPROG	zgpg30
TD	65536
SOLVENT	CDCl3
NS	1024
DS	4
SWH	25125.629 Hz
FIDRES	0.383387 Hz
AQ	1.3042164 sec
RG	8192
DW	19.900 usec
DE	6.00 usec
TE	300.0 K
D1	2.00000000 sec
d11	0.03000000 sec
d12	0.00002000 sec

---------- CHANNEL f1 ----------

NUC1	13C
P1	15.25 usec
PL1	3.00 dB
SF01	100.6237959 MHz

---------- CHANNEL f2 ----------

CPDPRG2	waltz16
NUC2	1H
PCPD2	107.50 usec
PL2	0.00 dB
PL12	24.00 dB
PL13	24.00 dB
SF02	400.1316005 MHz

F2 - Processing parameters

SI	32768
SF	100.6127290 MHz
WDW	EM
SSB	0
LB	1.00 Hz
GB	0
PC	1.40

1D NMR plot parameters

CX	20.00 cm
F1P	215.000 ppm
F1	21631.74 Hz
F2P	-5.000 ppm
F2	-503.06 Hz
PPMCM	11.00000 ppm/cm
HZCM	1106.73999 Hz/cm

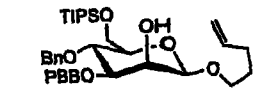

Intermediate to 2-8

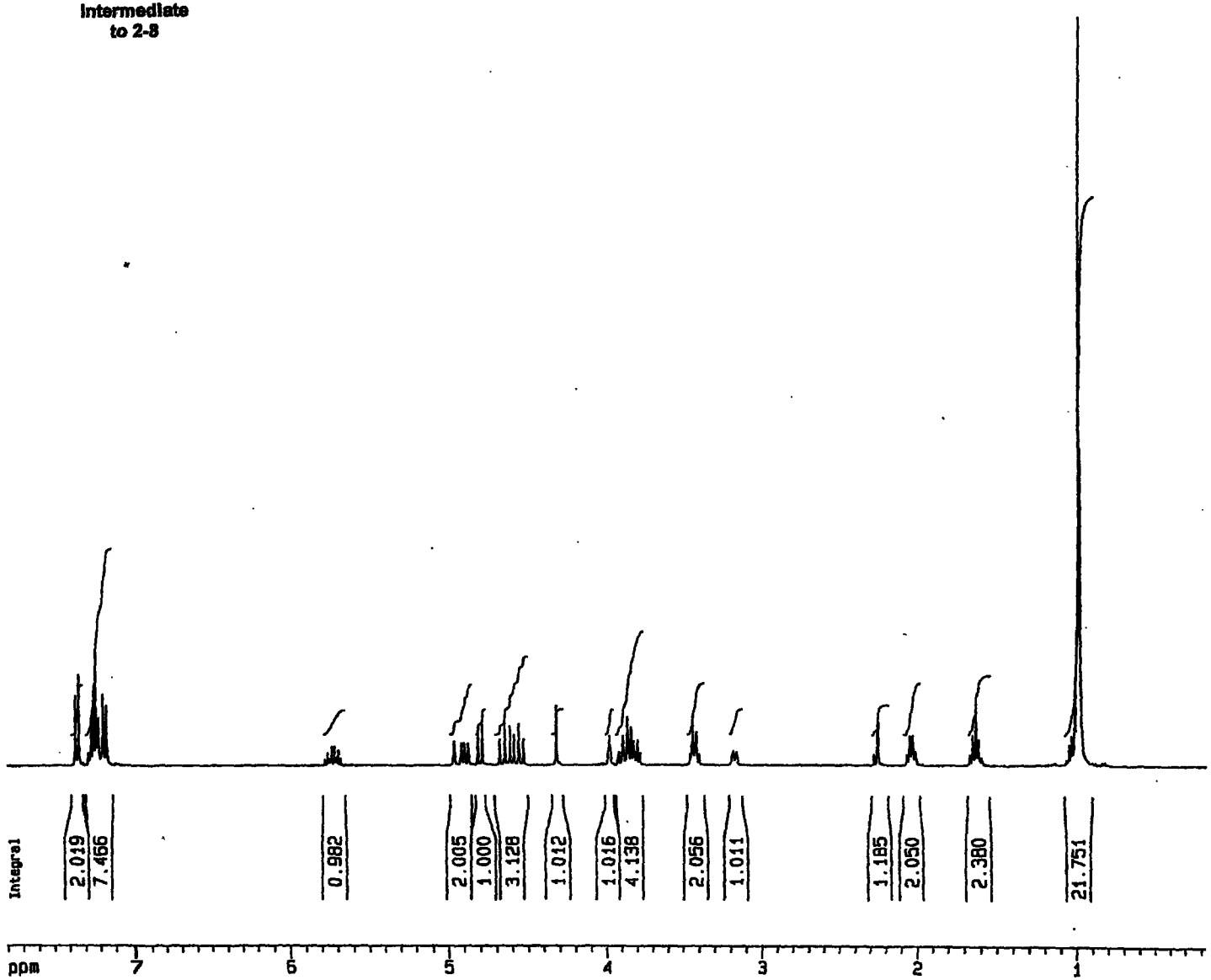


```
Current Data Parameters
NAME        DNR-I-NMR-101
EXPNO               10
PROCNO              1

F2 - Acquisition Parameters
Date_           20000405
Time              16.48
INSTRUM           spect
PROBHD     5mm BBO BB-1
PULPROG           zg30
TD                65536
SOLVENT           CDCl3
NS                16
DS                2
SWH           8278.146 Hz
FIDRES        0.126314 Hz
AQ            3.9564243 sec
RG                35.9
DW              60.400 usec
DE               6.00 usec
TE              300.0 K
D1           1.00000000 sec

========== CHANNEL f1 ========
NUC1              1H
P1               8.40 usec
PL1              0.00 dB
SF01        400.1324710 MHz

F2 - Processing parameters
SI                32768
SF          400.1300427 MHz
WDW               EM
SSB               0
LB               0.30 Hz
GB                0
PC               1.00

1D NMR plot parameters
CX               20.00 cm
F1P               7.804 ppm
F1              3122.64 Hz
F2P               0.177 ppm
F2               70.87 Hz
PPMCM         0.38135 ppm/cm
HZCM        152.58833 Hz/cm
```

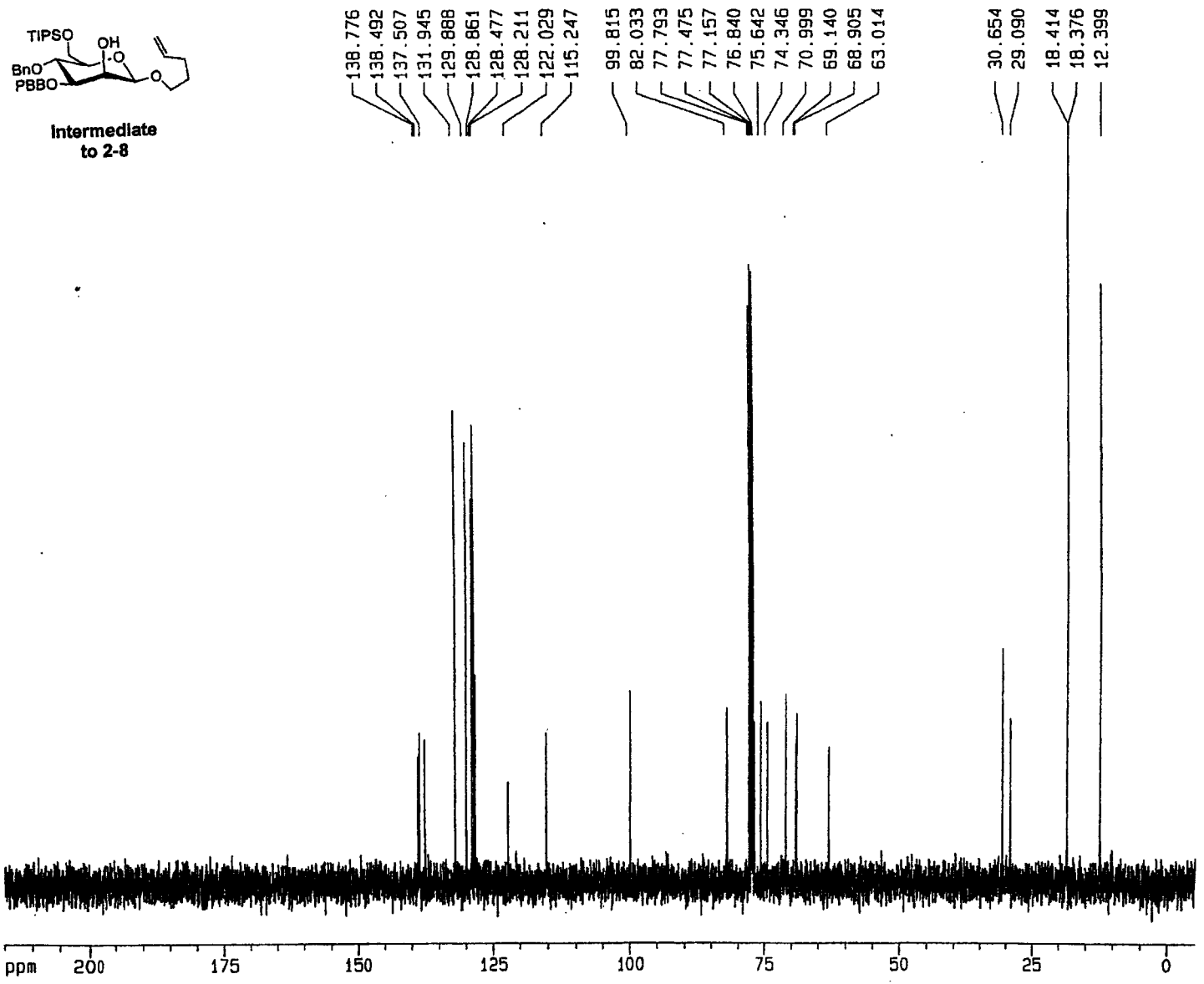

Current Data Parameters

NAME	DMR-I-NMR-101
EXPNO	12
PROCNO	1

F2 - Acquisition Parameters

Date_	20000405
Time	16.50
INSTRUM	spect
PROBHD	5mm BBO BB-1
PULPROG	zgpg30
TD	65536
SOLVENT	CDCl3
NS	32
DS	2
SWH	25125.629 Hz
FIDRES	0.383387 Hz
AQ	1.3042164 sec
RG	16384
DW	19.900 usec
DE	6.00 usec
TE	300.0 K
D1	2.00000000 sec
D11	0.03000000 sec
D12	0.00002000 sec

========== CHANNEL f1 ==========

NUC1	13C
P1	14.20 usec
PL1	3.00 dB
SFO1	100.6237959 MHz

========== CHANNEL f2 ==========

CPDPRG2	waltz16
NUC2	1H
PCPD2	107.50 usec
PL2	0.00 dB
PL12	24.00 dB
PL13	24.00 dB
SFO2	400.1316005 MHz

F2 - Processing parameters

SI	32768
SF	100.6127290 MHz
WDW	EM
SSB	0
LB	1.00 Hz
GB	0
PC	1.40

1D NMR plot parameters

CX	20.00 cm
F1P	215.000 ppm
F1	21631.74 Hz
F2P	-5.000 ppm
F2	-503.06 Hz
PPMCM	11.00000 ppm/cm
HZCM	1106.73999 Hz/cm

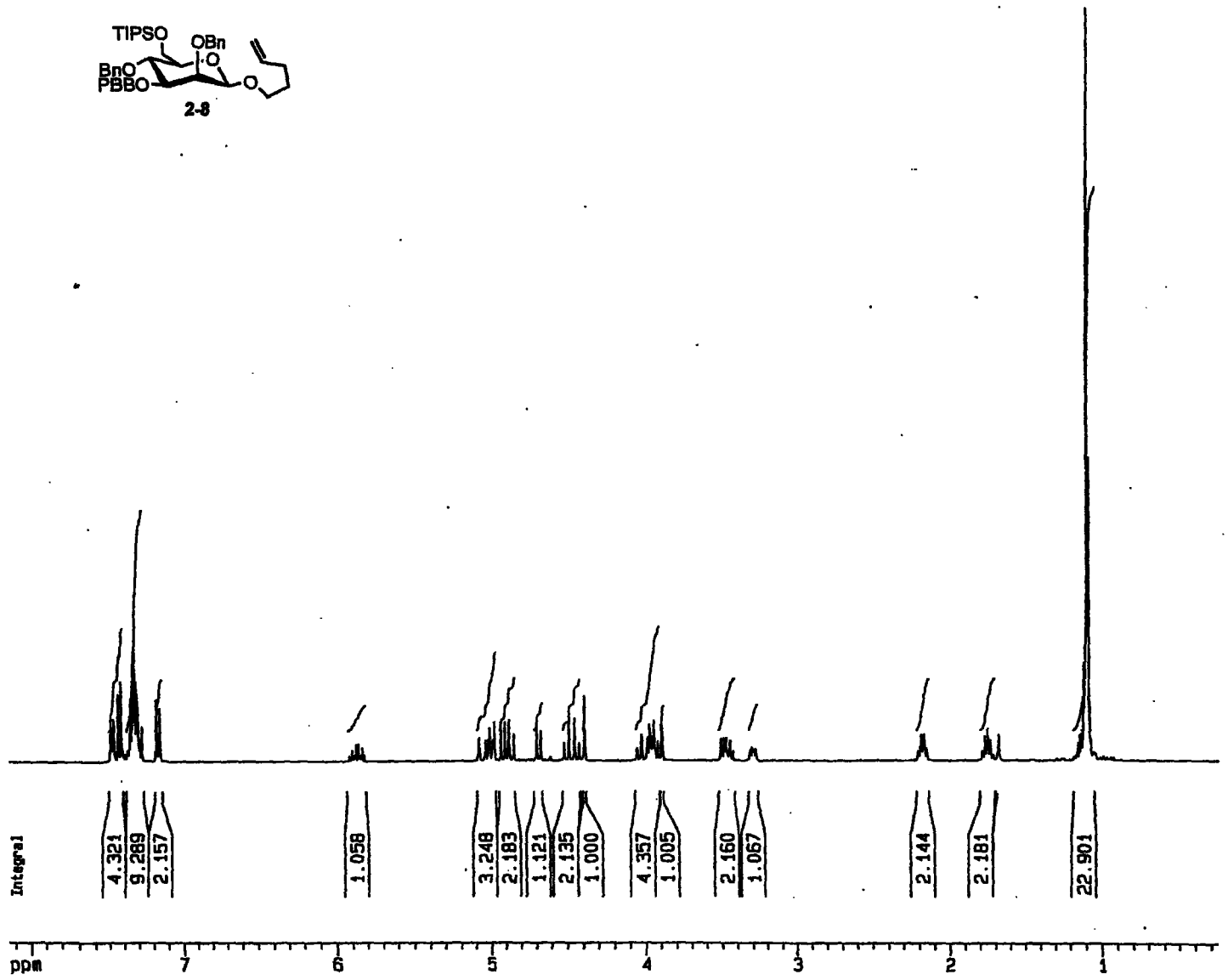

Current Data Parameters

NAME	DMR-I-265
EXPNO	10
PROCNO	1

F2 - Acquisition Parameters

Date_	20000918
Time	14.11
INSTRUM	spect
PROBHD	5mm BBO BB-1
PULPROG	zg30
TD	65536
SOLVENT	CDCl3
NS	16
DS	2
SWH	8278.146 Hz
FIDRES	0.126314 Hz
AQ	3.9684243 sec
RG	50.8
DW	60.400 usec
DE	6.00 usec
TE	300.0 K
D1	1.00000000 sec

========== CHANNEL f1 ==========

NUC1	1H
P1	7.90 usec
PL1	0.00 dB
SFO1	400.1324710 MHz

F2 - Processing parameters

SI	32768
SF	400.1300000 MHz
WDW	EM
SSB	0
LB	0.30 Hz
GB	0
PC	1.00

1D NMR plot parameters

CX	20.00 cm
F1P	8.139 ppm
F1	3256.72 Hz
F2P	0.261 ppm
F2	104.45 Hz
PPMCM	0.39391 ppm/cm
HZCM	157.61369 Hz/cm

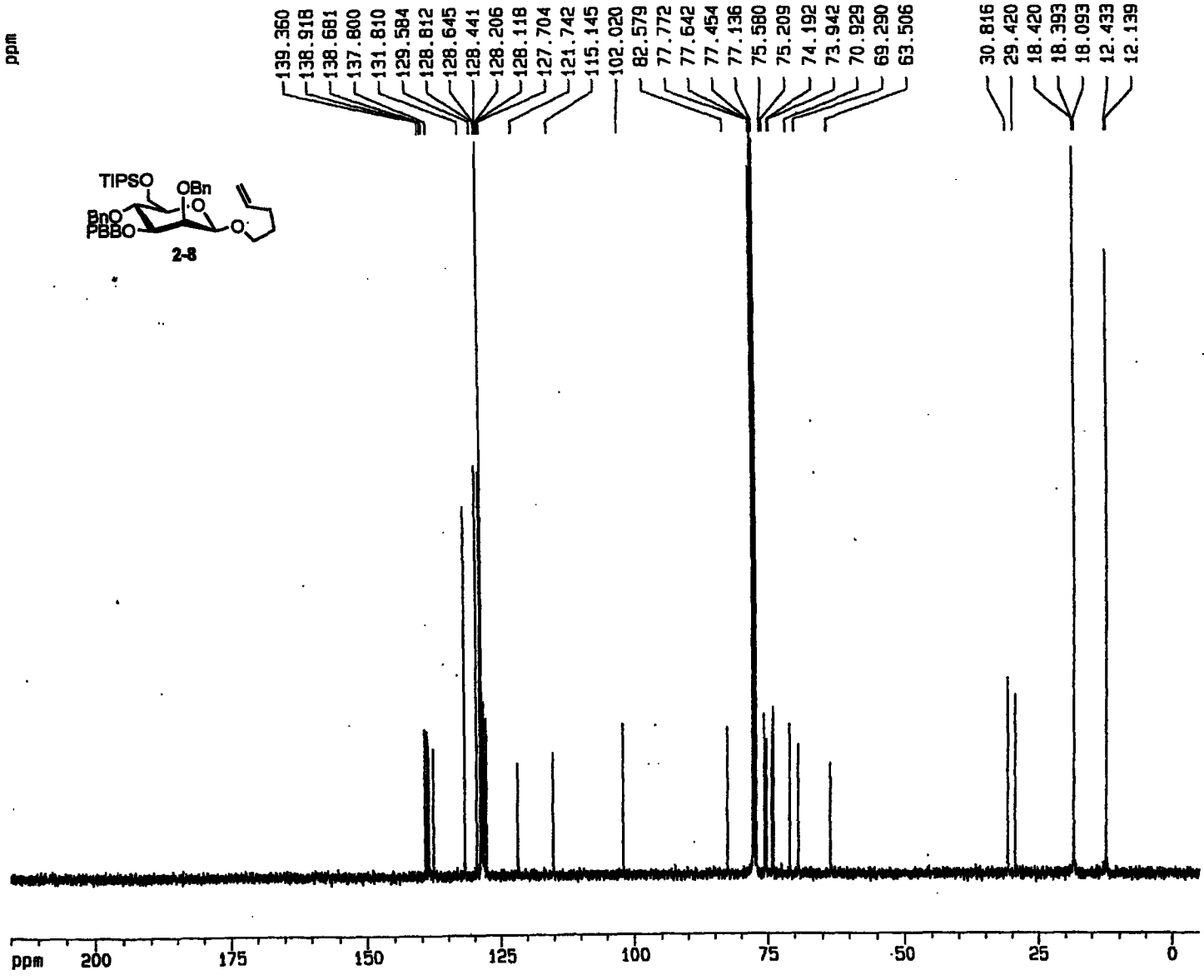

Current Data Parameters
NAME DMR-I-265
EXPNO 11
PROCNO 1

F2 - Acquisition Parameters
Date_ 20000918
Time 15.08
INSTRUM spect
PROBHD 5mm BBO BB-1
PULPROG zgpg30
TD 65536
SOLVENT CDCl3
NS 1024
DS 4
SWH 25125.629 Hz
FIDRES 0.383387 Hz
AQ 1.3042164 sec
RG 13004
DW 19.900 usec
DE 6.00 usec
TE 300.0 K
D1 2.00000000 sec
d11 0.03000000 sec
d12 0.00002000 sec

CHANNEL f1
NUC1 13C
P1 15.25 usec
PL1 3.00 dB
SF01 100.6237959 MHz

CHANNEL f2
CPDPRG2 waltz16
NUC2 1H
PCPD2 107.50 usec
PL2 0.00 dB
PL12 24.00 dB
PL13 24.00 dB
SF02 400.1316005 MHz

F2 - Processing parameters
SI 32768
SF 100.6127290 MHz
WDW EM
SSB 0
LB 1.00 Hz
GB 0
PC 1.40

1D NMR plot parameters
CX 20.00 cm
F1P 215.000 ppm
F1 21631.74 Hz
F2P -5.000 ppm
F2 -503.06 Hz
PPMCM 11.00000 ppm/cm
HZCM 1106.73999 Hz/cm

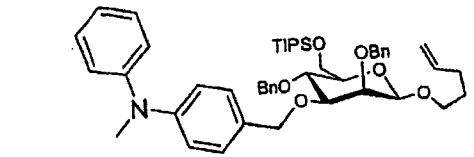

Intermediate to 2-14

Current Data Parameters

NAME	DMR-I-267
EXPNO	10
PROCNO	1

F2 - Acquisition Parameters

Date_	20000921
Time	12.15
INSTRUM	spect
PROBHD	5mm BBO BB-1
PULPROG	zg30
TD	65536
SOLVENT	CDCl3
NS	16
DS	2
SWH	8278.146 Hz
FIDRES	0.126314 Hz
AQ	3.9584243 sec
RG	57
DW	60.400 usec
DE	6.00 usec
TE	300.0 K
D1	1.00000000 sec

========== CHANNEL f1 ==========

NUC1	1H
P1	7.90 usec
PL1	0.00 dB
SFO1	400.1324710 MHz

F2 - Processing parameters

SI	32768
SF	400.1300000 MHz
WDW	EM
SSB	0
LB	0.30 Hz
GB	0
PC	1.00

1D NMR plot parameters

CX	20.00 cm
F1P	8.002 ppm
F1	3201.90 Hz
F2P	0.033 ppm
F2	13.08 Hz
PPMCM	0.39847 ppm/cm
HZCM	159.44110 Hz/cm

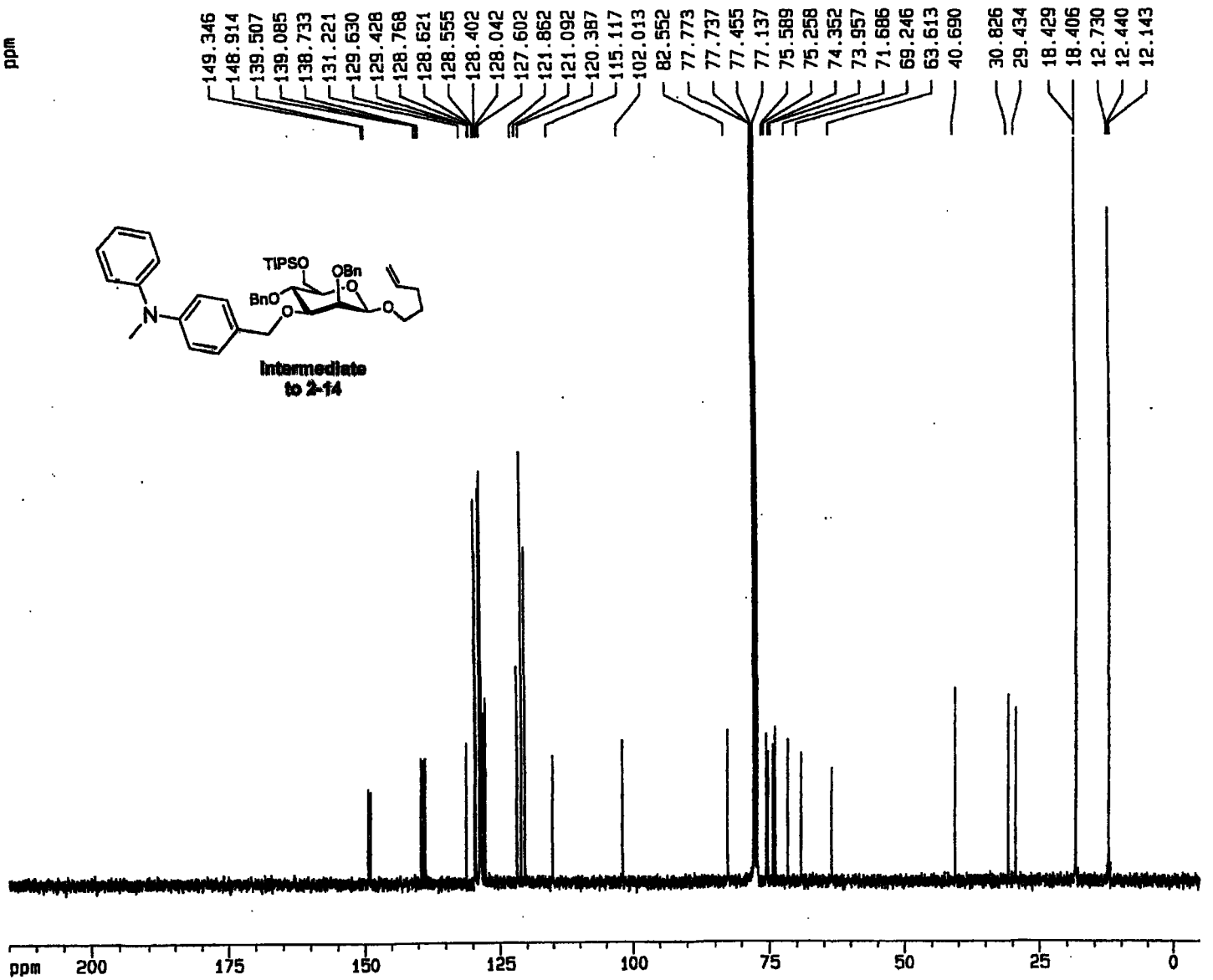


```
Current Data Parameters
NAME                  DMR-I-267
EXPNO                        20
PROCNO                        1

F2 - Acquisition Parameters
Date_                 20000921
Time                     13.12
INSTRUM                  spect
PROBHD     5mm BBO BB-1
PULPROG                 zgpg30
TD                       65536
SOLVENT                  CDCl3
NS                        1024
DS                           4
SWH                  25125.629 Hz
FIDRES                0.383367 Hz
AQ                    1.3042164 sec
RG                       18384
DW                       19.900 usec
DE                        6.00 usec
TE                       300.0 K
D1                    2.00000000 sec
d11                   0.03000000 sec
d12                   0.00002000 sec

======== CHANNEL f1 ========
NUC1                       13C
P1                       15.25 usec
PL1                       3.00 dB
SFO1                100.6237959 MHz

======== CHANNEL f2 ========
CPDPRG2                waltz16
NUC2                        1H
PCPD2                   107.50 usec
PL2                       0.00 dB
PL12                     24.00 dB
PL13                     24.00 dB
SFO2                400.1316005 MHz

F2 - Processing parameters
SI                         32768
SF                  100.6127290 MHz
WDW                           EM
SSB                            0
LB                        1.00 Hz
GB                             0
PC                         1.40

1D NMR plot parameters
CX                        20.00 cm
F1P                     215.000 ppm
F1                    21631.74 Hz
F2P                      -5.000 ppm
F2                     -503.06 Hz
PPMCM                 11.00000 ppm/cm
HZCM                1106.73999 Hz/cm
```

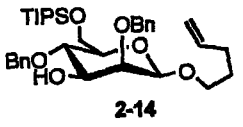

2-14


```
Current Data Parameters
NAME                  DMR-I-275
EXPNO                        10
PROCNO                        1

F2 - Acquisition Parameters
Date_                  20000923
Time                      14.01
INSTRUM                   spect
PROBHD      5mm BBO BB-1
PULPROG                   zg30
TD                       65536
SOLVENT                   CDCl3
NS                           16
DS                            2
SWH                 8278.146 Hz
FIDRES              0.126314 Hz
AQ                  3.9584243 sec
RG                         45.3
DW                    60.400 usec
DE                     6.00 usec
TE                     300.0 K
D1                  1.00000000 sec

========== CHANNEL f1 ========
NUC1                       1H
P1                     7.90 usec
PL1                    0.00 dB
SFO1           400.1324710 MHz

F2 - Processing parameters
SI                        32768
SF                 400.1300451 MHz
WDW                       EM
SSB                        0
LB                     0.30 Hz
GB                         0
PC                      1.00

1D NMR plot parameters
CX                     20.00 cm
F1P                    8.186 ppm
F1                   3275.57 Hz
F2P                   -0.126 ppm
F2                    -50.31 Hz
PPMCM                0.41560 ppm/cm
HZCM                166.29387 Hz/cm
```

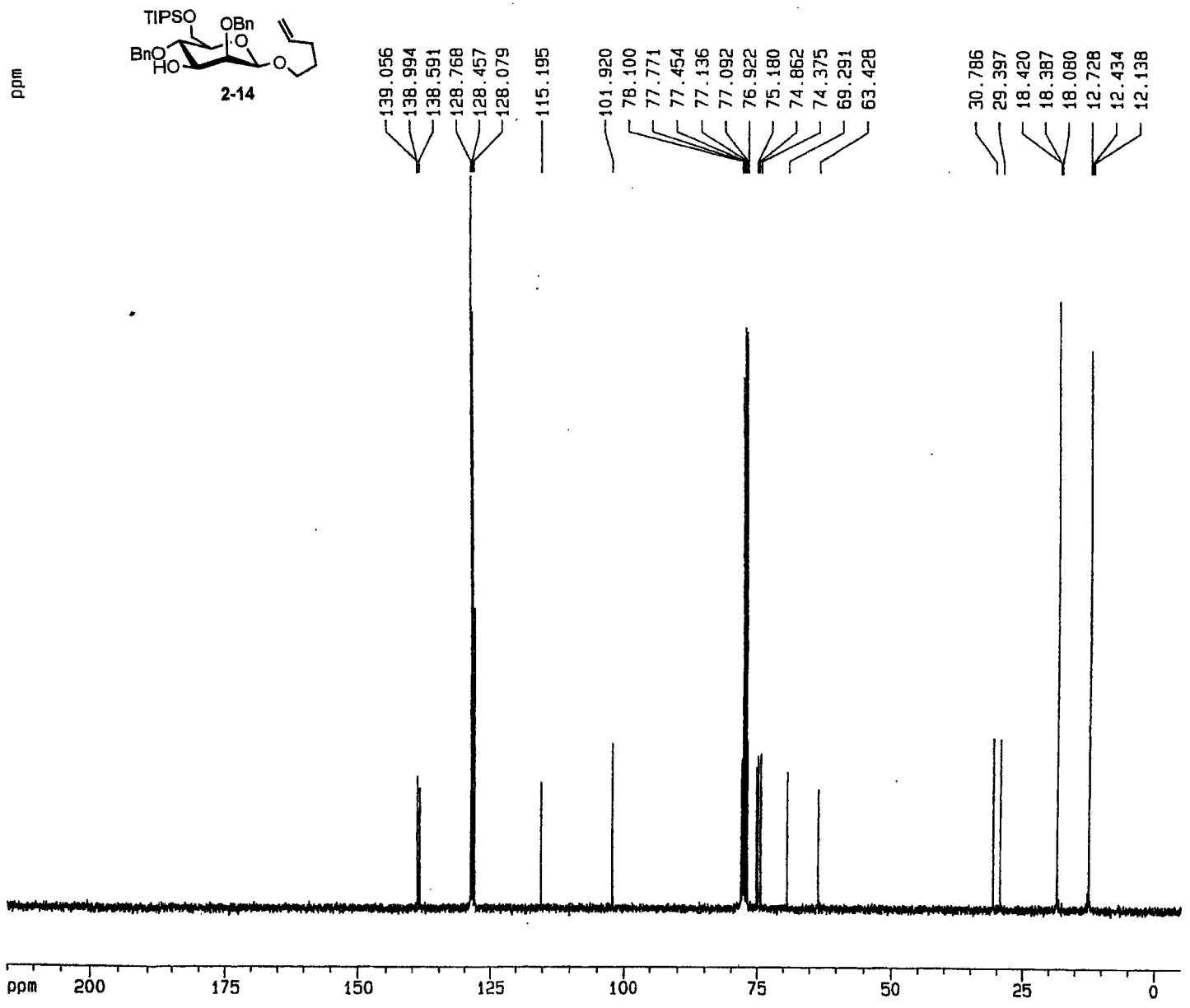

Current Data Parameters

NAME	DMR-I-275
EXPNO	11
PROCNO	1

F2 - Acquisition Parameters

Date_	20000923
Time	14.58
INSTRUM	spect
PROBHD	5mm BBO BB-1
PULPROG	zgpg30
TD	65536
SOLVENT	CDCl3
NS	1024
DS	4
SWH	25125.629 Hz
FIDRES	0.383387 Hz
AQ	1.3042164 sec
RG	16384
DW	19.900 usec
DE	6.00 usec
TE	300.0 K
D1	2.00000000 sec
d11	0.03000000 sec
d12	0.00002000 sec

CHANNEL f1

NUC1	13C
P1	15.25 usec
PL1	3.00 dB
SFO1	100.6237959 MHz

CHANNEL f2

CPDPRG2	waltz16
NUC2	1H
PCPD2	107.50 usec
PL2	0.00 dB
PL12	24.00 dB
PL13	24.00 dB
SFO2	400.1316005 MHz

F2 - Processing parameters

SI	32768
SF	100.6127290 MHz
WDW	EM
SSB	0
LB	1.00 Hz
GB	0
PC	1.40

1D NMR plot parameters

CX	20.00 cm
F1P	215.000 ppm
F1	21631.74 Hz
F2P	-5.000 ppm
F2	-503.06 Hz
PPMCM	11.00000 ppm/cm
HZCM	1106.73999 Hz/cm

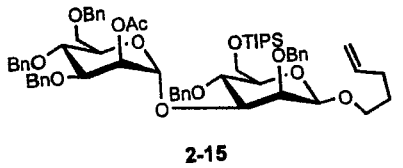

2-15

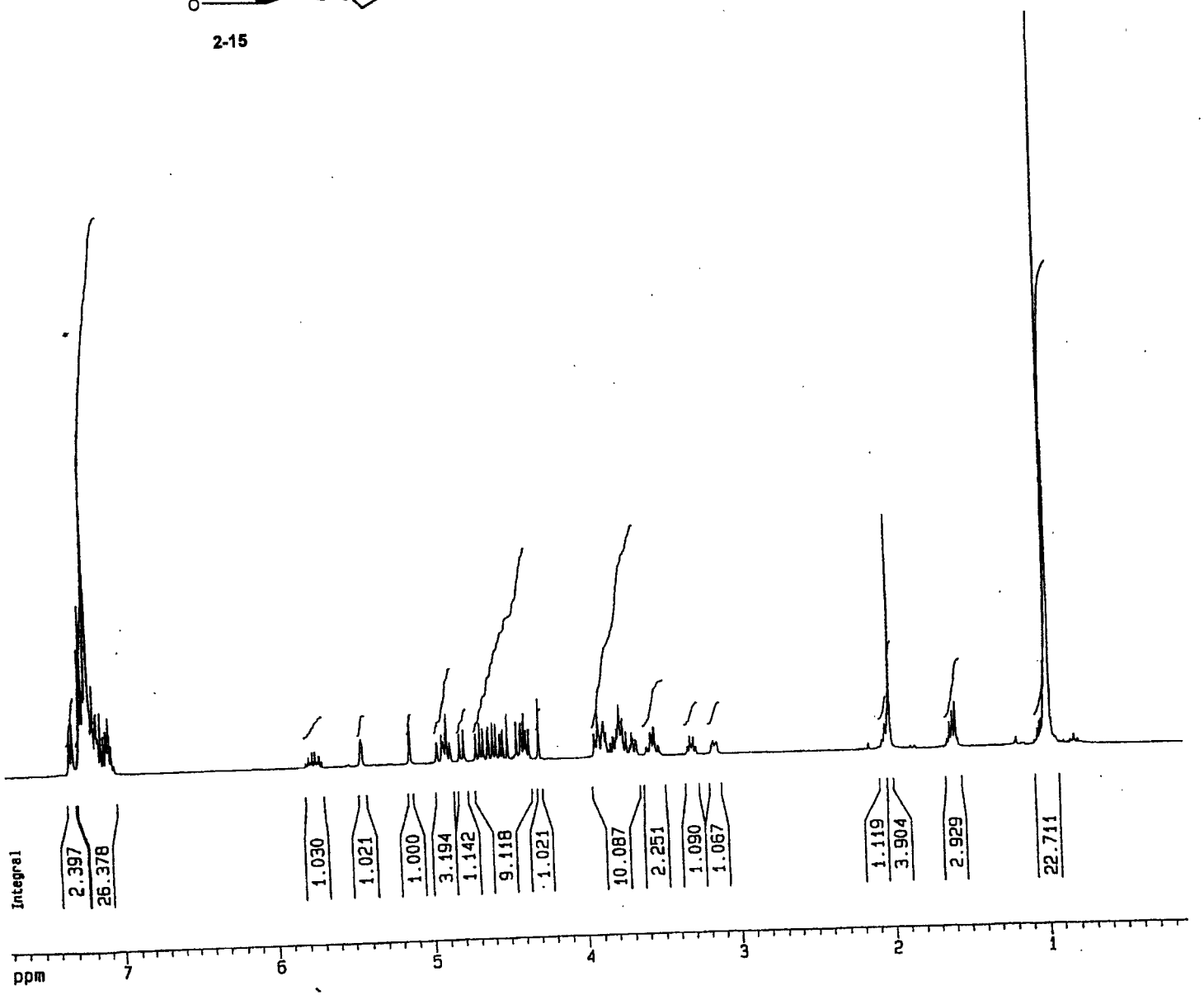

Current Data Parameters
NAME DMR-I-281
EXPNO 10
PROCNO 1

F2 - Acquisition Parameters
Date_ 20000927
Time 11.16
INSTRUM spect
PROBHD 5mm BBO BB-1
PULPROG zg30
TD 65536
SOLVENT CDCl3
NS 64
DS 0
SWH 8278.146 Hz
FIDRES 0.126314 Hz
AQ 3.9584243 sec
RG 35.9
DW 60.400 usec
DE 6.00 usec
TE 300.0 K
D1 2.00000000 sec

---------- CHANNEL f1 ----------
NUC1 1H
P1 7.90 usec
PL1 0.00 dB
SFO1 400.1324710 MHz

F2 - Processing parameters
SI 32768
SF 400.1300496 MHz
WDW EM
SSB 0
LB 0.30 Hz
GB 0
PC 1.00

1D NMR plot parameters
CX 20.00 cm
F1P 7.718 ppm
F1 3088.31 Hz
F2P 0.137 ppm
F2 54.81 Hz
PPMCM 0.37906 ppm/cm
HZCM 151.67464 Hz/cm

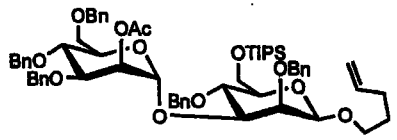

2-15

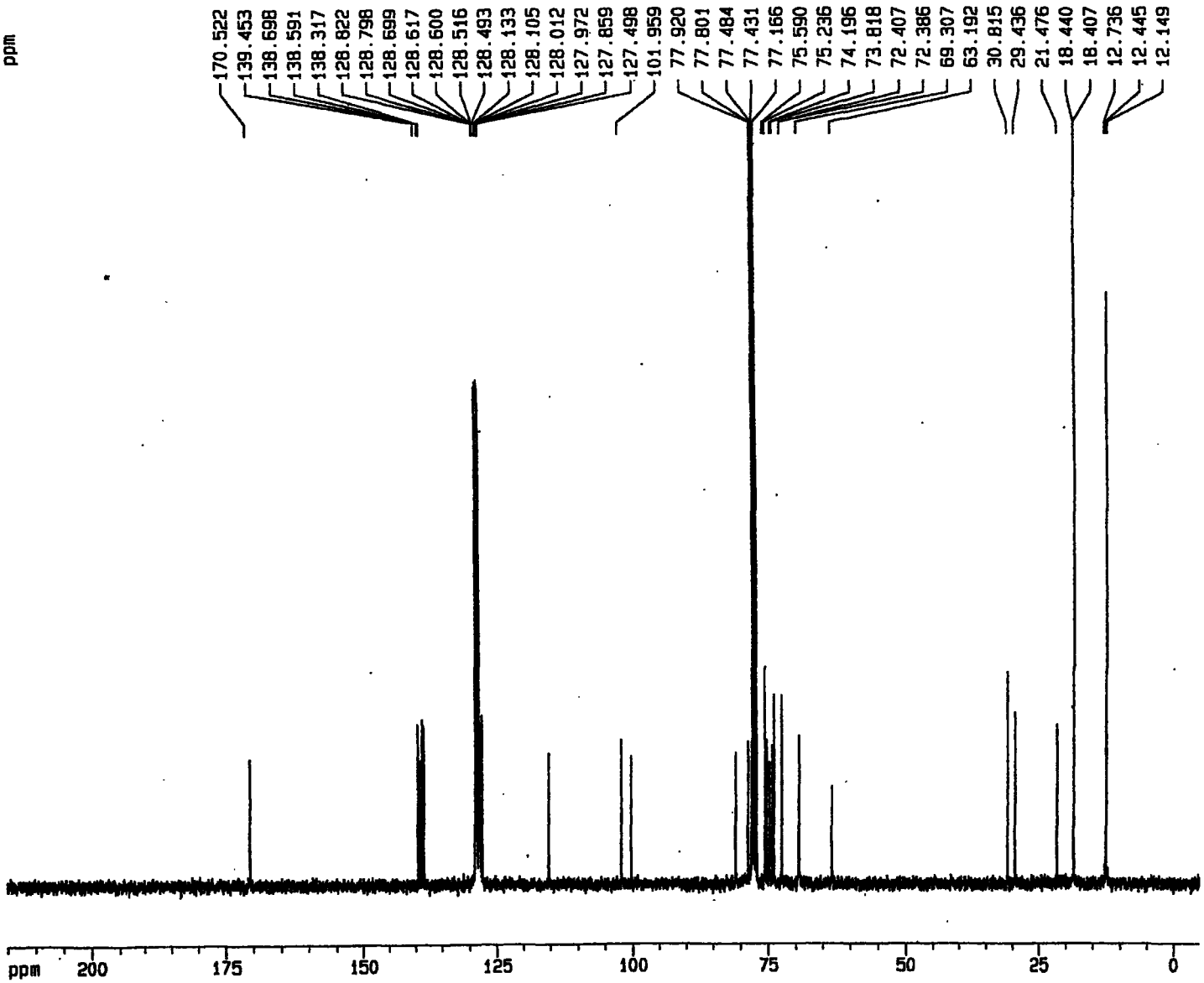


```
Current Data Parameters
NAME                  DNA-I-281
EXPNO                        20
PROCNO                        1

F2 - Acquisition Parameters
Date_                 20000927
Time                     12.13
INSTRUM                  spect
PROBHD     5mm BBO BB-1
PULPROG                zgpg30
TD                        65536
SOLVENT                   CDCl3
NS                         1024
DS                            4
SWH                  25125.629 Hz
FIDRES               0.383387 Hz
AQ                   1.3042164 sec
RG                        16384
DW                   19.900 usec
DE                    6.00 usec
TE                    300.0 K
D1                   2.00000000 sec
d11                  0.03000000 sec
d12                  0.00002000 sec

========== CHANNEL f1 ==========
NUC1                        13C
P1                    15.25 usec
PL1                    3.00 dB
SFO1               100.6237959 MHz

========== CHANNEL f2 ==========
CPDPRG2                waltz16
NUC2                        1H
PCPD2                 107.50 usec
PL2                    0.00 dB
PL12                  24.00 dB
PL13                  24.00 dB
SFO2               400.1316005 MHz

F2 - Processing parameters
SI                         32768
SF                 100.6127290 MHz
WDW                           EM
SSB                            0
LB                     1.00 Hz
GB                             0
PC                     1.40

1D NMR plot parameters
CX                    20.00 cm
F1P                  215.000 ppm
F1                 21631.74 Hz
F2P                   -5.000 ppm
F2                  -503.06 Hz
PPMCM                11.00000 ppm/cm
HZCM               1106.73999 Hz/cm
```

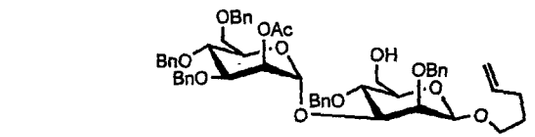

2-16

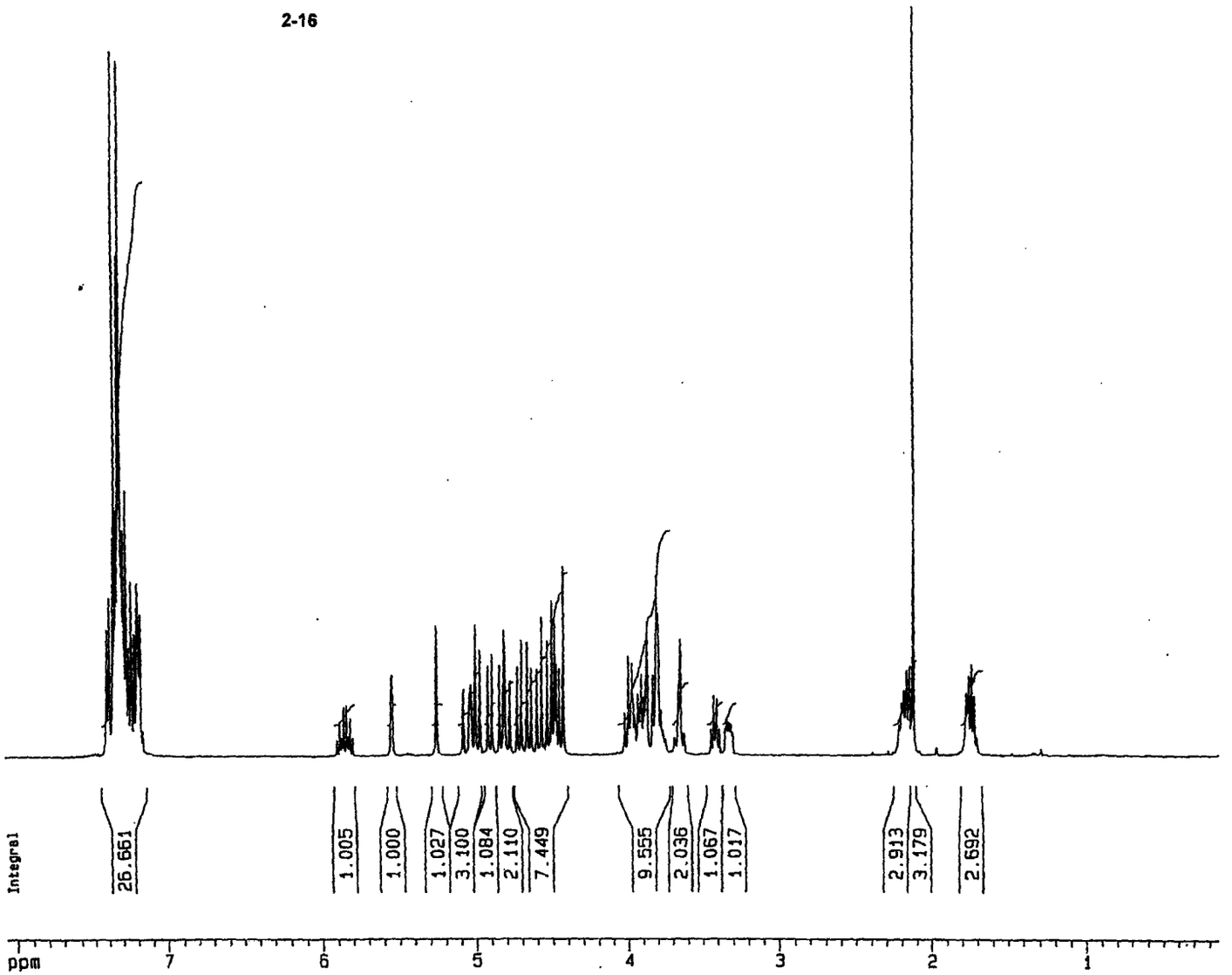


```
Current Data Parameters
NAME                  OHR-I-285
EXPNO                        10
PROCNO                        1

F2 - Acquisition Parameters
Date_                  20000930
Time                      13.39
INSTRUM                   spect
PROBHD      5mm BBO BB-1
PULPROG                   zg30
TD                       65536
SOLVENT                  CDCl3
NS                          64
DS                           0
SWH                 8278.146 Hz
FIDRES              0.126314 Hz
AQ                  3.9584243 sec
RG                          57
DW                     60.400 usec
DE                      6.00 usec
TE                     300.0 K
D1                  2.00000000 sec

========== CHANNEL f1 =========
NUC1                         1H
P1                      7.90 usec
PL1                     0.00 dB
SFO1               400.1324710 MHz

F2 - Processing parameters
SI                       32768
SF                 400.1300000 MHz
WDW                         EM
SSB                          0
LB                      0.30 Hz
GB                           0
PC                        1.00

1D NMR plot parameters
CX                      20.00 cm
F1P                     8.071 ppm
F1                    3229.31 Hz
F2P                     0.147 ppm
F2                      58.76 Hz
PPMCM                0.39619 ppm/cm
HZCM                158.52740 Hz/cm
```

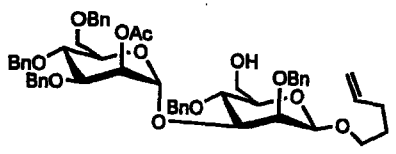

2-16

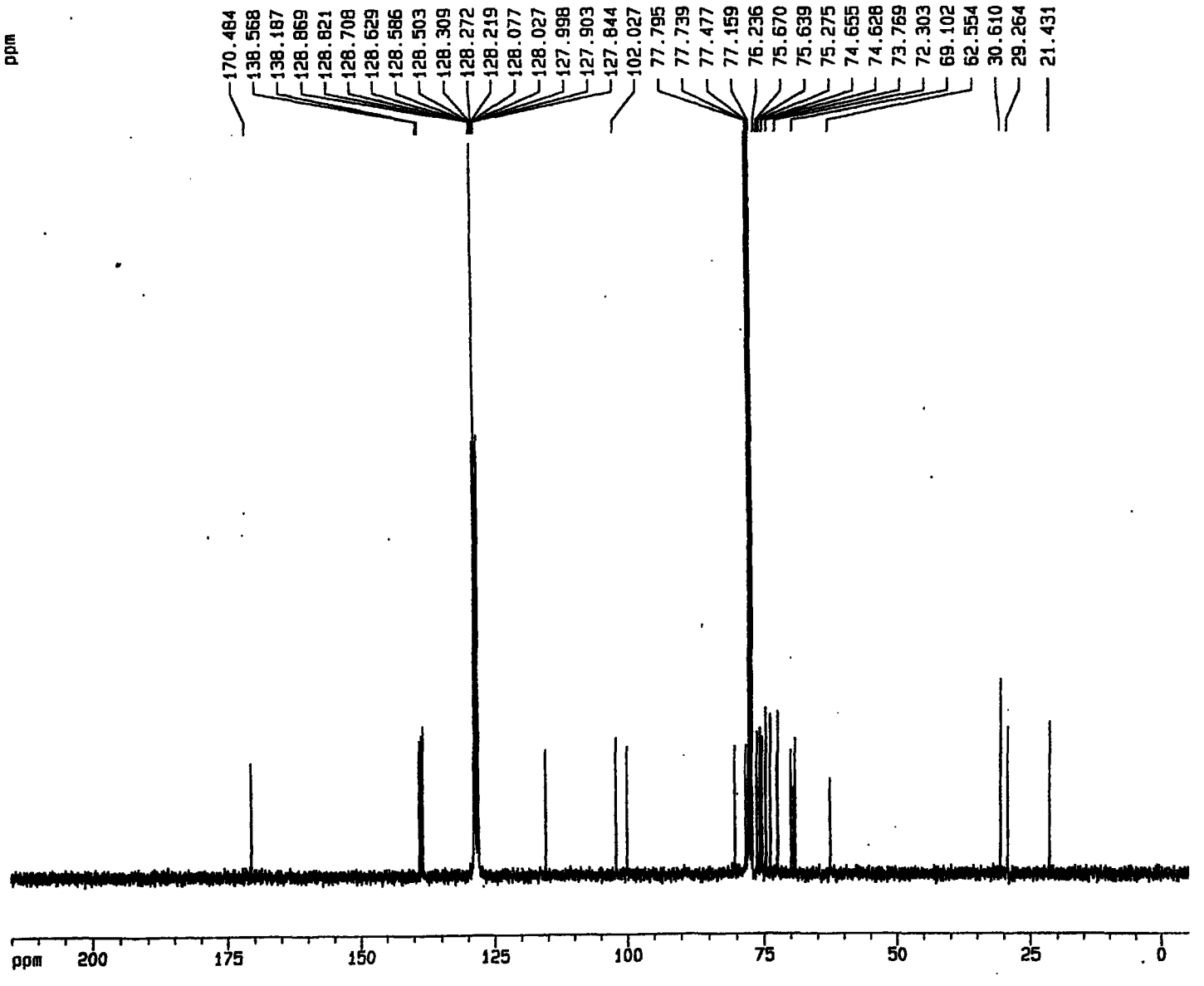


```
Current Data Parameters
NAME            OMR-I-285
EXPNO                  11
PROCNO                  1

F2 - Acquisition Parameters
Date_           20000930
Time                14.36
INSTRUM             spect
PROBHD     5mm BBO BB-1
PULPROG           zgpg30
TD                 65536
SOLVENT            CDCl3
NS                  1024
DS                     4
SWH           25125.629 Hz
FIDRES         0.383387 Hz
AQ             1.3042164 sec
RG                 16384
DW                19.900 usec
DE                 6.00 usec
TE                300.0 K
D1             2.00000000 sec
d11            0.03000000 sec
d12            0.00002000 sec

====== CHANNEL f1 ======
NUC1                13C
P1                15.25 usec
PL1                3.00 dB
SFO1         100.6237989 MHz

====== CHANNEL f2 ======
CPDPRG2          waltz16
NUC2                1H
PCPD2             107.50 usec
PL2                0.00 dB
PL12              24.00 dB
PL13              24.00 dB
SFO2         400.1316005 MHz

F2 - Processing parameters
SI                 32768
SF           100.6127290 MHz
WDW                  EM
SSB                   0
LB                 1.00 Hz
GB                    0
PC                 1.40

1D NMR plot parameters
CX                20.00 cm
F1P              215.000 ppm
F1             21631.74 Hz
F2P               -5.000 ppm
F2             -503.06 Hz
PPMCM          11.00000 ppm/cm
HZCM           1106.73998 Hz/cm
```

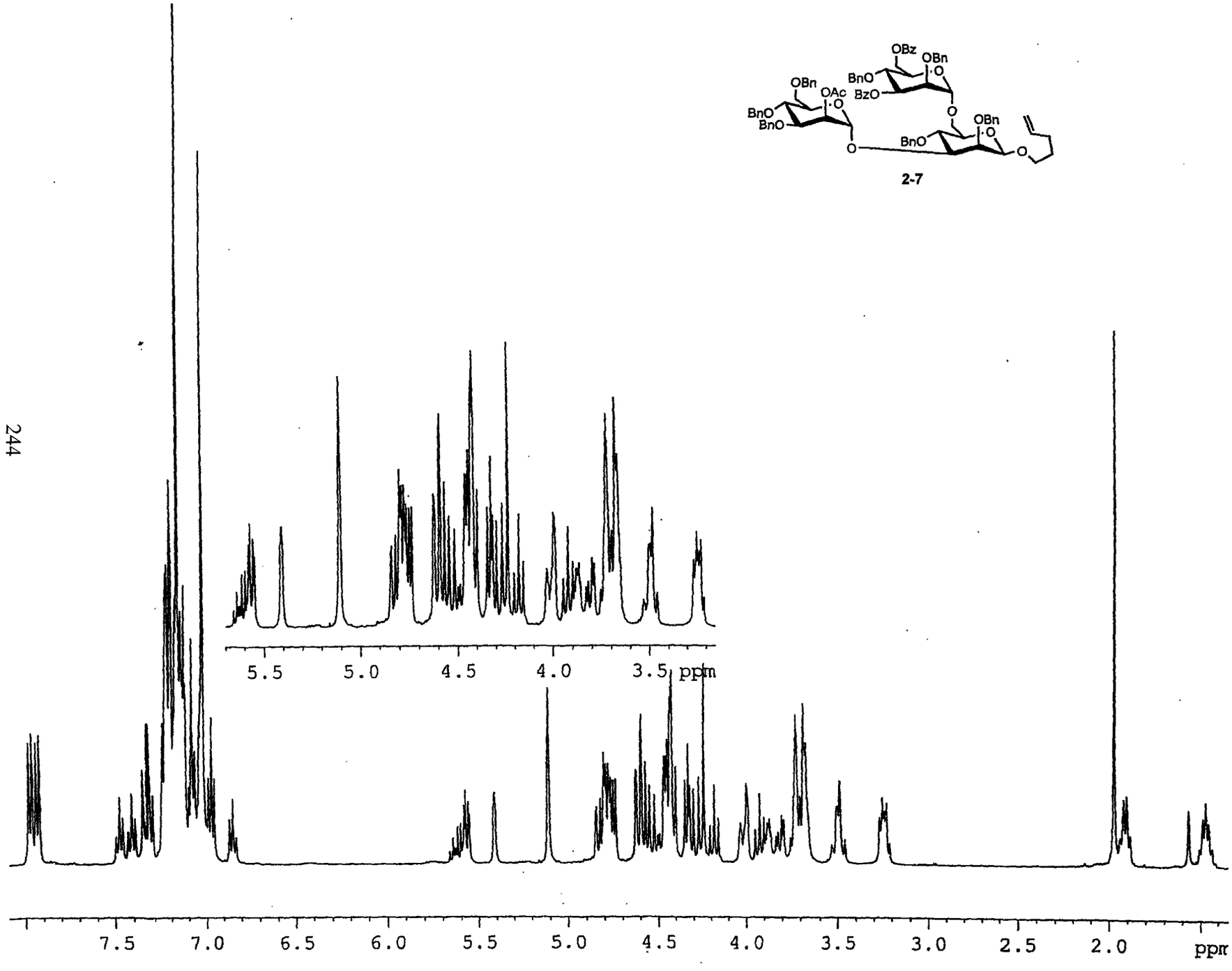
OBz
OBn
BnO
OBn
OAc
BzO
BnO
BnO
OBn
BnO
O
O
O
O
2-7
5.5
5.0
4.5
4.0
3.5
ppm
7.5
7.0
6.5
6.0
5.5
5.0
4.5
4.0
3.5
3.0
2.5
2.0
ppm

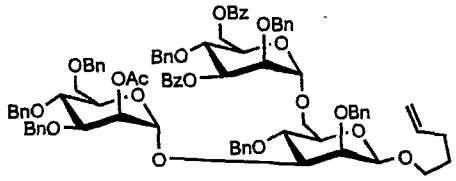

2-7

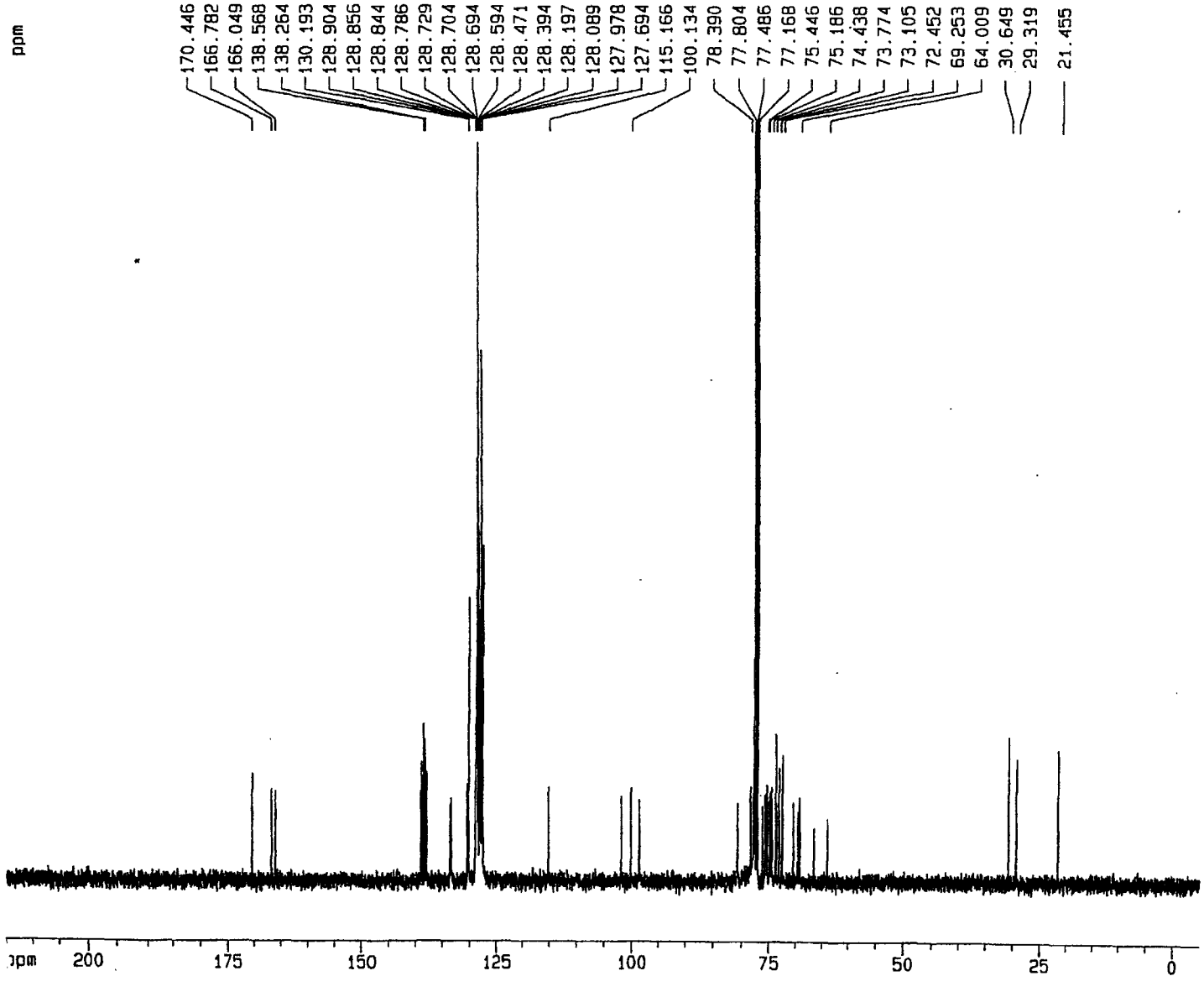

Current Data Parameters

NAME	DMA-II-61.prod
EXPNO	11
PROCNO	1

F2 - Acquisition Parameters

Date_	20010117
Time	18.25
INSTRUM	spect
PROBHD	5mm BBO BB-1
PULPROG	zgpg30
TD	65536
SOLVENT	CDCl3
NS	1024
DS	4
SWH	25125.629 Hz
FIDRES	0.383387 Hz
AQ	1.3042164 sec
RG	16384
DW	19.900 usec
DE	6.00 usec
TE	300.0 K
D1	2.00000000 sec
d11	0.03000000 sec
d12	0.00002000 sec

========== CHANNEL f1 ==========

NUC1	13C
P1	15.25 usec
PL1	3.00 dB
SFO1	100.6237959 MHz

========== CHANNEL f2 ==========

CPDPRG2	waltz16
NUC2	1H
PCPD2	107.50 usec
PL2	0.00 dB
PL12	24.00 dB
PL13	24.00 dB
SFO2	400.1316005 MHz

F2 - Processing parameters

SI	32768
SF	100.6127290 MHz
WDW	EM
SSB	0
LB	1.00 Hz
GB	0
PC	1.40

1D NMR plot parameters

CX	20.00 cm
F1P	215.000 ppm
F1	21631.74 Hz
F2P	-5.000 ppm
F2	-503.06 Hz
PPMCM	11.00000 ppm/cm
HZCM	1106.73999 Hz/cm

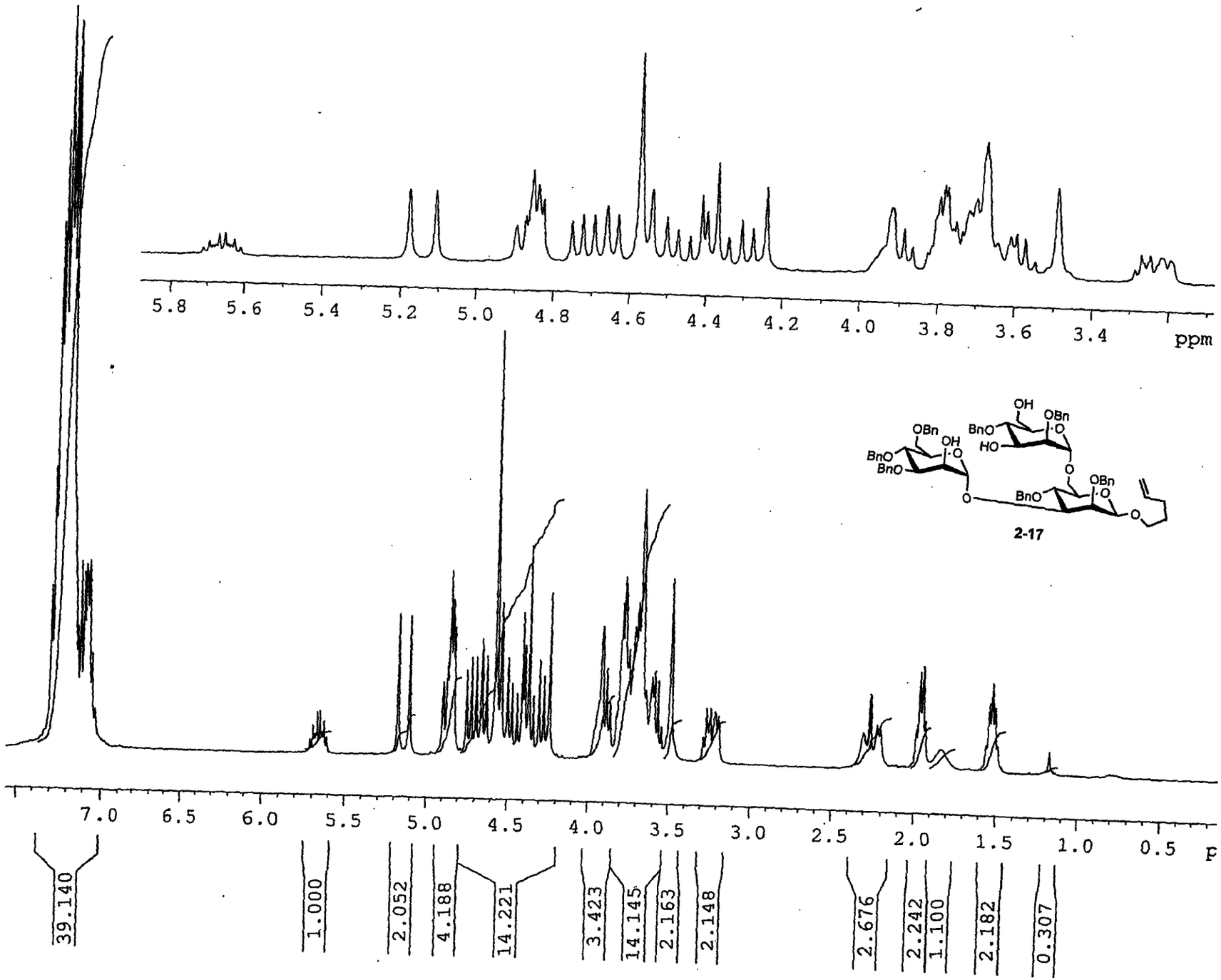
5.8
5.6
5.4
5.2
5.0
4.8
4.6
4.4
4.2
4.0
3.8
3.6
3.4
ppm
OH
OBn
BnO
HO
OBn
OH
BnO
BnO
OBn
BnO
2-17
7.0
6.5
6.0
5.5
5.0
4.5
4.0
3.5
3.0
2.5
2.0
1.5
1.0
0.5
39.140
1.000
2.052
4.188
14.221
3.423
14.145
2.163
2.148
2.676
2.242
1.100
2.182
0.307

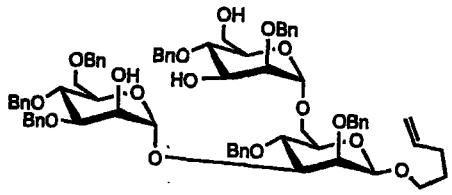

2-17

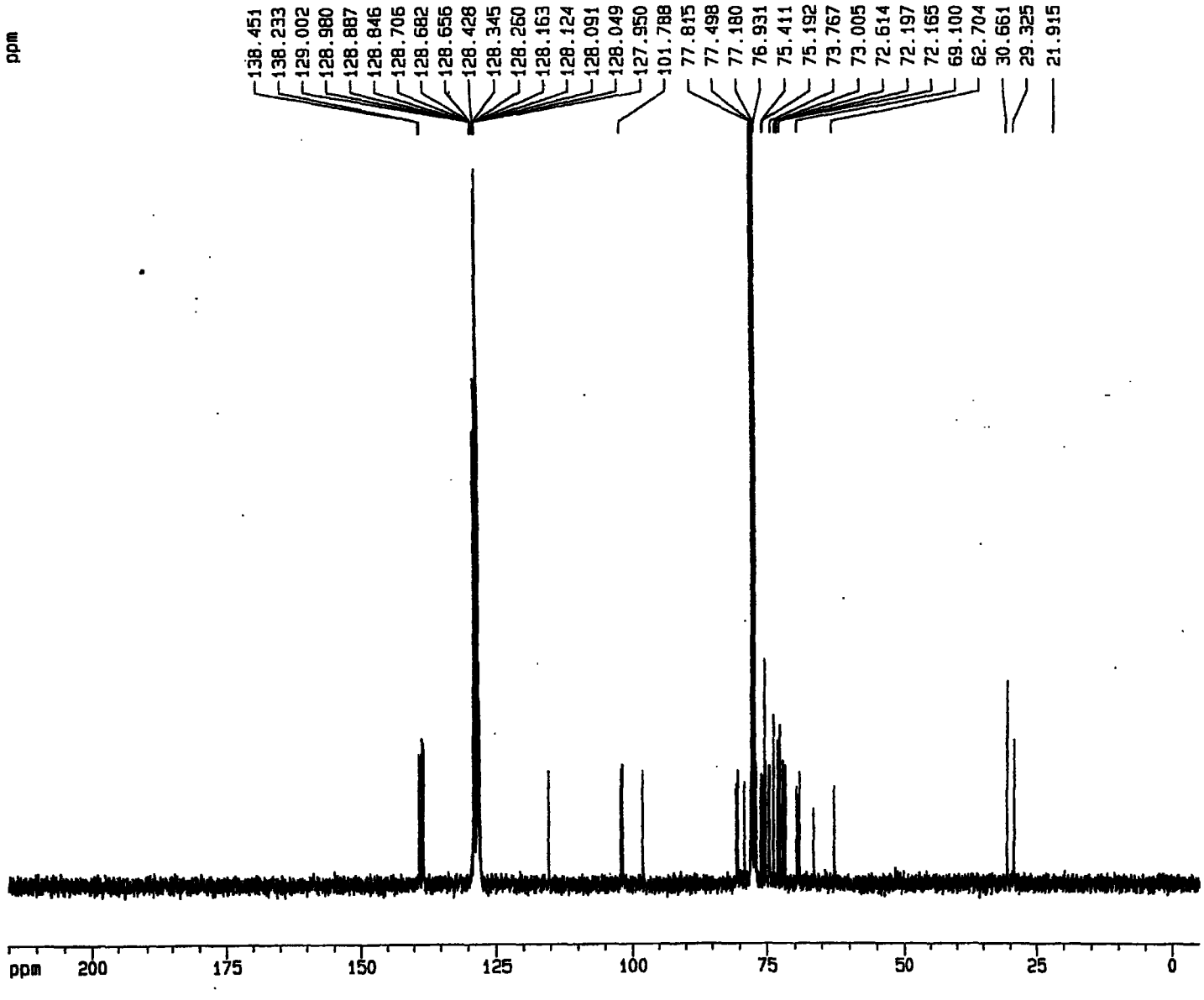


```
Current Data Parameters
NAME            DMR-II-65
EXPNO                  11
PROCNO                  1

F2 - Acquisition Parameters
Date_            20010120
Time                9.52
INSTRUM            spect
PROBHD     5mm BBO BB-1
PULPROG          zgpg30
TD                65536
SOLVENT           CDCl3
NS                 1024
DS                    4
SWH           25125.629 Hz
FIDRES        0.383387 Hz
AQ            1.3042164 sec
RG                16384
DW               19.900 usec
DE                6.00 usec
TE               300.0 K
D1            2.00000000 sec
d11           0.03000000 sec
d12           0.00002000 sec

========== CHANNEL f1 ==========
NUC1               13C
P1               15.25 usec
PL1               3.00 dB
SFO1         100.6237998 MHz

========== CHANNEL f2 ==========
CPDPRG2         waltz16
NUC2               1H
PCPD2           107.50 usec
PL2               0.00 dB
PL12             24.00 dB
PL13             24.00 dB
SFO2         400.1316005 MHz

F2 - Processing parameters
SI                32768
SF          100.6127290 MHz
WDW                EM
SSB                0
LB              1.00 Hz
GB                 0
PC              1.40

1D NMR plot parameters
CX              20.00 cm
F1P            215.000 ppm
F1           21631.74 Hz
F2P             -5.000 ppm
F2            -503.06 Hz
PPMCM          11.00000 ppm/cm
HZCM         1106.73999 Hz/cm
```

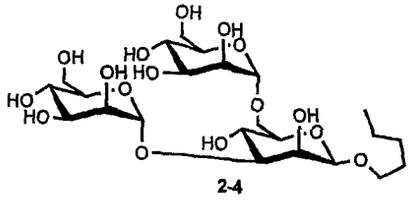

2-4

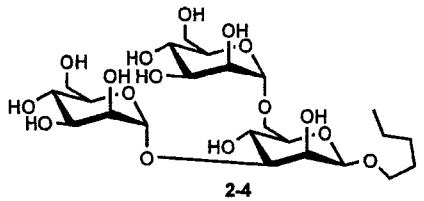
OH
OH
HO
OH
HO
HO
OH
HO
HO
O
O
OH
HO
O
O

2-4

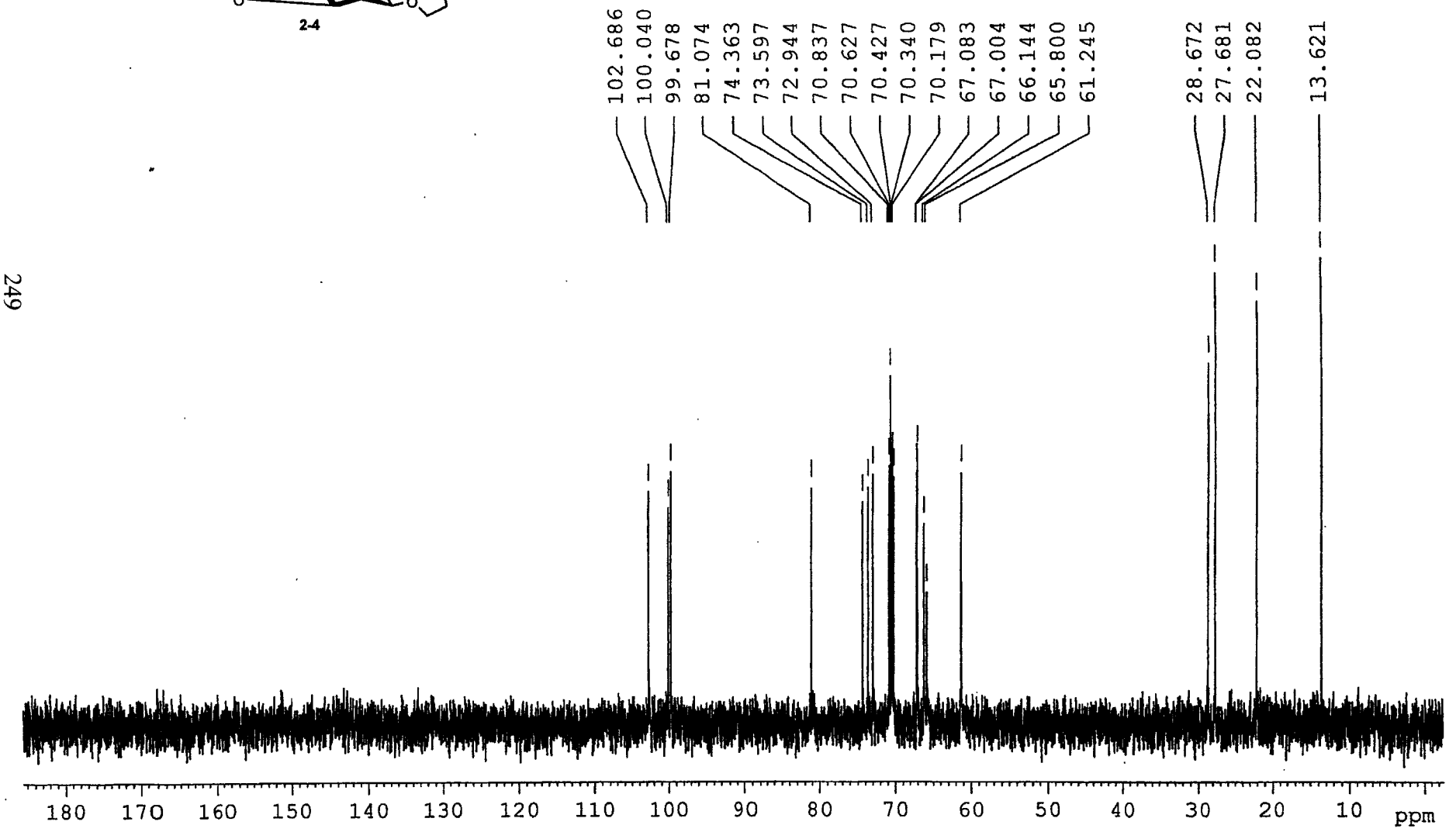
102.686
100.040
99.678
81.074
74.363
73.597
72.944
70.837
70.627
70.427
70.340
70.179
67.083
67.004
66.144
65.800
61.245
28.672
27.681
22.082
13.621
180
170
160
150
140
130
120
110
100
90
80
70
60
50
40
30
20
10
ppm

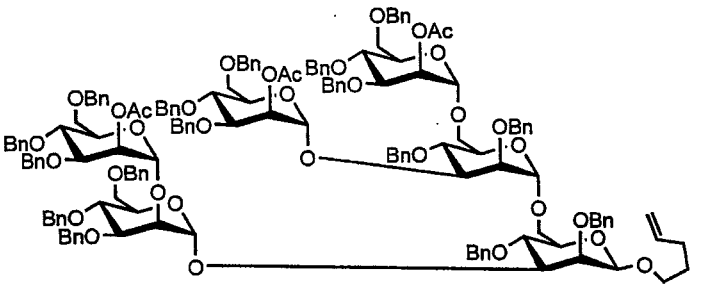
OBn
OAc
BnO
O

2-6

7
6
5
4
3
2
1
0
ppm
1.95
74.20
0.92
3.22
2.00
3.01
2.06
6.50
1.10
1.10
1.72
6.83
2.05
1.01
3.23
25
2.23

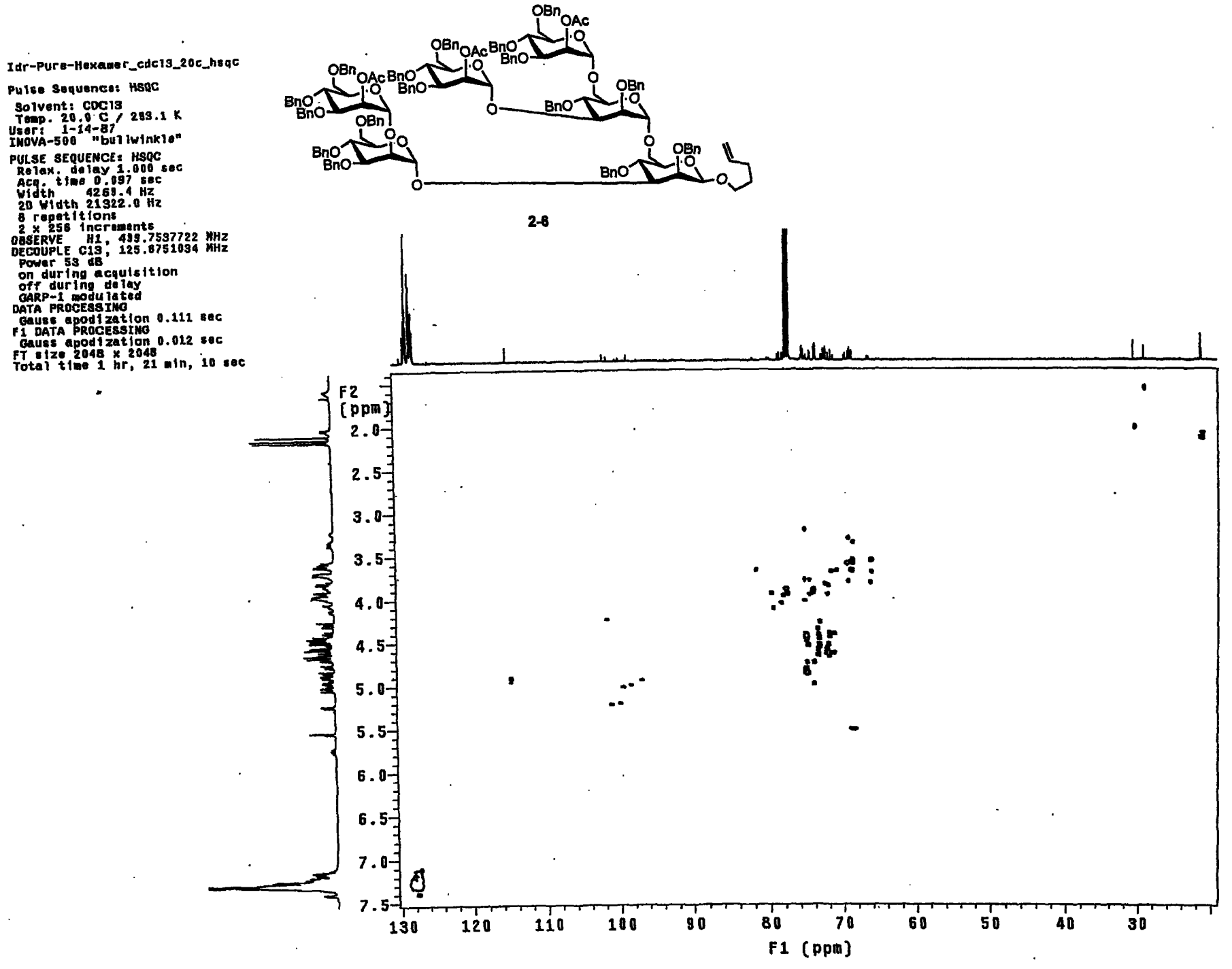
Idr-Pure-Hexamer_cdcl3_20c_hsqc
Pulse Sequence: HSQC
Solvent: CDCl3
Temp. 20.0 C / 293.1 K
User: 1-14-87
INOVA-500 "bullwinkle"
PULSE SEQUENCE: HSQC
Relax. delay 1.000 sec
Acq. time 0.097 sec
Width 4269.4 Hz
2D Width 21322.0 Hz
8 repetitions
2 x 256 increments
OBSERVE H1, 499.7537722 MHz
DECOUPLE C13, 125.6751034 MHz
Power 53 dB
on during acquisition
off during delay
GARP-1 modulated
DATA PROCESSING
Gauss apodization 0.111 sec
F1 DATA PROCESSING
Gauss apodization 0.012 sec
FT size 2048 x 2048
Total time 1 hr, 21 min, 10 sec
2-6
F2 (ppm)
F1 (ppm)

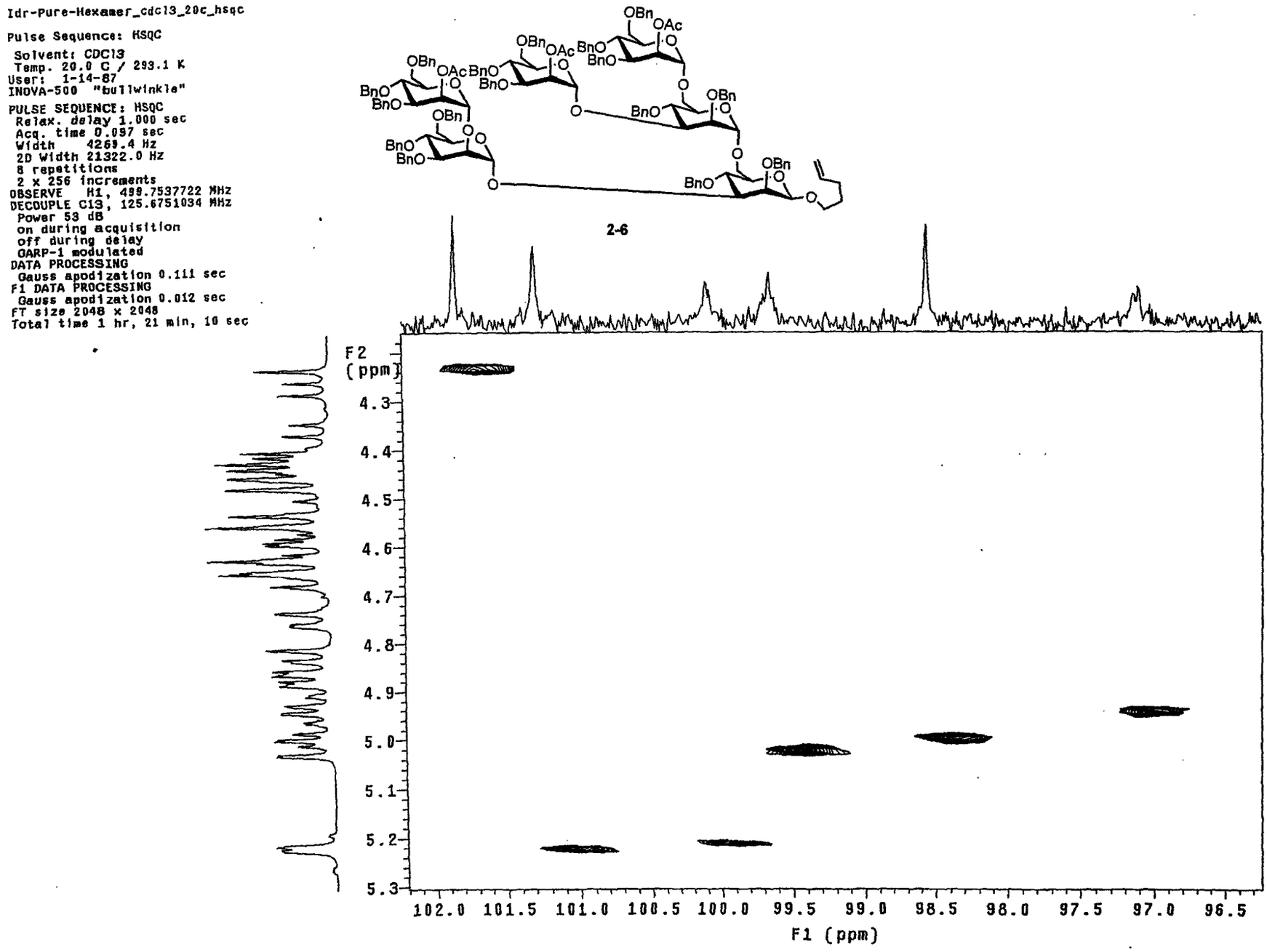
Idr-Pure-Hexamer_cdcl3_20c_hsqc
Pulse Sequence: HSQC
Solvent: CDCl3
Temp. 20.0 C / 293.1 K
User: 1-14-87
INOVA-500 "bullwinkle"
PULSE SEQUENCE: HSQC
Relax. delay 1.000 sec
Acq. time 0.097 sec
Width 4269.4 Hz
2D Width 21322.0 Hz
8 repetitions
2 x 256 increments
OBSERVE H1, 499.7537722 MHz
DECOUPLE C13, 125.6751034 MHz
Power 53 dB
on during acquisition
off during delay
GARP-1 modulated
DATA PROCESSING
Gauss apodization 0.111 sec
F1 DATA PROCESSING
Gauss apodization 0.012 sec
FT size 2048 x 2048
Total time 1 hr, 21 min, 10 sec
2-6
F2 (ppm)
4.3
4.4
4.5
4.6
4.7
4.8
4.9
5.0
5.1
5.2
5.3
102.0
101.5
101.0
100.5
100.0
99.5
99.0
98.5
98.0
97.5
97.0
96.5
F1 (ppm)

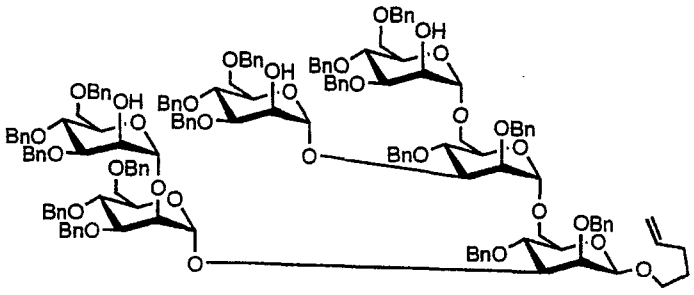

2-18

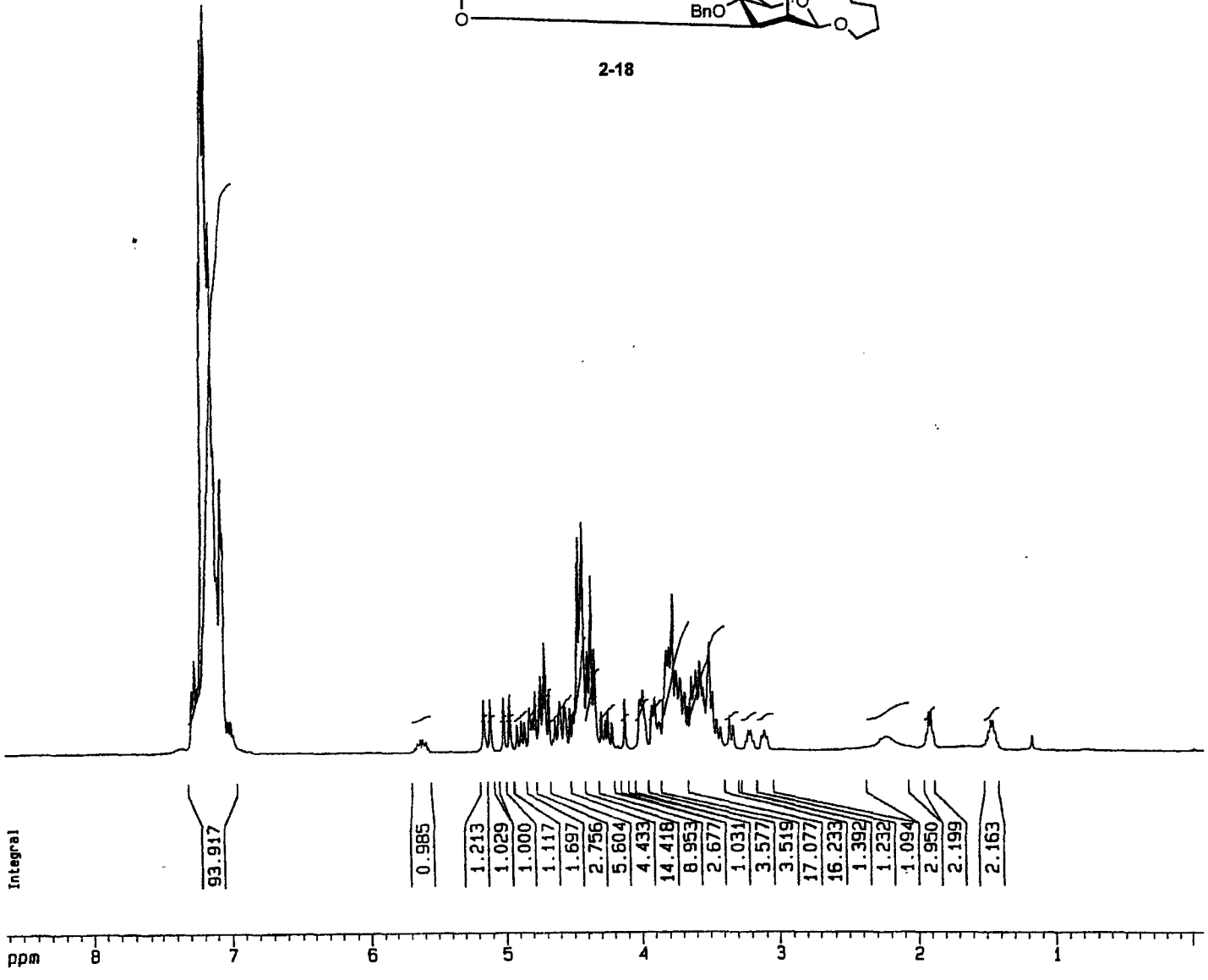


```
Current Data Parameters
NAME        OMA-II-55.2nd
EXPNO                  10
PROCNO                  1

F2 - Acquisition Parameters
Date_            20010106
Time                16.27
INSTRUM             spect
PROBHD     5mm BBO BB-1
PULPROG             zg30
TD                 65536
SOLVENT            CDCl3
NS                   128
DS                     0
SWH           8278.146 Hz
FIDRES        0.126314 Hz
AQ            3.9584243 sec
RG                 101.6
DW                60.400 usec
DE                 6.00 usec
TE                300.0 K
D1           2.00000000 sec

========== CHANNEL f1 ========
NUC1                   1H
P1                 7.90 usec
PL1                0.00 dB
SFO1         400.1324710 MHz

F2 - Processing parameters
SI                 32768
SF           400.1300450 MHz
WDW                   EM
SSB                    0
LB                 0.30 Hz
GB                     0
PC                 1.00

1D NMR plot parameters
CX                20.00 cm
F1P                8.623 ppm
F1              3450.18 Hz
F2P               -0.074 ppm
F2                -29.45 Hz
PPMCM          0.43481 ppm/cm
HZCM          173.98135 Hz/cm
```

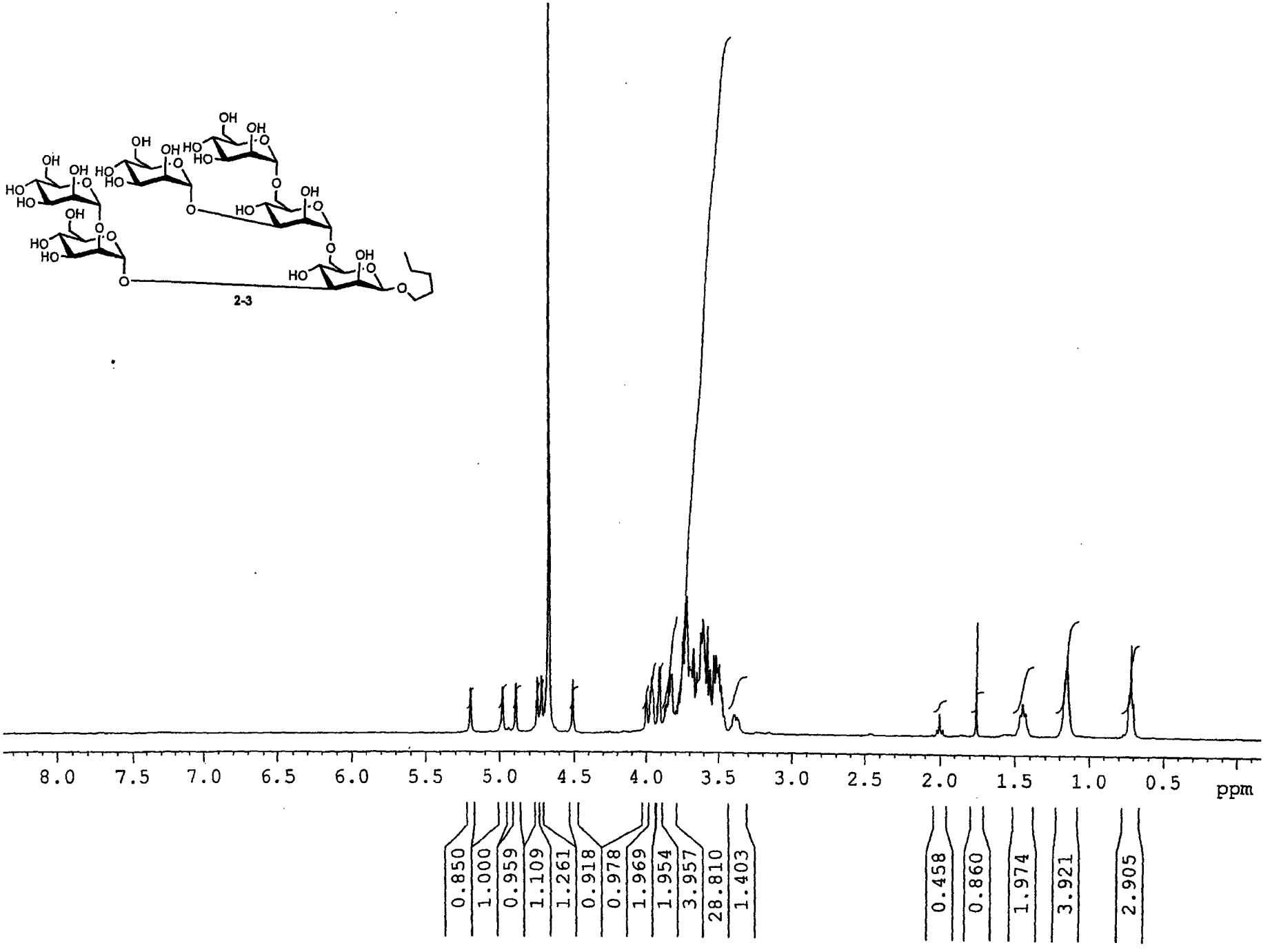
2-3
8.0
7.5
7.0
6.5
6.0
5.5
5.0
4.5
4.0
3.5
3.0
2.5
2.0
1.5
1.0
0.5
ppm
0.850
1.000
0.959
1.109
1.261
0.918
0.978
1.969
1.954
3.957
28.810
1.403
0.458
0.860
1.974
3.921
2.905

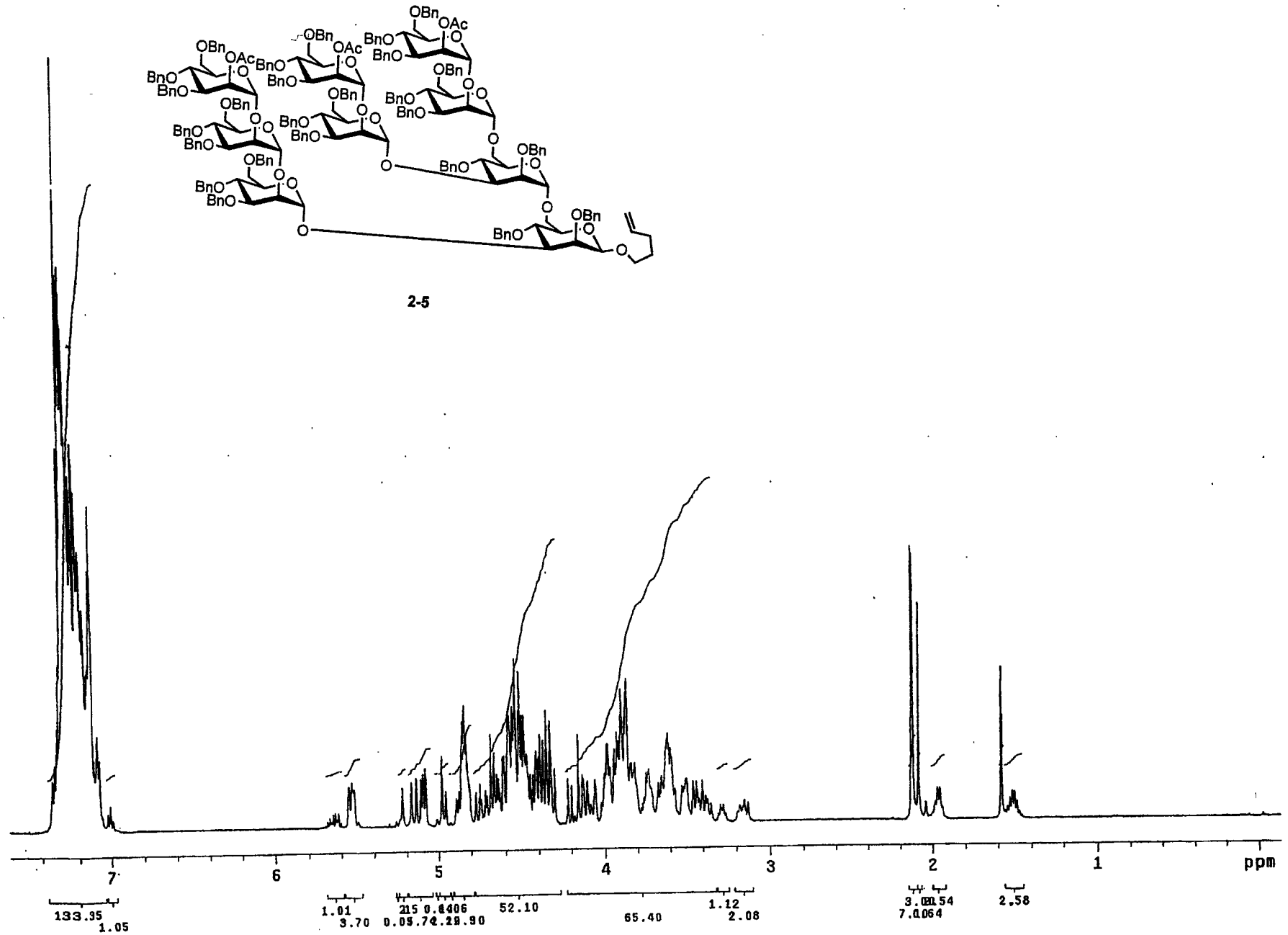
OBn
OAc
BnO
2-5
7
6
5
4
3
2
1
ppm
133.35
1.05
1.01
3.70
52.10
65.40
1.12
2.08
2.58

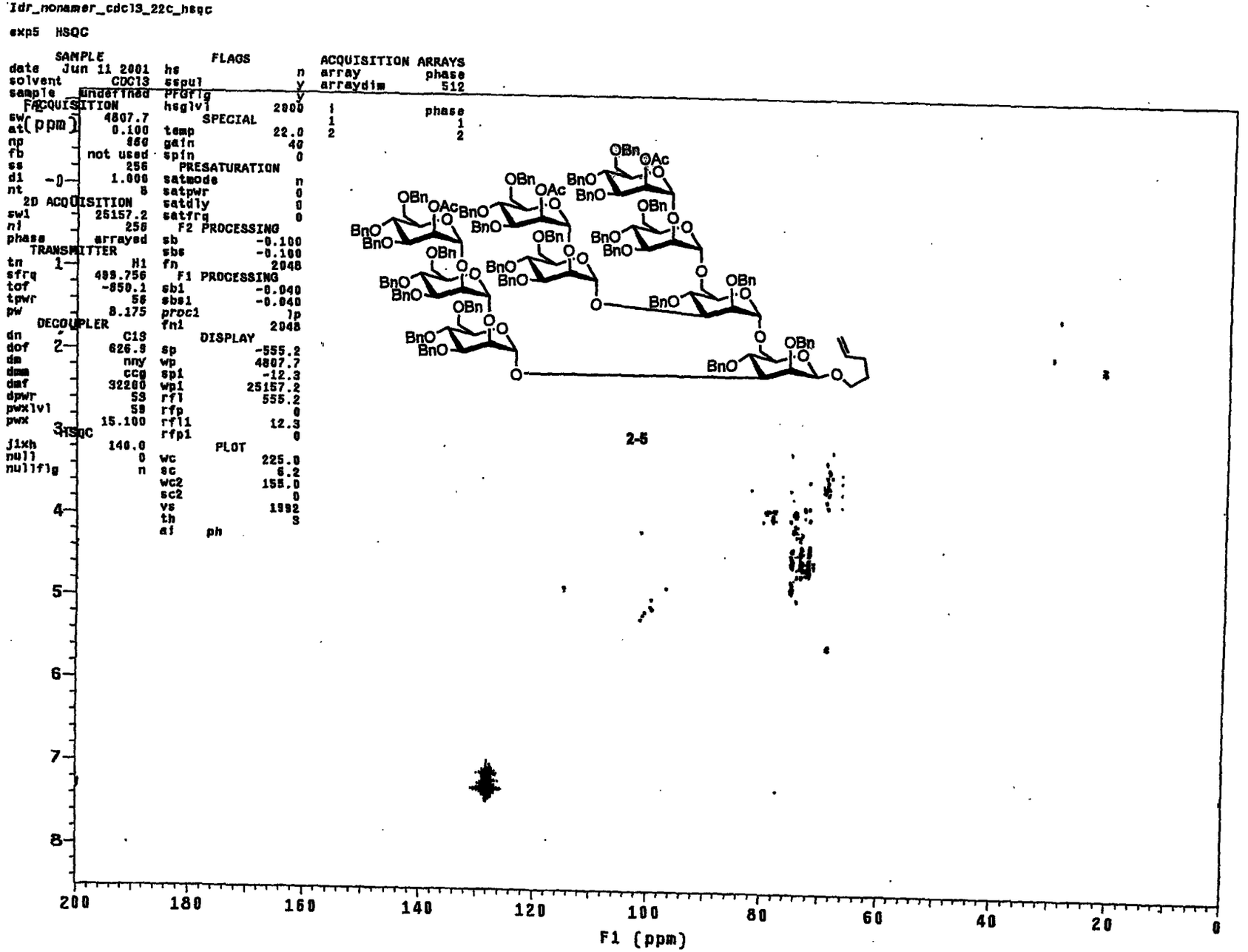
Idr_nonamer_cdcl3_22c_hsqc
exp5 HSQC
SAMPLE
date Jun 11 2001
solvent CDCl3
sample undefined
ACQUISITION
sw 4807.7
at(ppm) 0.100
np 860
fb not used
ss 256
d1 1.000
nt 8
2D ACQUISITION
swi 25157.2
ni 256
phase arrayed
TRANSMITTER
tn H1
sfrq 499.756
tof -850.1
tpwr 56
pw 8.175
DECOUPLER
dn C13
dof 626.9
dm nny
dmm ccg
dmf 32280
dpwr 53
pwxlvl 58
pwx 15.100
HSQC
jixh 140.0
null 0
nullflg n
FLAGS
hs n
sspul y
PFGflg y
hsglvl 2000
SPECIAL
temp 22.0
gain 40
spin 0
PRESATURATION
satmode n
satpwr 0
satdly 0
satfrq 0
F2 PROCESSING
sb -0.100
sbs -0.100
fn 2048
F1 PROCESSING
sb1 -0.040
sbs1 -0.040
proc1 lp
fn1 2048
DISPLAY
sp -555.2
wp 4807.7
sp1 -12.3
wp1 25157.2
rf1 555.2
rfp 0
rf11 12.3
rfp1 0
PLOT
wc 225.0
sc 6.2
wc2 155.0
sc2 0
vs 1992
th 3
ai ph
ACQUISITION ARRAYS
array phase
arraydim 512
i phase
1 1
2 2
2-5
200
180
160
140
120
100
80
60
40
20
0
F1 (ppm)

```
Idr_nonamer_cdcl3_22c_hsqc

Pulse Sequence: HSQC

Solvent: CDCl3
 Temp. 22.0 C / 295.1 K
File name: Idr_nonamer_cdcl3_22c_hsqc
INOVA-500  "zippy"

PULSE SEQUENCE: HSQC
 Relax. delay 1.000 sec
 Acq. time 0.100 sec
 Width     4807.7 Hz
 2D Width 25157.2 Hz
 8 repetitions
 2 x 256 increments
OBSERVE    H1, 499.7537722 MHz
DECOUPLE C13, 125.8757229 MHz
 Power 53 dB
 on during acquisition
 off during delay
 GARP-1 modulated
DATA PROCESSING
 Sq. sine bell 0.100 sec
  Shifted by -0.100 sec
F1 DATA PROCESSING
 Sq. sine bell 0.020 sec
  Shifted by -0.020 sec
FT size 2048 x 2048
Total time 1 hr, 22 min, 20 sec
```

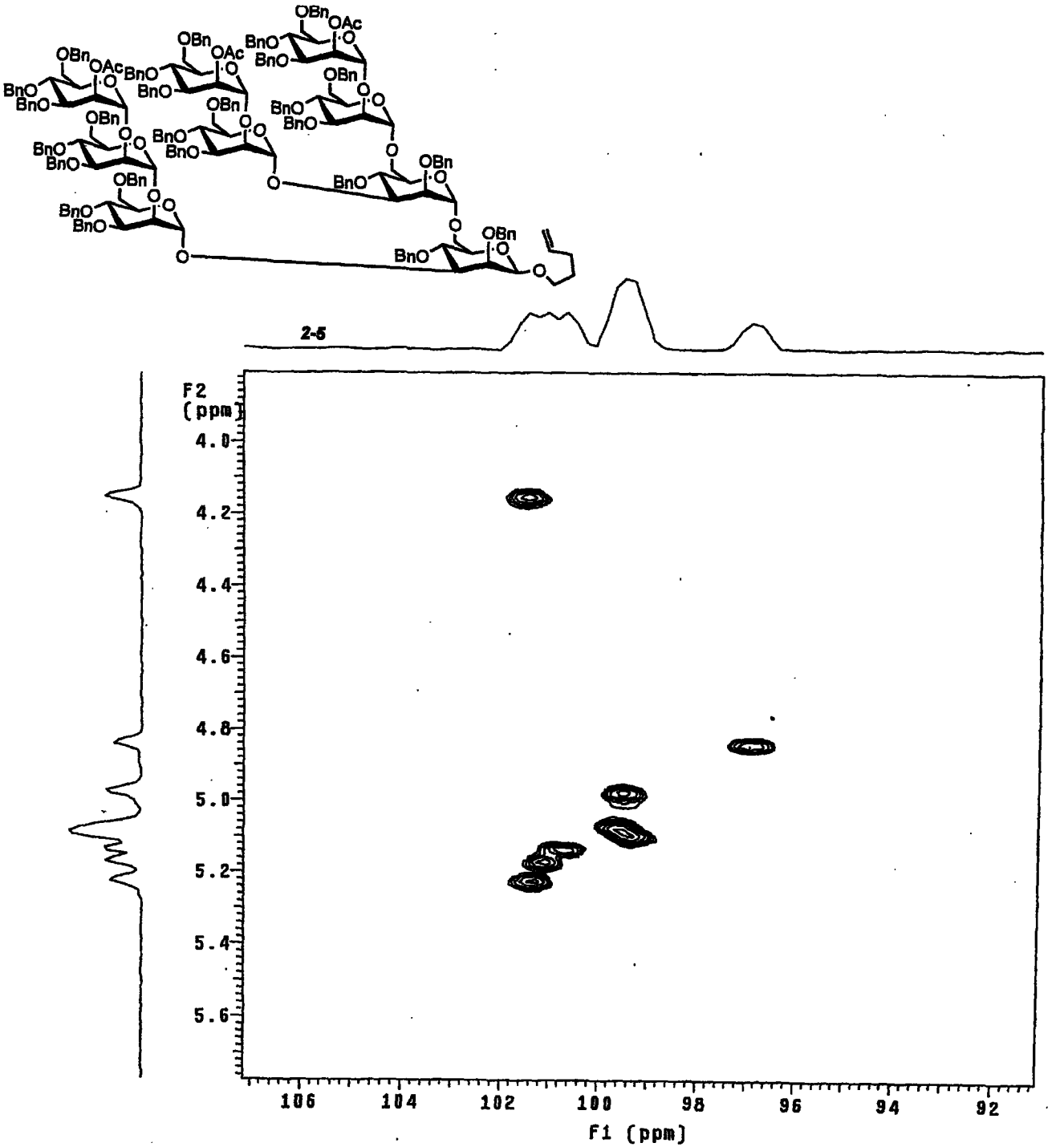

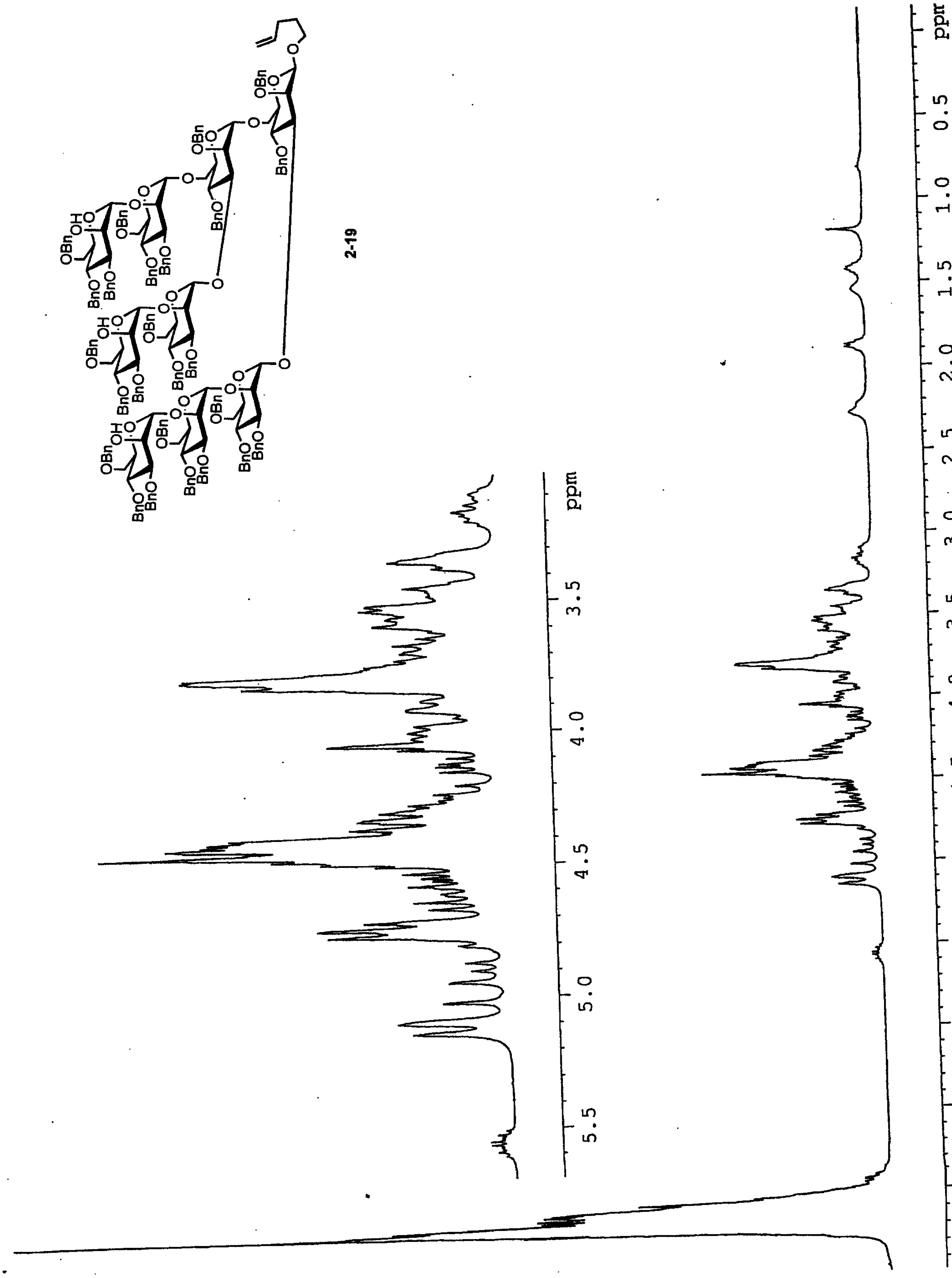
2-19
ppm
0.5
1.0
1.5
2.0
2.5
3.0
3.5
4.0
4.5
5.0
5.5
6.0
6.5
7.0

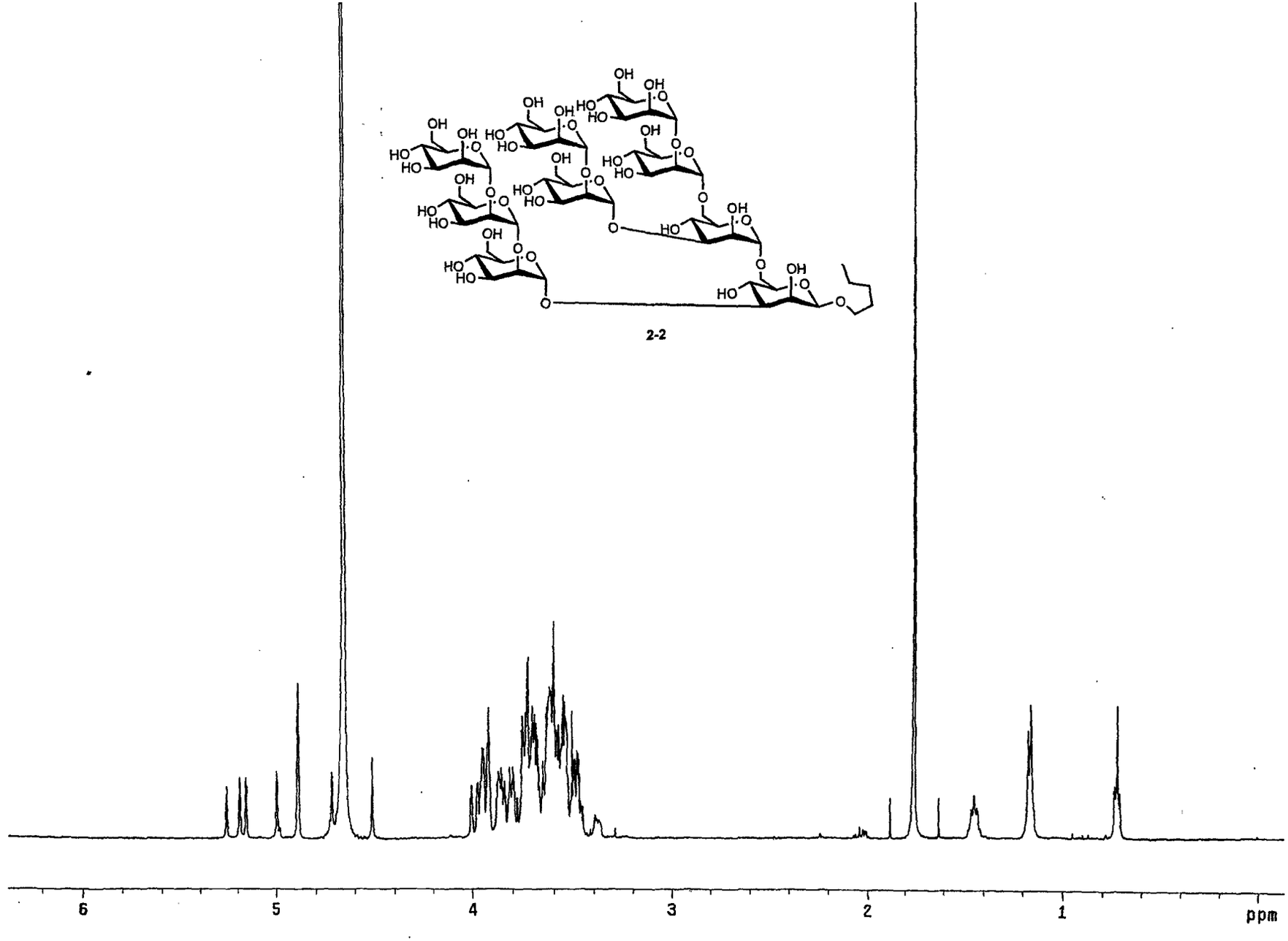
2-2
6
5
4
3
2
1
ppm

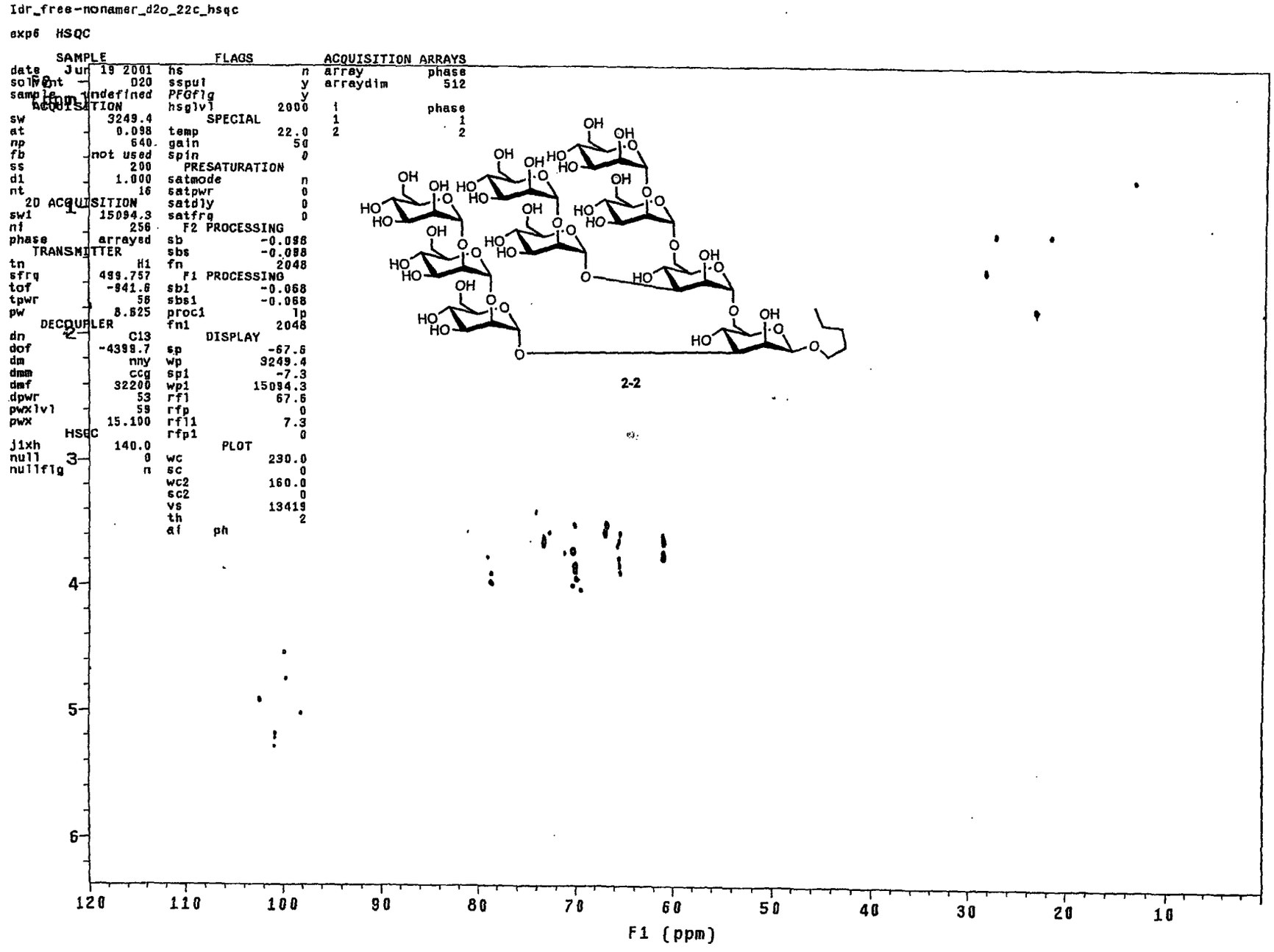
Idr_free-nonamer_d2o_22c_hsqc
exp6 HSQC
SAMPLE
date Jun 19 2001
solvent D2O
sample undefined
ACQUISITION
sw 3249.4
at 0.098
np 640
fb not used
ss 200
d1 1.000
nt 16
2D ACQUISITION
sw1 15094.3
nf 256
phase arrayed
TRANSMITTER
tn H1
sfrq 499.757
tof -941.6
tpwr 56
pw 8.525
DECOUPLER
dn C13
dof -4398.7
dm nny
dmm ccg
dmf 32200
dpwr 53
pwx1v1 59
pwx 15.100
HSQC
j1xh 140.0
null 0
nullflg n
FLAGS
hs n
sspul y
PFGflg y
hsglvl 2000
SPECIAL
temp 22.0
gain 50
spin 0
PRESATURATION
satmode n
satpwr 0
satdly 0
satfrq 0
F2 PROCESSING
sb -0.098
sbs -0.098
fn 2048
F1 PROCESSING
sb1 -0.068
sbs1 -0.068
proc1 lp
fn1 2048
DISPLAY
sp -67.6
wp 3249.4
sp1 -7.3
wp1 15094.3
rf1 67.6
rfp 0
rf11 7.3
rfp1 0
PLOT
wc 230.0
sc 0
wc2 160.0
sc2 0
vs 13419
th 2
ai ph
ACQUISITION ARRAYS
array phase
arraydim 512
i phase
1 1
2 2
2-2
F1 (ppm)

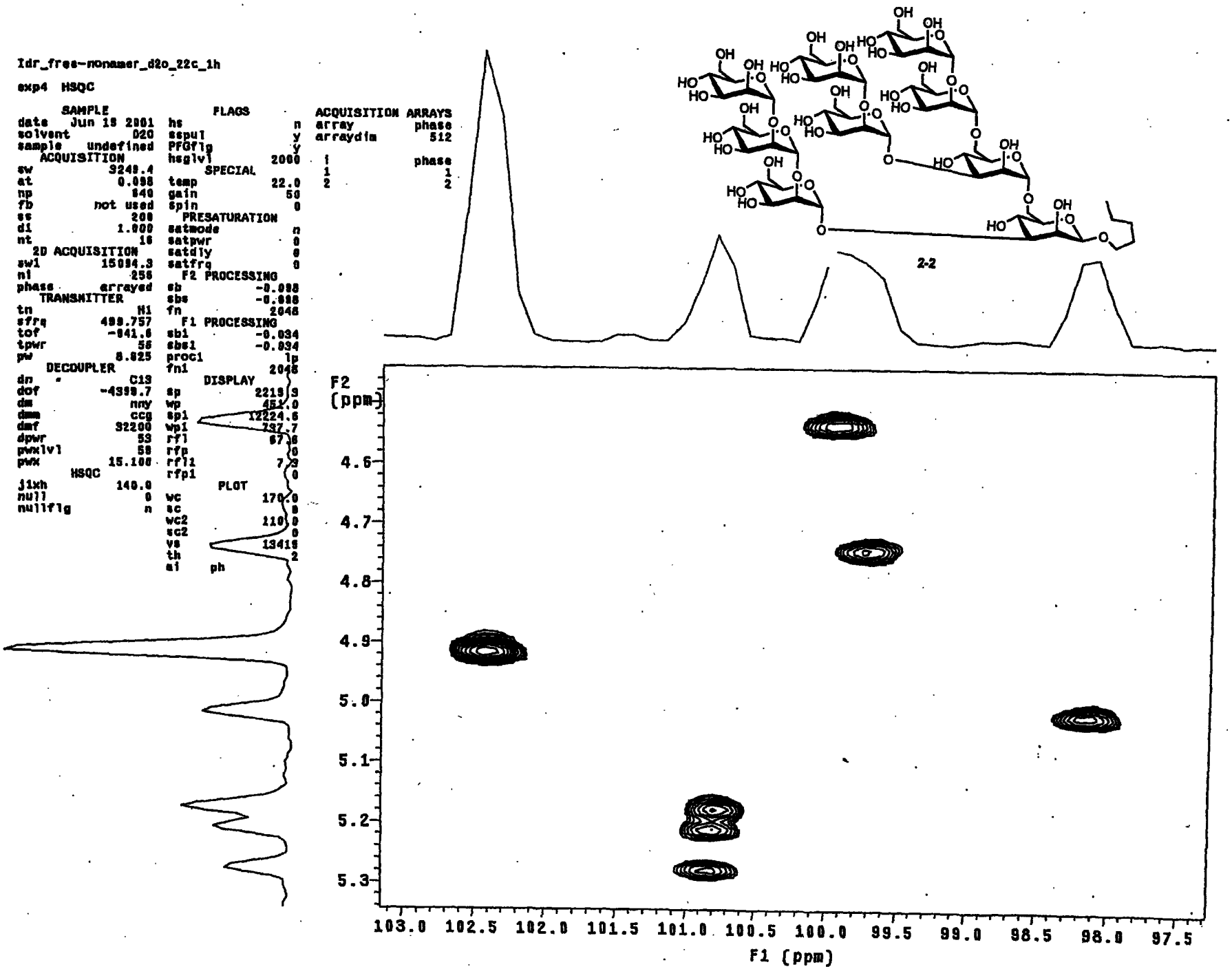
ldr_fres-nonamer_d2o_22c_1h
exp4 HSQC
SAMPLE
date Jun 15 2001
solvent D2O
sample undefined
ACQUISITION
sw 3249.4
at 0.098
np 640
fb not used
ss 208
d1 1.000
nt 16
2D ACQUISITION
sw1 15094.3
ni 256
phase arrayed
TRANSMITTER
tn H1
sfrq 499.757
tof -841.6
tpwr 58
pw 8.825
DECOUPLER
dn C13
dof -4398.7
dm nny
dmm ccg
dmf 32200
dpwr 53
pwxlvl 58
pwx 15.100
HSQC
j1xh 140.0
null 0
nullflg n
FLAGS
hs n
sspul y
PFGflg y
hsglvl 2000
SPECIAL
temp 22.0
gain 50
spin 0
PRESATURATION
satmode n
satpwr 0
satdly 0
satfrq 0
F2 PROCESSING
sb -0.098
sbs -0.098
fn 2048
F1 PROCESSING
sb1 -0.034
sbs1 -0.034
proc1 lp
fn1 2048
DISPLAY
sp 2219.9
wp 4514.0
sp1 12224.6
wp1 7377.7
rf1 67.6
rfp 0
rf1 7.3
rfp1 0
PLOT
wc 170.0
sc 0
wc2 110.0
sc2 0
vs 13415
th 2
ai ph
ACQUISITION ARRAYS
array phase
arraydim 512
i phase
1 1
2 2
2-2
F2 (ppm)
4.6
4.7
4.8
4.9
5.0
5.1
5.2
5.3
103.0 102.5 102.0 101.5 101.0 100.5 100.0 99.5 99.0 98.5 98.0 97.5
F1 (ppm)

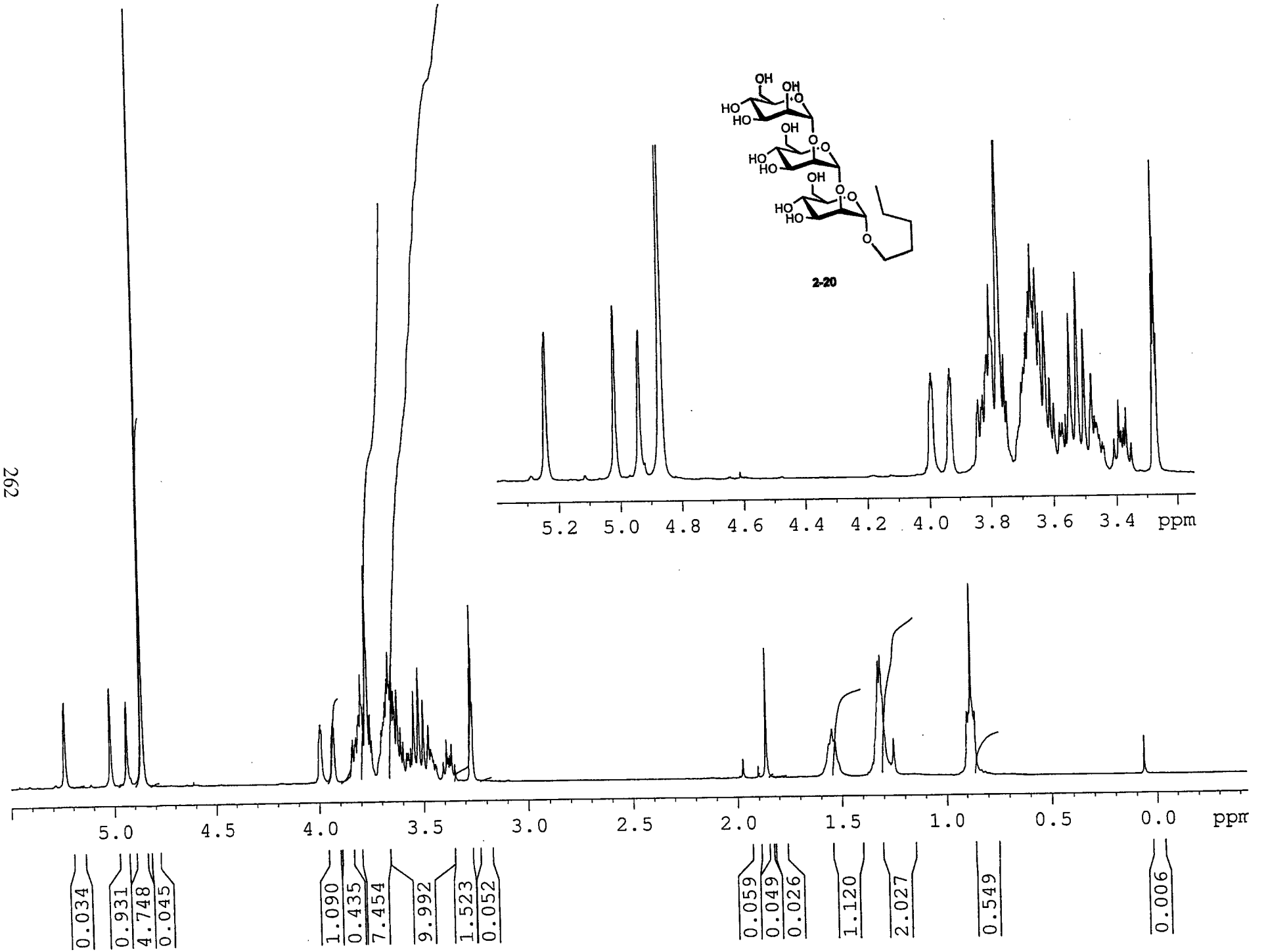
OH
OH
HO
HO
O
OH
HO
HO
O
OH
HO
HO
O
O
2-20
5.2 5.0 4.8 4.6 4.4 4.2 4.0 3.8 3.6 3.4 ppm
5.0 4.5 4.0 3.5 3.0 2.5 2.0 1.5 1.0 0.5 0.0 ppm
0.034
0.931
4.748
0.045
1.090
0.435
7.454
9.992
1.523
0.052
0.059
0.049
0.026
1.120
2.027
0.549
0.006

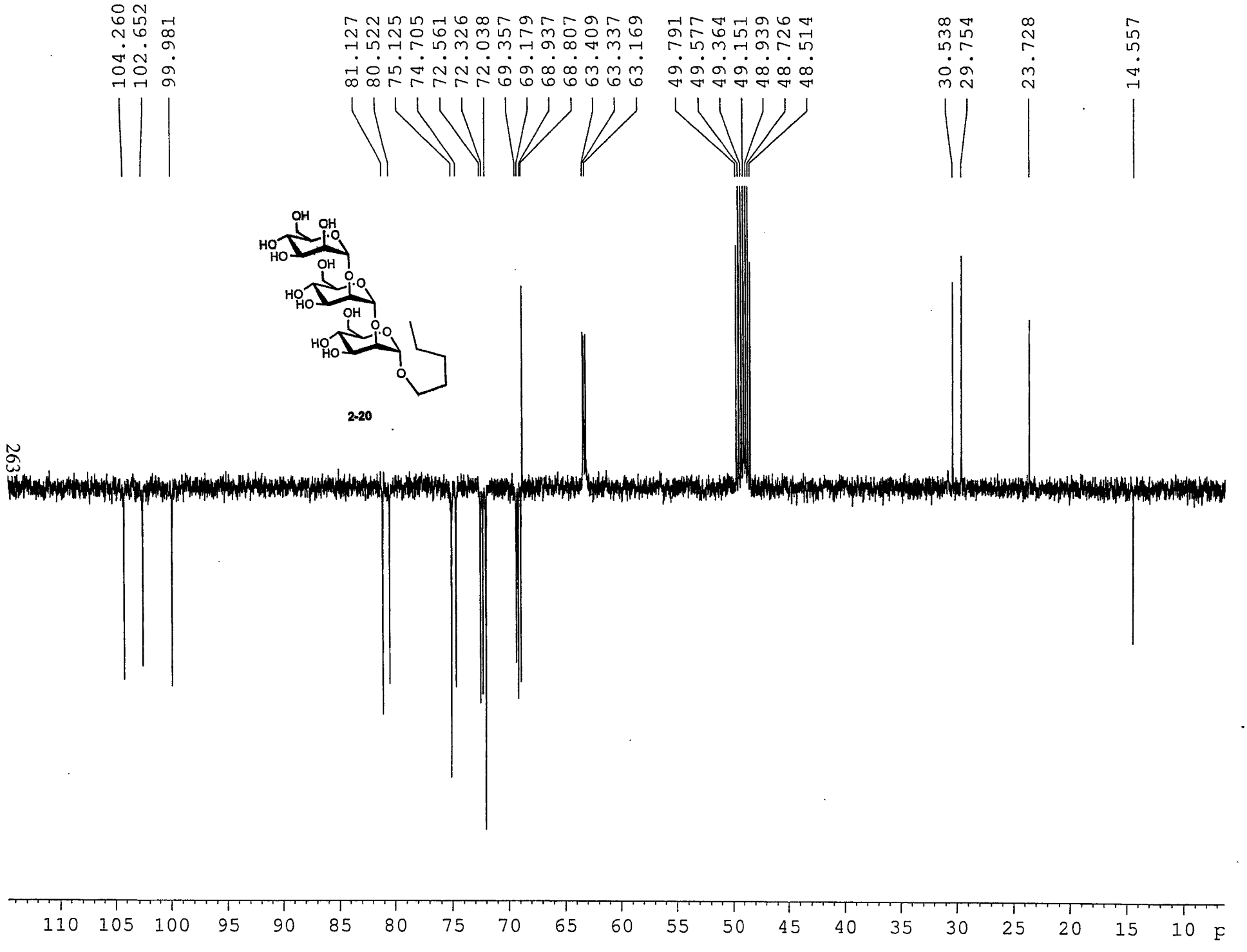
104.260
102.652
99.981
81.127
80.522
75.125
74.705
72.561
72.326
72.038
69.357
69.179
68.937
68.807
63.409
63.337
63.169
49.791
49.577
49.364
49.151
48.939
48.726
48.514
30.538
29.754
23.728
14.557
OH
HO
O
2-20
263
110 105 100 95 90 85 80 75 70 65 60 55 50 45 40 35 30 25 20 15 10 p

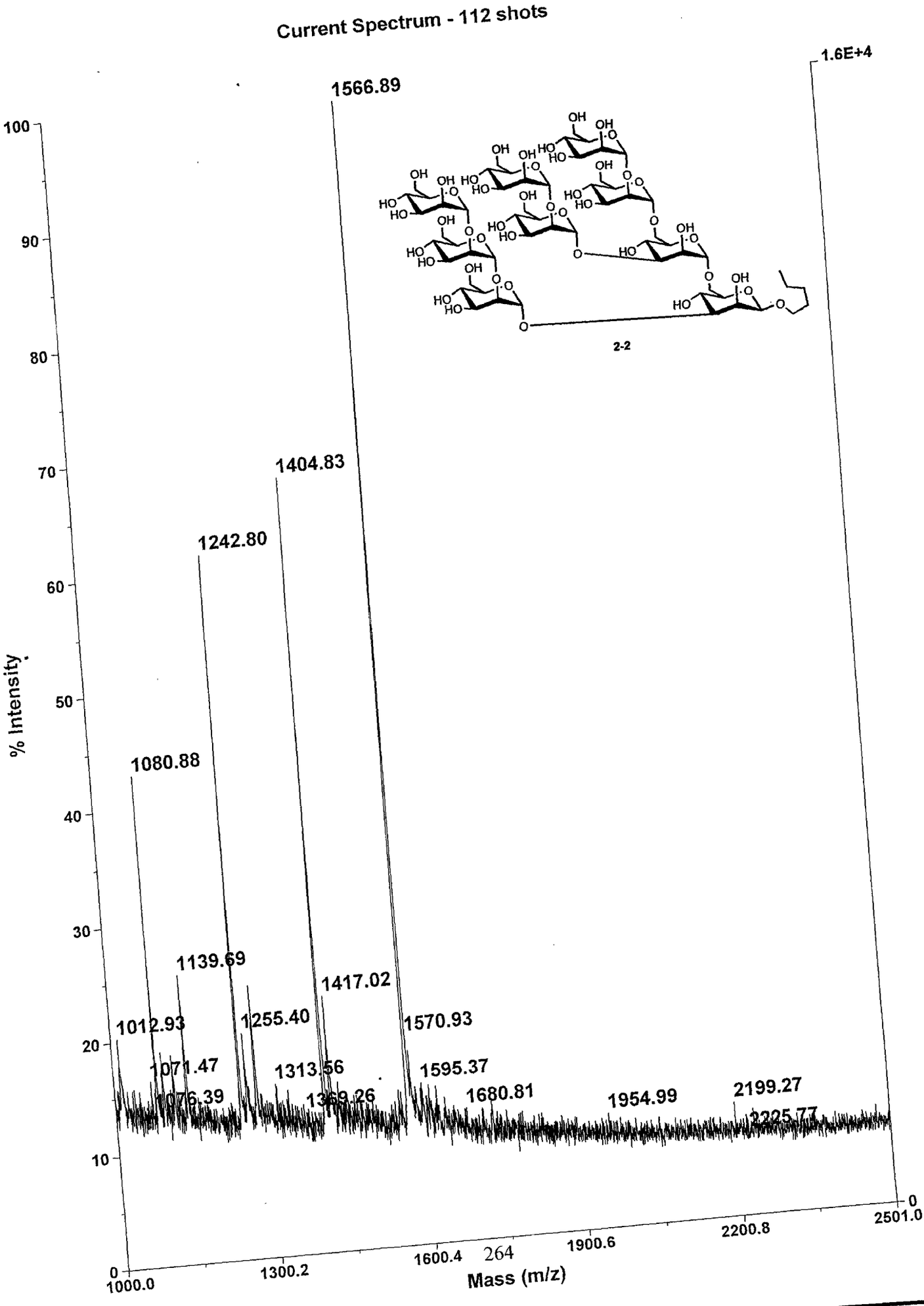
Current Spectrum - 112 shots
1.6E+4
1566.89
100
90
80
70
60
50
40
30
20
10
0
% Intensity
1404.83
1242.80
1080.88
1139.69
1417.02
1012.93
1255.40
1570.93
1071.47
1313.56
1595.37
1076.39
1369.26
1680.81
1954.99
2199.27
2225.77
1000.0
1300.2
1600.4
1900.6
2200.8
2501.0
Mass (m/z)
2-2

Appendix C.3

Selected Spectra – Chapter 3

3-7

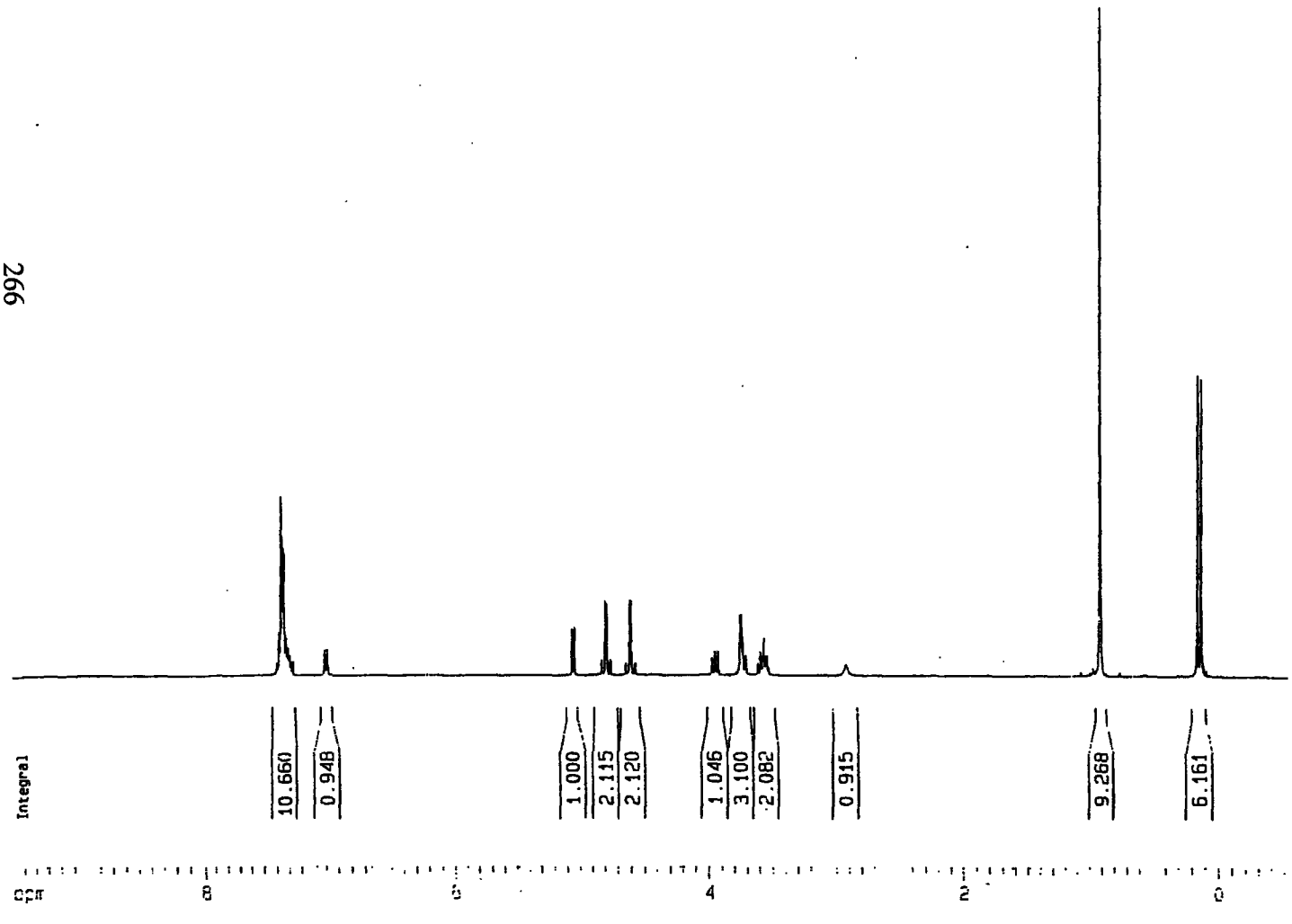


```
Current Data Parameters
NAME        ERS-III-238z
EXPNO                  1
PROCNO                 1

F2 - Acquisition Parameters
Date_           20030105
Time               20.14
INSTRUM            spect
PROBHD     5mm BBO BB-1
PULPROG            zg30
TD                40062
SOLVENT           CDCl3
NS                   16
DS                    2
SWH           4006.410 Hz
FIDRES        0.100005 Hz
AQ            4.9997878 sec
RG                   32
DW             124.800 usec
DE               6.00 usec
TE              300.0 K
D1           1.00000000 sec

========== CHANNEL f1 ==========
NUC1                 1H
P1                7.90 usec
PL1               0.00 dB
SFO1        400.1318006 MHz

F2 - Processing parameters
SI                32768
SF          400.1300054 MHz
WDW                  EM
SSB                   0
LB                0.30 Hz
GB                    0
PC                1.00

1D NMR plot parameters
CX               20.00 cm
F1P               9.493 ppm
F1              3798.43 Hz
F2P              -0.520 ppm
F2              -207.98 Hz
PPMCM         0.50064 ppm/cm
HZCM        200.32053 Hz/cm
```

3-7

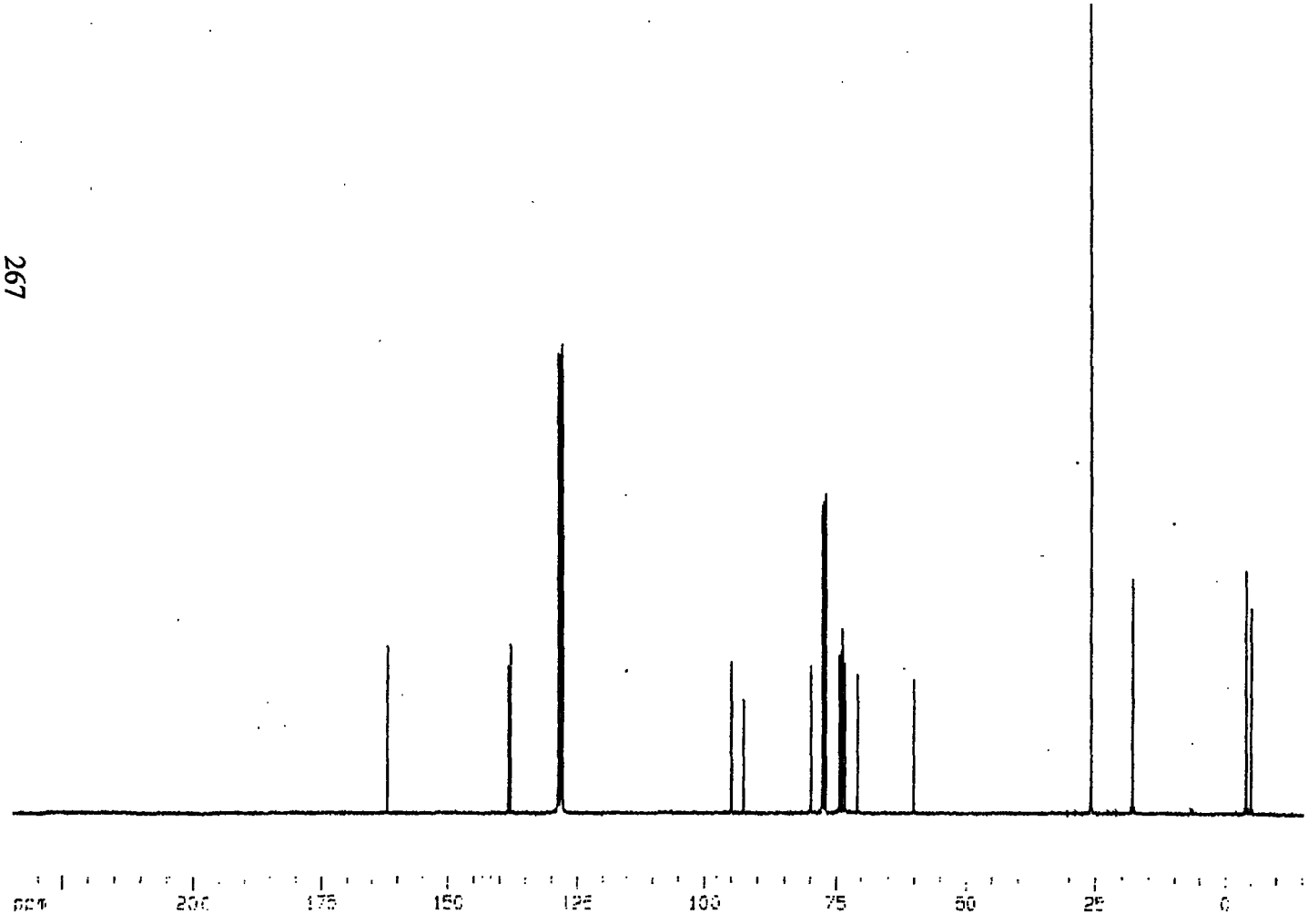


```
Current Data Parameters
NAME      ERS-III-239C13
EXPNO                 1
PROCNO                1

F2 - Acquisition Parameters
Date_          20030105
Time              21.16
INSTRUM           spect
PROBHD     5mm BBO BB-1
PULPROG          zgpg30
TD                65536
SOLVENT           CDCl3
NS                 1024
DS                    4
SWH           25125.629 Hz
FIDRES        0.383387 Hz
AQ            1.3042184 sec
RG               14596.5
DW               19.900 usec
DE                6.00 usec
TE              300.0 K
D1            2.00000000 sec
d11           0.03000000 sec
d12           0.00002000 sec

============ CHANNEL f1 =============
NUC1                13C
P1                15.25 usec
PL1               3.00 dB
SFO1         100.6237959 MHz

============ CHANNEL f2 =============
CPDPRG2          waltz16
NUC2                1H
PCPD2            107.50 usec
PL2               0.00 dB
PL12             24.00 dB
PL13             24.00 dB
SFO2         400.1316005 MHz

F2 - Processing parameters
SI                 32768
SF           100.6127614 MHz
WDW                  EM
SSB                   0
LB                1.00 Hz
GB                    0
PC                1.40

1D NMR plot parameters
CX               20.00 cm
F1P             234.536 ppm
F1             23597.30 Hz
F2P             -15.196 ppm
F2             -1528.33 Hz
PPMCM          12.48630 ppm/cm
HZCM           1256.28137 Hz/cm
```

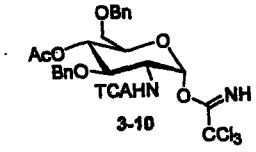

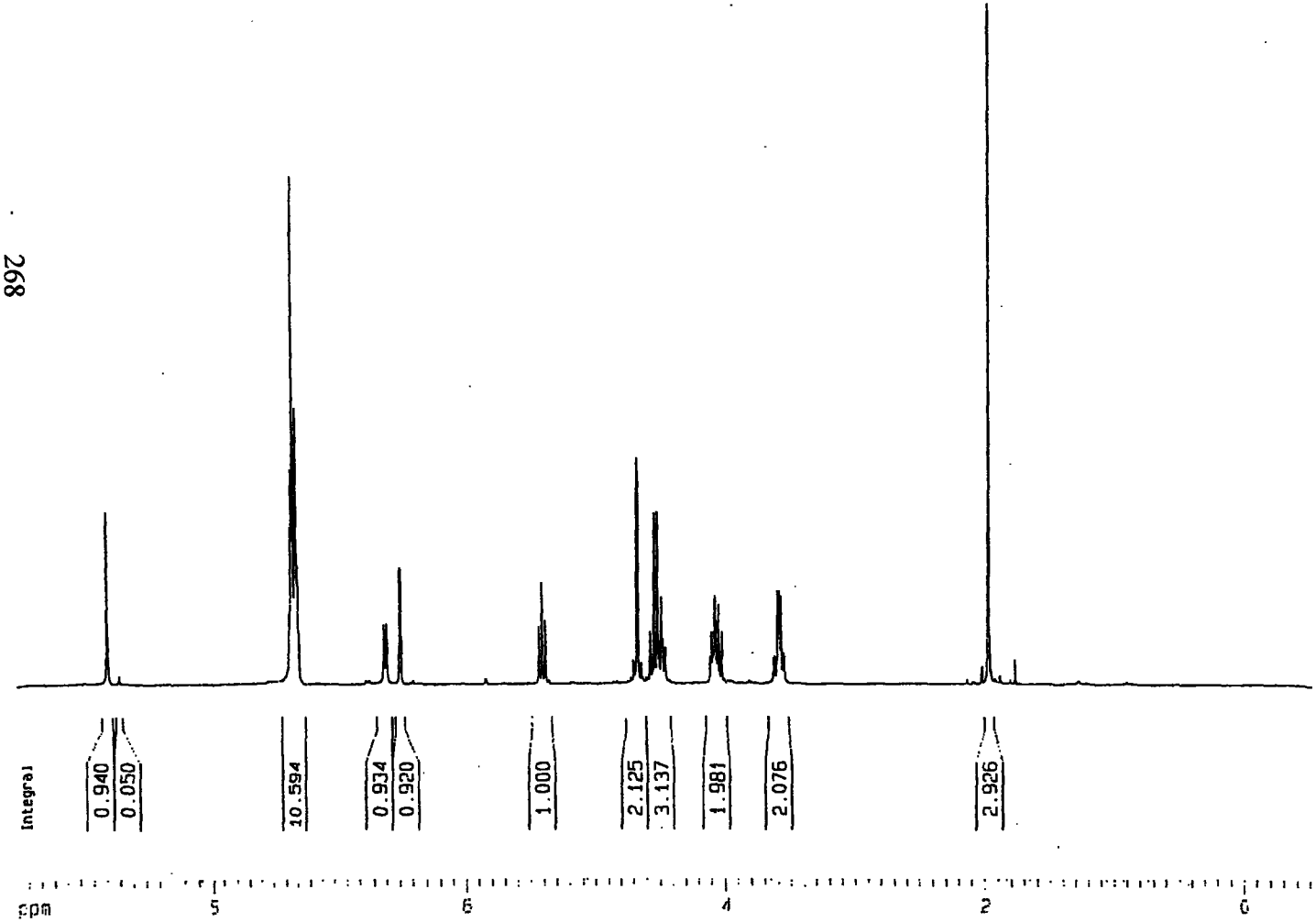


```
Current Data Parameters
NAME        ERS-IV-027z3
EXPNO                 1
PROCNO                1

F2 - Acquisition Parameters
Date_          20030120
Time              20.56
INSTRUM           spect
PROBHD     5mm BBO BB-1
PULPROG           zg30
TD               40062
SOLVENT          CDCl3
NS                  16
DS                   2
SWH           4006.410 Hz
FIDRES        0.100005 Hz
AQ            4.9997878 sec
RG                50.8
DW               124.800 usec
DE                6.00 usec
TE               300.0 K
D1            1.00000000 sec

========== CHANNEL f1 ==========
NUC1                 1H
P1                7.90 usec
PL1               0.00 dB
SFO1        400.1318006 MHz

F2 - Processing parameters
SI                32768
SF          400.1300056 MHz
WDW                  EM
SSB                   0
LB                0.30 Hz
GB                    0
PC                 1.00

1D NMR plot parameters
CX               20.00 cm
F1P               9.492 ppm
F1               3798.19 Hz
F2P              -0.520 ppm
F2               -206.23 Hz
PPMCM            0.50064 ppm/cm
HZCM          200.32053 Hz/cm
```

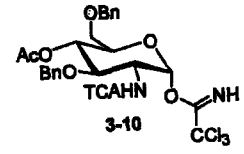

3-10

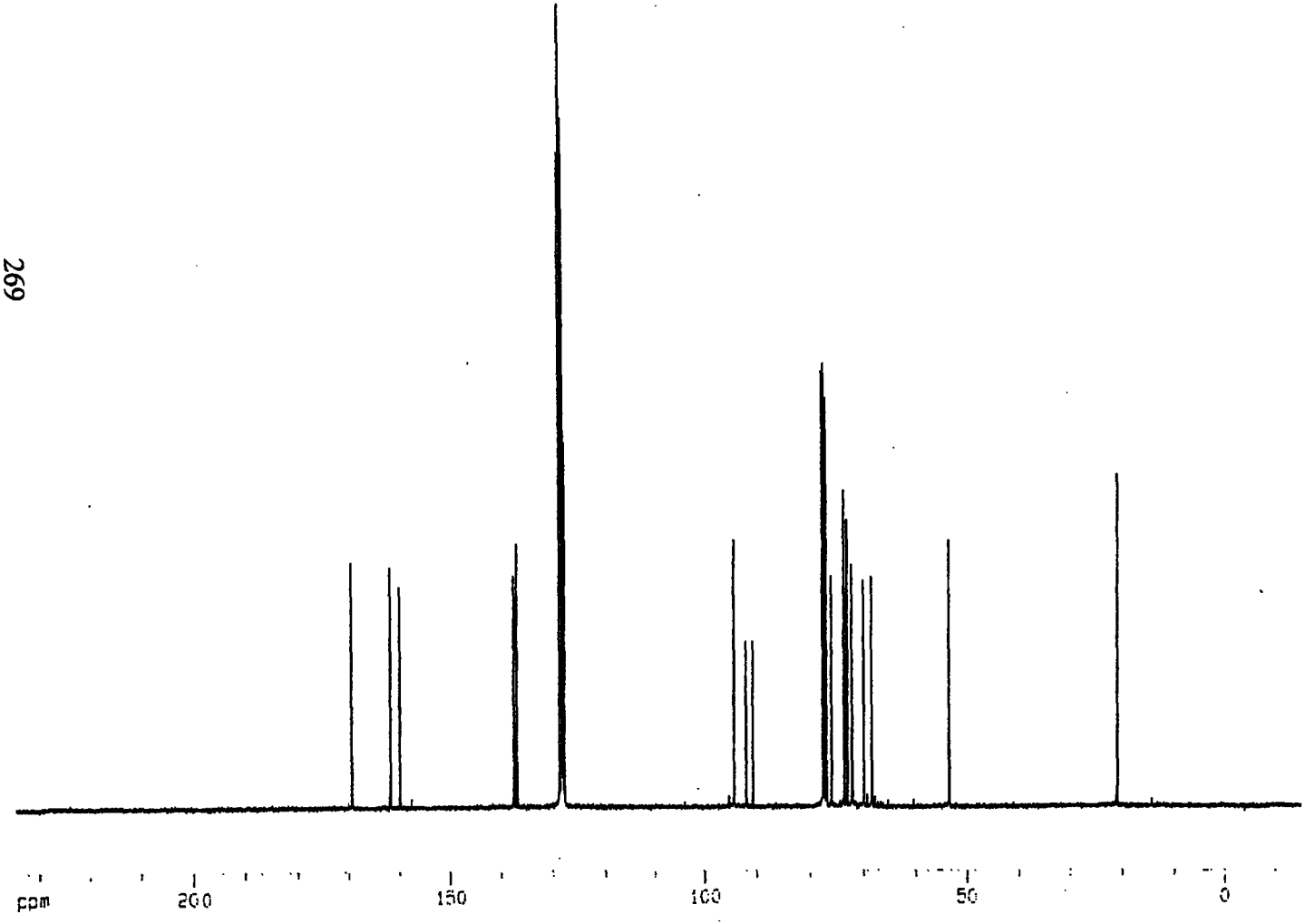


```
Current Data Parameters
NAME        ERS-IV-027C13
EXPNO                  1
PROCNO                 1

F2 - Acquisition Parameters
Date_           20030119
Time              18.24
INSTRUM           spect
PROBHD     5mm BBO BB-1
PULPROG         zgpg30
TD                65536
SOLVENT           CDCl3
NS                 1024
DS                    4
SWH           25125.629 Hz
FIDRES         0.383387 Hz
AQ             1.3042164 sec
RG                 2048
DW               19.900 usec
DE                6.00 usec
TE               300.0 K
D1             2.00000000 sec
D11            0.03000000 sec
D12            0.00002000 sec

============ CHANNEL f1 =============
NUC1               13C
P1               15.25 usec
PL1               3.00 dB
SFO1         100.6237959 MHz

============ CHANNEL f2 =============
CPDPRG2         waltz16
NUC2               1H
PCPD2           107.50 usec
PL2               0.00 dB
PL12             24.00 dB
PL13             24.00 dB
SFO2         400.1316005 MHz

F2 - Processing parameters
SI                32768
SF           100.6127691 MHz
WDW                EM
SSB                0
LB              1.00 Hz
GB                 0
PC              1.40

1D NMR plot parameters
CX              20.00 cm
F1P           234.459 ppm
F1           23589.62 Hz
F2P           -15.267 ppm
F2           -1536.01 Hz
PPMCM         12.48630 ppm/cm
HZCM        1256.28137 Hz/cm
```

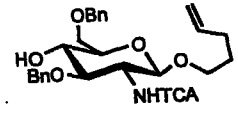

3-3

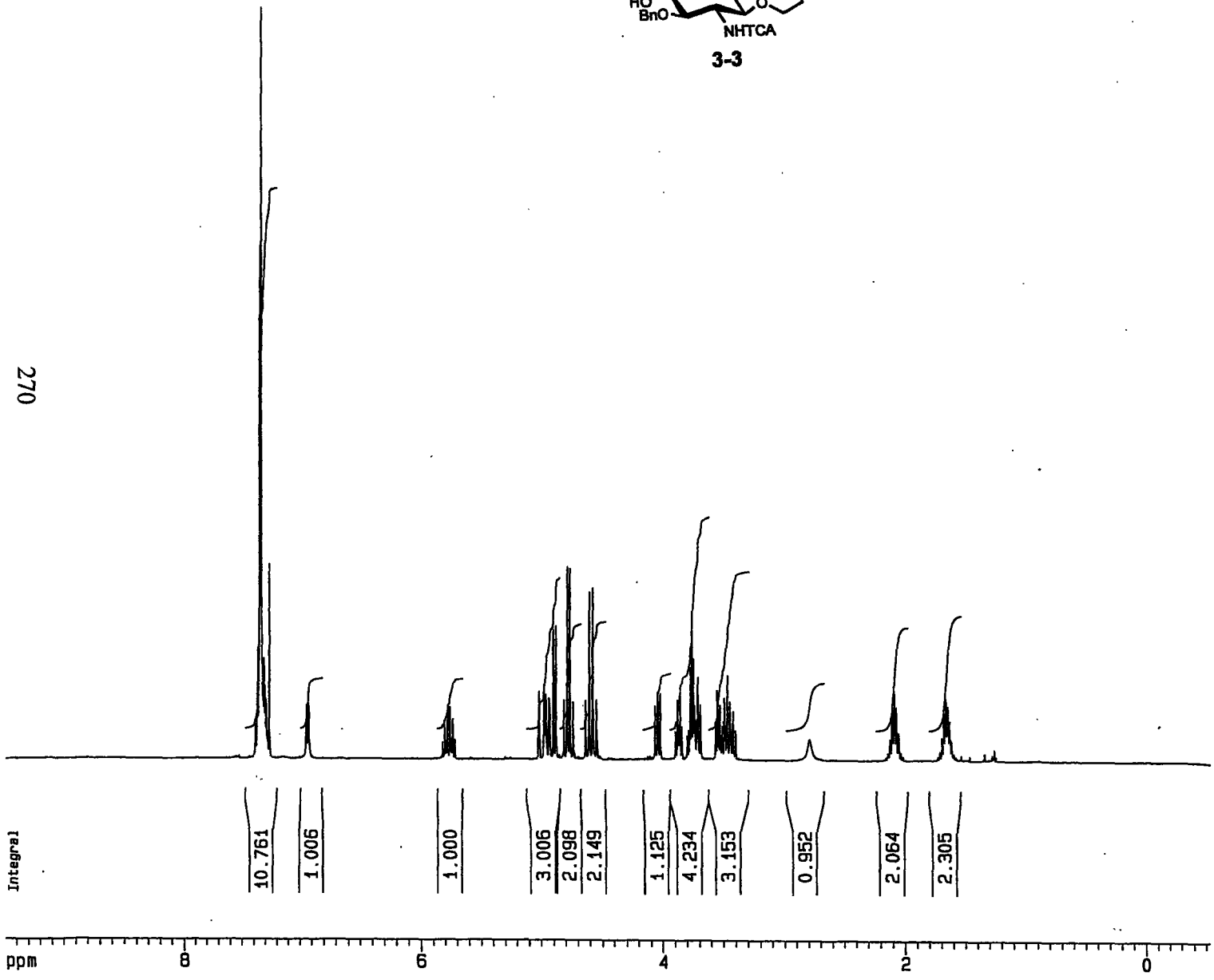


```
Current Data Parameters
NAME          ERS-III-234
EXPNO                   1
PROCNO                  1

F2 - Acquisition Parameters
Date_           20021021
Time               12.17
INSTRUM            spect
PROBHD     5mm BBO BB-1
PULPROG            zg30
TD                40062
SOLVENT           CDCl3
NS                   16
DS                    2
SWH          4006.410 Hz
FIDRES       0.100005 Hz
AQ           4.9997878 sec
RG                  128
DW            124.800 usec
DE              6.00 usec
TE             300.0 K
D1           1.00000000 sec

========== CHANNEL f1 ========
NUC1                 1H
P1                7.90 usec
PL1               0.00 dB
SFO1        400.1318006 MHz

F2 - Processing parameters
SI                32768
SF          400.1300060 MHz
WDW                  EM
SSB                   0
LB               0.30 Hz
GB                    0
PC                 1.00

1D NMR plot parameters
CX                20.00 cm
F1P               9.491 ppm
F1              3797.82 Hz
F2P              -0.521 ppm
F2              -208.59 Hz
PPMCM          0.50064 ppm/cm
HZCM          200.32051 Hz/cm
```

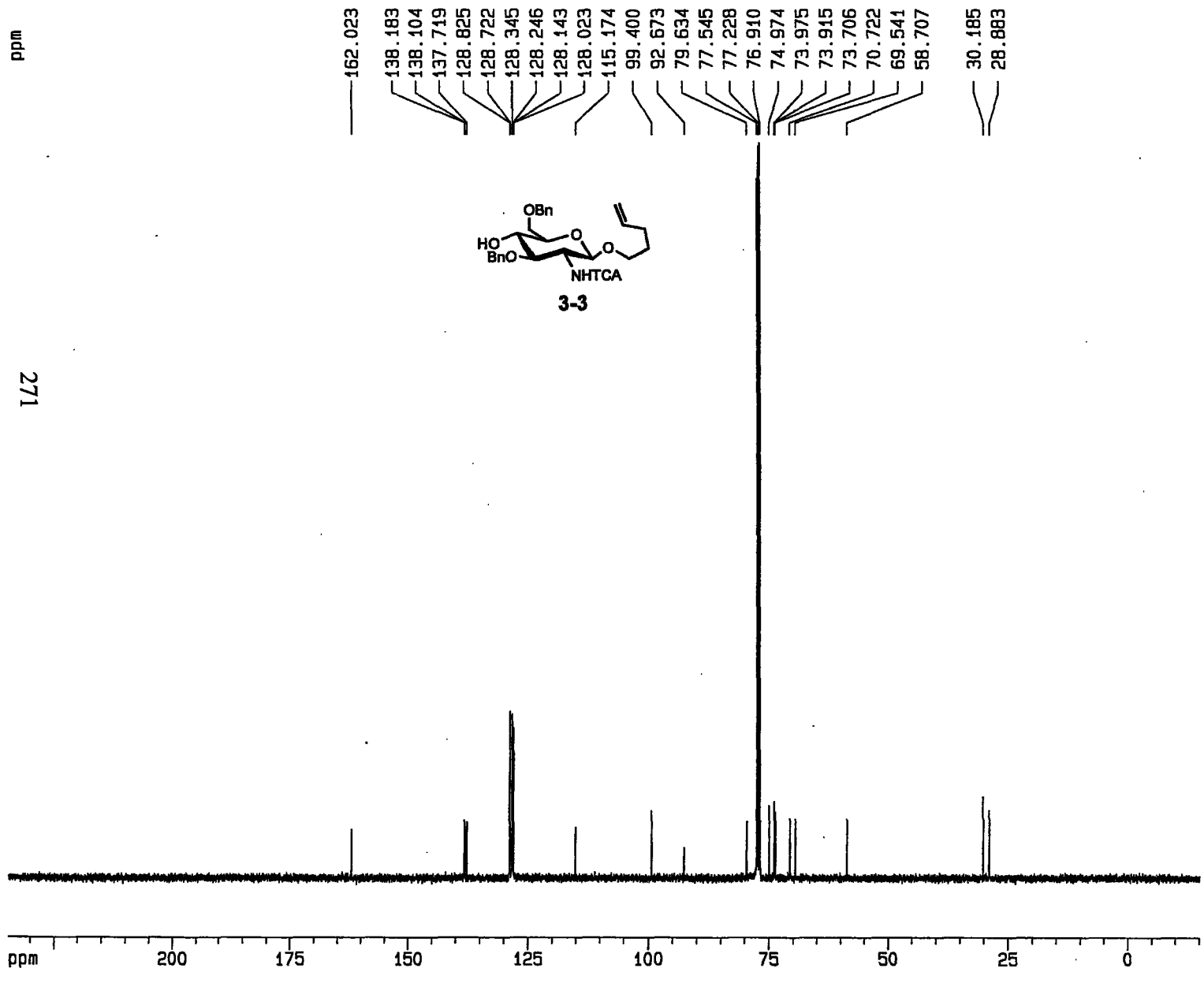

Current Data Parameters

NAME	ERS-III-234c13
EXPNO	1
PROCNO	1

F2 - Acquisition Parameters

Date_	20021021
Time	15.08
INSTRUM	spect
PROBHD	5mm BBO BB-1
PULPROG	zgpg30
TD	65536
SOLVENT	CDCl3
NS	1024
DS	4
SWH	25125.629 Hz
FIDRES	0.383387 Hz
AQ	1.3042164 sec
RG	1024
DW	19.900 usec
DE	6.00 usec
TE	300.0 K
D1	2.00000000 sec
d11	0.03000000 sec
d12	0.00002000 sec

========== CHANNEL f1 ==========

NUC1	13C
P1	15.25 usec
PL1	3.00 dB
SFO1	100.6237959 MHz

========== CHANNEL f2 ==========

CPDPRG2	waltz16
NUC2	1H
PCPD2	107.50 usec
PL2	0.00 dB
PL12	24.00 dB
PL13	24.00 dB
SFO2	400.1316005 MHz

F2 - Processing parameters

SI	32768
SF	100.6127515 MHz
WDW	EM
SSB	0
LB	1.00 Hz
GB	0
PC	1.40

1D NMR plot parameters

CX	20.00 cm
F1P	234.635 ppm
F1	23607.26 Hz
F2P	-15.091 ppm
F2	-1518.37 Hz
PPMCM	12.48630 ppm/cm
HZCM	1256.28137 Hz/cm

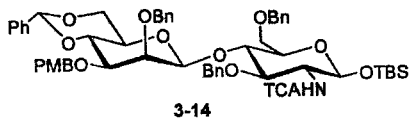

3-14

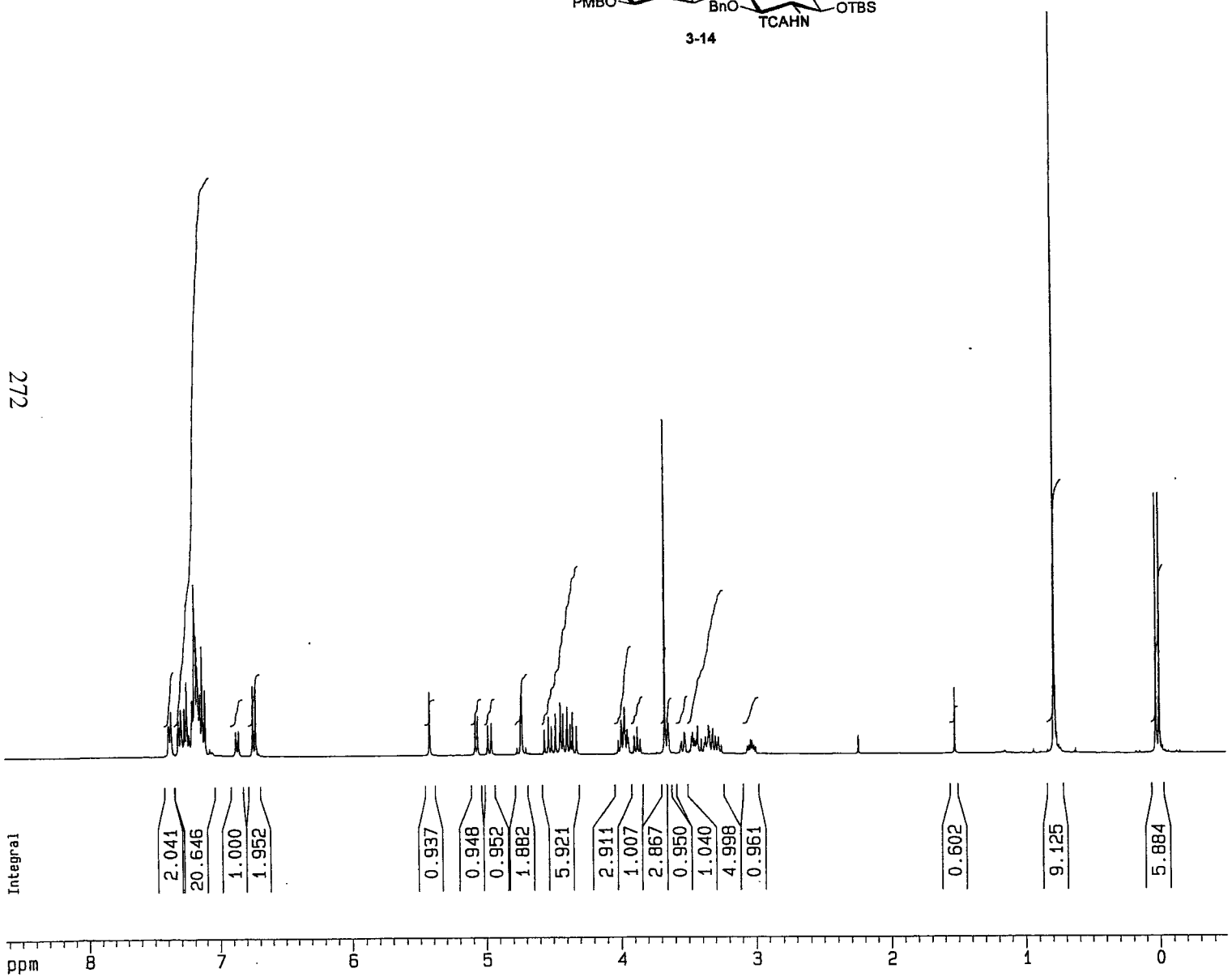

Current Data Parameters

NAME	Beta_dimer
EXPNO	10
PROCNO	1

F2 - Acquisition Parameters

Date_	20020612
Time	18.06
INSTRUM	spect
PROBHD	5mm BBO BB-1
PULPROG	zg30
TD	65536
SOLVENT	CDCl3
NS	32
DS	2
SWH	8278.146 Hz
FIDRES	0.126314 Hz
AQ	3.9584243 sec
RG	50.8
DW	60.400 usec
DE	6.00 usec
TE	300.0 K
D1	1.00000000 sec

========== CHANNEL f1 ========

NUC1	1H
P1	7.90 usec
PL1	0.00 dB
SF01	400.1324710 MHz

F2 - Processing parameters

SI	32768
SF	400.1300623 MHz
WDW	EM
SSB	0
LB	0.30 Hz
GB	0
PC	1.00

1D NMR plot parameters

CX	20.00 cm
F1P	8.626 ppm
F1	3451.63 Hz
F2P	-0.491 ppm
F2	-196.37 Hz
PPMCM	0.45585 ppm/cm
HZCM	182.39981 Hz/cm

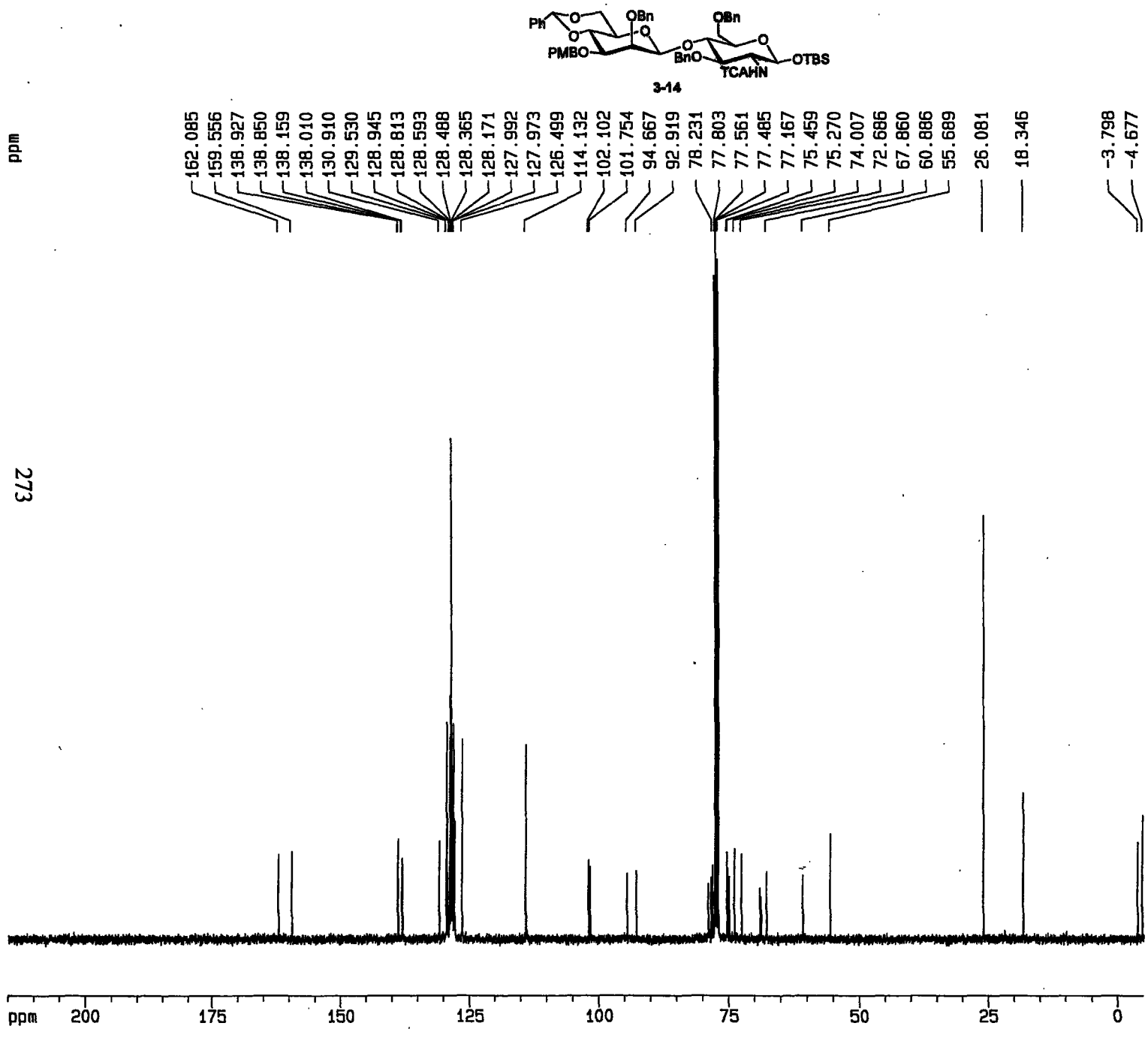

Current Data Parameters

NAME	Beta_dimer
EXPNO	12
PROCNO	1

F2 - Acquisition Parameters

Date_	20020612
Time	18.55
INSTRUM	spect
PROBHD	5mm BBO BB-1
PULPROG	zgpg30
TD	65536
SOLVENT	CDCl3
NS	768
DS	4
SWH	25125.629 Hz
FIDRES	0.383387 Hz
AQ	1.3042164 sec
RG	8192
DW	19.900 usec
DE	6.00 usec
TE	300.0 K
D1	2.00000000 sec
d11	0.03000000 sec
d12	0.00002000 sec

========== CHANNEL f1 ==========

NUC1	13C
P1	15.25 usec
PL1	3.00 dB
SFO1	100.6237959 MHz

========== CHANNEL f2 ==========

CPDPRG2	waltz16
NUC2	1H
PCPD2	107.50 usec
PL2	0.00 dB
PL12	24.00 dB
PL13	24.00 dB
SFO2	400.1316005 MHz

F2 - Processing parameters

SI	32768
SF	100.6127290 MHz
WDW	EM
SSB	0
LB	1.00 Hz
GB	0
PC	1.40

1D NMR plot parameters

CX	20.00 cm
F1P	215.000 ppm
F1	21631.74 Hz
F2P	-5.000 ppm
F2	-503.06 Hz
PPMCM	11.00000 ppm/cm
HZCM	1106.73999 Hz/cm

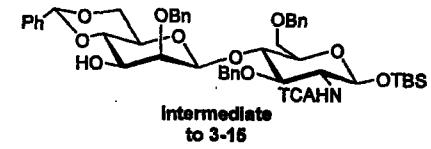

Intermediate
to 3-15

Integral

2.142 19.070 1.000 0.975 0.981 1.005 1.003 3.080 2.030 3.160 1.950 2.068 1.094 2.041 1.020 0.998 1.005 0.466 9.418 3.082 3.229

ppm 8 7 6 5 4 3 2 1 0

Current Data Parameters
NAME DMR-III-191
EXPNO 10
PROCNO 1

F2 - Acquisition Parameters
Date_ 20020614
Time 11.57
INSTRUM spect
PROBHD 5mm BBO BB-1
PULPROG zg30
TD 65536
SOLVENT CDCl3
NS 32
DS 2
SWH 8278.146 Hz
FIDRES 0.126314 Hz
AQ 3.9584243 sec
RG 45.3
DW 60.400 usec
DE 6.00 usec
TE 300.0 K
D1 1.00000000 sec

========== CHANNEL f1 ========
NUC1 1H
P1 7.90 usec
PL1 0.00 dB
SFO1 400.1324710 MHz

F2 - Processing parameters
SI 32768
SF 400.1300652 MHz
WDW EM
SSB 0
LB 0.30 Hz
GB 0
PC 1.00

1D NMR plot parameters
CX 20.00 cm
F1P 9.016 ppm
F1 3607.68 Hz
F2P -0.428 ppm
F2 -171.27 Hz
PPMCM 0.47222 ppm/cm
HZCM 188.94751 Hz/cm

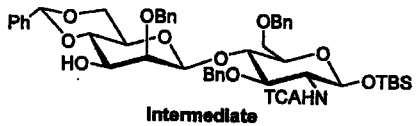

Intermediate to 3-15

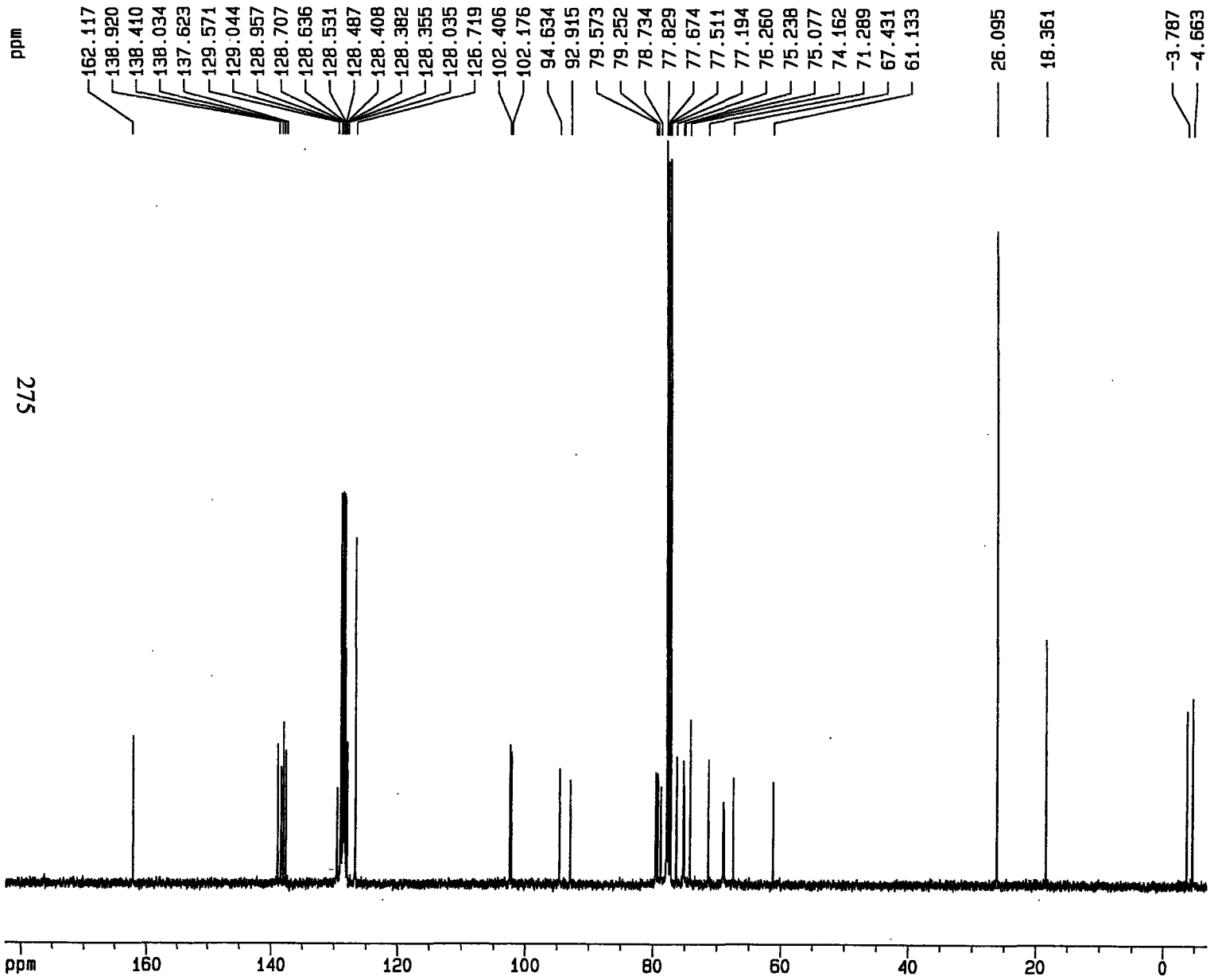

Current Data Parameters

NAME	DMR-III-191
EXPNO	12
PROCNO	1

F2 - Acquisition Parameters

Date_	20020614
Time	12.46
INSTRUM	spect
PROBHD	5mm BBO BB-1
PULPROG	zgpg30
TD	65536
SOLVENT	CDCl3
NS	768
DS	4
SWH	25125.629 Hz
FIDRES	0.383387 Hz
AQ	1.3042164 sec
RG	1625.5
DW	19.900 usec
DE	6.00 usec
TE	300.0 K
D1	2.00000000 sec
d11	0.03000000 sec
d12	0.00002000 sec

========== CHANNEL f1 ==========

NUC1	13C
P1	15.25 usec
PL1	3.00 dB
SFO1	100.6237959 MHz

========== CHANNEL f2 ==========

CPDPRG2	waltz16
NUC2	1H
PCPD2	107.50 usec
PL2	0.00 dB
PL12	24.00 dB
PL13	24.00 dB
SFO2	400.1316005 MHz

F2 - Processing parameters

SI	32768
SF	100.6127290 MHz
WDW	EM
SSB	0
LB	1.00 Hz
GB	0
PC	1.40

1D NMR plot parameters

CX	20.00 cm
F1P	182.360 ppm
F1	18347.70 Hz
F2P	-6.981 ppm
F2	-702.35 Hz
PPMCM	9.46702 ppm/cm
HZCM	952.50256 Hz/cm

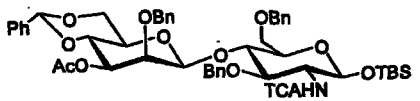

3-15

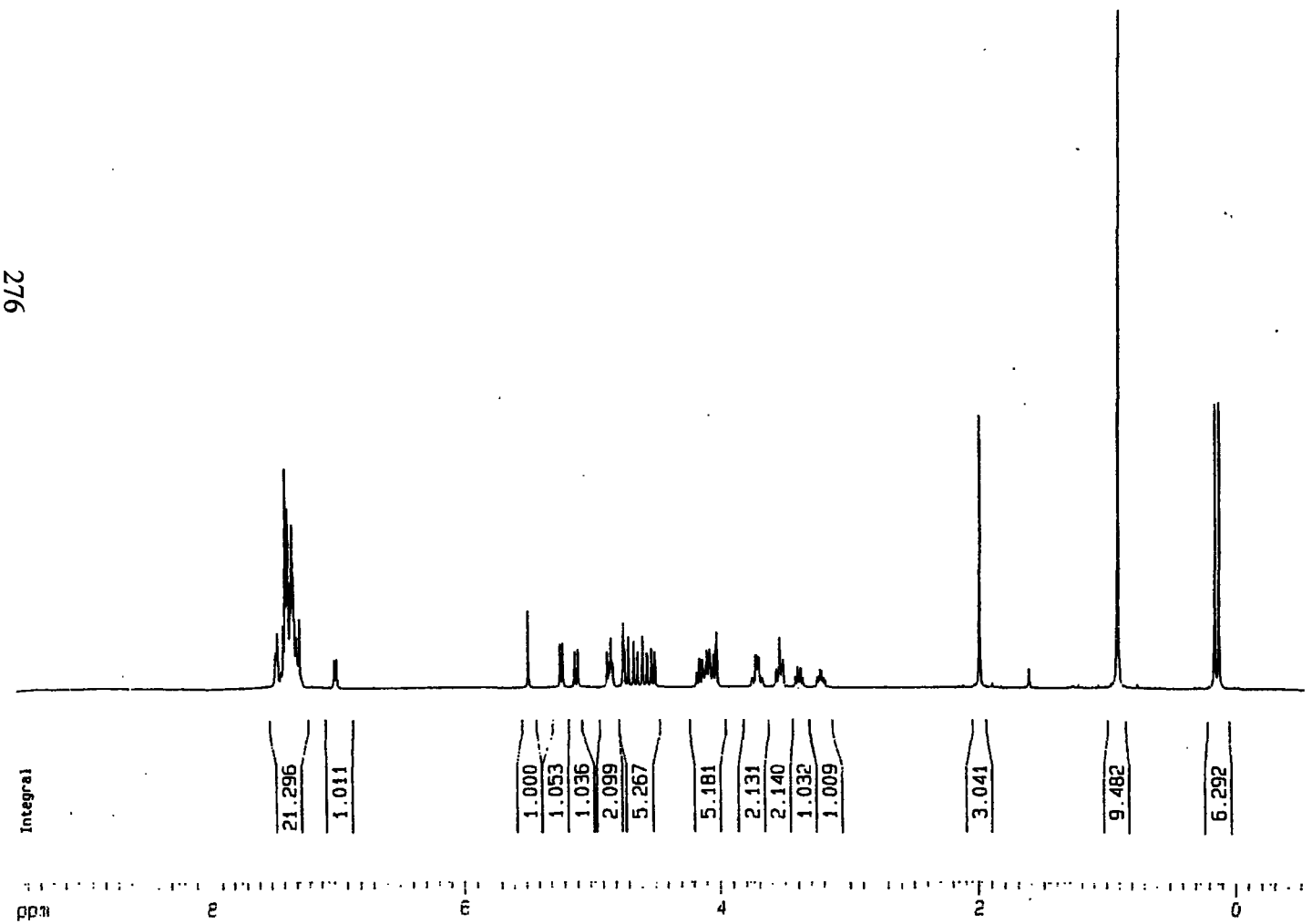


```
Current Data Parameters
NAME      ERS-III-242dry
EXPNO                  1
PROCNO                 1

F2 - Acquisition Parameters
Date_           20021028
Time               16.02
INSTRUM            spect
PROBHD     5mm BBO BB-1
PULPROG            zg30
TD                40062
SOLVENT           CDCl3
NS                   16
DS                    2
SWH           4006.410 Hz
FIDRES        0.100005 Hz
AQ            4.9997878 sec
RG                 80.6
DW              124.800 usec
DE                6.00 usec
TE.              300.0 K
D1            1.00000000 sec

============ CHANNEL f1 ============
NUC1                1H
P1                7.90 usec
PL1               0.00 dB
SFO1        400.1318006 MHz

F2 - Processing parameters
SI                 32768
SF          400.1300060 MHz
WDW                   EM
SSB                    0
LB                0.30 Hz
GB                     0
PC                1.00

1D NMR plot parameters
CX               20.00 cm
F1P              9.491 ppm
F1               3797.82 Hz
F2P              -0.521 ppm
F2               -208.59 Hz
PPMCM          0.50064 ppm/cm
HZCM          200.32053 Hz/cm
```

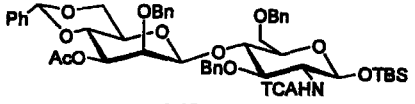

3-15

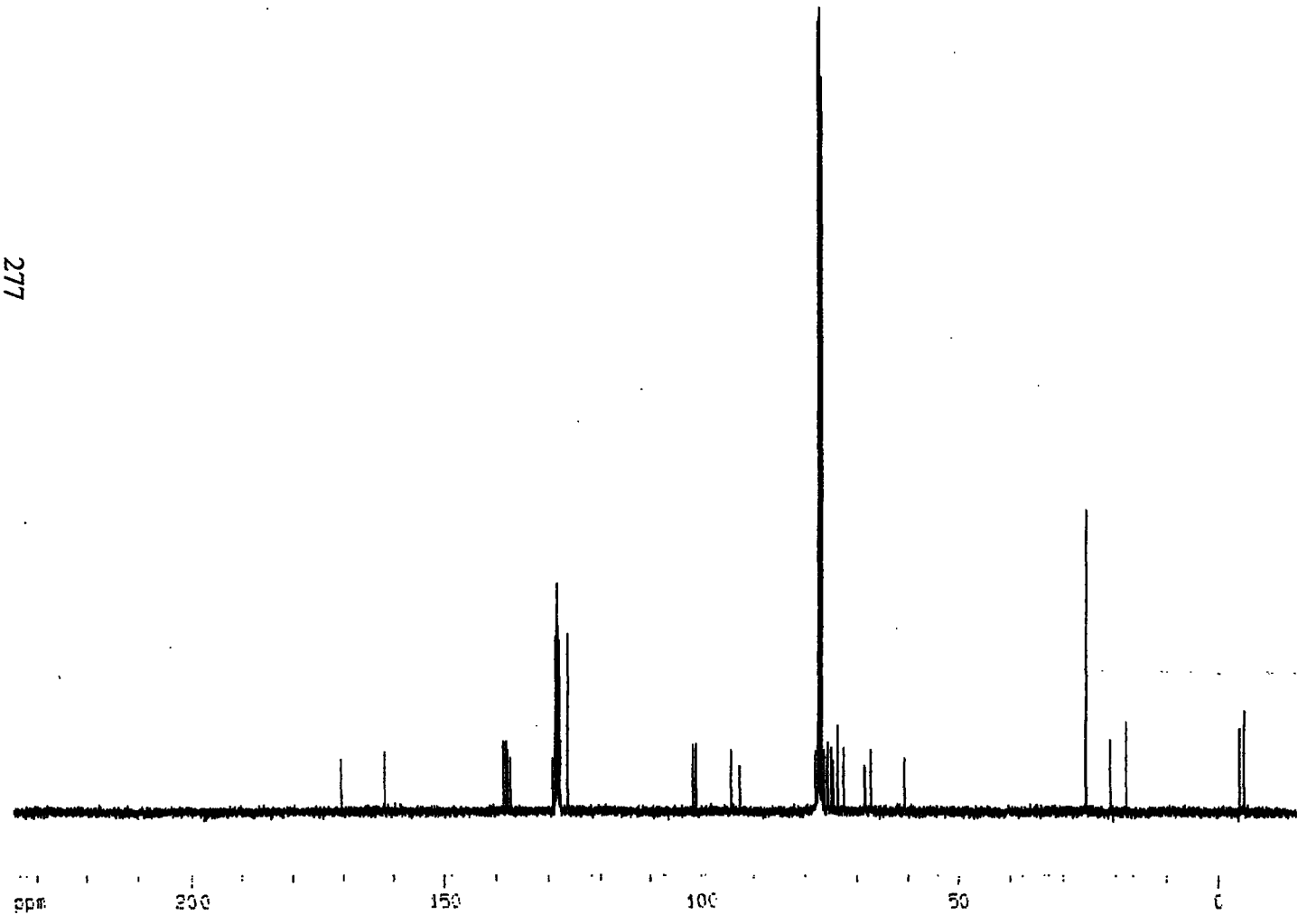


```
Current Data Parameters
NAME      ERS-III-242c13
EXPNO                  1
PROCNO                 1

F2 - Acquisition Parameters
Date_           20021028
Time               16.45
INSTRUM            spect
PROBHD     5mm BBO BB-1
PULPROG          zgpg30
TD                65536
SOLVENT            CDCl3
NS                   655
DS                     4
SWH           25125.629 Hz
FIDRES        0.383387 Hz
AQ            1.3042184 sec
RG                 16384
DW               19.900 usec
DE                6.00 usec
TE               300.0 K
D1            2.00000000 sec
d11           0.03000000 sec
d12           0.00002000 sec

============ CHANNEL f1 =============
NUC1                13C
P1                15.25 usec
PL1                3.00 dB
SFO1         100.6237959 MHz

============ CHANNEL f2 =============
CPDPRG2          waltz16
NUC2                1H
PCPD2            107.50 usec
PL2                0.00 dB
PL12              24.00 dB
PL13              24.00 dB
SFO2         400.1316005 MHz

F2 - Processing parameters
SI                 32768
SF           100.6127530 MHz
WDW                   EM
SSB                    0
LB                  1.00 Hz
GB                     0
PC                  1.40

1D NMR plot parameters
CX                 20.00 cm
F1P               234.620 ppm
F1              23605.72 Hz
F2P               -15.106 ppm
F2              -1519.90 Hz
PPMCM             12.48630 ppm/cm
HZCM           1256.28137 Hz/cm
```

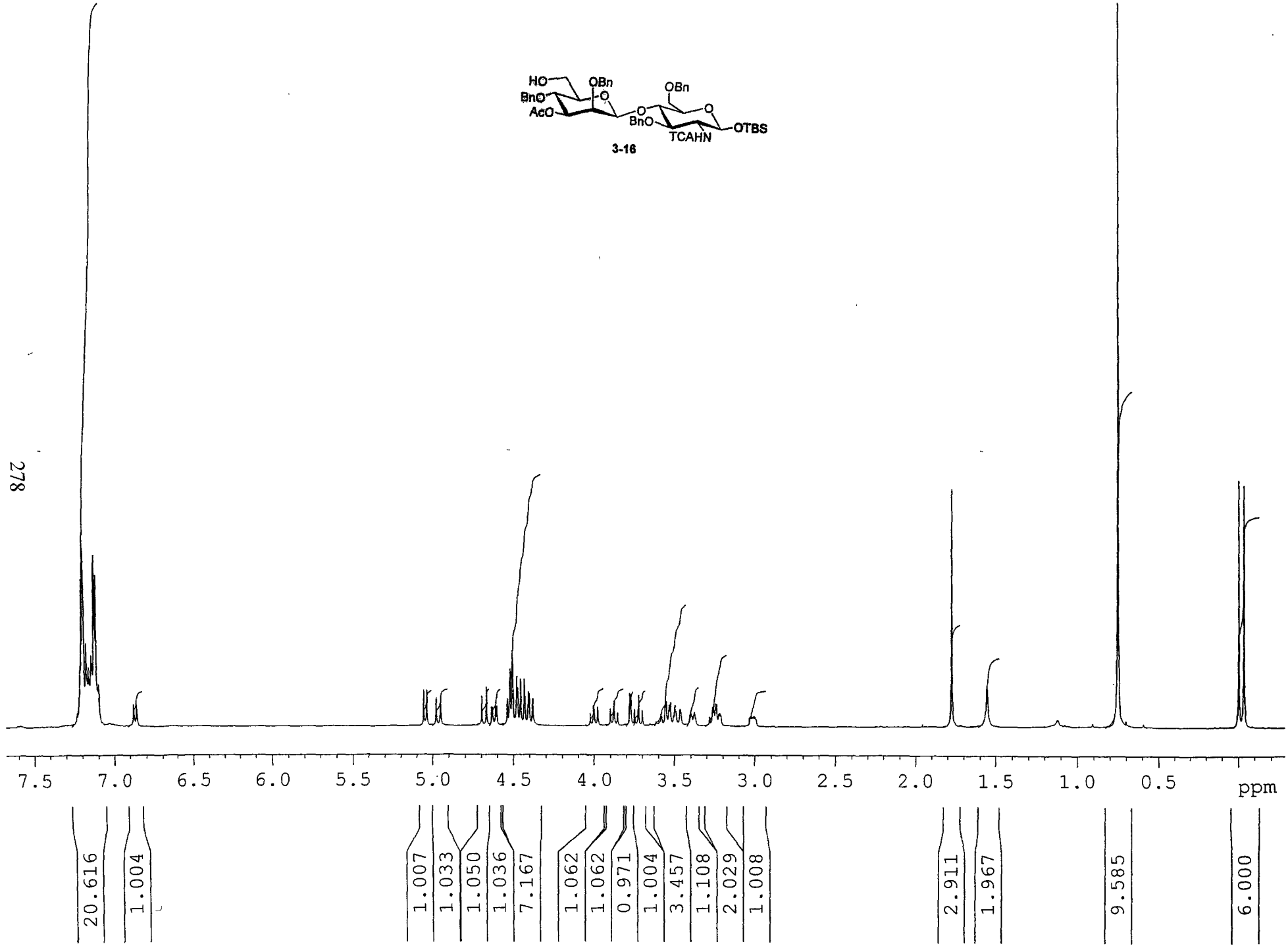
HO
OBn
BnO
AcO
O
O
OBn
O
BnO
TCAHN
OTBS
3-16
278
7.5
7.0
6.5
6.0
5.5
5.0
4.5
4.0
3.5
3.0
2.5
2.0
1.5
1.0
0.5
ppm
20.616
1.004
1.007
1.033
1.050
1.036
7.167
1.062
1.062
0.971
1.004
3.457
1.108
2.029
1.008
2.911
1.967
9.585
6.000

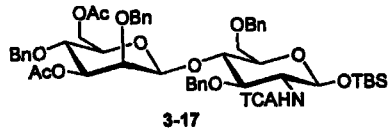

3-17

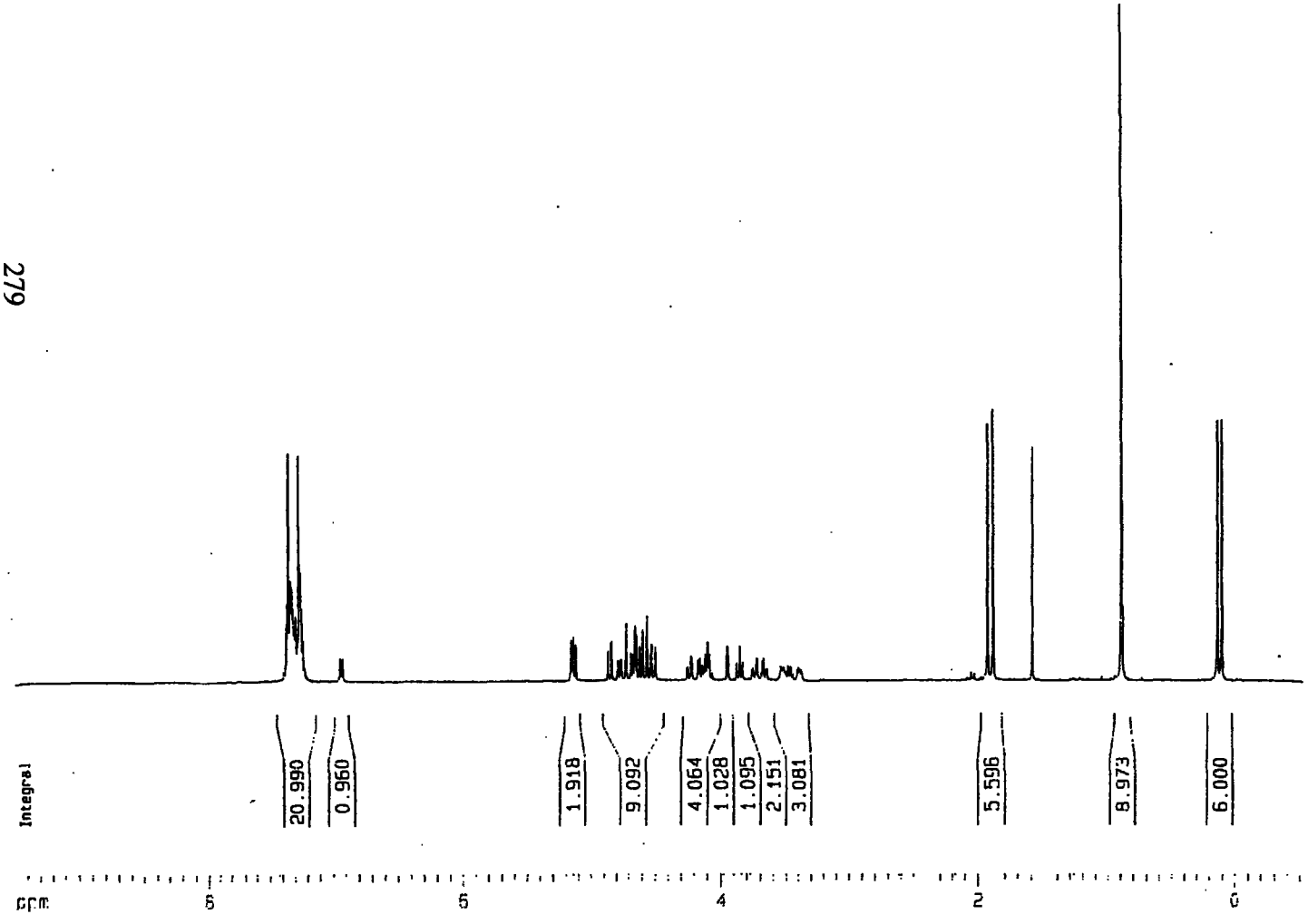


```
Current Data Parameters
NAME          ERS-III-168
EXPNO                   1
PROCNO                  1

F2 - Acquisition Parameters
Date_          20020903
Time              21.38
INSTRUM           spect
PROBHD     5mm BBO BB-1
PULPROG           zg30
TD               40062
SOLVENT          CDCl3
NS                  16
DS                   2
SWH           4006.410 Hz
FIDRES        0.100005 Hz
AQ            4.9997878 sec
RG                143.7
DW               124.800 usec
DE                6.00 usec
TE                300.0 K
D1            1.00000000 sec

========== CHANNEL f1 ============
NUC1                1H
P1               7.90 usec
PL1              0.00 dB
SFO1        400.1318006 MHz

F2 - Processing parameters
SI                32768
SF          400.1300057 MHz
WDW                 EM
SSB                  0
LB                0.30 Hz
GB                   0
PC                1.00

1D NMR plot parameters
CX               20.00 cm
F1P               9.492 ppm
F1             3798.06 Hz
F2P              -0.521 ppm
F2             -208.35 Hz
PPMCM         0.50064 ppm/cm
HZCM         200.32053 Hz/cm
```

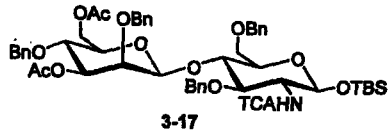

3-17

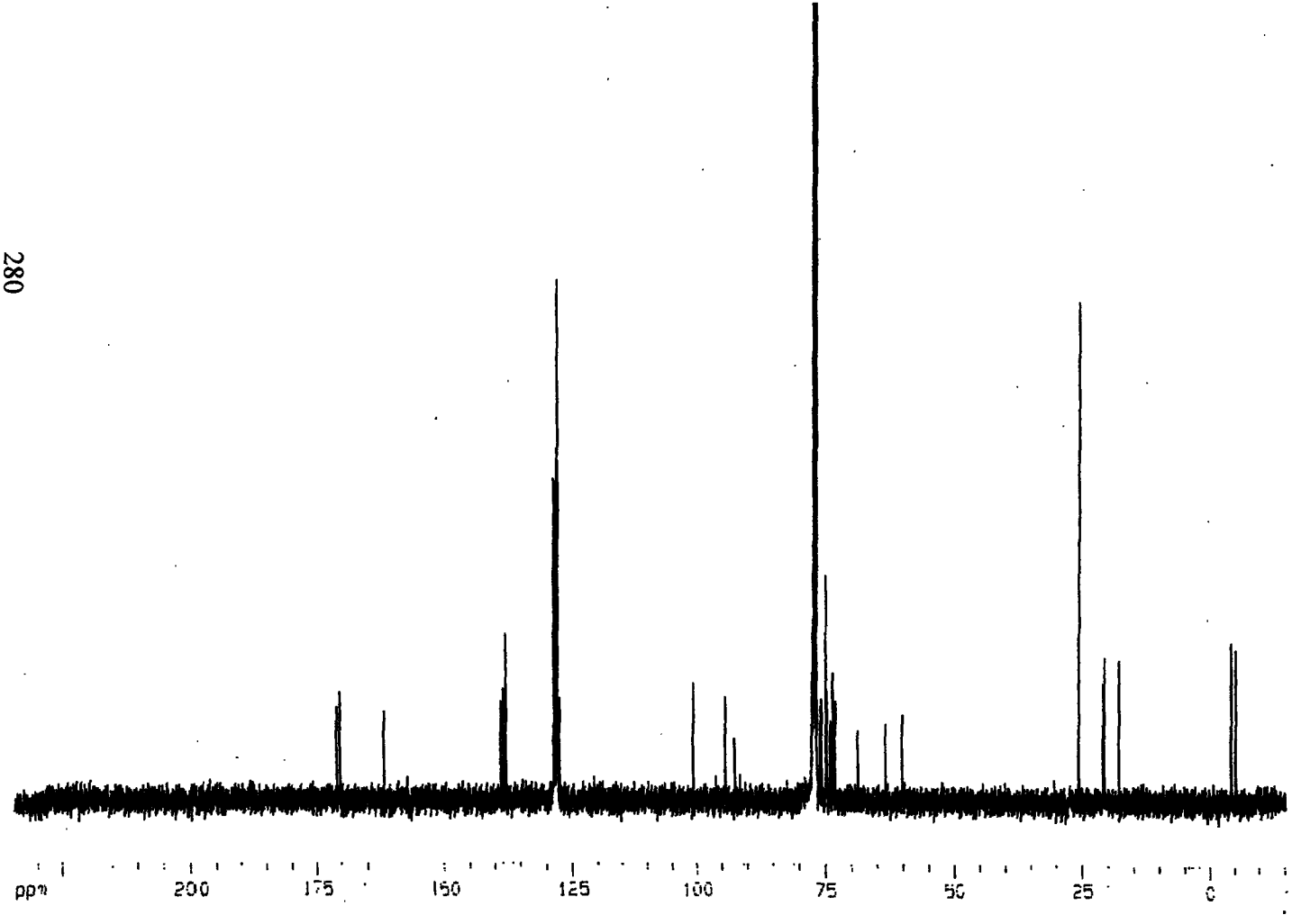


```
Current Data Parameters
NAME      EAS-III-168c13
EXPNO                  1
PROCNO                 1

F2 - Acquisition Parameters
Date_           20020904
Time                2.18
INSTRUM            spect
PROBHD     5mm BBO BB-1
PULPROG         zgpg30
TD               65536
SOLVENT          CDCl3
NS                2048
DS                   4
SWH          25125.629 Hz
FIDRES        0.383387 Hz
AQ           1.3042164 sec
RG                6502
DW              19.900 usec
DE               6.00 usec
TE              300.0 K
D1           2.00000000 sec
d11          0.03000000 sec
d12          0.00002000 sec

============ CHANNEL f1 ============
NUC1               13C
P1               15.25 usec
PL1               3.00 dB
SFO1        100.6237959 MHz

============ CHANNEL f2 ============
CPDPRG2         waltz16
NUC2                1H
PCPD2          107.50 usec
PL2               0.00 dB
PL12             24.00 dB
PL13             24.00 dB
SFO2        400.1316005 MHz

F2 - Processing parameters
SI                32768
SF          100.6127492 MHz
WDW                  EM
SSB                   0
LB                 1.00 Hz
GB                    0
PC                 1.40

1D NMR plot parameters
CX                20.00 cm
F1P              234.658 ppm
F1             23609.56 Hz
F2P              -15.068 ppm
F2             -1516.07 Hz
PPMCM            12.48630 ppm/cm
HZCM          1256.28137 Hz/cm
```

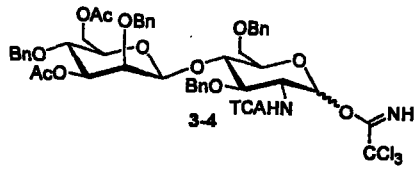

3-4

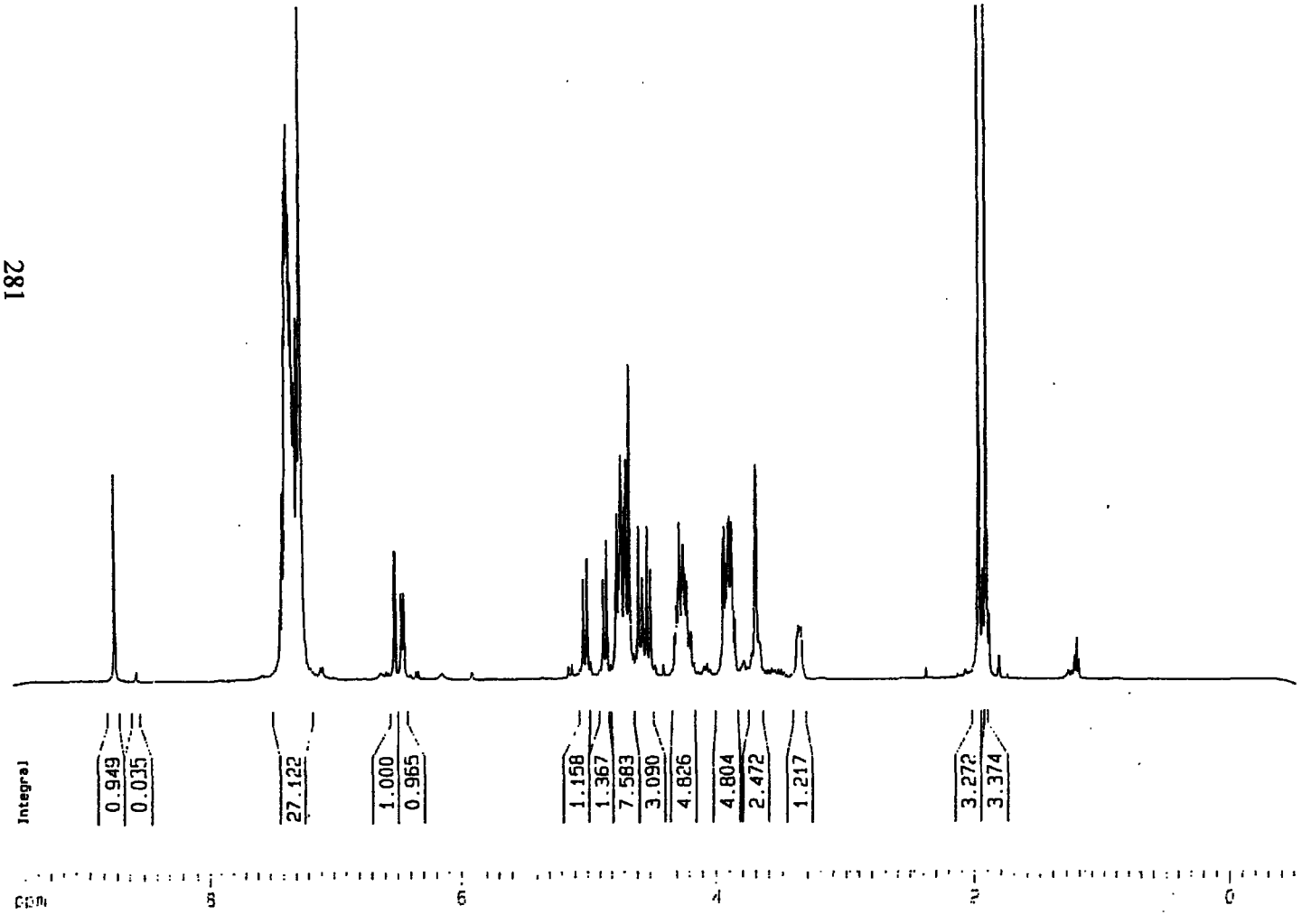


```
Current Data Parameters
NAME        ERS-III-176zz
EXPNO                   1
PROCNO                  1

F2 - Acquisition Parameters
Date_            20030122
Time                4.07
INSTRUM            spect
PROBHD     5mm BBO BB-1
PULPROG          zg30
TD                40062
SOLVENT           CDCl3
NS                   16
DS                    2
SWH           4006.410 Hz
FIDRES        0.100005 Hz
AQ            4.9997878 sec
RG                40.3
DW             124.800 usec
DE               6.00 usec
TE              300.0 K
D1           1.00000000 sec

========== CHANNEL f1 ==========
NUC1                 1H
P1                7.90 usec
PL1               0.00 dB
SFO1        400.1318006 MHz

F2 - Processing parameters
SI                32768
SF          400.1300055 MHz
WDW                  EM
SSB                   0
LB                0.30 Hz
GB                    0
PC                 1.00

1D NMR plot parameters
CX               20.00 cm
F1P               9.493 ppm
F1              3798.31 Hz
F2P              -0.520 ppm
F2              -208.10 Hz
PPMCM          0.50064 ppm/cm
HZCM          200.32053 Hz/cm
```

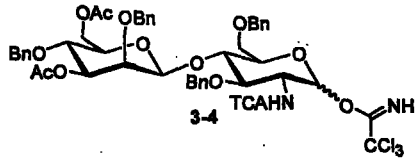

3-4

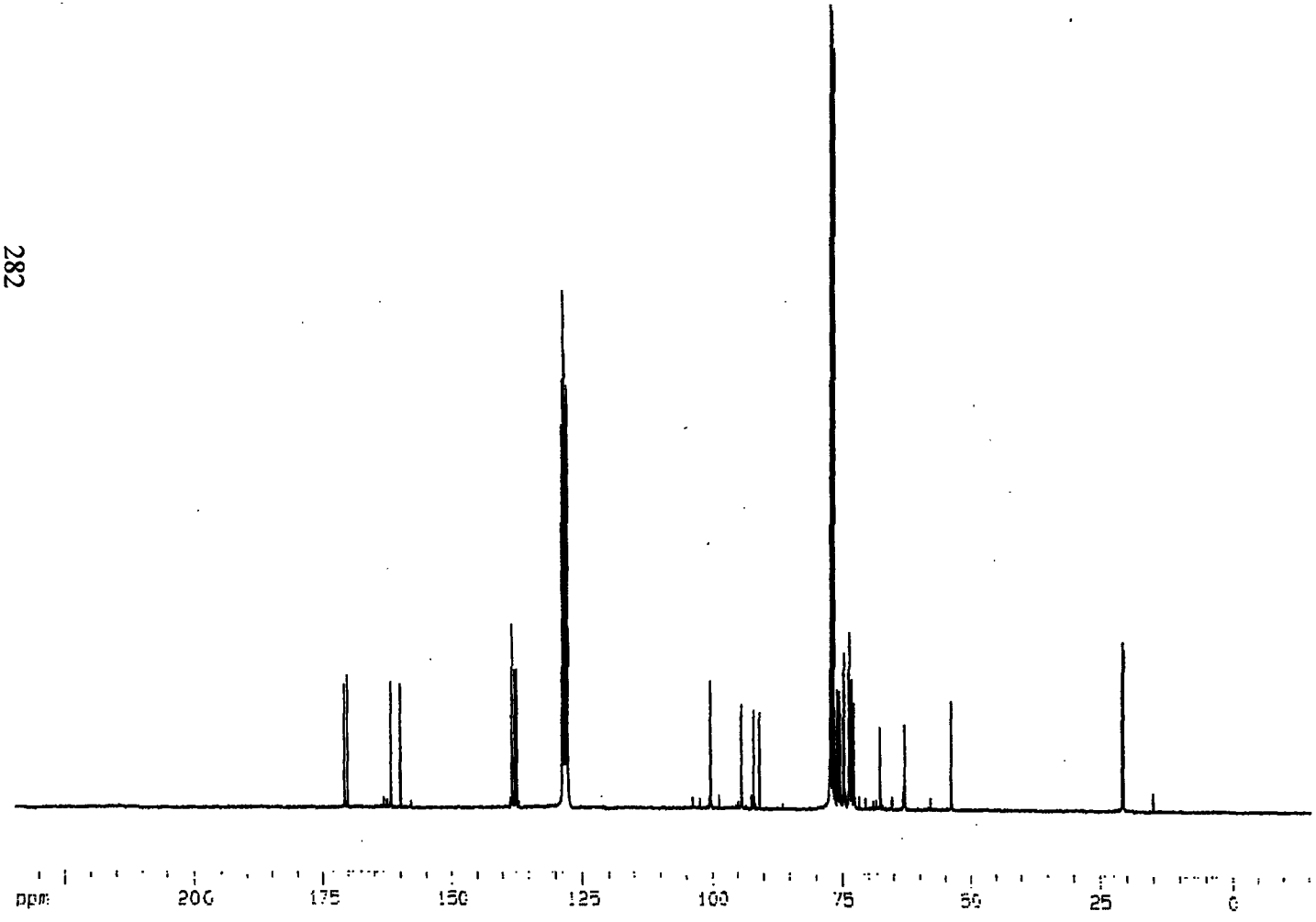


```
Current Data Parameters
NAME      ERS-III-176C13
EXPNO                  1
PROCNO                 1

F2 - Acquisition Parameters
Date_           20030122
Time               14.43
INSTRUM            spect
PROBHD     5mm BBO BB-1
PULPROG          zgpg30
TD                65536
SOLVENT           CDCl3
NS                11498
DS                    4
SWH           25125.629 Hz
FIDRES        0.383387 Hz
AQ            1.3042164 sec
RG                 4096
DW               19.900 usec
DE                6.00 usec
TE               300.0 K
D1            2.00000000 sec
D11           0.03000000 sec
D12           0.00002000 sec

============ CHANNEL f1 ============
NUC1               13C
P1               15.25 usec
PL1               3.00 dB
SFO1         100.6237959 MHz

============ CHANNEL f2 ============
CPDPRG2         waltz16
NUC2               1H
PCPD2           107.50 usec
PL2               0.00 dB
PL12             24.00 dB
PL13             24.00 dB
SFO2         400.1316005 MHz

F2 - Processing parameters
SI                32768
SF           100.6127607 MHz
WDW                  EM
SSB                   0
LB                 1.00 Hz
GB                    0
PC                 1.40

1D NMR plot parameters
CX                20.00 cm
F1P              234.543 ppm
F1             23598.08 Hz
F2P              -15.183 ppm
F2             -1527.57 Hz
PPMCM            12.48630 ppm/cm
HZCM          1256.28137 Hz/cm
```

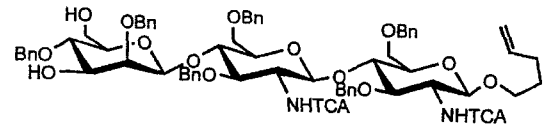
HO
OBn
OBn
OBn
BnO
HO
O
BnO
O
BnO
O
O
NHTCA
NHTCA

3-19

8
7
6
5
4
3
2
1
ppm
28.61
1.00
1.03
0.70
1.07
3.73
4.10
2.13
1.06
1.03
1.02
1.00
1.02
1.00
2.05
1.18
5.38
5.44
0.99
1.00
1.04
0.94
2.11
3.53
0.52

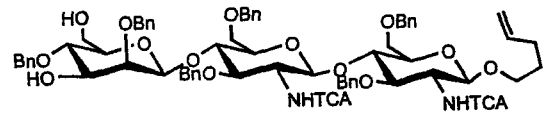
HO
OBn
OBn
OBn
BnO
HO
O
O
BnO
O
BnO
O
O
NHTCA
NHTCA

3-19

160
140
120
100
80
60
40
20
ppm

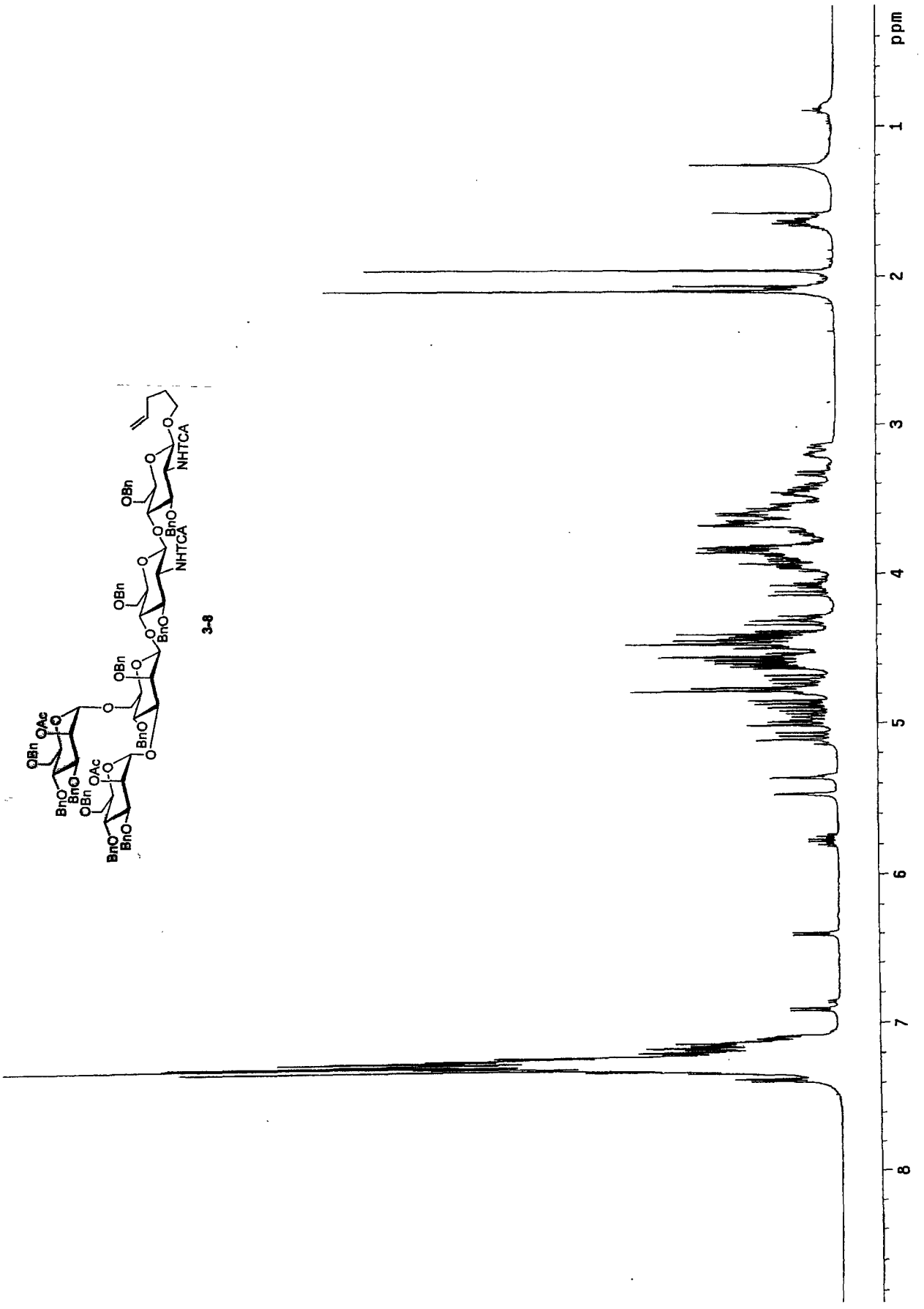
3-8
ppm

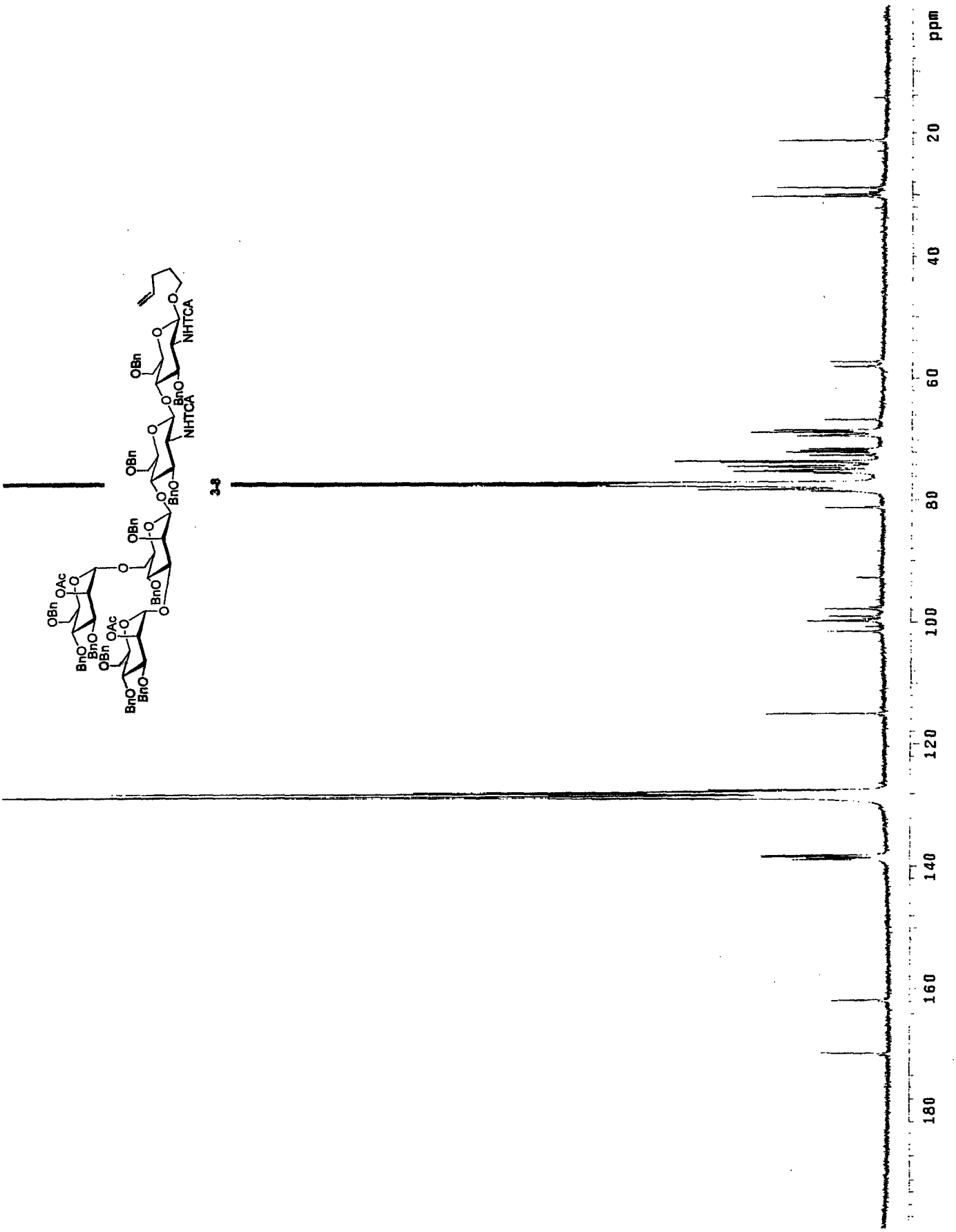
OBn
OAc
BnO
NHTCA
3-8
ppm
20
40
60
80
100
120
140
160
180

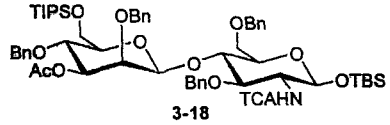

3-18

8 7 6 5 4 3 2 1 ppm

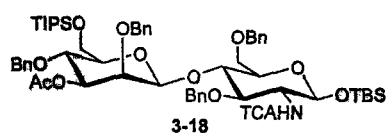

3-18

160 140 120 100 80 60 40 20 0 ppm

289

Integral

0.977 24.192 1.000 0.967 1.053 3.475 5.497 1.164 1.085 1.136 1.179 5.767 2.179 1.094 3.513 4.124 4.711 24.769 3.913

ppm 8 7 6 5 4 3 2 1 0

```
Current Data Parameters
NAME                  donor
EXPNO                    10
PROCNO                    1

F2 - Acquisition Parameters
Date_              20040731
Time                  17.01
INSTRUM               spect
PROBHD      5mm BBO BB-1
PULPROG               zg30
TD                   65536
SOLVENT              CDCl3
NS                      64
DS                       0
SWH              8278.146 Hz
FIDRES           0.126314 Hz
AQ               3.9584243 sec
RG                   228.1
DW                  60.400 usec
DE                   6.00 usec
TE                  300.0 K
D1               2.00000000 sec

============ CHANNEL f1 ========
NUC1                     1H
P1                    7.90 usec
PL1                   0.00 dB
SFO1           400.1324710 MHz

F2 - Processing parameters
SI                    32768
SF               400.1300380 MHz
WDW                      EM
SSB                      0
LB                    0.30 Hz
GB                       0
PC                    1.00

1D NMR plot parameters
CX                   20.00 cm
F1P                   9.437 ppm
F1                 3776.09 Hz
F2P                  -0.176 ppm
F2                  -70.60 Hz
PPMCM             0.48068 ppm/cm
HZCM            192.33441 Hz/cm
```

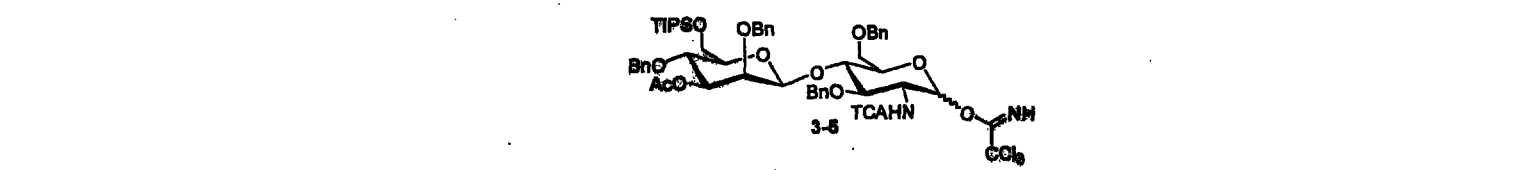

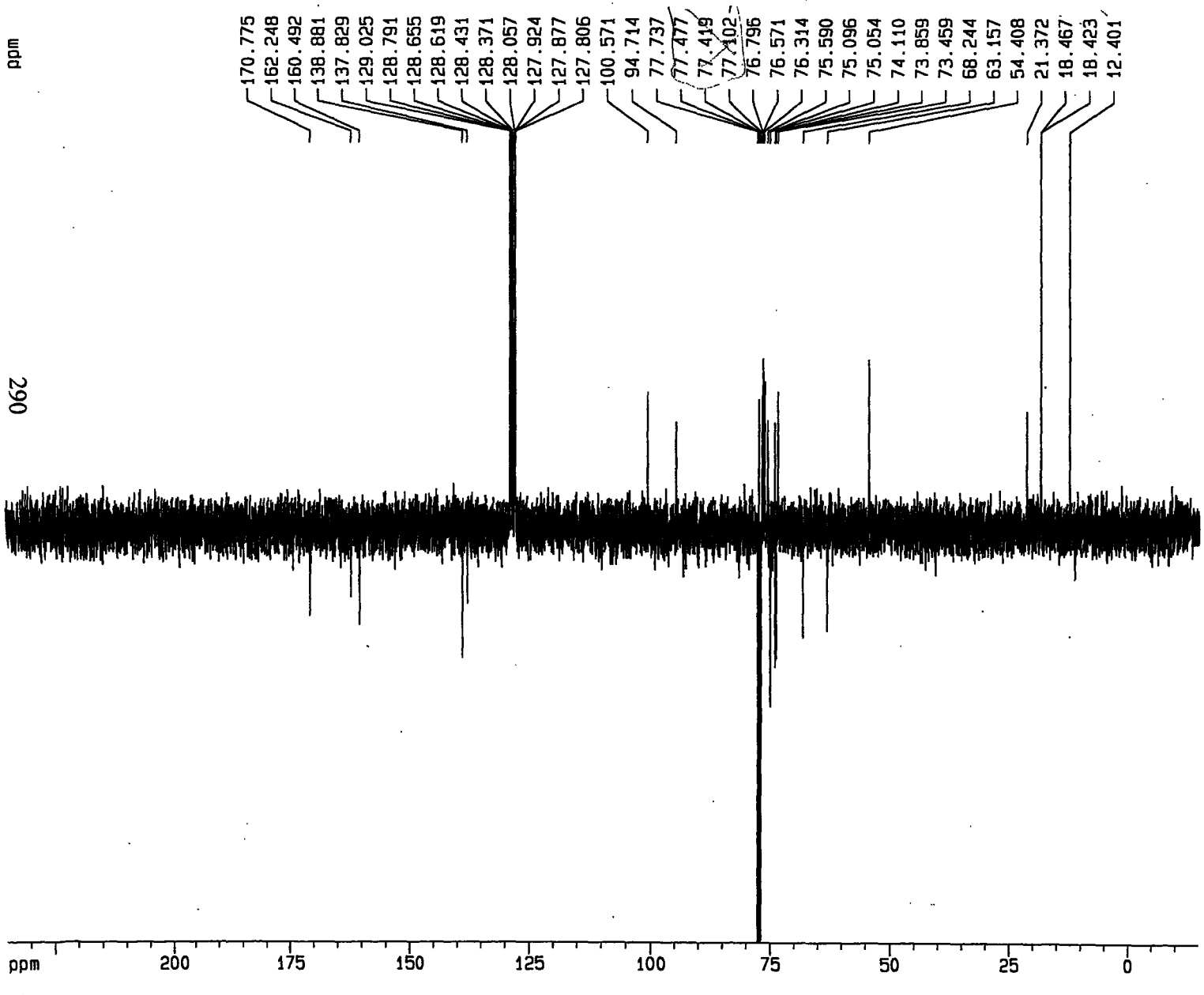

Current Data Parameters

NAME	donor
EXPNO	11
PROCNO	1

F2 - Acquisition Parameters

Date_	20040731
Time	17.30
INSTRUM	spect
PROBHD	5mm BBO BB-1
PULPROG	jmod
TD	65536
SOLVENT	CDCl3
NS	512
DS	4
SWH	25125.629 Hz
FIDRES	0.383387 Hz
AQ	1.3042164 sec
RG	14596.5
DW	19.900 usec
DE	6.00 usec
TE	300.0 K
CNST2	145.0000000
CNST11	1.0000000
D1	2.00000000 sec
d13	0.00000300 sec
d20	0.00689655 sec
DELTA	0.00001942 sec

========== CHANNEL f1 ==========

NUC1	13C
P1	15.25 usec
p2	30.50 usec
PL1	3.00 dB
SFO1	100.6237959 MHz

========== CHANNEL f2 ==========

CPDPRG2	waltz16
NUC2	1H
PCPD2	107.50 usec
PL2	0.00 dB
PL12	24.00 dB
SFO2	400.1316005 MHz

F2 - Processing parameters

SI	32768
SF	100.6127290 MHz
WDW	EM
SSB	0
LB	1.00 Hz
GB	0
PC	1.40

1D NMR plot parameters

CX	20.00 cm
F1P	234.844 ppm
F1	23628.35 Hz
F2P	-14.882 ppm
F2	-1497.28 Hz
PPMCM	12.48631 ppm/cm
HZCM	1256.28149 Hz/cm

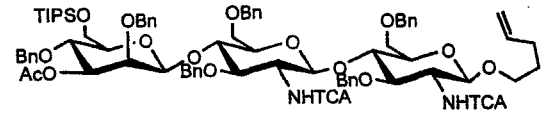
TIPSO
OBn
OBn
OBn
BnO
AcO
BnO
BnO
NHTCA
NHTCA

3-2

7
6
5
4
3
2
1
ppm
19.52 4.12 1.00 0.69 3.84 2.32 3.35 5.59 2.14 0.99 2.07 2.39
6.26 0.95 1.19 9.13 2.13 7.80 1.07 1.05 2.91 22.76

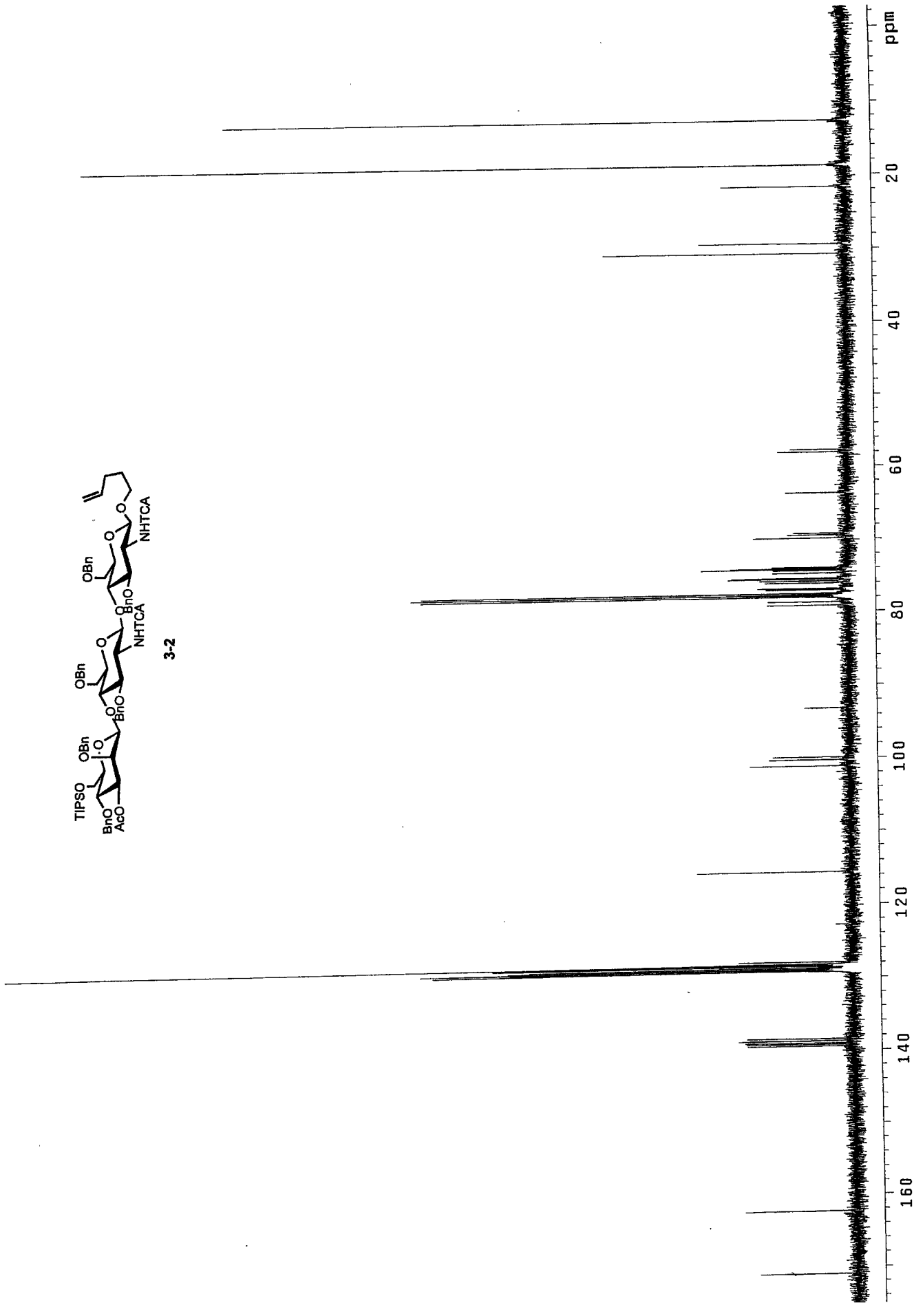
TIPSO
OBn
BnO
AcO
OBn
BnO
NHTCA
OBn
BnO
NHTCA
3-2
ppm
20
40
60
80
100
120
140
160

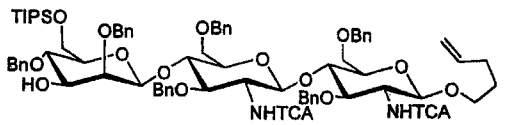
TIPSO
OBn
OBn
OBn
BnO
HO
O
BnO
BnO
NHTCA
NHTCA

3-20

7
6
5
4
3
2
1
ppm
17.45 4.17
76 0.91
0.22
1.00
0.78
3.61 2.53
1.18 0.23
4.56 3.12
0.93 1.96
1.28 0.92
1.34 2.16
6.48 1.77
5.81 1.37
1.00 0.99
0.89
2.38
3.44
19.80

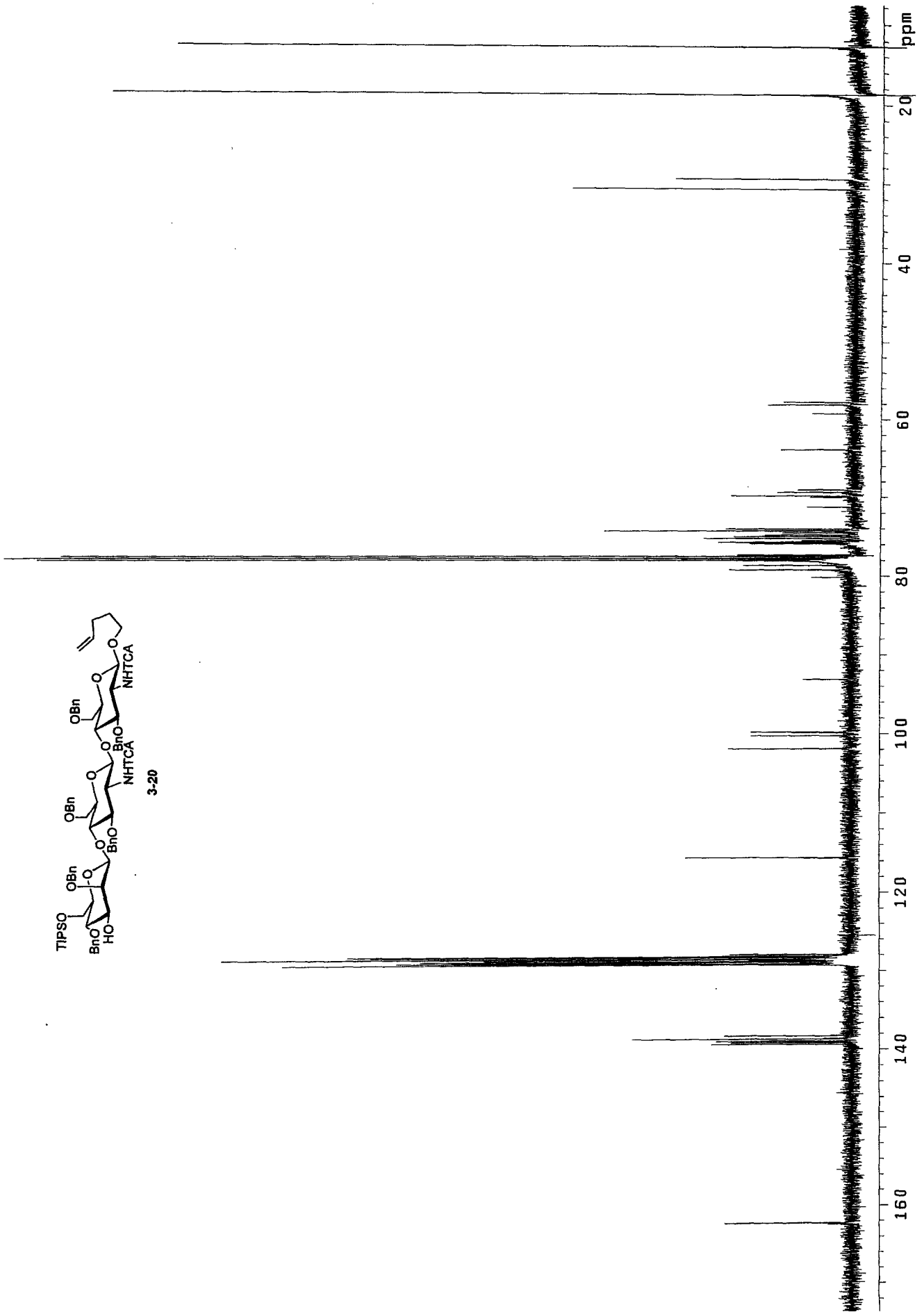
TIPSO
OBn
OBn
OBn
BnO
HO
BnO
NHTCA
BnO
NHTCA
3-20
ppm
20
40
60
80
100
120
140
160

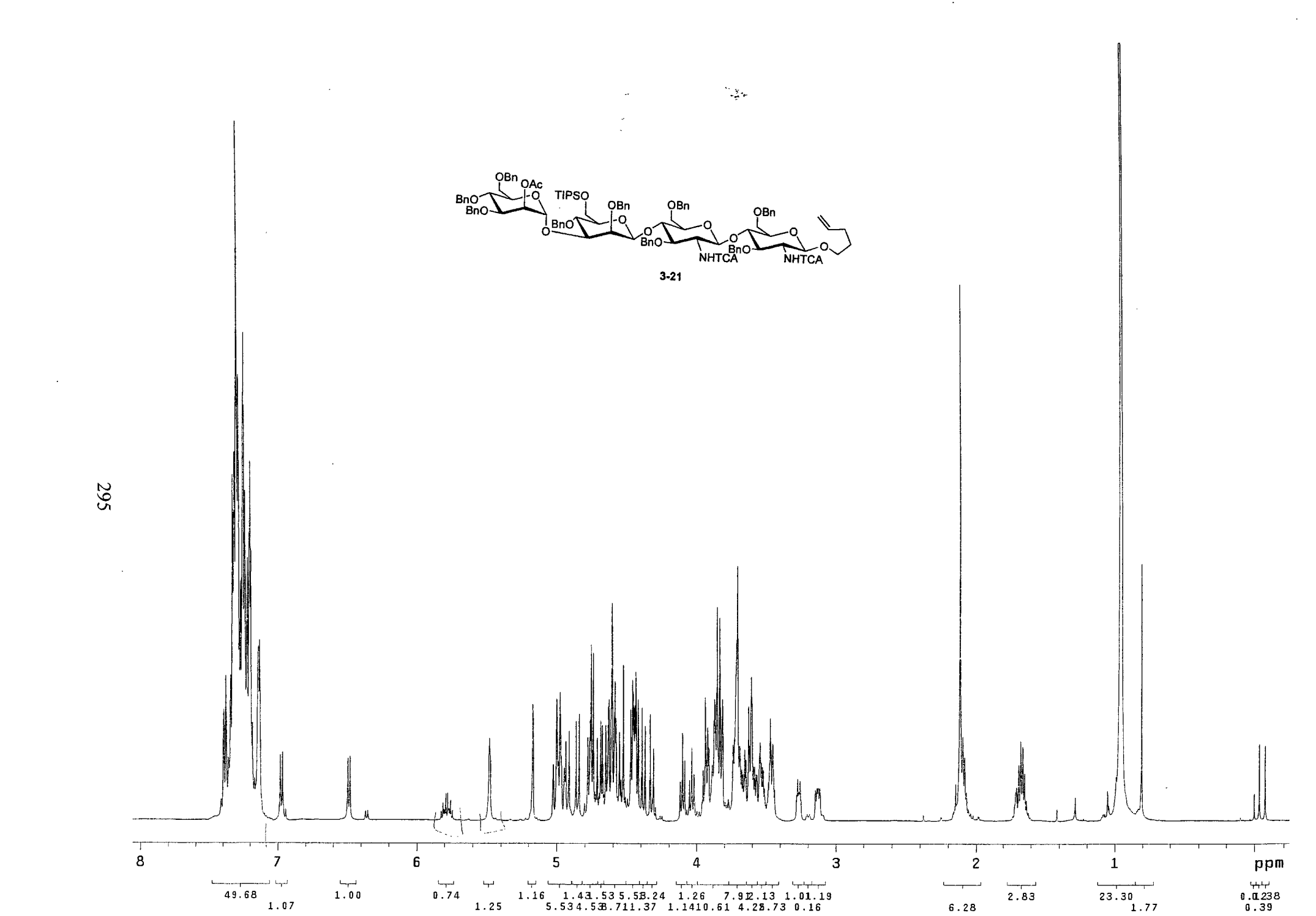
OBn
OAc
BnO
BnO
TIPSO
OBn
BnO
OBn
BnO
NHTCA
BnO
NHTCA
3-21
8
7
6
5
4
3
2
1
ppm
49.68
1.07
1.00
0.74
1.25
1.16
6.28
2.83
23.30
1.77
0.39

OBn
OAc
TIPSO
OBn
OBn
BnO
BnO
BnO
BnO
OBn
NHTCA
BnO
NHTCA
OBn
3-21

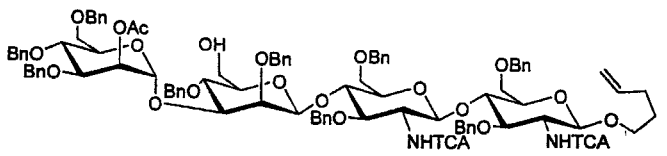
OBn
OAc
BnO
BnO
OH
OBn
OBn
OBn
BnO
BnO
BnO
NHTCA
NHTCA

3-22

7
6
5
4
3
2
1
ppm
4.49
40.88
1.00
1.03
0.68
1.07
1.03
3.86
2.91
3.55
5.98
1.01
2.62
3.43
3.49
1.03
1.06
1.22
5.95
2.59
1.04
3.43
3.62
9.46
1.03
1.20
5.44
2.37

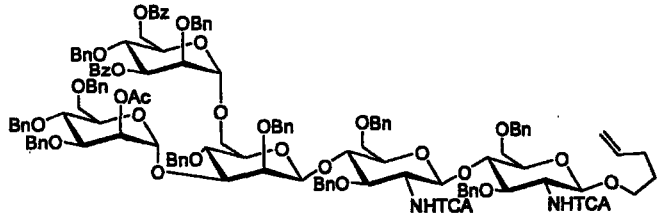

3-9


```
Current Data Parameters
NAME          core-ptenta
EXPNO                  10
PROCNO                  1

F2 - Acquisition Parameters
Date_           20030403
Time               10.27
INSTRUM            spect
PROBHD     5mm BBO BB-1
PULPROG            zg30
TD                65536
SOLVENT           CDCl3
NS                   32
DS                    0
SWH           8278.146 Hz
FIDRES        0.126314 Hz
AQ            3.9584243 sec
RG                 45.3
DW               60.400 usec
DE                6.00 usec
TE               300.0 K
D1            2.00000000 sec

========== CHANNEL f1 ========
NUC1                  1H
P1                 7.90 usec
PL1                0.00 dB
SFO1         400.1324710 MHz

F2 - Processing parameters
SI                 32768
SF           400.1300788 MHz
WDW                   EM
SSB                   0
LB                 0.30 Hz
GB                    0
PC                 1.00

1D NMR plot parameters
CX                20.00 cm
F1P                8.187 ppm
F1              3276.05 Hz
F2P               -0.298 ppm
F2              -119.39 Hz
PPMCM          0.42429 ppm/cm
HZCM          169.77216 Hz/cm
```

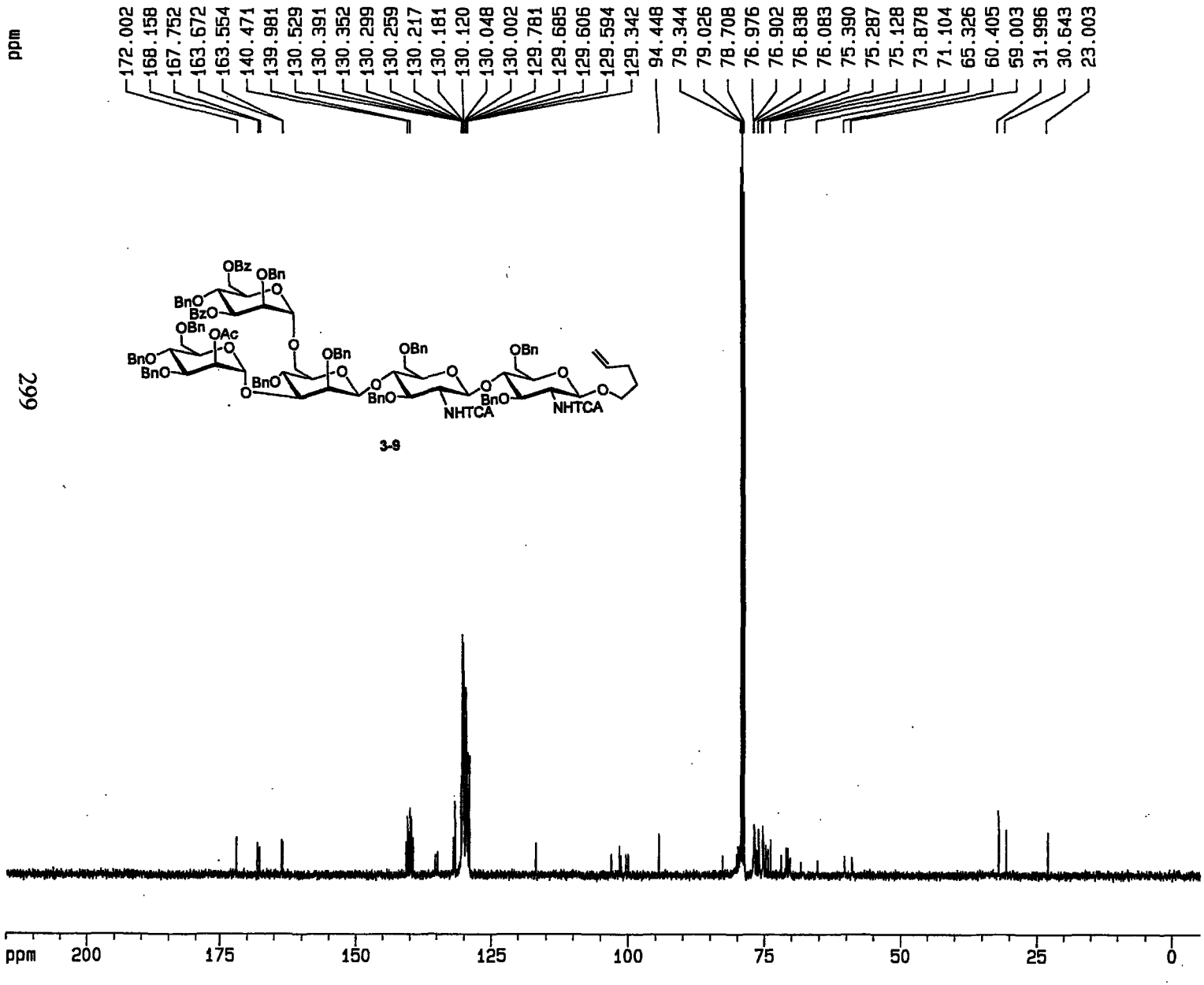

Current Data Parameters

NAME	core-ptenta
EXPNO	12
PROCNO	1

F2 - Acquisition Parameters

Date_	20030403
Time	11.40
INSTRUM	spect
PROBHD	5mm BBO BB-1
PULPROG	zgpg30
TD	65536
SOLVENT	CDCl3
NS	1024
DS	4
SWH	25125.629 Hz
FIDRES	0.383387 Hz
AQ	1.3042164 sec
RG	8192
DW	19.900 usec
DE	6.00 usec
TE	300.0 K
D1	2.00000000 sec
d11	0.03000000 sec
d12	0.00002000 sec

========== CHANNEL f1 ==========

NUC1	13C
P1	15.25 usec
PL1	3.00 dB
SFO1	100.6237959 MHz

========== CHANNEL f2 ==========

CPDPRG2	waltz16
NUC2	1H
PCPD2	107.50 usec
PL2	0.00 dB
PL12	24.00 dB
PL13	24.00 dB
SFO2	400.1316005 MHz

F2 - Processing parameters

SI	32768
SF	100.6125748 MHz
WDW	EM
SSB	0
LB	1.00 Hz
GB	0
PC	1.40

1D NMR plot parameters

CX	20.00 cm
F1P	215.000 ppm
F1	21631.71 Hz
F2P	-5.000 ppm
F2	-503.06 Hz
PPMCM	11.00000 ppm/cm
HZCM	1106.73828 Hz/cm

Appendix C.4

Selected Spectra – Chapter 4

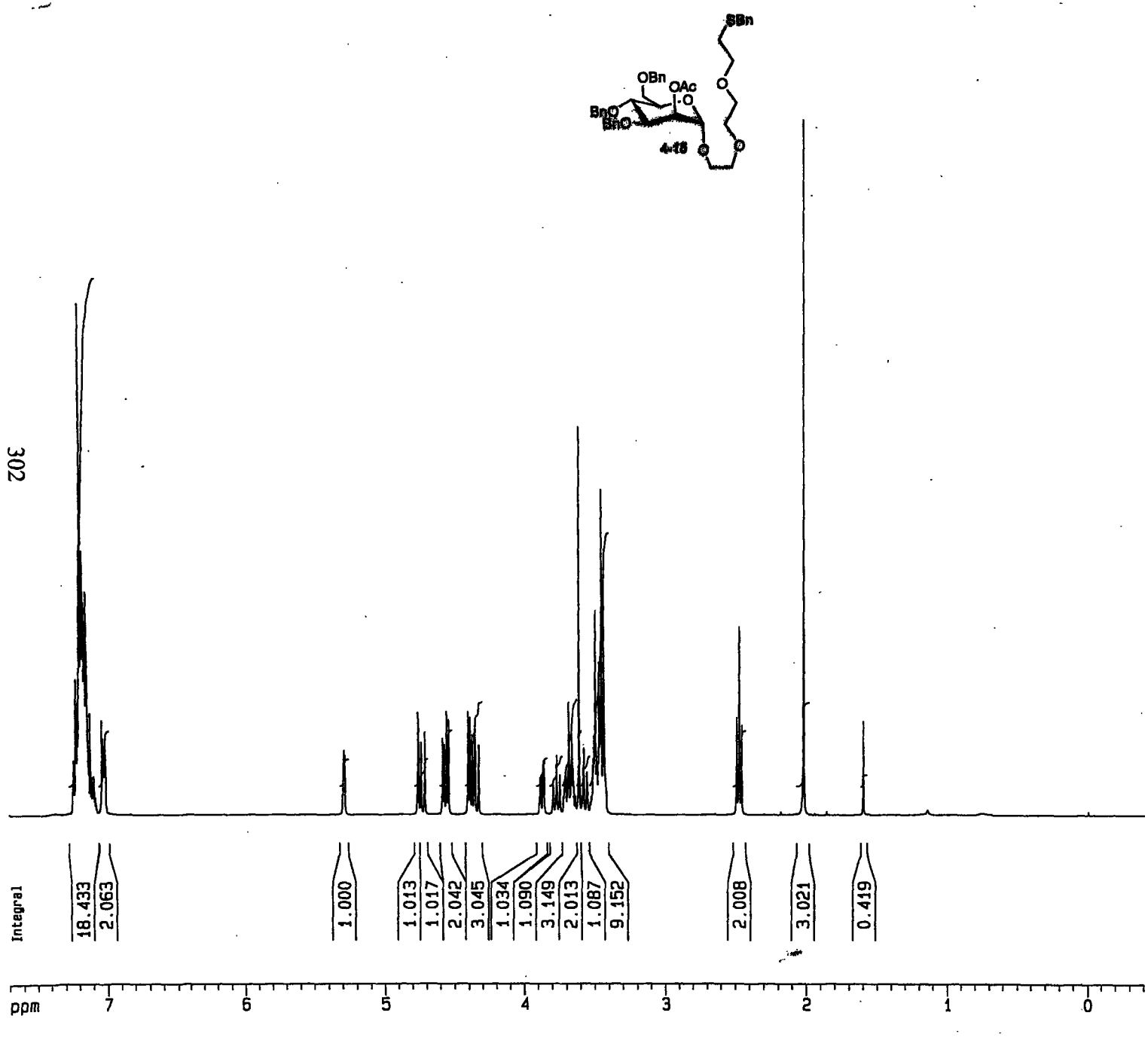

Current Data Parameters

NAME	Man-linker
EXPNO	10
PROCNO	1

F2 - Acquisition Parameters

Date_	20040805
Time	11.30
INSTRUM	spect
PROBHD	5mm BBO BB-1
PULPROG	zg30
TD	65536
SOLVENT	CDCl3
NS	64
DS	0
SWH	8278.146 Hz
FIDRES	0.126314 Hz
AQ	3.9584243 sec
RG	50.8
DW	60.400 usec
DE	6.00 usec
TE	300.0 K
D1	2.00000000 sec

========== CHANNEL f1 =========

NUC1	1H
P1	7.90 usec
PL1	0.00 dB
SFO1	400.1324710 MHz

F2 - Processing parameters

SI	32768
SF	400.1300644 MHz
WDW	EM
SSB	0
LB	0.30 Hz
GB	0
PC	1.00

1D NMR plot parameters

CX	20.00 cm
F1P	7.704 ppm
F1	3082.66 Hz
F2P	-0.402 ppm
F2	-160.98 Hz
PPMCM	0.40532 ppm/cm
HZCM	162.18222 Hz/cm

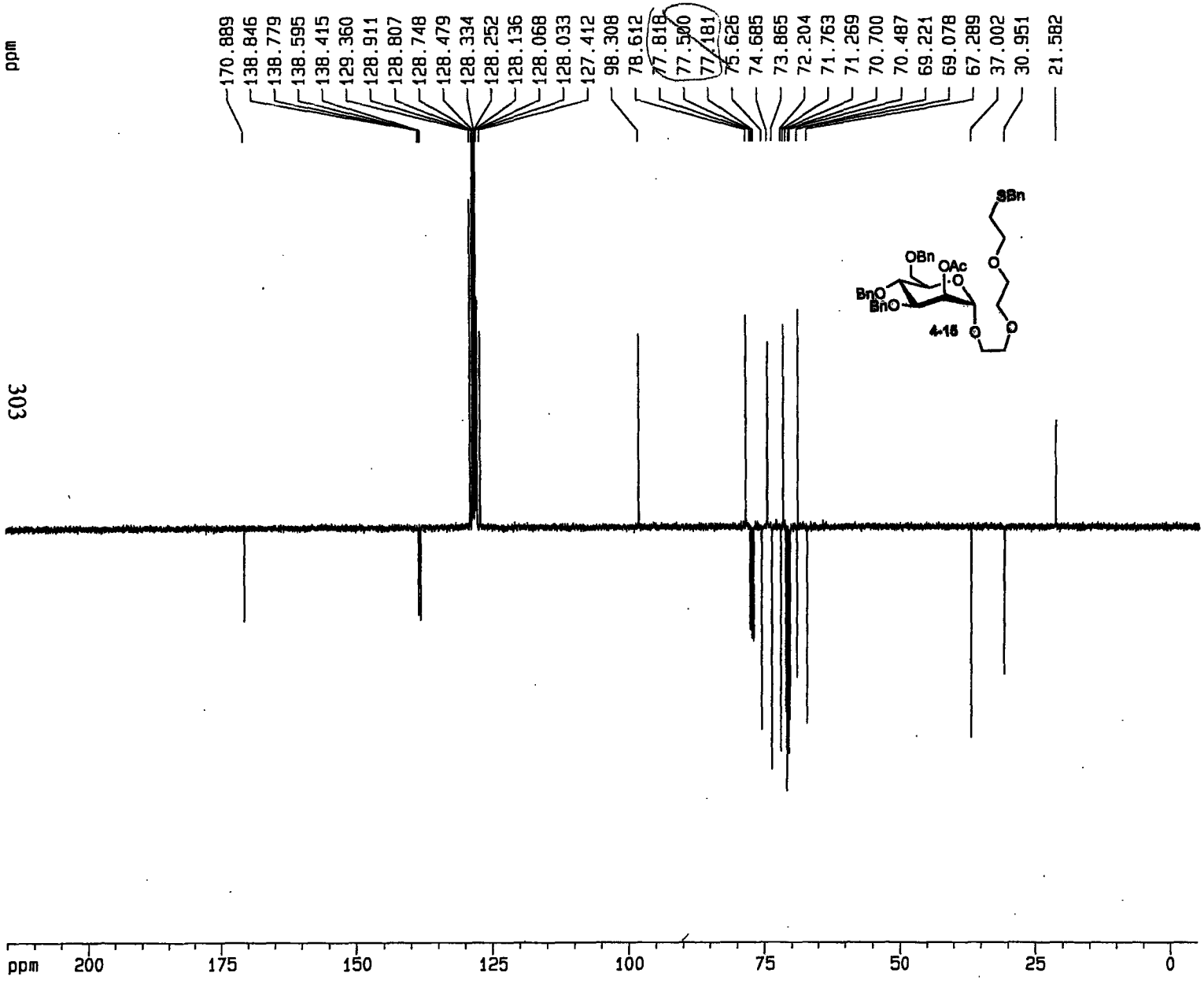

Current Data Parameters

NAME	Man-linker
EXPNO	11
PROCNO	1

F2 - Acquisition Parameters

Date_	20040805
Time	12.14
INSTRUM	spect
PROBHD	5mm BBO BB-1
PULPROG	jmod
TD	65536
SOLVENT	CDCl3
NS	768
DS	4
SWH	25125.629 Hz
FIDRES	0.383387 Hz
AQ	1.3042164 sec
RG	4096
DW	19.900 usec
DE	6.00 usec
TE	300.0 K
CNST2	145.0000000
CNST11	1.0000000
D1	2.00000000 sec
d13	0.00000300 sec
d20	0.00689655 sec
DELTA	0.00001942 sec

========== CHANNEL f1 ==========

NUC1	13C
P1	15.25 usec
p2	30.50 usec
PL1	3.00 dB
SFO1	100.6237959 MHz

========== CHANNEL f2 ==========

CPDPRG2	waltz16
NUC2	1H
PCPD2	107.50 usec
PL2	0.00 dB
PL12	24.00 dB
SFO2	400.1316005 MHz

F2 - Processing parameters

SI	32768
SF	100.6127290 MHz
WDW	EM
SSB	0
LB	1.00 Hz
GB	0
PC	1.40

1D NMR plot parameters

CX	20.00 cm
F1P	215.000 ppm
F1	21631.74 Hz
F2P	-5.000 ppm
F2	-503.06 Hz
PPMCM	11.00000 ppm/cm
HZCM	1106.73999 Hz/cm

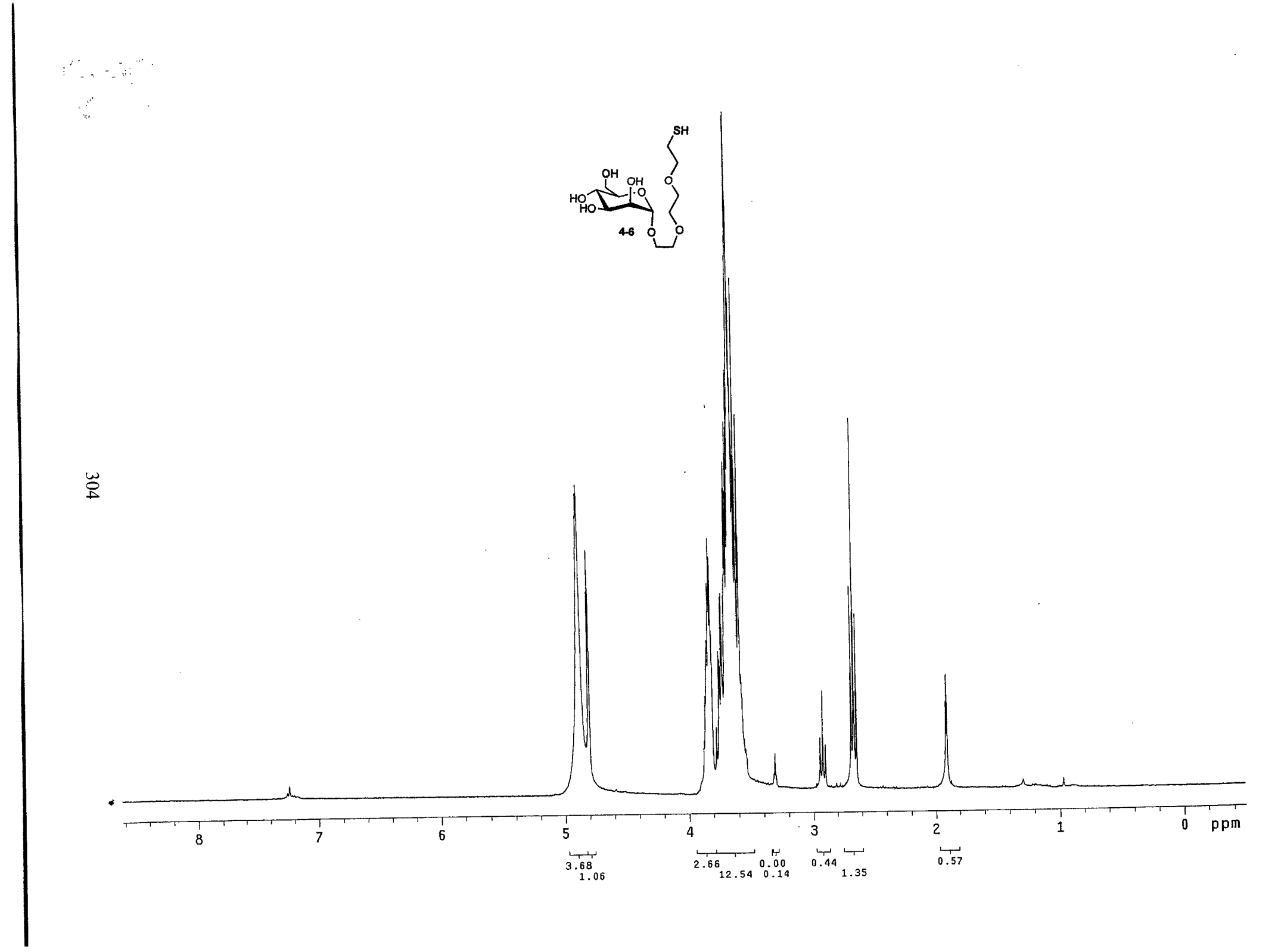
SH
OH
OH
HO
HO
O
O
O
O
4-6
8
7
6
5
4
3
2
1
0
ppm
3.68
1.06
2.66
12.54
0.00
0.14
0.44
1.35
0.57

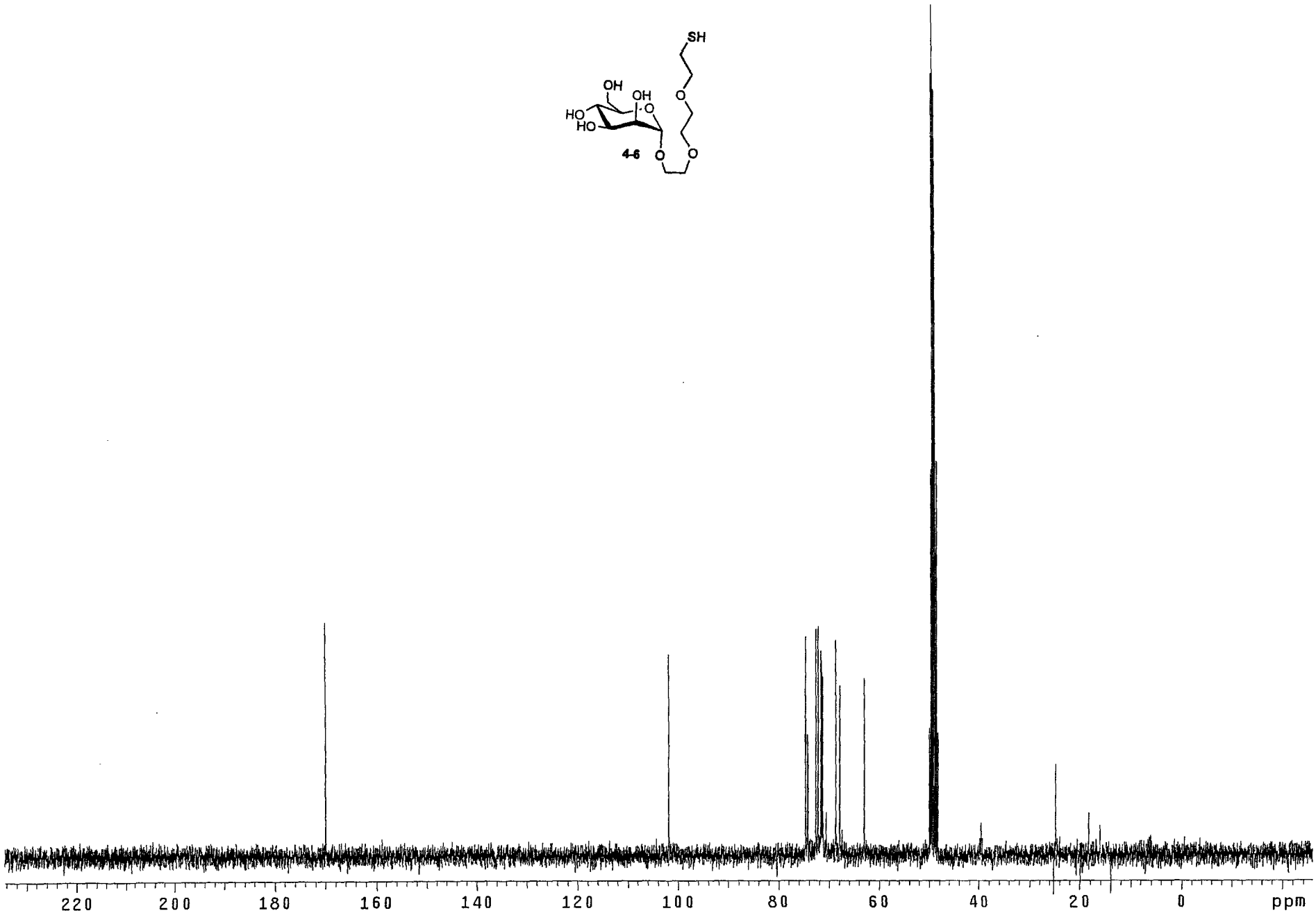
SH
OH
OH
HO
HO
O
O
O
O
4-6
220
200
180
160
140
120
100
80
60
40
20
0
ppm

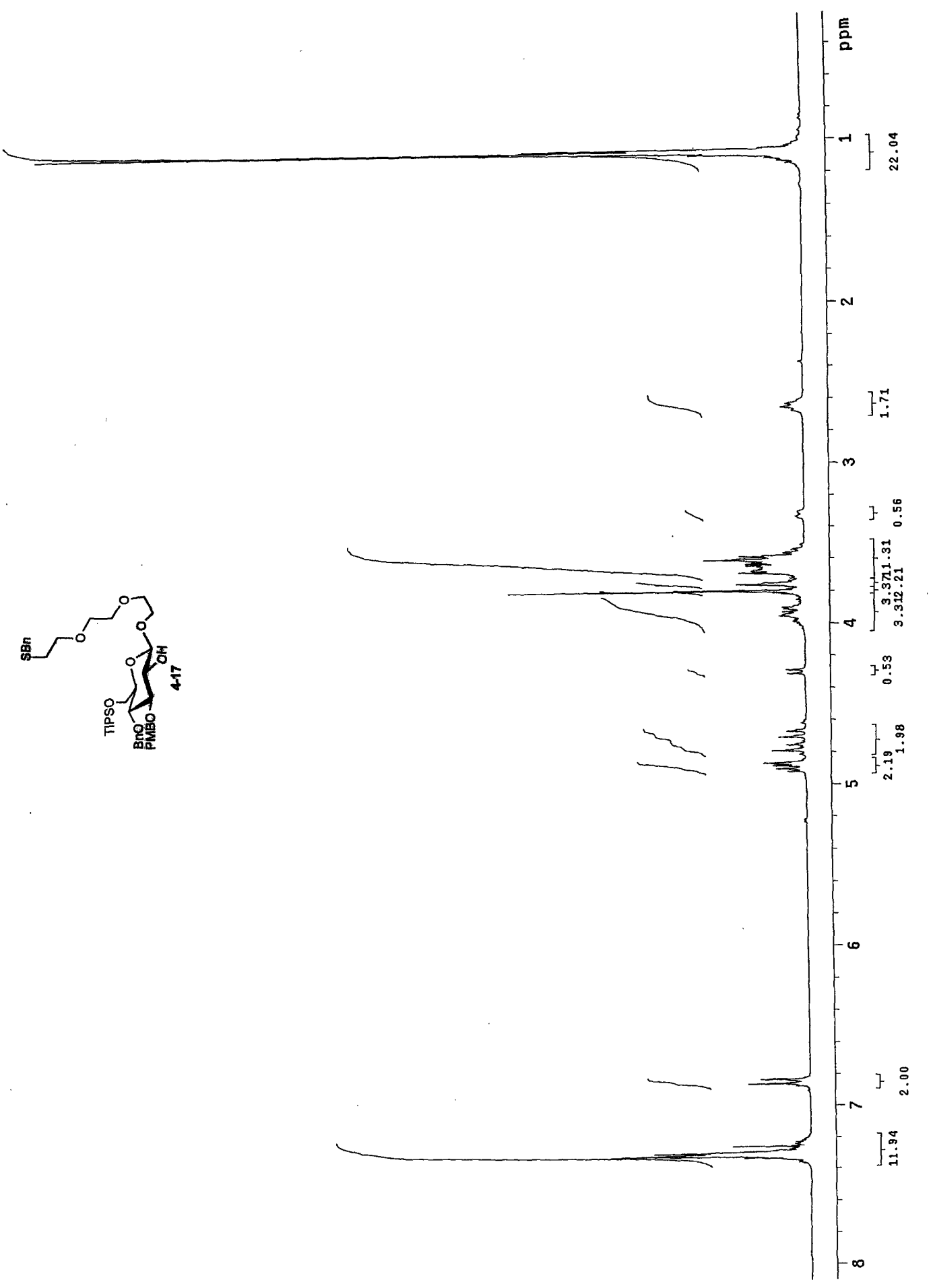
SBn
TIPSO
BnO
PMBO
OH
4-17
ppm
1
2
3
4
5
6
7
8
22.04
1.71
0.56
3.371
1.31
3.312
.21
0.53
2.19
1.98
2.00
11.94

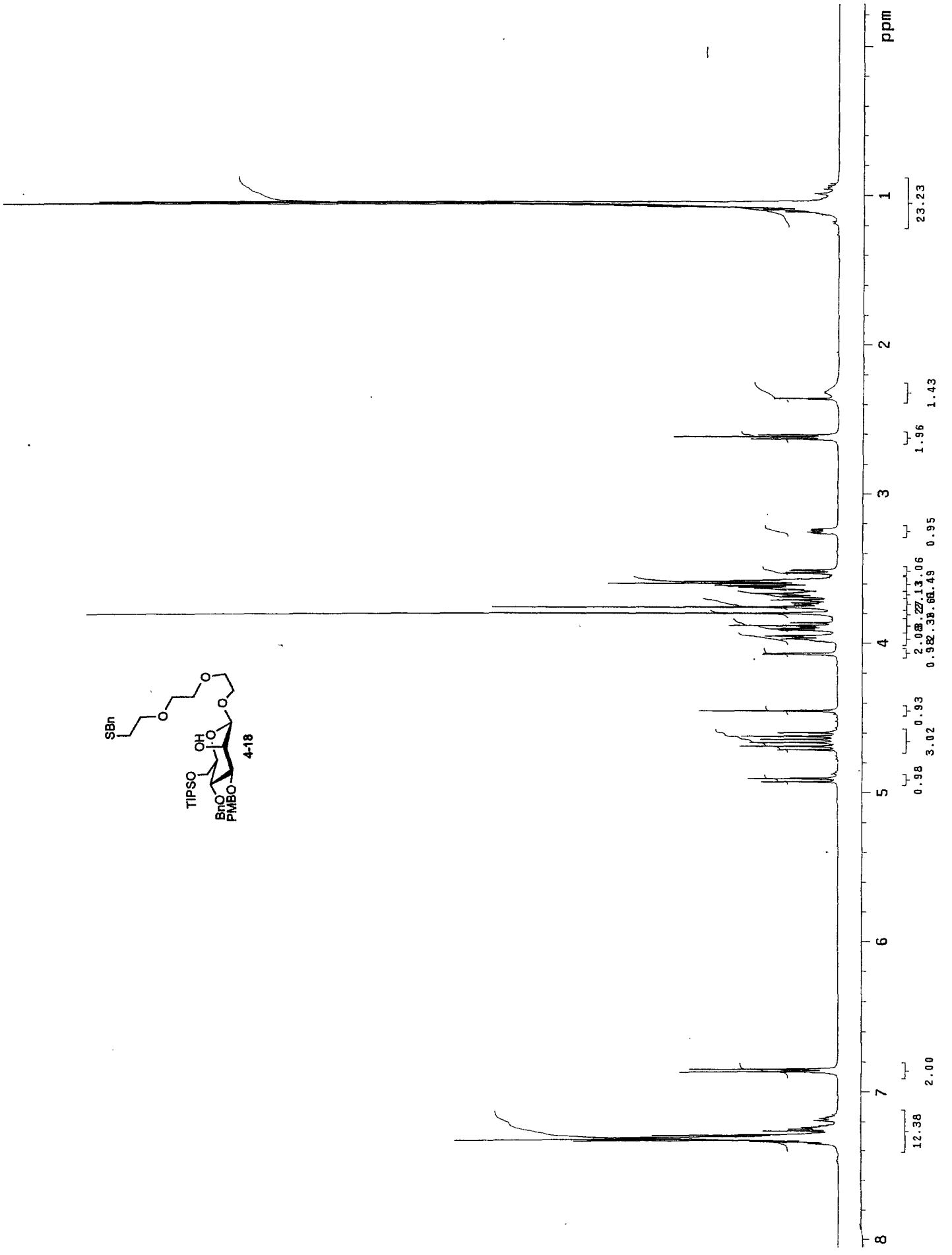
SBn
OH
TIPSO
BnO
PMBO
4-18
ppm
1
2
3
4
5
6
7
8
23.23
1.96
1.43
2.08
2.27
13.06
0.98
2.38
8.66
49
0.95
0.98
3.02
0.93
12.38
2.00

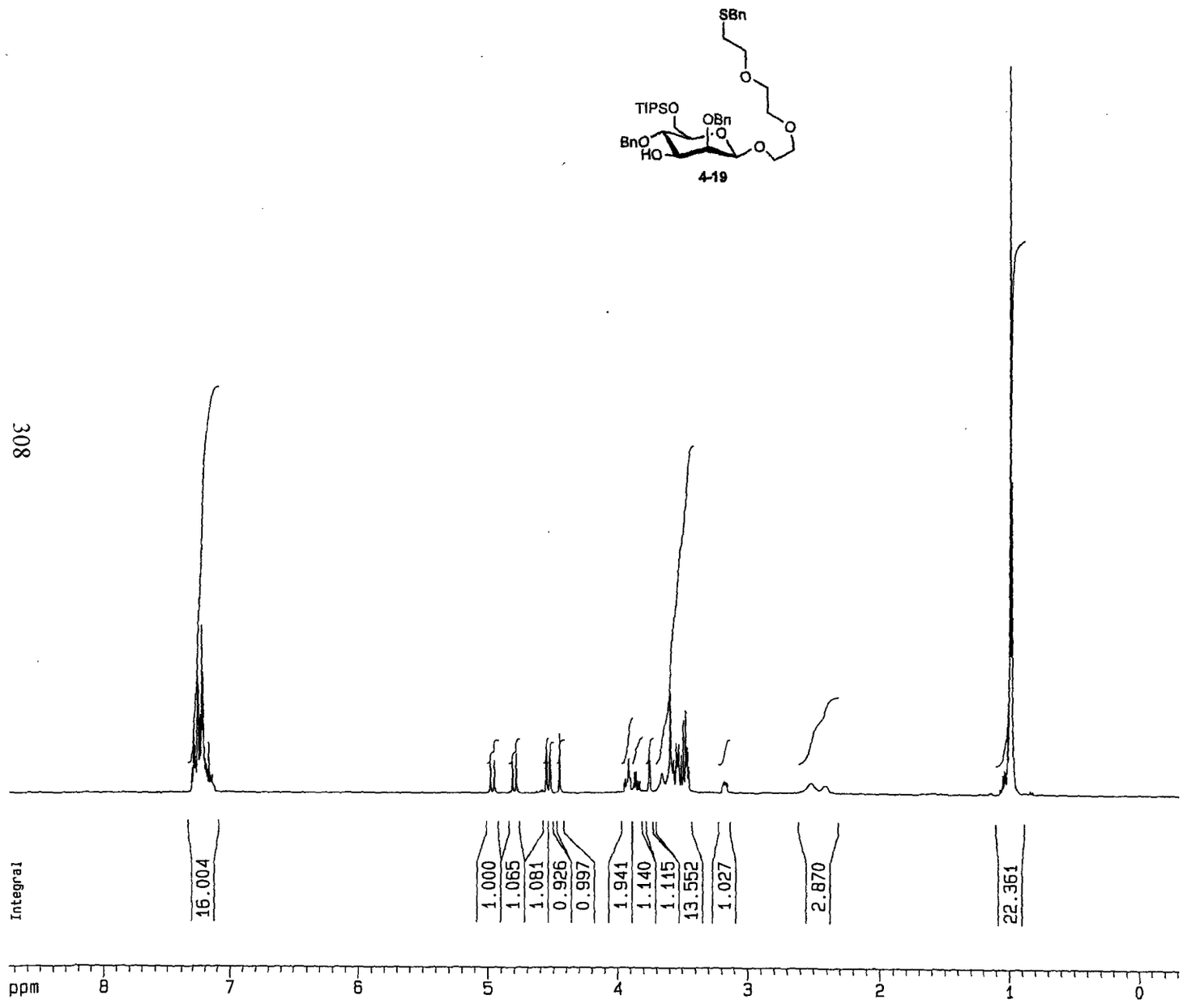


```
Current Data Parameters
NAME          DMR-III-299
EXPNO                  10
PROCNO                  1

F2 - Acquisition Parameters
Date_           20020912
Time               10.05
INSTRUM            spect
PROBHD     5mm BBO BB-1
PULPROG            zg30
TD                65536
SOLVENT           CDCl3
NS                   32
DS                    2
SWH           8278.146 Hz
FIDRES        0.126314 Hz
AQ            3.9584243 sec
RG                   57
DW              60.400 usec
DE               6.00 usec
TE              300.0 K
D1           1.00000000 sec

============ CHANNEL f1 ========
NUC1                 1H
P1                7.90 usec
PL1               0.00 dB
SFO1        400.1324710 MHz

F2 - Processing parameters
SI                32768
SF          400.1300445 MHz
WDW                  EM
SSB                   0
LB                 0.30 Hz
GB                    0
PC                 1.00

1D NMR plot parameters
CX                20.00 cm
F1P                8.741 ppm
F1              3497.47 Hz
F2P               -0.306 ppm
F2              -122.47 Hz
PPMCM          0.45234 ppm/cm
HZCM          180.99673 Hz/cm
```

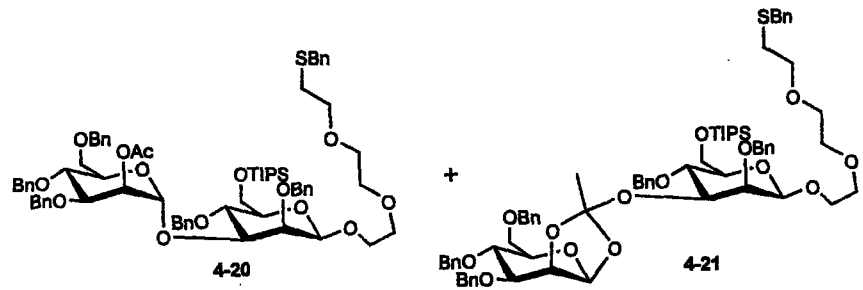

Current Data Parameters

NAME	DMR-IV-3
EXPNO	10
PROCNO	1

F2 - Acquisition Parameters

Date_	20020913
Time	8.04
INSTRUM	spect
PROBHD	5mm BBO BB-1
PULPROG	zg30
TD	65536
SOLVENT	CDCl3
NS	64
DS	2
SWH	8278.146 Hz
FIDRES	0.126314 Hz
AQ	3.9584243 sec
RG	45.3
DW	60.400 usec
DE	6.00 usec
TE	300.0 K
D1	1.00000000 sec

========== CHANNEL f1 ========

NUC1	1H
P1	7.90 usec
PL1	0.00 dB
SFO1	400.1324710 MHz

F2 - Processing parameters

SI	32768
SF	400.1300501 MHz
WDW	EM
SSB	0
LB	0.30 Hz
GB	.0
PC	1.00

1D NMR plot parameters

CX	20.00 cm
F1P	8.587 ppm
F1	3435.77 Hz
F2P	-0.297 ppm
F2	-118.69 Hz
PPMCM	0.44416 ppm/cm
HZCM	177.72290 Hz/cm

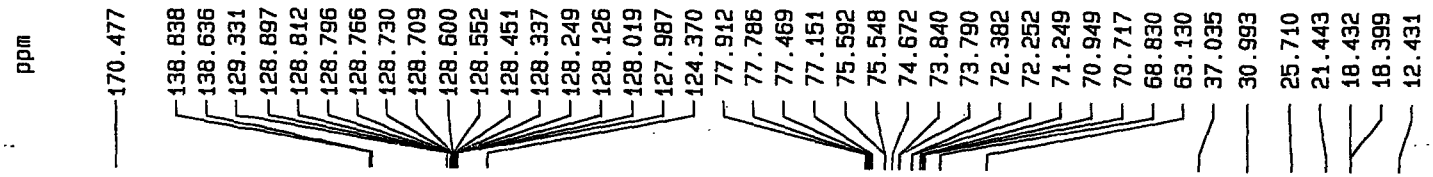

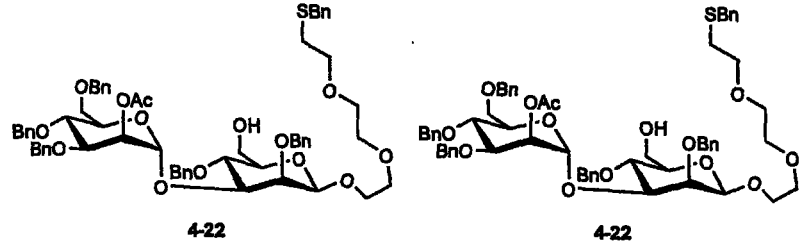

4-22 4-22

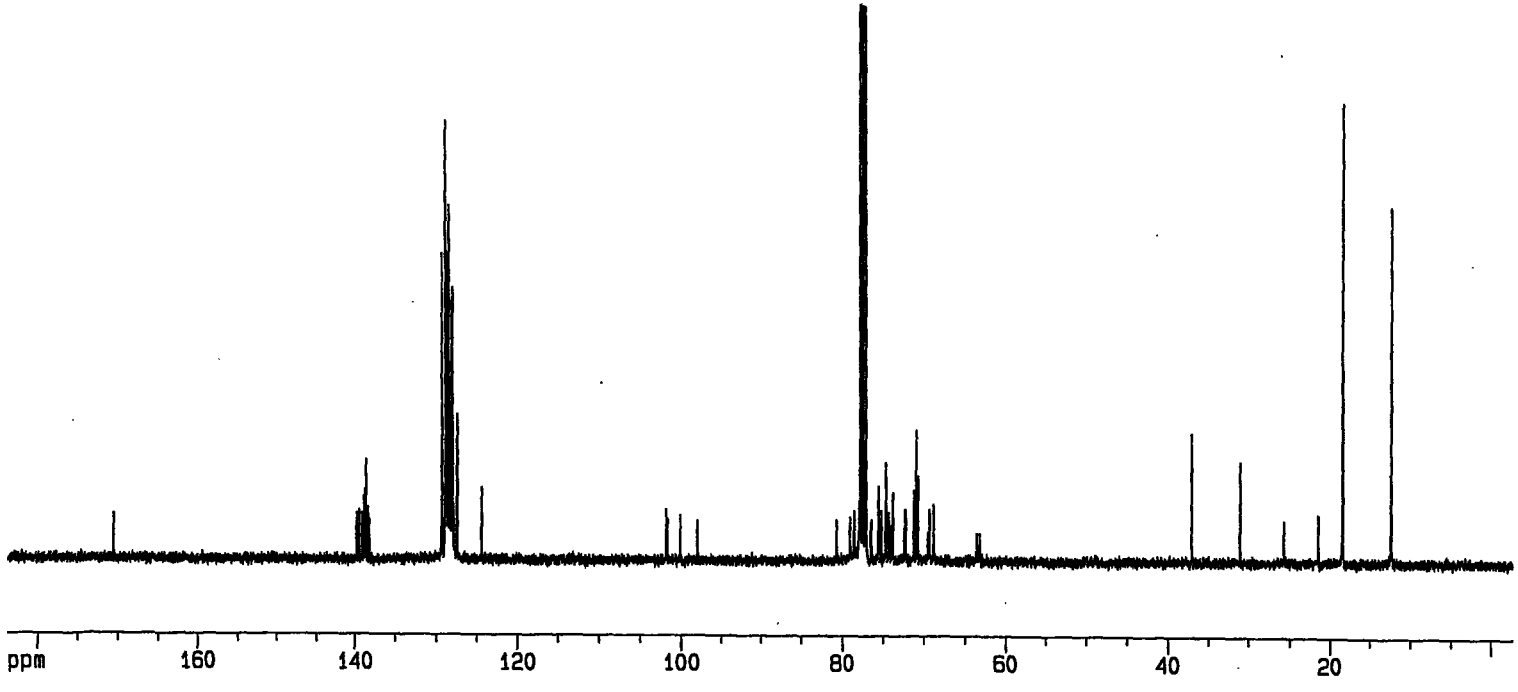


```
Current Data Parameters
NAME                  DMR-IV-3
EXPNO                       11
PROCNO                       1

F2 - Acquisition Parameters
Data_                 20020913
Time                      9.01
INSTRUM                  spect
PROBHD          5mm BBO BB-1
PULPROG                 zgpg30
TD                       65536
SOLVENT                  CDCl3
NS                        1024
DS                           4
SWH                  25125.629 Hz
FIDRES                0.383387 Hz
AQ                    1.3042164 sec
RG                        2048
DW                      19.900 usec
DE                        6.00 usec
TE                       300.0 K
D1                   2.00000000 sec
d11                  0.03000000 sec
d12                  0.00002000 sec

========== CHANNEL f1 ==========
NUC1                       13C
P1                       15.25 usec
PL1                       3.00 dB
SFO1                100.6237959 MHz

========== CHANNEL f2 ==========
CPDPRG2                waltz16
NUC2                       1H
PCPD2                   107.50 usec
PL2                       0.00 dB
PL12                     24.00 dB
PL13                     24.00 dB
SFO2                400.1316005 MHz

F2 - Processing parameters
SI                        32768
SF                  100.6127290 MHz
WDW                          EM
SSB                           0
LB                        1.00 Hz
GB                            0
PC                         1.40

1D NMR plot parameters
CX                       20.00 cm
F1P                     183.771 ppm
F1                    18489.66 Hz
F2P                      -2.748 ppm
F2                     -276.49 Hz
PPMCM                  9.32593 ppm/cm
HZCM                 938.30737 Hz/cm
```

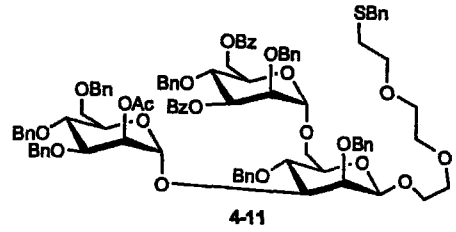

4-11


```
Current Data Parameters
NAME                  DMA-Ed-Tri
EXPNO                         10
PROCNO                         1

F2 - Acquisition Parameters
Date_                   20020917
Time                       15.59
INSTRUM                    spect
PROBHD      5mm BBO BB-1
PULPROG                    zg30
TD                        65536
SOLVENT                   CDCl3
NS                           32
DS                            0
SWH                  8278.146 Hz
FIDRES               0.126314 Hz
AQ                   3.9584243 sec
RG                           32
DW                     60.400 usec
DE                      6.00 usec
TE                      300.0 K
D1                   2.00000000 sec

========== CHANNEL f1 ========
NUC1                          1H
P1                      7.90 usec
PL1                      0.00 dB
SFO1                400.1324710 MHz

F2 - Processing parameters
SI                        32768
SF                  400.1300599 MHz
WDW                          EM
SSB                           0
LB                       0.30 Hz
GB                            0
PC                         1.00

1D NMR plot parameters
CX                      20.00 cm
F1P                      8.679 ppm
F1                    3472.73 Hz
F2P                     -0.321 ppm
F2                    -128.50 Hz
PPMCM                 0.45001 ppm/cm
HZCM                180.06137 Hz/cm
```

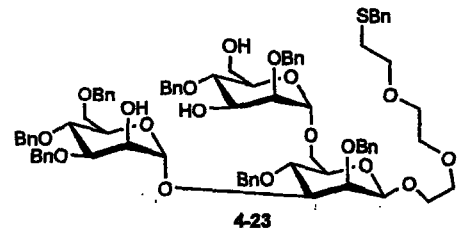

4-23


```
Current Data Parameters
NAME        OMR-IV-triol
EXPNO                 10
PROCNO                 1

F2 - Acquisition Parameters
Date_           20020919
Time               10.03
INSTRUM            spect
PROBHD     5mm BBO BB-1
PULPROG            zg30
TD                65536
SOLVENT           CDCl3
NS                   64
DS                    0
SWH           8278.146 Hz
FIDRES        0.126314 Hz
AQ           3.9584243 sec
RG                 28.5
DW              60.400 usec
DE               6.00 usec
TE              300.0 K
D1           2.00000000 sec

========== CHANNEL f1 ========
NUC1                  1H
P1                 7.90 usec
PL1                0.00 dB
SFO1        400.1324710 MHz

F2 - Processing parameters
SI                 32768
SF          400.1300672 MHz
WDW                   EM
SSB                   0
LB                 0.30 Hz
GB                    0
PC                 1.00

1D NMR plot parameters
CX                20.00 cm
F1P                8.123 ppm
F1              3250.22 Hz
F2P               -0.199 ppm
F2                -79.75 Hz
PPMCM          0.41611 ppm/cm
HZCM          166.49829 Hz/cm
```

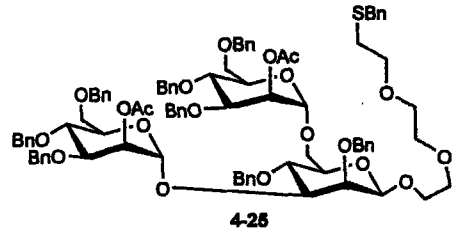

4-25


```
Current Data Parameters
NAME                  DMR-9-18.2
EXPNO                         10
PROCNO                         1

F2 - Acquisition Parameters
Date_                   20020918
Time                       15.36
INSTRUM                    spect
PROBHD          5mm BBO BB-1
PULPROG                    zg30
TD                        65536
SOLVENT                   CDCl3
NS                            32
DS                             2
SWH                 8278.146 Hz
FIDRES              0.126314 Hz
AQ                  3.9584243 sec
RG                         40.3
DW                    60.400 usec
DE                     6.00 usec
TE                     300.0 K
D1                  1.00000000 sec

========== CHANNEL f1 ========
NUC1                       1H
P1                     7.90 usec
PL1                    0.00 dB
SFO1              400.1324710 MHz

F2 - Processing parameters
SI                         32768
SF                400.1300560 MHz
WDW                        EM
SSB                         0
LB                     0.30 Hz
GB                          0
PC                      1.00

1D NMR plot parameters
CX                     20.00 cm
F1P                    8.385 ppm
F1                   3354.98 Hz
F2P                   -0.405 ppm
F2                   -162.06 Hz
PPMCM                0.43949 ppm/cm
HZCM                175.85214 Hz/cm
```

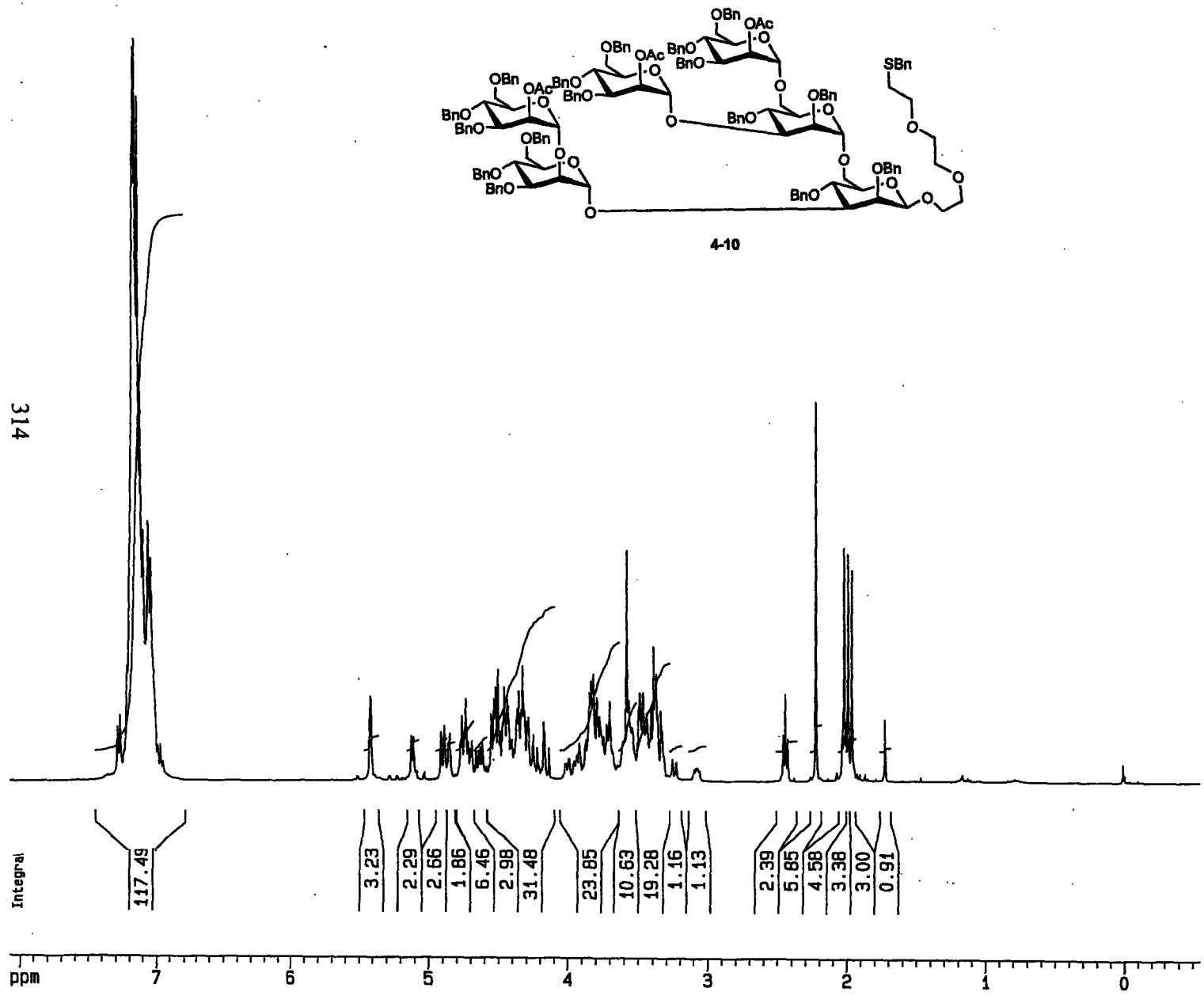

Current Data Parameters

NAME	hexa-SBn
EXPNO	10
PROCNO	1

F2 - Acquisition Parameters

Date_	20020920
Time	10.06
INSTRUM	spect
PROBHD	5mm BBO BB-1
PULPROG	zg30
TD	65536
SOLVENT	CDCl3
NS	64
DS	2
SWH	8278.146 Hz
FIDRES	0.126314 Hz
AQ	3.9584243 sec
RG	20.2
DW	60.400 usec
DE	6.00 usec
TE	300.0 K
D1	1.00000000 sec

========== CHANNEL f1 ========

NUC1	1H
P1	7.90 usec
PL1	0.00 dB
SFO1	400.1324710 MHz

F2 - Processing parameters

SI	32768
SF	400.1300964 MHz
WDW	EM
SSB	0
LB	0.30 Hz
GB	0
PC	1.00

1D NMR plot parameters

CX	20.00 cm
F1P	8.073 ppm
F1	3230.40 Hz
F2P	-0.553 ppm
F2	-221.17 Hz
PPMCM	0.43131 ppm/cm
HZCM	172.57829 Hz/cm

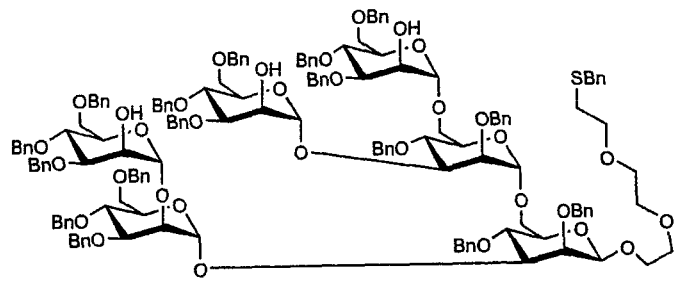
OBn
OH
BnO
BnO
SBn
O

4-26

8
7
6
5
4
3
2
1
ppm
81.19
2.00 6.78
2.14 1.10
27.29
3.40
23.54
28.35
0.83
2.32 0.95
2.78
1.50
0.28
0.17

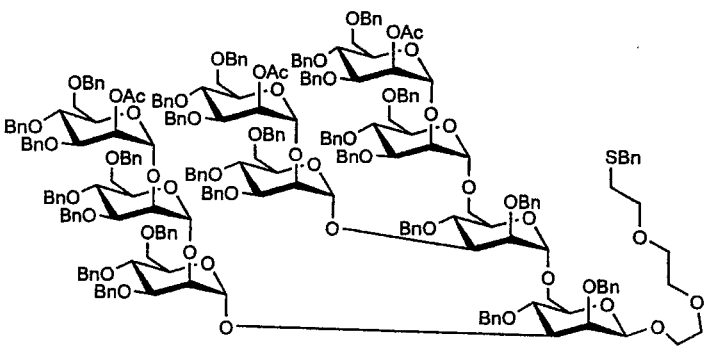

4-9

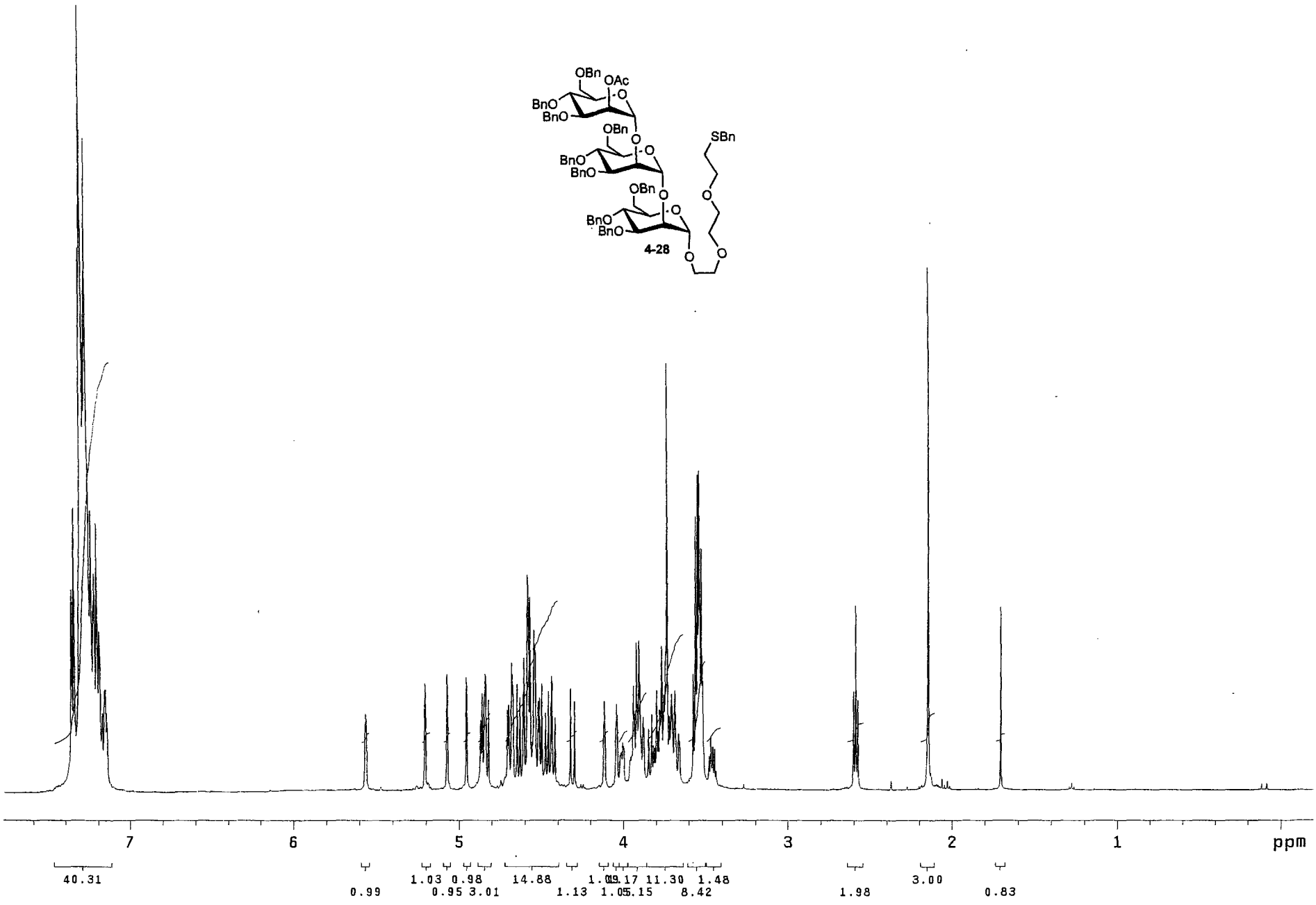
OBn
OAc
BnO
BnO
OBn
BnO
BnO
OBn
BnO
BnO
SBn
4-28
7
6
5
4
3
2
1
ppm
40.31
0.99
1.03
0.98
0.95
3.01
14.88
1.13
1.05
5.15
8.42
1.98
3.00
0.83

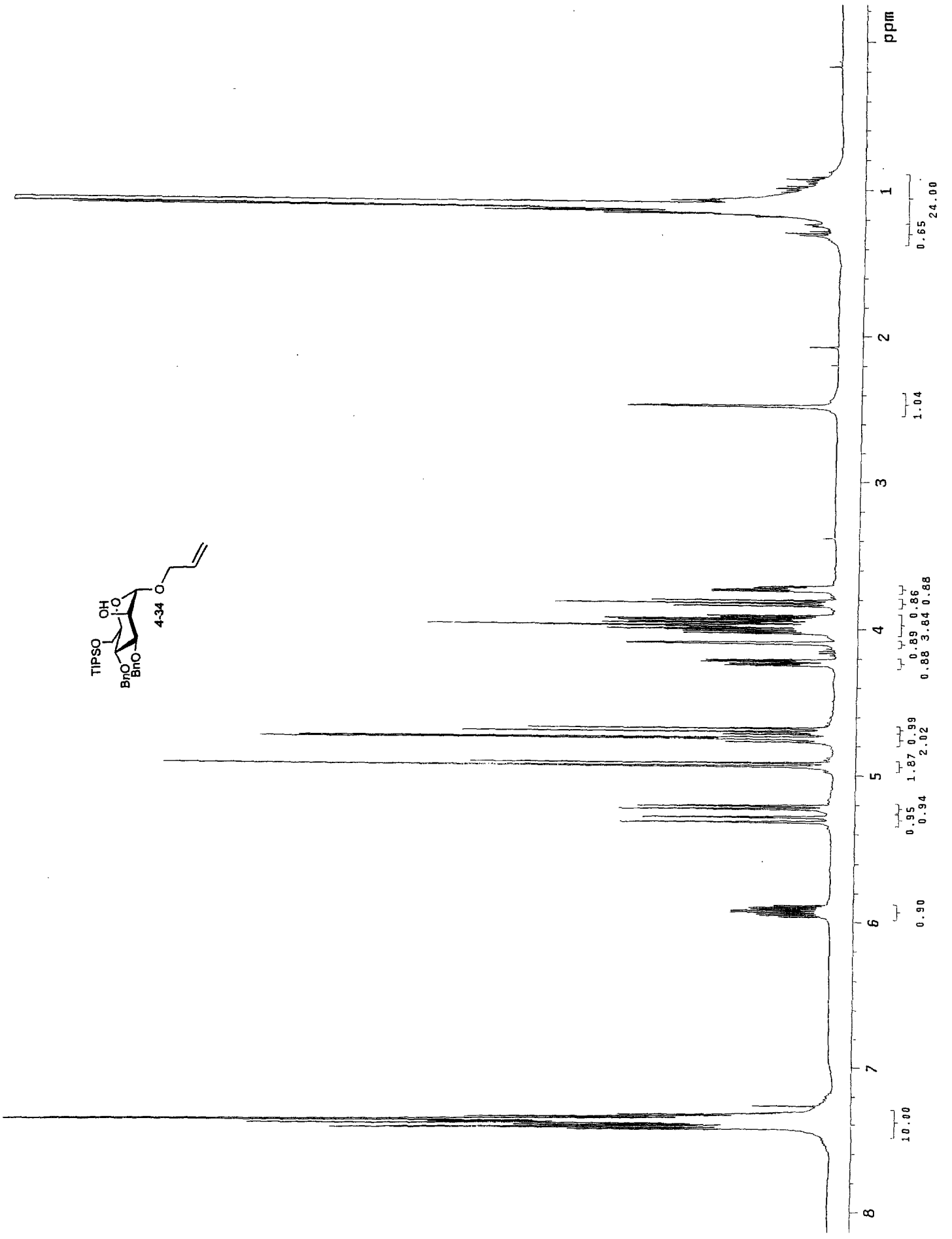
TIPSO
BnO
BnO
OH
4-34
O
ppm
1
2
3
4
5
6
7
8
0.65
24.00
1.04
0.89 0.86
0.88 3.84 0.88
0.95
0.94
1.87 0.99
2.02
0.90
10.00

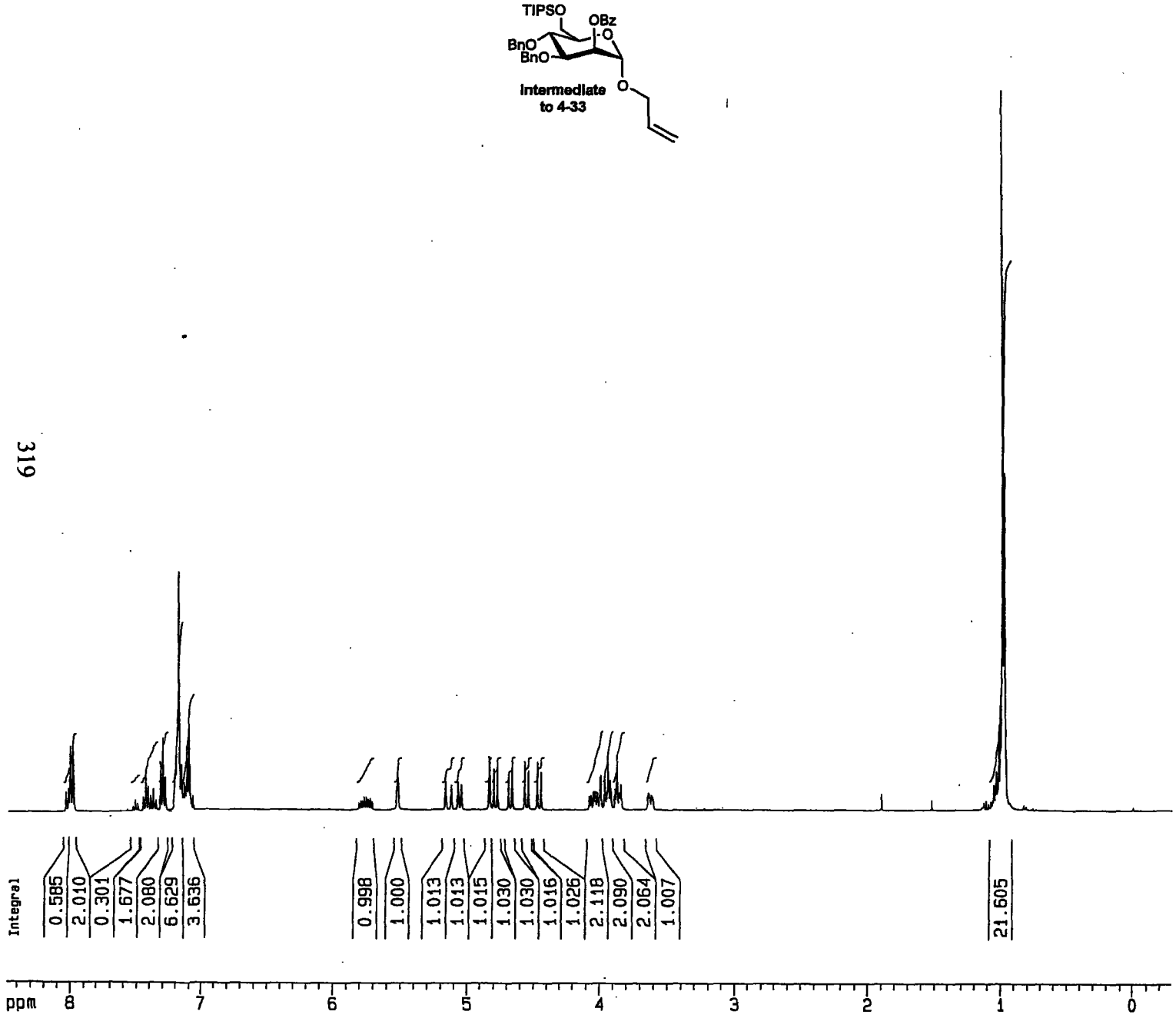

Current Data Parameters

NAME	DMR-V-9
EXPNO	10
PROCNO	1

F2 - Acquisition Parameters

Date_	20030531
Time	16.13
INSTRUM	spect
PROBHD	5mm BBO BB-1
PULPROG	zg30
TD	65536
SOLVENT	CDCl3
NS	64
DS	2
SWH	8278.146 Hz
FIDRES	0.126314 Hz
AQ	3.9584243 sec
RG	22.6
DW	60.400 usec
DE	6.00 usec
TE	300.0 K
D1	1.00000000 sec

========== CHANNEL f1 ========

NUC1	1H
P1	7.90 usec
PL1	0.00 dB
SFO1	400.1324710 MHz

F2 - Processing parameters

SI	32768
SF	400.1300846 MHz
WDW	EM
SSB	0
LB	0.30 Hz
GB	0
PC	1.00

1D NMR plot parameters

CX	20.00 cm
F1P	8.477 ppm
F1	3391.86 Hz
F2P	-0.289 ppm
F2	-115.83 Hz
PPMCM	0.43832 ppm/cm
HZCM	175.38445 Hz/cm

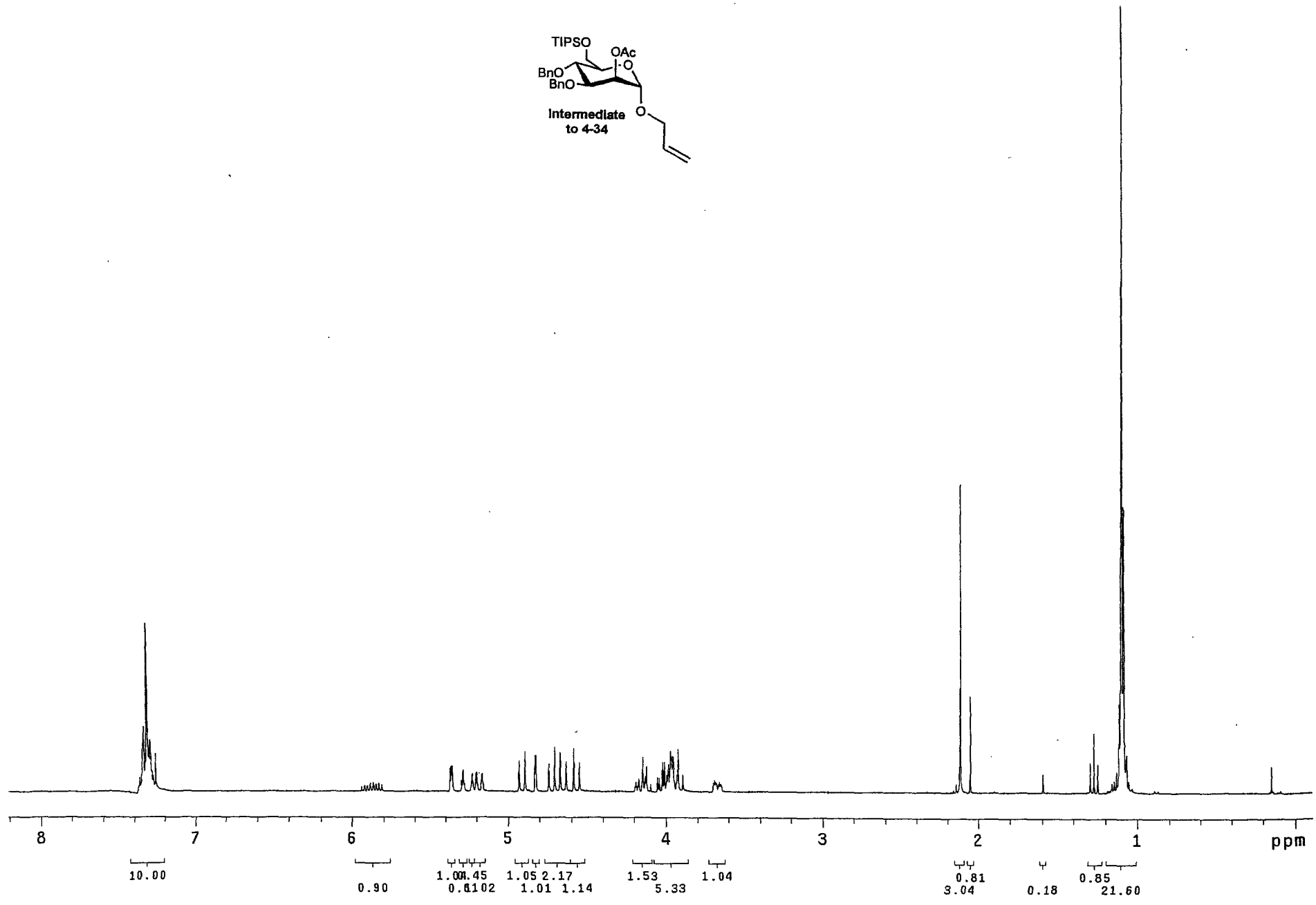
TIPSO
OAc
BnO
BnO
O
Intermediate
to 4-34
8
7
6
5
4
3
2
1
ppm
10.00
0.90
1.00 0.61 0.45 1.02
1.05 1.01 2.17 1.14
1.53 5.33
1.04
0.81 3.04
0.18
0.85 21.60

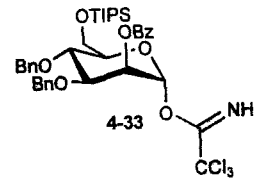
OTIPS
OBz
BnO
BnO
O
4-33
O
NH
CCl3

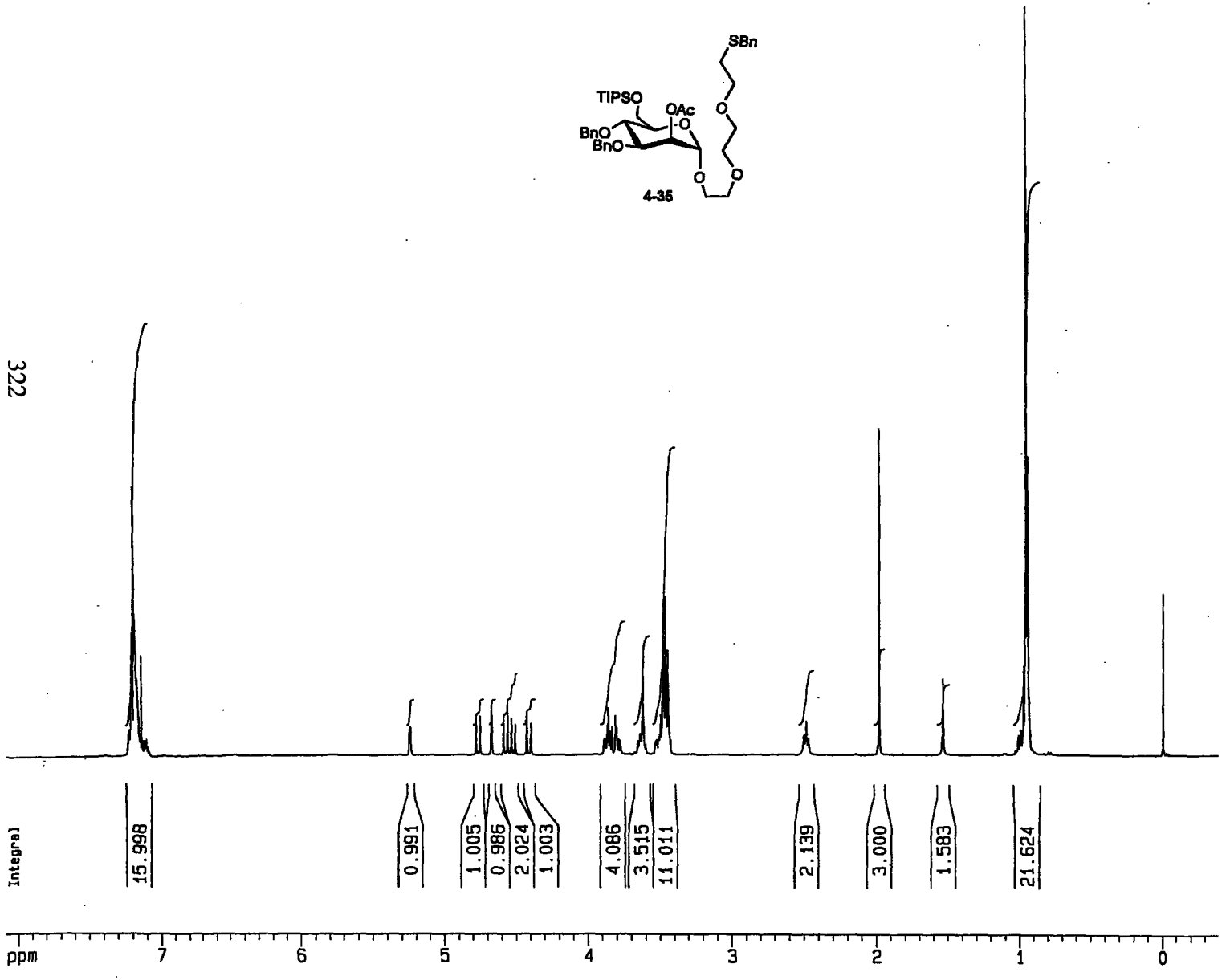


```
Current Data Parameters
NAME                  ac-tips
EXPNO                      10
PROCNO                      1

F2 - Acquisition Parameters
Date_               20040807
Time                   15.10
INSTRUM                spect
PROBHD      5mm BBO BB-1
PULPROG                zg30
TD                     65536
SOLVENT                CDCl3
NS                        64
DS                         2
SWH                 8278.146 Hz
FIDRES              0.126314 Hz
AQ                3.9584243 sec
RG                      90.5
DW                    60.400 usec
DE                     6.00 usec
TE                     300.0 K
D1                1.00000000 sec

============ CHANNEL f1 =========
NUC1                       1H
P1                     7.90 usec
PL1                    0.00 dB
SFO1              400.1324710 MHz

F2 - Processing parameters
SI                         32768
SF                400.1300583 MHz
WDW                        EM
SSB                         0
LB                     0.30 Hz
GB                          0
PC                      1.00

1D NMR plot parameters
CX                     20.00 cm
F1P                    8.085 ppm
F1                   3234.95 Hz
F2P                   -0.387 ppm
F2                   -154.88 Hz
PPMCM                0.42359 ppm/cm
HZCM               169.49185 Hz/cm
```

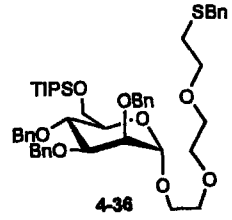

Current Data Parameters

NAME	bn-tips
EXPNO	10
PROCNO	1

F2 - Acquisition Parameters

Date_	20040807
Time	13.59
INSTRUM	spect
PROBHD	5mm BBO BB-1
PULPROG	zg30
TD	65536
SOLVENT	CDCl3
NS	64
DS	2
SWH	8278.146 Hz
FIDRES	0.126314 Hz
AQ	3.9584243 sec
RG	161.3
DW	60.400 usec
DE	6.00 usec
TE	300.0 K
D1	1.00000000 sec

========== CHANNEL f1 ========

NUC1	1H
P1	7.90 usec
PL1	0.00 dB
SFO1	400.1324710 MHz

F2 - Processing parameters

SI	32768
SF	400.1300395 MHz
WDW	EM
SSB	0
LB	0.30 Hz
GB	0
PC	1.00

1D NMR plot parameters

CX	20.00 cm
F1P	8.109 ppm
F1	3244.64 Hz
F2P	-0.089 ppm
F2	-35.55 Hz
PPMCM	0.40989 ppm/cm
HZCM	164.00961 Hz/cm

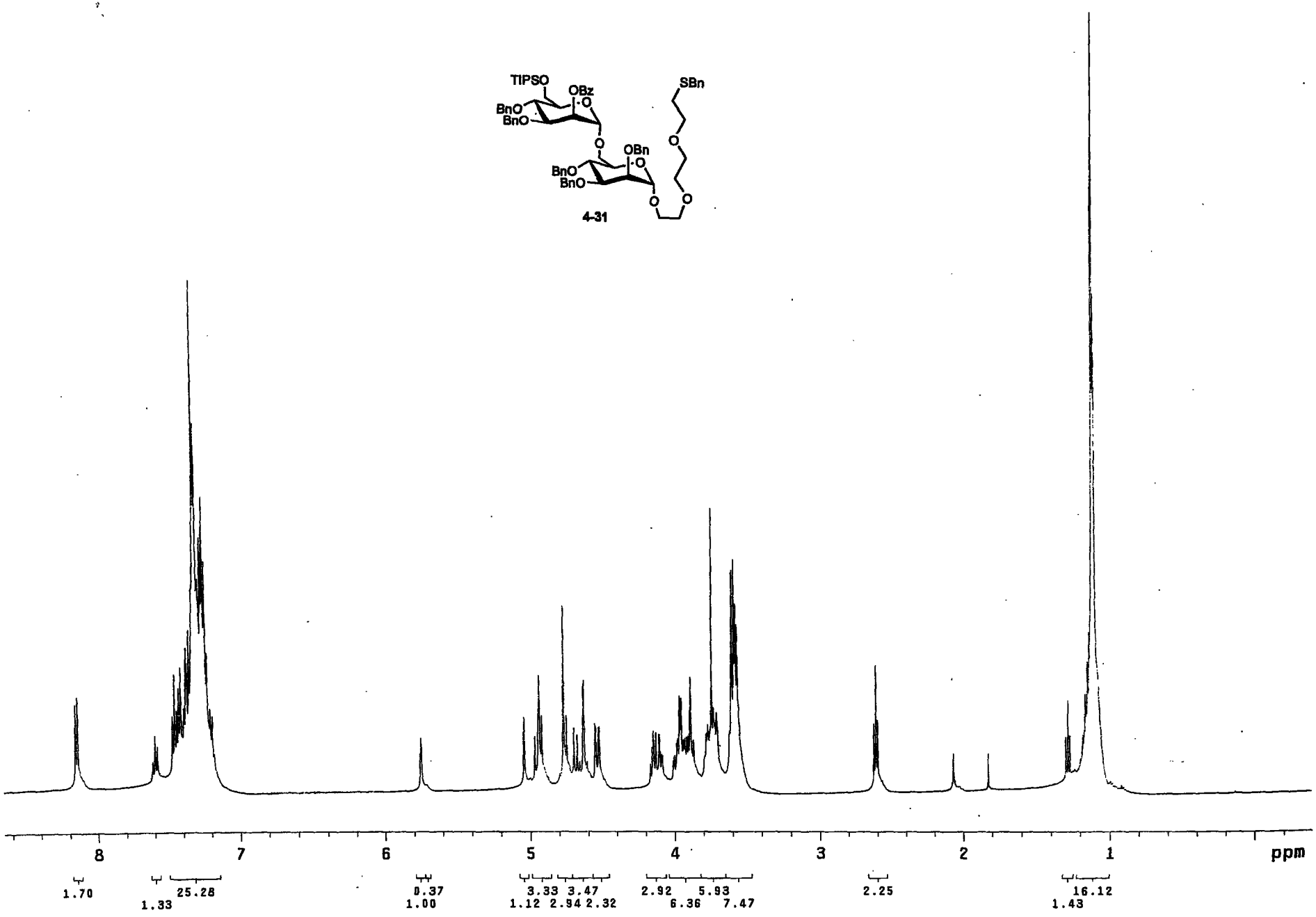
TIPSO
OBz
BnO
BnO
O
OBn
BnO
BnO
O
SBn
O
O
O
4-31
8
7
6
5
4
3
2
1
ppm
1.70
1.33
25.28
0.37
1.00
3.33
1.12
3.47
2.94
2.32
2.92
6.36
5.93
7.47
2.25
16.12
1.43

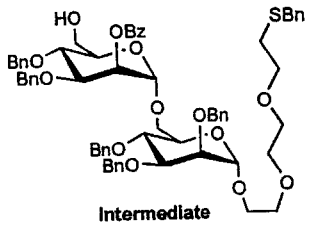

Intermediate
to 4-30

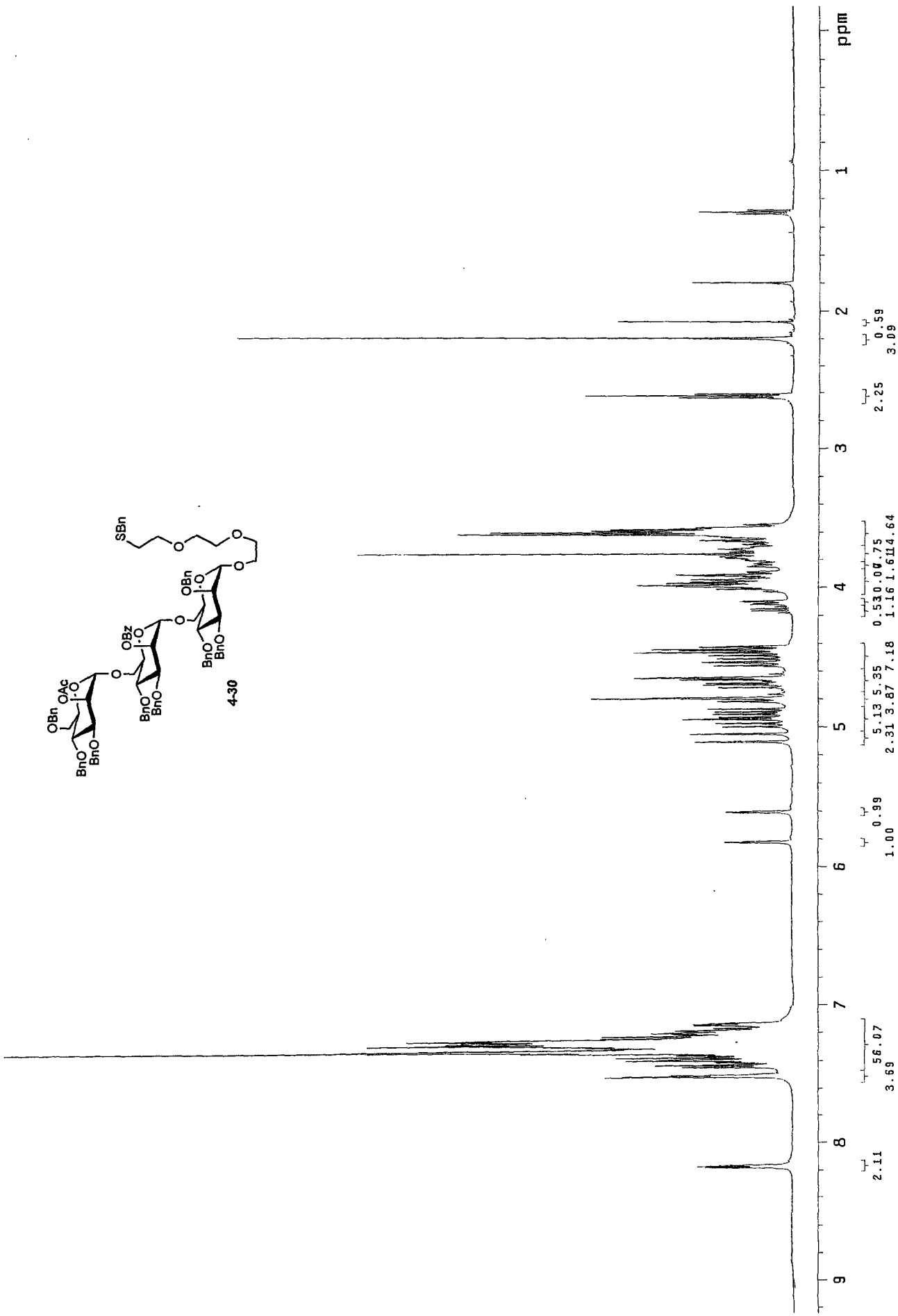
SBn
OBn
OBz
OAc
BnO
BnO
4-30
ppm
1
2
3
4
5
6
7
8
9
2.11
56.07
3.69
0.99
1.00
5.13 5.35
2.31 3.87 7.18
0.53 0.75
1.16 1.61 4.64
2.25
0.59
3.09

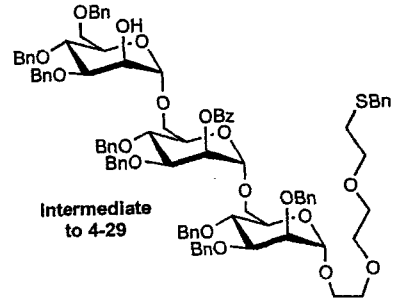

Intermediate to 4-29

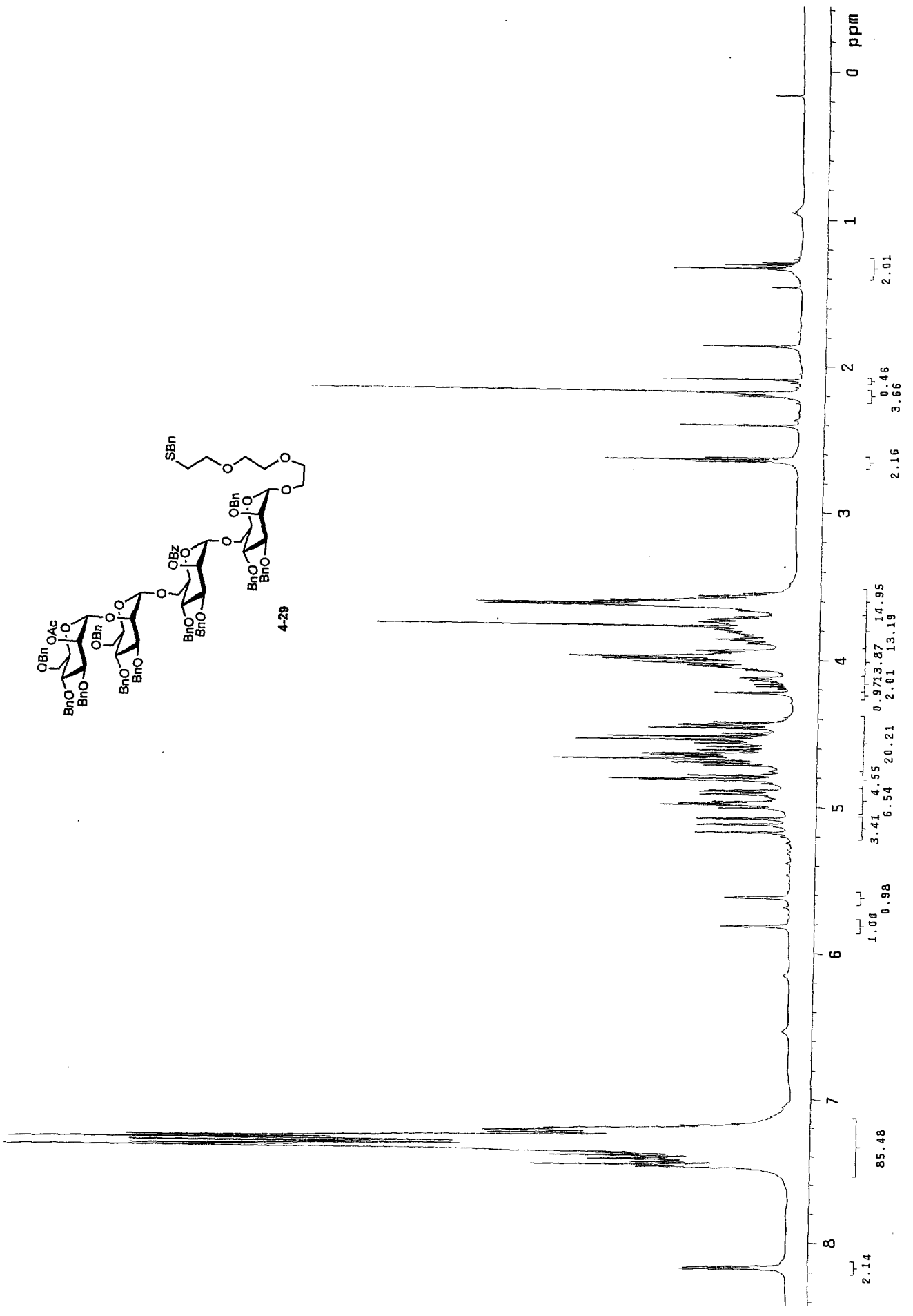
4-29
0 ppm

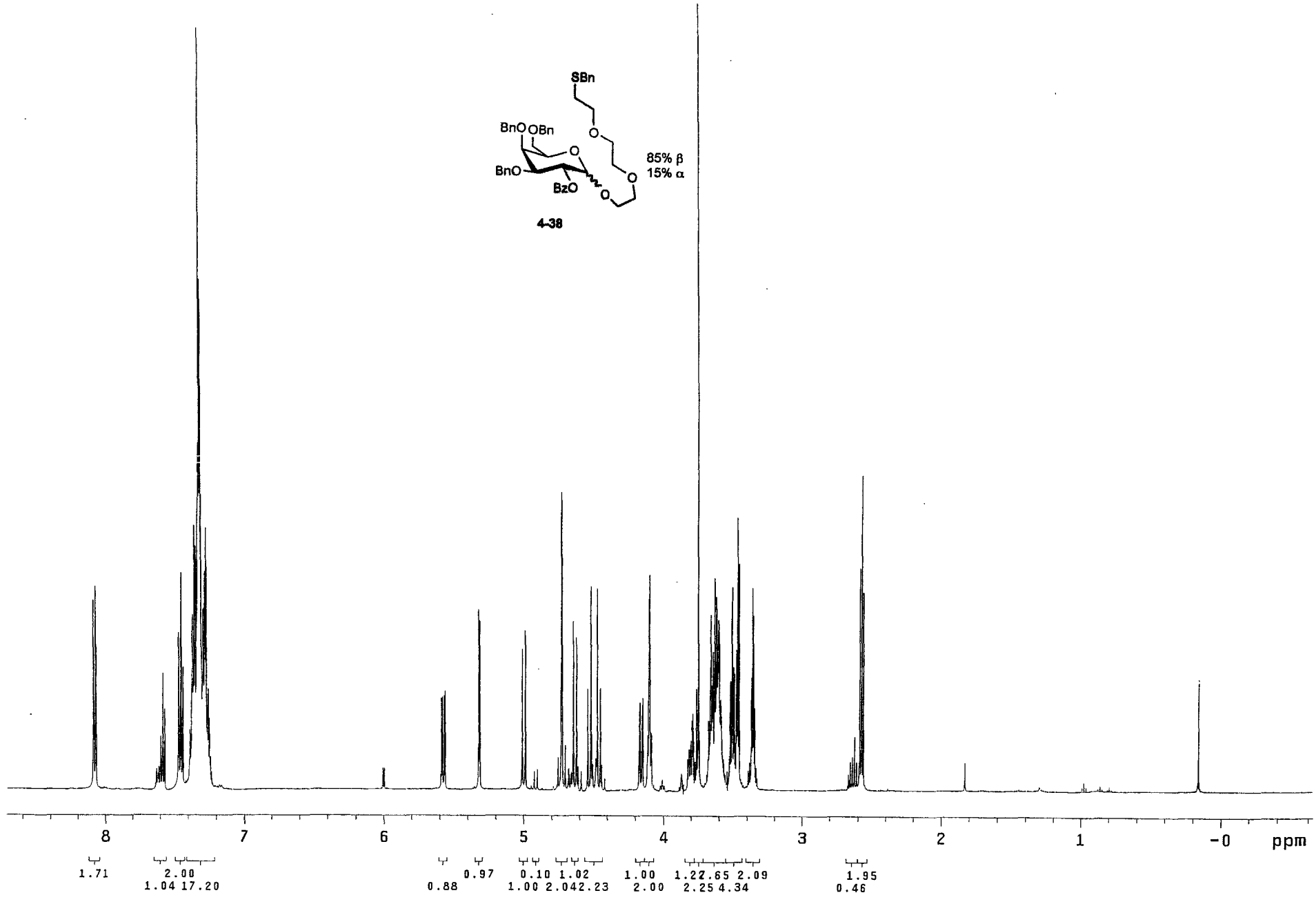
SBn
BnO
OBn
BnO
BzO
O
85% β
15% α
4-38
8
7
6
5
4
3
2
1
-0
ppm
1.71
2.00
1.04 17.20
0.88
0.97
0.10 1.02
1.00 2.04 2.23
1.00
2.00
1.22 2.65 2.09
2.25 4.34
1.95
0.46

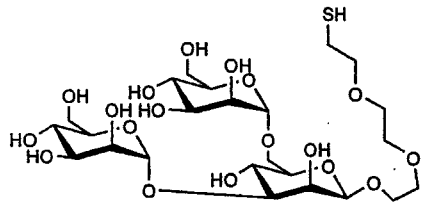
SH
OH
OH
HO
HO
OH
OH
HO
HO
HO
OH
O
O
O
O
O
O
O
O

4-3

5.5
5.0
4.5
4.0
3.5
3.0
2.5
2.0
ppm
1.00
10.80
1.12
0.93
0.93
2.02
1.18
5.70
9.16
9.94
0.87
0.66
1.12
3.02

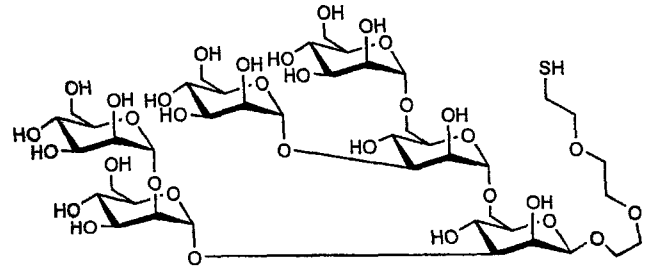

4-2

5.5
5.0
4.5
4.0
3.5
3.0
2.5
2.0
1.5
1.0
0.5
ppm
1.35
1.69
1.33
10.50
1.45
2.98
5.58
24.81
1.38
1.33
1.53
19.03

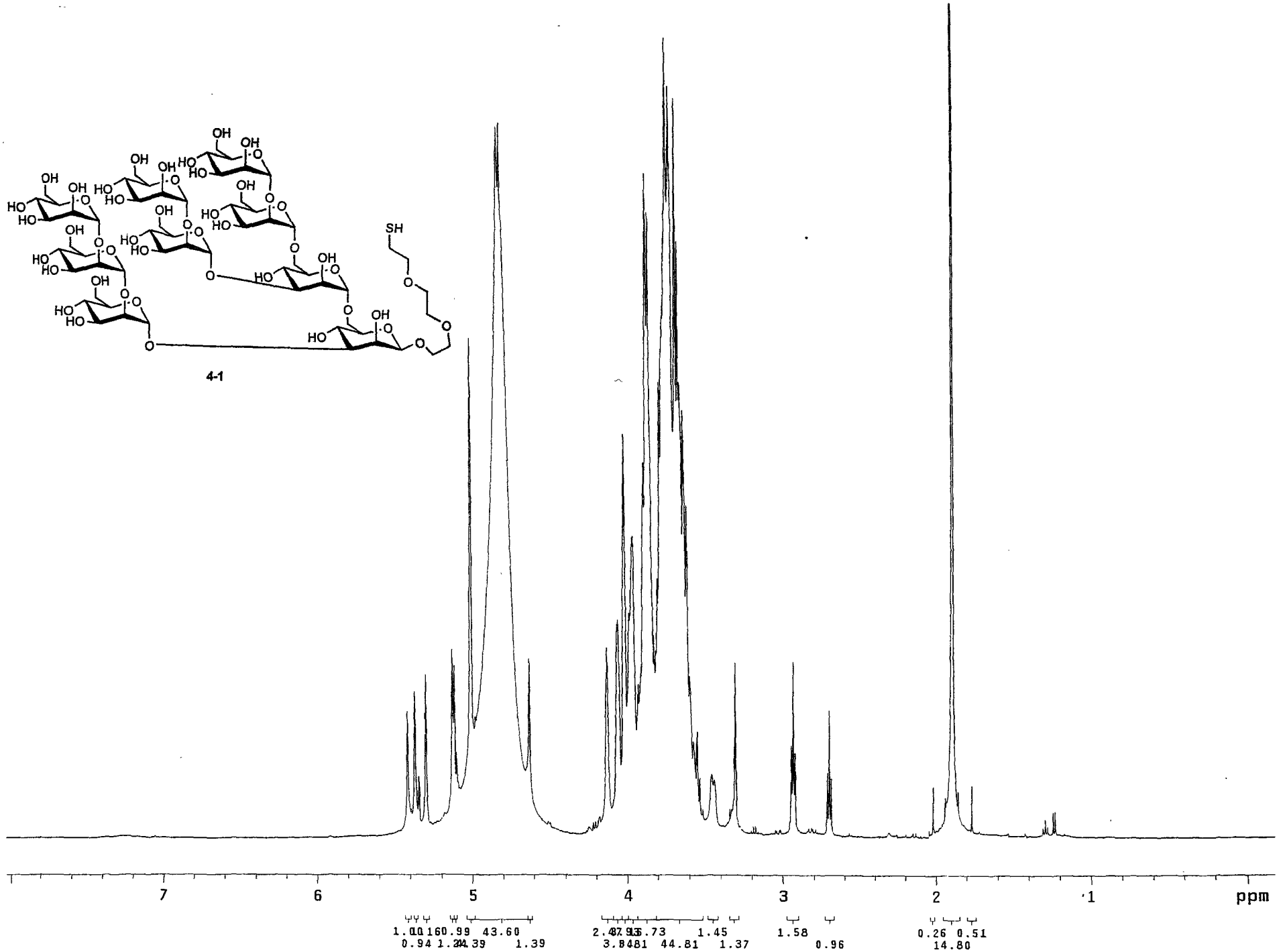
4-1
7
6
5
4
3
2
1
ppm

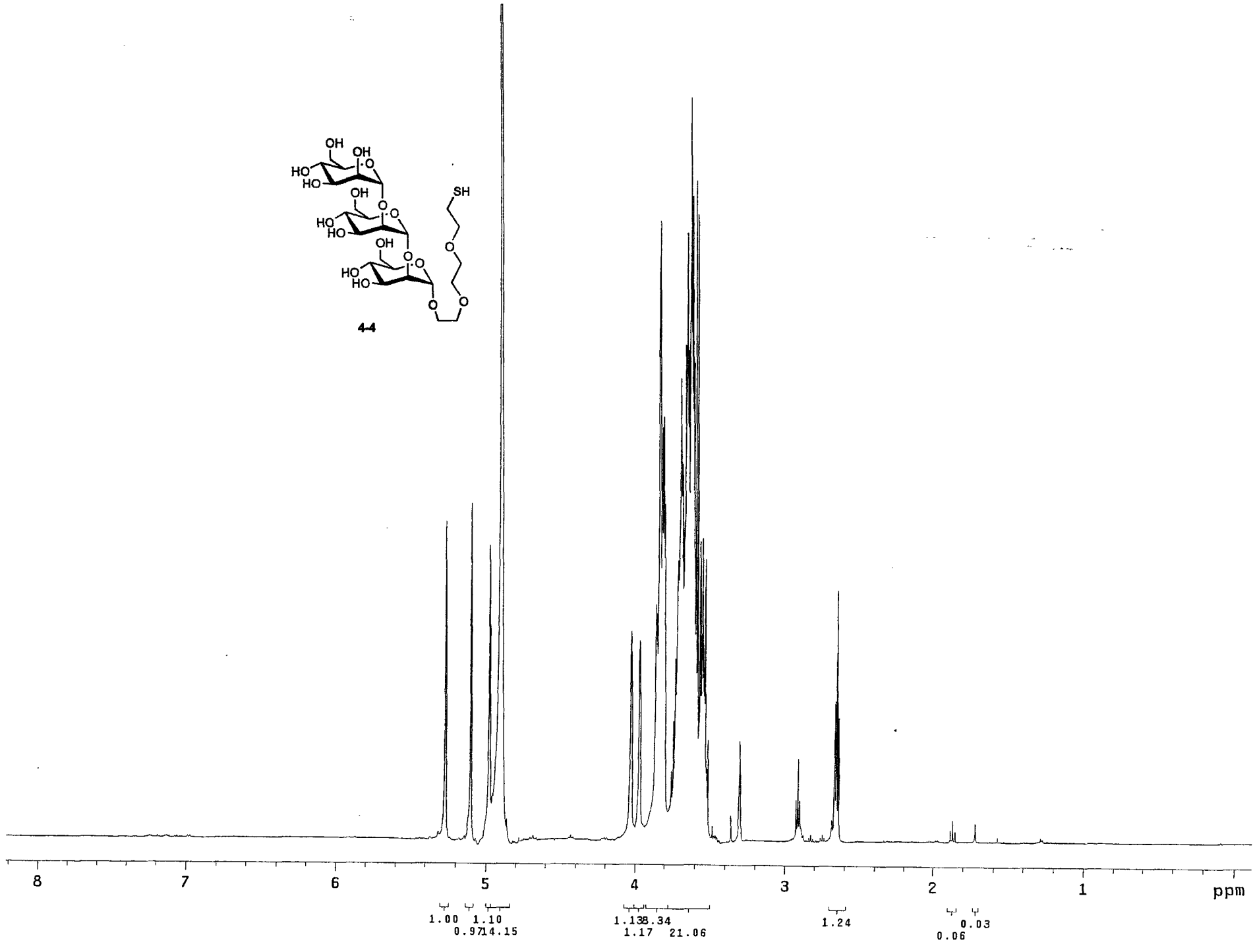
OH
OH
HO
HO
OH
HO
HO
OH
HO
HO
O
O
O
O
O
O
O
SH
4-4
8
7
6
5
4
3
2
1
ppm
1.00
1.10
0.97
14.15
1.13
8.34
1.17
21.06
1.24
0.03
0.06

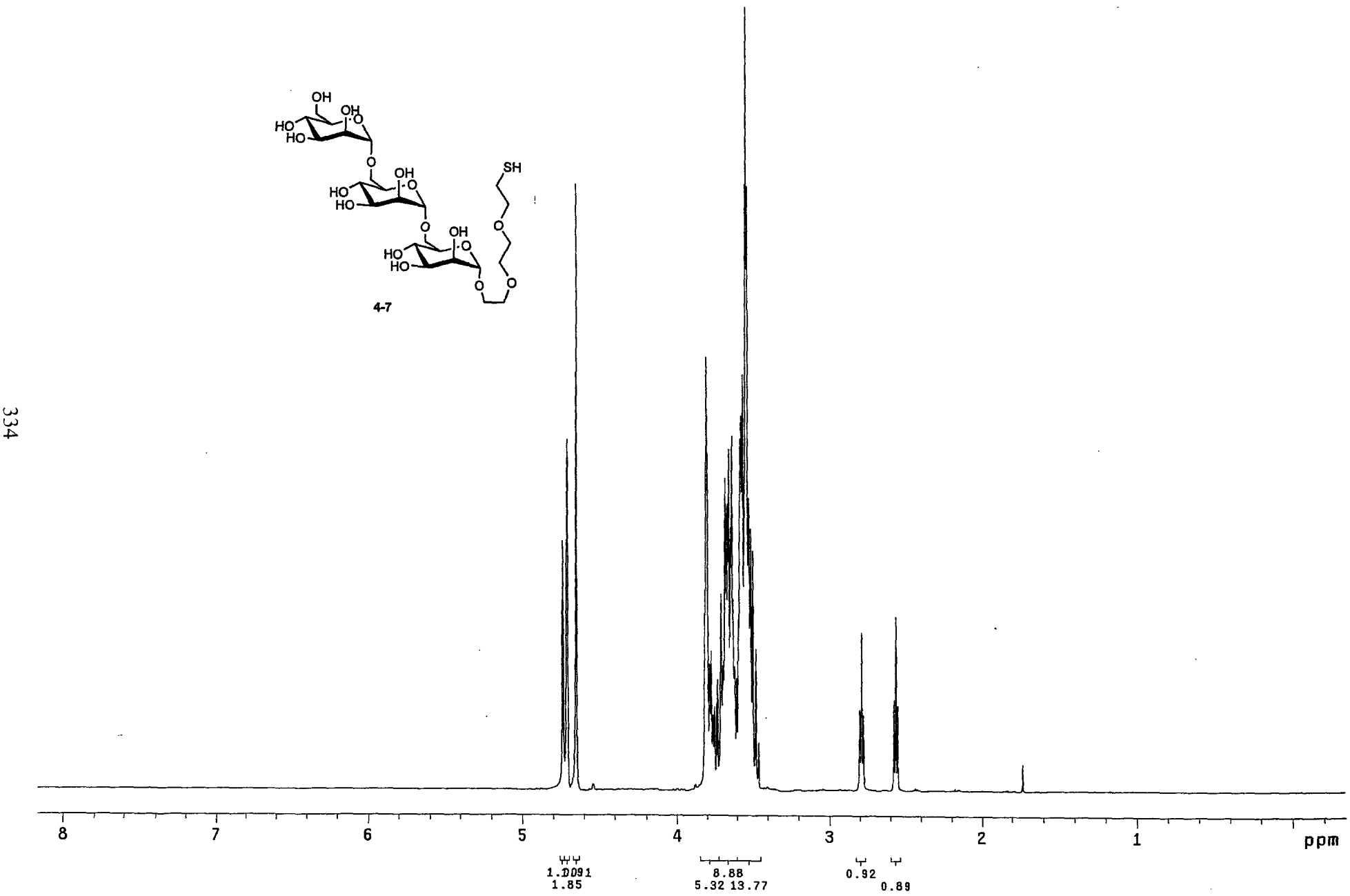
OH
OH
HO
HO
O
OH
HO
HO
O
OH
HO
HO
O
O
SH
O
O
O
4-7
8
7
6
5
4
3
2
1
ppm
1.0091
1.85
8.88
5.32 13.77
0.92
0.89

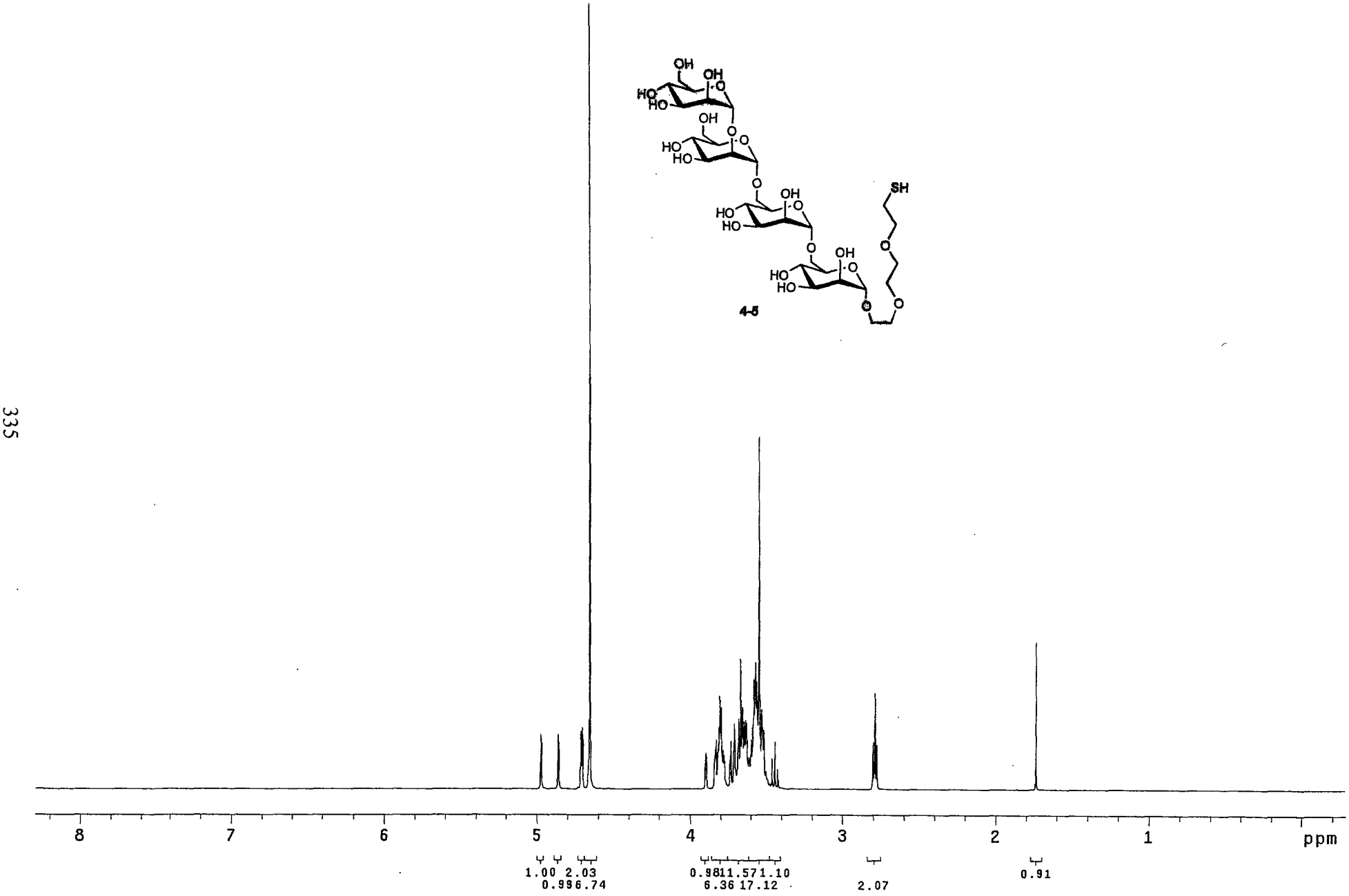
OH
HO
HO
OH
O
HO
HO
O
OH
HO
HO
O
OH
HO
HO
SH
O
O
O
4-5
8
7
6
5
4
3
2
1
ppm
1.00 2.03
0.996.74
0.9811.571.10
6.36 17.12
2.07
0.91

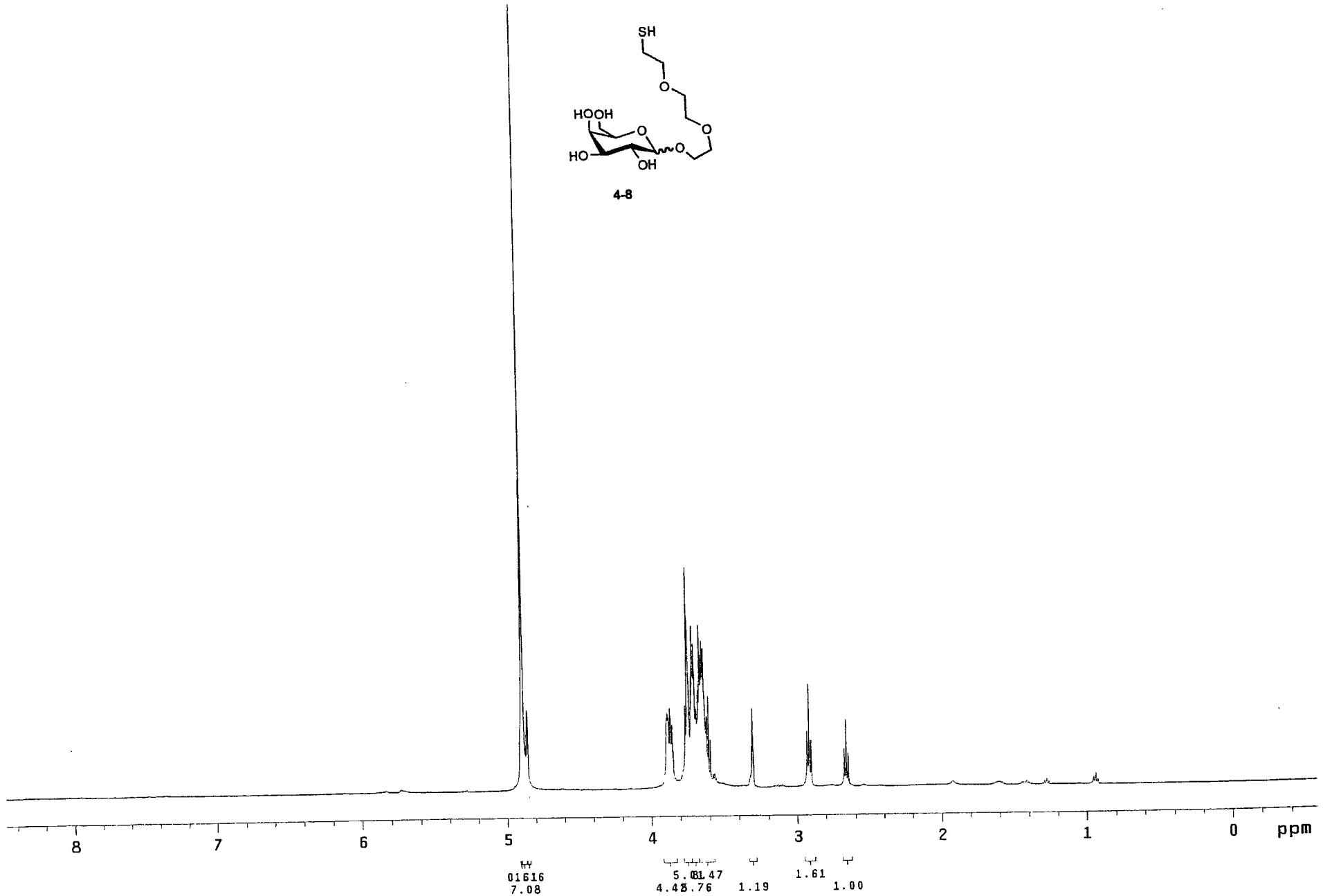
SH
O
O
O
HOOH
O
HO
OH
4-8
8
7
6
5
4
3
2
1
0
ppm
01616
7.08
5.08
4.43
1.47
3.76
1.19
1.61
1.00

Current Spectrum - 53 shots

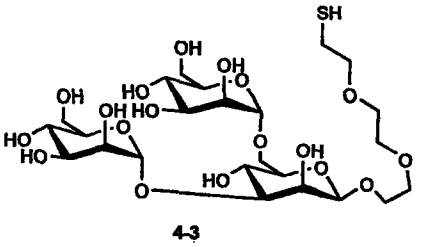

4-3

PE Biosystems Voyager System 102

Spec #1[BP = 1158.9, 13784]

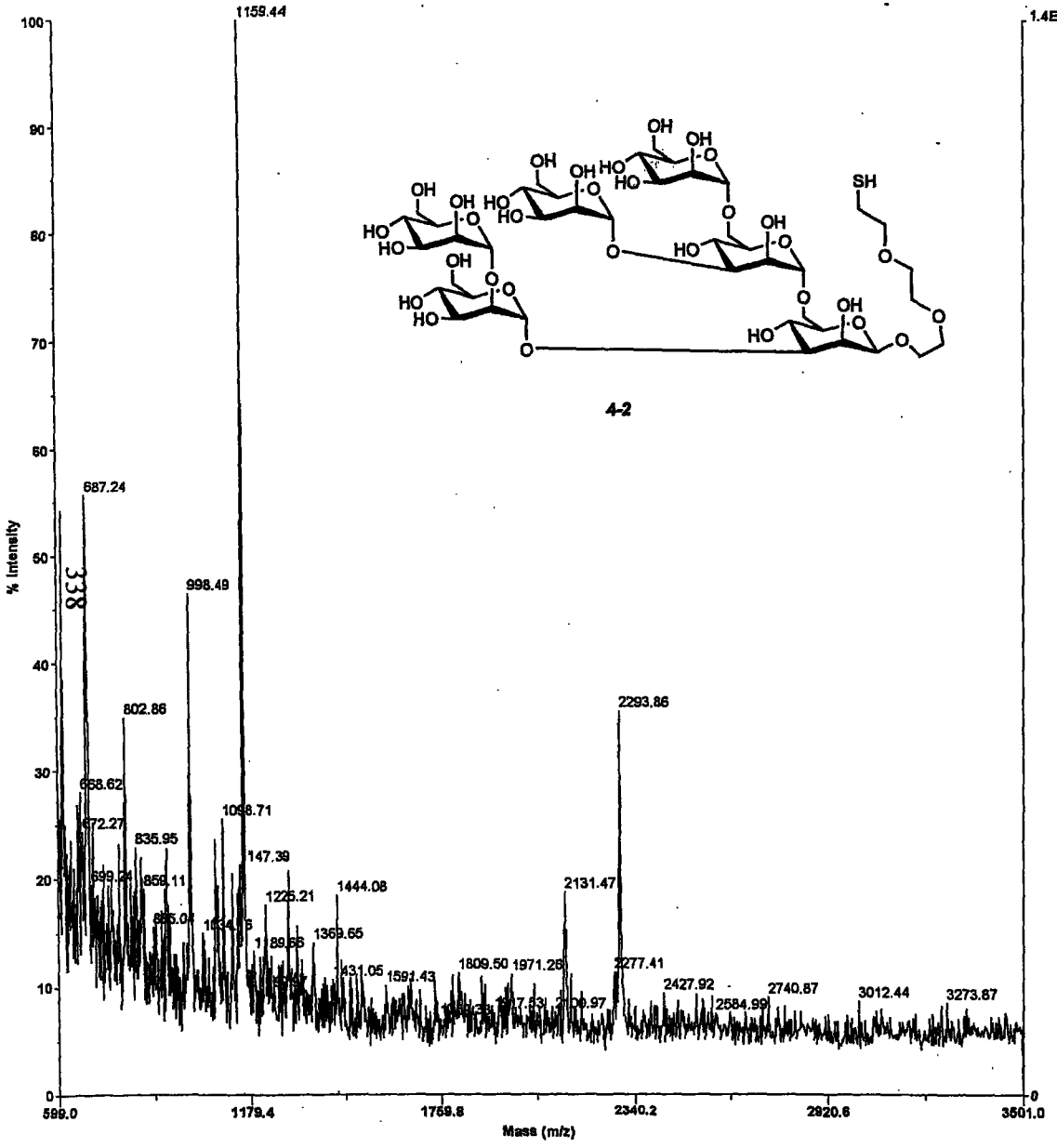

4-2

Mode of operation:	Linear
Extraction mode:	Continuous
Polarity:	Positive
Acquisition control:	Manual
Accelerating voltage:	22000 V
Grid voltage:	95%
Guide wire 0:	0.08%
Acquisition mass range:	600 – 3500 Da
Number of laser shots:	200/spectrum
Laser intensity:	2817
Calibration type:	External – D:\voyager backup\Data\Seeb,Imperial\Data\00016.cal
Calibration matrix:	2,5-Dihydroxybenzoic acid
Low mass gate:	400 Da
Digitizer start time:	23.3449
Bin size:	20 nsec
Number of data points:	5000
Vertical scale:	50 mV
Vertical offset:	0%
Input bandwidth:	500 MHz
Sample well:	43
Plate ID:	GENERIC
Serial number:	102
Instrument name:	Voyager-DE Elite
Plate type filename:	C:\VOYAGER\100 well plate.plt
Lab name:	PE Biosystems
Absolute x-position:	11855.8
Absolute y-position:	25762.8
Relative x-position:	108.316
Relative y-posititon:	-1224.68
Shots in spectrum:	148
Source pressure:	1.337e-007
Mirror pressure:	2.793e-008
TC2 pressure:	0.01923
TIS gate width:	30
TIS flight length:	1435

Acquired: 15:12, October 16, 2003
19mer–24min.
D:\voyager backup\Data\Seeb,Imperial\Data\A1.dat

Printed: 15:13, October 16, 2003

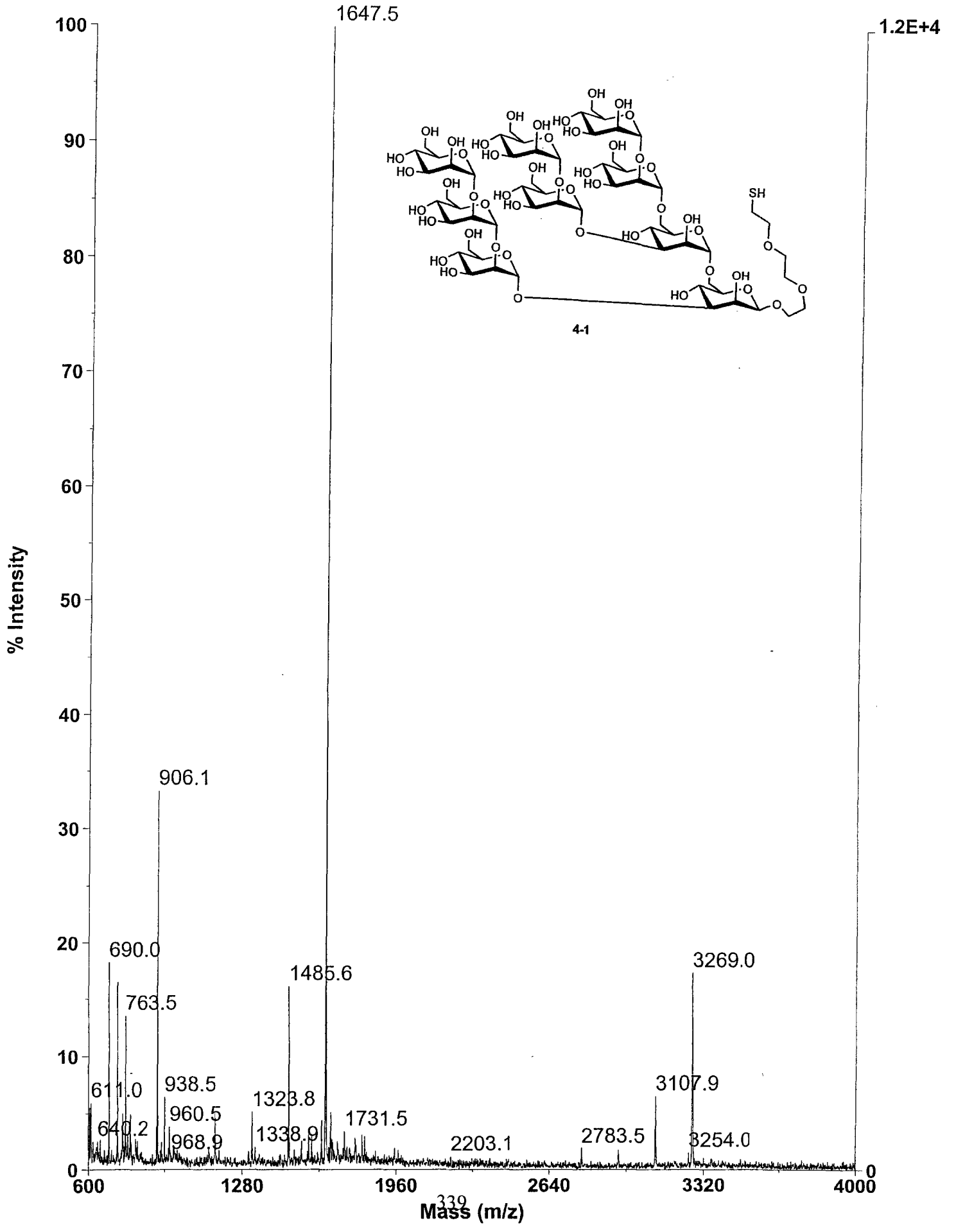
Current Spectrum - 145 shots
1647.5
1.2E+4
100
90
80
70
60
50
40
30
20
10
0
% Intensity
906.1
690.0
763.5
1485.6
3269.0
611.0
938.5
960.5
968.9
1323.8
1338.9
1731.5
2203.1
3107.9
2783.5
3254.0
640.2
600
1280
1960
2640
3320
4000
Mass (m/z)
4-1

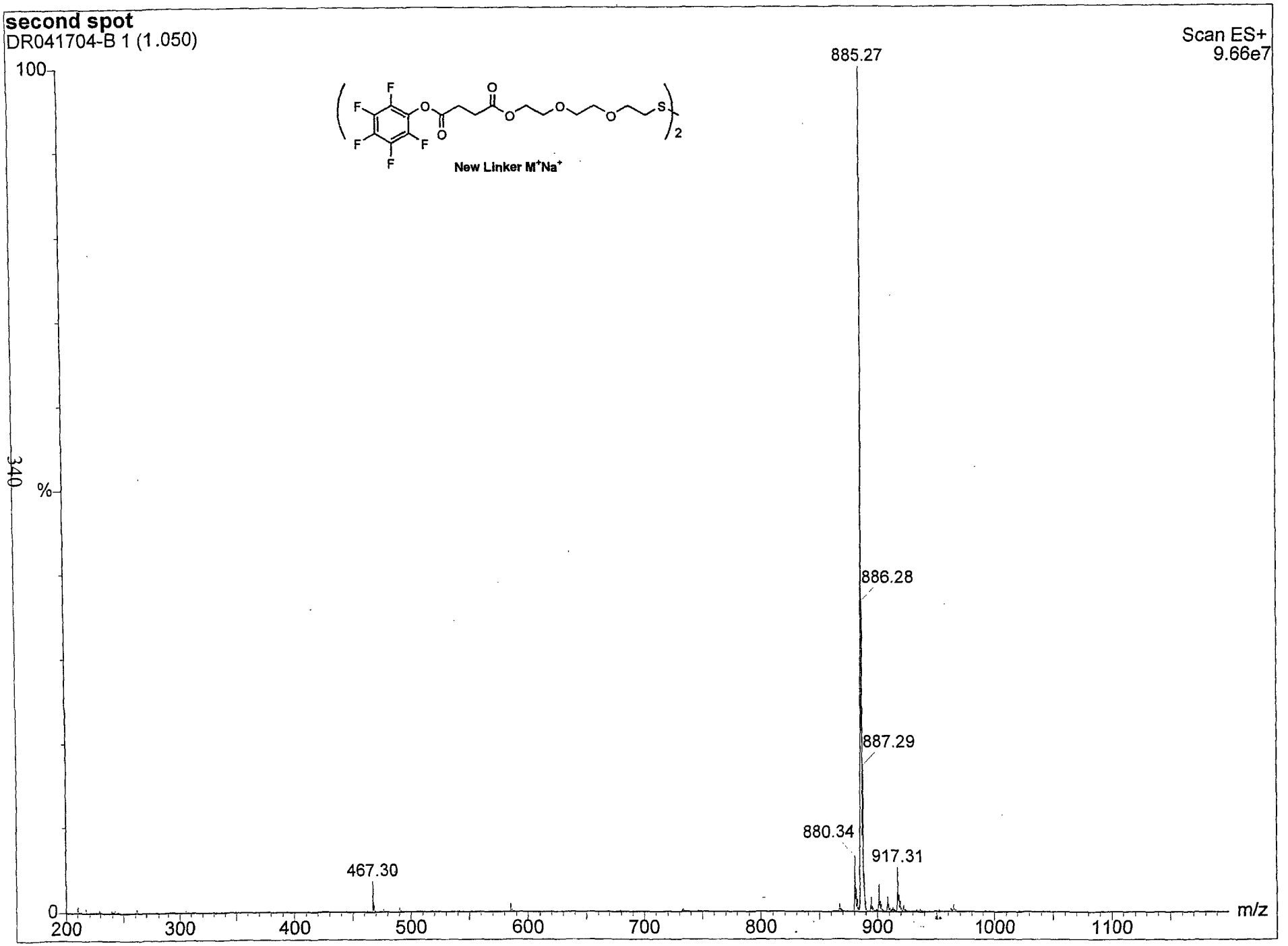
second spot
DR041704-B 1 (1.050)
Scan ES+
9.66e7
100
%
0
340
885.27
886.28
887.29
880.34
917.31
467.30
200
300
400
500
600
700
800
900
1000
1100
m/z
New Linker M+Na+

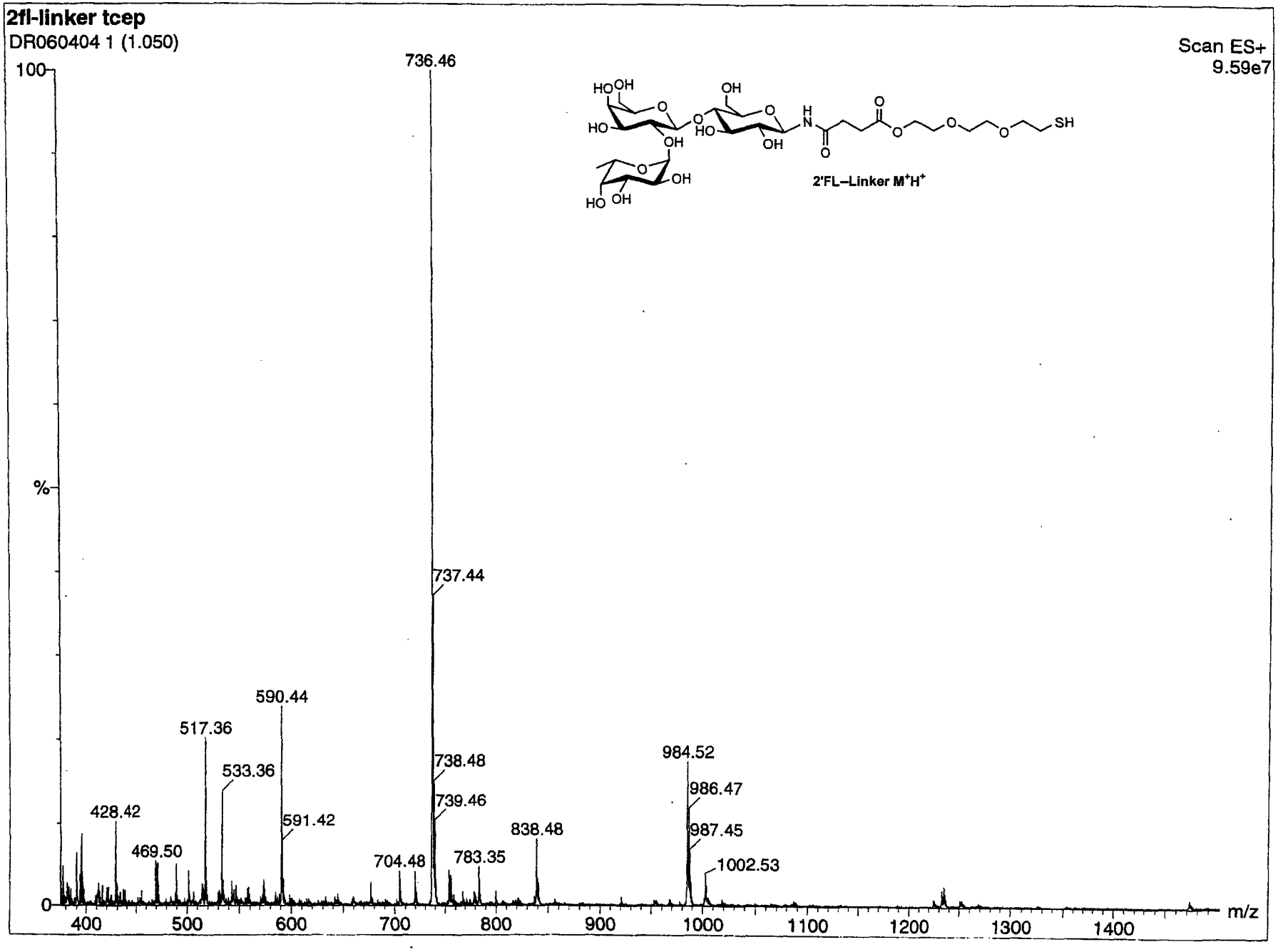
2fl-linker tcep
DR060404 1 (1.050)
Scan ES+
9.59e7
100
%
0
736.46
737.44
590.44
517.36
533.36
428.42
469.50
591.42
704.48
738.48
739.46
783.35
838.48
984.52
986.47
987.45
1002.53
400
500
600
700
800
900
1000
1100
1200
1300
1400
m/z
2'FL–Linker M+H+

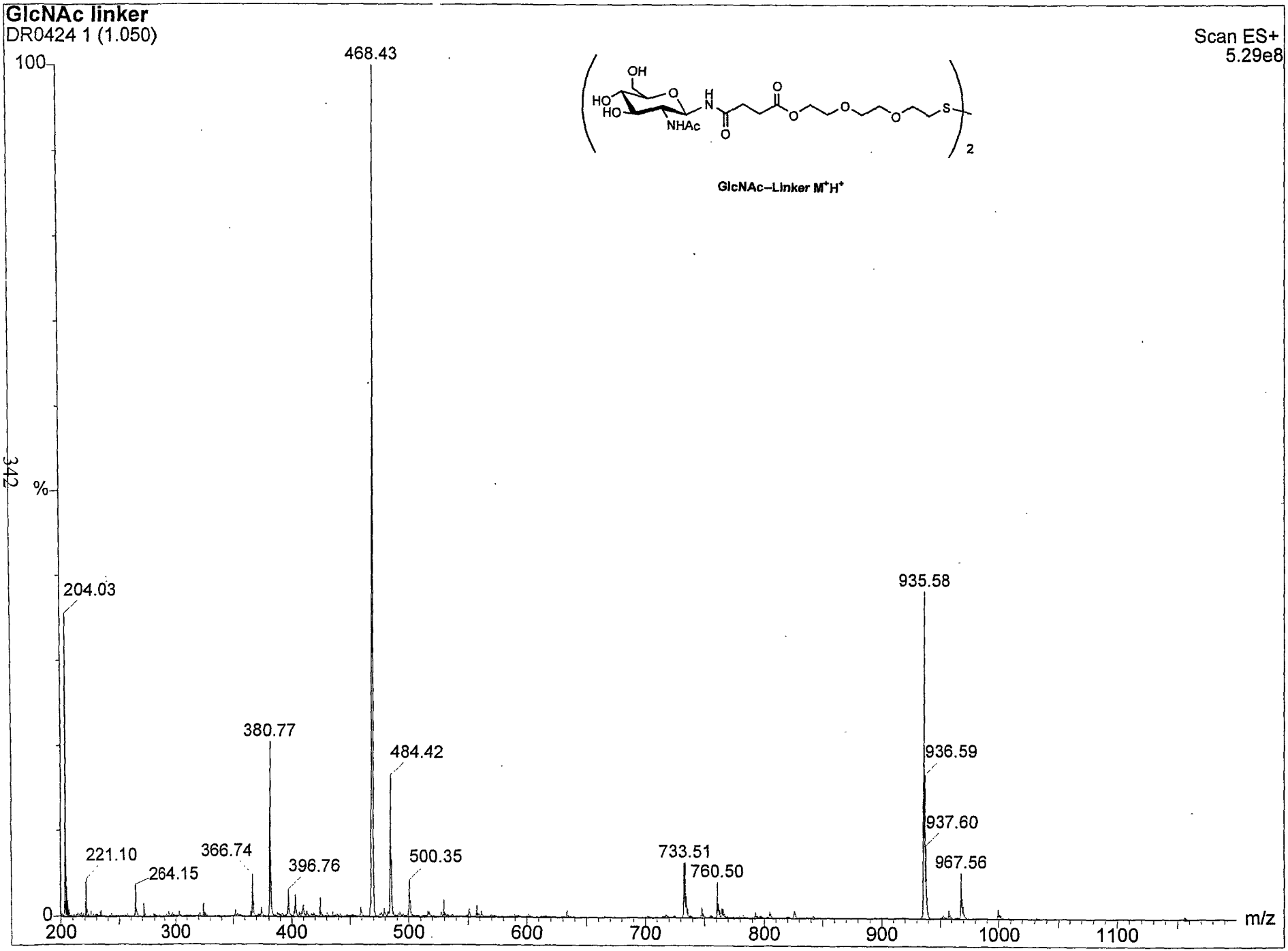
GlcNAc linker
DR0424 1 (1.050)
Scan ES+
5.29e8
100
%
0
342
468.43
204.03
380.77
484.42
935.58
936.59
937.60
967.56
221.10
264.15
366.74
396.76
500.35
733.51
760.50
200
300
400
500
600
700
800
900
1000
1100
m/z
OH
HO
HO
O
NHAc
H
N
O
O
O
O
O
O
S
2
GlcNAc–Linker M+H+

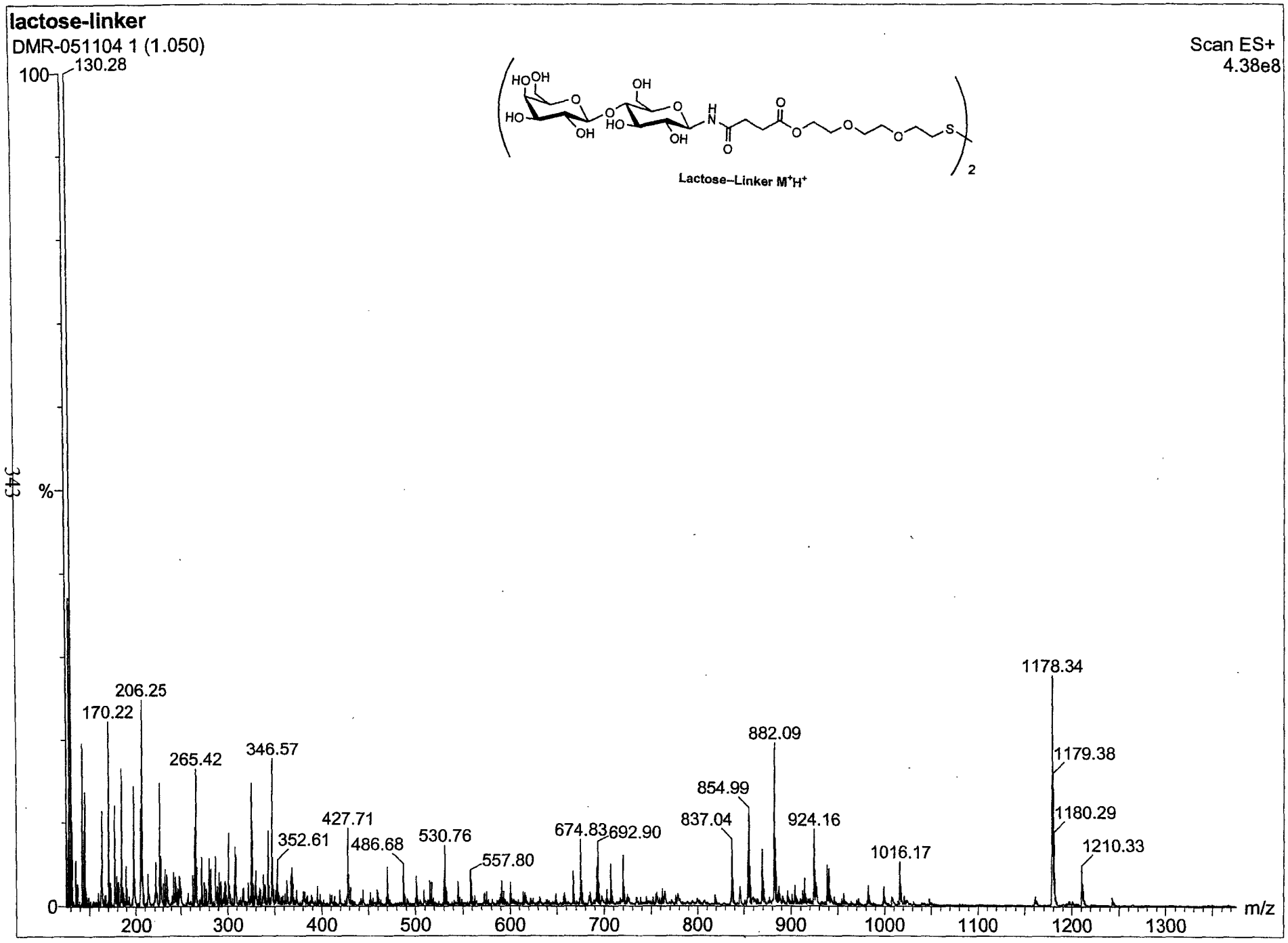
lactose-linker
DMR-051104 1 (1.050)
Scan ES+
4.38e8
100
130.28
%
0
343
206.25
170.22
265.42
346.57
427.71
352.61
486.68
530.76
557.80
674.83
692.90
837.04
854.99
882.09
924.16
1016.17
1178.34
1179.38
1180.29
1210.33
200
300
400
500
600
700
800
900
1000
1100
1200
1300
m/z
Lactose–Linker M+H+

Appendix C.5

Selected Spectra – Chapter 5

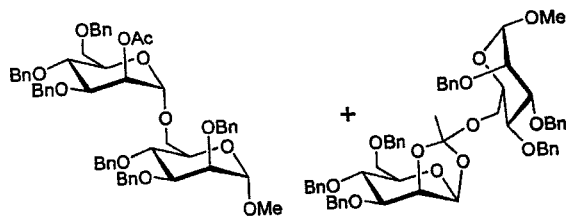

5-7 5-8

Current Data Parameters

NAME	DMA-V-229
EXPNO	10
PROCNO	1

F2 - Acquisition Parameters

Date_	20040416
Time	11.02
INSTRUM	spect
PROBHD	5mm BBO BB-1
PULPROG	zg30
TD	65536
SOLVENT	CDCl3
NS	32
DS	2
SWH	8278.146 Hz
FIDRES	0.126314 Hz
AQ	3.9584243 sec
RG	32
DW	60.400 usec
DE	6.00 usec
TE	300.0 K
D1	1.00000000 sec

========== CHANNEL f1 ========

NUC1	1H
P1	7.90 usec
PL1	0.00 dB
SFO1	400.1324710 MHz

F2 - Processing parameters

SI	32768
SF	400.1300000 MHz
WDW	EM
SSB	0
LB	0.30 Hz
GB	0
PC	1.00

1D NMR plot parameters

CX	20.00 cm
F1P	8.482 ppm
F1	3393.78 Hz
F2P	-0.333 ppm
F2	-133.11 Hz
PPMCM	0.44072 ppm/cm
HZCM	176.34460 Hz/cm

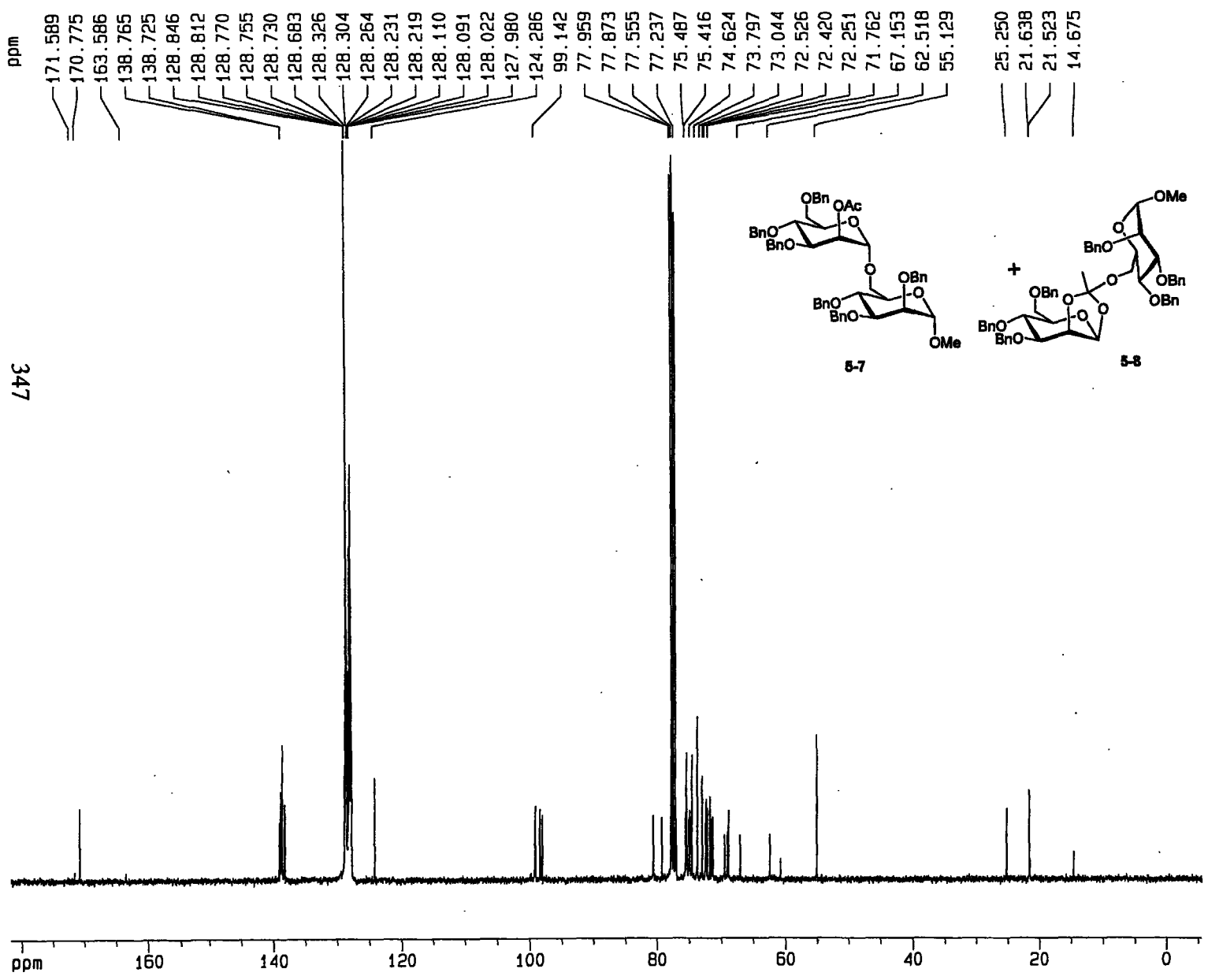

Current Data Parameters

NAME	OMR-V-229
EXPNO	11
PROCNO	1

F2 - Acquisition Parameters

Date_	20040416
Time	12.00
INSTRUM	spect
PROBHD	5mm BBO BB-1
PULPROG	zgpg30
TD	65536
SOLVENT	CDCl3
NS	1024
DS	4
SWH	25125.629 Hz
FIDRES	0.383387 Hz
AQ	1.3042164 sec
RG	8192
DW	19.900 usec
DE	6.00 usec
TE	300.0 K
D1	2.00000000 sec
d11	0.03000000 sec
d12	0.00002000 sec

========== CHANNEL f1 ==========

NUC1	13C
P1	15.25 usec
PL1	3.00 dB
SFO1	100.6237959 MHz

========== CHANNEL f2 ==========

CPDPRG2	waltz16
NUC2	1H
PCPD2	107.50 usec
PL2	0.00 dB
PL12	24.00 dB
PL13	24.00 dB
SFO2	400.1316005 MHz

F2 - Processing parameters

SI	32768
SF	100.6127290 MHz
WDW	EM
SSB	0
LB	1.00 Hz
GB	0
PC	1.40

1D NMR plot parameters

CX	20.00 cm
F1P	181.647 ppm
F1	18275.98 Hz
F2P	-5.510 ppm
F2	-554.38 Hz
PPMCM	9.35784 ppm/cm
HZCM	941.51782 Hz/cm

Appendix C.6

Selected Spectra – Appendix B

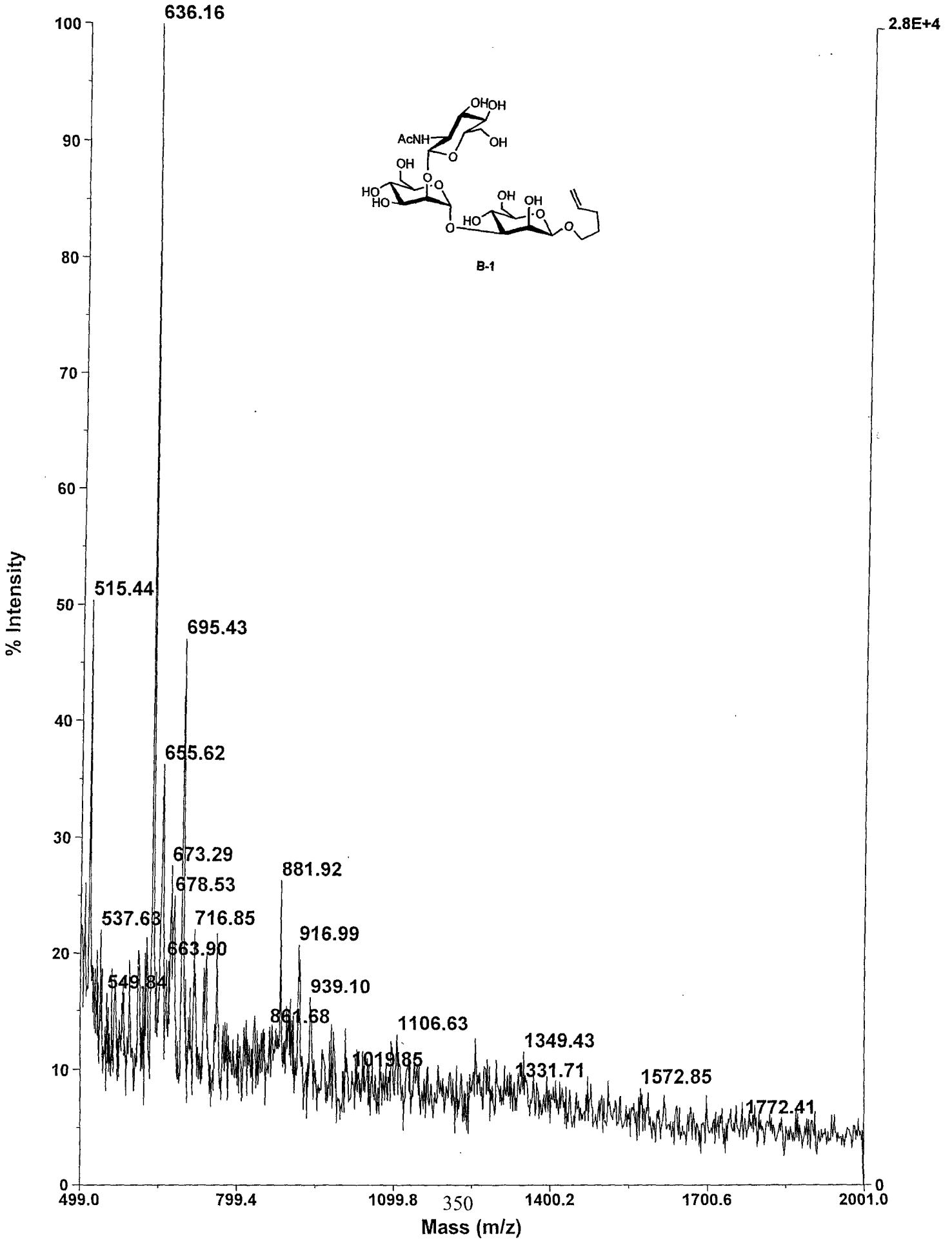
Current Spectrum - 103 shots
636.16
2.8E+4
B-1
515.44
695.43
655.62
673.29
678.53
881.92
537.63
716.85
916.99
663.90
549.84
939.10
861.68
1106.63
1349.43
1019.85
1331.71
1572.85
1772.41
% Intensity
Mass (m/z)
499.0
799.4
1099.8
1400.2
1700.6
2001.0
0
10
20
30
40
50
60
70
80
90
100

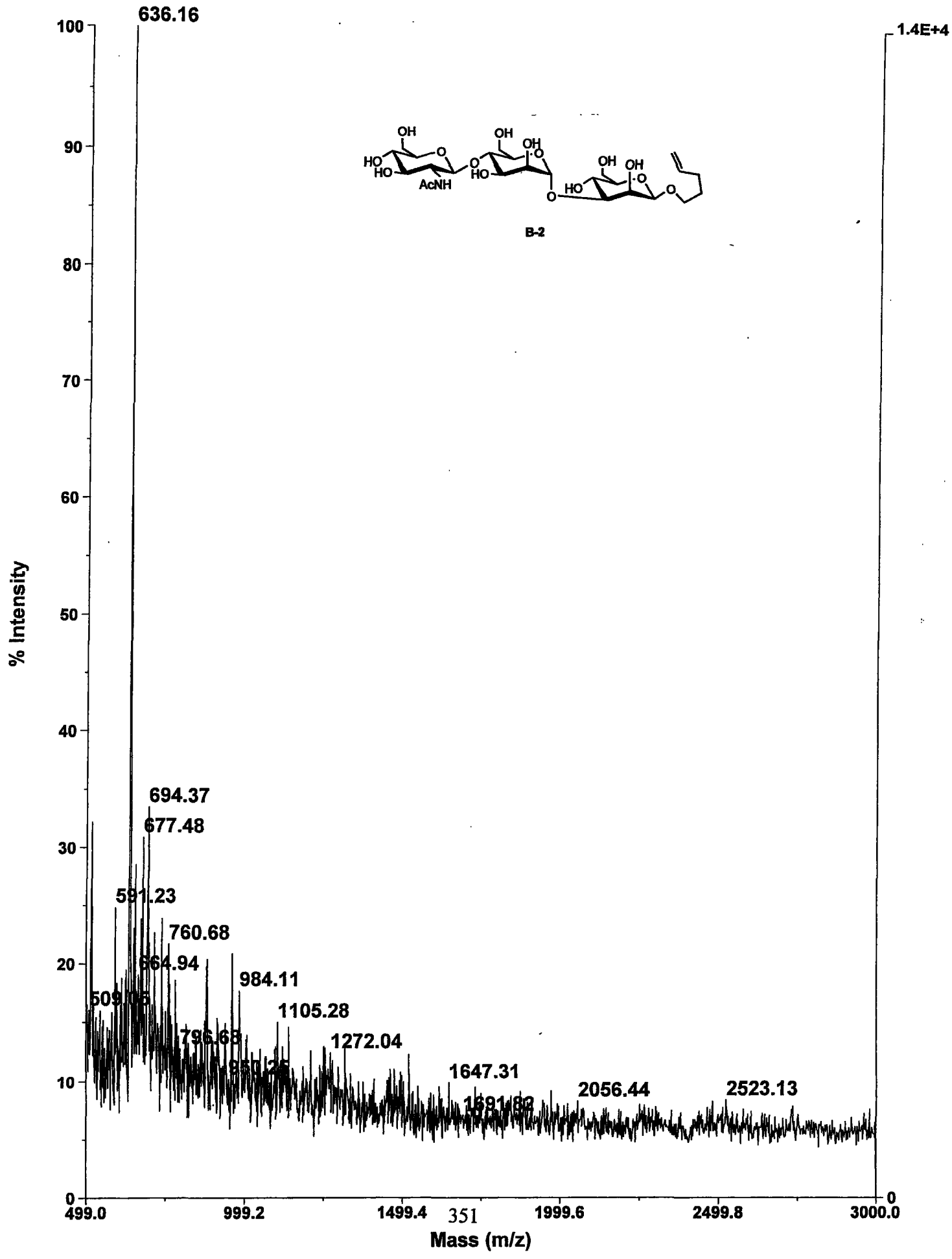
Current Spectrum - 131 shots
636.16
694.37
677.48
591.23
760.68
664.94
984.11
1105.28
1272.04
1647.31
2056.44
2523.13
% Intensity
Mass (m/z)
1.4E+4
100
90
80
70
60
50
40
30
20
10
0
499.0
999.2
1499.4
1999.6
2499.8
3000.0
OH
HO
AcNH
B-2

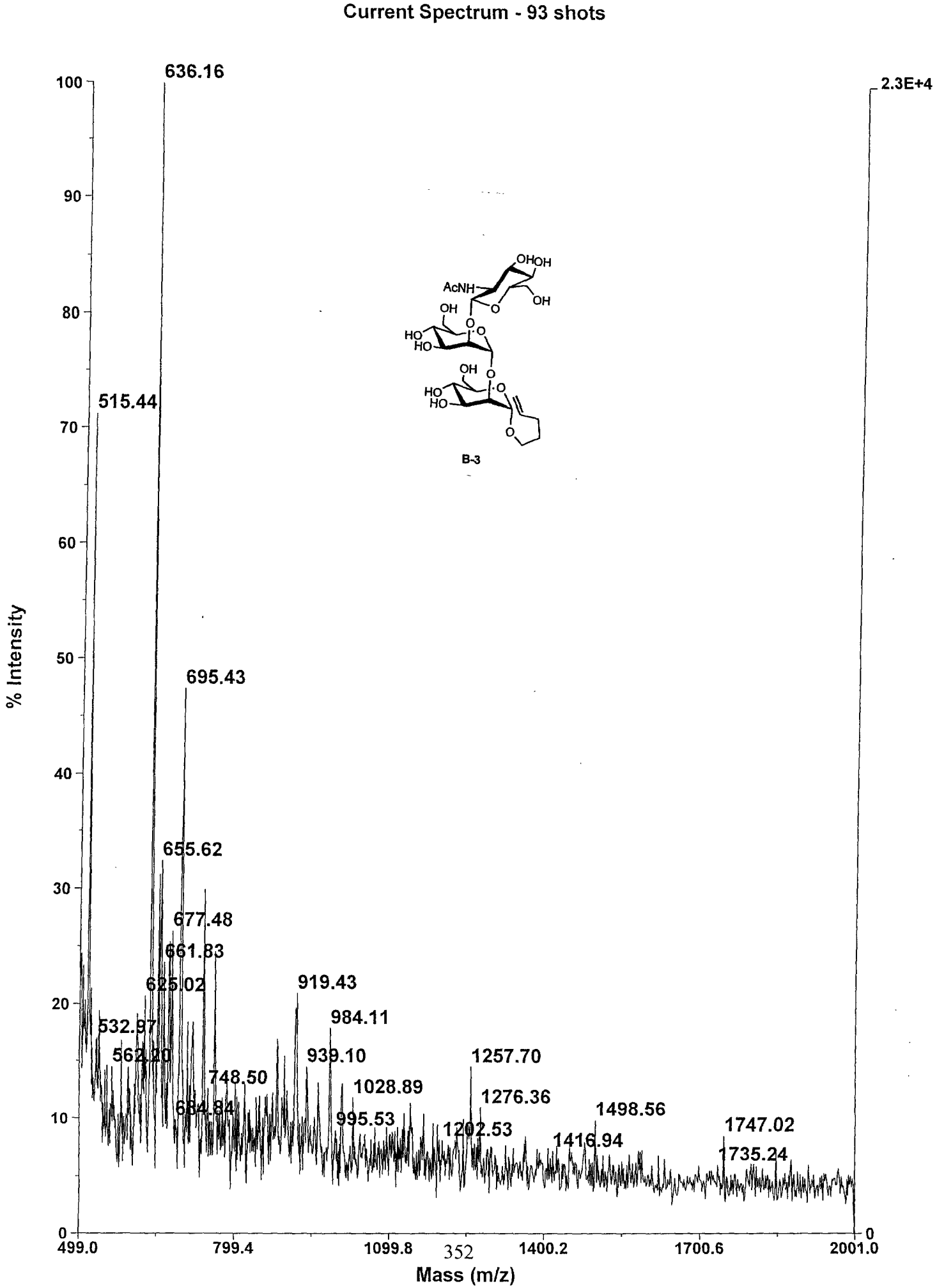
Current Spectrum - 93 shots
636.16
515.44
695.43
655.62
677.48
661.83
625.02
919.43
984.11
532.97
562.20
939.10
1257.70
748.50
1028.89
1276.36
684.84
995.53
1202.53
1498.56
1416.94
1747.02
1735.24
2.3E+4
% Intensity
Mass (m/z)
499.0
799.4
1099.8
1400.2
1700.6
2001.0
B-3

Current Spectrum - 79 shots

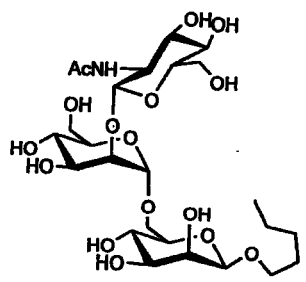

B-4

Daniel Martin Ratner

Education:

Ph.D. Organic Chemistry Massachusetts Institute of Technology	•September, 2004 •Thesis Advisor: Prof. Peter H. Seeberger
B.A., Chemistry Pomona College	•*Cum Laude*: May, 1999 •Thesis Advisor: Prof. Daniel J. O'Leary

Publications:

Ratner,* D. M.; Murphy,* E. R.; Jhunjhunwala, M.; Snyder, D. A.; Jensen, F. K.; Seeberger, P. H. Glycosylation as a Challenge for Microreactor-based Reaction Optimization in Organic Chemistry. *Submitted for Review.*

Ratner, D. M.; Adams, E. W.; Disney, M. D.; Seeberger, P. H. Tools for Glycomics: Mapping Interactions of Carbohydrates in Biological Systems. *ChemBioChem*, **2004**, in press.

Adams,* E. W.; Ratner,* D. M.; Bokesch, H. R.; McMahon, J. B.; O'Keefe, B. R.; Seeberger, P.H. Oligosaccharide and Glycoprotein Microarrays as Tools in HIV-Glycobiology: A Detailed Analysis of Glycan Dependent gp120 / Protein Interactions. *Chem. Biol.* **2004**, *11*, 875-881.

Ratner, D. M.; Adams, E. W.; Su, J.; O'Keefe, B. R.; Mrksich, M.; Seeberger, P. H. Probing Protein-Carbohydrate Interactions with Microarrays of Synthetic Oligosaccharides. *ChemBioChem.* **2004**, 5, 379-383.

Ratner, D. M.; Swanson, E. R.; Seeberger, P. H. Automated Synthesis of the *N*-linked Core Pentasaccharide. *Org. Lett.* **2003**, *5*, 4717-4720.

Adams, E. W.; Uberfeld, J.; Ratner, D. M.; O'Keefe, B. R.; Walt, D, R.; Seeberger, P. H. Encoded Fiber-Optic Microsphere Arrays for Probing Protein-Carbohydrate Interactions. *Angew. Chem. Int. Ed.* **2003**, *42*, 5317-5320.

Ratner, D. M.; Seeberger, P. H. Octenediol. *Encyclopedia of Reagents for Organic Synthesis.* **2003**.

Barrientos, L. G.; Louis, J. M.; Ratner, D. M.; Seeberger, P. H.; Gronenborn, A. M. Solution Structure of a Circular-permuted Variant of the Potent HIV-inactivating Protein Cyanovirin-*N*: Structural Basis for Protein Stability and Oligosaccharide Interaction. *J. Mol. Biol.* **2003**, *325*, 211-223.

Shenoy, S. R.; Barrientos, L. G.; Ratner, D. M.; O'Keefe, B. R.; Seeberger, P. H.; Gronenborn, A. M.; Boyd, M. R. Multisite and Multivalent Binding Between Cyanovirin-*N* and Branched Oligomannosides: Calorimetric and NMR Characterization. *Chem. Biol.* **2002**, *9*, 1109-1118.

Botos, I.; O'Keefe, B. R.; Shenoy S. R.; Cartner, L. K.; Ratner, D. M.; Seeberger, P. H.; Boyd, M. R.; Wlodawer, A. Structures of the Complexes of a Potent Anti-HIV Protein Cyanovirin-*N* and High-Mannose Oligosaccharides. *J. Biol. Chem.* **2002**, *277*, 34336-34342.

Ratner, D. M.; Plante, O. J.; Seeberger, P. H.; A Linear Synthesis of Branched High-Mannose Oligosaccharides from the HIV-1 Viral Surface Envelope Glycoprotein gp120. *Eur. J. Org. Chem.* **2002**, *5*, 826-833.

Patents:

• Seeberger, P. H.; Ratner, D. M.; Adams, E. W. " Carbohydrate Arrays," provisional application filed March 6, 2003.

Presentations:

• Talk, "The Linear Synthesis of HIV-1 Viral Surface Envelope Glycoprotein Oligosaccharides: Towards Automation and the Creation of Carbohydrate Arrays." NIH, Biotechnology Training Program Retreat, Spring 2003.

• Talk, "Linear Synthesis of Branched High-Mannose Oligosaccharides from the HIV-1 Viral Surface Envelope Glycoprotein gp120." American Chemical Society National Meeting, Boston 2002.

Teaching Experience:

- MIT - Graduate Resident Tutor, Residential Life Programs, 2001-2004
- MIT - Head TA, 5.12 Organic Chemistry I, Prof. Barbara Imperiali, Spring 2002
- MIT - TA, 5.12 Organic Chemistry I, Prof. Daniel S. Kemp, Fall 1999
- American Red Cross – Instructor, Emergency Response and CPR for the Professional Responder, Spring 1999

Honors:

- Excellence in Teaching by a Graduate Student, MIT 2002
- NIH Research Fellowship, Biotechnology Training Program, 2000
- Phi Beta Kappa, 1999